ERDC/CRREL MP-22-2



US Army Corps
of Engineers®
Engineer Research and
Development Center



Interior Alaska DoD Training Land Wildlife Habitat Vulnerability to Permafrost Thaw, an Altered Fire Regime, and Hydrologic Changes

Thomas A. Douglas, M. Torre Jorgenson, Hélène Genet,
Bruce G. Marcot, and Patricia Nelsen

January 2022

Cold Regions Research and Engineering Laboratory

Approved for public release; distribution is unlimited.

REPORT DOCUMENTATION PAGE

Form Approved
OMB No. 0704-0188

The public reporting burden for this collection of information is estimated to average 1 hour per response, including the time for reviewing instructions, searching existing data sources, gathering and maintaining the data needed, and completing and reviewing the collection of information. Send comments regarding this burden estimate or any other aspect of this collection of information, including suggestions for reducing the burden, to Department of Defense, Washington Headquarters Services, Directorate for Information Operations and Reports (0704-0188), 1215 Jefferson Davis Highway, Suite 1204, Arlington, VA 22202-4302. Respondents should be aware that notwithstanding any other provision of law, no person shall be subject to any penalty for failing to comply with a collection of information if it does not display a currently valid OMB control number.
PLEASE DO NOT RETURN YOUR FORM TO THE ABOVE ADDRESS.

1. REPORT DATE *(DD-MM-YYYY)*	2. REPORT TYPE	3. DATES COVERED *(From - To)*
31/01/2022	SERDP Final Report	

4. TITLE AND SUBTITLE

Interior Alaska DoD Training Land Wildlife Habitat Vulnerability to Permafrost Thaw, an Altered Fire Regime, and Hydrologic Changes

5a. CONTRACT NUMBER

5b. GRANT NUMBER

5c. PROGRAM ELEMENT NUMBER

6. AUTHOR(S)

Thomas Douglas:U.S. Army ERDC Cold Regions Research and Engineering Laboratory

Bruce Marcot: U.S. Forest Service

Merritt Turetsky: University of Colorado, Boulder

Mark Jorgenson: Alaska Ecoscience

Helene Genet: University of Alaska Fairbanks

5d. PROJECT NUMBER
RC18-1170

5e. TASK NUMBER

5f. WORK UNIT NUMBER

7. PERFORMING ORGANIZATION NAME(S) AND ADDRESS(ES)
U.S. Army ERDC Cold Regions Research and Engineering Laboratory
Army/Corps of Engineers
PO Box 35170
Fort Wainwright, AK 99703

8. PERFORMING ORGANIZATION REPORT NUMBER
ERDC/CRREL MP-22-2

9. SPONSORING/MONITORING AGENCY NAME(S) AND ADDRESS(ES)
Office of the Deputy Assistant Secretary of Defense (Energy Resilience & Optimization)
3500 Defense Pentagon, RM 5C646
Washington, DC 20301-3500

10. SPONSOR/MONITOR'S ACRONYM(S)
SERDP

11. SPONSOR/MONITOR'S REPORT NUMBER(S)
RC18-1170

12. DISTRIBUTION/AVAILABILITY STATEMENT

DISTRIBUTION STATEMENT A. Approved for public release: distribution unlimited.

13. SUPPLEMENTARY NOTES

14. ABSTRACT

Climate change and intensification of disturbance regimes are increasing the vulnerability of interior Alaska Department of Defense (DoD) training ranges to widespread land cover and hydrologic changes. This is expected to have profound impacts on wildlife habitats, conservation objectives, permitting requirements, and military training activities. The objective of this three-year research effort was to provide United States Army Alaska Garrison Fort Wainwright, Alaska (USAG-FWA) training land managers a scientific-based geospatial framework to assess wildlife habitat distribution and trajectories of change and to identify vulnerable wildlife species whose habitats and resources are likely to decline in response to permafrost degradation, changing wildfire regimes, and hydrologic reorganization projected to 2100. We linked field measurements, data synthesis, repeat imagery analyses, remote sensing measurements, and model simulations focused on land cover dynamics and wildlife habitat characteristics to identify suites of wildlife species most vulnerable to climate change. From this, we created a robust database linking vegetation, soil, and environmental characteristics across interior Alaska training ranges. The framework used is designed to support decision making for conservation management and habitat monitoring, land use, infrastructure development, and adaptive management across the interior Alaska DoD cantonment and training land domain.

15. SUBJECT TERMS

Infrastructure, wildland fires, arctic infrastructure, installation resilience, monitoring, habitat, fire, Climatic changes; Habitat (Ecology); Endangered species; Environmental management; Fort Wainwright (Alaska)

16. SECURITY CLASSIFICATION OF:			17. LIMITATION OF ABSTRACT	18. NUMBER OF PAGES	19a. NAME OF RESPONSIBLE PERSON
a. REPORT	b. ABSTRACT	c. THIS PAGE			Thomas Douglas
UNCLASS	UNCLASS	UNCLASS	UNCLASS	323	19b. TELEPHONE NUMBER *(Include area code)* 907-361-9555

The U.S. Army Engineer Research and Development Center (ERDC) solves the nation's toughest engineering and environmental challenges. ERDC develops innovative solutions in civil and military engineering, geospatial sciences, water resources, and environmental sciences for the Army, the Department of Defense, civilian agencies, and our nation's public good. Find out more at www.erdc.usace.army.mil.

To search for other technical reports published by ERDC, visit the ERDC online library at https://erdclibrary.on.worldcat.org/discovery.

Strategic Environmental Research and Development Program

ERDC/CRREL MP-22-2
January 2022

Interior Alaska DoD Training Land Wildlife Habitat Vulnerability to Permafrost Thaw, an Altered Fire Regime, and Hydrologic Changes

Thomas A. Douglas and Patricia Nelsen
Cold Regions Research and Engineering Laboratory
U.S. Army Engineer Research and Development Center
9th Avenue, Building 4070, Fort Wainwright, AK 99703

M. Torre Jorgenson
Alaska Ecosience
2332 Crodes Way, Fairbanks, AK 99709

Bruce G. Marcot
U.S. Forest Service Pacific Northwest, Portland Forestry Sciences Laboratory
620 SW Main St #400, Portland, OR 97205

Helene Génèt
Institute of Arctic Biology, University of Alaska Fairbanks
2140 Koyukuk Drive, Fairbanks, AK 99775

Final report

Approved for public release; distribution is unlimited.

Prepared for Washington, DC 201314
Under U.S. Army Corps of Engineers
SERDP Project RC18-C2-1170

Preface

This study was conducted for the U.S. Army Corps of Engineers under the U.S. Department of Defense Strategic Environmental Research and Development Program (SERDP), Project RC18-C2-1170.

The work was performed by U.S. Army Engineer Research and Development Center, Cold Regions Research Engineering Laboratory (ERDC-CRREL), Alaska Ecospecie, the U.S. Forest Service, and the University of Alaska Fairbanks. At the time of publication of this paper, the acting deputy director for ERDC-CRREL was Mr. Bryan E. Baker and the director was Dr. Joseph Corriveau.

This paper was originally published as *SERDP Final Report RC18-C2-1170* on 20 August 2021.

COL Teresa A. Schlosser was the ERDC commander, and the director was Dr. David W. Pittman.

DISCLAIMER: The contents of this report are not to be used for advertising, publication, or promotional purposes. Citation of trade names does not constitute an official endorsement or approval of the use of such commercial products. All product names and trademarks cited are the property of their respective owners. The findings of this report are not to be construed as an official Department of the Army position unless so designated by other authorized documents.

DESTROY THIS REPORT WHEN NO LONGER NEEDED. DO NOT RETURN IT TO THE ORIGINATOR.

TABLE OF CONTENTS

Table of Contents 1
List of Figures 5
List of Tables 16
EXECUTIVE SUMMARY 17
List of acronyms 20
1. OBJECTIVES 23
2. TECHNICAL APPROACH 27
2.1 Study Design and Field sites 27
2.2 Schedule 29
2.3 Task 1.1 31
2.3.1 Geospatial Measurements 31
2.3.2 Remote Sensing Measurements 36
2.3.3 Thermokarst Feature Development 37
2.4 Task 1.2 59
2.4.1 Background 59
2.4.2 Methods 60
2.4.2.1 Study Design 60
2.4.2.2 Image Compilation and Georectification 60
2.4.2.3 Ecological Classification and Change Detection 61
2.4.2.4 Historical Transition Probabilities 65
2.4.2.5 Climate Trends 65
2.4.2.6 Modeled Ecosystem Transitions 66
2.4.3 Results 66
2.4.3.1 Historical Ecotype Changes 66
2.4.3.2 Drivers of Change 72
2.4.3.3 Accuracy Assessment of Historical Changes 76
2.4.3.4 Climate Trends and Projections 78
2.4.3.5 Projected Ecotype Changes 79
2.4.4 Remote Sensing of Targeted Fen Changes 82
2.4.5 Remote Sensing of NDVI Change 82
2.5 Task 1.3 85
2.6 Task 1.4 88
2.6.1 An Aerial Photograph Transect Study of Interior Alaska training lands 88
2.6.1.1 Structure and Methods of the Aerial Photo Transect Study 89
2.6.2 Landscape Conditions Represented in the Photo Series 91
2.6.3 Archival Access of Photo Series Results 94
2.6.4 Examples of Comparing Previous and Current Site Conditions 94
2.6.5 Examples of Use of Nadir Photos to Create Panoramic Images 95
2.6.6 Examples of Use of Nadir Photo Series to Create Flight Path Animations 96

2.6.7 High-resolution DSLR Photography 97
2.7 Task 2.1 101
2.7.1 Model developments 101
2.7.2 Analysis of historical postfire trajectory using remote sensing data 102
2.7.2.1 Context 102
2.7.2.2 Approach 102
2.7.2.3 Description of the fire regime 103
2.7.2.4 Land cover change resulting from wildfire 104
2.7.2.5 The impact of climate on thermokarst occurrence 106
2.8 Task 2.2 110
2.8.1 Description of the Model 110
2.8.2 Description of the Model Simulations using historical probabilities 112
2.8.3 Description of the Model Inputs 113
2.8.4 Results 117
2.8.4.1 Effect of Constant Historical Probability of Ecotype Change 117
2.8.4.2 Effect of Explicit Fire Frequency and Severity on Ecotype Change 121
2.8.4.3 Effect of Climate Change and Vegetation Productivity on Ecotype Change 121
2.8 Task 2.3 123
2.9 Task 3.1 128
2.9.1 Overview of the Wildlife Analyses 128
2.9.2 Wildlife Species occurrence and Habitat Projections 128
2.9.2.1 What is Presented in This Section 128
2.9.2.2 How This Section Relates to Project Objectives and Hypotheses 128
2.9.3 Overall Work Flow of the Wildlife Analyses 129
2.9.3.1 Overall Objectives 129
2.9.3.2 Guiding Assumptions 129
2.9.3.3 Overall Work Flow: Identifying Species-Habitat Relationships and Projecting Habitat Changes 130
2.9.4 Wildlife Species Occurring in the Project Area 132
2.9.4.1Amphibians 132
2.9.4.2 Birds 133
2.9.4.3 Mammals 135
2.9.4.4 Total Wildlife Species 138
2.9.4.5 Sign of Species Occurrence 139
2.9.4.6 Taxa Not Considered 142
2.9.5 Wildlife Species-Ecotype Relationships 144
2.9.5.1 Ecotypes Used 144
2.9.5.2 Use of Ecotypes by Wildlife Species 144
2.9.6 Bioacoustics of Interior Alaska Training Lands 161

2.9.6.1 Identification of Wildlife Species and Other Site Conditions Through Bioacoustic Recordings 161
2.9.6.2. Sampling Design Used for the Bioacoustic Recordings 161
2.9.6.3. Site Conditions of the Bioacoustic Recording Locations 163
2.9.8 Ecoacoustic Study of the Soundscapes of USAG-AK Training Lands 171
2.9.8.1 Audio Recordings Analyzed as Indices of Soundscape Conditions 171
2.9.8.2 Categories of Ecoacoustics 171
2.9.8.3 Examples of Ecoacoustic Categories 172
2.9.8.4 Analysis of Ecoacoustic Indices 177
2.10 Task 3.2 180
2.10.1 Species Habitats Over Past, Current, and Future Time Periods by Ecotype Projection Scenario 180
2.10.2 Integrating Ecotype Areas by Time Period 180
2.10.3 Species Habitats Over Past, Current, and Future Time Periods 183
2.10.3.1 Wood frog 183
2.10.3.2 Birds 184
2.10.3.3 Mammals 190
2.10.4. Patterns of Soundscapes in the Study Area and Implications for Wildlife Management 194
2.10.4.1 Overview of Ecoacoustic Indices by Soundscape Categories 194
2.10.4.2 The Daily Cycle of Sounds 195
2.10.4.3 The Seasonal Cycle of Sounds 197
2.10.4.4 Influence of Vegetation Conditions on Sounds 199
2.10.4.5 Influence on Sounds from Proximity to Human Activities 201
2.10.4.6 How Sounds Varied By Sampled Site 208
2.11 Task 3.3 210
2.11.1 Habitat Trends of Key Selected Wildlife Species and Species Groups by Scenario 210
2.11.1.1 Bird Migrant Stopover Species Groups 210
2.11.1.2 Bird Game Species 213
2.11.1.3 Bird Habitat Specialists 213
2.11.1.4 Other Bird Species Groups 214
2.11.1.5 Mammal Game Or Subsistence Species 220
2.11.1.6 Mammal Habitat Specialists 221
2.11.1.7 Mammal Carnivores And Top Predators 222
2.11.1.8 Examples Of Trends Of Mammals By Time Period 223
2.12 Task 4 229
2.12.1 Discussion and Management Implications of the Wildlife Habitat Analyses 229
2.12.1.1 Assumptions and Caveats 229
2.12.1.2 Expectations of Ecotype Projection Scenarios 230
2.12.1.3 Species-Rich Ecotypes Depict Spatial Variability in Drivers of Vulnerability 230

2.12.1.4 Understanding the Relationship Between Changing Climate and Key Ecological Processes 230
2.12.1.5 Habitat Futures for Game and Subsistence Species 231
2.12.1.6 Conservation and Protection of Key Ecotypes for the Most Vulnerable Species 231
2.12.1.7 Effects on Wildlife Habitat From Environmental Disturbances 232
2.12.1.8 Considering Habitat Fragmentation and Connectivity 232
2.12.1.9 How Wildlife Behaviors Can Alter Habitat 232
2.12.3 Discussion and Potential Implications for Future Inventory, Monitoring, and Research 233
2.12.4 Conclusions and Management Implications of the Soundscape Analyses 233
2.12.5 Applications for Future Change-Detection Studies 234
3. CONCLUSIONS AND RECOMMENDATIONS FOR TRAINING RANGE MANAGEMENT 235
REFERENCES CITED 238
4. ADDRESSING COMMENTS FROM THE INTERIM REPORT 250
SERDP INTERIM REPORT COMMENTS 250
ACKNOWLEDGMENTS 257
PEER REVIEWED PUBLICATIONS AND PRESENTATIONS SUPPORTED BY THIS PROJECT 258
5. APPENDICES 263
Appendix A.1. References Consulted for Determining Wildlife Species Occurrence and Habitat Use on Fort Wainwright 263
Appendix A.2. Issue with Cornell Swift ARU audio recording anomalies 297

LIST OF FIGURES

Figure 1. A map of the training area domain from Douglas et al., 2014. Boundaries of the major state and federal government landowners. The majority of the non-Federal and non-State of Alaska lands are owned privately or by Alaska Native Corporations. 24
Figure 2. Predominant land cover classes for the Tanana Flats and surrounding areas of interior Alaska from Douglas et al., 2014. From the Alaska 2001 National Land Cover Database (Homer et al., 2007) including evergreen (34%) and deciduous (12%) forest, shrubland (24%), woody wetland (13%), and barren (7%). Percentages are calculated from DoD owned lands within the visible domain. 25
Figure 3. An overview map of the main field sites that were the focus of this study. 29
Figure 4. Map of point locations where data was collected on environmental, soil, and vegetation characteristics across the training lands. These data were put into the Microsoft access relational database, and were used to inform Task 1.2. 32
Figure 5. Screenshot of the relationships and linkages among data and reference tables in the Access relational database used for compiled field site information for DoD lands. 33
Figure 6. A map of Interior Alaska DoD lands (red bounding boxes) with some of the high-resolution images we collected and processed for our study sites. 37
Figure 7. A repeat LiDAR analysis of the Husky Drop Zone showing surface elevation changes between 2017 and 2018. Positive values identify the amount of subsidence. Negative values, identifying areas where elevation increased, are predominantly associated with higher water level elevations in small ponds at the site. From Josh Busby, USAG-FWA Range Control. 39
Figure 8. Repeat LiDAR analysis of the Creamer's Field site. Yellow to orange colored regions exhibited ground subsidence between 2010 and 2020. In some cases, it was as much as a meter of displacement. The blue circle denotes the location of the thermistors presented in Figures 9 and 10. 40
Figure 9. Repeat photos of a site at the Creamer's Field Migratory Refuge where degradation of ice wedge polygons has occurred over the past six years. 41
Figure 10. Soil thermal measurements from two thermistors at site CF2a which is located in the middle of a degrading high-centered polygon surrounded by ice wedges. Thermistor locations are shown in the photos in Figure 6. Note that the thermistor at 1.2 meters depth is approaching 0 ºC. 42
Figure 11. Soil thermal measurements from two thermistors at site CF2b which is located in an ice wedge along the sides that constrain a degrading high-centered polygon. Thermistor locations are shown in the photos in Figure 6. Note that the thermistor at 1.2 meters depth is approaching 0 ºC. 43
Figure 12. Soil temperature measurements at 1.2 m depth from October 1, 2013 to October 1, 2019 for the three study sites. Mean annual ground temperature (MAGT) values at 1.2 m for the period of record are also provided. 44
Figure 13. The Creamer's Field transect from 0 to 246 m. Image a) is a Worldview 2 (© Digital Globe) true color image of the transect with terrain features and core locations (circles) identified, b) LiDAR, c) repeat thaw depth measurements in 2014, d) repeat active layer depth measurements from 2014-2019, and e) a 246 m electrical resistivity tomography transect corrected for ground surface elevation with boreholes identified as black boxes to true depth and numbers corresponding to the distance (in meters) of the borehole location along the transect. Stars with a "T" denote a thermistor location. 45

Figure 14. The Creamer's Field transect from 252 to 498 m. Image a) is a Worldview 2 (© Digital Globe) true color image of the transect with terrain features and core locations (circles) identified, b) May 2020 LiDAR, c) repeat thaw depth measurements in 2014, d) repeat active layer depth measurements from 2014-2019, and e) is a 246 m ERT transect corrected for ground surface elevation with boreholes identified as black boxes to true depth and numbers corresponding to the distance (in m) of the borehole location along the transect. Stars with a "T" denote a thermistor location. 46
Figure 15. The Farmer's Loop 1 transect. Image a) is a Worldview 2 (© Digital Globe) true color image of the transect with terrain features and core locations (circles) identified, b) May 2020 LiDAR, c) repeat thaw depth measurements in 2014, d) repeat active layer depth measurements from 2014-2019, and e) a 410 m ERT transect corrected for ground surface elevation with boreholes identified as black boxes to true depth and numbers corresponding to the distance (in m) of the borehole location along the transect. Stars with a "T" denote a thermistor location. ... 47
Figure 16. The Farmer's Loop 2 transect. Image a) is a Worldview 2 (© Digital Globe) true color image of the transect with terrain features and core locations (circles) identified, b) May 2020 LiDAR, c) repeat thaw depth measurements in 2014, d) repeat active layer depth measurements from 2014-2019, and e) a 492 m ERT transect corrected for ground surface elevation with boreholes identified as black boxes to true depth and numbers corresponding to the distance (in m) of the borehole location along the transect. Stars with a "T" denote a thermistor location. ... 48
Figure 17. The Permafrost Tunnel transect. Image a) is a Worldview 2 (© Digital Globe) true color image of the transect with terrain features and core locations (circles) identified, b) May 2020 LiDAR, c) repeat thaw depth measurements in 2014, d) repeat active layer depth measurements from 2014-2019, and e) a 410 m ERT transect corrected for ground surface elevation with boreholes identified as black boxes to true depth and numbers corresponding to the distance (in m) of the borehole location along the transect. Stars with a "T" denote a thermistor location. 49
Figure 18. A time series of repeat photos from a lowland site on the Tanana Flats Training Area, experiencing degradation of ice rich permafrost and commensurate habitat change. Long-term monitoring of permafrost degradation at this site since 1994 has documented widespread thawing and collapse of permafrost. At this soil temperature monitoring site in a birch forest (T1-Bir1), the ground surface has collapsed underwater. The Campbell datalogger network was replaced with a simpler, lower cost, Onset Hobo network as part of a previous SERDP project (RC-2110). While the photos are from different angles, the tree in the center is the same. By 2011, the site was already flooded with water. 57
Figure 19. Long-term monitoring of soil surface (-5 cm depth) and permafrost (-1 m depth) temperatures in black spruce ecosystems on the Tanana Flats indicates that permafrost has reached a tipping point. Before 2015, permafrost regularly decreased to minus 2-3 °C during winter, indicating stable permafrost. During the last few years, temperatures at depth have risen above 0 °C during summer and have not cooled below 0 °C during winter, indicating accumulation of unfrozen water that prevents hard freezeback..... 58
Figure 20. Sampling grids (yellow with grid ID) used for assessing landscape change within the Tanana Flats Training Area, Yukon Training Area, and Donnelly Training Ageas East and West near Fort Greely, central Alaska. 61
Figure 21. Photographic examples of the six physiographic landscapes in central Alaska comprising a wide diversity of boreal ecotypes (photos by Richard Murphy)..... 68

Figure 22. An example of a time-series of imagery for a lowland grid (#10) on the Tanana Flats from 1949, 1978, 2007, and 2017 used for quantifying ecotype changes. Crosshairs are sampling points used for photo-interpretation and are color-coded to indicate change driver associated with changes. Dominant lowland ecotypes are highlighted on imagery..... 69
Figure 23. Mean changes (n=22 grids) in area (%) of 61 ecotypes from 1949 to 2017 (median years for periods). Bars are 95% confidence intervals, but shown only for seven ecotypes that showed significant trends (P<0.05, repeated measures ANOVA)..... 70
Figure 24. Photographs illustrating ecological processes driving change, including thermokarst, fire, post-fire succession, river erosion/deposition, land clearing, and trail development (photos by T. Jorgenson)..... 73
Figure 25. Mean (n=22 grids, ±95% CI) areal extent and annual rates of change affected by 17 drivers (plus 4 combinations) of ecotype changes for three time-intervals. Note the difference in scales between charts. 74
Figure 26. Areal extent of fires within the study area by year (top), the annual average by interval and landscape (middle), and the reburn occurrence of fires since ~1920..... 76
Figure 27. Historical (Fairbanks) and projected climate warming during summer (based on thawing degree-days, base 0 °C) for the RCP4.5 (low), RCP6.0 (medium), and RCP8.5 (high) scenarios (data from SNAP, 2021). 78
Figure 28. Projected ecotype changes (left) as percent of total study area from 2017 to 2100 based on the time (circle), RCP4.0 (gray bar) and RCP8.0 (black bar) temperature models, and the driver-adjusted RCP6.0 temperature (diamond) models. Relative change (percent difference from initial area) for the driver-adjusted RCP6.0 temperature model is at right. Note different scales for decreases and increases in relative change (right graph). Area (km^2) in 2017 is included with ecotype name..... 80
Figure 29. Map of centerlines and fen width measurement locations for three fen systems on the Tanana Flats. Red denotes wide fens and yellow denotes narrow fens. 83
Figure 30. Landsat derived NDVI change over a 31-year period of record. 84
Figure 31. Comparison of observed wetland formation that occurred between 1984 and 2014 (assessed from Wang et al., 2019) and predicted thermokarst vulnerability from (A) Genet et al., 2014 and (B) Olefeldt et al., 2016..... 86
Figure 32. Comparison of observed wetland formation that occurred between 1984 and 2014 (assessed from Wang et al., 2019), reburn distribution (assessed from the MTBS database) and the distribution of riverine features (assessed from Jorgenson et al., 2008). The purple ellipse represents transitions to water that can be attributed to stream or river channel movement. The green ellipse represents transitions to wetland and water that can be attributed to moderately ice-rich permafrost in alluvial fan..... 87
Figure 33. Flight paths used for the low-level aerial photographic transect of the study area on 4 June 2019, showing the main training areas intersected. TFTA = Tanana Flats Training Area, YTA = Yukon Training Area, DTA = Donnelly Training Area..... 89
Figure 34. Flight paths (blue lines) and flight profiles of velocity (light blue curve) and ASL (altitude above sea level, purple curve) of the two flights conducted for the low-level aerial photographic transect of the study area on 4 June 2019. 90
Figure 35. An example of intersecting GIS data vegetation and land cover mapping on the training lands (Ostrom 2020) with a low-level aerial transect photograph taken during two flight transects on 4 June 2019 (upper-right inset; TFTA = Tanana Flats Training Area, YTA = Yukon Training Area), superimposed here over a recent Google Earth image. The actual flight-line

GoPro photograph is shown offset above the mapped coverage for that photo for comparison. The light white squares show outlines of adjacent time-lapse photographs taken on that transect flight line. 92
Figure 36. Two examples of matching GoPro photographs taken from this study's low-level aerial photographic transects conducted 4 June 2019 (imaged on the right), with prior year conditions from Google Earth imagery (imaged on the left). Top: an example of changes in major riverine flood levels, meanders, sandbar, and riparian conditions (Tanana River near Sam Charley Island). Bottom: impacts of aspen leaf miner (Phyllocnistis populiella) on stands of trembling aspen (Populus tremuloides). 95
Figure 37. Panorama image stitched from 5 sequential GoPro 5 photos of the Tanana River taken on flight path 2, centered on the example image shown in Figure D.4.1. 96
Figure 38. Panorama image stitched from 5 sequential GoPro 5 photos of drainage wetlands and thermokarst ponds in western Tanana River Training Area, taken on flight path 2 (Figure 33).. 96
Figure 39. a) Photographs of dominant drivers of landscape change in central Alaska, including thermokarst on the Tanana Flats (above) and fire on morainal uplands near Ft. Greely (below). 98
Figure 40. Comparison of observed and modeled rate of loss of permafrost plateau resulting from thermokarst disturbance in the TFTA. Red symbols represent rates of loss in validation plots (independent observations). Blue symbols represent rates of loss in plots used for model development. The circles represent rates of loss of permafrost plateau inside the plateau. The dots represent rates of loss of permafrost plateau on the edges of the plateau. Vertical and horizontal lines represent modeled and observed standard deviation respectively. 101
Figure 41. Representation of land cover change and fire regime from 2001 to 2016 in the training area. (A, B) land cover distribution from the NLCD from 2001 and 2016 respectively. (C, D) fire distribution and severity assessed from the Monitoring Trends in Burn Severity database from 2001 to 2016. Deep red sheds in panel c represent areas of re-burn. The purple patch in panel (c) indicates the footprint of the 2001 Survey Line fire that was not reported in the MTBS database. 103
Figure 42. Effect of wildfire frequency on land cover dynamic between 2001 and 2016: (a) percent of area that did not change land cover class, (b) major land cover changes (> 1% cover) in unburned, burned once and reburned areas. 105
Figure 43. Effect of burn severity on land cover dynamic between 2001 and 2016: (a) percent of area that did not change land cover class, (b) major land cover changes (> 1% cover) by severity class. 106
Figure 44. Annual climate records for Fairbanks from 1950 to 2020, corresponding to the period of the repeated imagery analysis presented in Task 1.2. Horizontal lines in each panel represent historical means. Seasons acronyms are W for winter, SP for spring, SM for summer and F for fall. DD = degree days. 107
Figure 45. Location of the soil temperature and active layer depth monitoring sites used for the climate analysis of abrupt increase in active layer depth. 108
Figure 46. Influence of summer precipitation from the current year (a) and from the previous year (b), and heating degree days on the occurrence of abrupt 109
Figure 47. Representation of the ecotypes in (a) lowland, (b) upland and (c) riverine landform and the possible drivers of transitions. F = fire, PFS = post-fire succession, TK = thermokarst, PAE = early paludification, PAL=late paludification, RD = river deposit, RE = river erosion, PS = post-disturbance succession. These diagrams have been simplified for clarity. 111

Figure 48. Diagram representing the coupling of ATM with a disturbance model (ALFRESCO) and a biosphere model (TEM). 113
Figure 49. The 2017 ecotype map used for model initialization. 114
Figure 50. Percent cover by ecotype computed for the 2017 initialization land cover map shown in Figure 49. 115
Figure 51. ALFRESCO projections of (a) cumulated area burned (km^2) and (b) the proportion of high severity fires, from 2017 to 2100, for the ten climate scenarios tested. 116
Figure 52. Projected change in organic layer thickness from 2017 for fen wetlands in response to the 10 climate scenarios tested (5 global circulation models (GCM) for 2 emissions scenarios (rcp4.5 and rcp 8.5) simulated by TEM. 117
Figure 53. (a) Most abundant and (b) less abundant drivers of ecotype change simulated from 2017 to 2100 using constant probabilities of ecotype change computed from repeated historical imagery analysis. BASELINE, MIN, and MAX simulations used averaged, minimum and maximum values of probabilities of change from the three periods of observation respectively. 118
Figure 54. Change in area of the (a) most abundant and (b) less abundant ecotypes, simulated from 2017 to 2100 using constant probabilities of ecotype change computed from repeated historical imagery analysis. BASELINE, MIN, and MAX simulations used averaged, minimum and maximum values of probabilities of change from the three periods of observation, respectively. 120
Figure 55. Projected relative change in vegetation groups as a function of total area burn from 2017 to 2100. Every point represents an entire simulation. Only vegetation groups that were correlated to total area burned are shown. 121
Figure 56. Vulnerability map for a moderate warming scenario (i.e. IPSL-CM5A-LR model for RCP4.5 emissions scenario, warming trend of 2.7 °C/century). Colors locate pixels that experienced land cover change between 2017 and 2100, and the driver of this change. 126
Figure 57. Flow chart of sources and use of information for determining the occurrence of wildlife species occurrence in the study area, their relationships to ecotypes, their current and projected habitat extent, wildlife habitat gainers and losers, wildlife habitat generalist and specialists, wildlife species-rich and species-poor ecotypes, and depictions of soundscapes in the training land study area. Note that multiple sources of information were used to determine species occurrence, including literature, peer reviews, use of field audio recordings, and direct observation. 131
Figure 58. Wood frog (Rana sylvatica), family Ranidae. (A) Adult wood frog (source: National Park Service; photo by Jakara Hubbard), (B) Wood frog with egg mass in pond (source: USAG-FWA Natural Resources). Public domain photo from: https://www.nps.gov/media/photo/gallery-item.htm?pg=919109&id=194a4069-64f5-4004-a207-fcfd63f62f57&gid=AB7AC107-EBD4-441D-8723-3559B3490DE3. 133
Figure 59. Numbers of species and taxonomic families of amphibians, birds, and mammals, by categories mentioned in the text. 134
Figure 60. Immature bald eagle (Haliaeetus leucocephalus, family Accipitridae) observed over the Tanana River within the study area. Although bald eagles were removed from protection under the Endangered Species Act, they are still protected under the Bald and Golden Eagle Protection Act (Alaska Department of Fish and Game, http://www.adfg.alaska.gov/index.cfm?adfg=baldeagle.management). Bald eagle is included on the list of species occurring within the study area. Photos by Bruce G. Marcot. 135

Figure 61. Muskrats (Ondatra zibethicus) occur broadly throughout subarctic Alaska and have been an important element in the fur trade. Photo by M. Torre Jorgenson. 136
Figure 62. Museum occurrence locations of singing vole (*Microtus miurus*) denoting occurrence within the study area. Source: A. Gunderson, Collection Manager, Museum of the North, University of Alaska Fairbanks, contacted April 2021..... 137
Figure 63. Museum occurrence locations of tundra shrew (Sorex tundrensis) denoting occurrence within the study area. Source: A. Gunderson, Collection Manager, Museum of the North, University of Alaska Fairbanks, contacted April 2021..... 138
Figure 64. Examples of wildlife sign found within the study area: (A) down log torn apart likely by an American black bear (Ursus americanus) on the hunt for grubs to eat; (B) tracks of American black bear along a pond shoreline; (C) track of moose (Alces alces) along a river bank; (D) scat (droppings) of moose in an open black spruce woodland); (E) cavity and bark shredded in a cottonwood (Populus balsamifera) tree likely by an American three-toed woodpecker (Picoides dorsalis). Photos by Bruce G. Marcot. 140
Figure 65. Further examples of wildlife sign found within the study area: (A) midden with multiple burrow entrances of an arctic ground squirrel colony (Urocitellus [Spermophilus] parryii) including a cache of spruce cones on top, in black spruce forest; (B) scat (droppings) of red fox (Vulpes vulpes); (C) browse of branches by snowshoe hare (Lepus americanus) who remove bark from low-hanging small branches of deciduous trees; (D) scat pile of snowshoe hare; (E) stream dam created by American beaver (Castor canadensis). Photos by Bruce G. Marcot. 141
Figure 66. Example of a potentially key pollinator of flowering plants of the region is this butterfly, a common alpine (Erebia epipsodea, family Nymphalidae). Photo by Bruce G. Marcot. 142
Figure 67. Extracted example of the wildlife species-ecotype relationships tables used to denote use levels of each ecotype by each species. This example shows only a partial list of the 61 ecotypes and 124 bird species in the study area. Within the Table, 0 denotes that an ecotype is generally not used by the species; 1 denotes secondary use; and 2 denotes primary use for resources. The full set of all ecotypes used by a given species at levels 1 or 2 (thus, omitting 0-coded entries) constitutes that species' habitat within the study area. 145
Figure 68. Ecotypes used by wood frogs in the study area, at use levels 1 (secondary habitat use) and 2 (primary habitat use). Blanks after ecotype names denote that they are generally not used. 147
Figure 69. Bird species richness by ecotype and level of use (1 = secondary, 2 = primary)..... 149
Figure 70. Total bird species richness (no. of species) combining secondary and primary habitat use levels of ecotypes, of the study area, based on vegetation maps of 2017, updated with recent fire events and other disturbances, and cross-indexed to the ecotypes used in this study..... 150
Figure 71. Number of migrant stopover bird groups by ecotype. See Table 13 for general categories of habitat associations, and Appendix Table 2 for the list of bird species in each migrant stopover group. 151
Figure 72. Number of migrant stopover bird groups' combined secondary and primary habitat use levels of ecotypes, of the study area, based on vegetation maps of 2017, updated with recent fire events and other disturbances, and cross-indexed to the ecotypes used in this study. 152
Figure 73. Mammal species richness by ecotype and level of use (1 = secondary, 2 = primary). 153

Figure 74. Total mammal species richness (no. of species) combining secondary and primary habitat use levels of ecotypes, of the study area, based on vegetation maps of 2017, updated with recent fire events and other disturbances, and cross-indexed to the ecotypes used in this study. 154
Figure 75. Total wildlife species richness, of all taxonomic groups (amphibian, birds, and mammals) by ecotype and level of use (1 = secondary, 2 = primary). 155
Figure 76. Total wildlife species richness (no. of species) of amphibians (wood frog) and all birds and mammals, combining secondary and primary habitat use levels of ecotypes, of the study area, based on vegetation maps of 2017, updated with recent fire events and other disturbances, and cross-indexed to the ecotypes used in this study..... 156
Figure 77. Frequency distribution of bird habitat use breadth, measured as number of ecotypes use as secondary or primary (level 1 or 2) habitat. This graph shows that most bird species each used < 20 ecotypes, and very few species used a broader set of ecotypes, e.g., > 30 ecotypes. 157
Figure 78. Bird species habitat use breadth, shown as number of ecotypes used at secondary or primary levels (use levels 1 or 2, respectively), of the top 10 generalists (most ecotypes used) and the top 10 specialists (least ecotypes used). 158
Figure 79. Frequency distribution of mammal habitat use breadth, measured as number of ecotypes use as secondary or primary (level 1 or 2) habitat. This graph shows that most mammal species use either a relatively few or many ecotypes, with fewer mammal species using a moderate number of ecotypes, suggesting greater degrees of habitat specialization and generalization than with birds (Figure 77). 159
Figure 80. Mammal species habitat use breadth, shown as number of ecotypes used at secondary or primary levels (use levels 1 or 2, respectively), of the top 10 generalists (most ecotypes used) and the top 10 specialists (least ecotypes used). 160
Figure 81. A true color image of the region around Fairbanks and Fort Wainwright, Alaska identifying locations of the Automated Recording Units. 164
Figure 82. Deployment locations of 24 automated audio recording units (ARUs) in the study area for the bioacoustic recording study. (A) With satellite view from Google Earth; see Table 15 for code names, and landscape and successional stages at each site. (B) With North American Land Change Monitoring System (NALCMS) land cover conditions, with ARU placement locations shown as white circles. 165
Figure 83. Example of photograph documentation done at each deployment site of the automated audio recording units (ARUs), showing four horizontal images taken at 90-degree intervals clockwise around each ARU unit lashed to trees at approximately head height, and images at zenith and nadir orientations to document canopy cover and ground cover, respectively. 166
Figure 84. Examples of vegetation conditions within 0.5-km of four placements of automated audio recording units (ARUs) located in lowland landscapes of western Yukon Training Area (YTA). TFTA = Tanana Flats Training Area. Dots are the specific locations of the ARUs (see Table 3.2.1). LDTL = Lowland Deep Thermokarst Lake, LDSB = Lowland Dwarf Scrub Bog, LWNF = Lowland Wet Needleleaf Forest, LWBF = Lowland Wet Broadleaf Forest. The 0.5-km radius approximates the effective recording distance from each ARU location. 167
Figure 85. Examples of wildlife sound spectrograms of recordings from automated audio recording units (ARUs). (A) black-capped chickadee, (B) chipping sparrow,(C) northern waterthrush, (D) varied thrush (continued below). Ecotype associations: (A, D) Upland Moist Needleleaf Forest; (B) Lowland Deep Thermokarst Lake; (C) Upland Shallow Thermokarst Lake..... 169

Figure 86. Categories of ecoacoustic sounds used in the soundscape analyses. Sounds can be generally classified as natural and anthropogenic (human-caused). Natural sounds can be further classified as caused by living organisms, including wildlife (biophony) or by abiotic conditions (geophony). Anthropogenic sounds can be further classified as sounds of people (anthrophony) or of their technologies, including vehicles (technophony). Sounds play important roles in ecological systems such as for species identification, and potentially as undue noise disturbance on wildlife from anthropogenic sources. See Appendix Table 15 for a variety of values for each ecoacoustic sound. 172
Figure 87. Examples of sound spectrograms of geophony conditions. (A) intermittent blustery wind, (B) rain, (C) heavy rain downpour, (D) thunder, (E) silence. The red traces at the top of each image denote sound amplitude, and the bottom part of the images denote frequency distributions, both as a function of time (x-axis). Continued below. 173
Figure 88. Examples of a sound spectrogram of an anthrophony condition of people talking and walking. Vocalizations produce the lower-frequency bands < ~1kHz, and walking -- here, through shrubs and vegetation cover, stepping on down twigs and branches -- appear as vertical bands covering a wide range of frequencies. 174
Figure 89. Examples of sound spectrograms of technophony conditions. (A) large jet aircraft, (B) small propeller airplane, (C) helicopter, (D) road vehicles. (continued below) 175
Figure 90. An example of expanding the bird-ecotype relationships table (Figure 66) to include projections of the area coverage of each ecotype by 8 past, current, and future projected time periods. This example pertains to future projections (years 2040 to 2100) under the climate model RCP 4.5 scenario, and this figure shows just a small corner of the much larger table that includes 61 ecotypes (rows) and 124 bird species (columns). Ecotype amounts are the same under all four future climate projection scenarios for time periods 1949 to 2017, and they differ among all four scenarios for the future time periods of 2040 to 2100. In general, this table structure allows for matching of each wildlife species' ecotype use (at levels 1 and 2, secondary and primary habitats, respectively) for efficient calculation of total habitat areas by past, current, and future time period. 181
Figure 91. An example of using the table structure in Figure 90 to track the area of each ecotype, as used by each wildlife species, for the 8 time periods. This example shows the expected use of each ecotype by a bird species, violet-green swallow, for both secondary and primary levels of habitat use. Additional, similar tables track use for secondary and primary use levels separately; this table summed them. For the future time period values, this example pertains to the ecotype projections under the climate model RCP 4.5. The other projection scenarios are tracked in similarly-structured tables. 182
Figure 92. An example showing summed ecotype areas used by each species, by each time period, as measures of their total habitat area. This example shows habitat area based on secondary and primary use levels (levels 1 and 2 in the species-ecotype relationships tables), and the future time periods are based on the climate model 4.5 projection scenario. This is only a small part of the fuller table of all 124 bird species. Also shown in the right three columns are examples of calculated percent changes of habitat areas of each species, for three selected time-period comparisons. 183
Figure 93. Projections of percent change in total habitat area for wood frog from 2017 to 2100, under the 4 ecotype projection scenarios. Note how the scenarios differ in degrees of changes in the ecotypes contributing to habitat for this species, and vary from essentially no change to as

much as an 11% decline. These differences are due to the assumptions and factors considered in each of the ecotype projection scenarios. 184
Figure 94. The top ten bird habitat "gainer" species and top ten "loser" species, over the historic time period of 1949 to 2017. Gainers generally include associates of lowland bogs, fens, wet meadows, and low and tall scrub that have increased in the study area. Losers include associates of other post-fire scrub conditions and needleleaf woodlands and forests that have decreased in area as they gave way to vegetation succession and other changes (see 2.4.3.1 Historical Ecotype Changes). Other bird species had less extreme habitat changes in the study area over this time period (Appendix Table 4). 185
Figure 95. Top 10 bird species habitat gainers and top 10 habitat losers for the projected future time period of 2017 to 2100, among the four ecotype projection scenarios: (A) climate model RCP 4.5, (B) driver-adjusted climate model RCP 6.0, (C) climate model RCP 8.5, and (D) time model based on historic rates. Gainer and loser bird species varied among the projection scenarios depending on the severity of changes among ecotype conditions and disturbances considered in each scenario. 187
Figure 96. Examples of some bird species projected to gain habitat within the study area from 2017 to 2100 under one or more of the ecotype projection scenarios: (A) arctic tern, (B) green-winged teal, (C) dunlin, (D) horned grebe, (E) least sandpiper, (F) red-winged blackbird. Photos by Bruce G. Marcot. 188
Figure 97. Examples of some bird species projected to lose habitat within the study area from 2017 to 2100 under one or more of the ecotype projection scenarios: (A) herring gull, (B) wandering tattler, (C) ruffed grouse, (D) spotted sandpiper, (E) golden-crowned sparrow, (F) harlequin duck, (G) bald eagle, (H) bufflehead. Photos by Bruce G. Marcot. 189
Figure 98. The top ten mammal habitat "gainer" species and top ten "loser" species, over the historic time period of 1949 to 2017. During this time period, no mammal species was projected to have lost habitat within the study area. Several small mammals (lemmings, shrews, voles) gained habitat conditions as a result of post-fire recovery of open, short-vegetation ecotypes, which also benefited grazing caribou. Most of the other mammal species had modest gains in their habitat conditions over this time period (Appendix Table 5). 190
Figure 99. Top 10 mammal species habitat gainers and top 10 habitat losers for the projected future time period of 2017 to 2100, among the four ecotype projection scenarios: (A) climate model RCP 4.5, (B) driver-adjusted climate model RCP 6.0, (C) climate model RCP 8.5, and (D) time model based on historic rates. As with the bird species (Figure 95), gainer and loser mammal species and the severity of projected habitat changes varied among the projection scenarios depending on the intensity of changes among ecotype conditions and disturbances considered in each scenario. 192
Figure 100. Examples of some mammal species projected to gain or lose habitat within the study area from 2017 to 2100 under one or more of the ecotype projection scenarios: (A) arctic ground squirrel, habitat gainer; (B) porcupine, habitat loser; (C) caribou, habitat loser; (D) black bear, habitat loser. Porcupine photo by M. Torre Jorgenson; other photos by Bruce G. Marcot. 193
Figure 101. Example of variation in the values of two ecoacoustic indices — Acoustic Diversity Index (ADI) and Normalized Difference Soundscape Index (NDSI) — over the course of the 24-hour daily cycle. Curved lines are mean values and vertical bars are ±1 SD. 196
Figure 102. Values of the Acoustic Diversity Index (ADI) by date from April to September 2020, for four landscapes. Curved lines are mean values and vertical bars are ±1 SD. 198

Figure 103. Values of the Acoustic Diversity Index (ADI) among all 24 automated audio recording unit (ARU) locations (Table 15), by 8 vegetation and ground cover covariates, from June-August 2019 audio recordings. Lines are best-fit linear regressions, dots are individual ARU locations. Patterns using the April-September 2020 ARU recordings also produced essentially the same patterns. 200
Figure 104. Values of the Normalized Difference Soundscape Index (NDSI) among all 24 automated audio recording unit (ARU) locations (Table 15), by 8 vegetation and ground cover covariates, from June-August 2019 audio recordings. Lines are best-fit linear regressions, dots are individual ARU locations. Patterns using the April-September 2020 ARU recordings also produced essentially the same patterns. 201
Figure 105. Locations of key human-created features in the portion of the study area with 24 automated audio recording units (ARUs). This was used to analyze the potential effects of distance to these features on soundscape attributes at each ARU location. The radial flight lines are from Fairbanks International Airport; flight lines on the right are military training flight paths. 202
Figure 106. Values of the Acoustic Diversity Index (ADI) among all 24 automated audio recording unit (ARU) locations (Table 15), by distance from the recorder location to 9 categories of human activity (anthropogenic disturbance covariates), from June-August 2019 audio recordings. Lines are best-fit power regressions, dots are the individual ARU locations. 204
Figure 107. Values of the Normalized Difference Soundscape Index (NDSI) among all 24 automated audio recording unit (ARU) locations (Table 15), by distance from the recorder location to 9 categories of human activity (anthropogenic disturbance covariates), from June-August 2019 audio recordings. Lines are best-fit power regressions, dots are individual ARU locations. 205
Figure 108. Areas within the study area within buffer threshold distances of four anthropogenic sound sources of primary roads (5,000 m), firing sites (5,000 m), main airports (15,000 m), and flight lines (1,000 m). These are sounds sources for which the Acoustic Diversity Index (ADI) shows curvilinear threshold distances within which effects on sound diversity greatly increase. Overlapping areas have >1 sound source within their respective threshold distances, and white areas are further than the threshold distances to all four of these sound sources where wildlife are likely the least impacted by noise of these human activities. 207
Figure 109. Variation in values of two ecoacoustic indices — Acoustic Diversity Index (ADI) and Normalized Difference Soundscape Index (NDSI) — among the 5 main geographic locations of deployment of the automated audio recording units (Table 15) during June-August 2019 and April-September 2020. (Note that, because of recorder scheduling problems, Creamer's field and the Permafrost Tunnel were inadequately sampled during 2020.) Center lines in the boxes are median values, box lengths are the range within the central 50% of values, and asterisks are outside values. 209
Figure 110. Past, present, and future habitat area of bird migrant stopover species groups (see Appendix Table 2 for species lists) under four ecotype projections: (A) climate model RCP 4.5, (B) driver-adjusted climate model RCP 6.0, (C) climate model RCP 8.5, (D) time model based on historic rates. 212
Figure 111. Percent change in future habitat, 2017 to 2100, of 25 bird game species (as listed by Alaska Department of Fish and Game; see Appendix A.1), under four ecotype projection scenarios. Note that most projections result in minor declines, no changes, or increases in habitat

areas except for some scenarios projecting habitat decreases for harlequin duck and two species each of grouse and ptarmigan. 213
Figure 112. Percent change in future habitat, 2017 to 2100, of 14 habitat-specialist bird species, under four ecotype projection scenarios. Here, bird habitat specialists are defined as those species using 5 or fewer ecotype categories. Projections predict high increases in habitat for some aquatic-associated species, and possible declines for wetland and other wet-site vegetated conditions. 214
Figure 113. Percent change in future habitat, 2017 to 2100, of selected groups of bird species of potential management or conservation interest, under four ecotype projection scenarios: (A) waterfowl (ducks, geese), (B) grouse and ptarmigan, (C) raptors, (D) owls, (E) woodpeckers, (F) thrushes and flycatchers, (G) warblers, (H) sparrows, finches, and allies. 219
Figure 114. Percent change in future habitat, 2017 to 2100, of rusty blackbird, under four ecotype projection scenarios. Projections predict at much as a 10% increase or a 10% decrease depending on the scenario. 220
Figure 115. Percent change in future habitat, 2017 to 2100, of 9 mammal game or subsistence species (as listed by Alaska Department of Fish and Game; see Appendix A.1), under four ecotype projection scenarios. Note the projected, potential habitat decline for caribou, beaver, and black bear, although percent changes vary significantly among the four ecotype projection scenarios. 221
Figure 116. Percent change in future habitat, 2017 to 2100, of 9 mammal habitat specialist species, under four ecotype projection scenarios. Here, mammal specialists are defined as those species using 10 or fewer ecotype categories. Most species are projected with stable to increasing habitat amounts. 222
Figure 117. Percent change in future habitat, 2017 to 2100, of 12 species of mammalian carnivores, under four ecotype projection scenarios. The species listed here all belong to order Carnivora and in the families Canidae, Felidae, Ursidae, and Mustelidae. 223
Figure 118. Past, present, and future habitat area of small mammals (lemmings and voles) and muskrat, under four ecotype projections: (A) climate model RCP 4.5, (B) driver-adjusted climate model RCP 6.0, (C) climate model RCP 8.5, (D) time model based on historic rates. 225
Figure 119. Past, present, and future habitat area of ungulate species, under four ecotype projections: (A) climate model RCP 4.5, (B) driver-adjusted climate model RCP 6.0, (C) climate model RCP 8.5, (D) time model based on historic rates. 227

LIST OF TABLES

Table 1. Training range land uses and the potential vulnerabilities and risks for wildlife habitats on those range areas in a projected future warmer climate. 26
Table 2. Hypotheses and Tasks of the proposed research. 27
Table 3. A Gantt chart style schedule of the proposed three-year effort. 30
Table 4. Number of sites compiled in the database listed by training area and type of data collected. 34
Table 5. Example characteristics measured in the field and compiled in the database. The soil stratigraphy characteristics were measured for each horizon layer present in the soil pit, and the vegetation characteristics measured for each species observed at a site. 35
Table 6. A summary of the thaw depth measurements by ecotype and results from a means comparison using a student's t-test. Among a given ecotype different and year the letters identify statistically significantly different means. Mean values for a given ecotype and year with similar letters have similar means. 51
Table 7. A summary of thermistor measurements from 1.2m depth at the study site transects. Mean annual temperature (MAT) values for each of six individual years are presented as well as the six-year global mean annual temperature for each site. 54
Table 8. Coding system used for classifying landscape change. 63
Table 9. Crosswalk of statewide ecotypes used in grid sampling with ecotypes described for the TFTA and YTA near Fort Wainwright (Jorgenson et al., 1999) and DTAW and DTAE near Fort Greely (Jorgenson et al., 2001). 64
Table 10. Explanation for cumulative historical and projected landscape change (driver-adjusted climate model RCP6). 71
Table 11. Accuracy assessment comparing mapped versus ground determinations. See Table 8 for codes. 77
Table 12. Distribution of area burned by severity class and by landform. 104
Table 13. Categories of migrant stopover bird species (see Appendix Table 2) by habitat associations. 134
Table 14. Numbers of wildlife species and taxonomic families included in the habitat projections. 139
Table 15. Deployment of 24 automated audio recording units (ARUs) in the study area. ARUs were used during field seasons 2019 (June-August) and 2020 (April-September) to record sounds useful for identifying wildlife species and soundscape conditions (discussed in section 2.10.4). 162
Table 16. Ecoacoustic indices calculated from field sound recordings. These 13 indices represent various dimensions of soundscape conditions, or patterns of sound frequencies, amplitudes, and temporal variations, from various natural and anthropogenic (human-caused) sources. 178
Table 17. Regions of the study area that are within threshold distances of four anthropogenic sound sources or combinations thereof, that display distance threshold influences on the Acoustic Diversity Index (see Figure 106). Shown are non-mutually exclusive total areal coverage and percent of the total study area of each sound source individually and where they spatially overlap. Threshold buffer distances from each sound source are: primary road, 5,000 m; firing site, 5,000 m; main airport, 15,000 m; flight line, 1,000 m. 206

EXECUTIVE SUMMARY

Climate change and intensification of disturbance regimes are increasing the vulnerability of interior Alaska Department of Defense (DoD) training ranges to widespread land cover and hydrologic changes (Lara et al., 2016; Jorgenson et al., 2020; Douglas et al., 2019; 2021). This is expected to have profound impacts on wildlife habitats, conservation objectives, permitting requirements, and military training activities. The objective of this three-year research effort was to provide United States Army Alaska Garrison Fort Wainwright, Alaska (USAG-FWA) training land managers a scientific-based geospatial framework to assess wildlife habitat distribution and trajectories of change and to identify vulnerable wildlife species whose habitats and resources are likely to decline in response to permafrost degradation, changing wildfire regimes, and hydrologic reorganization projected to 2100. We linked field measurements, data synthesis, repeat imagery analyses, remote sensing measurements, and model simulations focused on land cover dynamics and wildlife habitat characteristics to identify suites of wildlife species most vulnerable to climate change. From this, we created a robust database linking vegetation, soil, and environmental characteristics across interior Alaska training ranges. The framework used is designed to support decision making for conservation management and habitat monitoring, land use, infrastructure development, and adaptive management across the interior Alaska DoD cantonment and training land domain.

This Report provides a summary of project activities and outcomes for the three-year project "Interior Alaska DoD training land wildlife habitat vulnerability to permafrost thaw, an altered fire regime, and hydrologic changes," Strategic Environmental Research and Development Program (SERDP) project RC18-C2-1170. This project was initiated in March 2018 and ended in late July, 2021. There were no Go/No-Go decision points associated with the project.

This Report starts with an overall introduction to the research problems addressed along with information about our field sites. From there, the main content in this Report is provided as standalone sections, keyed to major project Tasks, that provide the roadmap for the project work and results. Each Task is presented first as a succinct itemization of the main goals and activities. From this, Task achievements are summarized with a focus on the new science developed, the results, and the overall interpretation. The Report concludes with a set of conclusions and recommendations for training land management.

The focused objective of this project was to answer the question: "*where, when, and how will projected climate warming on Interior Alaska DoD training lands affect habitat access, suitability, and use?*" The major conclusions with broad ramifications for training land management and decision making include:

1) Across the military training lands and cantonments in central Alaska, ecosystems form a highly diverse mosaic of patches at varying successional stages following disturbance. The main disturbance drivers include fire, thermokarst development, river erosion and deposition, vegetation succession, and human impacts. This diversity, patchiness, and the varying successional stages help maintain a fairly stable composition of ecotypes over time. However, there can be wide and unpredictable short-term fluctuations, particularly from fire and infrastructure development (fire breaks, roads, and trails).
2) To assess the patterns and rates of change across the landscape, we quantified the extent of ecotypes, and the fire history and biophysical factors affecting change, through photo-interpretation of 2,200 systematically distributed points on a time-series (~1949, ~1978, ~2007, ~2017) of geo-rectified imagery across all central Alaska Army lands. Overall,

67.9% (n=2,200) of the study area had changes in ecotypes over the entire 68-yr interval, with net changes of 49.6%, 52.4%, and 25.0%, respectively, during the 1949-1978, 1978-2007, and 2007-2017 time intervals. Most of these changes resulted from increases in upland and lowland forest types, with an accompanying decrease in upland and lowland scrub types as post-fire succession led to late-successional stages. There also were smaller losses of forest ecotypes to river erosion, and increases in riverine scrub with accompanying decreases in riverine gravelly barrens. Fire was by far the largest driver of landscape change, affecting 47.3% of the region overall from 1949 to 2017. Thermokarst was notable in that affected areas have nearly doubled from 3.7% area in 1949 to 6.0% in 2017, likely due to a warming climate. River erosion, deposition, and early succession following disturbance affected 1.2% of the area.

3) When evaluating the relative effects of climate change we found fire, thermokarst, hydrology, and human activities interact to complicate analysis of effects of climate change, and that these interactions vary across the landscape. The local climate is projected to warm by 4-6 °C over the next 80 years and precipitation is projected to increase modestly. While the current paradigm is that fire frequency and severity will increase with climate warming we found fires were much more extensive in the early 1900s in both upland and lowland landscapes. This set the stage for the current abundance of mid- to late-successional ecosystems that are now providing more fuels for recent fires. In addition, a substantial portion of the fires on military lands are caused by humans and fire control greatly affects fire extent. Thermokarst, which is much more abundant in lowlands than other landscapes, increased from 3.7% in 1949 to 6.0% of the overall area by 2017 and our modeling projects thermokarst features to increase to up to 26% of the area by 2100.
4) Hydrologic changes associated with this increase in thermokarst development will lead to increased wetlands (bogs and fens) where lowlands subside. Increased glacial runoff and extreme precipitation will increase rates of river erosion and deposition within the more limited riverine landscape. Overall, while fires are more widespread and subject to substantial human influence, thermokarst will occur at accelerating rates and be more transformative.
5) State-transition modeling based on historical rates, RCP4.5 and RCP8.0 summer temperature projections, and a driver-adjusted RCP6.0 temperature model projects that ~38 ecotypes will gain area and ~24 will lose area by 2100. This will substantially affect the habitat availability of a large number of wildlife species.
6) To investigate how changing ecotypes will affect habitats, the ultimate objective of this effort, we first identified and listed all wildlife species (non-fish vertebrates) occurring in the study from published literature and reports, by using in-field automated audio recording units, and from direct observations of species and their signs. To assess the effects of habitat (ecotype) changes we project to occur over the next 80 years, we then compiled habitat (ecotype) use information on 193 species. This included 1 amphibian, 151 birds, and 41 mammals present across 61 ecotypes. From this, we identified a variety of species of concern for land management that might lose the most habitat over the coming century, particularly under the climate model RCP 6.0 projections. These include wood frogs, woodland birds (e.g., yellow warbler, northern waterthrush), porcupine, caribou, and marten. The birds and mammals that we expect to gain habitats are associated with lowland bogs, fens, wet meadows, scrub, and post-fire recovery of open,

short-vegetation types. We projected habitat changes for various species groups (migrant-stopover bird species, bird and mammal game or subsistence species, and others), especially for wildlife habitat specialists (identified by their narrow habitat-use breadth), under each ecotype projection scenario. Among habitat specialists, potential habitat-losers, to varying degrees, include wood frog, rusty blackbird, caribou, pica, and others. Although by 2100 we project some substantial declines compared to historic (1949-2017) habitat availability (e.g., > 25%) for some bird species, overall, few wildlife species are projected to suffer major habitat loss over the coming century.

7) We also analyzed audio recordings to characterize the degree to which wildlife and natural soundscapes are potentially influenced by human (anthropogenic) activities, and mapped areas with greater noise disturbance. Planning for future linear and horizontal infrastructure development could include at least maintaining the more vulnerable habitats and species, avoiding undue human activities in least-disturbed locations, and maintaining the existing diversity and connectivity of ecotypes.

LIST OF ACRONYMS

ABoVE	Arctic Boreal Vulnerability Experiment
ABR	Alaska Biological Research
ACI	Acoustic Complexity Index
ACT	Activity Index
ADI	Acoustic Diversity Index
AEI	Acoustic Evenness Index
AFB	Air Force Base
AGL	Above Ground Level
AHAP	Alaska High Altitude Aerial Photography
AKCSC	USGS Alaska Climate Science Center
ALFD	Alaska Large Fire Database
ALFRESCO	ALaska FRame-based EcoSystem COde
ANOVA	Analysis of variance
APEX	Alaska Peatland Experiment
AR	Assessment Report
ARU	automated audio recording unit
ASL	Above Sea Level
ATM	Alaska Thermokarst Model
B&W	Black and white
BGN	Background Noise Index
BI	Bioacoustic Index
BLM	Bureau of Land Management
CALM	Circumpolar Active Layer Monitoring
Co-PI	Co-Principal Investigator
CCSM4	Community Climate System Model 4
CENT	Concentration Index
CF	Creamer's Field Migratory Refuge
CIR	Color infrared
COE	U.S. Army Corps of Engineers
CRREL	U.S. Army Cold Regions Research and Engineering Laboratory
CRU TS4.0	Climate Research Unit Timeseries
DEM	Digital elevation model
DoD	Department of Defense
DGGS	The State of Alaska Division of Geological and Geophysical Surveys
DTAE	Donnelly Training Area East
DTAW	Donnelly Training Area West
EIS	Environmental Impact Statement
ERDAS	Earth resources data analysis system
ERDC	Engineer Research and Development Center
ERT	Electrical resistivity tomography
EVN	Events Index
EXIF	Exchangeable Image File Format
FDD	Freezing degree day
G-LiHT	Goddard LiDAR, Hyperspectral and Thermal
GEE	Google Earth Engine

GEAR	Geocentric Environment for Analysis and Reasoning
GFDL-CM	Geophysical Fluid Dynamics Laboratory Climate Model
GIS	Geographic Information systems
GISMO	Geographic Information Systems- Management and Operations Alaska
GISS-E2	Goddard Institute for Space Studies E2-R Model
GPS	Global Positioning System
HDD	Heating degree day
HFCI	High-frequency Cover Index
IEM	Integrated Ecosystem Model
IKONOS	Greek for “image”
IPCC	Intergovernmental Panel on Climate Change
IPSL-CM	Institut Pierre Simon Laplace Coupled Earth System Model
JPARC	Joint Pacific Alaska Range Complex
LCC	Landscape Conservation Cooperative
LDSB	Lowland Dwarf Scrub Bog
LDTL	Lowland Deep Thermokarst Lake
LFC	Low-frequency Cover Index
LiDAR	Light Detection and Ranging
LLSD	Lowland Low Scrub Fire-Disturbed
LTER	Long Term Ecological Research
LWBF	Lowland Wet Broadleaf Forest
LWNF	Lowland Wet Needleleaf Forest
LTER	Long term ecological research
MAAT	Mean annual air temperature
MAT	Mean annual temperature
MAGT	Mean annual ground temperature
MFC	Mean fire cycle
MFCI	Mid-frequency Cover Index
MRI-CGCM3	Meteorological Research Institute Coupled Global Climate Model 3
MTBS	Monitoring Trends in Burn Severity
NALCMS	North American Land Change Monitoring System
NASA	National Aeronautics and Space Administration
NCAR-CCSM4	National Center for Atmospheric Research Coupled Global Climate Model 4
NDSI	Normalized Difference Soundscape Index
NDVI	Normalized difference vegetation index
NED	National elevation dataset
NEPA	National Environmental Policy Act
NGA	National Geospatial Intelligence Agency
NLCD	National land cover database
NPP	Net primary production
NRCS	National Resources Conservation Service
NSF	National Science Foundation
PAE	Early paludification
PAL	Late paludification
PFS	Post-fire succession
PI	Principal Investigator

PS	Psot-disturbance sucession
RCP	Representative Concentration pathway
RCSON	Resource Conservation Statement of Need
RD	River deposit
RE	River erosion
RMBF	Riverine Moist Broadleaf Forest
RMNF	Riverine Moist Needleleaf Forest
RMS	Root mean squared
RMTS	Riverine Moist Tall Scrub
SD	Standard deviation
SDSWCD	Salcha-Delta Soil and Water Conservation District
SAR	Synthetic aperture radar
SERDP	Strategic Environmental Research and Development Program
SNAP	Scenarios Network for Alaska Planning
SNR	Signal to Noise Ratio Index
SON	Statement of Need
TB	Terabyte
TEM	Terrestrial Ecosystem Model
TDD	Thawing degree day
TFTA	Tanana Flats Training Area
TK	Thermokarst
UAF	University of Alaska Fairbanks
UMBF	Upland Moist Broadleaf Forest
UMNF	Upland Moist Needleleaf Forest
UMTLS	Upland Moist Tall and Low Scrub
USAG-FWA	United States Army Garrison Fort Wainwright, Alaska
USDAFS	U.S. Department of Agriculture Forest Service
USFWS	United States Fish and Wildlife Service
USGS	United States Geological Survey
USTL	Upland Shallow Thermokarst Lake
WV	Worldview
YTA	Yukon Training Area

1. OBJECTIVES

This project was designed to address all four Research Objectives in RCSON-18-C2 through a multidisciplinary three-year effort focused on identifying habitat and wildlife vulnerability to landscape change on Interior Alaska DoD training lands. Specific to the Statement of Need (SON), this project was focused on (underlined text in quotes is from SERDP RCSON-18-C2):

1) "Assessing habitat vulnerability to climate change and identify the factors that drive vulnerability."

2) "Developing an improved understanding of the spatial variability in drivers of vulnerability across a species' range."

3) "Developing an improved understanding of the relationship between changing climate and key ecological processes such as fire regimes, hydrological regime or food webs."

4) We are "developing methodologies, tools, and guidance that translates research on these issues into practical information that will improve adaptive management of these sensitive habitats to meet conservation objectives."

Our effort was structured around three major hypotheses (listed below and linked to project Tasks in Table 1) and their attendant research tasks, each with specific objectives designed to collect and evaluate data for hypothesis testing. The hypotheses were designed to address the four Research Objectives identified in SERDP RCSON-18-C2. They were tested through a series of focused tasks consisting of field measurements, repeat imagery analyses, and geospatial information synthesis to develop ecotype and habitat models and analyses on the training ranges.

Hypothesis 1: (a) Fire is the most rapid driver of ecological changes compared to other primary geomorphologic drivers such as thermokarst development (resulting in formation of thermokarst landforms) and hydrologic change on interior Alaska DoD lands. (b) But thermokarst, driven by a set of physical characteristics including altered surface vegetation from wildfires or changing environmental conditions, will lead to the most dramatic, long-lasting ecological changes.

Hypothesis 2: (a) With projected climate warming ecotypes will experience changes in their areal extent by 2050 and 2100 driven by fire, thermokarst, and hydrologic change. (b) These drivers interact to accelerate or reduce the rates of ecotype changes over time.

Hypothesis 3: Wildlife habitats will be affected by climate, fire, thermokarst, and other drivers, resulting in increases and decreases of populations dependent on those habitats, but some species may have some degree of ecological flexibility to help buffer habitat declines.

From the perspective of training range managers the variety of landscapes, ecosystem properties, and ecosystem services provide different characteristics in terms of the seasonality of access, the type of training that can be used to support the mission, and the potential for adverse conditions for people, infrastructure, and habitat functions. Alaska training ranges are well known for their all season training capabilities, large remote areas, and, increasingly for their ability to support multi-force and international scale exercises. Figure 1 provides a large scale overview map of the training area lands as well as physiographic information and major place names. Table 1 provides a summary of the main landscape uses and the attendant risks from a warmer future climate that provided the motivation for this research project. Figure 2 shows the wide variety of land cover across the training area domain. This land cover and the variety of ecosystem properties and processes controlling habitat use were the focus of this research effort.

Specifically, we attempted to answer the question: "*where, when, and how will projected climate warming in the area affect habitat access, suitability, and use?*"

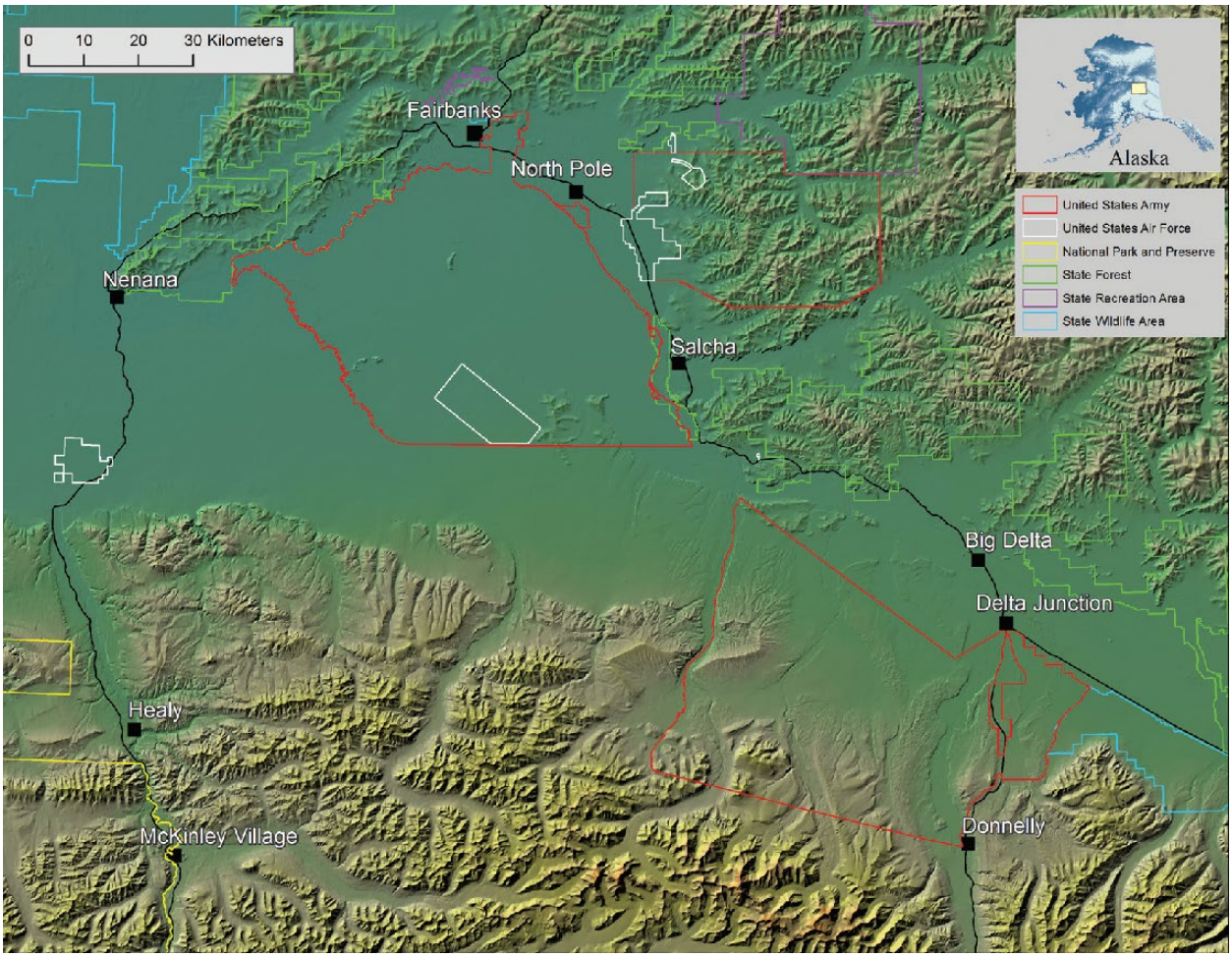


Figure 1. A map of the training area domain from Douglas et al., 2014. Boundaries of the major state and federal government landowners. The majority of the non-Federal and non-State of Alaska lands are owned privately or by Alaska Native Corporations.

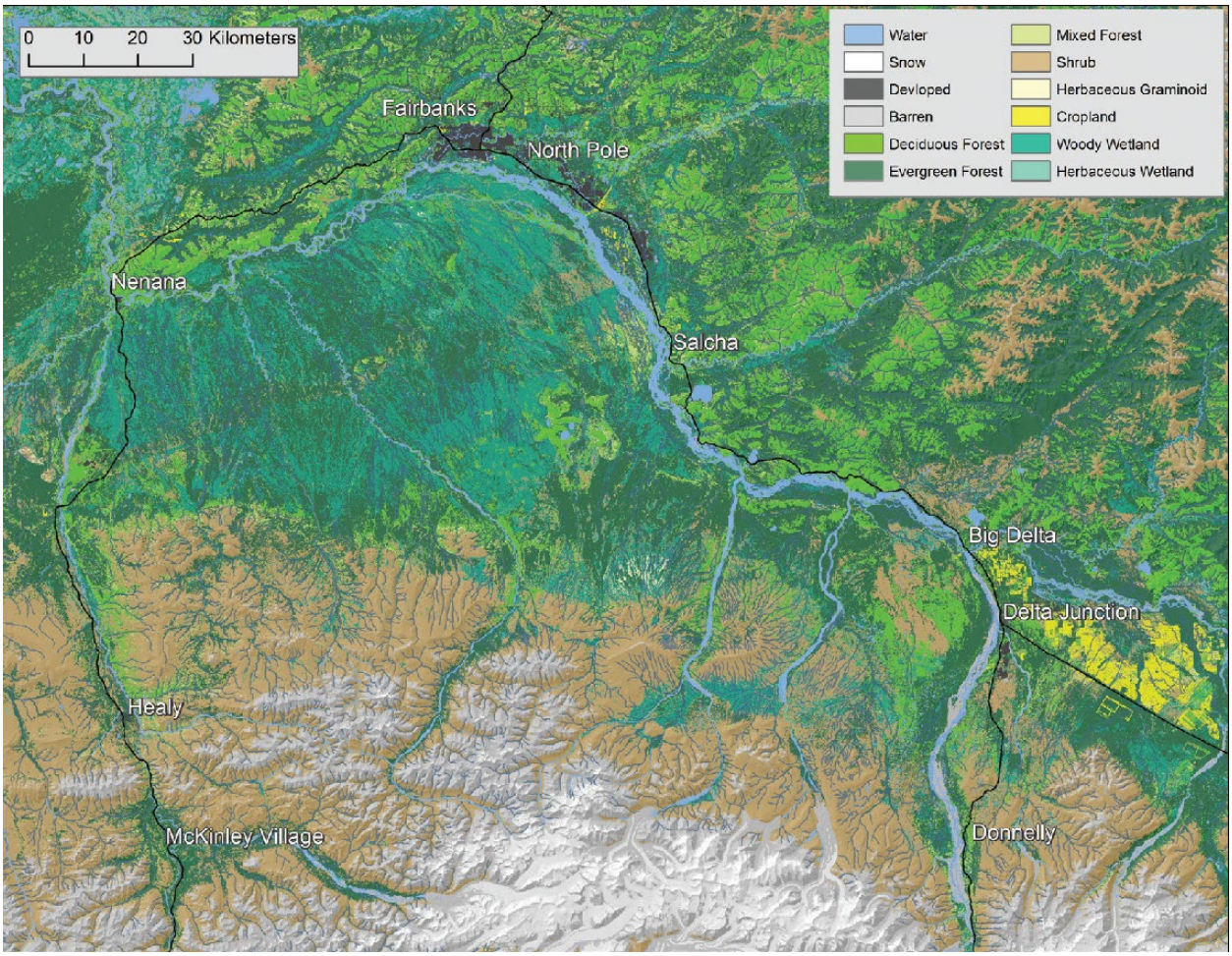


Figure 2. Predominant land cover classes for the Tanana Flats and surrounding areas of interior Alaska from Douglas et al., 2014. From the Alaska 2001 National Land Cover Database (Homer et al., 2007) including evergreen (34%) and deciduous (12%) forest, shrubland (24%), woody wetland (13%), and barren (7%). Percentages are calculated from DoD owned lands within the visible domain.

Table 1. Training range land uses and the potential vulnerabilities and risks for wildlife habitats on those range areas in a projected future warmer climate.

Landscape type and DoD land use function	Risk of ecotype change and vulnerability of wildlife habitat
Upland terrain- drop zones, mobility training, firing points, observation points, hunting, wildlife viewing and hiking recreation	Drying, increased fire risk, increasing shrub cover, changing hydrology, potential increase in thermal erosion; effects on stream water quality for fish, and browsing density for mammals like moose or snowshoe hares,
Lowland conifer permafrost plateau forests- roads and trails, runways, winter trail access for training and recreation	Increased fire risk and management requirements; thermokarst damage to infrastructure; loss of old growth forest important to songbirds
Lowland birch permafrost islands- winter mobility training, roads and trails, winter access for training and recreation	Training activities; thermokarst; they provide the critical land-water margins for bogs and fens used by large mammals and birds
Lowland riparian zone- drop zones, impact/target areas, hunting, fishing	Drying, altered discharge, increased fire risk could limit live fire training; habitats for birds, mammals, amphibians, fish
Lowland streams- low water crossings; winter ice roads, fishing, boating	Changing discharge, increased erosion and bed load sediments could alter suitability for salmon spawning habitat
Grassland tundra- drop zones, impact/target areas, winter mobility training, winter recreation	Conversion to shrub and forest eliminates prey for mesocarnivores and predators, alters food web in trophic cascades
Lakes- habitat protection, fishing, recreation	Lake drying, loss of fish and waterbird habitat

2. TECHNICAL APPROACH

2.1 Study Design and Field sites

This study combined database development, focused field measurements, remote sensing acquisitions, and repeat imagery analyses with a variety of permafrost, ecological, and habitat modeling efforts. The project was designed and implemented to address three hypotheses, each with multiple Tasks (Table 2).

Table 2. Hypotheses and Tasks of the proposed research.

Hypothesis	Objectives
H1: (a) Fire is the most rapid driver of ecological changes compared to other primary drivers such as thermokarst processes (resulting in thermokarst landforms) and hydrologic change on interior Alaska DoD lands. (b) But thermokarst, driven by a set of physical characteristics including altered surface vegetation from wildfires or changing environmental conditions, will lead to the most dramatic, long-lasting ecological changes.	
	Task 1.1 Development of a database of critical environmental characteristics useful in evaluating the distribution and classification of thermokarst formation across main ecological units.
	Task 1.2: Analyze historical rates of change in the **abundance of ecotypes,** in response to fire, thermokarst and hydrologic change by field survey and photointerpretation of a time-series of high-resolution imagery from the 1950s to the late 2010s.
	Task 1.3: Validate and improve geospatial models characterizing current/baseline **landscape vulnerability to thermokarst** disturbance.
	Task 1.4: **Visually document** current conditions and historical changes of ecotypes through high-quality photography for use in outreach to stakeholders, managers, and the public.
H2: (a) With projected climate warming ecotypes will experience changes in their areal extent by 2050 and 2100 driven by fire, thermokarst, and hydrologic change. (b) These drivers interact to accelerate or reduce the rates of ecotype changes over time.	
	Task 2.1: Integrate effects of the static physical drivers (Task 1.1) and dynamic drivers such as fire, thermokarst and hydrologic change (Task 1.2) in the **Alaska Thermokarst Model (ATM)**
	Task 2.2: **Simulate thermokarst and ecotype dynamics** between 2000, 2050 and 2100 using the improved version of the ATM, in response to an ensemble of climate and fire scenarios.
	Task 2.3: Assess **the relative effect of climate change, fire and thermokarst** disturbances on projected ecotypes dynamic.
H3. Wildlife habitats will be affected by climate, fire, thermokarst, and other drivers, resulting in increases and decreases of populations dependent on those habitats, but some species may have some degree of ecological flexibility to help buffer habitat declines.	
	Task 3.1: Assess **wildlife use of ecotypes as habitats**, and determine factors affecting their potential vulnerability or flexibility to change.
	Task 3.2: Evaluate effects of projected change in ecotype distribution (Task 2.3) on wildlife.

	Task 3.3: Project and map the **future distributions of wildlife habitats** and assess changes in wildlife species' vulnerability by 2050 and 2100 through state-transition modeling and assess sensitivity of models to historical rates, temperature, and driver parameterization.
	Task 4: Develop technologies and **methodologies for transferring results** into operational routines useful for training land planning. Develop adaptive management strategies to minimize impacts to vulnerable populations.

Our project sites are located across the vast training ranges spread south of Fairbanks, Alaska. The region has a continental climate with a mean annual air temperature of -2.4 °C, typical mean summer temperatures of 20 °C, mean winter temperatures of -20 °C, and yearly extremes ranging from 38 °C to -51 °C (Jorgenson et al., 2001a; 2020). Mean annual precipitation is 28.0 cm (Wendler and Shulski, 2009) with a typical annual snowfall of 1.7 m (Jorgenson et al., 2001a) that represents 40-45% of the annual precipitation (Liston and Hiemstra, 2011). Discontinuous permafrost features in the area are up to 60 meters thick and are located primarily in lowlands, along north-facing slopes, and where soils or vegetation provide adequate thermal protection (Racine and Walters, 1994; Jorgenson et al., 2008; Douglas et al., 2014). Permafrost at our field sites is Pleistocene syngenetic ice-rich "yedoma" formed through repeated deposition of windblown loess and organic matter (Shur and Jorgenson, 2007; Douglas et al., 2011; Strauss et al., 2016). Almost a third (181000 km^2) of the global yedoma permafrost is in Alaska and of that the majority is in a swath of central Alaska between the Brooks Range to the north and the Alaska Range to the south (Strauss et al., 2016). Carbon content in the permafrost of 2–5% (~10 kg m^{-3}) is up to 30 times greater than unfrozen mineral soil (Strauss et al., 2013).

Targeted field surveys and monitoring were conducted at a variety of sites that characterize long-term trajectories of ecotypes that have been disturbed by thermokarst or fire and to compare these to undisturbed areas. Due to the vast and largely inaccessible nature of the Interior Alaska training land domain some of our field sites are not readily accessible by vehicle. Figure 3 provides an overview map identifying the major study site locations. Eight existing thermokarst monitoring sites were resurveyed by maintaining currently deployed field instrumentation (soil temperature and water level dataloggers, time-lapse cameras), light detection and ranging (LiDAR) and/or drone mapping for digital elevation model (DEM) creation, and electrical resistivity tomography (ERT) surveys. These sites include the U.S. Army Cold Regions Research and Engineering Laboratory (CRREL) Permafrost Tunnel and Farmer's Loop sites and the Creamer's Field Migratory Refuge (CF) where a 10 year record of seasonal thaw, soil and permafrost temperatures, and snowpack characteristics have been collected. A variety of sites on the Tanana Flats Training Area (TFTA) represent a series of fens (kilometers long linear hydrologic features) and areas burned by wildfire at different times in the past 70 years. The sites were selected based on their ability to represent a variety of vegetation, soil, and hydrologic conditions as well as disturbed and undisturbed areas. We also sought to address locations where measurements have been lacking and/or where future training range expansion is proposed as is the case for the southeastern portion of the TFTA. A recently finished bridge over the Tanana River provided access to a planned road route to the Blair Lakes area.

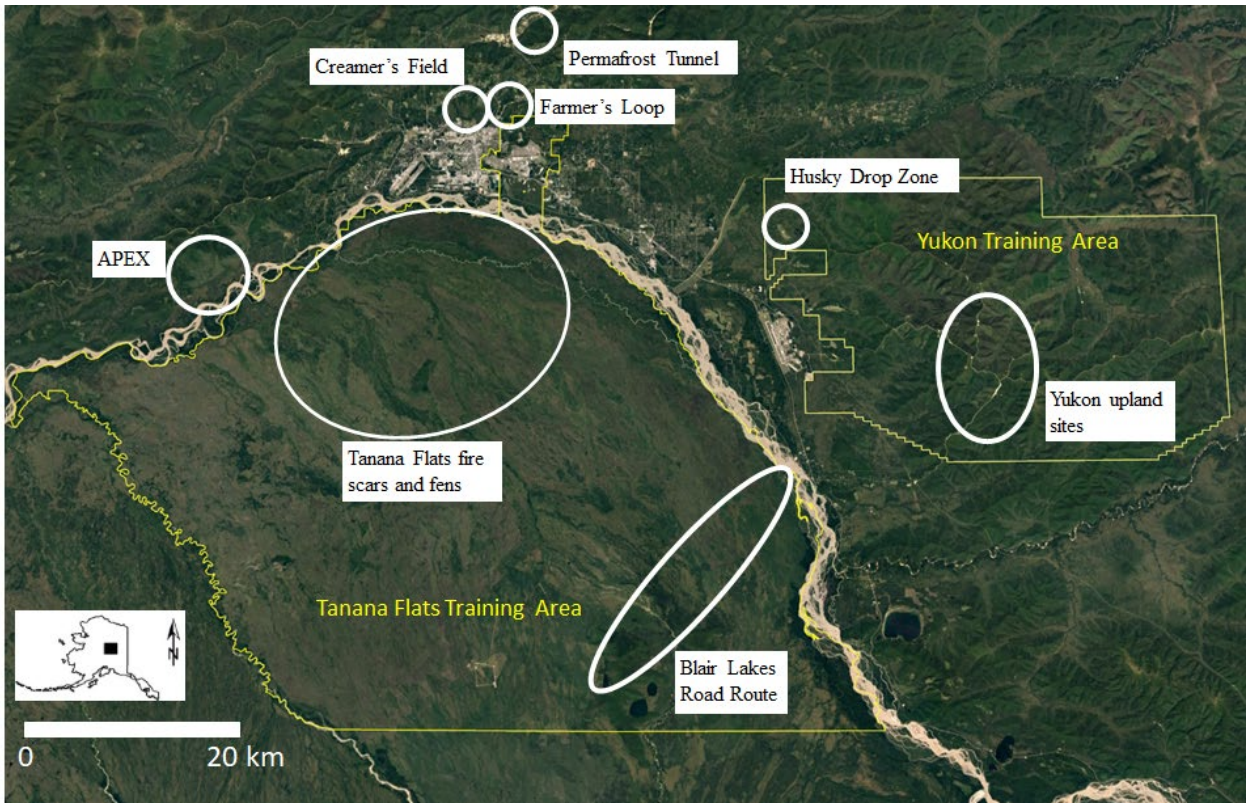


Figure 3. An overview map of the main field sites that were the focus of this study.

2.2 Schedule

Table 3 provides a detailed Gantt style chart of project activities. These are mapped to address the three main project Hypotheses. Due to setbacks from the COVID-19 pandemic we pushed back our year three schedule by six months. No project Tasks or other efforts were unfinished due to this extension. Activities and results for each project Task are provided in Task order below.

Table 3. A Gantt chart style schedule of the proposed three-year effort.

Research Focus or Activity	3/1/18-12/31/19				2/1/19-1/31/20				2/1/20-1/31/21				2/1/21-8/20/21	
Calendar year quarter: 1) Jan.-Mar.; 2) Apr.-Jun.; 3) Jul.-Sep.; 4) Oct.-Dec.[1]	1	2	3	4	1	2	3	4	1	2	3	4	1	2
Meet with stakeholders/partners, compile data from other projects and collaborators. Meet with U.S. Army AK bi-monthly.														
T1.1 Develop a database of physical environmental characteristics, thermokarst distribution, and ecotypes														
T1.2 Analyze historical rates of change in distribution of ecotypes														
T1.3 Validate and improve geospatial models of landscape vulnerability to thermokarst														
T1.4 Visual documentation of locations exhibiting varying ecotype change														
T2.1 Integrate results into the ATM and simulate fire, thermokarst, and hydrologic change														
T2.2 Simulate thermokarst vulnerability and ecotype change using ATM														
T2.3 Assess relative effects of climate change, fire, and thermokarst disturbance on projected ecotype dynamics														
T3.1 Assess wildlife use of habitats and factors affecting wildlife vulnerability to change														
T3.2 Evaluate effects of projected changes in ecotype distribution														
T3.3 Project future distributions of wildlife habitat suitability and vulnerability between 2000 and 2100 through state-transition modeling														
T4 Develop technologies and methodologies to transition results to U.S. Army AK land managers; develop adaptive management strategies and guidance to minimize impact to vulnerable populations														
Develop, submit peer reviewed papers														
Reporting: presentation to SERDP (1), interim report (2), final report (3)				1			2	1						3

2.3 Task 1.1

Development of a database of critical environmental characteristics useful in evaluating the distribution and classification of thermokarst formation across main ecological units.

We compiled a broad variety of geospatial information for the training lands and field sites that represent training land permafrost, ecology, and hydrology. The most relevant environmental characteristics for thermokarst assessment include topography, temperature, permafrost ice content, soil composition, vegetation cover, and hydrologic conditions. Data from field surveys and instrumentation deployed at point locations were compiled into several relational databases in ArcGIS and Microsoft Access. Spatial data involving remote sensing imagery and geographic information systems (GIS) vector data were compiled into geodatabases. Field surveys of seasonal thaw depths, permafrost geophysical characteristics and borehole samples were used to quantify rates of top-down and lateral thaw and to track thermokarst feature development. The field measurements and database properties are described first and some field site measurements of thermokarst processes follow.

2.3.1 Geospatial Measurements

A wide variety of field data from numerous sources were compiled into relational databases. Figure 4 and Table 4 provide information for site specific environmental, soil, and vegetation characteristics across the training lands. These data include information on site environmental characteristics, soil stratigraphy, soil physical and chemical laboratory results, ^{14}C radiocarbon dating, and vegetation composition and structure. The database comprises eight main data tables that are supported by 39 reference tables that describe the fields, variable attributes, and units (Figure 5). Additional data from topographic surveys and soil temperatures were compiled into Excel databases that are more favorable for maintaining active formulas and cell referencing. Currently, there are data on 3888 sites in the database (Table 4). These data were compiled from projects over the past decade as well as field measurements of environmental, soil, and vegetation characteristics provided by USAG-FWA, Salcha-Delta Soil and Water Conservation District (SDSWCD), the National Aeronautics and Space Administration (NASA) Arctic Boreal Vulnerability Experiment (ABoVE), NASA Goddard LiDAR, Hyperspectral and Thermal (G-LiHT), the National Geospatial Intelligence Agency (NGA), the National Resource Conservation Service (NRCS), Alaska Biological Research (ABR) environmental studies, and fire management efforts by the Bureau of Land Management (BLM) and the State of Alaska. The environmental characteristics captured in the field included general site information, physiography, geomorphology, topography, hydrology, and wetland, ecotype, and Viereck classification as just a few of the fields described (Table 5).

The soil stratigraphy field measurements contain information about each soil horizon following the NRCS soil survey guidelines, and specifically attempt to capture depth of permafrost, if present. However, some of the sources' data did not collect data deep enough to identify whether there was permafrost or not, or were not able to classify permafrost early on in the field season. The vegetation field measurements compiled into the database list all vegetation species present at the site by their percent cover and average height. Some of this information is presented in the studies by Burkert et al. (2018), Treat et al. (2019), Jorgenson et al. (2020), and Douglas et al. (2021) which were supported by this project. With data coming from many sources, it was a major effort to review consistency in coding, resolve differences in terminology among datasets, and identify and resolve outliers/errors in the data. In addition, not all data

sources collected all fields present in the database, thus some site data are more informative than others. These data were used for analysis of biophysical factors affecting soil temperatures, permafrost stability, and thermokarst formation (for example, Jorgenson et al.,2020 and Douglas et al., 2021).

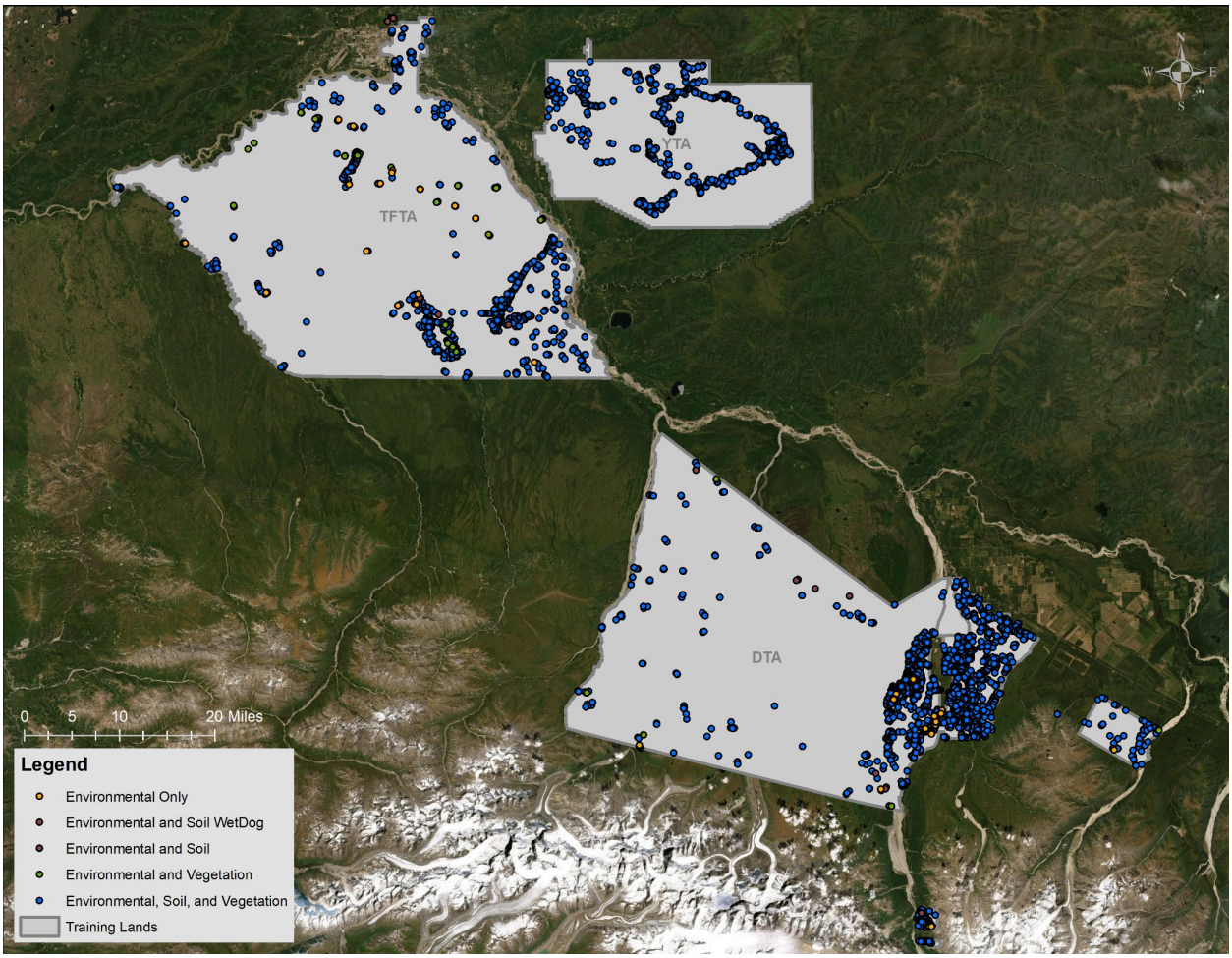


Figure 4. Map of point locations where data was collected on environmental, soil, and vegetation characteristics across the training lands. These data were put into the Microsoft access relational database, and were used to inform Task 1.2.

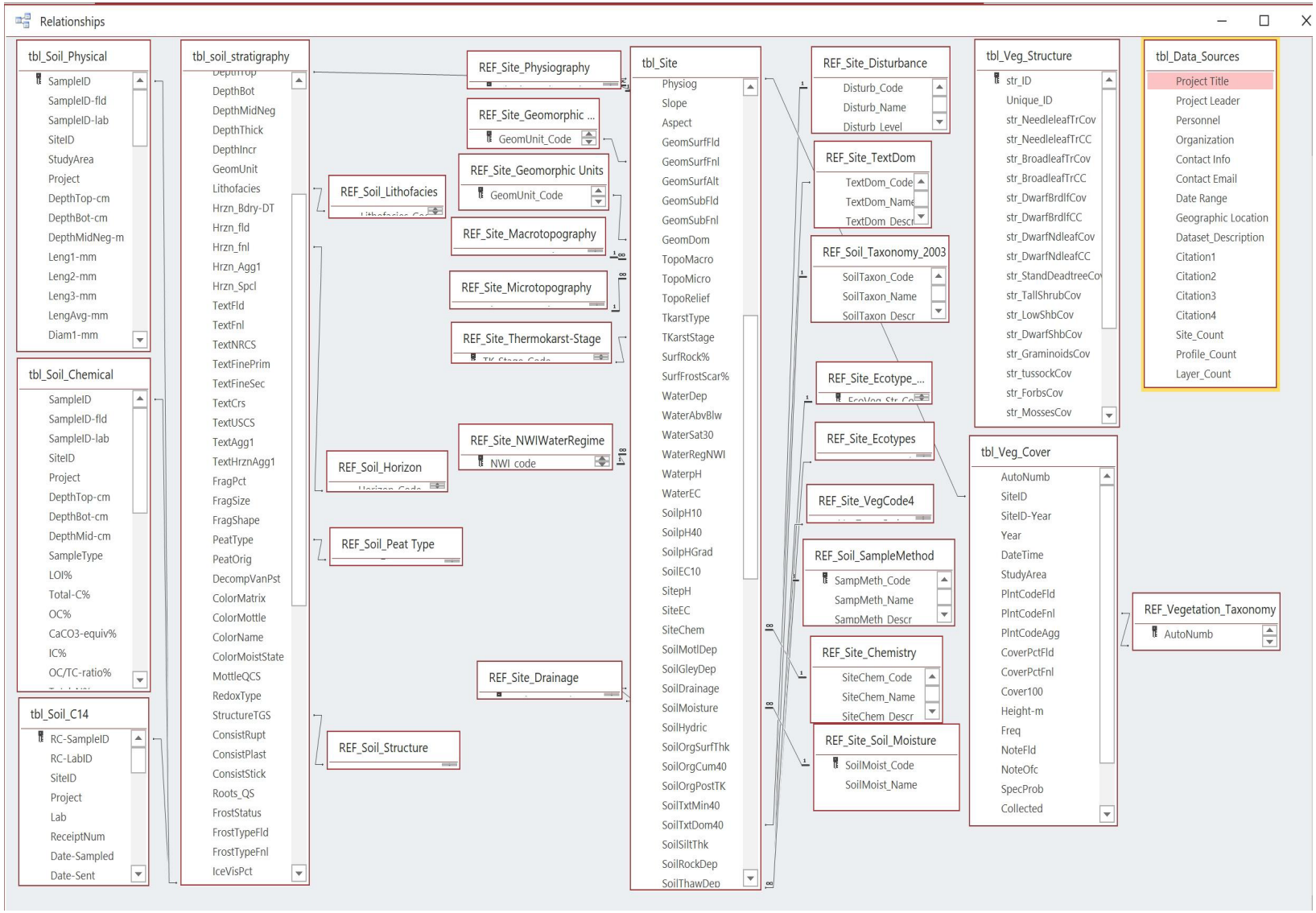


Figure 5. Screenshot of the relationships and linkages among data and reference tables in the Access relational database used for compiled field site information for DoD lands.

Table 4. Number of sites compiled in the database listed by training area and type of data collected.

Data Collected	Tanana Flats	Yukon	Donnelly West	Donnelly East	Gerstle River	Black Rapids	Total
Environmental Only	18	0	29	0	1	1	**49**
Environmental and Soil	10	0	6	0	1	1	**18**
Environmental and Vegetation	34	0	5	0	1	2	**42**
Environmental, Soil, and Vegetation	665	722	1204	1030	58	100	**3779**
Total	**727**	**722**	**1244**	**1030**	**61**	**104**	**3888**

Table 5. Example characteristics measured in the field and compiled in the database. The soil stratigraphy characteristics were measured for each horizon layer present in the soil pit, and the vegetation characteristics measured for each species observed at a site.

Environmental	Soil Stratigraphy	Vegetation
Location	Soil layer	Plant species
Date	Layer depth	Estimated percent cover
Project	Layer thickness	Plant height
Elevation	Geomorphic stratigraphic unit	
Physiography	Horizon boundary	
Slope	NRCS horizon designation	
Aspect	Soil texture	
Geomorphology	Coarse fragment modifier	
Topography	Fragment percent	
Relief	Fragment size	
Thermokarst type	Fragment shape	
Surface fragments	Peat type	
Water presence	Matrix color	
Soil saturation	Mottle color	
Water conductivity	Mottle quantity	
Water pH	Mottle contrast	
Soil conductivity	Mottle size	
Soil pH	Redoximorphic status	
NWI hydrology regime	Structure type	
Soil drainage	Frost status	
Soil moisture	Visible ice percentage	
Soil hydric	Ice lens size	
Organic material thickness		
Soil thaw depth		
Permafrost presence		
Viereck vegetation class		
Disturbance class		
Disturbance year		
Ecotype		

2.3.2 Remote Sensing Measurements

A major focus was placed on acquiring clear sky satellite imagery over our main project field sites because this allowed for comparison with historical measurements and imagery. A number of new stereo pair Worldview 2 (WV2) and WV3 images were collected, at our request, over the past two years. Spring and early summer clear sky conditions allowed for collection of a number of high-quality snow-on and snow-off stereo pairs. Another request through DoD's partnership with Airbus yielded excellent Pleiades high-resolution stereo-pairs for March, June, and September 2019 at no cost to the project. LiDAR data from The State of Alaska Division of Geological and Geophysical Surveys (DGGS) and USAG-FWA were acquired during our project. CRREL paid for a LiDAR acquisition over five of our field sites in May, 2020 using Army Basic Research Program funds. Some of our sites were part of the July, 2019 NASA ABoVE airborne campaign. A NASA proposal was submitted and funded (PI-Hiemstra) to collect Synthetic Aperture Radar (SAR) data in December 2019, March-April 2020, and August-September 2020 over our research sites. These measurements, combined with machine learning analyses, allowed for an assessment of the role snow plays in ecosystem processes (Douglas and Zhang, 2021). Figure 6 includes an image of the Interior Alaska DoD lands (red boundary) with the training range lands where our work was focused, presented as high resolution photos.

Multiple Pleiades high-resolution stereo images, free to the project, were collected for a number of our sites in September following leaf off. Some WorldView imagery was also collected. A time series of 42 summer (June, July, August) surface reflectance Landsat data scenes that stretch from 1984 to 2017) and cover almost all our sites were also collected and orthorectified. A time series analysis on these images has been used to identify locations where landscape change has occurred/is occurring over time or where landscapes are stable. This will be used to check model outputs for permafrost degradation and thermokarst development.

We have compiled a corrected surface reflectance Landsat imagery time series from 1984-2017. This enables normalized difference vegetation index (NDVI) trend assessments over the training range domain over time. Nearly two terabytes (Tb) of high-resolution Digital Globe and Airbus imagery collections have been obtained and tasked to assess ecotype distributions and changes from 2002-2019. As a DoD-funded project, we were able to task stereo collections of Worldview and Pleiades imagery over our field sites (Figure 6) to represent all seasons. Hundreds of Digital Globe images are available for 2001-present through the NGA archives. The data and imagery has been georeferenced and terrain corrected. Three papers (Anderson et al., 2019; McPartland et al., 2019; and Douglas and Zhang, 2021) present some of the remotely sensed measurements and geospatial analyses developed through this Task.

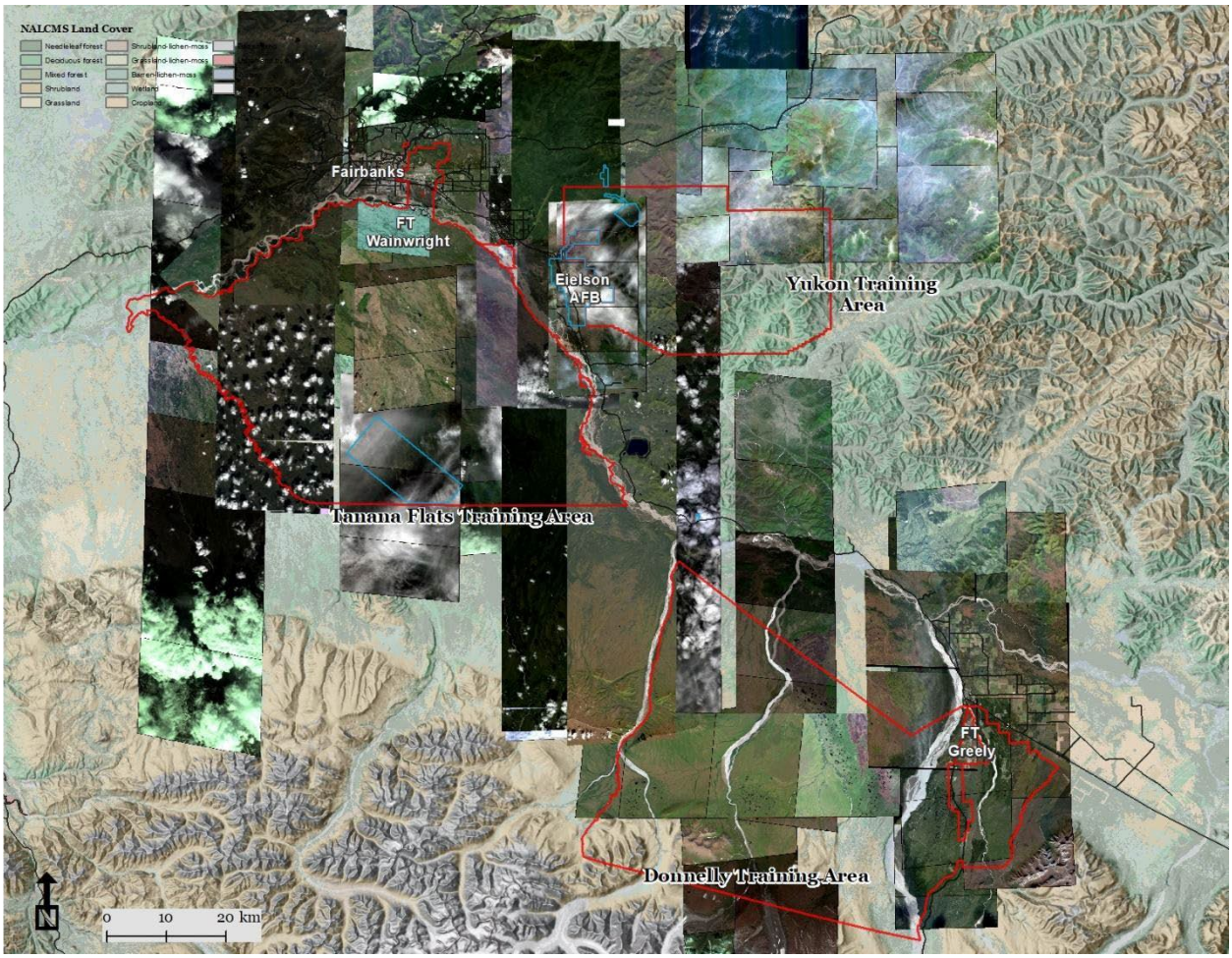


Figure 6. A map of Interior Alaska DoD lands (red bounding boxes) with some of the high-resolution images we collected and processed for our study sites.

2.3.3 Thermokarst Feature Development

The thermal state of near surface permafrost is controlled by topography, slope, aspect, soil texture, ground ice content, air temperature, hydrology, land cover, snow depth and timing, and liquid precipitation (Osterkamp and Romanovsky, 1999; Jorgenson and Osterkamp, 2005; Myers-Smith et al., 2008; Loranty et al., 2018). In relatively warm areas like Interior Alaska, the permafrost is "ecosystem protected" (Shur and Jorgenson, 2007) by an insulating organic-rich soil, plant litter, and vegetation surface layer. Disturbance to this insulating layer from climate warming, infrastructure development, or wildfire increases ground heat flux and promotes top down, lateral, and bottom-up thaw (Viereck et al., 1993; Yoshikawa et al., 2003; Nossov et al., 2013).

Commonly, the first signal of an altered permafrost thermal state is an increased seasonally-thawed "active" layer (Hinkel et al., 2003; Shiklomonov et al., 2010). Seasonal trends in active layer depth, particularly across a variety of ecotypes, can provide information on how and where permafrost degradation features initiate and expand. Low-ice content dry sandy soils typically have deeper active layers than ice-rich silt or organic-rich soils (Brown et al., 2015; Loranty et al., 2018). As such, active layer measurements can infer information about subsurface soil characteristics. When top-down permafrost degradation occurs, the active layer depth may

increase before any readily identifiable change in surface vegetation or geomorphology occurs. The most pronounced terrain surface features form when thaw of ice-rich permafrost leads to thermokarst (hollows formed by ground subsidence following thaw of ice-rich permafrost; Kokelj and Jorgenson, 2013; Brown et al., 2015; Douglas et al., 2016). Thermokarst features include lakes, bogs, fens, and pits in lowlands and thaw slumps and active layer detachments in uplands (Smith et al., 2005; Jorgenson et al., 2013).

Thermokarst features can form rapidly over the course of a few weeks where gradients, slope failures, or movement of surface and shallow subsurface water can drive erosion. They can also form slowly over the course of many years due to top-down thaw of permafrost or the lateral expansion of thawed regions (Douglas et al., 2021). As such, a key part of classifying thermokarst features is the application of remotely sensed and ground surveying protocols to track feature development.

There is a need to broadly apply remotely-sensed analyses to identify high ice content permafrost at risk of top down and lateral thaw degradation to support ecological, hydrologic, and engineering investigations. Identifying risk factors for thermokarst initiation typically requires combining ground-based surveys and remotely-sensed measurements. Where permafrost is associated with surface biophysical characteristics that can be measured remotely, standoff detection tools like airborne LiDAR and repeat imagery analysis can be applied toward tracking trajectories of change over large regions (Jones et al., 2013; Chasmer and Hopkinson, 2016; Lewkowicz and Way, 2019). Geophysical techniques, predominantly ERT, have been recently coupled with airborne and active layer measurements to detect thermokarst development and associate ice content with terrain geomorphology (Yoshikawa et al., 2006; Douglas et al., 2008; Lewkowicz et al., 2011; Hubbard et al., 2013; Minsley et al., 2015) and biophysical characteristics (Douglas et al., 2016) at broader scales. A combination of repeat active layer measurements, geophysical surveys, and airborne LiDAR have been used to map subsurface permafrost bodies, quantify top-down thaw, and identify locations where thermokarst features have been initiated or expanded (Douglas et al., 2016; Rey et al., 2020). Long-term ground-based time series measurements can be combined with ERT to quantify top down thaw, track the initiation and lateral expansion of thermokarst features, and identify where ecosystem characteristics influence the permafrost thermal regime. Further, extents of the base and sides of discontinuous permafrost bodies with geophysical measurements confirmed with deep boreholes is needed to monitor and better model lateral and bottom-up thaw.

As part of this project we continued long term end of summer season thaw depth measurements of the “active layer” at multiple focus sites We combined those measurements with repeat airborne LiDAR, geophysical measurements, and deep boreholes to get a holistic view of the changing surface conditions at three different sites near Fairbanks, Alaska (Douglas et al., 2021). Repeat airborne LiDAR measurements are optimal for rapidly identifying changes in surface elevations over space and time. From this, focused field measurements can determine what terrain characteristics are leading to the landscape change. For example, Figure 7 shows the results of a repeat LiDAR analysis of the Husky Drop Zone on the Yukon Training Area (YTA). It is clear that large scale subsidence (red zreas) occurred at the site over the span of just one year. Regions in blue identify increased surface water elevations between the two acquisitions.

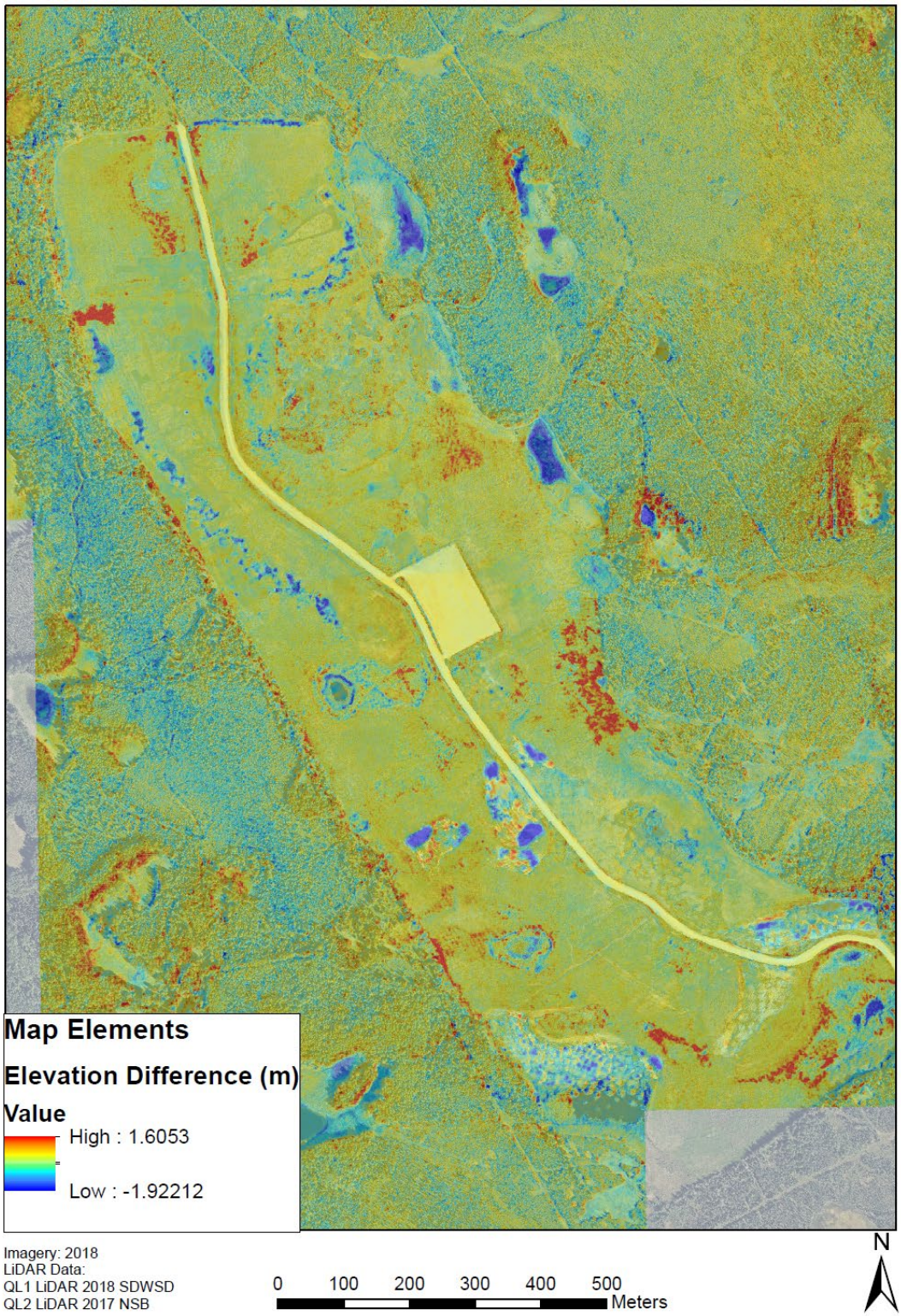


Figure 7. A repeat LiDAR analysis of the Husky Drop Zone showing surface elevation changes between 2017 and 2018. Positive values identify the amount of subsidence. Negative values, identifying areas where elevation increased, are predominantly associated with higher water level elevations in small ponds at the site. From Josh Busby, USAG-FWA Range Control.

In Figure 8, a repeat LiDAR map of the Creamer's Field site, the yellow and orange regions identify areas that experienced more than 1.5 meters of surface subsidence between 2010 and 2020. Thermistors installed into the top of what was stable permafrost in 2013 have warmed considerably (Figures 9-11). Across the Creamer's Field, Farmer's Loop, Permafrost Tunnel, and Husky Drop Zone sites (locations in Figure 3) there is a general warming of permafrost in a variety of ecotypes (Figure 12). At locations where the steady warming has been retarded at ~-0.1 °C, likely due to latent heat effects associated with the phase change of ground ice in the transient layer and below, future warming above 0 °C will slow the process of winter freezeback (Boike et al., 1998; Shur et al., 2005).

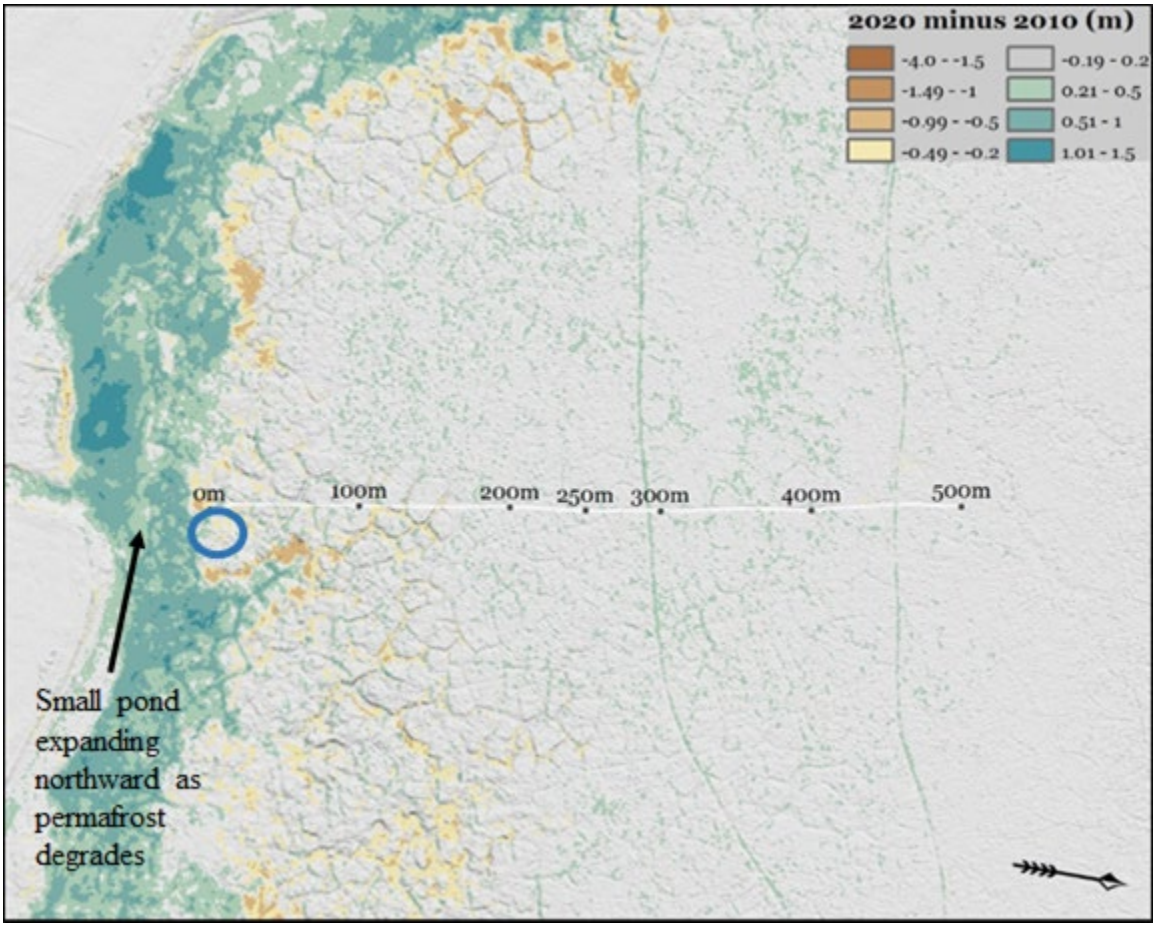


Figure 8. Repeat LiDAR analysis of the Creamer's Field site. Yellow to orange colored regions exhibited ground subsidence between 2010 and 2020. In some cases, it was as much as a meter of displacement. The blue circle denotes the location of the thermistors presented in Figures 9 and 10.



Figure 9. Repeat photos of a site at the Creamer's Field Migratory Refuge where degradation of ice wedge polygons has occurred over the past six years.

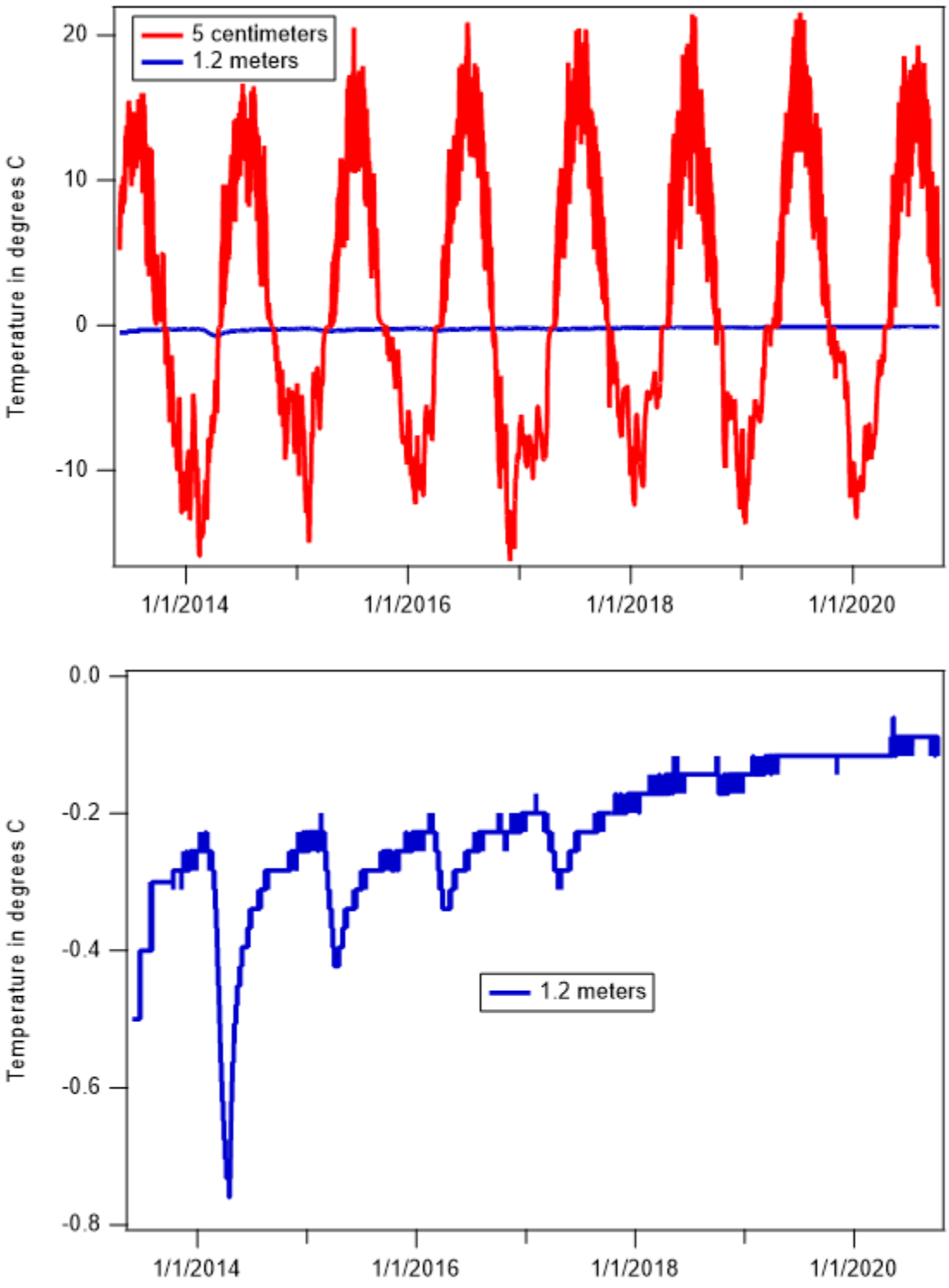


Figure 10. Soil thermal measurements from two thermistors at site CF2a which is located in the middle of a degrading high-centered polygon surrounded by ice wedges. Thermistor locations are shown in the photos in Figure 6. Note that the thermistor at 1.2 meters depth is approaching 0 ºC.

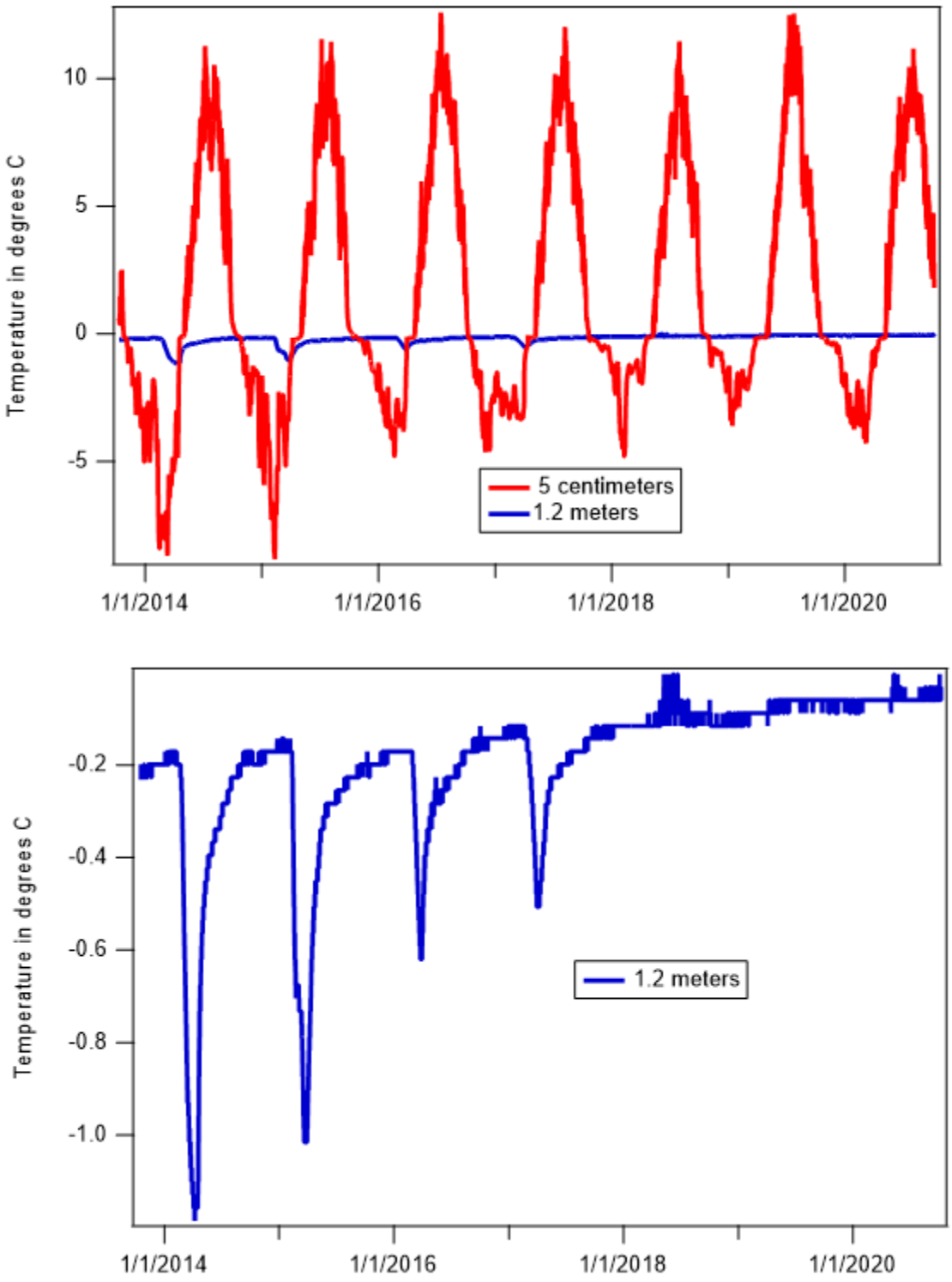


Figure 11. Soil thermal measurements from two thermistors at site CF2b which is located in an ice wedge along the sides that constrain a degrading high-centered polygon. Thermistor locations are shown in the photos in Figure 6. Note that the thermistor at 1.2 meters depth is approaching 0 ºC.

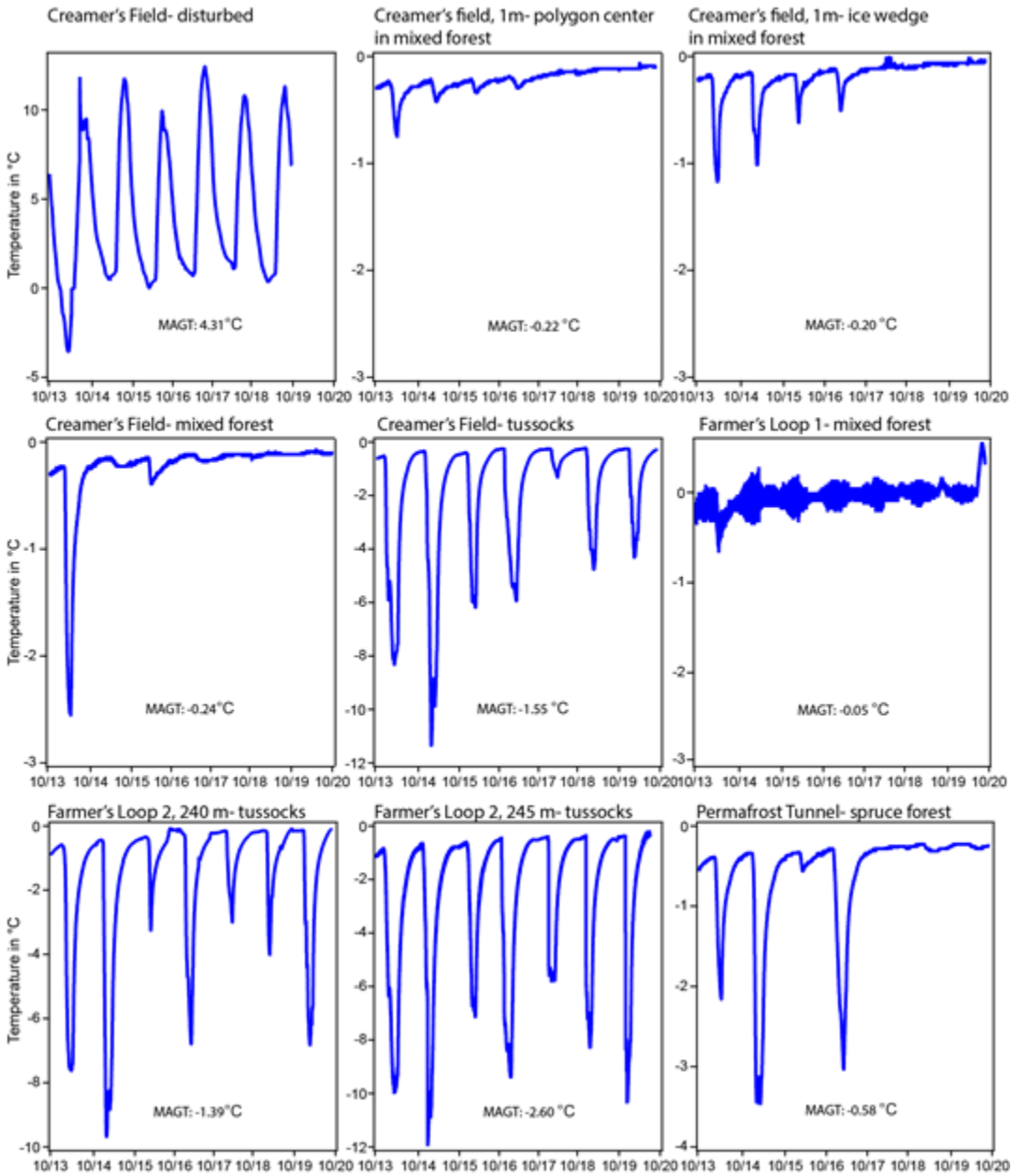


Figure 12. Soil temperature measurements at 1.2 m depth from October 1, 2013 to October 1, 2019 for the three study sites. Mean annual ground temperature (MAGT) values at 1.2 m for the period of record are also provided.

Figures 13-17 provide a series of detailed site specific summaries of both top-down thaw and thermokarst development at the Creamer's Field, Farmer's Loop, and Permafrost Tunnel sites. In all five Figures, panel c shows the downward progression of seasonal thaw during the summer of 2014 while panel d provides an 8-year record of active layer depths at the sites. It is clear that across all five transect sessions top-down thaw of permafrost has increased the active layer depths by between 5o and 100 percent (d panels). Lateral thaw of thermokarst features is also evident as shown by the increasing thaw depths along the margins of thawed features as well as low resistivity regions (yellow and red zones in e panels).

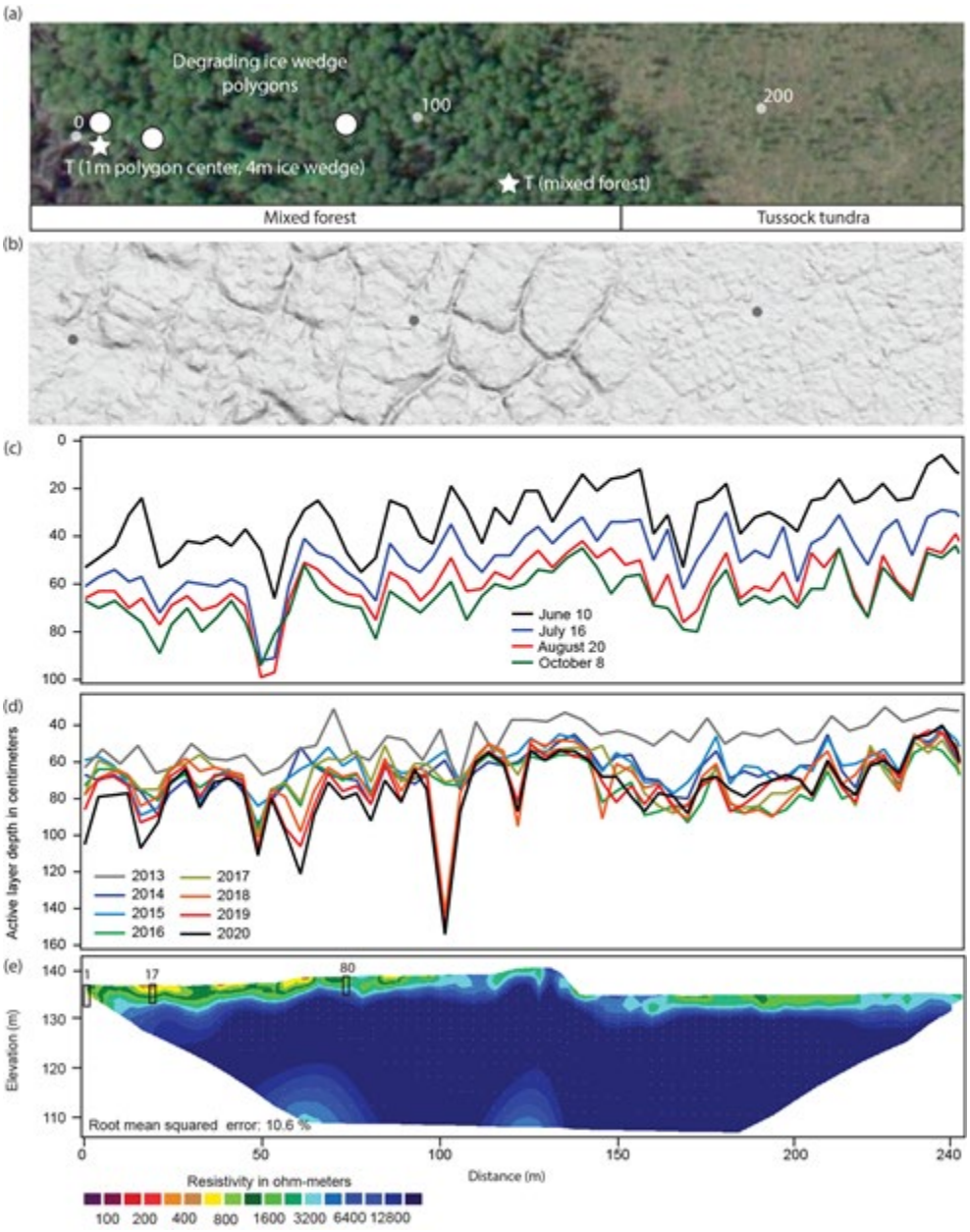


Figure 13. The Creamer's Field transect from 0 to 246 m. Image a) is a Worldview 2 (© Digital Globe) true color image of the transect with terrain features and core locations (circles) identified, b) LiDAR, c) repeat thaw depth measurements in 2014, d) repeat active layer depth measurements from 2014-2019, and e) a 246 m electrical resistivity tomography transect corrected for ground surface elevation with boreholes identified as black boxes to true depth and numbers corresponding to the distance (in meters) of the borehole location along the transect. Stars with a "T" denote a thermistor location.

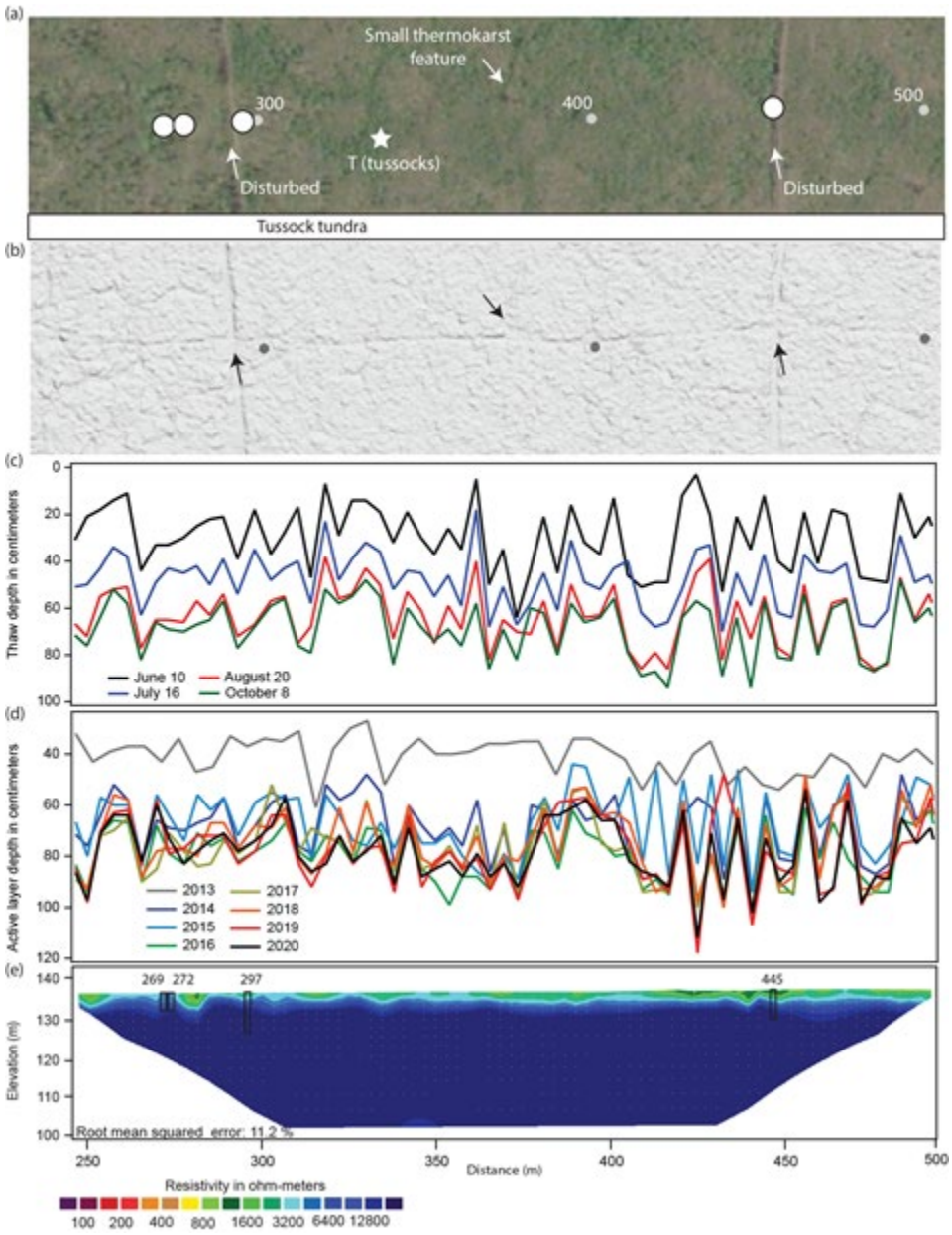


Figure 14. The Creamer's Field transect from 252 to 498 m. Image a) is a Worldview 2 (© Digital Globe) true color image of the transect with terrain features and core locations (circles) identified, b) May 2020 LiDAR, c) repeat thaw depth measurements in 2014, d) repeat active layer depth measurements from 2014-2019, and e) is a 246 m ERT transect corrected for ground surface elevation with boreholes identified as black boxes to true depth and numbers corresponding to the distance (in m) of the borehole location along the transect. Stars with a "T" denote a thermistor location.

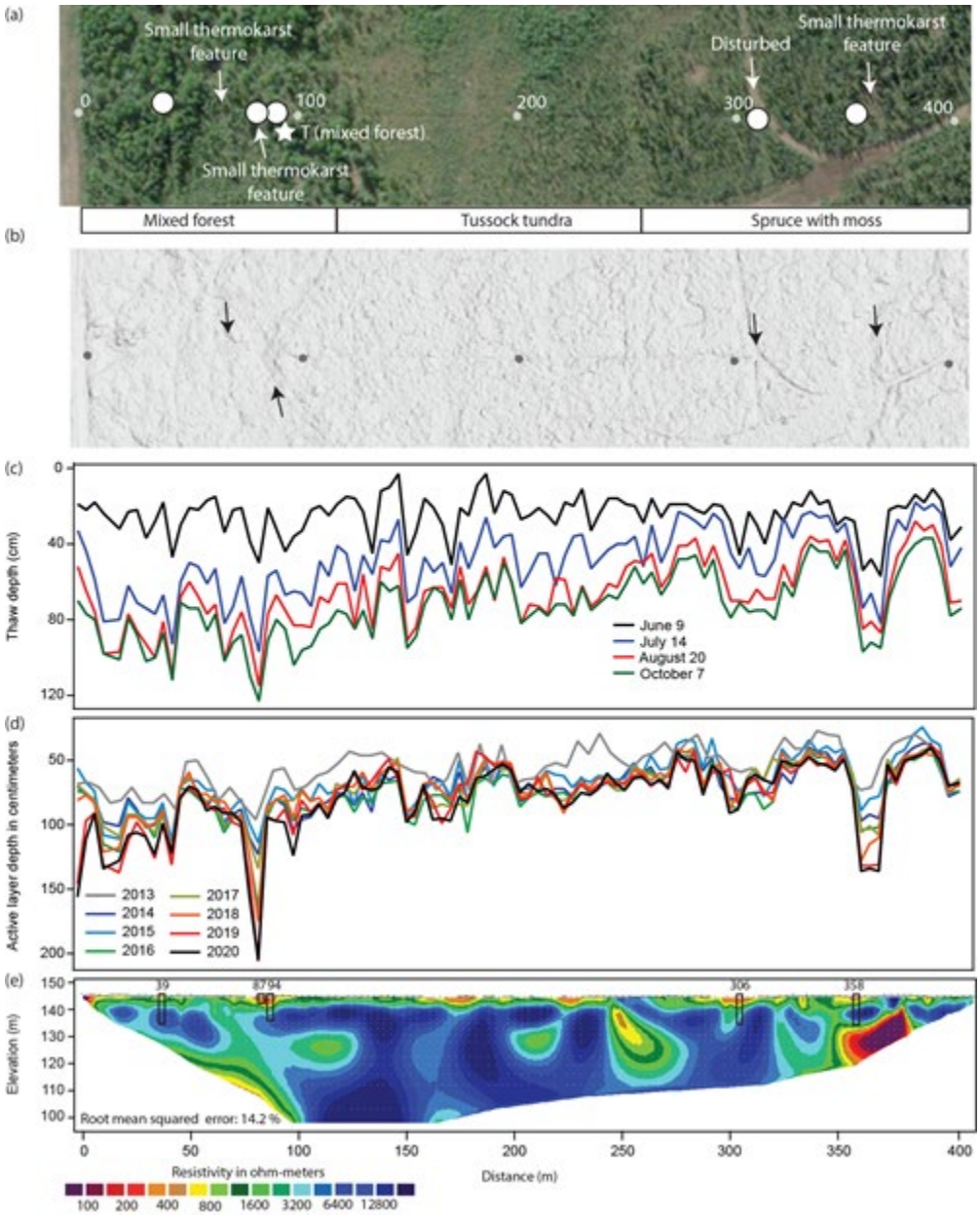


Figure 15. The Farmer's Loop 1 transect. Image a) is a Worldview 2 (© Digital Globe) true color image of the transect with terrain features and core locations (circles) identified, b) May 2020 LiDAR, c) repeat thaw depth measurements in 2014, d) repeat active layer depth measurements from 2014-2019, and e) a 410 m ERT transect corrected for ground surface elevation with boreholes identified as black boxes to true depth and numbers corresponding to the distance (in m) of the borehole location along the transect. Stars with a "T" denote a thermistor location.

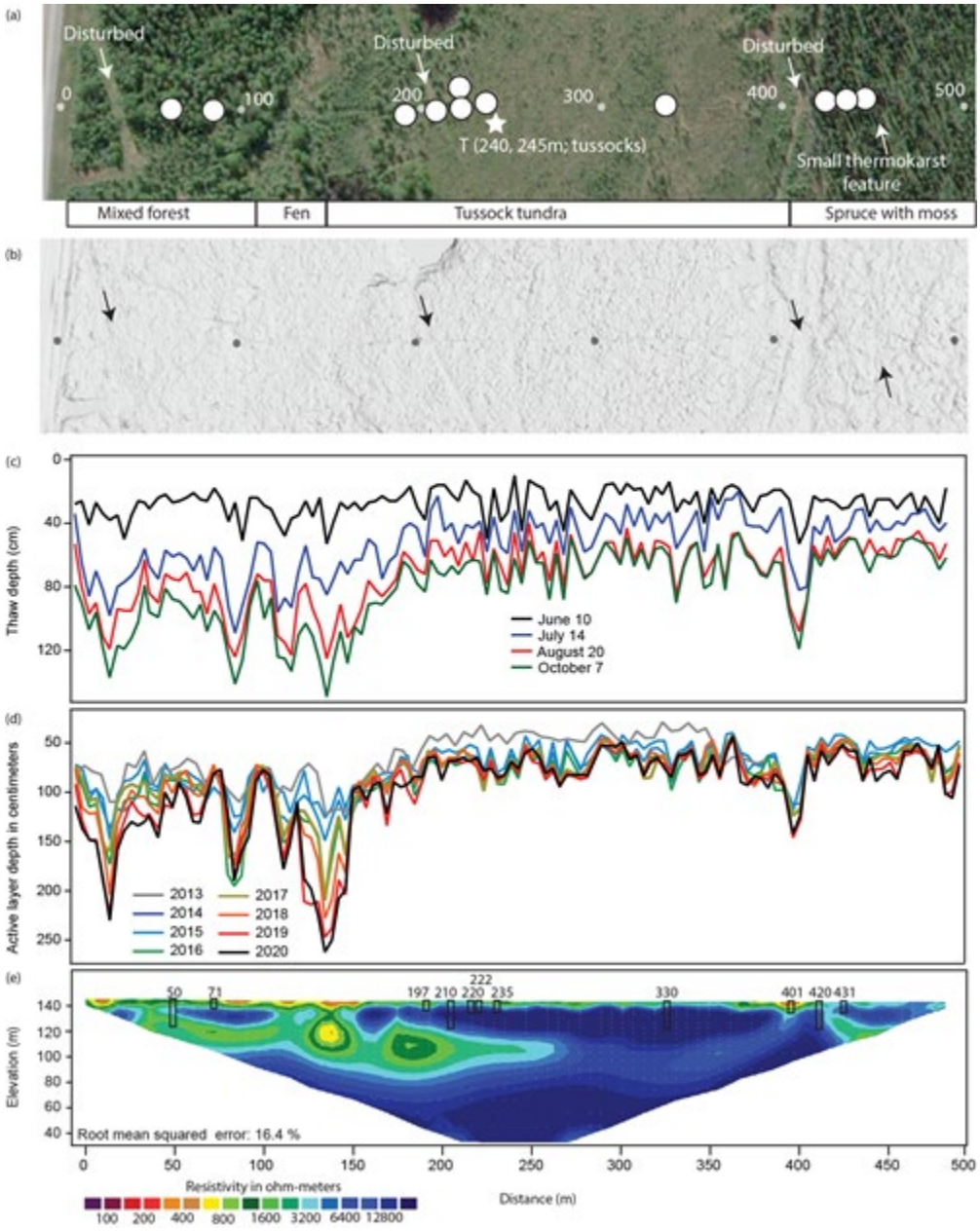


Figure 16. The Farmer's Loop 2 transect. Image a) is a Worldview 2 (© Digital Globe) true color image of the transect with terrain features and core locations (circles) identified, b) May 2020 LiDAR, c) repeat thaw depth measurements in 2014, d) repeat active layer depth measurements from 2014-2019, and e) a 492 m ERT transect corrected for ground surface elevation with boreholes identified as black boxes to true depth and numbers corresponding to the distance (in m) of the borehole location along the transect. Stars with a "T" denote a thermistor location.

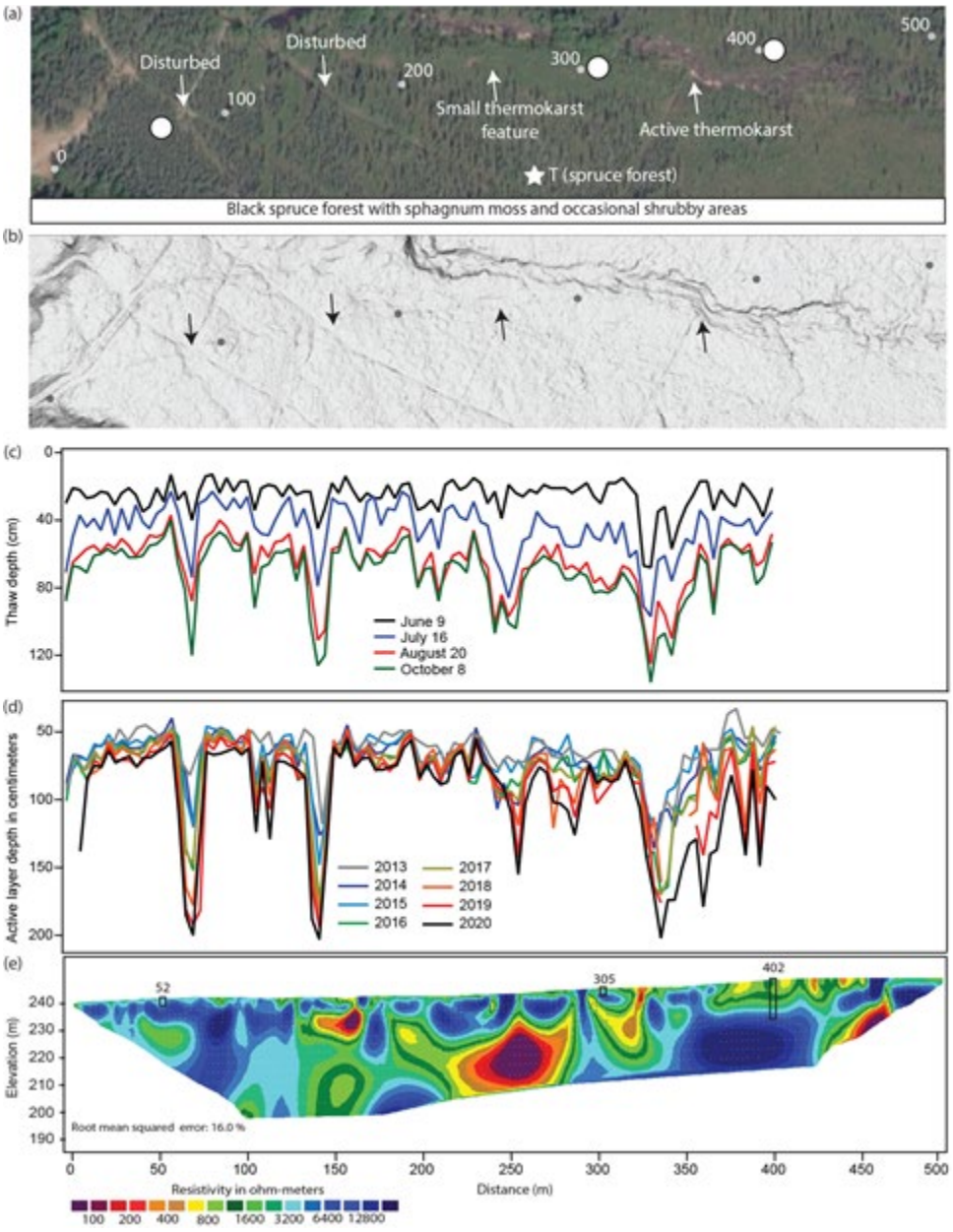


Figure 17. The Permafrost Tunnel transect. Image a) is a Worldview 2 (© Digital Globe) true color image of the transect with terrain features and core locations (circles) identified, b) May 2020 LiDAR, c) repeat thaw depth measurements in 2014, d) repeat active layer depth measurements from 2014-2019, and e) a 410 m ERT transect corrected for ground surface elevation with boreholes identified as black boxes to true depth and numbers corresponding to the distance (in m) of the borehole location along the transect. Stars with a "T" denote a thermistor location.

The results from our focused field measurements at the Husky Drop Zone, Creamer's Field, Farmer's Loop, and Permafrost Tunnel sites clearly show, through a variety of corroborating measurements, ice-rich permafrost in the area around Fairbanks, Alaska has been warming and actively degrading in numerous locations. Four major lines of evidence show permafrost thaw degradation has been initiated and is likely increasing at our sites. First, active layer measurements show thaw depths have been increasing across all ecotypes since 2013, however, some ecotypes experience deeper seasonal thaw than others. Table 6 provides a summary of statistical analyses of the repeat thaw depth measurements made between 2013 and 2020.

Table 6. A summary of the thaw depth measurements by ecotype and results from a means comparison using a student's t-test. Among a given ecotype different and year the letters identify statistically significantly different means. Mean values for a given ecotype and year with similar letters have similar means.

	Year	N	Mean (cm)	Standard deviation	Means comparison	% increase 2013-2020
Tussock	2013	126	45.0	10.9	F	
	2014	153	67.7	12.2	D	50
	2015	153	63.3	12.6	E	41
	2016	153	75.3	12.1	A	67
	2017	153	72.2	13.8	B, C	60
	2018	153	69.5	13.3	C, D	54
	2019	153	72.8	13.9	A, B	62
	2020	153	73.5	13.4	A, B	63
Wetland	2013	41	71.5	24.4	D	
	2014	48	91.4	23.5	B, C	28
	2015	48	82.7	18.6	C, D	16
	2016	48	104.9	30.0	A, B	47
	2017	46	96.9	30.4	B, C	36
	2018	47	103.1	39.2	A, B	44
	2019	47	113.3	49.4	A	59
	2020	47	113.6	51.5	A	59

Table 6. Continued

	Year	N	Mean (cm)	Standard deviation	Means comparison	% increase 2013-2020
Disturbed	2013	35	75.5	23.8	C	
	2014	67	85.8	20.4	C	14
	2015	58	84.2	21.1	C	11
	2016	60	99.9	28.8	B	32
	2017	51	101.9	33.0	B	35
	2018	56	104.3	35.0	B	38
	2019	55	118.4	42.4	A	57
	2020	56	117.1	44.3	A	55
Mixed forest	2013	57	64.4	17.9	D	
	2014	75	81.4	19.0	B, C	27
	2015	75	75.1	17.2	C	17
	2016	75	85.1	27.1	B	32
	2017	75	79.5	24.0	B, C	24
	2018	74	84.9	25.7	B	32
	2019	74	93.4	29.0	A	45
	2020	74	97.4	30.2	A	51
Moss spruce	2013	86	54.6	13.3	E	
	2014	111	59.7	10.7	C, D	9
	2015	120	56.5	12.6	D, E	3
	2016	118	64.0	11.6	B	17
	2017	124	62.5	12.2	B, C	14
	2018	115	64.9	14.8	B	19
	2019	119	70.1	16.0	A	28
	2020	115	72.5	18.7	A	33

Previous studies have established that vegetation provides a range of "ecosystem protection" properties for permafrost (Shur and Jorgenson, 2007; Loranty et al., 2018). Recent measurements confirm this and identify strong links between different ecotypes and top-down thaw of permafrost in Interior Alaska (Yi et al., 2018; Douglas et al., 2020; Jorgenson et al., 2020; Kropp et al., 2020). Our measurements show that some ecotypes are associated with consistently deeper active layer measurements over time. Disturbances, like trail crossings, have dramatically deeper seasonal thaw than any other ecotypes and some of them are also expanding laterally. Removal or alteration of the organic soil layer or moss ground cover increases the ground heat flux and promotes more rapid seasonal and permafrost thaw (Nicholas and Hinkel, 1996) due to the loss of the ecosystem protection of permafrost in the area (Shur and Jorgenson, 2007). In many locations at our field sites, active layer depths have increased since 2013 to greater than 2 m, which is greater than typical winter freezeback. Infrastructure development and wildfire are the most likely ways for land cover to change to a disturbed ecotype. Post-fire forest succession to a mixed forest, which is increasingly occurring across Interior Alaska and much of the boreal biome, will also undoubtedly lead to warmer surface soils and more top-down permafrost thaw (Kasischke and Johnstone, 2005; Johnstone et al., 2010; Jafarov et al., 2013; Brown et al., 2015). Tussock tundra and some of the spruce forest sites yield the shallowest active layer depths. As such, if vegetation were to change from tussocks or spruce to a mixed forest or disturbed (i.e. no moss or forest vegetation) land cover the potential risk of top-down permafrost thaw would increase considerably.

Our results support recent work at our study sites that show the disturbed, mixed forest, and wetland ecotypes exhibit the deepest active layers (Douglas et al., 2020). That study presents measurements from 2014 to 2017 at the same sites presented here and links deeper active layer depths with wetter summers. The four additional years presented here show the thaw front has continued to migrate downward despite the lack of anomalously wet summers in 2018 and 2019. At most sites the 2020 active layer depths are the deepest in the record and the comparatively shallower thaw depths measured in 2013 have not been repeated at any site since then.

The increase in active layer depths we measured at our sites since 2013 is similar to the longer-term trend represented at all six Circumpolar Active Layer Monitoring (CALM) sites spread across 500,000 km^2 of central Alaska (the east-west swath south of the Brooks Range and North of the Alaska Range; CALM, 2020). At most sites a steady increase in active layer depth was initiated around 2010 and has continued since.

The second piece of evidence indicating thaw of near-surface permafrost at our sites includes some thermistor measurements showing at 1.2 m depth approaching and eventually warming above 0 °C (Figure 12, Table 7) at some sites. Mixed forest sites have warmed the most and all three of our 1.2 m deep thermistors in this ecotype exhibit a steady warming that has been retarded at ~-0.1 °C, likely due to latent heat effects associated with the phase change of ground ice in the transient layer and below (Boike et al., 1998; Shur et al., 2005). The tussock and spruce forest ecotypes do not show the steady increases in permafrost temperatures, however, the overall trend in mean annual temperatures at 1.2 m depth at these sites is increasing (Table 7).

Table 7. A summary of thermistor measurements from 1.2m depth at the study site transects. Mean annual temperature (MAT) values for each of six individual years are presented as well as the six-year global mean annual temperature for each site.

Creamer's Field, disturbed		MAT °C	Creamer's Field, 1m-polygon center		MAT °C	Creamer's Field, 1m-ice wedge in mixed forest		MAT °C
10/01/13	09/30/14	2.78	10/01/13	09/30/14	-0.36	10/01/13	09/30/14	-0.37
10/01/14	09/30/15	4.57	10/01/14	09/30/15	-0.29	10/01/14	09/30/15	-0.33
10/01/15	09/30/16	3.85	10/01/15	09/30/16	-0.26	10/01/15	09/30/16	-0.23
10/01/16	09/30/17	4.91	10/01/16	09/30/17	-0.23	10/01/16	09/30/17	-0.20
10/01/17	09/30/18	5.15	10/01/17	09/30/18	-0.16	10/01/17	09/30/18	-0.10
10/01/18	09/30/19	4.61	10/01/18	09/30/19	-0.13	10/01/18	09/30/19	-0.08
10/01/19	09/30/20	N/A	10/01/19	09/30/20	-0.11	10/01/19	09/30/20	-0.06
	6 year mean	4.31		7 year mean	-0.22		7 year mean	-0.20
Creamer's Field-mixed forest		MAT °C	Creamer's Field-tussocks		MAT °C	Farmer's Loop 1-mixed forest		MAT °C
10/01/13	09/30/14	-0.72	10/01/13	09/30/14	-2.85	10/01/13	09/30/14	-0.21
10/01/14	09/30/15	-0.20	10/01/14	09/30/15	-3.03	10/01/14	09/30/15	-0.08
10/01/15	09/30/16	-0.23	10/01/15	09/30/16	-1.63	10/01/15	09/30/16	-0.07
10/01/16	09/30/17	-0.15	10/01/16	09/30/17	-0.34	10/01/16	09/30/17	-0.04
10/01/17	09/30/18	-0.13	10/01/17	09/30/18	-0.51	10/01/17	09/30/18	-0.02
10/01/18	09/30/19	-0.12	10/01/18	09/30/19	-1.31	10/01/18	09/30/19	0.00
10/01/19	09/30/20	-0.11	10/01/19	09/30/20	-1.15	10/01/19	09/30/20	0.06
	7 year mean	-0.24		7 year mean	-1.55		7 year mean	-0.05

Table 7. Continued

Creamer's Field- mixed forest		MAT °C	Creamer's Field- tussocks		MAT °C	Farmer's Loop 1- mixed forest		MAT °C
10/01/13	09/30/14	-0.72	10/01/13	09/30/14	-2.85	10/01/13	09/30/14	-0.21
10/01/14	09/30/15	-0.20	10/01/14	09/30/15	-3.03	10/01/14	09/30/15	-0.08
10/01/15	09/30/16	-0.23	10/01/15	09/30/16	-1.63	10/01/15	09/30/16	-0.07
10/01/16	09/30/17	-0.15	10/01/16	09/30/17	-0.34	10/01/16	09/30/17	-0.04
10/01/17	09/30/18	-0.13	10/01/17	09/30/18	-0.51	10/01/17	09/30/18	-0.02
10/01/18	09/30/19	-0.12	10/01/18	09/30/19	-1.31	10/01/18	09/30/19	0.00
10/01/19	09/30/20	-0.11	10/01/19	09/30/20	-1.15	10/01/19	09/30/20	0.06
	7 year mean	-0.24		7 year mean	-1.55		7 year mean	-0.05
Farmer's Loop 2, 240m- tussocks		MAT °C	Farmer's Loop 2, 245m- tussocks		MAT °C	Permafrost Tunnel- spruce forest		MAT °C
10/01/13	09/30/14	-2.29	10/01/13	09/30/14	-3.70	10/01/13	09/30/14	-0.74
10/01/14	09/30/15	-2.62	10/01/14	09/30/15	-3.20	10/01/14	09/30/15	-1.17
10/01/15	09/30/16	-0.68	10/01/15	09/30/16	-2.16	10/01/15	09/30/16	-0.40
10/01/16	09/30/17	-1.45	10/01/16	09/30/17	-2.98	10/01/16	09/30/17	-0.98
10/01/17	09/30/18	-0.63	10/01/17	09/30/18	-1.80	10/01/17	09/30/18	-0.28
10/01/18	09/30/19	-0.55	10/01/18	09/30/19	-2.21	10/01/18	09/30/19	-0.27
10/01/19	09/30/20	-1.51	10/01/19	09/30/20	-2.16	10/01/19	09/30/20	-0.25
	7 year mean	-1.39		6 year mean	-2.60		7 year mean	-0.58

The third indication of near-surface permafrost thaw and lowering of the permafrost table is the widespread development of a permanent residual thaw layer between the top of permafrost and the base of seasonally frozen ground at our sites indicated by SIPRE cores collected in 2017 and 2018. At many locations, the seasonal thaw has proven to be deeper than the depth of winter freeze-back. Residual thaw layers are located predominantly in the mixed forest and disturbed ecotypes. These areas contain the warmest near surface permafrost and in some cases, the low ice content sandy silts have a higher thermal conductivity that promotes the movement of heat

into the ground. At some of these sites where the thaw front has penetrated to a depth of 1.2 m, we have had to augment the instrumentation by installing deeper thermistors (i.e. 2 to 2.5 m) to maintain temperature measurements of the near surface permafrost. Since thaw depths increased in 2019 and 2020 it is likely residual thaw layers have increased in thickness and lateral extent. At locations where the thaw front has extended below 1.5 to 2 m it is likely that taliks (unfrozen zones between the bottom of the seasonal freeze and the top of permafrost) have formed.

Numerous lines of visual evidence provide the fourth indication of active permafrost thaw in our research area. The most dramatic is that of the ground subsidence associated with permafrost thaw in the mixed forest region of the Creamer's Field transect. Ice wedge polygons in the area have warmed steadily since 2013 and repeat LiDAR analysis shows high-centered polygon development has expanded due to melting ice wedges (Figures 8 and 9). This suggests potential hydrologic and soil thermal process changes are ongoing in that area (Liljedahl et al., 2016). Anomalous thaw depths coinciding with recent development of thermokarst pits are evident in airborne LiDAR and true color images at all of our sites. At the Creamer's Field site, degradation of ice wedge polygons is evident in our repeat LiDAR analysis, and the most striking thaw subsidence occurred in the mixed forest area along the first 150 m of this transect. The near surface permafrost soils in this area, comprised of lower ice content silts and sands, are warmer than nearby permafrost overlain by tussocks and high-centered polygons had already begun to develop before we initiated our study. Some of the low-lying troughs between polygons, particularly those along the thaw front next to the ponded area to the west, have settled by 1-1.5 m in the decade from 2010 to 2020. For some areas in the vicinity of this transect the ground elevations of the polygon troughs increased between 2010 and 2020, but we attribute this to the area being extremely low-lying and to more standing water in the troughs from greater snowmelt in May 2020 compared to that in 2010. Due to this standing water, we could not ascertain whether the ice wedges in this area had melted or not.

Another means of documenting permafrost thaw and permafrost degradation is through the use of repeat photography. Repeat photos and a long-term thermistor dataset from a site on the northern boundary of the Tanana Flats Training Area (TFTA) show increases in ground thermal conditions and thermokarst development in a lowland wet birch forest (Figure 18). An example of long-term soil temperature monitoring in a lowland black spruce forest at the site is provided in Figure 19. This is clearly an area where rapid warming and thawing of ice rich permafrost has led to ground subsidence. In addition, we established pairs of burned/unburned plots at three north-facing black spruce sites with permafrost in 2018. These upland wet needleleaf forests are an under-studied ecotype compared to the lowland terrains. Soil temperature dataloggers monitored soil surface and permafrost temperatures over the course of this project.



Figure 18. A time series of repeat photos from a lowland site on the Tanana Flats Training Area, experiencing degradation of ice rich permafrost and commensurate habitat change. Long-term monitoring of permafrost degradation at this site since 1994 has documented widespread thawing and collapse of permafrost. At this soil temperature monitoring site in a birch forest (T1-Bir1), the ground surface has collapsed underwater. The Campbell datalogger network was replaced with a simpler, lower cost, Onset Hobo network as part of a previous SERDP project (RC-2110). While the photos are from different angles, the tree in the center is the same. By 2011, the site was already flooded with water.

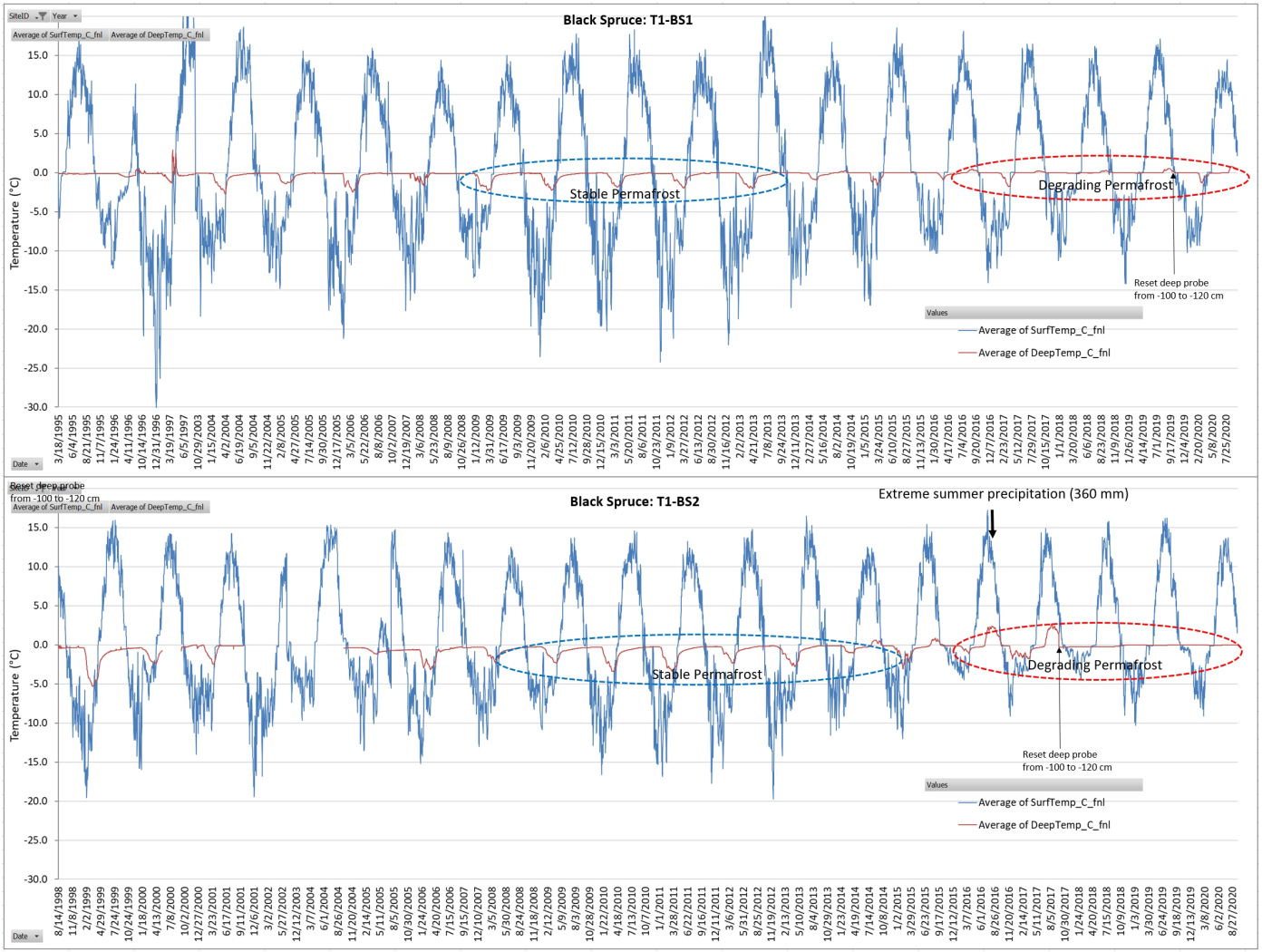


Figure 19. Long-term monitoring of soil surface (-5 cm depth) and permafrost (-1 m depth) temperatures in black spruce ecosystems on the Tanana Flats indicates that permafrost has reached a tipping point. Before 2015, permafrost regularly decreased to minus 2-3 °C during winter, indicating stable permafrost. During the last few years, temperatures at depth have risen above 0 °C during summer and have not cooled below 0 °C during winter, indicating accumulation of unfrozen water that prevents hard freezeback.

2.4 Task 1.2

Analyze historical rates of change in the abundance of ecotypes, in response to fire, thermokarst and hydrologic change by field survey and photointerpretation of a time-series of high-resolution imagery from the 1950s to the late 2010s.

2.4.1 Background

Ecosystems over large regions are highly diverse owing to gradients in environmental conditions and disturbance regimes. As a consequence, they can be expected to respond differently to climate warming. In arctic and boreal biomes a wide range of atmospheric, hydrologic, geomorphic, fire, biotic, and anthropogenic drivers can affect ecological patterns and processes that raise concern for ecosystem management and subsistence resources (Chapin et al., 2006; Martin et al., 2009). To project future change in central Alaska from climate warming, we addressed the complexity of diverse ecosystems and biophysical drivers by using a state-transition modeling approach that incorporates a large number of historical observations of past rates of change. Projection of future trends based on state-transition modeling then can help land managers identify, avoid, and minimize activities in areas of concern.

The factors affecting ecological responses to climate change are being assessed on many fronts. Warming air temperatures have led to changing water balance (Riordan et al., 2006) and surface and subsurface hydrology (Walvoord et al., 2012). Permafrost degradation has increased (Jorgenson et al., 2006; Grosse et al., 2011), which radically reorganizes hydrologic flow paths, soil processes, and vegetation (Jorgenson et al.,2001; 2013, Schuur and Mack, 2018). Compositional shifts or biomass changes in vegetation are occurring through nutrient cycling and competitive interactions among plant species (Potter et al., 2013), snow cover change (Sturm et al., 2005), and herbivory (Joly et al., 2009). Increasing fire frequency and severity associated with climate warming and human activity may lead to a shift in forest composition and distribution (DeWilde and Chapin, 2006, Barrett et al., 2011; Johnstone et al., 2019) and permafrost stability (Jafarov et al., 2013, Nossov et al., 2013; Genet et al., 2013; Douglas et al., 2021). Forest and shrub migration into new areas, altitudinal increases in treeline, and shifts in dominance within plant communities have altered canopy dominance and understory composition (Suarez et al., 1999; Sturm et al., 2001; Myers-Smith et al., 2012). Insect outbreaks, particularly the spruce bark beetle, have killed the spruce overstory in large areas in Alaska (Berg et al., 2006). River erosion and deposition replace late-successional ecosystems with water and barren fluvial deposits, followed by primary succession on riverbars (Van Cleve et al., 1996; Nilsson et al., 2013; Brown et al., 2020). Lake area has increased through shore erosion and decreased from drainage associated with permafrost degradation (Jones et al., 2011; Nitze et al., 2017), evaporative loss and paludification (Roach et al., 2011; Jorgenson et al., 2012). Glacier melting has exposed new barren alpine areas subject to primary succession (Arendt et al., 2002) and affected the geomorphology of glacier-fed river systems (Moore et al., 2009). Increasing human populations and industrial activities also contribute to environmental changes (Raynolds et al., 2014; Trammel and Aisu, 2015). Collectively, these drivers contribute to a diverse mosaic of early to late-successional ecosystems where change can occur abruptly (pulse) through disturbance events or gradually (press) through successional processes or chronic stressors (Chapin et al., 2006; Fresco, 2019).

To assess historical patterns and rates of landscape change in central Alaska and project future changes to 2100, we used a time-series of historical airphotos and recent satellite images to quantify changes in local-scale ecosystems (ecotypes) through photo-interpretation of points

systematically distributed across military lands in the Tanana Kuskowkim Lowlands, Yukon Tanana Uplands and Alaska Range of central Alaska. We then used past transition rates in a state-transition modeling approach to project future changes in response to climate change and geomorphic and ecological drivers of change. Specific objectives of the study were to: (1) compile and geo-rectify imagery from ~1949, ~1978, ~2007, and ~2017; (2) photo-interpret ecosystem type, permafrost status, and drivers of change at 22 systematically distributed grids of 100 points; (3) quantify past rates of ecotype change and identify the ecological drivers of change; and (4) develop a state-transitions model to project future changes from 2017 to 2100.

2.4.2 Methods

2.4.2.1 Study Design

The study was designed to quantify ecotype changes across four major military training areas, TFTA, YTA, Donnelly Training Area East (DTAE), and Donnelly Training Area West (DTAW), that are situated within the Tanana-Kuskokwim Lowlands, Yukon-Tanana Uplands, and Alaska Range of central Alaska (Figures 1 and 20). The sampling used a photo-interpretation and point-intercept technique involving 20 grids (1.8 x 1.8 km) randomly selected from a set of 65 grids systematically distributed in 10-km intervals within the sampling domain, with a randomly assigned starting point. In addition, we added two targeted grids to sample riverine and alpine landscapes not adequately sampled by the random grids in order to have sufficient data for the state-transition modeling. For each of the 22 grids, 100 points were established at 200 m spacing, for a total of 2200 points.

2.4.2.2 Image Compilation and Georectification

Historical airphotos and recent satellite images were acquired for each grid for four time periods, 1949-1952 (median year 1949), 1978-1980 (1978), 2006-2011 (2007), and 2013-2020 (2017). Using the median year for each period (hereafter referred to by median year) to simplify analysis, the imagery allowed us to quantify change for three time-intervals 1949-1978 (29 yrs), 1978-2007 (20 yrs), and 2007-2017 (10 yrs). For the 1949 period, black and white airphotos (scale 1:40,000 to 1:50,000) were identified from the United States Geological Survey (USGS) Earth Explorer web site and USGS scanned them at 14 micron for ~0.7 m pixel resolution. For the 1978 period, the false color infrared (CIR) Alaska High Altitude Aerial Photography (AHAP) airphotos (scale ~1:63,000) were acquired from Earth Explorer at a high-resolution scan (25 micron) for ~1.7 m pixel resolution. For both the 1949 and 1978 periods, orthomosaics (3.3 m and 2.5 m resolution, respectively) processed by the Alaska Satellite Facility also were utilized. For the 2007 and 2017 periods, high-resolution satellite imagery, including Quickbird (0.7 m pixel resolution), Nextview (1.2 m mosaic), Worldview (0.6 m), and IKONOS (1.0 m panchromatic-fused), were acquired from the NGA by CRREL. Recent orthoimagery (0.6 m resolution) processed by the NRCS were also acquired through the Alaska Statewide Digital Mapping Initiative.

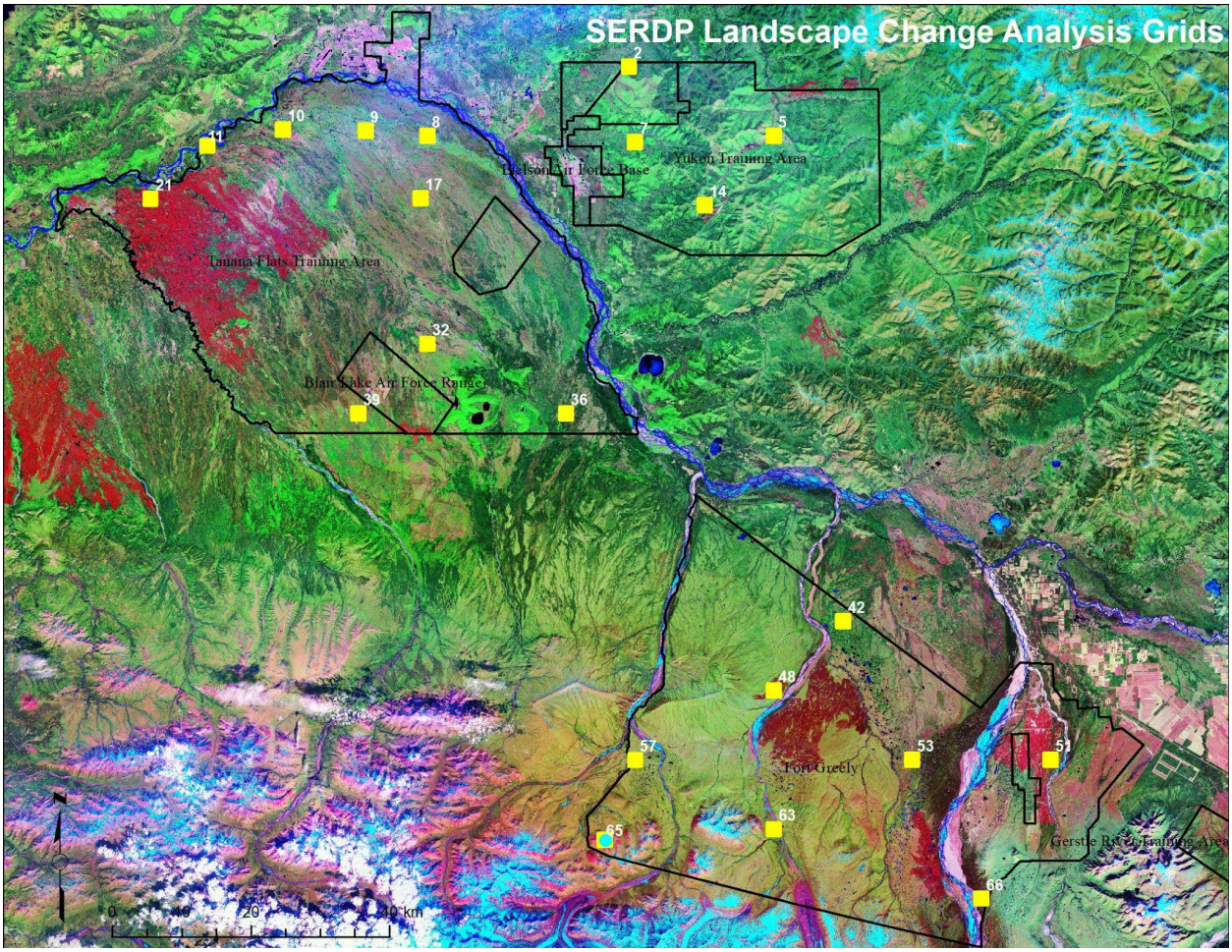


Figure 20. Sampling grids (yellow with grid ID) used for assessing landscape change within the Tanana Flats Training Area, Yukon Training Area, and Donnelly Training Ageas East and West near Fort Greely, central Alaska.

The raw imagery from the YTA, DTAW and DTAE was orthorectified using Earth resources data analysis system (ERDAS) Imagine software with the national elevation dataset (NED), and the raw imagery from the TFTA was georeferenced using ArcMap. Control points (distinct terrain features) were obtained from a 1999 panchromatic, orthorectified airphoto mosaic (Aerometrics, Anchorage, Alaska) for the Tanana Flats and Yukon Training Area, and from the Nextview orthorectified mosaics and other recent imagery available for DTAW and DTAE. Camera model calibrations were used in rectifying the airphotos when available. Otherwise, imagery was orthorectified or georeferenced primarily utilizing second order polynomial transformations. Georectification errors for the 1949 (RMS 0.1-3.5 m), 1978 (0.2-3.7 m), 2007 (0.0-6.0 m) and 2017 (0.5-3.7 m) periods were small relative to the photo-interpretation sampling area (10 m for shrub and forest determinations).

2.4.2.3 Ecological Classification and Change Detection

The detection of change at each point involved photo-interpreting multiple terrain characteristics mostly used established classifications (Table 8). We developed a new multi-level ecological land classification that better integrated classifications developed for TFTA near Fort

Wainwright (Jorgenson et al.,1999), DTAW and DTAE near Fort Greely (Jorgenson et al.,2001), and northwest Alaska (Jorgenson et al., 2009), which incorporated physiography, soil texture, moisture, and vegetation structure into the ecological classification (Table 9). For the geomorphology (surficial geology, terrain units) classification, we used the system from the ecological land classifications for the military lands (Jorgenson et al.,1999, 2001), which was modified from the terrain-unit classification of Kreig and Reger (1982). For permafrost/thermokarst conditions, we modified the classification of Jorgenson and Osterkamp (2005). Thermokarst features were identified by their collapse form and vegetation, and in areas without thermokarst the presence or absence of permafrost was interpreted through vegetation-landform association described in Jorgenson et al. (1999). For assigning ecological drivers to ecotype changes, we used the system developed by Jorgenson et al. (2015). To assign fire age, we used the fire history maps of the Alaska Interagency Coordination Center (http://afsmaps.blm.gov/imf/imf.jsp?site=firehistory). For older fires before 1950, we used vegetation successional status and changes in fire scars between image dates to roughly estimate fire year. We assigned a fire year of 1930 when ecotype (BLSP) was still in post-fire shrub stage on the 1949 airphotos, 1900 when the ecotype was in younger broadleaf/mixed/needleleaf stage with older needleleaf stands evident nearby, and 1850 when the ecotype was in the oldest needleleaf stage with younger needleleaf stands were evident nearby fire scars. Even with more recent fire perimeters in the fire history database we needed photo-interpretation to establish whether a site was burned or not within the perimeter.

For photo-interpretation, the terrain classification was conducted onscreen at ~1:2000 scale using the center of cross-hair created with the GIS for the sampling point. For shrub and forest types, the ecotype was based on a 10-m diameter circle, because the forest classification was based on canopy cover, and for meadow/tundra types the interpretation was done for the cross-hairs, because classification does not depend on shrub/forest canopy percentages. If more than one ecotype was evident within the circle, the ecotype encompassing the cross-hair was used. For thermokarst features, the classification was done at the cross-hair. We first interpreted the most recent high-quality imagery and proceeded to earlier imagery. For the early black and white photography the image quality was poor, consequently, we were only able to differentiate large structural changes in vegetation (e.g., shrub to forest) and relied on ecotype interpretations from later imagery. Changes in the early airphotos were assigned only when there were distinct changes, thus biasing the sampling toward no change. The photo-interpreter (Jorgenson) was able to apply experience gained from 25 years of ecological land classification and mapping at TFTA, YTA, DTAW, and DTAE (Jorgenson et al., 1999; 2000; 2001; 2020).

To analyze landscape change, we cross-tabulated ecotypes by time-interval, change driver, and landscape. We also aggregated the points by grid so that the grid became the sample unit for assessing variability, and tested for significant differences ($P<0.05$) among intervals using a repeated measures analysis of variance (ANOVA).

Table 8. Coding system used for classifying landscape change.

Code	Statewide Ecotype (Lvl 8)
BADPV	Boreal Alpine Dry Barrens
BADSD	Boreal Alpine Dry Dwarf Scrub
BADSL	Boreal Alpine Dry Low Scrub
BAMSD	Boreal Alpine Moist Dwarf Scrub
BAMSL	Boreal Alpine Moist Low Scrub
BASP	Boreal Alpine Post-fire Scrub
BAWMT	Boreal Alpine Wet Tussock Meadow
BAWSL	Boreal Alpine Wet Low Scrub
BLBD	Boreal Lowland Bog Dwarf Scrub
BLBM	Boreal Lowland Bog Meadow
BLBT	Boreal Lowland Bog Tussock Scrub
BLDSL	Boreal Lowland Dry Low Scrub
BLDWB	Boreal Lowland Dry Broadleaf Woodland
BLDWM	Boreal Lowland Dry Mixed Woodland
BLMWN	Boreal Lowland Moist Needleleaf Woodland
BLNM	Boreal Lowland Fen Meadow
BLNS	Boreal Lowland Fen Low Scrub
BLPU	Boreal Lowland Human-modified Barrens
BLSP	Boreal Lowland Post-fire Scrub
BLSU	Boreal Lowland Human-modified Scrub
BLWSL	Boreal Lowland Wet Low Scrub
BLWST	Boreal Lowland Wet Tall Scrub
BLWWB	Boreal Lowland Wet Broadleaf Woodland
BLWWM	Boreal Lowland Wet Mixed Woodland
BLWWN	Boreal Lowland Wet Needleleaf Woodland
BPLD	Boreal Lacustrine Deep Lake
BPLS	Boreal Lacustrine Shallow Lake
BPNM	Boreal Lacustrine Fen Meadow
BPWMG	Boreal Lacustrine Wet Grass Meadow
BRDMG	Boreal Riverine Dry Grass Meadow
BRDPV	Boreal Riverine Dry Barrens
BRDSD	Boreal Riverine Dry Dwarf Scrub
BRDSL	Boreal Riverine Dry Low Scrub
BRDWB	Boreal Riverine Dry Broadleaf Woodland
BRDWM	Boreal Riverine Dry Mixed Woodland
BRDWN	Boreal Riverine Dry Needleleaf Woodland
BRLS	Boreal Riverine Shallow Lake
BRMFB	Boreal Riverine Moist Broadleaf Forest
BRMFM	Boreal Riverine Moist Mixed Forest
BRMFN	Boreal Riverine Moist Needleleaf Forest
BRMPV	Boreal Riverine Moist Barrens
BRMST	Boreal Riverine Moist Tall Scrub
BRRW	Boreal Riverine River
BRSP	Boreal Riverine Post-fire Scrub
BRWMS	Boreal Riverine Wet Sedge Meadow
BRWSL	Boreal Riverine Wet Low Scrub
BSMST	Boreal Subalpine Moist Tall Scrub
BSMWN	Boreal Subalpine Moist Needleleaf Woodlanc
BUDPV	Boreal Upland Dry Barrens
BUDSL	Boreal Upland Dry Low Scrub
BUDWB	Boreal Upland Dry Broadleaf Woodland
BUDWM	Boreal Upland Dry Mixed Woodland
BUDWM	Boreal Upland Dry Needleleaf Woodland
BUMFB	Boreal Upland Moist Broadleaf Forest
BUMFM	Boreal Upland Moist Mixed Forest
BUMFN	Boreal Upland Moist Needleleaf Forest
BUMSL	Boreal Upland Moist Low Scrub
BUMST	Boreal Upland Moist Tall Scrub
BUPU	Boreal Upland Human-modified Barrens
BUSP	Boreal Upland Post-fire Scrub
BUSU	Boreal Upland Human-modified Scrub
BUWWN	Boreal Upland Wet Needleleaf Woodland

Code	Permafrost Status
BL	Block Landslide
BS	Beaded Stream
CBS	Collapse-block Shore
CP	Collapsed Pingo
CTM	Conical Thermokarst Mounds
DS	Detachment Slide
DTL	Deep Thermokarst Lake
GL	Glacial Thermokarst
GTL	Glacial Thermokarst Lake
ITM	Irregular Thermokarst Mounds
PA	Permafrost aggrading
PL	Permafrost Likely
PS	Permafrost Stable
SH	Sink Holes
STL	Shallow Thermokarst Lake
TDB	Thermokarst Deep Basin
TB	Thermokarst Bog
TEG	Thermal Erosion Gully
TF	Thermokarst Fen
THS	Thermokarst Shore Bog
TLB	Thermokarst-lake Basin
TP	Thermokarst Pits
TSK	Thaw Sink
TSL	Thaw Slump
TTP	Thermokarst Troughs and Pits
TWT	Thermokarst Water Track
UL	Unfrozen Likely
US	Unfrozen Stable

Code	**Geomorphic Unit (for year 1949)**
Nn	Metamorphic-noncarbonate
Ch	Hillslope Colluvium
Ell	Lowland Loess
Elu	Upland Loess
Elui	Upland Loess, ice-rich (yedoma)
Fmra	Meander active channel (point bar)
Fmrb	Meander Abandoned Channel (gravelly, sandy)
Fmri	Meander Inactive Channel Deposits
Fmoi	Meander Inactive Overbank Deposits
Fmob	Mean. Abandoned Overbank Deposits
Fbrag	Braided gravelly active channel
Fbrb	Braided Abandoned Channel (gravelly, sandy)
Fboi	Braided Inactive Overbank Deposits
Fbob	Braided Abandoned Ovrbank Deposits
Fhl	Headwater Lowland Floodplain
Fhm	Headwater Mod. Steep Floodplain (2–6% grad.)
Fhmo	Headwater Moderately Steep Overbank Dep.
Gfo	Glaciofluvial Outwash
Ldmy	Drained Lake, morainal, young
Ldmo	Drained Lake, morainal, old
Fsl	"Lowland" Retransported deposits
Of	Organic Fens
Ob	Bogs
Wrlg	Lower Perennial, glacial
Wrln	Lower Perennial, non-glacial
Wldit	Deep Isolated Lake, Thaw
Wlsit	Shallow Isolated Lake, Thaw
Wldm	Deep Lake, morainal
Wlsir	Shallow Isolated Lake, Riverine

Code	Change Type
AL	Acidification-leaching
CD	Coastal deposition
CE	Coastal erosion
DL	Drained Lake
DM	Drainage & migration
DMS	Drying/moisture Stress
F	Fire
F-VFE	Fire and Post Fire Succession
FV	Fire-Very Old (Before 1949)
FO	Fire-old (1950-1978)
FI	Fire-intermediate (1978 to 2005))
FR	Fire-recent (>2005)
FM	Fire-multiple (after 1950)
FTK	Fire and Thermokarst
GM	Glacier melting
H	Human development
Ha	Agriculture
Hc	Clearings
Hl	Logging
He	Excavations
Hf	Fill/Roads
Ht	Trails
ID	Insect Damage
LF	Landslides/fans
N	None
VPE	Vegetation Paludification-early
VPL	Vegetation Paludification-Late
VFE	Veg. Fire succession-early (to shrub, broadleaf)
VFL	Veg. Fire succession-late (to mixed, needleleaf)
VFM	Vegetation Fire Succession-multipe
Voe	Vegetation, other expansion
VSE	Vegetation Shrub Expansion
VTE	Vegetation Tree Expansion
VRE	Vegetation Riverine Succession-Early
VRL	Vegetation Riverine Succession-Late
RD	River deposition
RE	River erosion
TK	Thermokarst
PFA	Permafrost Aggradation
Wb	Wildlife Beaver
VLE	Vegetation, lacustrine succession-early
VLL	Vegetation, lacustrine succession-late
	Bogs, Fens assumed unburned

Code	**Fire Regime**
R	Recent >2005
I	Intermediate-age, 1986-2005
O	Old 1950-80: assigned
V	Very Old, <1950, evident old forest near fire scars
M	Multiple fires since 1900s
U	Unburned, late successional ecotype, fire <1900

Code	**Fire Year**
Year	Enter year of fire for each interval. 0=no fire

Table 9. Crosswalk of statewide ecotypes used in grid sampling with ecotypes described for the TFTA and YTA near Fort Wainwright (Jorgenson et al., 1999) and DTAW and DTAE near Fort Greely (Jorgenson et al., 2001).

Statewide Ecotypes Level 8 2020	Ft Wainwright Ecotype 1999	Ft Greely Ecotype 2001
Boreal Alpine Dry Barrens	NA	Alpine Rocky Dry Barrens
Boreal Alpine Dry Dwarf Scrub	Alpine Rocky Dry Dwarf Scrub	Alpine Rocky Dry Dwarf Scrub
Boreal Alpine Dry Low Scrub	NA	Upland Rocky Dry Low Scrub
Boreal Alpine Moist Dwarf Scrub	NA	NA
Boreal Alpine Moist Low Scrub	Alpine Rocky Moist Tall and Low Scrub	Alpine Rocky Moist Low Scrub
Boreal Alpine Post-fire Scrub	NA	NA
Boreal Alpine Wet Tussock Meadow	NA	Alpine Wet Tussock Meadow
Boreal Alpine Wet Low Scrub	NA	Alpine Wet Low Scrub
Boreal Alpine Wet Sedge Meadow	NA	Alpine Wet Meadow
Boreal Lowland Bog Dwarf Scrub	Lowland Bog Meadow	Lowland Dwarf Scrub Bog
Boreal Lowland Bog Meadow	Lowland Bog Meadow	Lowland Dwarf Scrub Bog
Boreal Lowland Bog Tussock Scrub	Lowland Tussock Bog	Lowland Tussock Scrub Bog
Boreal Lowland Dry Low Scrub	NA	Lowland Gravelly Moist Low Scrub
Boreal Lowland Dry Broadleaf Woodland	Lowland Gravelly Moist Broadleaf Forest	Lowland Gravelly Dry Broadleaf Forest
Boreal Lowland Dry Mixed Woodland	Lowland Gravelly Moist Mixed Forest	Lowland Gravelly Dry Mixed Forest
Boreal Lowland Moist Needleleaf Woodland	Lowland Gravelly Moist Needleleaf Forest	Lowland Gravelly Needleleaf Forest
Boreal Lowland Fen Meadow	Lowland Fen Meadow	Lowland Fen Meadow
Boreal Lowland Fen Low Scrub	Lowland Scrub Fen	NA
Boreal Lowland Human-modified Barrens	Human Modified	Human Disturbed Scrub
Boreal Lowland Post-fire Scrub	Lowland Wet Low Scrub	Lowland Low Scrub-Disturbed
Boreal Lowland Human-modified Scrub	Human Modified	Human Disturbed Scrub
Boreal Lowland Wet Low Scrub	Lowland Wet Low Scrub	Lowland Wet Low Scrub
Boreal Lowland Wet Low Scrub	Lowland Gravelly Wet Low Scrub	Lowland Wet Low Scrub
Boreal Lowland Wet Tall Scrub	Lowland Wet Tall Scrub	Lowland Moist Tall Scrub
Boreal Lowland Wet Broadleaf Woodland	Lowland Wet Broadleaf Forest	Lowland Wet Broadleaf Forest
Boreal Lowland Wet Mixed Woodland	Lowland Wet Mixed Forest	Lowland Wet Mixed Forest
Boreal Lowland Wet Needleleaf Woodland	Lowland Wet Needleleaf Forest	Lowland Wet Needleleaf Forest
Boreal Lacustrine Deep Lake	Lakes and Ponds	Lakes and Ponds
Boreal Lacustrine Shallow Lake	Lakes and Ponds	Lakes and Ponds
Boreal Lacustrine Fen Meadow	Lacustrine Fen Meadow	Lacustrine Fen Meadow
Boreal Lacustrine Wet Grass Meadow	Lowland Moist Meadow	Lacustrine Moist Meadow
Boreal Riverine Dry Grass Meadow	NA	Riverine Gravelly Dry Meadow
Boreal Riverine Dry Barrens	NA	Riverine Gravelly Barrens
Boreal Riverine Dry Dwarf Scrub	NA	Riverine Gravellly Dry Dwarf Scrub
Boreal Riverine Dry Low Scrub	NA	Riverine Gravelly Low and Tall Scrub
Boreal Riverine Dry Broadleaf Woodland	NA	Riverine Gravelly Dry Broadleaf Forest
Boreal Riverine Dry Mixed Woodland	NA	Riverine Gravelly Dry Mixed Forest
Boreal Riverine Dry Needleleaf Woodland	NA	Riverine Gravelly Needleleaf Forest
Boreal Riverine Shallow Lake	Lakes and Ponds	Lakes and Ponds
Boreal Riverine Moist Broadleaf Forest	Riverine Moist Broadleaf Forest	Riverine Moist Broadleaf Forest
Boreal Riverine Moist Mixed Forest	Riverine Moist Mixed Forest	Riverine Moist Mixed Forest
Boreal Riverine Moist Needleleaf Forest	Riverine Moist Needleleaf Forest	Riverine Moist Needleleaf Forest
Boreal Riverine Moist Barrens	Riverine Barrens	Riverine Gravelly Barrens
Boreal Riverine Moist Tall Scrub	Riverine Moist Tall Scrub	Riverine Moist Tall and Low Scrub
Boreal Riverine River	Lower Perennial River	Upper Perennial River
Boreal Riverine Post-fire Scrub	NA	NA
Boreal Riverine Marsh	Riverine Marsh (not mapped)	NA
Boreal Riverine Wet Sedge Meadow	Riverine Wet Meadow	Riverine Wet Meadow
Boreal Riverine Wet Low Scrub	Riverine Wet Low Scrub	Riverine Moist Tall and Low Scrub
Boreal Subalpine Moist Tall Scrub	Alpine Rocky Moist Tall and Low Scrub	Alpine Rocky Moist Low Scrub
Boreal Subalpine Moist Needleleaf Woodland	NA	NA
Boreal Upland Dry Barrens	NA	Upland Rocky Dry Barrens (not described)
Boreal Upland Moist Grass Meadow	NA	Upland Moist Meadow
Boreal Upland Dry Low Scrub	Upland Rocky Dry Meadow	Upland Rocky Dry Meadow
Boreal Upland Dry Broadleaf Woodland	Upland Moist Broadleaf For. (south-facing	Upland Rocky Dry Broadleaf Forest
Boreal Upland Dry Mixed Woodland	Upland Moist Mixed Forest (south-facing)	NA
Boreal Upland Dry Needleleaf Woodland	Upland Moist Needleleaf Forest	NA
Boreal Upland Moist Broadleaf Forest	Upland Moist Broadleaf Forest	Upland Moist Broadleaf Forest
Boreal Upland Moist Mixed Forest	Upland Moist Mixed Forest	Upland Moist Mixed Forest
Boreal Upland Moist Needleleaf Forest	Upland Moist Needleleaf Forest	Upland Moist Needleleaf Forest
Boreal Upland Moist Low Scrub	Upland Moist Low Scrub	Upland Moist Low and Tall Scrub
Boreal Upland Moist Tall Scrub	Upland Moist Tall Scrub	Upland Moist Low and Tall Scrub
Boreal Upland Human-modified Barrens	Human Modified	Human Disturbed Barrens
Boreal Upland Post-fire Scrub	Upland Moist Low Scrub	Upland Moist Low and Tall Scrub-disturbed
Boreal Upland Human-modified Scrub	Human Modified	NA
Boreal Upland Wet Needleleaf Woodland	Upland Wet Needleleaf Forest	Upland Wet Needleleaf Forest

2.4.2.4 Historical Transition Probabilities

A comprehensive set of transitions from one ecotype to another were developed for each ecotype, as well biophysical factors associated with each transition. First, an initial set of all possible transitions was developed from the transitions documented in the data sets. Second, we assigned drivers associated with each change attributed by the photo-interpreter. Third, we then made minor additions to the list of transitions and drivers using information from: (1) scoping workshops for long-term ecological monitoring in Alaska (Martin et al., 2009); and (2) our extensive field experience in the region. Overall, we identified 269 possible transitions (including no-change possibility) for 62 ecotypes; one ecotype was added that was not observed from the grid sampling.

Transition probabilities for each possible state change over the three intervals were first calculated to estimate the fraction of each ecotype that transitioned from the original ecotype normalized to the interval years. For the no-change probability (sampling without replacement) we used the formula TransProb =(count of individual partial transition/count of all partial transitions)^(1/(yrs)). For the remaining partial transitions, we used TransProb=(1 - no-change probability)*(count of individual partial transition/(count of all partial transitions - count of individual partial transition)). We then averaged the transition probabilities for the three time-intervals. Because the averages from the partial transitions did not always add up to 1 (100%), we frequently had to adjust the value for the no-change transition so that all partial transitions added to 1. For some transitions for which we had few data, or for transitions that we know to happen for which we had no data, we used transition rates from other similar transitions within our database or from other studies (compiled by Jorgenson et al., 2015) to adjust the rates. When no data were available for a particular transition from one ecotype to another, we assigned values based on our field experience. These assigned values generally were very small because they were sufficiently rare to have no observations.

2.4.2.5 Climate Trends

We analyzed trends in air temperatures from two long term weather station records near the study area, Fairbanks (1904-2020) and Big Delta (1917-2020), using climate data obtained from the Western Regional Climate Center (www.wrcc.dri.edu/summary/ Climsmak.html). For each station, we calculated daily and seasonal thawing (TDD) and freezing (FDD) degree-days (base 0 °C), as well as summer (May–September) cumulative precipitation (mm). We then calculated mean temperature (TDD) for each of the three time-intervals. For future projections, we compiled data for decadal downscaled climate projections for 2010-2100 from the Scenario Network for Alaska Planning (SNAP; https://uaf-snap.org/get-data/) based on the RCP 4.5 (low), 6.0 (middle), 8.5 (high) according to the Intergovernmental Panel on Climate Change (IPCC) Assessment Report (AR5) Synthesis Report (2014). The SNAP modeling selected the five Global Climate Models (GCM) that performed best in Alaska and the Arctic (Walsh et al., 2018). Outputs from these models were downscaled using PRISM data, which accounts for slope, elevation, and proximity to coastlines. The final SNAP products were high-resolution monthly climate data for ~1901-2100 for Alaska and large regions of Canada. We used the projected decadal averages for each month to calculate seasonal TDD (monthly average × days in each month).

2.4.2.6 Modeled Ecosystem Transitions

State-transition modeling of future changes for four intervals (2017–2040, 2040–2060, 2060–2080 and 2080–2100) were calculated in Excel spreadsheets for a time model, RCP 4.5 and RCP 8.5 temperature models, and a driver-adjusted RCP6.5 temperature model that adjusted change rates based on perceived climate sensitivity of the driver to climate warming. The time model, which predicts future changes will occur at the same rate over future 20-yr intervals as during the past 68-yr period, involved: (1) calculating partial areas resulting from the transition of each ecotype into other ecotypes by multiplying the beginning total area by the transition probabilities; (2) summing the partial areas of the resulting transitions into a new total area for each ecotype for the specific time interval; and (3) iteratively calculating changes for each 20-yr period based on the total area from the previous interval.

The temperature models involved increasing transition probabilities as a function of the rate of change of temperature, assuming that summer TDD is the primary driver of all transitions and that the rate of change will increase linearly with temperature increase. We used transition rate increases of 1.05, 1.09, 1.12, and 1.13x in TDD for the RCP4.5 temperature model, 1.04, 1.08, 1.15, and 1.17x for the RCP6.0 model, and 1.05, 1.15, 1.22, and 1.30x for the RCP8.0 mode for the four respective time-intervals based on the SNAP projections.

In the rate-adjusted RCP6.0 model, transition probabilities were calculated the same as for the temperature model with the addition of a change-rate factor used to scale changes that were generally believed to be slow to change with temperature (i.e., plant migration and plant dominance shifts affected by numerous interacting factors and negative feedbacks) and to accelerate changes that have strong positive feedbacks due to interaction with surface water and are therefore highly sensitive to temperature (i.e., for glacier melting, and most types of thermokarst). Six type of driver adjustments were made: (1) removal of temperature rate (factor inverse of TDD rate increase) because temperature has a negligible effect (e.g., human activity); (2) no adjustment (factor=1) assuming biological/geomorphic processes respond linearly to temperature; (3) elimination of transition (factor=0), e.g., when no further permafrost aggradation is possible; (4) rates accelerate slowly (e.g., tree and shrub expansion, factors 1.5, 2, 2.5, 3x during 4 intervals); (5) rates accelerate rapidly (e.g, permafrost degradation 2, 4, 6, 8x during 4 intervals) due to strong positive feedbacks; (5) rates have a step change (e.g., spruce bark beetle invasion, factor=5) from insect outbreaks. While there is a theoretical justification in the literature for this scaling, no data were available to constrain the values and we view them as working hypotheses. From a practical aspect, the scaling was limited so that transition probabilities driven by large driver adjustments did not exceed 100% by the end of the four intervals.

The amount of change (final area minus beginning area in ha) was summarized for each ecotype and time-interval as: (1) absolute percent change calculated as a proportion of the total study area, which is useful for comparing changes among ecotypes and identifying which are causing the largest overall changes; and (2) as relative percent change calculated as a proportion of initial ecotype area, which is useful for comparing relative effects among ecotypes. Cumulative net change in area was calculated as the sum of all positive changes in area.

2.4.3 Results

2.4.3.1 Historical Ecotype Changes

Photointerpretation of the occurrence of ecotypes on high-resolution imagery at 22 grids (100 points/grid) during four periods (median years 1949, 1978, 2007, 2017) documented

changes in 61 ecotypes responding to 17 drivers across the 657,495 ha study area. Some representative photos of the different landscape types with diverse ecotypes are provided in Figure 21 and an example of changes in a lowland grid on the Tanana Flats is provided in Figure 22. Overall, 67.9% (n=2200) of the region had changes in ecotypes over the entire 68-yr interval. When comparing the 1949-1978, 1978-2007, and 2007-2017 time-intervals, ecotype changes occurred over 49.6%, 52.4%, and 25.0% of the study area, respectively.

When comparing ecotypes, gains in area over the entire 1949-2017 interval were dominated by Lowland Wet Low Scrub (11.0% of total area) that had recovered after extensive fires before 1949, with lesser gains in Lowland Bog Tussock Scrub (1.4%), Lowland Wet Tall Scrub (1.4%), Lowland Wet Broadleaf Woodland (1.4%), Lowland Wet Mixed Woodland (1.3%), and Upland Dry Mixed Woodland (1.3%; Figure 23). Decreases in area were dominated by Lowland Post-fire Scrub (-20.0%), with lesser losses for Upland Post-fire Scrub (-3.1%), Upland Moist Broadleaf Forest (-1.7%), Alpine Post-fire Scrub (-1.4%), and Riverine Moist Mixed Forest (-0.7%). However, significant changes ($P<0.05$, repeated measures ANOVA) were found only for Lowland Fen Meadow, Lowland Human-modified Scrub, Lowland Wet Low Scrub, Lowland Post-fire Scrub, Lowland Wet Tall Scrub, and Lowland Wet Mixed Woodland, with marginally significant changes for Lowland Bog Meadow ($P=0.06$) and Upland Dry Mixed Woodland ($P=0.08$). Our interpretations of what caused the areal changes for each ecotypes are presented in Table 10.



Figure 21. Photographic examples of the six physiographic landscapes in central Alaska comprising a wide diversity of boreal ecotypes (photos by Richard Murphy).

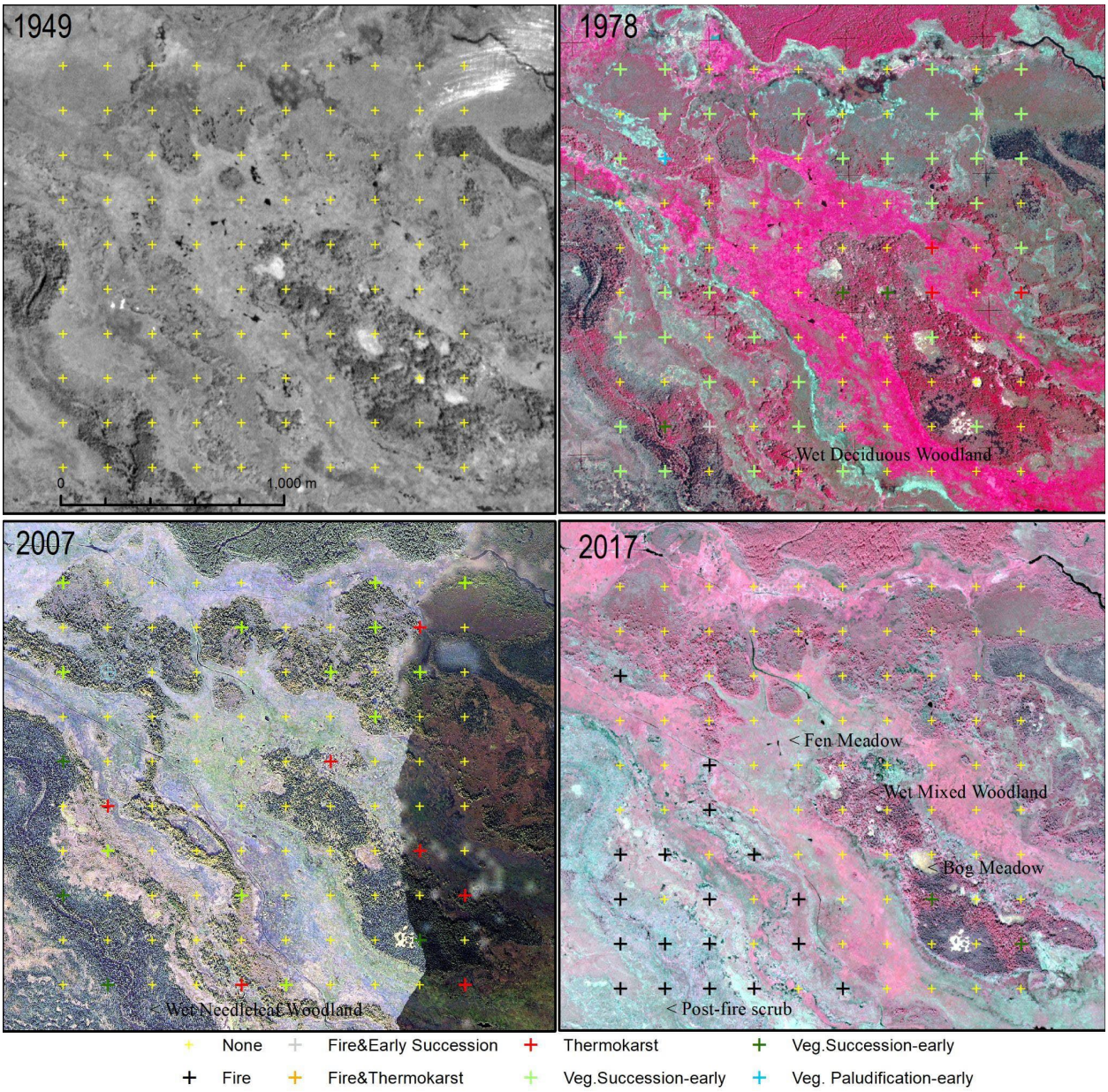


Figure 22. An example of a time-series of imagery for a lowland grid (#10) on the Tanana Flats from 1949, 1978, 2007, and 2017 used for quantifying ecotype changes. Crosshairs are sampling points used for photo-interpretation and are color-coded to indicate change driver associated with changes. Dominant lowland ecotypes are highlighted on imagery.

Relative change, based on initial area of each ecotype, provides a measure of how much each ecotype changed independent of overall area. The largest relative gains occurred for Lowland Dry Broadleaf Woodland (1900%), Upland Moist Tall Scrub (1000%), Lowland Wet Low Scrub (968%), Upland Moist Low Scrub (650%), Lowland Wet Tall Scrub (620%), and Lowland Human-modified Scrub (500%). The largest relative losses were for Alpine Post-fire Scrub (-100%), Riverine Dry Grass Meadow (-66.7%), Riverine Moist Barrens (-66.7%), Riverine Moist Tall Scrub (-58.3%), Upland Post-fire Scrub (-51.9%), Riverine Dry Barrens (-50.0%) and Lacustrine Deep Lake (-50.0%).

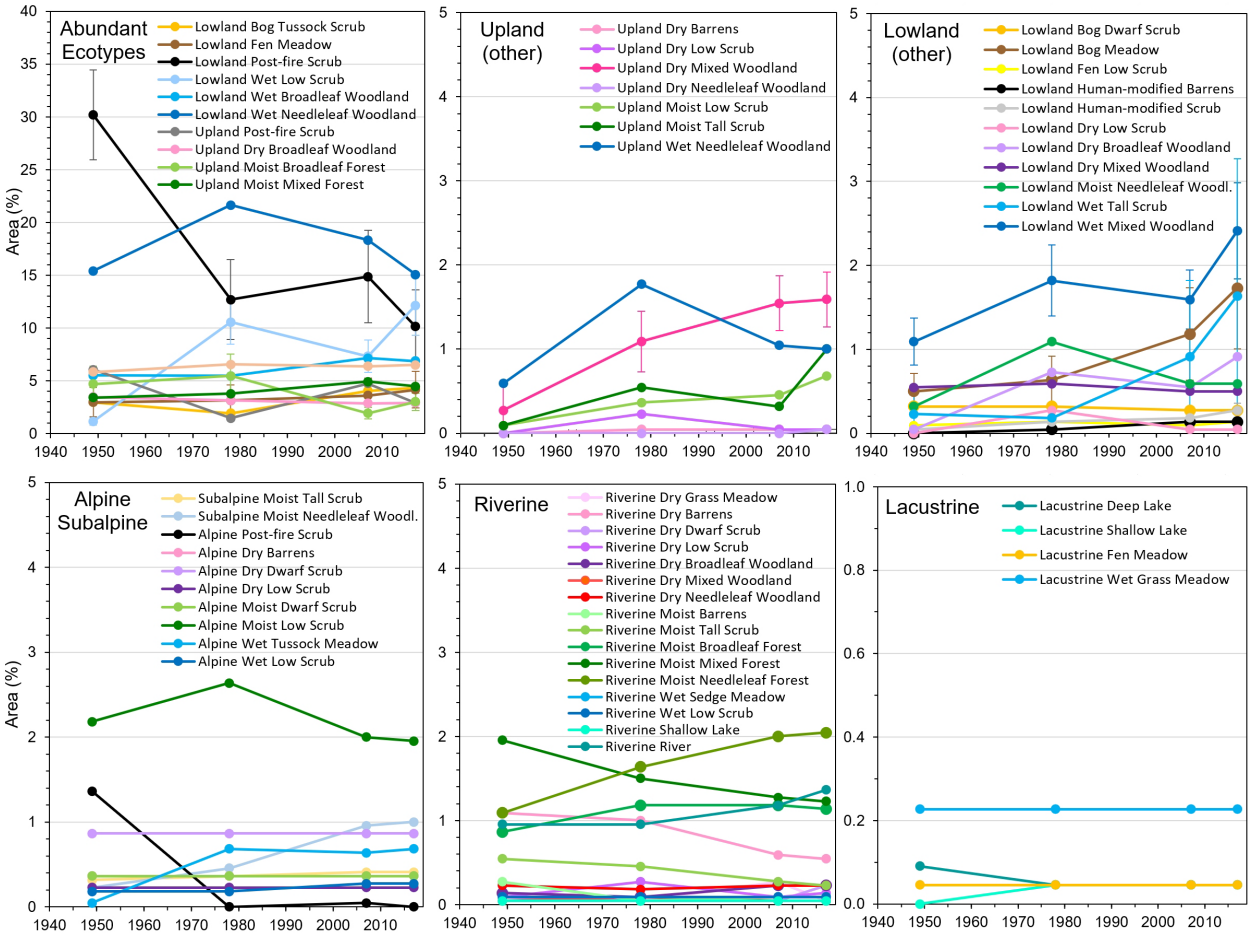


Figure 23. Mean changes (n=22 grids) in area (%) of 61 ecotypes from 1949 to 2017 (median years for periods). Bars are 95% confidence intervals, but shown only for seven ecotypes that showed significant trends (P<0.05, repeated measures ANOVA).

Table 10. Explanation for cumulative historical and projected landscape change (driver-adjusted climate model RCP6).

Ecotype Name	Area (%)	Explanation for Change
Alpine Dry Barrens	0.0	near steady state
Alpine Dry Dwarf Scrub	-0.1	near steady state
Alpine Dry Low Scrub	0.0	near steady state
Alpine Moist Dwarf Scrub	0.0	near steady state
Alpine Moist Low Scrub	-0.9	initial fire related oddity from burned subalpine woodlands returning to alpine scrub, then loss from shrub/tree expansion,
Alpine Post-fire Scrub	-1.3	initial big drop after early fire hit one of the grids, very slow increase later
Alpine Wet Tussock Mead.	0.7	big increase after early fire, then steady, oddity of fire on few grids
Alpine Wet Low Scrub	0.2	slow increase from thermokarst water-track formation, also extreme precip. event
Lowland Bog Dwarf Scrub	-0.1	birch/spruce colonization extremely slow, permafrost aggradation and forest stablishment eliminated
Lowland Bog Meadow	8.8	large increase from strongly accelerating thermokarst
Low. Bog Tussock Scrub	0.7	recovery after early fire, then very slow decreased from thermokarst
Lowland Dry Low Scrub	0.1	initial small fire-related increase due to one big fire, otherwise near steady state
Lowland Dry Broadleaf Woodland	0.9	large increase after mid-interval fire, then steady
Low. Dry Mixed Woodl.	0.2	near steady stage balancing successional gains and losses
Lowland Moist Needleleaf Woodland	2.2	increased after early fire, then decrease from late 1900s fires, then large increase from permafrost thaw/soil drainage
Lowland Fen Meadow	11.9	large increase from accelerating thermokarst from climate warming and groundwater
Lowland Fen Low Scrub	0.5	slow increase for paludification after thermokarst
Lowland Human-modified Barrens	0.2	mid-interval increase, then steady
Lowland Post-fire Scrub	-21.3	huge 1949 extent after 1930s fires, then loss from late succession, then slowly decrease as flammable lowland ecotypes lost to thermokarst
Lowland Human-modified Scrub	0.4	slight increase from expanded clearings related to military training, and shrub recovery
Lowland Wet Low Scrub	3.6	large increase after extensive early fires, then decrease after replacement with woodlands, then rapid decrease due to thermokarst
Lowland Wet Tall Scrub	0.6	increase after early fire, then loss to succession and thermokarst
Lowland Wet Broadleaf Woodland	-4.3	increase after early fires, then accelerating loss from thermokarst
Lowland Wet Mixed Woodland	3.8	low after early fires, increasing expansion of birch into lowland black spruce even with loss from thermokarst
Lowland Wet Needleleaf Woodland	-8.4	initial big recovery after 1930s fires, with subsequent loss from later fires, then accelerating loss from thermokarst and loss to mixed forests from thaw/drainage
Lacustrine Deep Lake	0.2	initially slight loss to lake drainage, but later small increase from deep lakes forming in yedoma
Lacustrine Shallow Lake	0.2	slight gain from partial lake drainage from deep lakes overcoming loss from lake drainage
Lacustrine Fen Meadow	0.0	near steady state, but few samples,
Lacustrine Wet Grass Mead	-0.1	near steady state, but few samples, lacustrine low shrub transition missing
Riverine Dry Grass Meadow	0.0	big increase in 2007 perhaps from extreme flooding events, not predictable in broad transition intervals
Riverine Dry Barrens	-0.7	loss from extreme flooding events, then near steady state, large changes not predictable in broad transition intervals
Riverine Dry Dwarf Scrub	0.0	changes from extreme flooding events, not predictable in broad transition intervals
Riverine Dry Low Scrub	0.1	changes from extreme flooding events, not predictable in broad transition intervals
Riverine Dry Broadleaf Woodland	0.0	changes from extreme flooding events, not predictable in broad transition intervals
Riverine Dry Mixed Woodland	0.1	near steady state
Riverine Dry Needleleaf Woodland	-0.1	near steady state
Riverine Shallow Lake	0.0	near steady state

2.4.3.2 Drivers of Change

Changes in ecotypes were attributed to 17 (plus 4 combinations) drivers associated with ecological and geomorphic processes (Figures 24 and 25). Change drivers during 1949-1978 were dominated by post-fire early succession (28.5% of total area) and fires (14.1%). Drivers affecting smaller areas included post-fire late succession (2.7%), riverine early succession (0.9%), riverine late succession (0.6%), river erosion (0.3%), and thermokarst (0.4%). During 1978-2007, areas affected by fire (19.4%) increased moderately, while post-fire early succession (10.5%) decreased nearly two-thirds, and post-fire late succession (6.3%) increased two-fold. Areas affected by lesser drivers included fire and post-fire early succession combined (2.0%), thermokarst (1.1%), riverine early succession (0.7%), riverine late succession (0.8%), and river erosion (0.4%). Areas affected by human activity (fill, trails, clearing combined) increased from 0.2% to 0.3% over the two intervals. During 2007-2017, post-fire succession (13.9%) increased slightly and fire (7.3%) decreased by nearly two-thirds, while post-fire late succession (1.3%), thermokarst (1.1%), riverine early succession (0.4%), river erosion (0.3%) and deposition (0.2%) caused small changes.



Figure 24. Photographs illustrating ecological processes driving change, including thermokarst, fire, post-fire succession, river erosion/deposition, land clearing, and trail development (photos by T. Jorgenson).

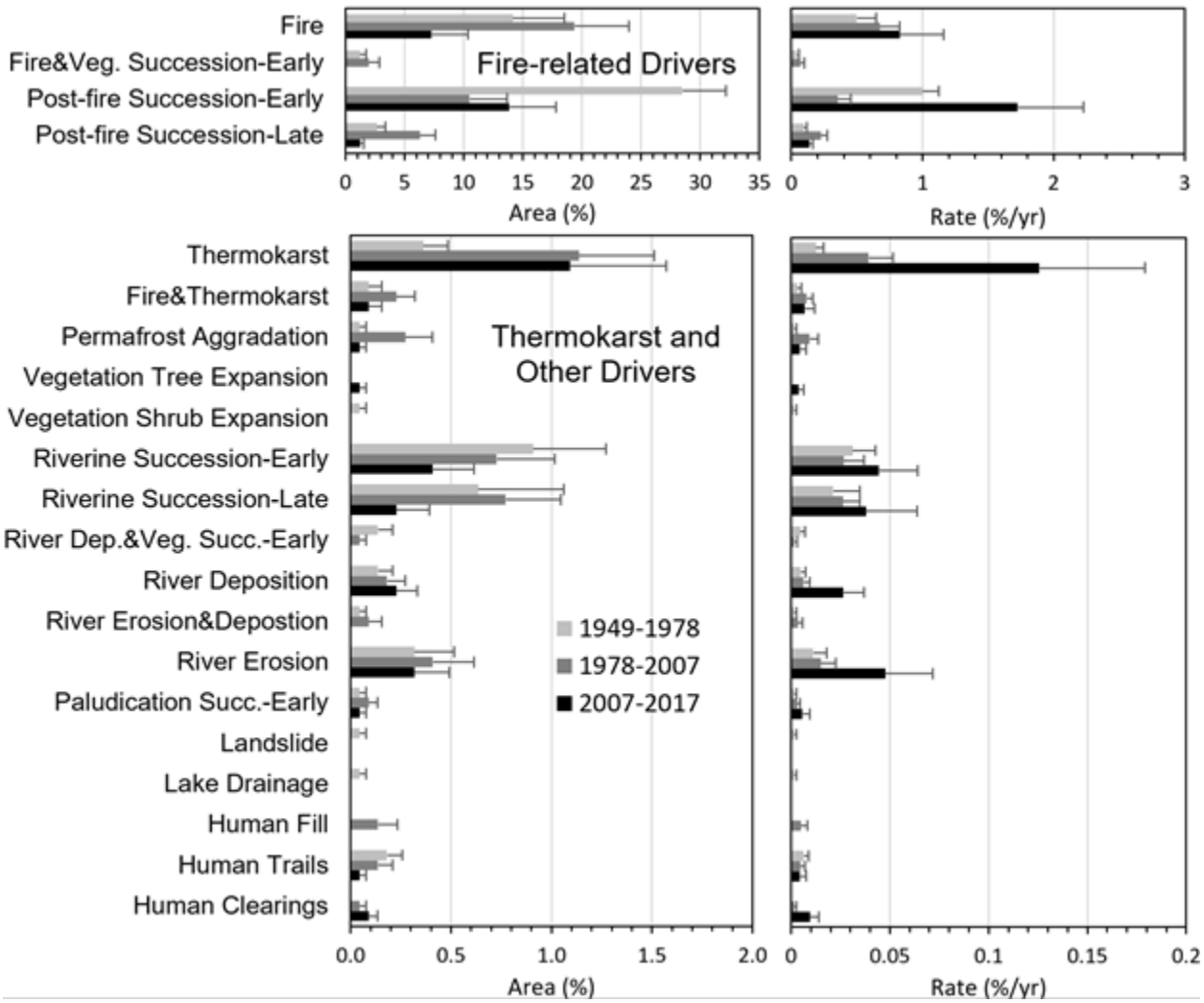


Figure 25. Mean (n=22 grids, ±95% CI) areal extent and annual rates of change affected by 17 drivers (plus 4 combinations) of ecotype changes for three time-intervals. Note the difference in scales between charts.

When comparing annual rates of change for the three intervals of differing lengths, fire change was slightly higher during the last interval (0.8% of absolute area/yr) compared to previous intervals (0.5-0.7%/yr). Annual rates of post-fire early succession (0.4-1.7%/yr) were highly variable among intervals depending on fire occurrence. Thermokarst showed accelerating rates, increasing ten-fold from the early (0.01%/yr) to the last interval (0.13%/yr). Both early (0.03-0.04%/yr) and late (0.02-0.03%/yr) riverine vegetation succession showed only minor variation among intervals. Both river erosion and deposition showed a three- to five-fold increase during the last interval compared to earlier intervals. Human clearings showed a six-fold increase during the last interval, while other human activities were variable and showed only minor changes among intervals.

Fire was by far the dominant driver of ecotype changes, affecting 72.1% of the area since ~1920, but it was highly variable over time and across the study area. During the interval of recorded observations (1949-2019), fires occurred during 23 of the 70 years of records and affected 47.3% of the area, with 2001 having the largest extent (7.1%). When comparing the 1949-1978, 1979-2007, and 2008-2017 intervals, fire occurred in 6, 12, and 5 of the years, and

covered 17.5%, 22.2%, and 7.7% of the area, respectively. In the 1949 period, 49% of the landscape was in an early successional state after fire, which we interpreted as evidence that fire occurred on the grids during 1920-1948. Many of the early fires we documented on our grids were not in the individual fire perimeter database maintained by the Alaska Interagency Coordination Center (https://fire.ak.blm.gov/predsvcs/maps.php). In addition, the fire perimeter data overestimate the area burned by fires because unburned patches usually exist within the fire perimeters.

Across all intervals (1920-2017) and landscapes, fires overall burned an annual average of 1.00%/yr of the study area (Figure 26). When comparing intervals, annual fire extent during the 1920-1948 interval (1.76%/yr) was two- to three-fold higher than the annual average extent of other intervals. When comparing landscapes for the entire 1920-2017 interval, overall annual average fire extent was four-fold higher in lowland (0.78%/yr) than in upland (0.19%/yr) landscapes, with fires affecting negligible areas in riverine (0.01%/yr), lacustrine (0.002%/yr) and alpine (0.02%/yr) landscapes. Since ~1920, fires that burned an area only once affected 44.0% of the area, while areas that reburned twice or three times covered 22.1% and 6.0% of the area, respectively. The mean fire cycle (MFC), as defined as the average time required to burn an area equal to the entire study area, was 100 yrs overall for the entire 1920-2017 interval. When comparing shorter intervals, the MFC varied three-fold from 57 yrs during 1920-1948 to 166 yrs during 1949-1978. When comparing MFC within landscapes for the entire 1920-2017 interval, MFC was 78 yrs for lowland (61.3% of study area), 132 yrs for upland (24.5%), 194 yrs for lacustrine (0.4%), 400 yrs for alpine (6.2%), and 785 yrs for riverine (7.7%) landscapes. Permafrost and thermokarst extent were quantified during the grid sampling by photo-interpreting permafrost and thermokarst status in the 1978 and 2017 periods. Areas interpreted to have stable permafrost (as indicated by stable land when nearby areas had evident thermokarst indicative to ice-rich terrain) decreased slightly from 67.5% to 64.7% of the area. Areas where permafrost had recently aggraded (from thermokarst fen to forest on permafrost plateaus) increased from 0.05% to 0.4%. Thermokarst fens increased from 2.9% to 4.0% and thermokarst bogs increased from 0.9% to 2.0% during this 39-yr interval. Very small incidences of thaw slumps (0.05%) and thermokarst water tracks (0.1%) were evident in the 2017 that were not evident in 1949.

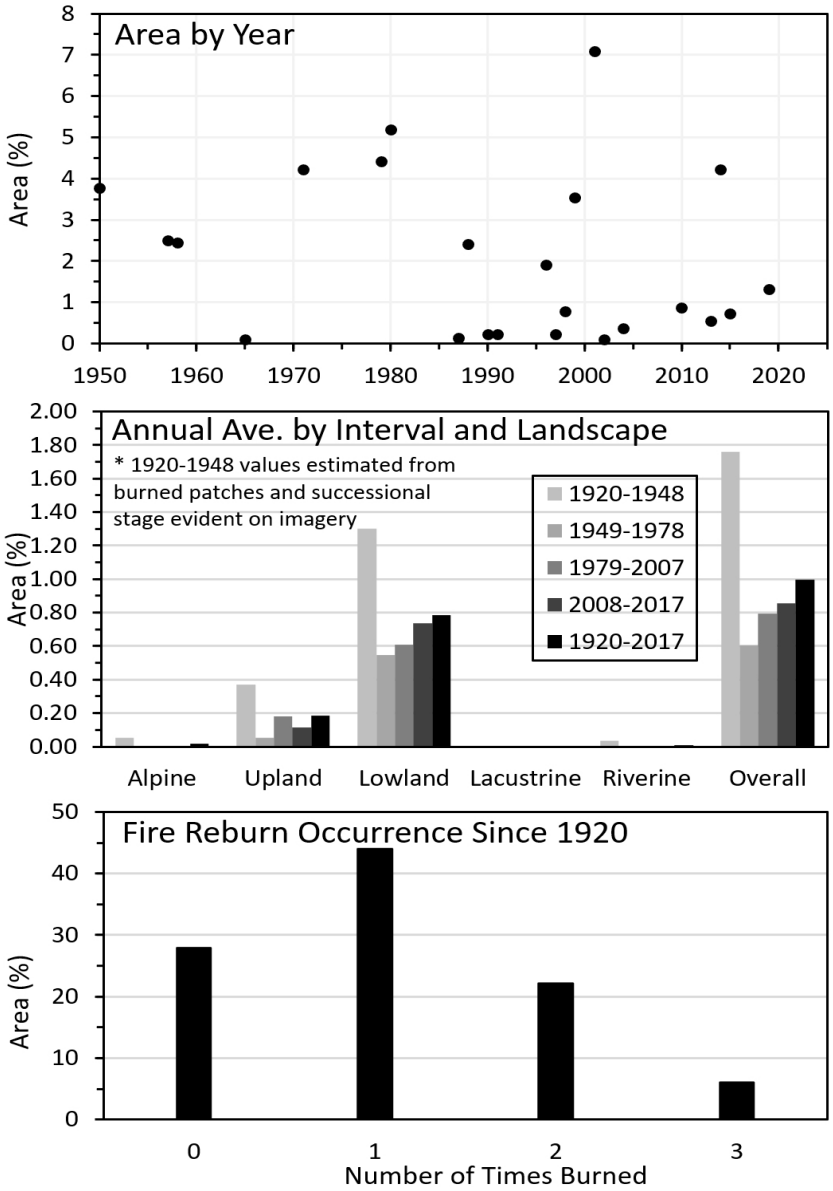


Figure 26. Areal extent of fires within the study area by year (top), the annual average by interval and landscape (middle), and the reburn occurrence of fires since ~1920.

2.4.3.3 Accuracy Assessment of Historical Changes

The overall accuracy of the photo-interpretation was 77% based on 127 ground determinations at 10 grids made in 2012 for 17 classes compared to photo-interpretations made using imagery from the 2017 period (Table 11). Most of the errors of commission (user's accuracy) were due to: photo-interpreted lowland wet mixed forest (n=8 points) being found on the ground to be lowland wet broadleaf forest (2) and lowland wet needleleaf forest (1); lowland wet needleleaf forest (37) found to be lowland wet low scrub (2) and lowland wet tall scrub (2); and upland moist mixed forest (15) found to be upland moist needleleaf forest (5) and upland moist broadleaf forest (2). Overall, the main problems were distinguishing canopy coverage among broadleaf, mixed, and needleleaf forests where the understory and overstory trees lead to errors when observed from above the canopy (photo-interpretation) and below the canopy (ground), and to frequent scrub calls when tree cover was low.

Another approach to assessing the accuracy of the photo-interpretation is to compare the results of ecotype abundance from the photo-interpretation with that obtained by previous mapping based on very different methods. The systematic grid sampling identified 61 ecotypes within the study area, compared to the more comprehensive survey of 71 ecotypes (after crosswalking to unified statewide system) identified in the field ecological land surveys for YTA and TFTA near Fort Wainwright (Jorgenson et al., 1999) and DTAE and DTAW near Fort Greely (Jorgenson et al., 2001), which involved more effort to distinguish rocky and gravelly ecotypes that were combined in the photo-interpretation analysis. The relative abundance of ecotypes from the photo-interpretation grid sampling for the 1978 period was similar in extent to the area of most ecotypes mapped (using 1980s imagery) for lands near Fort Wainwright and Fort Greely. For example, values were similar for Lowland Wet Needleleaf Forest (21.6% vs 20.1% mapped), Lowland Wet Low Scrub (10.5% vs 13.4%), Lowland Wet Broadleaf Woodland (5.5% vs 5.1%), Upland Moist Mixed Forest (3.8% vs 4.3%), Upland Moist Needleleaf Forest (6.5% vs 3.0%), and Upland Dry Broadleaf Woodland (3.1 vs 2.7%). There were, however, a couple of ecotypes with widely varying extents between the two methods, including Lowland Bog Tussock Scrub (1.9% vs 10.3%) and Lowland Post-fire Scrub (12.7% vs 1.3%), which we attribute to misclassification between these two classes during automated spectral image classification. Overall, this indicates that the results from systematic gridding was broadly representative of the terrain conditions quantified through intensive mapping.

Table 11. Accuracy assessment comparing mapped versus ground determinations. See Table 8 for codes.

	Ground Determination																		
Mapped	BLBT	BLNM	BLSP	BLSU	BLWSL	BLWST	BLWWB	BLWWM	BLWWN	BUDWB	BUDWM	BUMFB	BUMFM	BUMFN	BUMST	BUSP	BUWWN	Total	User's Accuracy
BLBT	**5**				1													6	83
BLMFN									1									1	0
BLMST					1													1	0
BLMWB							1											1	0
BLNM		**2**																2	100
BLNS		1					1											2	0
BLSP	1		**9**													1		11	82
BLSU				**1**														1	100
BLWSL					**4**													4	100
BLWWB							**5**											5	100
BLWWM							2	**4**	1			1						8	50
BLWWN				1	2	2	1		**30**			1						37	81
BUDWB										**8**								8	100
BUDWM										1	**2**			1				4	50
BUMFB												**3**						3	100
BUMFM												2	**8**	5				15	53
BUMFN														**10**			1	11	91
BUMST															**1**			1	100
BUSP																**6**		6	100
Grand Total	6	3	9	2	8	2	10	4	32	9	2	7	8	16	1	7	1	127	
Producers Accuracy	83	67	100	50	50	0	50	100	94	89	100	43	100	63	100	86	0		77

2.4.3.4 Climate Trends and Projections

Historical air temperature data from Fairbanks showed mean annual thawing degree-day (TDD) values of 1901, 1961, and 2034 for the 1949–1978, 1979–2007, and 2008–2017 time-intervals (Figure 27). Relative to the 1949–1978 baseline interval, TDD increased by 1.03x for the 1979–2007 interval and by 1.07x for the 2008–2017 interval. When considering individual years from 1949 to 2019, regression analysis evaluating TDD over time found that the TDD trend increased 1.11x from 1838 to 2045 for the Fairbanks station. This was similar to the increase in TDD trendline of 1.06x from 1839 to 1945 at the Big Delta station over the same interval. Winter air temperatures for Fairbanks as summarized by FDD, however, warmed at substantially higher rates 0.72x from -2970 to -2162. The overall regression trend in mean annual air temperature (MAAT) indicates that MAAT increased by 1.8 °C from 1905 to 2020, for an average increase of 0.3 °C/20 yrs.

Projected summer air temperatures (TDD) from 2010–2100 modeled by SNAP (Walsh et al., 2018) increased relative to the 2010–2019 baseline period by 1.05, 1.09, 1.12, and 1.13x for the RCP4.5 temperature model, by 1.04, 1.08, 1.15, and 1.17x for the RCP6.0 model, and by 1.05, 1.15, 1.22, and 1.30x for the RCP8.0 mode for the four respective time-intervals (Figure 27). These relative increases were used for the temperature effects on transition rates in the state-transition modeling.

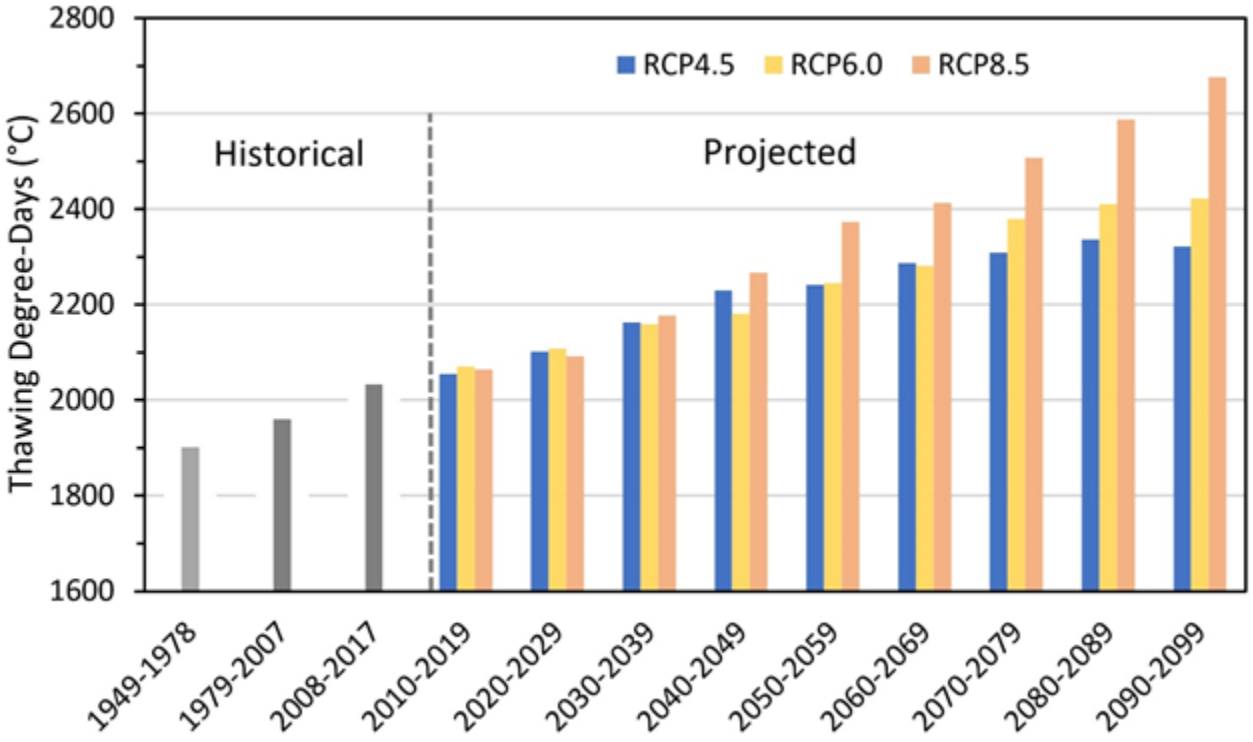


Figure 27. Historical (Fairbanks) and projected climate warming during summer (based on thawing degree-days, base 0 °C) for the RCP4.5 (low), RCP6.0 (medium), and RCP8.5 (high) scenarios (data from SNAP, 2021).

2.4.3.5 Projected Ecotype Changes

The net changes in ecotype abundance over the entire 2017–2100 interval, or the amount of area that changed ecotypes, was nearly three times higher for the driver-adjusted RCP6.0 temperature model (30.6%) compared to the time model (11.5%), RCP4.5 (12.4%), and the RCP8.0 (14.7%) temperature models. The time model, which assumes future transitions occur at the same rate as past transitions, projected 38 ecotypes will gain area and 24 will lose area by 2100 (Figure 28). Note that during the 1949–2017 time-interval from which the historical transition rates were developed, TDD increased by 1.11x over 68 yrs. This model provides a baseline of the minimum areal changes in ecotypes projected to occur by 2100. The temperature and driver-adjusted temperature models show similar numbers of ecotypes gaining (37–39) and losing area (23–25). The much higher changes in the driver-adjusted RCP6.0 model were primarily due to rapidly accelerating thermokarst in lowland ecotypes.

When comparing net change by landscapes, most of the projected changes during 2017–2100 in the driver-adjusted RCP6.0 model (most likely scenario) occurred in lowland (23.9% of total area changed), upland (3.9%) and riverine (1.6%) landscapes, while there was little area affected by change in alpine (0.3%) subalpine (0.4%) and lacustrine (0.3%) landscape. When changes were calculated in proportion to the extent of each landscape, lacustrine (82.5%) and subalpine (73.3%) landscapes had the greatest change. Lowland (39.0%), riverine (20.7%), and upland (15.9%) landscapes had intermediate levels of change, while the alpine (5.4%) landscape had little projected change.

In comparing changes in individual ecotypes from the driver-adjusted RCP6.0 model, we present results in terms of changes in: (1) area as a percent of the total study area to highlight changes that affect large areas; and (2) relative percent for each ecotype to highlight changes that may affect small areas, but may dramatically change the extent of particular ecotypes. Results from the other two models are presented in Figure 28.

Ecotypes projected to experience large increases in area as a percent of the total area during 2017–2100 in the driver-adjusted RCP6.0 model (Figure. 28) included Lowland Bog Meadow (7.6%) and Lowland Fen Meadow (10.7%) due to accelerating thermokarst and Lowland Wet Mixed Woodland (2.5%) due to increased soil drainage from thaw and deciduous tree expansion. Ecotypes losing the most area included Lowland Wet Needleleaf Woodland (-8.0%), Lowland Wet Low Scrub (-7.4%), and Lowland Wet Broadleaf Woodland (-5.6%) due mostly to thermokarst, and Upland Moist Needleleaf Forest (-2.1%) due to fire. Abundant ecotypes (>10,000 ha) that were projected to have small gains included only Upland Moist Broadleaf Forest (1.8%). Abundant ecotypes with projected small losses included Lowland Post-fire Scrub (-1.3%), Lowland Wet Tall Scrub (-0.8%), and Lowland Bog Tussock Scrub (-0.7%) from loss of fire-prone lowlands, Riverine Moist Needleleaf Forest (-1.0%) from river erosion, Upland Dry Broadleaf Woodland (-1.2%) from late succession and fire, and Alpine Moist Dwarf Scrub (-0.7%) from tree and shrub expansion. See Table 2 for more detail on attribution of factors affecting change.

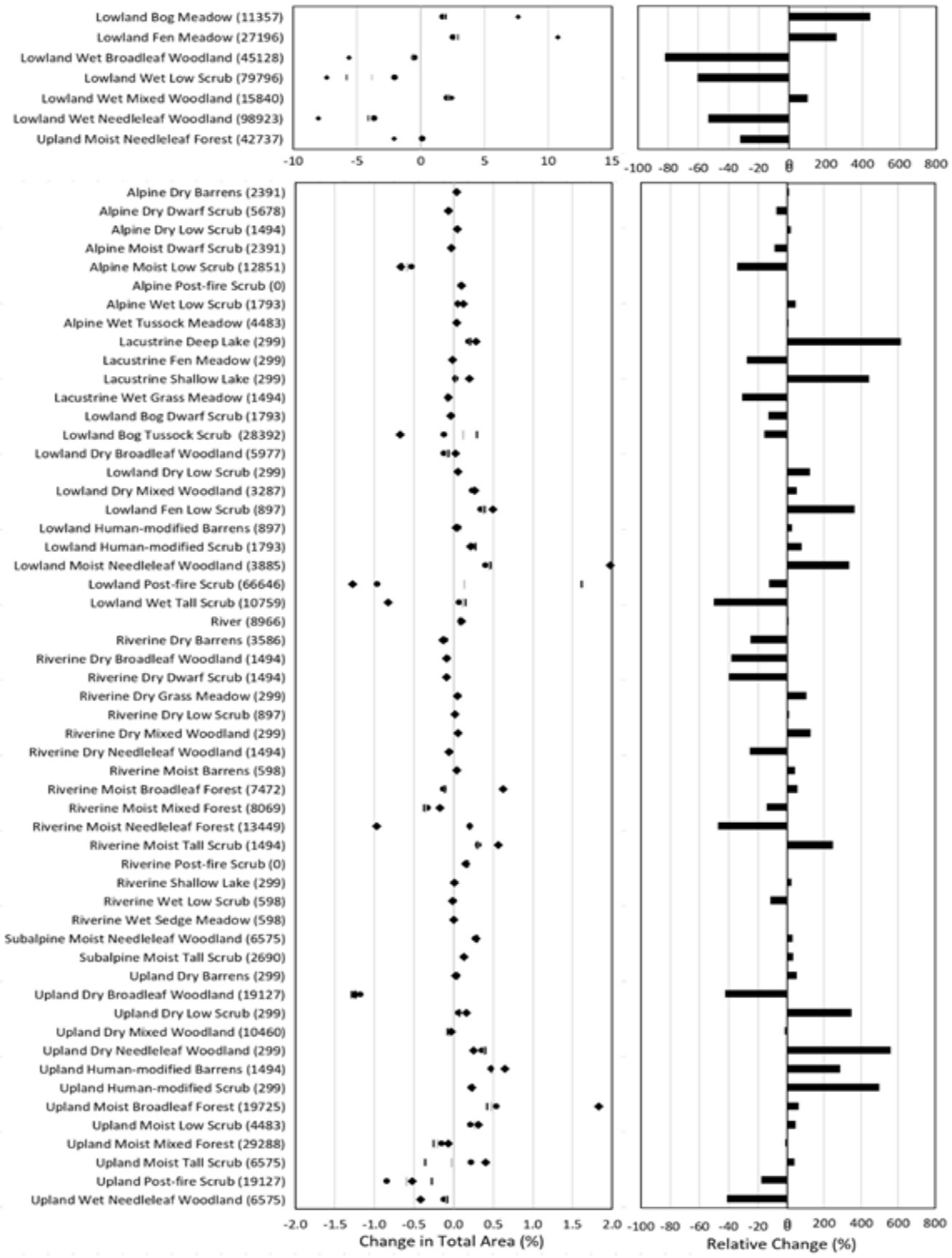


Figure 28. Projected ecotype changes (left) as percent of total study area from 2017 to 2100 based on the time (circle), RCP4.0 (gray bar) and RCP8.0 (black bar) temperature models, and the driver-adjusted RCP6.0 temperature (diamond) models. Relative change (percent difference from initial area) for the driver-adjusted RCP6.0 temperature model is at right. Note different scales for decreases and increases in relative change (right graph). Area (km^2) in 2017 is included with ecotype name.

When considering relative changes (% of initial area by ecotype), several ecotypes, often covering relatively small areas, had large projected increases by 2100 (Figure 28), including: Lacustrine Deep Lake (616%), Lacustrine Shallow Lake (443%), and Lowland Bog Meadows (441%) from thermokarst, Upland Dry Needleleaf Woodland (561%) from late succession, and Upland Human-modified Scrub (498%) from early succession. Large relative losses were projected for Lowland Wet Broadleaf Woodland (-82%), Lowland Wet Low Scrub (-61%), Lowland Wet Needleleaf Woodland (-54%), and Lowland Wet Tall Scrub (-50%) due to thermokarst. Other large relative losses were projected for Alpine Moist Low Scrub (-34%) from tree and tall shrub expansion, Lacustrine Wet Grass Meadow (-31%) from early succession, Riverine Dry Dwarf Scrub (-40%) from early succession, Riverine Moist Needleleaf Forest (--47%) from river erosion, Upland Dry Broadleaf Woodland (-43%), and Upland Wet Needleleaf Woodland (-41%) from soil drainage after permafrost thaw.

Numerous factors affect the reliability of our analysis of historical changes and future projections based on state-transition modeling. The reliability of detecting historical changes was limited by: (1) the modest sample size of 22 grids (2200 points); (2) the high variability in ecotypes across grids and over time; and the (3) modest photo-interpretation accuracy. Given the large number of ecotypes (61) across the study area, the 22 grids were insufficient to adequately sample all ecotypes, and the highly patchy nature of fires over time and space created large swings in ecotype composition that limited our ability to statistically detect change. While the overall photo-interpretation accuracy was 77%, we consider this to be quite acceptable given the high number of ecotypes that needed to be differentiated. As for limitations of future projections, the temperature models used an overly simplified approach to increasing state-transition rates of ecosystems to climate warming, but they are at least presented in relation to the time model that projects future changes to occur at the same rates as historical changes. Furthermore, the driver-adjusted RCP6.0 model relied on the expert judgement as to the relative sensitivity of the change drivers to temperatures, with human activities being not sensitive to climate warming while thermokarst being highly sensitive to warming. Overall, while this model lacks a mechanistic approach for biogeochemical factors affecting ecosystem change, its strength lies in its foundation of historical transition rates, its recognition that diverse ecosystems respond very differently, and the incorporation of a wide range of ecological factors that drive change. Knowledge of the magnitude and directions of landscape changes can help inform land management decisions on military lands. Fire is by far the most prevalent driver of change and is the subject of intensive fire-fighting and land management decisions statewide. Fire is a natural process that is essential to maintaining the diversity and health of boreal ecosystems (Chapin et al., 2006), but has the risks of damaging human infrastructure. Current land management strategies are directed toward allowing human-made and natural fires to burn on military lands, unless they endanger military facilities and private lands adjacent to military lands. Thermokarst has been expanding in response to longer-term climate warming since the Little Ice Age (Jorgenson et al., 2001) and to recent anthropogenic-induced warming (Grosse et al., 2011). Thermokarst is projected to greatly increase in the driver-adjusted RCP6.0 model, with Lowland Bog Meadows and Lowland Fen Meadows associated with thermokarst projected to cover 18% of the military lands by 2100. Thus, while fire is more extensive, thermokarst will be more transformative affecting up to 26% of the landscape by 2100. Although land management strategies can do little to affect ongoing thermokarst, activities on ice-rich permafrost can be avoided or minimized during training exercises and infrastructure development. Similarly, land use on dynamic floodplains also can be avoided or minimized.

2.4.4 Remote Sensing of Targeted Fen Changes

As part of our effort to quantify rates of historical habitat changes, a remote sensing analysis was conducted to evaluate changes in fen ecotypes (Figure 29). The remote sensing of fen changes at 88 cross-sections using a time-series of high-resolution imagery from 1949 to 2018 revealed that the fen systems were highly variable spatially and highly dynamic over time. A repeated measures statistical analysis found that mean widths significantly varied two-fold among the three fens systems (P=0.04). Overall, mean fen widths increased from 214.6 m in 1949 to 263.9 m in 2018, but the differences among years were not significant (P=0.20) due to the high variability among cross-sections. When calculated as a lateral degradation rate per year for each margin, the overall lateral degradation rate for the three fens was 0.36 m/yr over the 69 yrs, and varied only from 0.32 m/yr to 0.39 m/yr among the three fens. When comparing among years, mean rates showed different patterns for each fen: for fen 1 rates decreased and then increased; for fen 2 rates decreased every year; and for fen 3 rates increased and then decreased. Across all fens and all periods, rates varied five-fold from 0.13 to 0.64 m/yr.

A time-series analysis of historical transition rates for 45 ecotypes was developed for interior and northwest Alaska using imagery for the 1950s, 1980s, and 2000s by Jorgenson et al., (2001; 2015). We updated this to a fourth period using 2017-2018 high-resolution satellite imagery. We have compiled new imagery with peak summer, cloudless scenes and have georectified imagery from previous image sets. Photo-interpretation of changes in ecotypes and assignment of change drivers and analysis of ecotype changes relative to climate (temperature, precipitation trends), terrain (geomorphology, topography), fire history, and other change drivers were completed as part of Tasks 1.2. Figures 21 and 24 (earlier in this section) provide some images of a field site on the TFTA where thermokarst has led to dramatic landscape change processes.

2.4.5 Remote Sensing of NDVI Change

GEE is being leveraged to build annual land cover maps from Landsat and Sentinel-2 cloud-free imagery composites, which will be analyzed to parameterize modeled rates of land cover change, especially thermokarst, in response to fire. Clear-sky summer USGS Analysis Ready Landsat Thematic Mapper data spanning 1986-2017 has been obtained and time series analyses are ongoing. This Figure (30) shows the longest comparison span from 1984-2013 in the dataset. This dataset provides a coarse-scale view of potential landscape changes on Alaska DoD training ranges. Data will be statistically assessed for a dense network of points. In addition, results from this analysis can be compared with high-resolution site analyses to assess sensitivity of coarse-scale data and potential thresholds of change detection.

Figure 30 provides the results of a Landsat derived NDVI change map from 1986 to 2017. Of particular note is that the southern portion of Tanana Flats has experienced a small to moderate increase in NDVI over the time of record. This is an area with ice rich permafrost that has been identified for expanded infrastructure including 40 km of potential all season road access and Air Force targeting facilities.

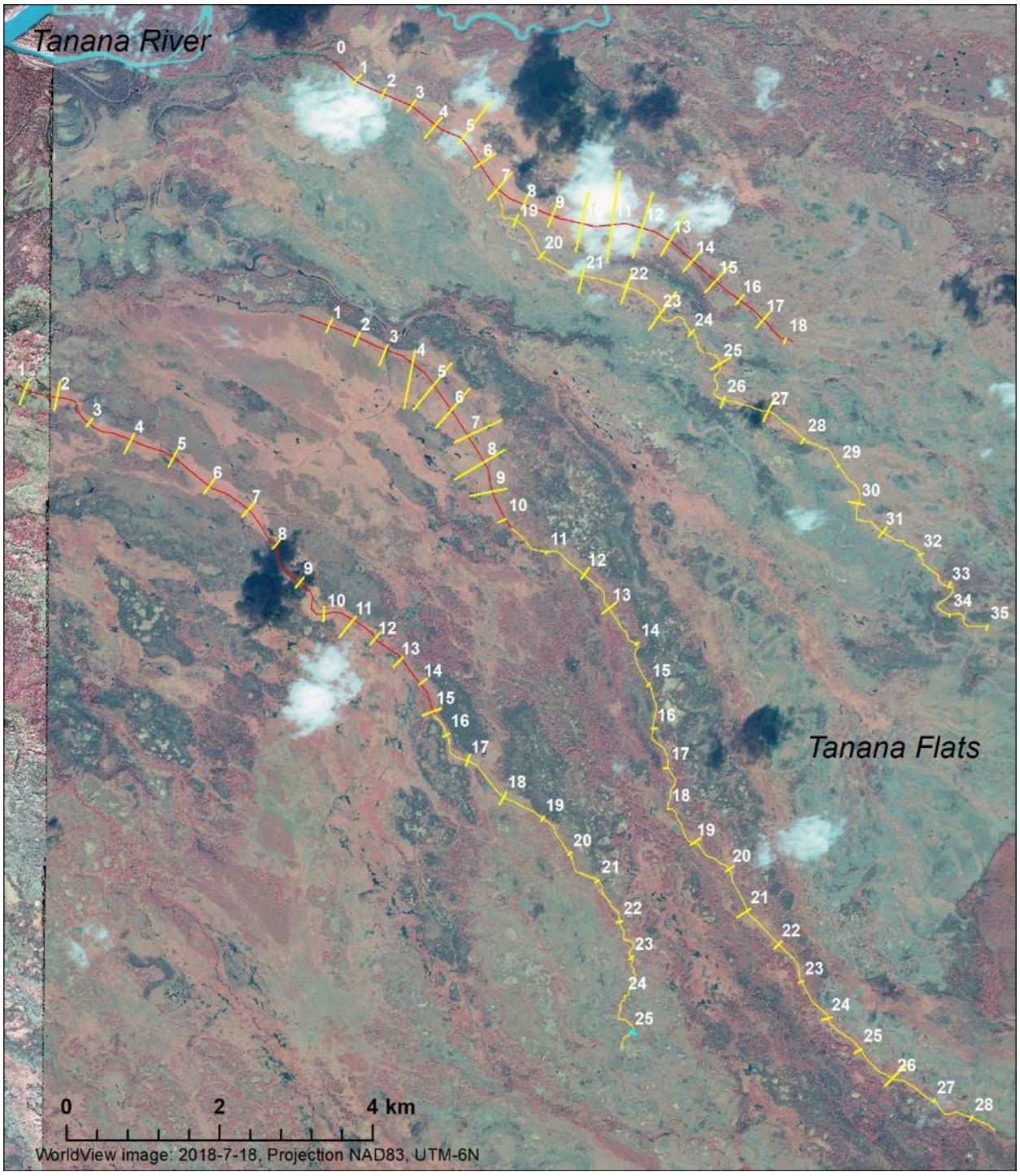


Figure 29. Map of centerlines and fen width measurement locations for three fen systems on the Tanana Flats. Red denotes wide fens and yellow denotes narrow fens.

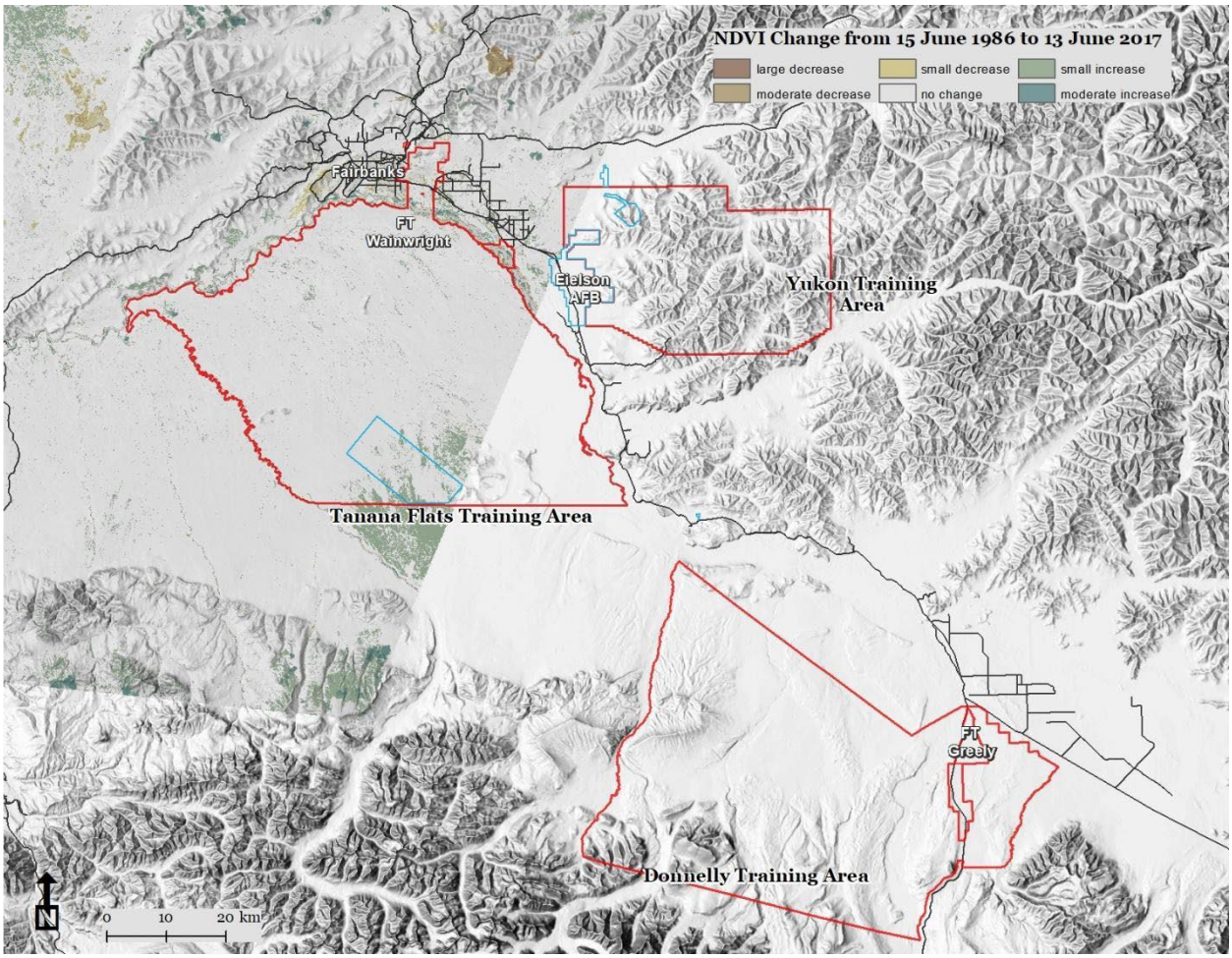


Figure 30. Landsat derived NDVI change over a 31-year period of record.

2.5 Task 1.3

Validation and improvement of geospatial models characterizing thermokarst vulnerability.

Two geospatial models predicting static landscape vulnerability to thermokarst formation have been used for this Task: the first was developed as part of the Integrated Ecosystem Model for Alaska and Northwest Canada (Genet et al., 2014). The second was developed as part of the National Science Foundation (NSF) Permafrost Research Network for the circum-arctic region (Olefeldt et al., 2016). Both models are static. We compared these models with the distribution of wetland formation assessed from 30-m resolution Landsat-derived annual dominant land cover maps from 1984 to 2014 produced by Wang et al., (2019) as part of the NASA ABoVE program.

Wetland/water transition was defined as all pixels that were classified as non-wetland types in the 1984 land cover map and were classified as wetland types or water in the 2014 land cover map. Most wetland formation that occurred in the Tanana Flats and Yukon Training Areas were located in areas predicted to show moderate to high vulnerability to thermokarst formation in the Genet and Olefeldt models (Figure 31 a, b). However, large proportions of wetland formations and transition to water that occurred in the Donnelly Training Area were located in areas that were predicted to be low vulnerability by both models. The potential causes of this discrepancy are (1) the transition to wetland in this area is not caused by thermokarst, (2) the predisposition models are underestimating landscape vulnerability to thermokarst disturbance in this area, (3) the land cover maps are overestimating wetland formation in this area.

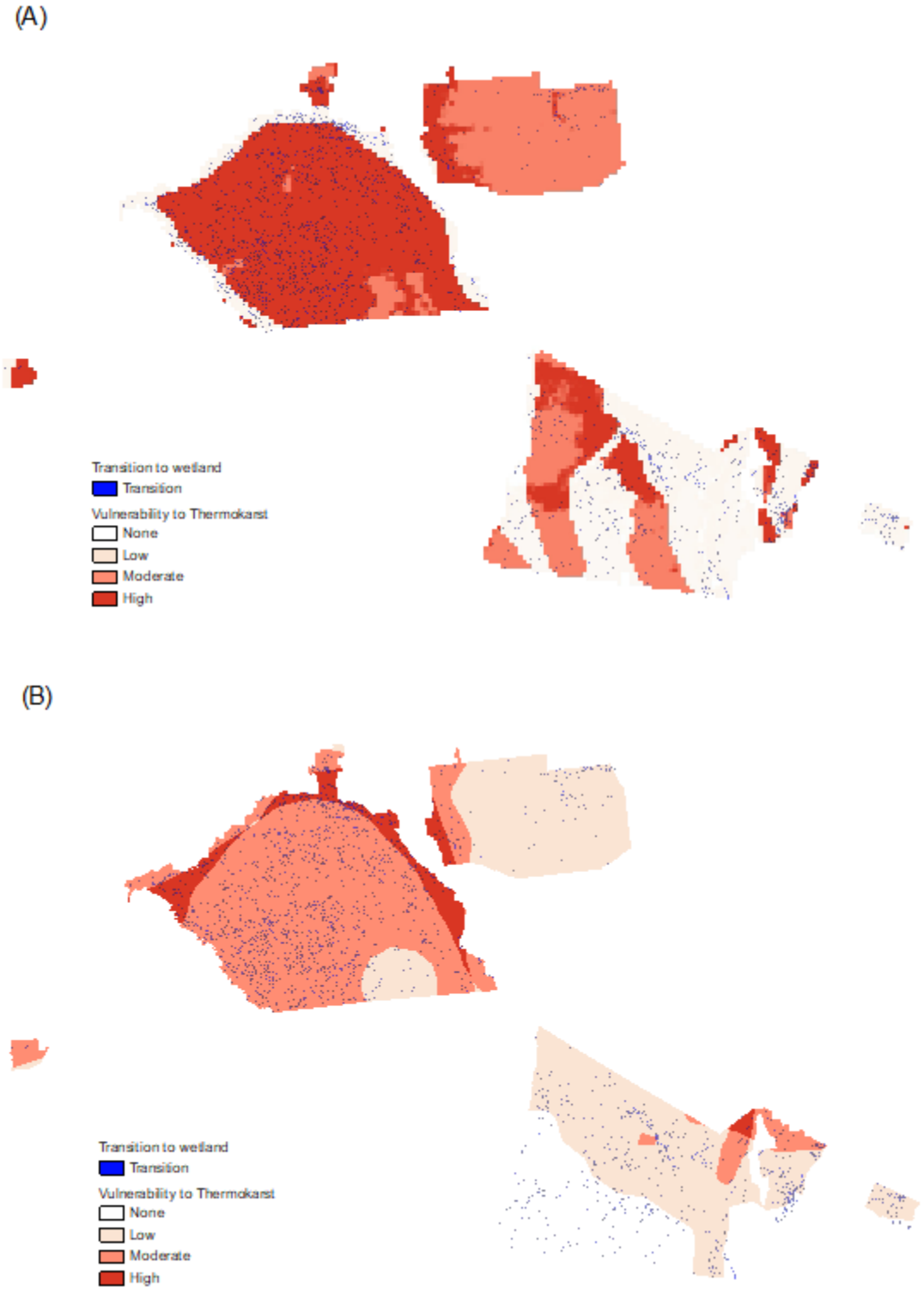


Figure 31. Comparison of observed wetland formation that occurred between 1984 and 2014 (assessed from Wang et al., 2019) and predicted thermokarst vulnerability from (A) Genet et al., 2014 and (B) Olefeldt et al., 2016.

The information on permafrost ice content from the SDSWCD and FWA databases was only available for 5 out of the 4,088 sites and could not be used to relate the occurrence of transition to wetlands with permafrost ice content. However, we assessed the distribution of burn and re-burn distribution across the landscape using MTBS data (see section 2.7.2. for further details), and were able to associate the occurrence of transition to wetlands in the Donnelly Training Area with areas of exceptionally high fire frequency (Figure 32). We also looked at the distribution of streams and riverine landforms to attribute transitions to water to river and stream channel movements (Figure 32, purple ellipse for example).

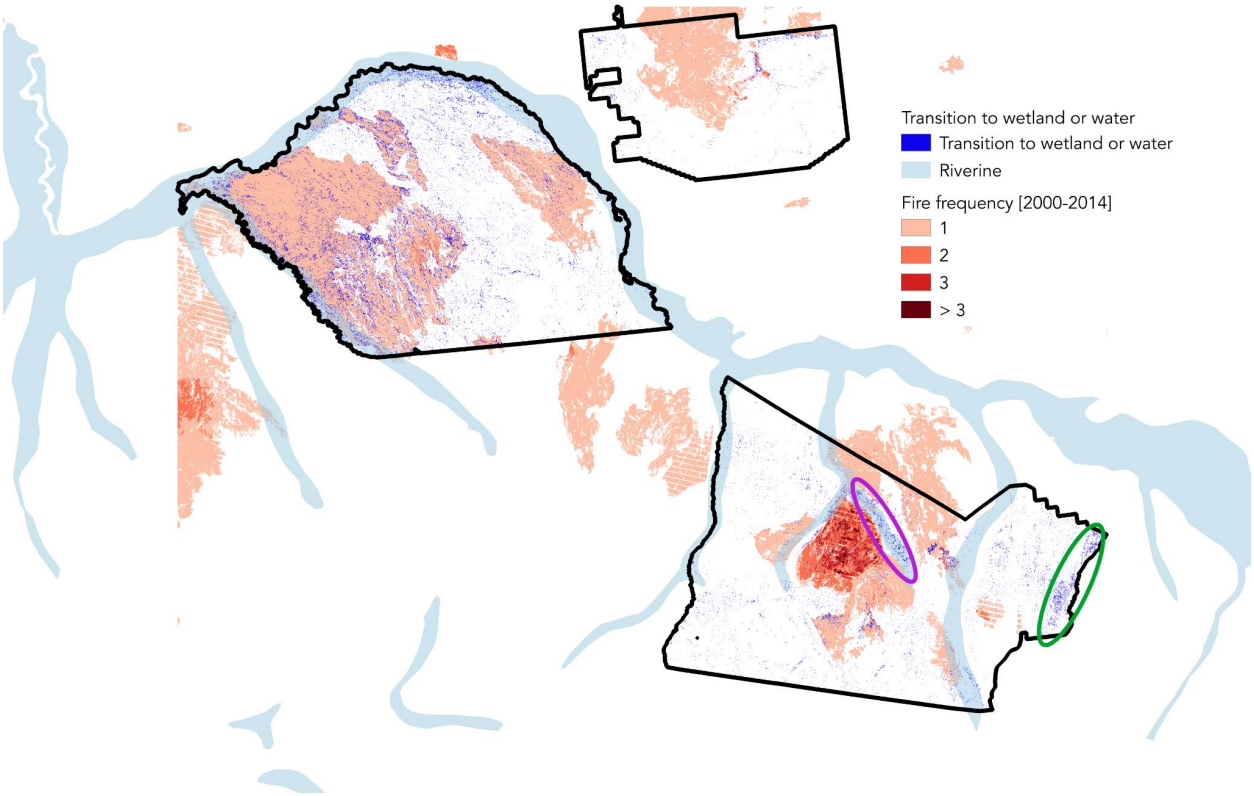


Figure 32. Comparison of observed wetland formation that occurred between 1984 and 2014 (assessed from Wang et al., 2019), reburn distribution (assessed from the MTBS database) and the distribution of riverine features (assessed from Jorgenson et al., 2008). The purple ellipse represents transitions to water that can be attributed to stream or river channel movement. The green ellipse represents transitions to wetland and water that can be attributed to moderately ice-rich permafrost in alluvial fan.

When compared to historical assessment of transition to wetland and water from remote-sensing land cover time series (Wang et al., 2019), both static vulnerability maps were able to represent the higher proportion of transitions to wetland and water in the Tanana Flat compared to the two other training areas. However, the map from Genet et al., identified slightly better the vulnerability to thermokarst disturbance of moderately ice rich permafrost in alluvial fan (Figure 32, green circle). This spatial comparison suggests that repeated fire can potentially trigger thermokarst disturbance in lowlands, even on permafrost with low to moderate ice content.

2.6 Task 1.4

Visually document ecotype changes through high quality photography for use in outreach to stakeholders, managers, and the public.

We acquired thousands of high-quality airborne and field based photographs of habitat changes and drivers behind those changes to provide visual documentation for outreach to stakeholders, managers, and the public. An aerial reconnaissance survey was made with a fixed-wing airplane to photograph ecosystems and examples of drivers affecting ecosystem change. We coordinated with USAG-FWA Range Control to gain permission for the flights. Photographs were geotagged, date and time stamped, corrected for lens distortion, and denoted on flight lines. All photos and global positioning system (GPS) flight lines are accessible in databases through an ArcMap layer. Results provide high-resolution imagery of current conditions that can be repeated over later intervals for future change-detection studies as a legacy dataset.

The aerial photo transect was conducted 4 June 2019 by team members Bruce Marcot, Torre Jorgenson, and Richard Murphy. Cameras used included two GoPro cameras clamped to the underwing and rear landing gear of the Cessna fixed-wing airplane, and three hand-held digital cameras in the cabin for mostly oblique but some nadir photos. The GoPro cameras were set for 5-second time-lapse nadir photos, producing approximately 1/3 overlap of images between successive photographs to ensure continuous image coverage along the flight transects. The time-lapse interval was based on photogrammetric calculations from mean flight altitude (~90 knots) and speed (~300 m above ground level; AGL) (as detailed in Marcot et 2014). Two flights were conducted, in morning and afternoon, totaling ~6 hrs & 783 km (487 mi), covering most of the ecotypes of the study area, from TFTA, and portions of YTA, DTAW, and DTAE, south to the Alaska Range.

The flight transect tracks were GPS-tagged and saved in gpx, csv, and shp file formats. The flight transects resulted in: 6,063 GoPro photos (135 GB), each of which are GPS-tagged, date- and time-stamped Exchangeable Image File Format (EXIF data), contrast & gamma enhanced, and corrected for wide-angle lens distortion (Table 3, Figure 7); and 1,493 hand-held oblique photos of selected land cover conditions taken by Marcot with a Panasonic Lumix digital camera.

2.6.1 An Aerial Photograph Transect Study of Interior Alaska training lands

This section presents methods and findings from a low-level photographic aerial transect of the four major training lands managed by U.S. Army Fort Wainwright (USAG-AK). Presented here are: (1) the structure of the aerial photo transect study; (2) a summary of the vegetation and landscape conditions represented in the photo series; (3) archival access of the photo series results; (4) examples of comparing previous and current site conditions; (5) examples of use of nadir photos to create panoramic images; (6) examples of use of nadir photos series to create flight path animations.

The objectives of conducting a low-level aerial photographic transect of the study area were to document current vegetation and landscape conditions along the flight paths, and to provide a baseline from which future replication of the transects can be used in change-detection studies.

2.6.1.1 Structure and Methods of the Aerial Photo Transect Study

On 4 June 2019, we chartered Mallen Air LLC (pilot Mike Allen), Fairbanks, to conduct a day's overflight of the study area on two flight paths intersecting portions of Tanana Flats Training Area, Yukon Training Area, and Donnelly Training Area (Figure 33). The flights were conducted out of Fairbanks. Flight path 1 began 20:13 GMT (12:13 Alaska Time) and flight path 2 began 23:53 GMT (15:53 Alaska Time), and totaled 487 miles (784 km) with a return to Fairbanks between the two flights (Figure 34). The aircraft used was a Cessna 180.

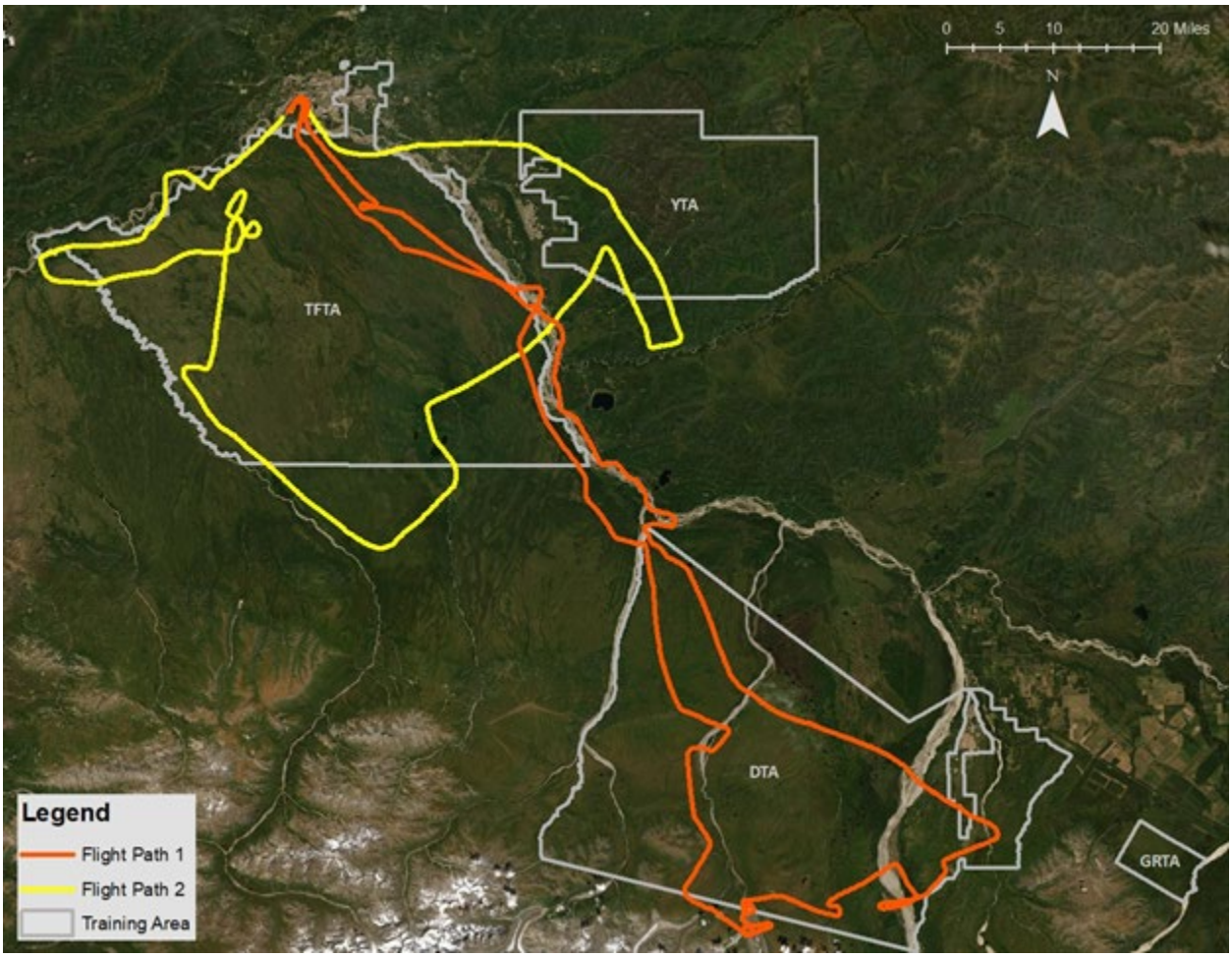


Figure 33. Flight paths used for the low-level aerial photographic transect of the study area on 4 June 2019, showing the main training areas intersected. TFTA = Tanana Flats Training Area, YTA = Yukon Training Area, DTA = Donnelly Training Area.

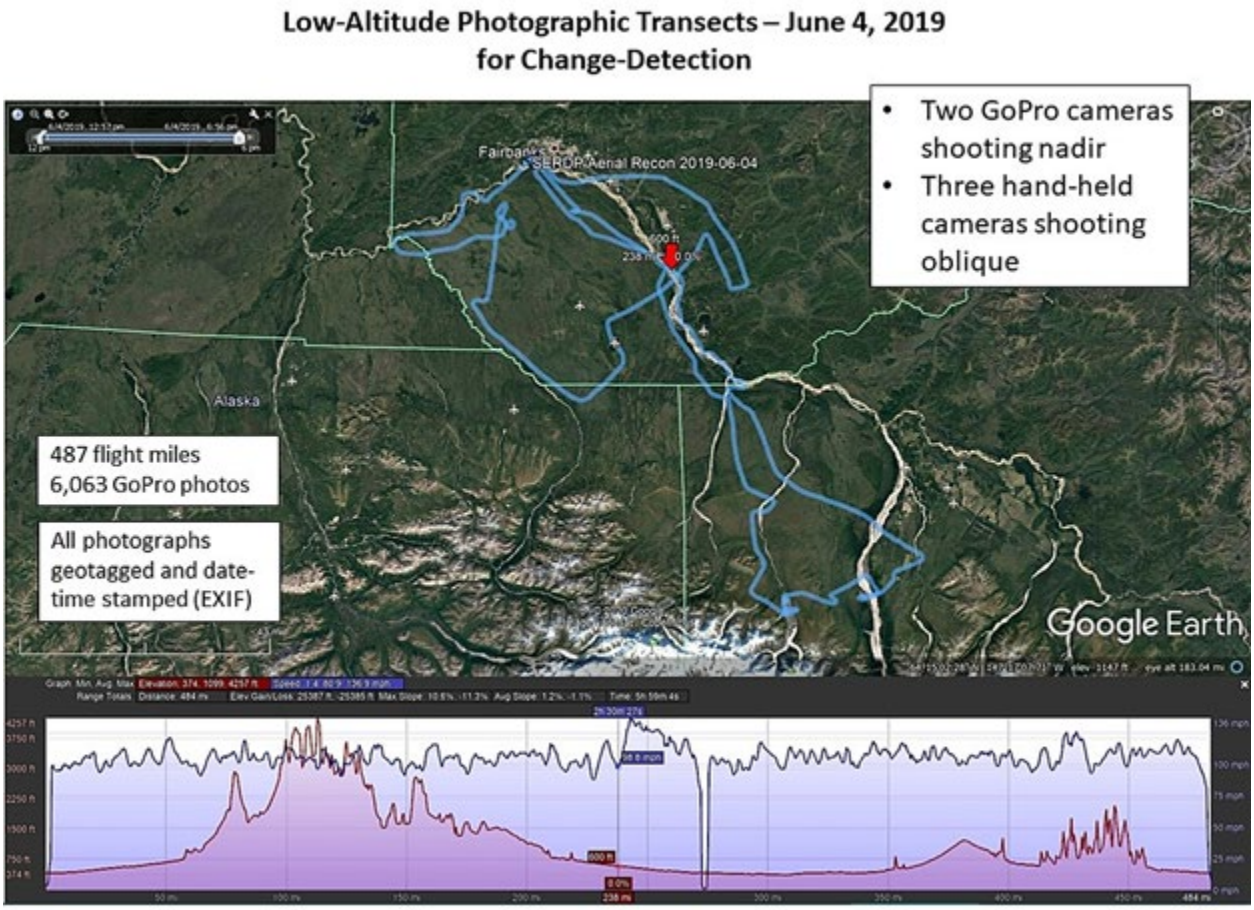


Figure 34. Flight paths (blue lines) and flight profiles of velocity (light blue curve) and ASL (altitude above sea level, purple curve) of the two flights conducted for the low-level aerial photographic transect of the study area on 4 June 2019.

The intent of the flights was to provide photographic documentation of landscape conditions. We affixed two GoPro cameras (a GoPro3 and a GoPro5) to the under-struts of the aircraft and set each camera for 5-second interval time-lapse photos, shooting mostly at nadir angles but slightly offset from one another to provide complementary imagery. Both cameras were set to wide-angle (170 °) mode. The 5-second interval was set so as to provide subsequent photos that roughly overlapped by at least a third of the frame so as to later facilitate stitching adjacent photos into panorama images, and was calculated using a similar, previous flight transect conducted in northwest Alaska (Marcot et al., 2014). Additionally, three of us (Marcot, Jorgenson, and contractor photographer Richard Murphy) shot photos with hand-held cameras from the plan cabin shooting oblique at selected landscape, ground cover, and vegetation conditions.

The specific flight paths were selected to intersect the greatest variety of land cover and ecotype conditions. The flight path respected a temporary flight restriction for a fire in northern Donnelly Training Area, and was generally restricted over eastern Yukon Training Area. Locations of the flight lines were documented by two concurrent GPS units and saved in gpx, csv, and shp file formats. We directed the pilot to generally fly at approximately 1000 ft (300 m) AGL (above ground level) and a ground speed of approximately 100 mph (160 kph or 86 kn) to facilitate the GoPro time-lapse calculations (see Appendix 1 in Marcot et al., 2014).

A total of 6,063 photos were taken by the two GoPro cameras over the two flight paths, in addition to the hand-held photos that included 706 oblique photos taken by Marcot with a Panasonic Lumix digital camera. Additional GoPro time-lapse photos included takeoff and landing situations not useful for change-detection imagery, and are excluded in this tally. All photos were then GPS-tagged, date- and time-stamped (stored in each photo file's EXIF data), saved as JPG format, and are available for public access. We also corrected each GoPro photo for lens distortion and cropped the superfluous edges of each image. This served to reduce the coverage angle to about 2/3 of the original images, and resulted in an effective image coverage of about 115°. All GoPro photos were taken at 4000 x 3000 pixels (12 megapixel images) with an aspect ratio of 4:3. After lens distortion correction and cropping, at the average flight altitude AGL, each GoPro image covered on average 175 ac (71 ha). The area represented in each photo varied depending on the specific altitude AGL, whether the plane was turning in flight, and whether the camera was positioned slightly off true nadir, as angling the cameras perfectly at nadir was not possible given the limitations of the attachments to the plane's undercarriage struts and the objective of slightly offsetting the frames to provide complementary imagery. Regardless, this setup sufficed for successfully gauging relative representations of vegetation and land cover conditions in the photos.

2.6.2 Landscape Conditions Represented in the Photo Series

Next, we intersected the GPS point (latitude, longitude) of each photo with GIS data on 44 current vegetation and land cover conditions data provided from USAG-AK Directorate of Public Works Environmental (Ostrom 2020). We used this land cover and vegetation classification because of its availability in GIS coverage format for the area needed. An example for one photo is illustrated in Figure 35.

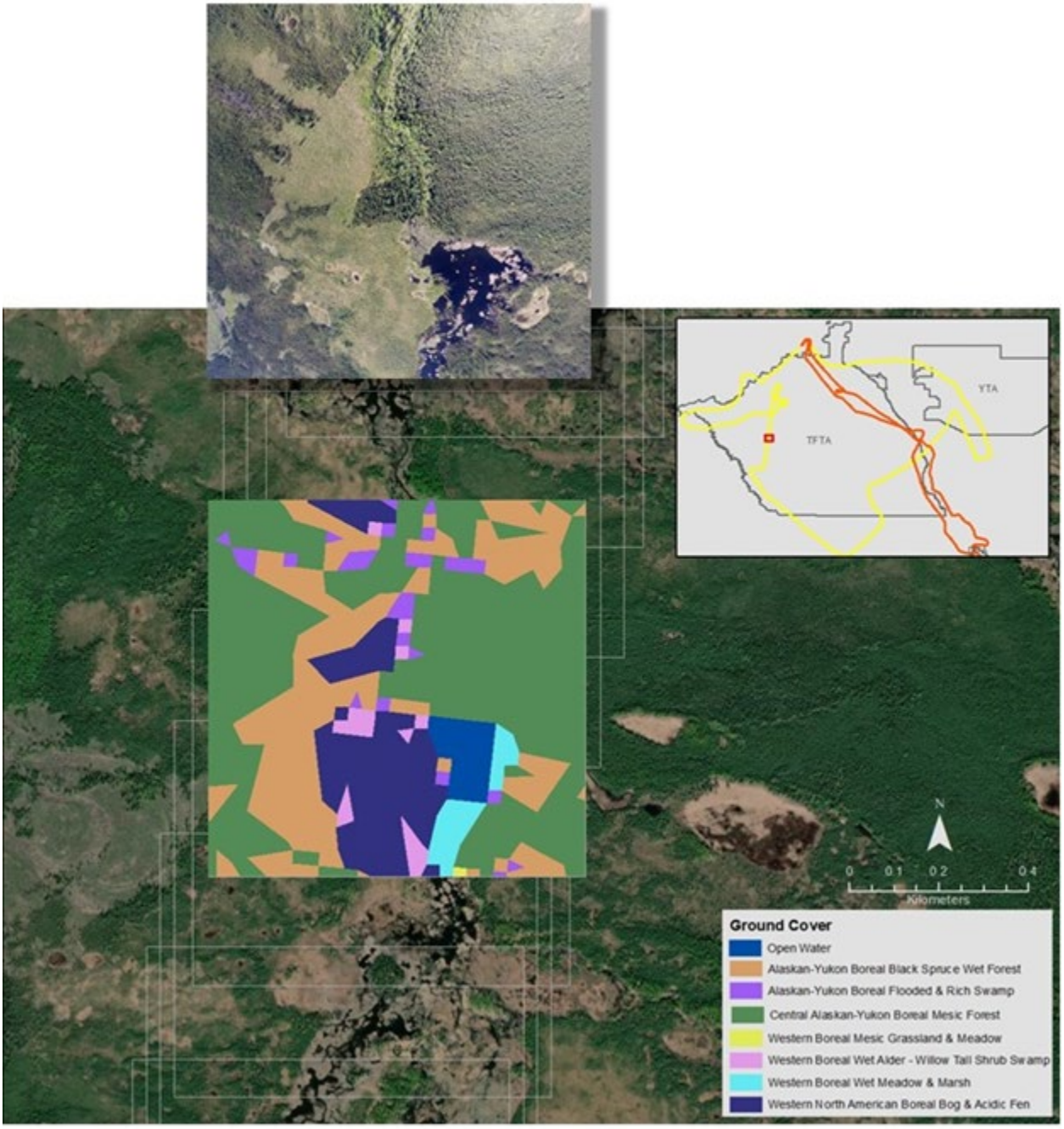


Figure 35. An example of intersecting GIS data vegetation and land cover mapping on the training lands (Ostrom 2020) with a low-level aerial transect photograph taken during two flight transects on 4 June 2019 (upper-right inset; TFTA = Tanana Flats Training Area, YTA = Yukon Training Area), superimposed here over a recent Google Earth image. The actual flight-line GoPro photograph is shown offset above the mapped coverage for that photo for comparison. The light white squares show outlines of adjacent time-lapse photographs taken on that transect flight line.

We then tallied the areal coverage of each of the 44 vegetation and land cover condition categories shown in each photo based on an approximate 175 ac (71 ha) square area centered on each photo's GPS point. We then summed the areas of each category across all photos for each

camera and each transect flight path as a measure of relative areal coverage represented in the photo series.

In total, the GoPro photos represented 38 of the 44 cover categories represented in the GIS map. Among all 6,063 GoPro photos, and on each of the two flight paths, the most common vegetation conditions, in decreasing order of area photographed, were:

- Central Alaskan-Yukon Boreal Mesic Forest,
- Western North American Boreal Bog and Acidic Fen,
- Alaskan-Yukon Boreal Black Spruce Wet Forest,
- Western Boreal Alpine Mesic Dwarf Birch - Willow Shrubland, and
- Open Water.

The 6 categories not represented in any photo included:

- Alaskan Maritime Western Hemlock - Sitka Spruce Rainforest,
- Alaska-Yukon Northern Boreal Mesic Woodland,
- Recently Disturbed Other-Herb and Grass Cover,
- Recently Disturbed Other-Shrub Cover,
- Recently Logged-Shrub Cover, and
- Southern Alaskan Boreal Mesic Forest.

Along flight path 1 ─ with 3,829 GoPro photos that covered northeast Tanana Flats Training Area, Donnelly Training Area, and the Tanana River between these area ─ the 5 most commonly photographed conditions were (in decreasing order of area photographed):

- Central Alaskan-Yukon Boreal Mesic Forest,
- Western Boreal Alpine Mesic Dwarf Birch - Willow Shrubland,
- Western North American Boreal Bog and Acidic Fen,
- Open Water, and
- Alaskan-Yukon Boreal Black Spruce Wet Forest.

The 5 least commonly photographed conditions (excluding the 6 not-represented categories listed above) in flight path 1 were (in increasing order of area photographed):

- Agriculture-Cultivated Crops and Irrigated Agriculture,
- Western North American Boreal Alkaline Fen,
- Alaskan Boreal Dry Aspen Forest,
- North American Glacier and Ice Field, and
- Arctic Herbaceous Tundra.

Along flight path 2 ─ with 2,234 GoPro photos that covered the remaining perimeters of Tanana Flats Training Area, and the western portion of Yukon Training Area ─ the 5 most commonly photographed conditions were (in decreasing order of area photographed):

- Central Alaskan-Yukon Boreal Mesic Forest,
- Western North American Boreal Bog and Acidic Fen,
- Alaskan-Yukon Boreal Black Spruce Wet Forest,
- Western Boreal Wet Alder - Willow Tall Shrub Swamp, and
- Open Water.

The 5 least commonly photographed conditions (excluding the 6 not-represented categories listed above) in flight path 2 were (in increasing order of area photographed):

- Agriculture-Pasture and Hay,
- Western Boreal Alpine Acidic Mesic Meadow,
- Arctic Herbaceous Tundra,
- Alaskan Boreal Dry Aspen Forest, and
- Western North American Boreal Alkaline Fen.

A full summary of land cover and vegetation conditions represented by each flight path and camera system is shown in Appendix Figure 7.

2.6.3 Archival Access of Photo Series Results

As of this writing, we are seeking a best location for archiving all material associated with this project for public and research access for future change-detection studies. Materials include: GPS flight line data; all photographs GPS-tagged, date- and time-stamped, and GoPro photos corrected for lens distortion and cropped; and documentation of methods and results.

2.6.4 Examples of Comparing Previous and Current Site Conditions

As part of the change-detection study theme intended for this project is a comparison of the photos taken on the flight path transects to past aerial or remote-sensing images taken at the same locations. Here we present two examples using selected transect photos paired to previous-year images from Google Earth. These examples serve to illustrate landscape changes under various disturbance or environmental developmental conditions and processes.

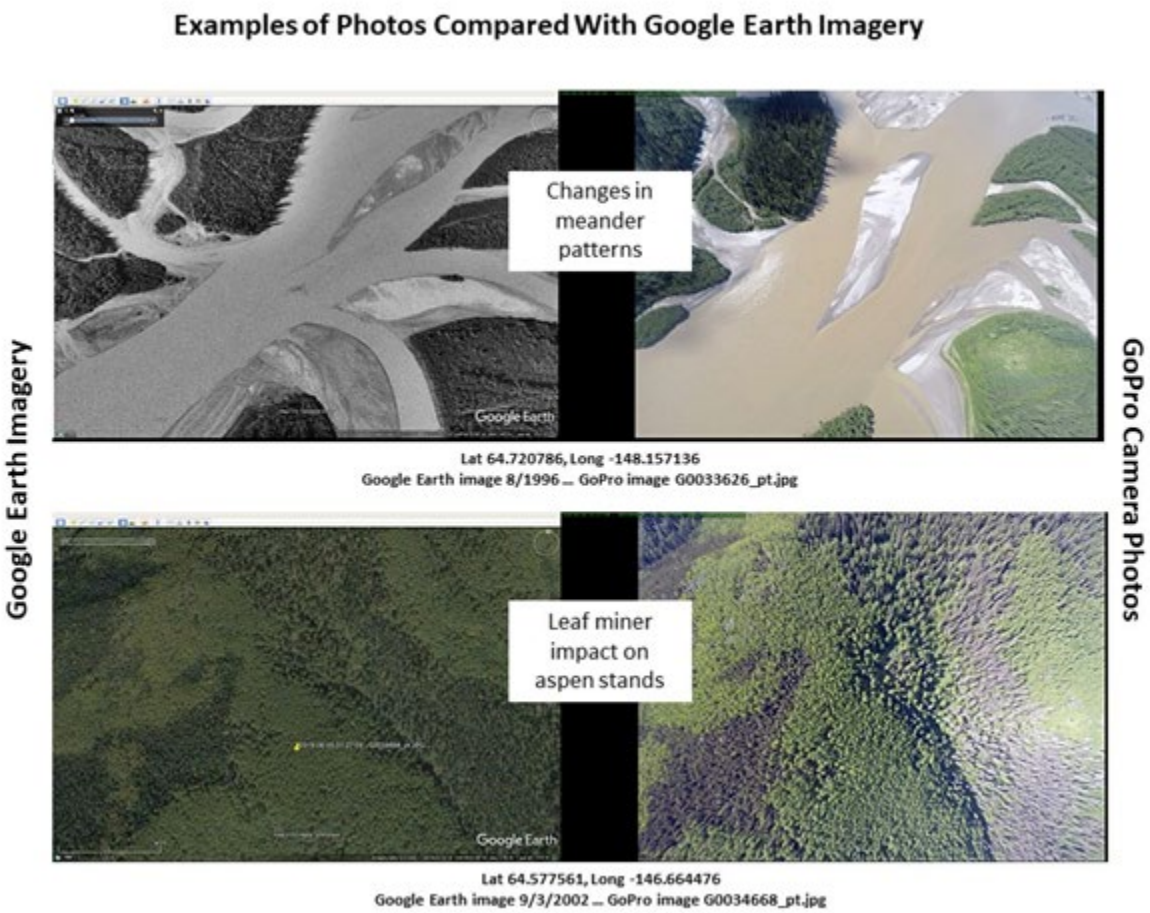


Figure 36. Two examples of matching GoPro photographs taken from this study's low-level aerial photographic transects conducted 4 June 2019 (imaged on the right), with prior year conditions from Google Earth imagery (imaged on the left). Top: an example of changes in major riverine flood levels, meanders, sandbar, and riparian conditions (Tanana River near Sam Charley Island). Bottom: impacts of aspen leaf miner (Phyllocnistis populiella) on stands of trembling aspen (Populus tremuloides).

2.6.5 Examples of Use of Nadir Photos to Create Panoramic Images

The GoPro photos were taken at time-lapse intervals of 5 seconds, and at the specified flight altitude AGL and ground speed, sequential images generally overlapped by about one-third. This affords the opportunity to stitch together sequential images into panoramas of however many photos are desired, although resulting panoramas are more useful from photos taken during level flight.

Here, we present two examples of panoramic images each stitched from 5 sequential photos. Figure 37 shows a panorama of the Tanana River centered on the GoPro photo from the upper part of Figure 36, above, and turned 90-degrees. Figure 38 is a panorama centered on drainage wetlands and thermokarst ponds in the western section of Tanana River Training Area (Figure 33). Both panorama examples shown here are from GoPro 5 photos taken on flight path 2.



Figure 37. Panorama image stitched from 5 sequential GoPro 5 photos of the Tanana River taken on flight path 2, centered on the example image shown in Figure D.4.1.



Figure 38. Panorama image stitched from 5 sequential GoPro 5 photos of drainage wetlands and thermokarst ponds in western Tanana River Training Area, taken on flight path 2 (Figure 33).

As shown above, creating selected panorama images may be a useful means of displaying the broader landscape context of specific sites and features. This may be helpful for interpreting causal events and identifying disturbances in future change-detection studies.

2.6.6 Examples of Use of Nadir Photo Series to Create Flight Path Animations

A final potential use of the aerial photo transect images is to create animations of the flight path nadir images. This can be accomplished using video editing software or even by combining sequential photos into animated gif image. Animating photos in this way can also helpfully display the broader landscape context of a given image or feature, to give a quick visual overview of selected flight path segments, and also to generally elicit interest during presentations of project results.

2.6.7 High-resolution DSLR Photography

During the project, Richard Murphy, photographed examples of the various ecosystem types on military lands and these photos highlight examples of landscapes that are changing due to fire, thermokarst, hydrologic shifts, and other drivers. A total of 2,883 photographs were taken during four field trips, including a team introductory field reconnaissance in May 2018 (438 photos), fieldwork in May 2019 (591), an airborne reconnaissance photo mission in June 2019 (1,939, see Figure 33 for flight route) and an airborne reconnaissance photo mission on the Tanana Flats in October 2020. All photographs are GPS-tagged with positional information so they can be replicated over time for change-detection studies. The photography collection was reviewed to identify the best photographs to represent ecotypes and change drivers (Figure 39a-c). This reduced set of photos were labeled and purchased for the project. This photography provides a high impact means of conveying to stakeholders the diversity of boreal ecosystems in central Alaska and illustrating the wide range of disturbance drivers that are changing Alaska's landscape. A poster with highlights of the photography was presented at the IBFRA21 conference of the International Boreal Forest Research Association in August 2021, and the poster has been provided to Ft Wainwright Natural Resources Office.



Figure 39. a) Photographs of dominant drivers of landscape change in central Alaska, including thermokarst on the Tanana Flats (above) and fire on morainal uplands near Ft. Greely (below).



Figure 39b. Photographs of ecotypes, including Alpine Dry Barrens near Ft. Greely (top) and Upland Wet Needleleaf Woodland and Alpine Moist Low Scrub in the YTA (below).



Figure 39c. Photographs of Lacustrine Wet Grass Meadow and Lacustrine Shallow Lake near Ft. Greely (above) and Lowland Fen Meadow on Tanana Flats (below).

2.7 Task 2.1

Integrate the effect of the static and dynamic drivers of ecotype change in the Alaska Thermokarst Model.

2.7.1 Model developments

The ATM was originally developed as a state-and-transition model representing spatial and temporal patterns of ecotype transitions resulting from thermokarst disturbance. This original version was applied across the TFTA, the area predicted to be the most vulnerable for thermokarst formation in future years due to the presence of lowland ice rich permafrost (Figure 40). Simulations were conducted from 1950 to 2015 using historical climate records from the Climate Research Unit Timeseries (CRU) TS4.0. These historical simulations were compared with observed land cover transitions from repeated imagery analysis (Lara et al., 2016) to evaluate the capacity of the model to reproduce historical thermokarst disturbances. Observed and modeled rates of loss of permafrost plateau resulting from thermokarst disturbance were compared in 25 plots located in the Tanana Flats training area. Fifteen of these plots were used to develop the predictive models, and 10 of these plots provided independent observations for model validation. This comparison shows that the thermokarst model is successfully representing historical loss of permafrost resulting from thermokarst disturbance.

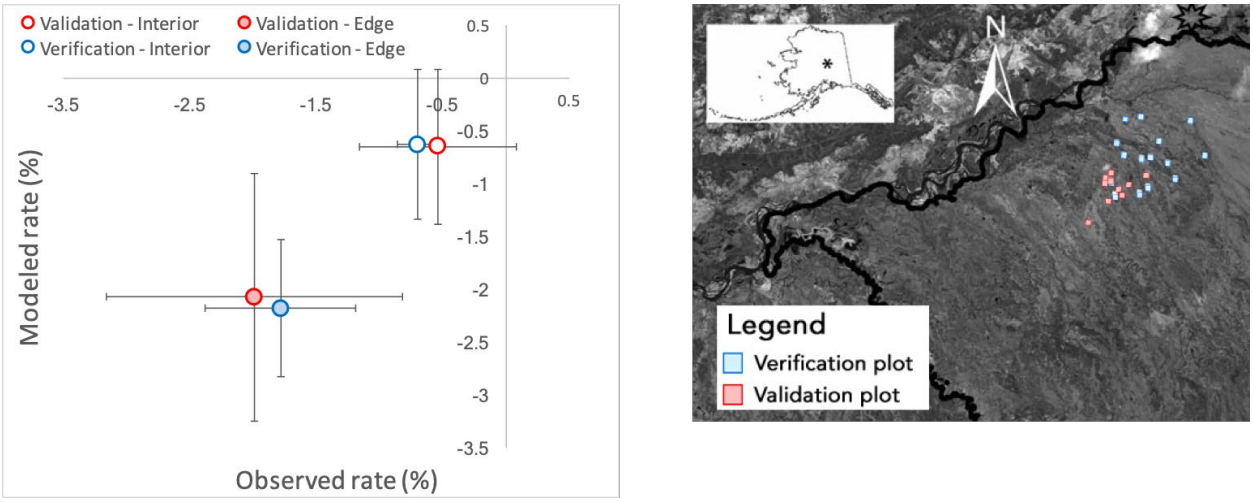


Figure 40. Comparison of observed and modeled rate of loss of permafrost plateau resulting from thermokarst disturbance in the TFTA. Red symbols represent rates of loss in validation plots (independent observations). Blue symbols represent rates of loss in plots used for model development. The circles represent rates of loss of permafrost plateau inside the plateau. The dots represent rates of loss of permafrost plateau on the edges of the plateau. Vertical and horizontal lines represent modeled and observed standard deviation respectively.

From the ecotype surveys performed in Task 1.4 we realized the importance of other drivers of land cover change that are at play not only in the lowlands of the TFTA, but also in the uplands of the YTA, DTAE, and DTAW. Therefore, we decided to expand the ATM to include other drivers of change in addition to thermokarst alone. We integrated all drivers of land cover change presented in Task 2.1 (below) in the state and transition model. The new drivers of change represented in the model include: primary succession, wildfire, paludification, infrastructure development, river deposition, drainage, and landslide. We also developed the model parameterization to characterize landscape heterogeneity using ecotype classes rather than

only land cover classes. The advantages of this change include: (1) a better characterization of the landscape heterogeneity and (2) an easier integration and valorization of the observations collected in Task 1.2. Compared to land cover classes that are mostly based on the characterization of the vegetation, ecotype classes integrate vegetation, landform, geological deposits, drainage conditions and disturbance. Therefore, we developed ATM's parameterization so it now simulates all the 62 ecotype classes described in Task 1.2 (Table 9).

We also synthesized the latest remote sensing landscape products of landscape characterization and in-situ ecological monitoring data to refine some of the rules driving disturbance regimes and landscape dynamics in ATM. Specifically, we used the latest products of the Monitoring Trends in Burn Severity (MTBS) and the National Land Cover Database (NLCD) to better characterize the impact of fire distribution and fire severity on landcover dynamic (see 2.7.2). We also synthesized in-situ soil moisture, soil temperature and active layer monitoring measurements collected by our team and a variety of collaborators working across Alaska to better characterize the environmental controls of abrupt permafrost thaw driving thermokarst occurrence (see Figure 45 at the end of this section).

Finally, we coupled the ATM with two other models to better represent the biogeophysical processes driving the effect of projected climate change on landscape dynamics. We used the Alaska Frame Based Ecosystem Code (ALFRESCO; Rupp et al., 2000; Johnstone et al., 2011; Gustine et al., 2014) to integrate spatially explicit simulations of fire occurrence and fire severity in response to multiple climate change scenarios. We also used spatially explicit simulations of permafrost and vegetation dynamics from the Terrestrial Ecosystem Model (TEM; Raich et al., 1991; Yi et al., 2009; Euskrichen et al., 2009; Genet et al., 2013) to represent the effect of permafrost thaw and changes in soil moisture and organic layer thickness on land cover dynamics.

2.7.2 Analysis of historical postfire trajectory using remote sensing data

2.7.2.1 Context

The probabilities of land cover change computed from the repeated imagery analysis presented in Task 1.2 can characterize the effect of wildfire occurrence at the regional level. The sampling design of this analysis did not allow to attribute temporal variations in the fire-related probabilities of land cover change to change in total area burn, change in fire spatial distribution, or change in fire severity. As such, using these probabilities in a model such as ATM that represents the spatial distribution of wildfire might result in an underestimation of fire-related land cover change. Fire related probabilities of change from the repeated imagery analysis are based on 2,200 sampling points, including burned unburned sites, that are part of our geospatial database. In ATM, fire related probabilities of change are exclusively applied to areas/pixels that actually burn. As such, these probabilities need to be computed from a sampling exclusively of burned sites.

2.7.2.2 Approach

In order to cover the diversity of the landscape, and the diversity of post-fire land cover trajectories we used remote sensing data to assess historical fire-related land cover change across the area of interest. We used annual land cover maps from the NLCD (Selkowitz et al., 2011) for Alaska from 2001 and 2016 (Figures 41 A and B) and wildfire distributions from the MTBS (Eidenshink et al., 2007) from 2001 to 2016 (Figures 41 C and D) to assess pre- and post-fire

land cover change between 2001 and 2016 and to assess the influence of re-burn and fire severity on these changes.

The effect of fire was assessed (Figure 41) using the MTBS database rather than the Alaska Large Fire Database (ALFD, Bureau of Land Management, https://www.frames.gov/catalog/10465) because the MTBS provides assessment of fire severity and the ALFD tends to overestimate the area that actually burned. As the MTBS data were compiled from 2001 to 2016, we noticed that the footprint of the 2001 Survey Line fire (Manies et al., 2014) was missing from the database. We used the ALFD to include the footprint of this fire in our analysis of post-fire land cover change. However, since we did not have information on the severity of the fire, it was excluded from our analysis on fire severity. In reburned areas, fire severity was computed as a rounded average of the fire severity class of the multiple fires.

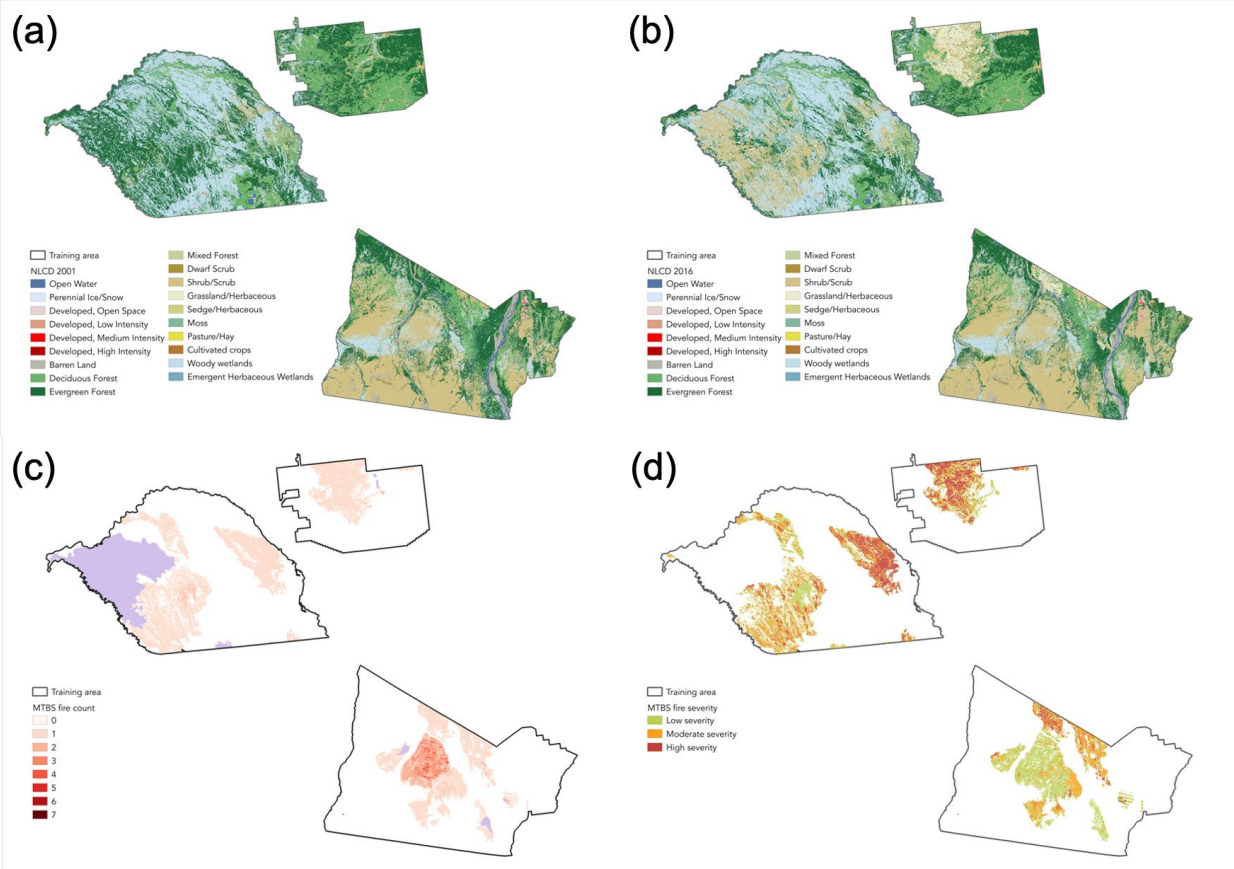


Figure 41. Representation of land cover change and fire regime from 2001 to 2016 in the training area. (A, B) land cover distribution from the NLCD from 2001 and 2016 respectively. (C, D) fire distribution and severity assessed from the Monitoring Trends in Burn Severity database from 2001 to 2016. Deep red sheds in panel c represent areas of re-burn. The purple patch in panel (c) indicates the footprint of the 2001 Survey Line fire that was not reported in the MTBS database.

2.7.2.3 Description of the fire regime

Across the four training ranges, 1,592 km^2 burned once, and the footprint of the reburns was 141 km^2 (8.4%) between 2001 and 2016. The maximum re-burn frequency was 7 times during this period. When re-burn frequency is taken into consideration, the re-burn area totaled

339 km^2 (18.0%). Most of the re-burns were anthropogenic and concentrated in impact areas located in DTAW. Only 0.6% and 3.7% of the total area burned occurred in lacustrine and riverine environments, usually at low severity. For this reason, we decided to focus our analysis on uplands and lowlands exclusively. Across the total area burned, 46.7%, 30.4% and 22.9% of the area burned at low, moderate and high severity. The highest proportion of high severity fires were found in upland (i.e. 34.4%, Table 12).

Table 12. Distribution of area burned by severity class and by landform.

Fire severity	Percent of area burned	
	Lowland	Upland
Low	48.1	39.9
Moderate	31.6	25.7
High	20.3	34.4

2.7.2.4 Land cover change resulting from wildfire

Land cover changes assessed between 2001 and 2016 from NLCD land cover maps were the most abundant in areas that burned once (Figure 42 A). Land cover changes were slightly more abundant in re-burned than in unburned areas. The relatively low proportion of land cover changes in re-burned areas compared to areas that burned once is likely due to the fact that these areas burned prior to 2001 and the major land cover transitions associated with fire already happened.

Fire-related land cover changes were almost 75% more abundant in uplands than in lowlands. (44.6% and 77.9% in lowland and upland respectively). Fire-related land cover changes were dominated by transitions from evergreen forest to shrubland, evergreen forest to grassland, deciduous forest to shrubland, and evergreen forest to shrub wetland. In uplands, wildfires mainly resulted in transitions from evergreen and deciduous forests to grasslands and shrublands (Figure 42 B). Transitions from evergreen forest to shrublands were largely dominating fire-related land cover dynamics in lowlands.

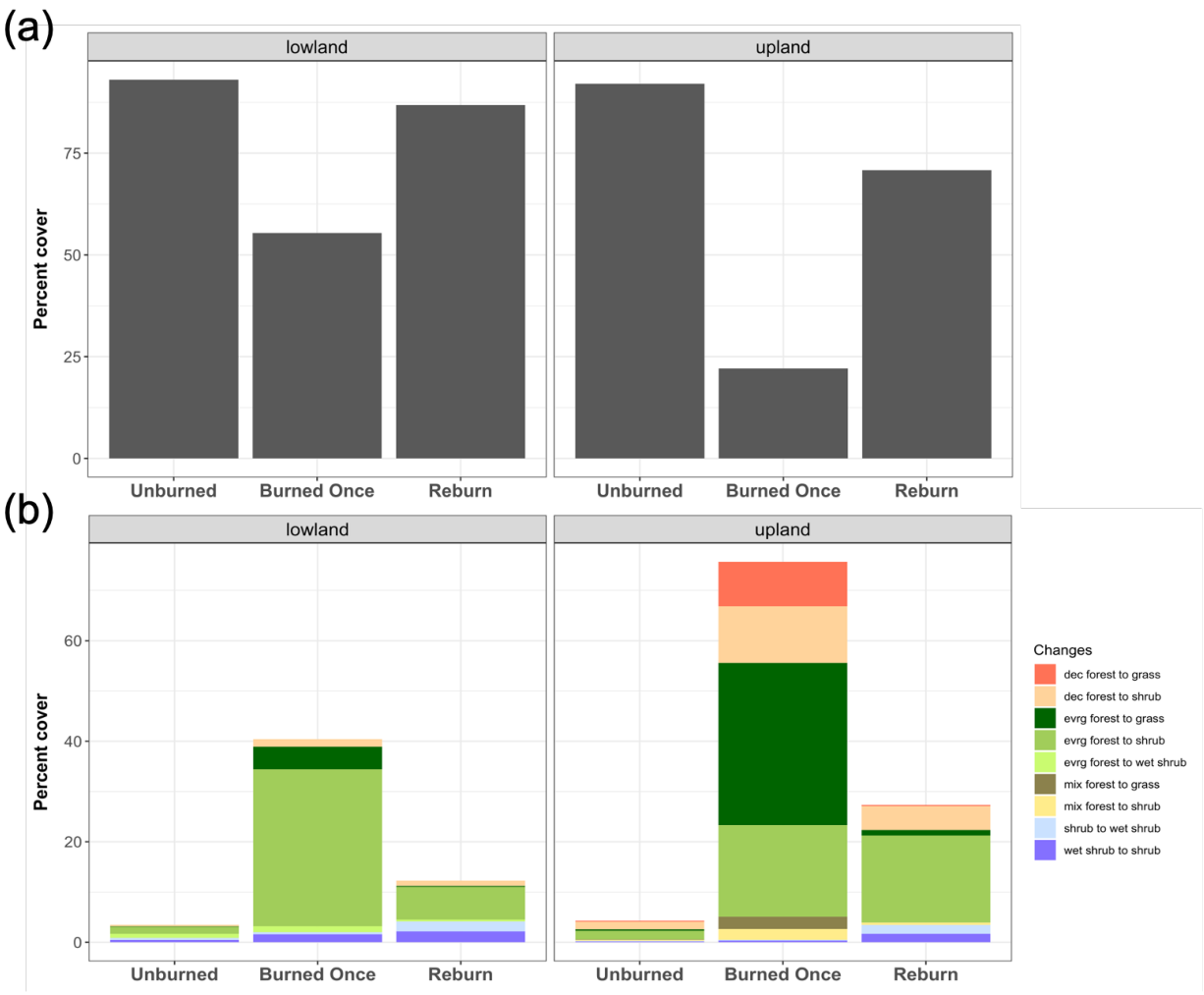


Figure 42. Effect of wildfire frequency on land cover dynamic between 2001 and 2016: (a) percent of area that did not change land cover class, (b) major land cover changes (> 1% cover) in unburned, burned once and reburned areas.

Increasing fire severity was associated with increasing land cover change (Figure 43a). While low severity fires resulted in land cover changes across 27.7% and 61.7% of the area burned in lowland and upland respectively, high severity fires resulted in 54.9% and 93.6% of land cover change in lowland and upland respectively. Increasing fire severity was also associated with increasing proportion of transitions from evergreen forest to grassland in both uplands and lowlands (Figure 43).

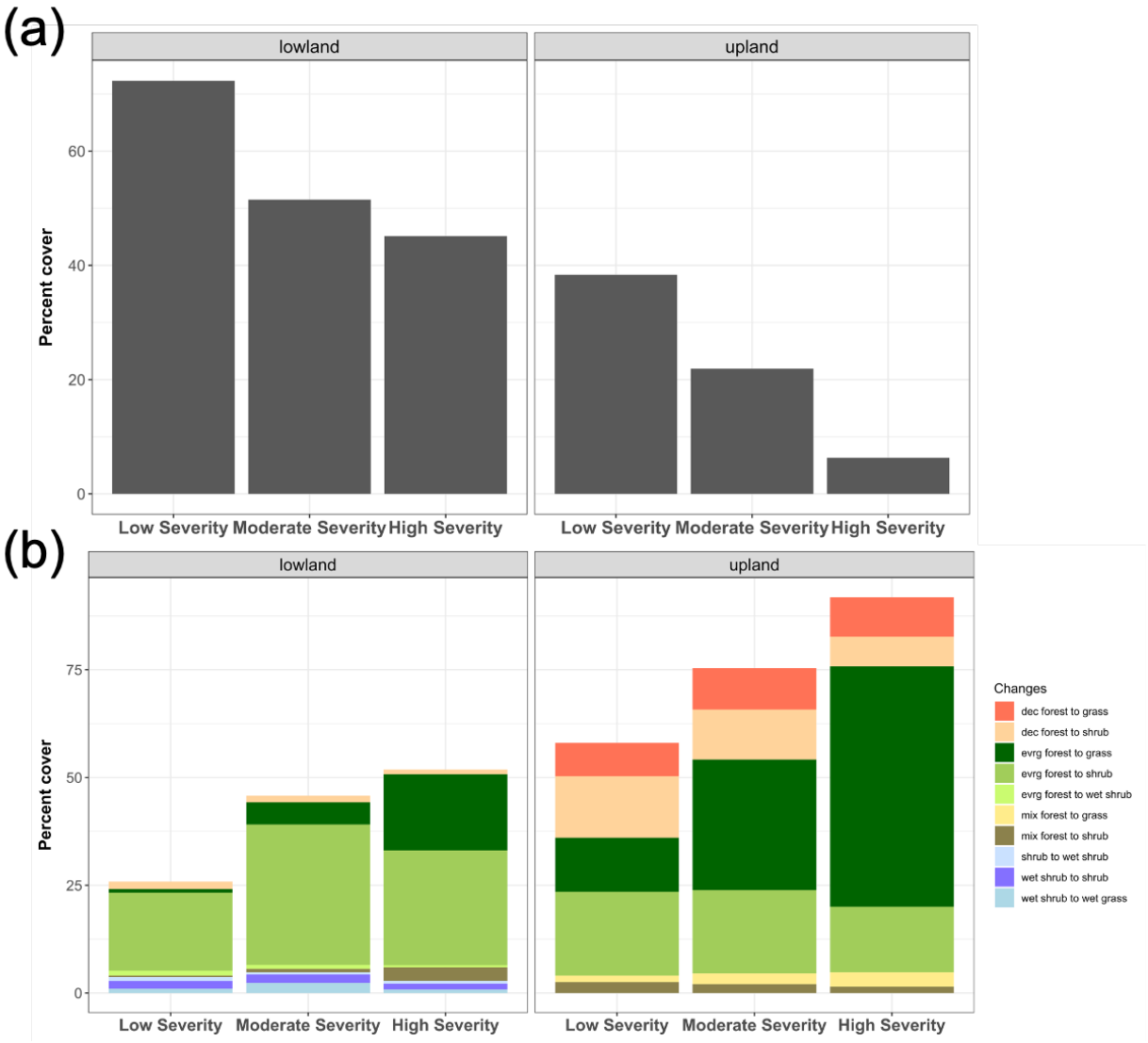


Figure 43. Effect of burn severity on land cover dynamic between 2001 and 2016: (a) percent of area that did not change land cover class, (b) major land cover changes (> 1% cover) by severity class.

2.7.2.5 The impact of climate on thermokarst occurrence

A previous imagery analysis conducted on the northern part of the Tanana Flats suggested that precipitation plays a primary role in thermokarst dynamics in the region, warming being a secondary factor of thermokarst occurrence (Lara et al., 2016). The analysis of the historical climate records for Fairbanks (Figure 44), reveal that the increase in thermokarst occurrence observed in the current study from the first observation [1950-1980] (0.36%) to the second and third more recent periods of observation [1980-2000] (1.04%) and [2000-2017] (1.09%) corresponds to an increase in heating degree days (i.e. a warming trend) and an increase in summer precipitation (Figure 44 B, E).

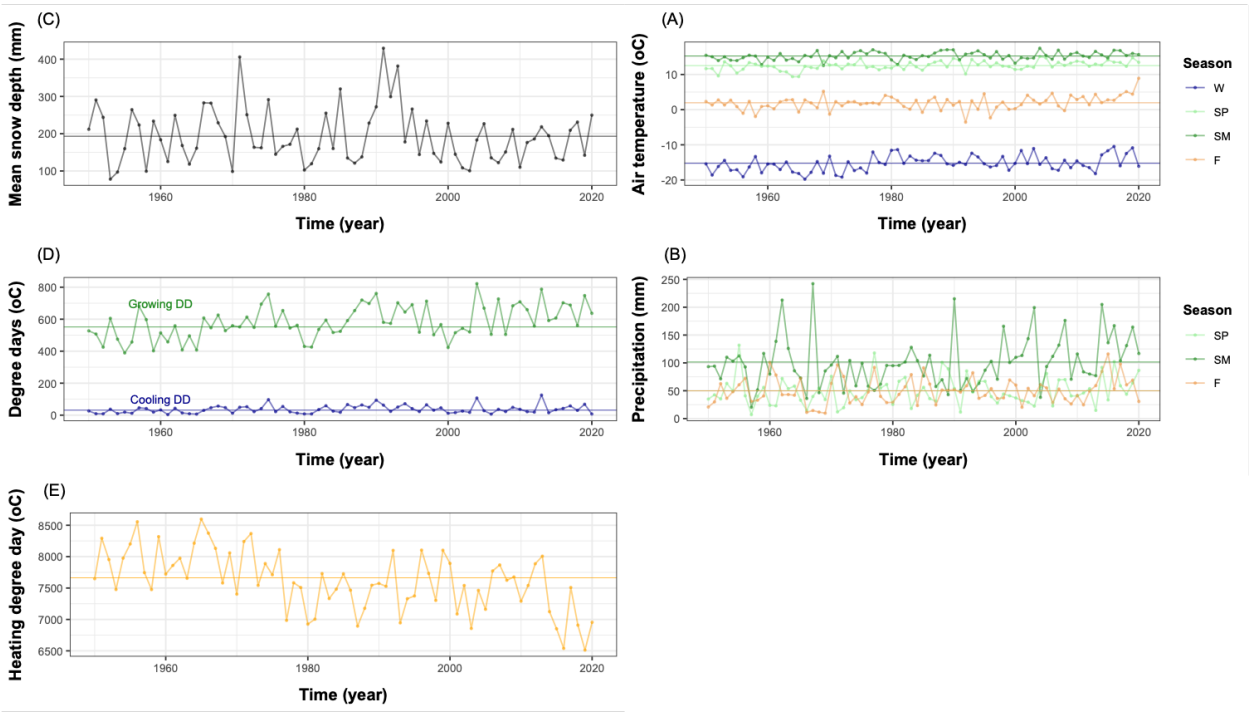


Figure 44. Annual climate records for Fairbanks from 1950 to 2020, corresponding to the period of the repeated imagery analysis presented in Task 1.2. Horizontal lines in each panel represent historical means. Seasons acronyms are W for winter, SP for spring, SM for summer and F for fall. DD = degree days.

To further quantify the effect of precipitation and warming on thermokarst disturbance, we synthesized soil temperature and active layer observations from 34 sites across Interior Alaska (Figure 45) located in regions moderately to highly vulnerable to thermokarst. We looked at the impact of climate on abrupt increase in active layer depth for these sites. We defined abrupt increases in active layer depth as an increase higher than the 80% quantile value of the observed interannual changes in active layer depth (i.e. the 20% highest increase in active layer depth from one year to the next). In addition, we noticed a few sites presenting high interannual variability in active layer depth (i.e. not likely to show persisting permafrost degradation). To exclude these events from the analysis, we added another parameter to the identification of abrupt increase in active layer depth, which is temporal persistence. Abrupt increase in active layer depth was therefore define as an increase in active layer depth higher than the 80% quantile value of the observed interannual changes in active layer depth across sites, and with a persisting increase in active layer for 3 years (the limitation to three years is justified by the relative shortness of the time series).

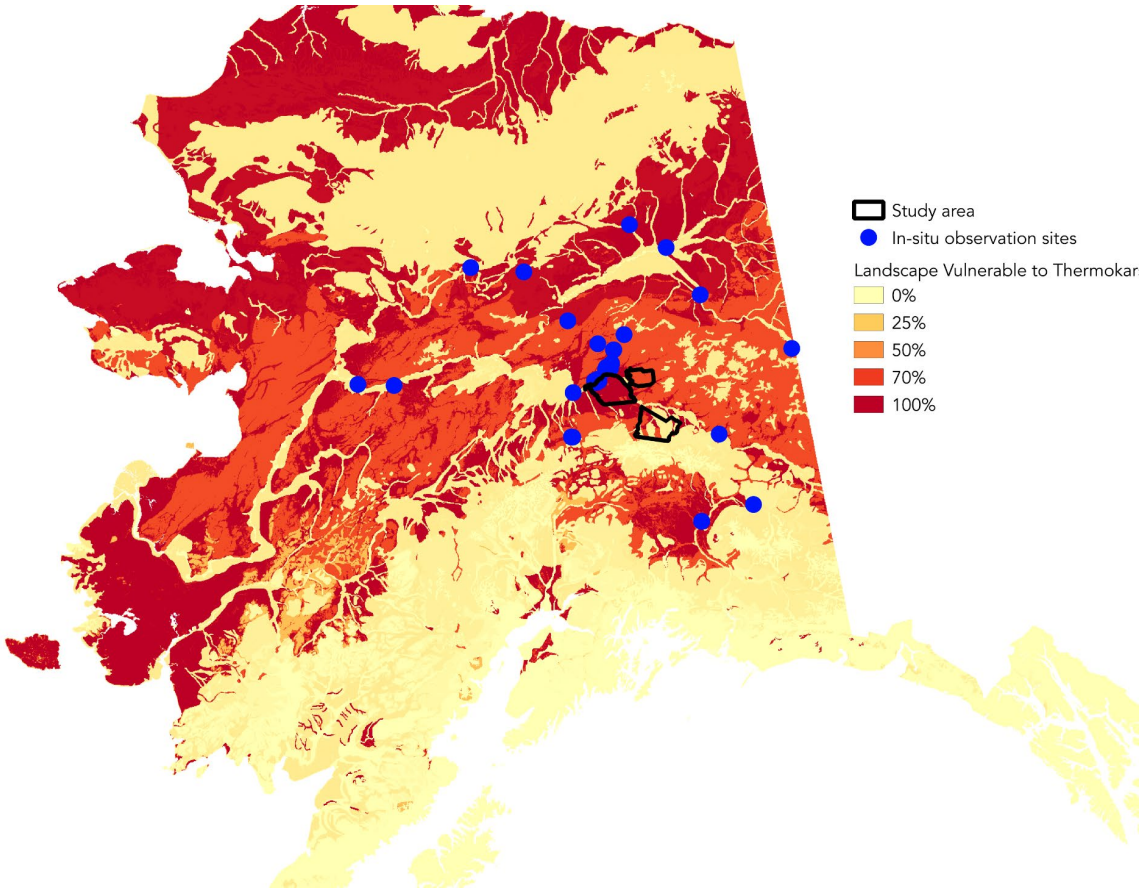


Figure 45. Location of the soil temperature and active layer depth monitoring sites used for the climate analysis of abrupt increase in active layer depth.

We used a mixed regression model to assess the combined influence of seasonal precipitation totals, seasonal air temperature means, winter snow depth and length and annual heating degree days, growing and freezing degree days on the occurrence of abrupt thaw. We accounted for the differences between sites as random effect in the mixed model. The final model explained 36.5 % of the total variance of abrupt thaw occurrences with summer precipitation from the current and previous years and annual heating degree days as the three significant drivers of abrupt thaw (Figure 46).

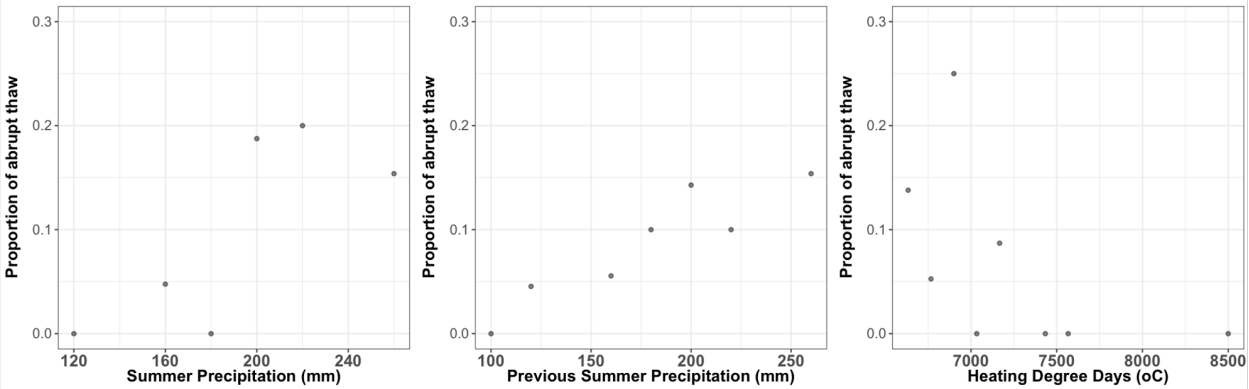


Figure 46. Influence of summer precipitation from the current year (a) and from the previous year (b), and heating degree days on the occurrence of abrupt

The final model was used to represent the effect of precipitation and warming on thermokarst probability as follows (HDD: heating degree day):

Tkp= - 8.254 10-5 * HDD + 1.459 10-3 * PS + 9.088 10-4 * PS1 + 0.00274

Where tkp is the probability of thermokarst, HDD is the annual heating degree days, PS and PS1 are summer precipitations of the current and previous year.

Because HDD was not directly available for climate projections (which only produced monthly mean temperature), we used the climate records analyzed in this study to compute HDD from mean annual temperature (R2=0.997) as:
HDD= - 361.63 * MAT + 6704.9

where MAT is mean annual temperature.

2.8 Task 2.2

Simulation of thermokarst and ecotype dynamics from 2000 to 2100 using the Alaska Thermokarst Model

2.8.1 Description of the Model

The Alaska thermokarst model is a state and transition probabilistic model that predicts change in ecotype distribution on an annual basis, at a 30-m resolution. Currently, the model represents the effect of wildfire, thermokarst, permafrost aggradation, river movement, succession, lake drainage, human activities (e.g. trails and clearings), shrubification and forest advancement on ecotype dynamic. The set of possible ecotype transitions and their associated drivers are separated by landform, namely alpine, upland, lowland, riverine, and lacustrine landforms. Figure 47 represents the ecotype transitions that were documented from the repeated imagery analysis and integrated in ATM.

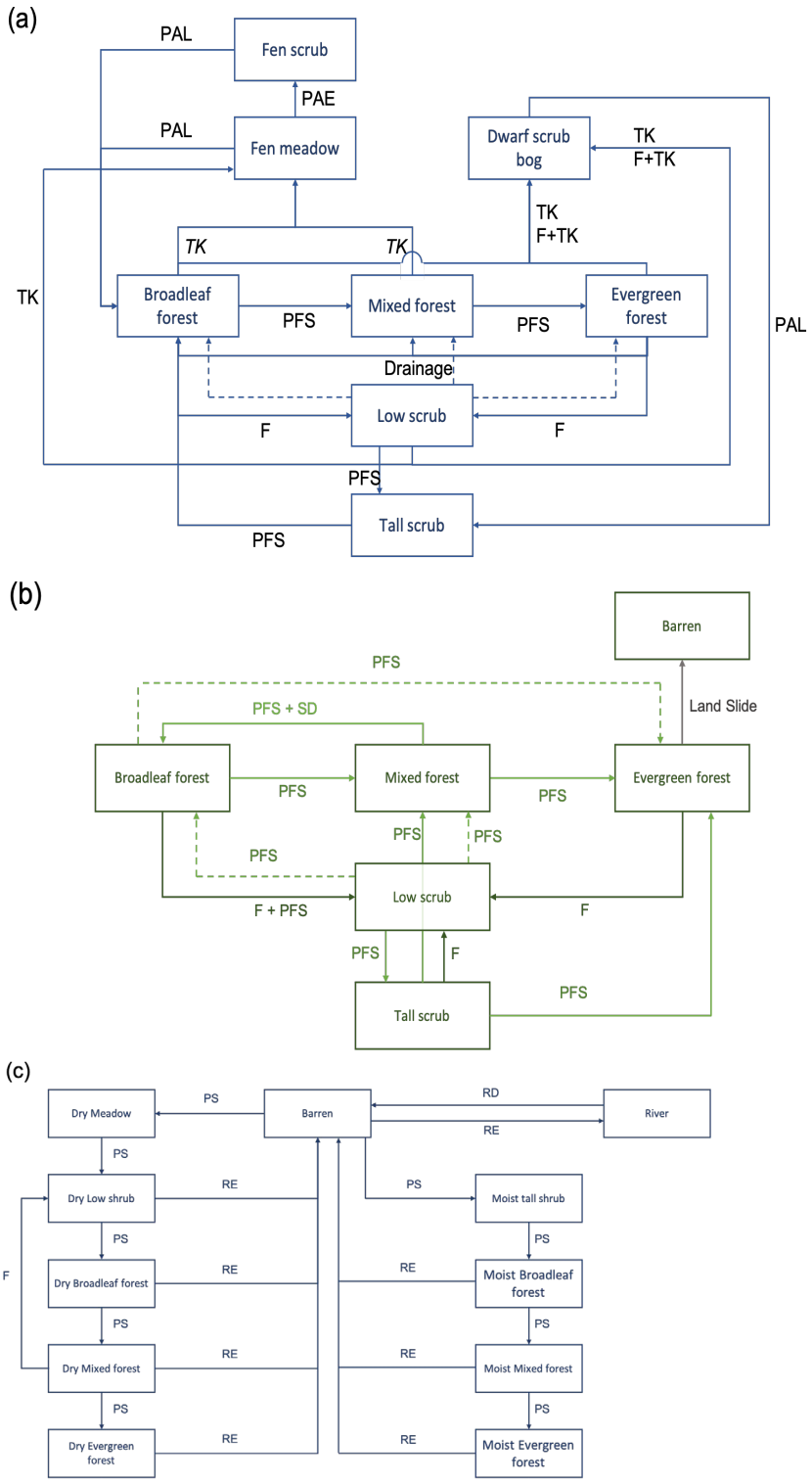


Figure 47. Representation of the ecotypes in (a) lowland, (b) upland and (c) riverine landform and the possible drivers of transitions. F = fire, PFS = post-fire succession, TK = thermokarst, PAE = early paludification, PAL=late paludification, RD = river deposit, RE = river erosion, PS = post-disturbance succession. These diagrams have been simplified for clarity.

2.8.2 Description of the Model Simulations using historical probabilities

1- Constant historical probabilities: A set of three model simulations were first conducted using constant probabilities of ecotype change computed from the repeated imagery analysis presented in Task 1.2. Simulations were conducted using mean, maximum and minimum probabilities of change computed across the three periods of observations (i.e., 1950 to 1980, 1980 to 2000 and 2000 to 2017).
The probabilities were computed from the 2,200 points of observations, based on the laws of probability for sampling without replacement. This computation was conducted in two steps:

1. compute the probability of no ecotype change (pnc), where A_{start} and A_{end} are the area of ecotype A at the start and the end of the observation period and n is the length of the observation period in years.
$$pnc = (A_{end} / A_{start})^{(1/n)}$$

2. compute the probability/ies of change (pc), where AB is the area of ecotype A that transitioned to ecotype B during the period of observation.
$$pc = (1-pnc) * (AB / (A_{start} - A_{end}))$$

2- Explicit representation of fire occurrence and fire severity: all the historical probabilities of ecotype change associated with fire were replaced by the fire-related probabilities of transitions computed in Task 2.1.2. Fire-related probabilities of transition were also modified by fire severity. A simulation was produced for every wildfire projection from ALFRESCO, i.e. ten simulations in total (see input description below).

3- Fully dynamic projections: a final set of simulations included the explicit effect of wildfire, wildfire severity, climate and organic layer dynamic on ecotype change. Climate directly affected the probability of abrupt thaw and thermokarst as presented in section 2.1.3. Climate also affected fire occurrence and severity as formulated in the ALFRESCO model. Finally climate and wildfire affected vegetation productivity and organic layer thickness, as formulated in the TEM model (Figure 48).

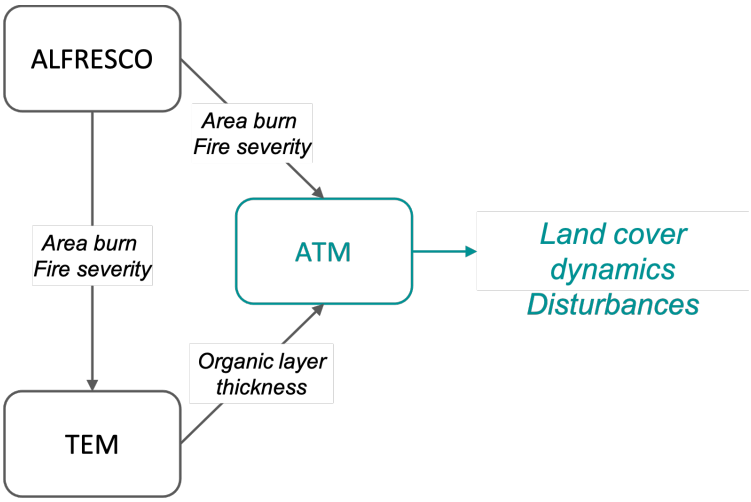


Figure 48. Diagram representing the coupling of ATM with a disturbance model (ALFRESCO) and a biosphere model (TEM).

2.8.3 Description of the Model Inputs

Ecotype initialization: Model projections were produced from 2017 to 2100. All projections were conducted at a 30m resolution. Ecotype initialization was done using the 2017 ecotype map (Figure 49) that we developed based on the original ecotype map for the three training areas (Jorgenson et al., 2001), updated with the impact of the most recent fires and the NLCD 2016 land cover maps.

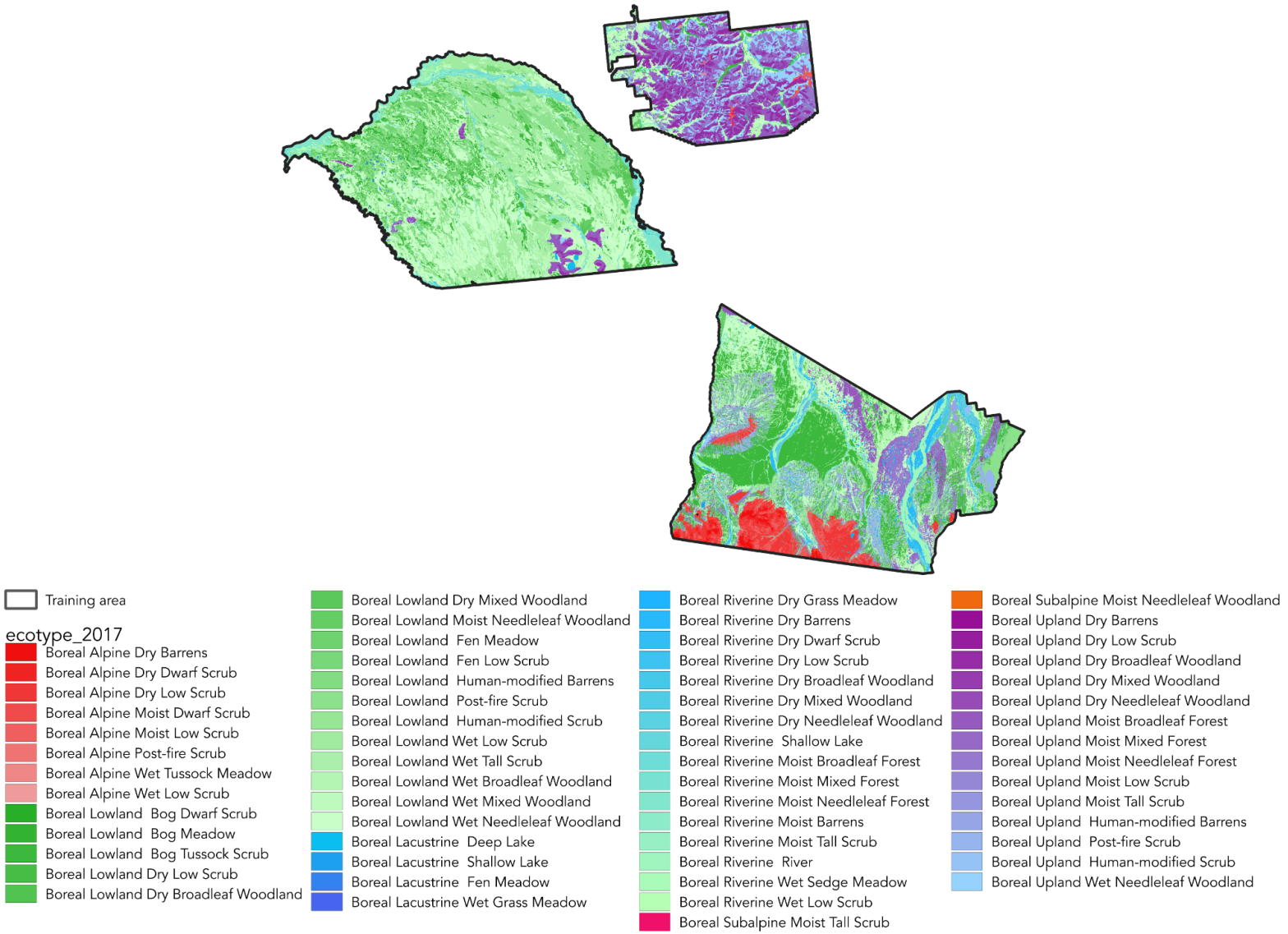


Figure 49. The 2017 ecotype map used for model initialization.

Since lowlands are the most abundant landform across the training ranges, ecotypes associated with this landform are dominating the landscape. Boreal lowland wet needleleaf forest, wet low scrub, post-fire scrub and bog tussock scrubs are the most abundant ecotypes in lowlands. Broadleaf, and needleleaf forests and shrublands are the most abundant in uplands (Figure 50).

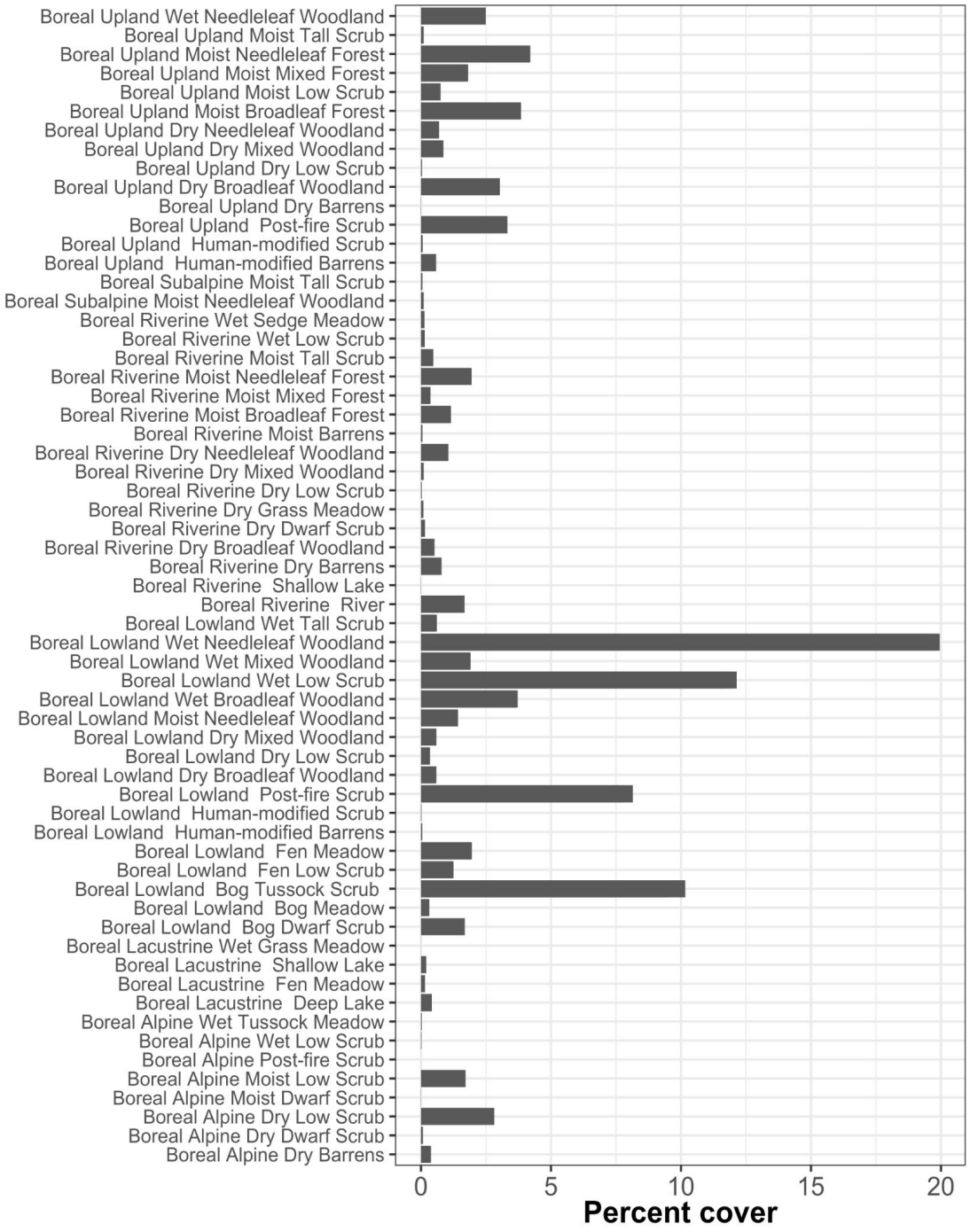


Figure 50. Percent cover by ecotype computed for the 2017 initialization land cover map shown in Figure 49.

Climate projections: Projections of the effect of climate on ecotype change were simulated for a total of ten climate scenarios, from five global circulation models (CCSM4, GISS-E2, MRI-CGC, GFDL-CM, IPSL-CM) in response to two emission scenarios (rcp 4.5 and rcp 8.5). Climate data were available on a monthly basis, from the Scenario Network for Alaska Planning data portal (http://ckan.snap.uaf.edu/dataset). The climate data was provided at a 1km-resolution and resampled to 30m-resolution to match the ecotype map.

Fire projections: Projections of annual distribution of fire scars and fire severities were assessed using ALFRESCO simulations for each of the ten climate scenarios used in this study. ALFRESCO simulations were conducted at a 1km-resolution and resampled to 30m-resolution to match the ecotype map. Between 2017 and 2100, a total of 2,000 to 4,196 km^2 is projected to burn across the three training ranges, depending on the scenario considered (Figure 51 A). The proportion of high severity fires was quite variable between ALFRESCO simulations, and ranged from 8.3% to 35.6% of the area burned (Figure 51 B).

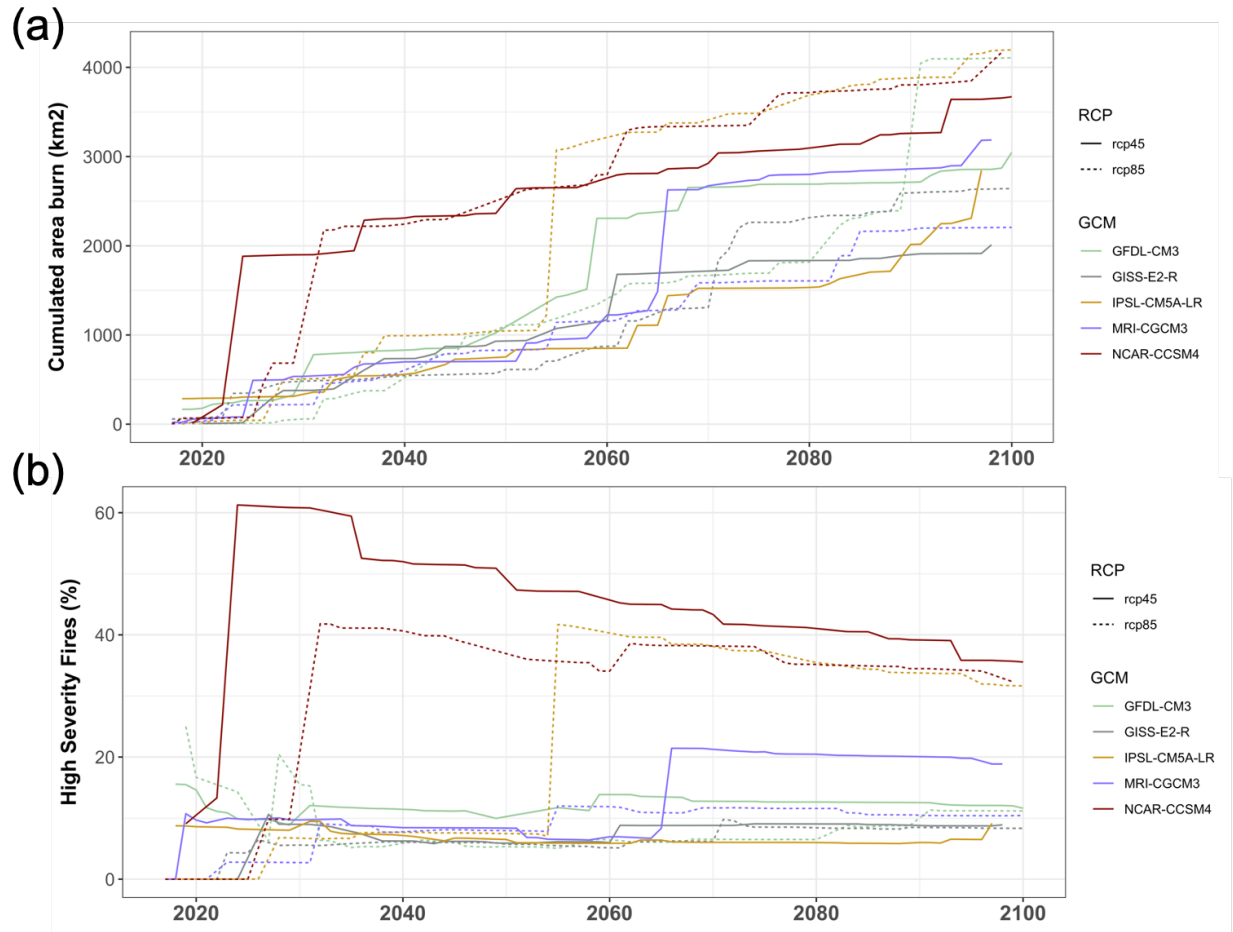


Figure 51. ALFRESCO projections of (a) cumulated area burned (km^2) and (b) the proportion of high severity fires, from 2017 to 2100, for the ten climate scenarios tested.

Vegetation productivity and organic layer dynamics: Projections of annual vegetation net primary productivity (NPP in $gC/m^2/yr$) and organic layer thickness (cm) were assessed using TEM simulations for each of the ten climate scenarios used in this study. TEM simulations were conducted at a 1km-resolution and resampled to 30m-resolution to match the ecotype map. Change in organic layer thickness is driven by NPP through litterfall, mineralization and wildfire consumption. Across the 10 climate scenarios we tested, organic layer in fens increased by 35.98% from 2017 to 2100 (Figure 52).

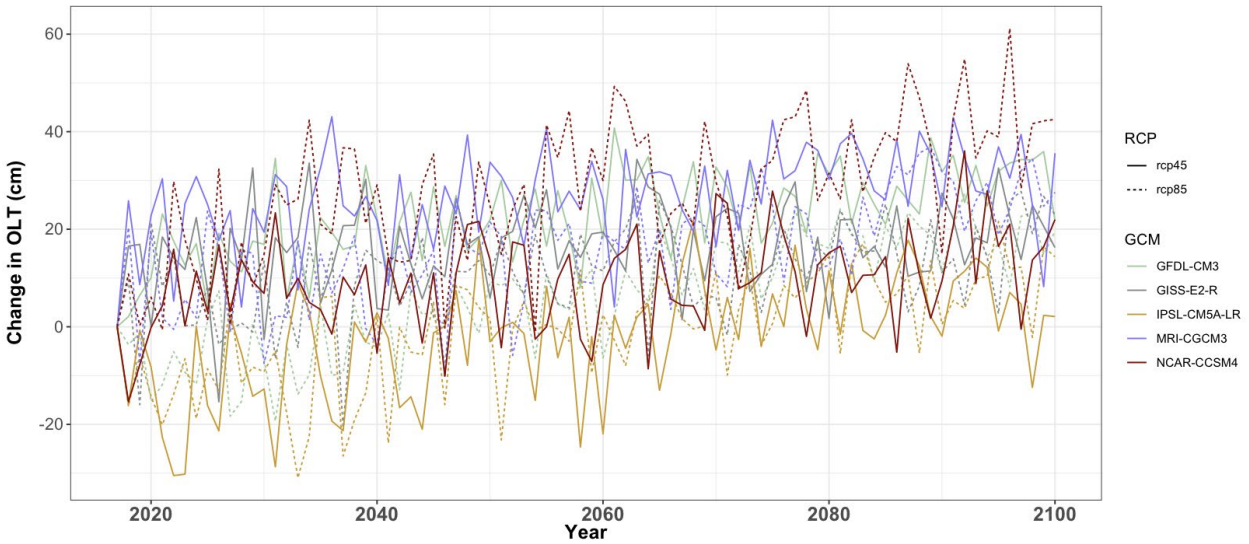


Figure 52. Projected change in organic layer thickness from 2017 for fen wetlands in response to the 10 climate scenarios tested (5 global circulation models (GCM) for 2 emissions scenarios (rcp4.5 and rcp 8.5) simulated by TEM.

2.8.4 Results

2.8.4.1 Effect of Constant Historical Probability of Ecotype Change

Simulations using the minimum, average and maximum values of historical probabilities of transitions resulted in 285.7km^2 (4.5%), 326.1 km^2 (5.2%) and 1,105.6km^2 (17.7%) of ecotype change respectively, across the three training ranges between 2017 and 2100.

Ecotype dynamics from 2017 to 2100 using constant historical probabilities of change were mostly driven by fire activity and post-fire vegetation transitions (Figure 53). To a lesser extent, thermokarst disturbance and river dynamics had a secondary impact on ecotype distribution. The extent of the landscape impacted by fire and post-fire transitions decreases over time as fire prone vegetation such as evergreen forest decreases in extent (see next paragraph and Figure 54). In all three scenarios, thermokarst disturbances increase over the 21st Century and are more frequent than permafrost aggradation (Figure 53).

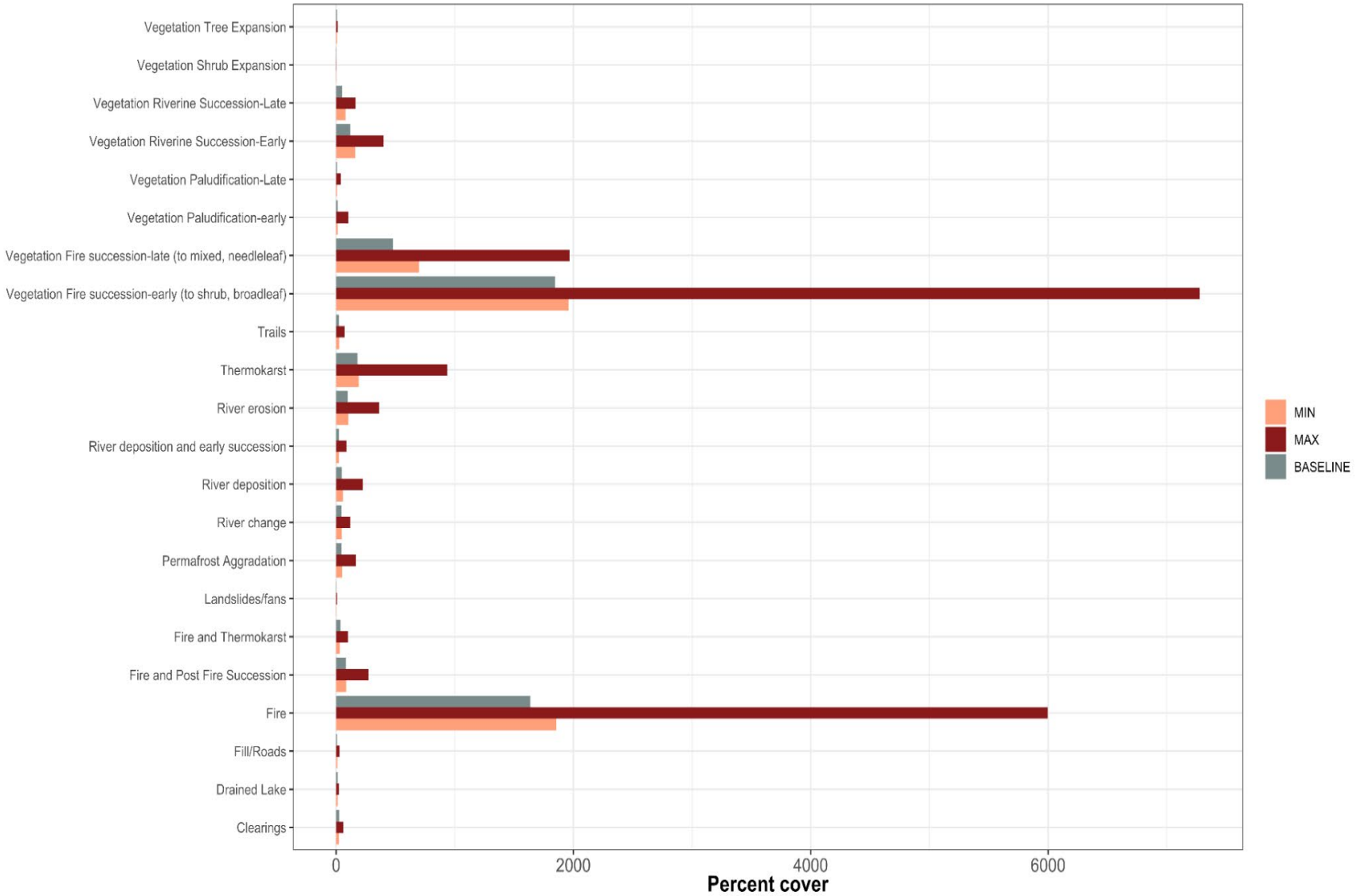


Figure 53. (a) Most abundant and (b) less abundant drivers of ecotype change simulated from 2017 to 2100 using constant probabilities of ecotype change computed from repeated historical imagery analysis. BASELINE, MIN, and MAX simulations used averaged, minimum and maximum values of probabilities of change from the three periods of observation respectively.

Frequent fires resulted in substantial transitions from needleleaf forests to deciduous vegetation (scrubs, forest) in lowlands (Figure 54 A). Lowland wildfires also resulted in a decrease in tussock scrub bogs (Figure 54 B). In addition to the increasing ecotype transitions associated with paludification, thermokarst disturbances resulted in increasing extent of fen and bog meadows in lowlands. Ecotype distribution in uplands was dominated by post-fire succession, a legacy of intense historical fires. As a result, the extent of post-fire scrubs and broadleaf and mixed forests decreased to the benefit of needleleaf forest characteristic of mid- and late successional stage. Ecotype distributions in riverine landform remained relatively stable as it has a low probability of burning and vegetation transitions associated with river erosion and river deposition are occurring at similar rates.

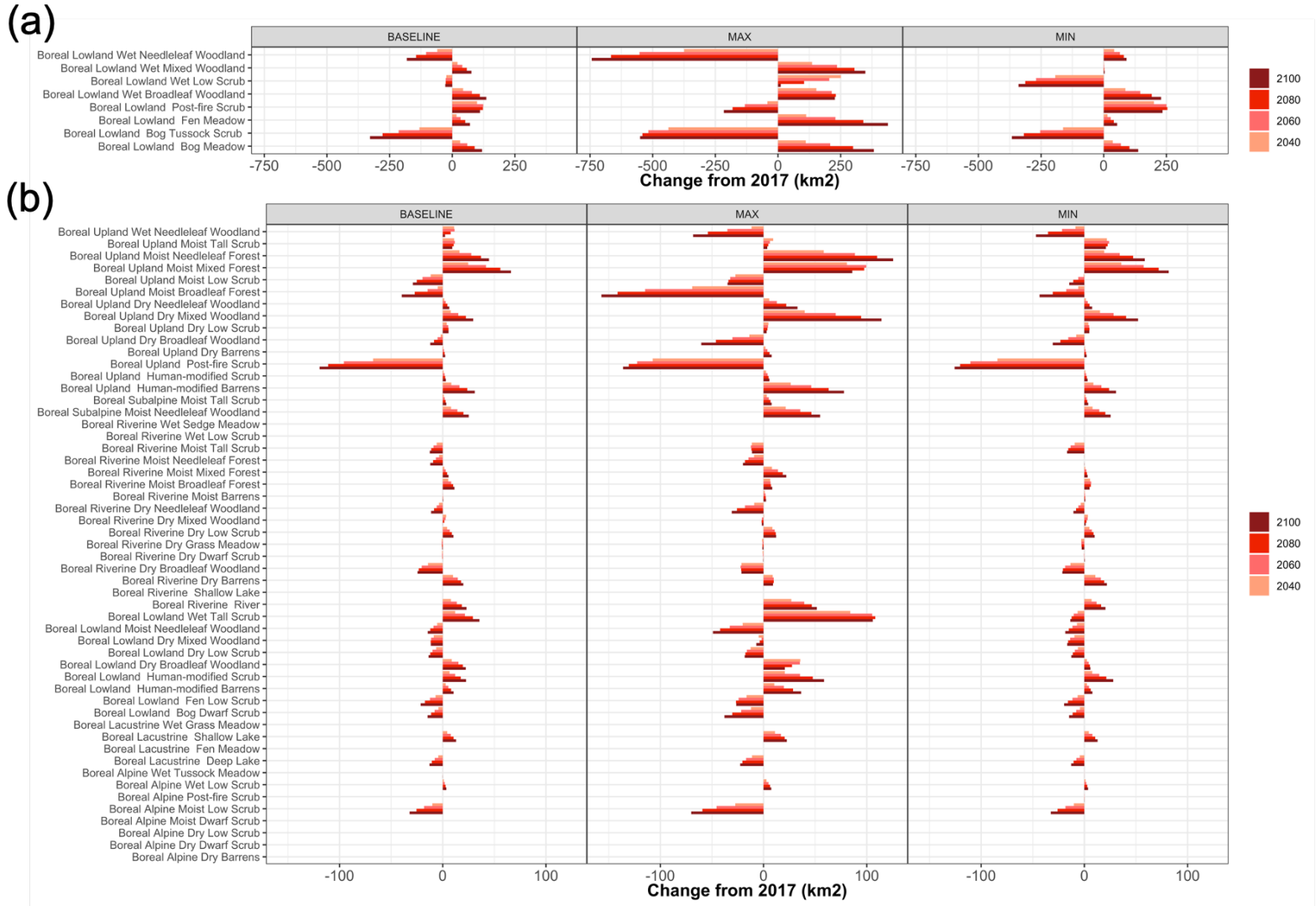


Figure 54. Change in area of the (a) most abundant and (b) less abundant ecotypes, simulated from 2017 to 2100 using constant probabilities of ecotype change computed from repeated historical imagery analysis. BASELINE, MIN, and MAX simulations used averaged, minimum and maximum values of probabilities of change from the three periods of observation, respectively.

2.8.4.2 Effect of Explicit Fire Frequency and Severity on Ecotype Change

We conducted ten simulations with explicit fire occurrence and severity using ALFRESCO outputs. Each of these simulations corresponded to different climate projections. These simulations allowed for a direct quantification of the projected change in fire regimes on ecotype distribution. To summarize the results in a clear way, we grouped ecotypes by classes of vegetation with similar flammability, i.e. deciduous shrub/forest, evergreen forest, wetland, grassland, barren, lake, river. As expected, the increase in area burned resulted in a decrease in fire-prone evergreen vegetation and an increase in post-fire deciduous shrubs and forest and wetlands when fires trigger thermokarst disturbance (Figure 55).

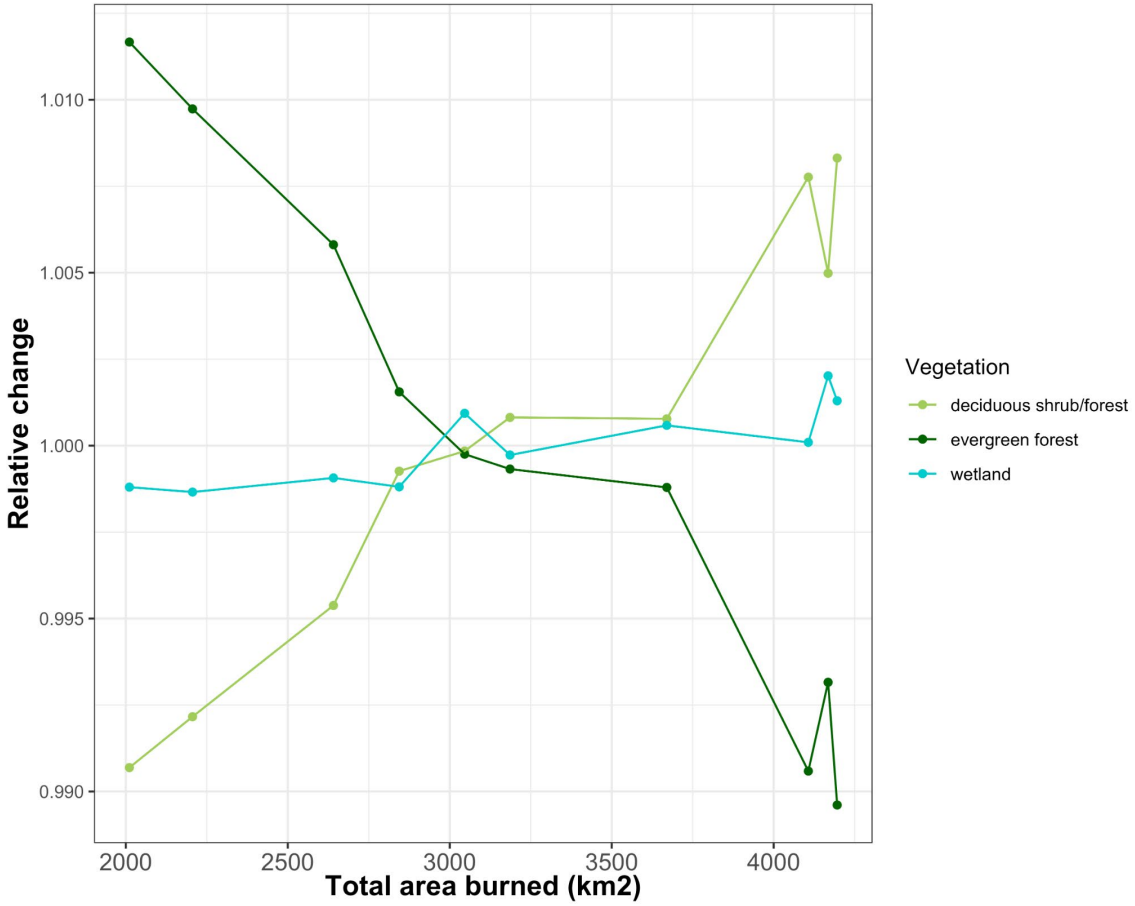


Figure 55. Projected relative change in vegetation groups as a function of total area burn from 2017 to 2100. Every point represents an entire simulation. Only vegetation groups that were correlated to total area burned are shown.

2.8.4.3 Effect of Climate Change and Vegetation Productivity on Ecotype Change

As explained in section 2.7.2.5, increases in precipitation and temperature increase thermokarst disturbance. However, changes in NPP and associated change in organic layer thickness affect rates of paludification. Across the 10 climate scenarios we tested, climate warming and increases in precipitation resulted in a 32.73 % increase in thermokarst disturbance on average (s.d. 28.49 %), compare to the baseline simulation (using historical mean probabilities of change) by 2100. As a result of this expansion of thermokarst features, boreal

lowland fen meadows and boreal lowland dwarf scrub bogs increased in areal extent by 26.44% (s.d. 21.87 %) and 19.70% (20.01%) on average by 2100 compared to the baseline

The increase in organic layer thickness simulated by TEM for boreal lowland fen meadows resulted in an increase in early and late paludification by 22.75% (s.d. 18.41 %) on average by 2100 compare to the baseline simulation.

2.8 Task 2.3

Assessing the relative effect of climate change, fire, and thermokarst disturbances on projected ecotype dynamics.

When evaluating the relative effects of climate change, fire, thermokarst, hydrology, and human activities interact to compound or obscure the effects of climate change, and that these interactions vary across the landscape. Boreal ecosystems form a diverse and highly patchy mosaic in central Alaska in response to a wide variety of biophysical drivers. While 67% of the study area had changes in ecotypes over the entire 68-yr interval, recovery after disturbance across the patchy mosaic of differing-aged disturbances led to a remarkably stable overall composition of ecotypes over time, although there were some large fluctuations for a few ecotypes among time-intervals. Significant ($P<0.05$) changes were found for only for 6 of 61 ecotypes during 1949-2017, mostly from a large increase in Lowland Wet Low Scrub (from 1.1% to 12.1%) associated with a large decrease in Lowland Post-fire Scrub (from 30.2% to 10.1%), while Lowland Fen Meadow (from 3.0 to 4.1%), Lowland Human-modified Scrub (from 0.0 to 0.3%), Lowland Wet Tall Scrub (from 0.2% to 1.6%), and Lowland Wet Mixed Woodland (1.1% to 2.4%) had small but consistent increases. By far, most of the areal change was associated with fire and post-fire vegetation succession, while thermokarst and river erosion and deposition also affected substantial areas during the three time intervals. Thermokarst was unique in that it showed a consistent increase over time in comparison to the highly variable effects of fluctuating fire and river dynamics over time. Thus, while fire is much more widespread, thermokarst is becoming increasingly more transformative, with almost no recovery toward initial ecotypes within the 68-yr observation period.

Climate is projected to warm by 4-6 °C in central Alaska over the next century, with precipitation increasing modestly. We accounted for the projected climate change in our state-transition modeling by using increases in summer temperatures, as quantified as summer thawing-degree days, to increase the rates of ecotype transitions, based on the widely accepted assumption/concept that climate change will increase rates of change. In our modeling, the effects of climate warming on overall net changes in ecotype abundance from 2017 to 2100 were relatively small from RCP4.5 (12.4%), and the RCP8.0 (14.7%) temperature models compared to the time model (11.5%) based on historical change rates. This indicates that temperature alone is not a significant driver of ecotype changes over the next century. However, when transition rates were adjusted for anticipated positive and negative feedbacks on ecological and geomorphic drivers of change, net change was nearly three times higher for the driver-adjusted RCP6.0 temperature model (30.6%). The relative importance of fire, thermokarst, and hydrology on landscape change are discussed below.

Fire was by far the largest driver of landscape change, affecting 47.3% of the region overall from 1949 to 2017. When the post-fire scrub present in the 1949 period was used to infer fire occurrence shortly before then, we estimate that 49% of the area was burned during 1920-1948 and thus 72.1% of the area (some reburned) has been fire-affected since ~1920. We speculate the unusually large extent of fires during 1920-1948 was due to human-caused fire during a time of extensive settlement, mining, and steamboat traffic in the early 1900s. A large fire on the Tanana Flats reportedly occurred in 1941. Also, indigenous peoples reportedly purposely set fire for habitat manipulation. This early large fire extent set the stage for subsequent: (1) diminished fire activity as fire-susceptible ecotypes were diminished; (2) a large decrease in Lowland Post-fire Scrub; (3) a large increase in Lowland Wet Needlefeaf Forest

from post-fire succession that provided renewed fuel buildup for later fires; and (4) the prevalence of mid- to late successional upland forests during recent time intervals. The large extent of early fires and indistinct trends during recent periods is at odds with recent analyses of fire history that indicates that fire frequency and extent has substantially increased since the 1980s, while the proportion of human-caused fires has remained relatively low in the last few decades (Kasischke et al., 2005; 2010). Distinguishing between short-term (decadal) and long-term (centennial) effects are important, however. Our historical analysis found large variations in fire-affected areas among years, showing the effects that large fire years, or periods of frequent fires, have on ecotype abundance. There was little difference in fire occurrence among the decadal time-intervals, however. Over the long term, the extremely patchy nature of the diverse mosaic of boreal ecosystems of varying ages of post-fire disturbance and recovery causes the gain and loss in ecotypes to balance out without long-term directional trends. This is consistent with the results of our state-transition modeling that showed little direction change in fire-affected ecotypes, in part because the model used transition rates based on long-term averages (1949-2017) and was not able to incorporate effects of unpredictable extreme fire years.

The link between fire frequency and severity to climate change in the study area is difficult to quantify because of the large role of human in fire initiation and suppression. Our historical analyses show a much higher abundance of fires early in the 1900s, presumably due to both more human-caused fires and lack of fire suppression. Even now a large percentage of the fires in the study area are human caused, part of which were initiated by military training activities. The Oklahoma Impact Area in the center of DTAW has fires almost every year (Figure 41C). Because the training lands have substantial human settlements and infrastructure fires in the area are controlled. In our modeling approach, we allowed fires to increase slightly in proportion to projected TDD increase (default condition) as we had no basis for projecting increased or decreased fire frequency.

Thermokarst is typically associated with ice-rich permafrost, especially in lowland environments that frequently have organic-rich silty soils (Jorgenson et al., 2008). In our study, thermokarst (lowland bogs and fens) affected only 6.0% of the overall area by 2017, but nearly doubled from 3.7% area in 1949. Thermokarst was mostly located on the Tanana Flats portion of the study area, but also occurs in the loess belt near Eielson AFB and in valley bottoms in the YTA. The estimate for our study area is similar to the 5% estimated for thermokarst extent across the broader zone of discontinuous permafrost in Alaska (Jorgenson et al., 2008), but is much lower than the thermokarst extent of 47% estimated for a small rapidly degrading area observed on the Tanana Flats (Jorgenson et al., 2001b).

The state-transition models project a doubling of thermokarst extent by 2100 for the time model (11.2%), RCP4.5 temperature model (11.7%), and RCP8.0 temperature model (12.0%), and a four-fold increase for the rate-adjusted RCP6.0 temperature model (25.8%) based on the abundance of the various thermokarst associated ecotypes (see examples in Figure 56). Areas with stable permafrost, based on permafrost-ecotype associations, are projected to decrease slightly in area from 58.5% in 2017 to 53.0% in the time model, 52.5% in the RCP4.5 temperature model, and to 52.0% in the RCP8.0 model, and by a third to 36.6% in the rate-adjusted RCP6.0 temperature model. Our projected loss in permafrost is similar to the projected reduction of 48% in permafrost in the Intermontane Boreal region in Alaska by Pastick et al. (2015) based on the intermediate A1B scenario. Our projected permafrost loss, however, is much slower that results of permafrost thermal modeling by SNAP (http://data.snap.uaf.edu/data/IEM/Outputs/GIPL/Gen_1a/) that indicates nearly all permafrost (MAAT at 3 m depth >2 °C) is

eliminated by 2100 in the study area. Permafrost temperature modeling by Panda et al. (2014) for Denali National Park, which has similar terrain on its northern portion, also projects nearly total loss of permafrost in the region by 2100 based on a 5-GCM composite climate dataset for the A1B emission scenario.

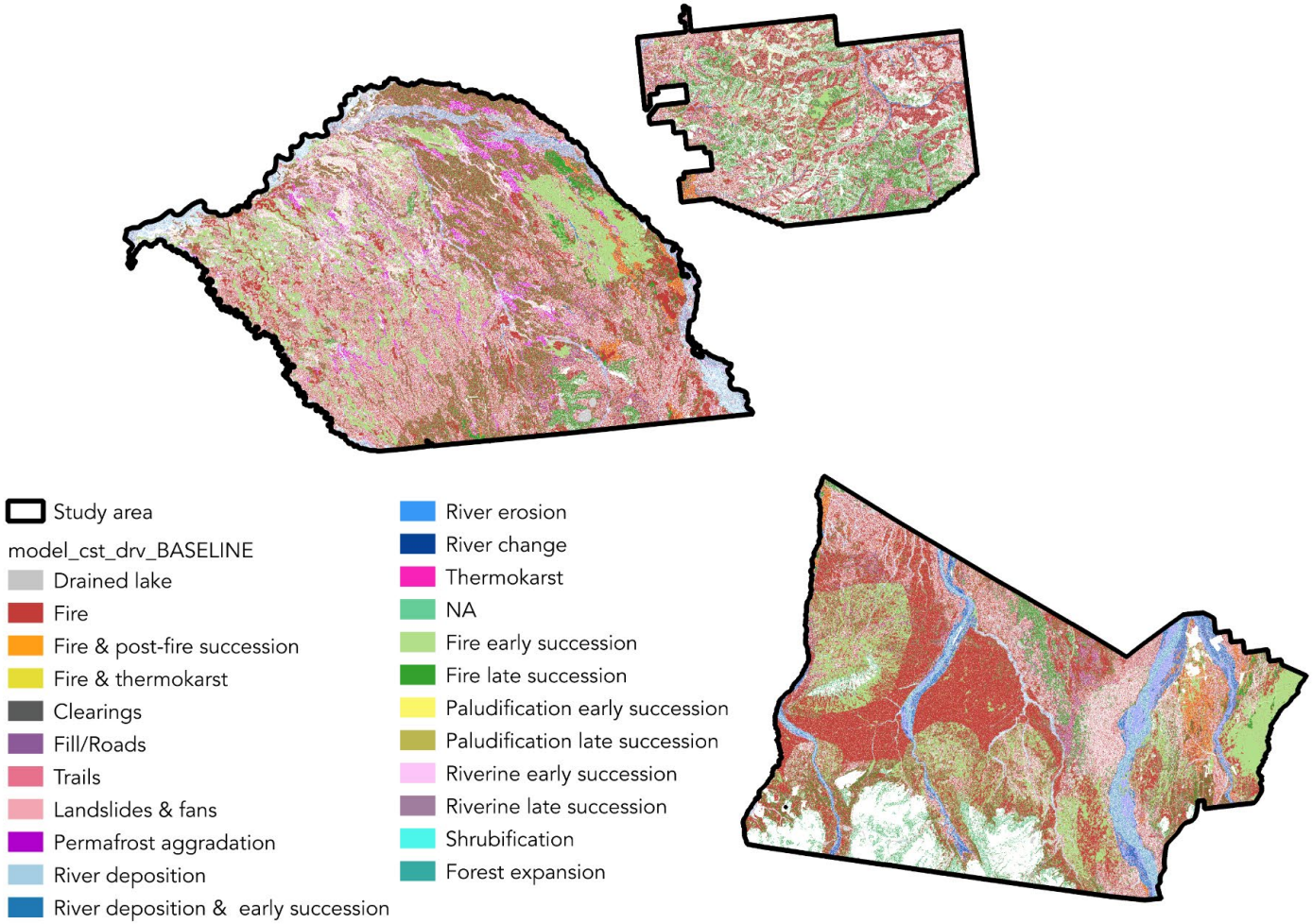


Figure 56. Vulnerability map for a moderate warming scenario (i.e. IPSL-CM5A-LR model for RCP4.5 emissions scenario, warming trend of 2.7 °C/century). Colors locate pixels that experienced land cover change between 2017 and 2100, and the driver of this change.

The large differences in permafrost loss among models based on very different approaches reveal the large uncertainty inherent in projecting permafrost responses to climate. First, there are strong negative feedbacks associated with vegetation structure and positive feedbacks from surface water that can cause mean annual surface temperatures to vary as much as 12 °C among ecotypes, an effect roughly twice as strong as expected climate warming (Jorgenson et al., 2010). Of particular interest is the resilience of permafrost associated with Lowland Bog Tussock Scrub (4.3% of area in 2017) because it has the lowest mean annual ground temperatures, it recovers quickly after fire, and it has been shown to persist in areas with mean annual air temperatures of up to +2 °C. Second, permafrost degradation in thermokarst bogs and fens is strongly driven by ground water, which is less affected by air temperatures (Jorgenson et al., 2020). Third, extreme precipitation events/summer are likely to contribute to permafrost degradation (Douglas et al., 2020). Fourth, the amount of ground ice greatly affects latent heat contents and slows the rate of soil thaw, which is largely unaccounted for in spatial thermal modeling. In these respects, historical rates of permafrost thaw provide a strong foundation for constraining projections of future changes because these factors are inherent in the historical observations.

The interactions between fire and thermokarst also are difficult to quantify. In our historical analysis, both fire and subsequent thermokarst combined as a driver contributed only 14% of the area affected by thermokarst. This is consistent with our observations that most thermokarst results from lateral thawing along the margins of thermokarst bogs and fens. In previous studies, however, in an earlier SERDP supported study (RC-2110), we found fire caused immediate (within a few years) thermokarst and led to forested ground collapsing below water level on Tanana Flats (Nossov et al., 2013; Douglas et al., 2016). Climate can also play a role, with thermal modeling indicating that fires during cold periods (1960s) have little effect on permafrost stability compared to fire during warmer (2010s) periods (Nossov et al., 2013).

Fluvial processes create highly dynamic environments associated with channel erosion and deposition, overbank flooding, and primary succession (Viereck et al., 1993; Van Cleve et al., 1996; Brown et al., 2020). In our study, riverine ecotypes covered 7.8% of the total area in 2017, while river erosion, deposition, and vegetation succession affected 1.2% of the total area, indicating the floodplains were highly dynamic. Interestingly, most of the change in total area during 1949-2017 resulted in loss of early successional Riverine Dry Grass Meadow and Riverine Dry Barrens (-0.5%) and gain of River water due to highly dynamic channel migration on braided gravelly floodplains near the mountains. In meandering floodplains with moist, silty overbank deposition, most ecotype loss was associated with loss of late-successional Riverine Moist Mixed Forest (-0.7%) due to erosion and late succession transition to Riverine Moist Mixed Forest, and loss of Riverine Moist Barrens (-0.2%) and Riverine Moist Tall Scrub (-0.3%) due to channel migration and early succession. We attribute the unusually large gain in Riverine Moist Needleleaf Forest (1.0%) to late succession of vegetation after a large proportion of this ecotype was cut to fuel steamboats along the Tanana River. We speculate the loss of highly disturbed gravelly barrens and the increase in early successional vegetation may be related to changes in the discharge of glacial rivers or recovery from past large flood events. While we were not able to explicitly link changes to extreme precipitation events, they undoubtedly play a major role in large, short term shifts in riverine extent.

2.9 Task 3.1

Assessment of wildlife use of habitats affecting vulnerability to change.

2.9.1 Overview of the Wildlife Analyses

A key aspect of linking potential ecotype change due to climate warming is to identify what species are associated with different habitat types so future projections of habitat change can also provide insight into habitat availability. For this Task, assessments of wildlife species, habitats, soundscapes, and photographic transects collectively provide methods, information, and results to support training land planning to test management strategies for wildlife and ecosystem conservation.

Here, we identify potentially vulnerable wildlife species based on multiple criteria such as the degree of habitat specialization, designated game and subsistence status, recognized vulnerability from small population size, recent habitat decline, potential future habitat decline, and other factors. We also identify patterns of soundscapes and identify locations where human activities may be introducing undue noise into the environment as a generally overlooked disturbance element. Additionally, we review our methods and results of conducting a low-level aerial photographic transect of the study area to provide a rich set of images of representative landscape conditions to serve as a baseline for future replication for change-detection studies.

This part of Task 3.1 contributes directly to Project Task 4 (Developing technologies and methodologies and transferring results into operational routines useful for training land planning and develop adaptive management strategies to minimize impacts to vulnerable populations).

2.9.2 Wildlife Species occurrence and Habitat Projections

2.9.2.1 What is Presented in This Section

Presented in this section are methods, results, and management implications of the wildlife species evaluations and wildlife habitat projections on the following topics: (1) overall work flow; (2) identification of wildlife species of occurrence in the project area; (3) the relationships of wildlife species to ecotypes, constituting each species' habitat; (4) projections of species habitats over previous, current, and future time periods, under the various ecotype projection models presented earlier in this report; (5) habitat trends of key selected wildlife species and species groups, and patterns of species richness among ecotypes; and (6) overall discussion of the results and their potential implications for planning and management.

The set of wildlife species in this analysis include all non-fish vertebrates known or expected to occur in the study area, that is, amphibians, birds, and mammals. Only one amphibian species occurs in the study area (wood frog), and no reptiles (lizards or snakes) occur. The analysis does not include fish or invertebrates.

2.9.2.2 How This Section Relates to Project Objectives and Hypotheses

The outcome of this part of the project pertains to much of the four main project objectives: 1) assessing habitat vulnerability to climate change and identifying the factors that drive vulnerability; 2) expanding our understanding of the spatial variability in drivers of vulnerability across a species' range; 3) improving our assessments of the relationship between changing climate and key ecological processes such as fire regimes, hydrological regime or food webs; and 4) developing methodologies, tools, and guidance to translate research on these issues into practical information for improving adaptive management of sensitive habitats to meet land management conservation objectives.

The outcomes also are useful for explicitly testing project Hypothesis 3, that wildlife habitats will be affected by climate, fire, thermokarst, and other drivers, resulting in increases and decreases of populations dependent on those habitats, but some species may have some degree of ecological flexibility to help buffer habitat declines.

The results presented in this section generally constitute working hypotheses of species-habitat relationships and future impacts of disturbances and climate change, as source material was not available to rigorously inventory each species' occurrence and to quantify species-ecotype relationships specific to the study area, such as with population size, density, and trend. Instead, such relationships had to be mostly inferred from general species habitat descriptions and from studies conducted elsewhere, as detailed below. We expect that some results and projections may change and be improved over time as new research results and field surveys of wildlife species-habitat relationships become available. With this in mind, we designed the analyses to foster updating of results. The major data tables presenting species-habitat relationships and calculations of habitat changes are archived at CRREL and are also available from Task lead Marcot upon request.

2.9.3 Overall Work Flow of the Wildlife Analyses

2.9.3.1 Overall Objectives

The overall objective of this portion of the study was to determine wildlife species-habitat relationships based on categories of ecotypes within the study area and project past and future habitat areal extents for individual species and selected species groups of potential conservation and management interest.

2.9.3.2 Guiding Assumptions

The main assumptions underlying this analysis include the following:

- Each wildlife species' habitat can be characterized by denoting the collective set of ecotype categories that each species would use for their main life history needs, including breeding, feeding, and cover.

Not addressed is the occasional use by an individual of other ecotypes and environmental conditions during some behaviors of dispersal, exploration, or migration, except for our grouping sets of bird species that use the area only or mostly for "pass-through migration." Overall, such use has been little studied and quantified, if at all, explicitly for the set of wildlife species analyzed in this report.

- The species-habitat relationships thus identified are assumed to not change over time, particularly into future decadal time periods.

This assumption is made because there is no empirical basis by which to predict changes (adaptive shifts, behavioral plasticity) of each species' habitat selection behaviors under stress of disturbances and climate change impacts.

The obvious exception are invasive species, or species currently (or expected to be) expanding their range into the study area, where they might use habitat conditions different than they use elsewhere in their range outside the study area. However, this has not been well studied and still does not provide a basis for predicting future adaptive shifts in habitat selection behaviors for those species.

2.9.3.3 Overall Work Flow: Identifying Species-Habitat Relationships and Projecting Habitat Changes

The overall work flow is depicted in Figure 57. The initial step was to list the set of wildlife (amphibian, bird, and mammal species) known or expected to occur within the training land study area (see section A.2 below), and then determine which ecotypes each species uses as habitat (see section A.3 below). The lists of species and their ecotype-habitat relationships were compiled using a variety of sources (Appendix A.1), including external peer review, published literature and reports, various professional web sites, and results of two field seasons' of automated audio recordings in selected landscapes within the study area to help confirm species presence (see 2.9.6, Bioacoustics of Interior Alaska Training Lands, below). Subsequent analyses summarized here were all conducted separately for amphibians, birds, and mammals, and in some cases further subsets of species as detailed further below.

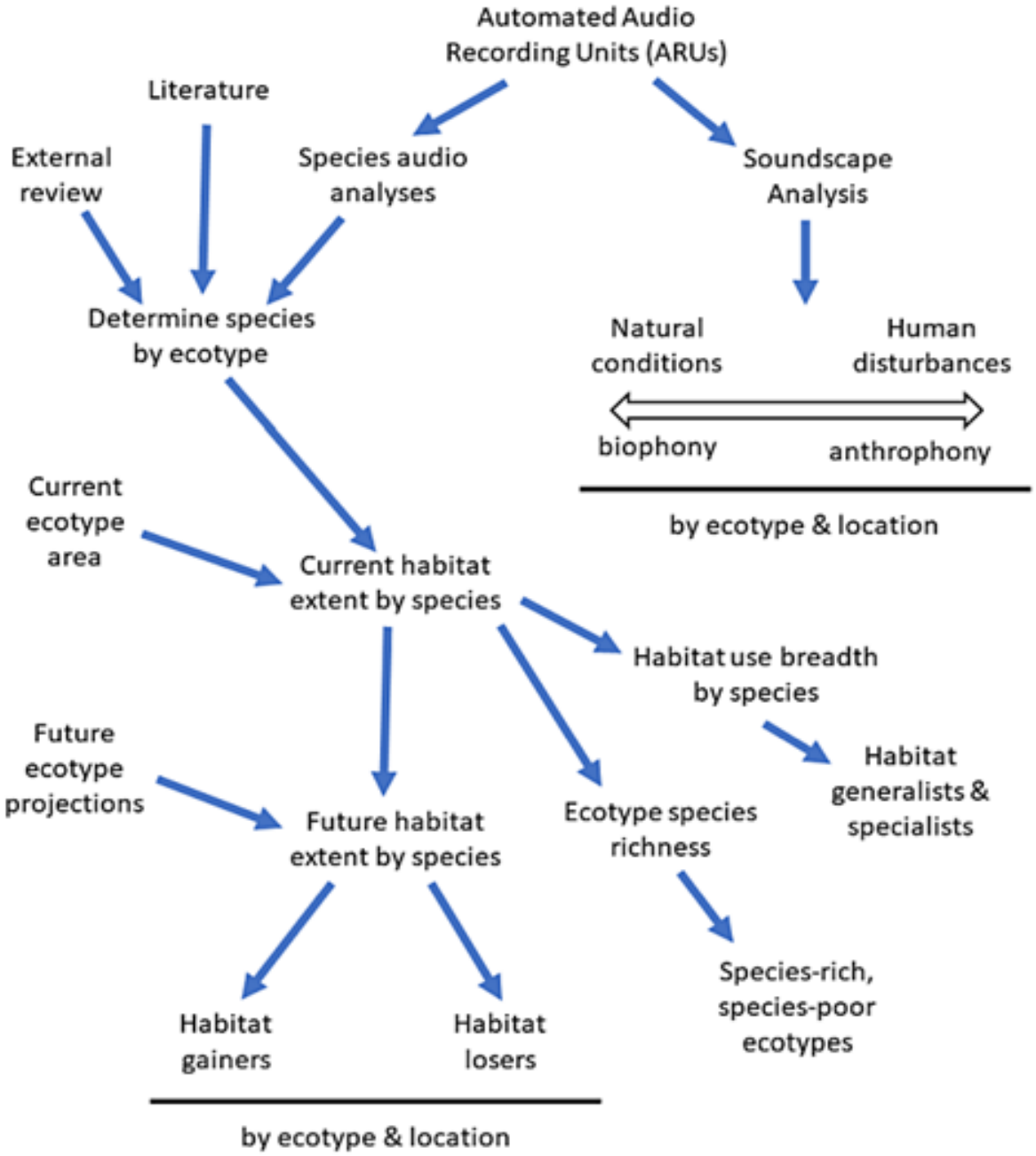


Figure 57. Flow chart of sources and use of information for determining the occurrence of wildlife species occurrence in the study area, their relationships to ecotypes, their current and projected habitat extent, wildlife habitat gainers and losers, wildlife habitat generalist and specialists, wildlife species-rich and species-poor ecotypes, and depictions of soundscapes in the training land study area. Note that multiple sources of information were used to determine species occurrence, including literature, peer reviews, use of field audio recordings, and direct observation.

Once the wildlife species lists and the species-ecotype relationships were developed, calculating the current habitat extent of each species was done by using the ecotype area data

provided by the evaluation of current ecotype coverage in the study area (see report section on ecotype area analyses). That is, the total current habitat of each species was the sum of the current area of each of the ecotypes the species uses as habitat.

Next, past habitat areas of each species were estimated by using the historic projections of ecotype areas, and future habitat areas of each species were estimated by using the state-transition models projecting future ecotype areas under four future scenarios (see report section on ecotype projections). Then, the percent change in habitat area for each species was calculated for historic to current periods, and, under each of the four ecotype projection scenarios, for historic to future and current to future periods. Species were then rank-ordered according to the percent changes of habitat over these time periods, by which to identify species most gaining habitat and those most losing habitat.

Further, tallying the number of ecotypes expected to be used by each species provided an index to wildlife species' habitat-use breadth. Species using the fewest number of ecotypes, that is, with the narrowest habitat-use breadth, were identified as habitat specialists, and those using the greatest number of ecotypes were identified as habitat generalists.

Additional community-level analyses were conducted based on the species-ecotype relationships information. These analyses included tallying the number of species (again, separately for birds and mammals; there was only one amphibian species occurring in the study area) using each ecotype, and then rank-ordering the ecotypes accordingly to identify those that are most species-rich and those most species-poor. Species-rich ecotypes were interpreted as those providing for the greater numbers of species, at least for part of the species' life needs. Also, the automated audio recordings (see section 2.9.6 Bioacoustics of Interior Alaska Training Lands, below) were further analyzed on a separate evaluation of so-called soundscape conditions for the selected landscapes used in that portion of the study. The soundscape analyses provided insights into which landscapes (and the associated selected ecotypes) consisted of more natural (biological) conditions, and which were more affected in terms of sounds created by human sources or disturbances. The potential impact of sounds on wildlife species is little studied in the training area, so this portion of the study provided initial working hypotheses of potential impacts from non-natural noise (e.g., from roads, aircraft, and other human disturbance events) and to help set a baseline from which potential future monitoring and research studies could be conducted on this topic.

The following sections provide further detail on methods and findings, and are summarized in terms of potential conclusions for management and planning considerations in the study area.

2.9.4 Wildlife Species Occurring in the Project Area

The initial step in this process was to list all amphibian, bird, and mammal species known or expected to occur in the study area, as outlined above. Multiple sources were consulted to develop the species lists (Appendix A.1).

2.9.4.1Amphibians

Only a single species of amphibian, wood frog (Rana sylvatica, family Ranidae), occurs in the study area (Figure 58), as noted in Chester (2016). They are listed as a “species of concern” in some areas.

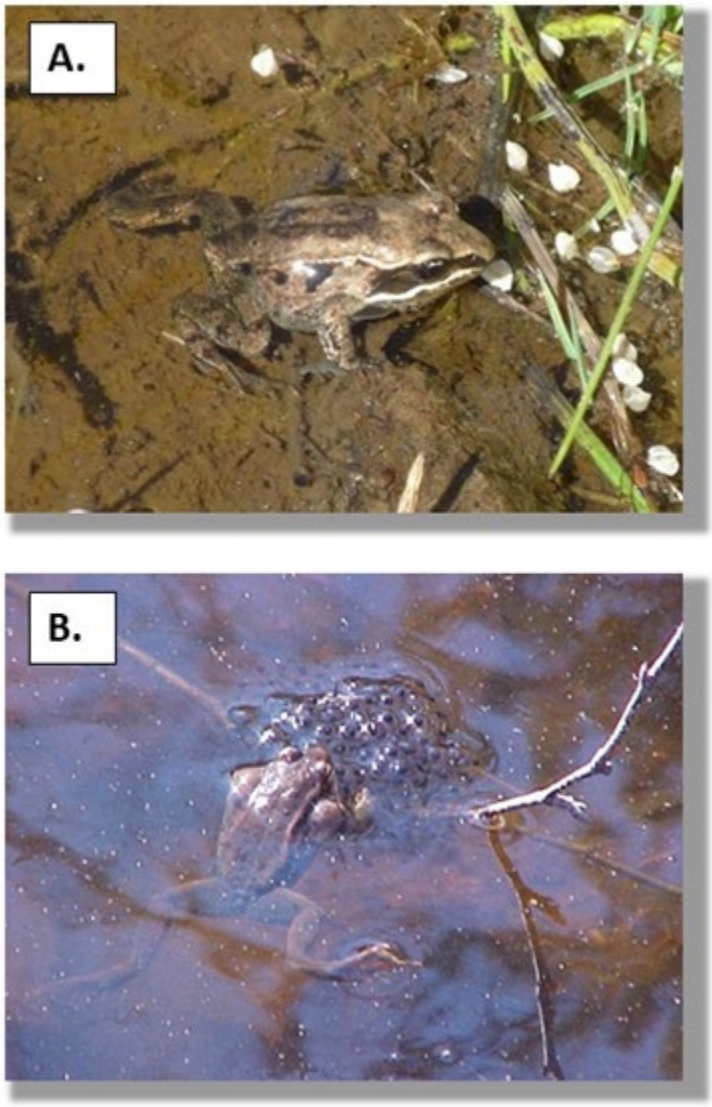


Figure 58. Wood frog (Rana sylvatica), family Ranidae. (A) Adult wood frog (source: National Park Service; photo by Jakara Hubbard), (B) Wood frog with egg mass in pond (source: USAG-FWA Natural Resources). Public domain photo from: https://www.nps.gov/media/photo/gallery-item.htm?pg=919109&id=194a4069-64f5-4004-a207-fcfd63f62f57&gid=AB7AC107-EBD4-441D-8723-3559B3490DE3.

2.9.4.2 Birds

Mostly breeding resident bird species.

-- Some 124 species of birds were identified as occurring in the study area as more than just occasional or intermittent migrant pass-throughs or stop-overs, and included 20 game species and 5 subsistence species as identified by Alaska Department of Fish and Game (Appendix Table 1). The 124 species represented 33 taxonomic families (Figure 59).

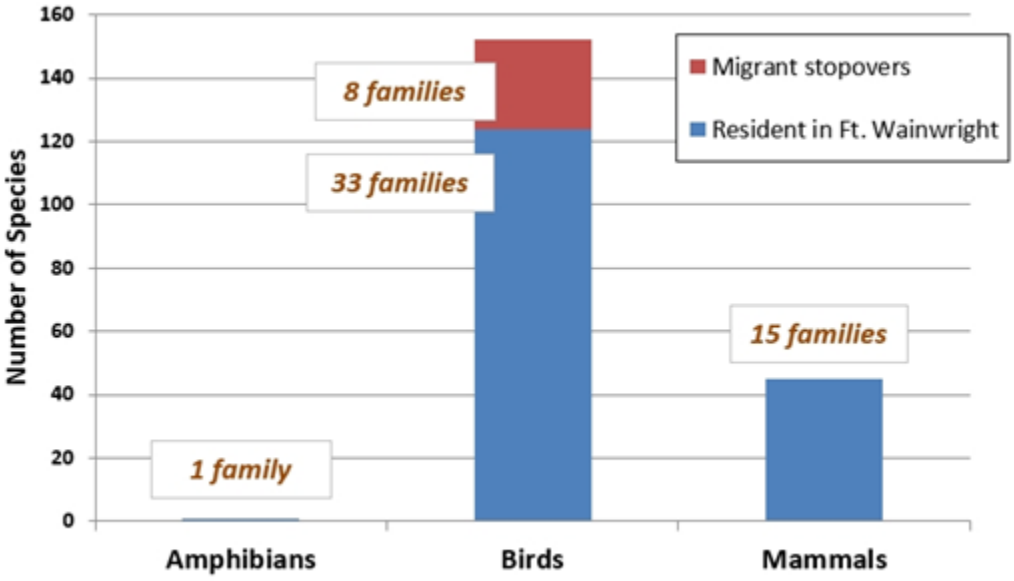


Figure 59. Numbers of species and taxonomic families of amphibians, birds, and mammals, by categories mentioned in the text.

Migrant stopover bird species.
-- An additional 27 bird species were identified as migrant stopovers that occur within the study area only during spring and/or fall seasons, generally enroute to or from breeding grounds further north (Appendix Table 2). These stopover species represented 8 taxonomic families (Figure 60), and generally consisted of waterfowl and shorebirds with just a few songbirds or woodland species (Appendix Table 2, Table 13).

Table 13. Categories of migrant stopover bird species (see Appendix Table 2) by habitat associations.

Migrant Stopover Group	Wetland, water associates	Wet open site associates	Dry open site associates	Woodland, forest associates	No. migrant stopover species
MSG1	X				9
MSG2		X			1
MSG3	X	X			10
MSG4			X		5
MSG5				X	1
MSG6		X	X		1
					27

Other suspected bird species.
-- A further list of 36 bird species, among 12 families, of suspected or hypothetical occurrence was investigated and rejected as at least currently occurring within the study area. This list was derived by comparing bird species listed in a previous study as occurring further north in the National Park Service's Arctic Network of northwest Alaska (Marcot et al., 2015).



Figure 60. Immature bald eagle (Haliaeetus leucocephalus, family Accipitridae) observed over the Tanana River within the study area. Although bald eagles were removed from protection under the Endangered Species Act, they are still protected under the Bald and Golden Eagle Protection Act (Alaska Department of Fish and Game, http://www.adfg.alaska.gov/index.cfm?adfg=baldeagle.management). Bald eagle is included on the list of species occurring within the study area. Photos by Bruce G. Marcot.

2.9.4.3 Mammals
Resident mammal species.
-- A total of 41 species of mammals among 15 families were identified as occurring in the study area (Figure 61), including 7 game species, 1 small game species, and 6 state subsistence species as listed by Alaska Department of Fish and Game (Appendix Table 3).



Figure 61. Muskrats (Ondatra zibethicus) occur broadly throughout subarctic Alaska and have been an important element in the fur trade. Photo by M. Torre Jorgenson.

Other suspected mammal species.
-- A further list of 9 mammal species, among 7 families, was investigated and rejected as at least currently occurring within the study area. The list of rejected mammal species is available from author Marcot upon request. This list was derived by comparing mammal species occurring in the National Park Service's Arctic Network of northwest Alaska (Marcot et al., 2015) and from discussion with local biologists hypothesizing on the potential but unverified occurrence of some species.

Museum specimens of mammal species.
-- Recorded, mapped occurrences of selected mammal species were provided from the University of Alaska Fairbanks, Museum of the North (A. Gunderson, Collection Manager, pers. comm.). As examples, museum location records of singing vole and tundra shrew suggested occurrence within the study area (Figures 62 and 63) and thus both species were included in the mammal species list (Appendix Table 3).

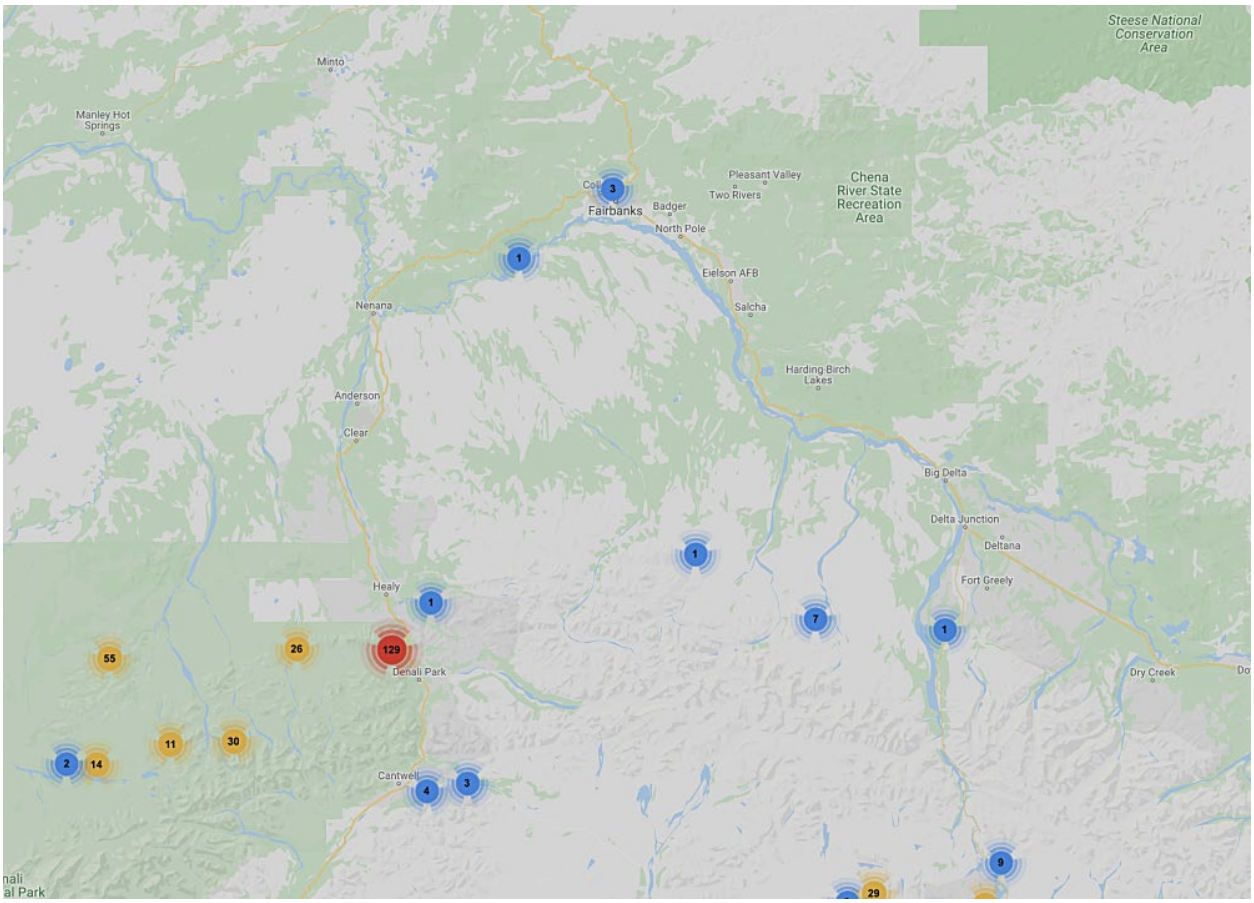


Figure 62. Museum occurrence locations of singing vole (*Microtus miurus*) denoting occurrence within the study area. Source: A. Gunderson, Collection Manager, Museum of the North, University of Alaska Fairbanks, contacted April 2021.

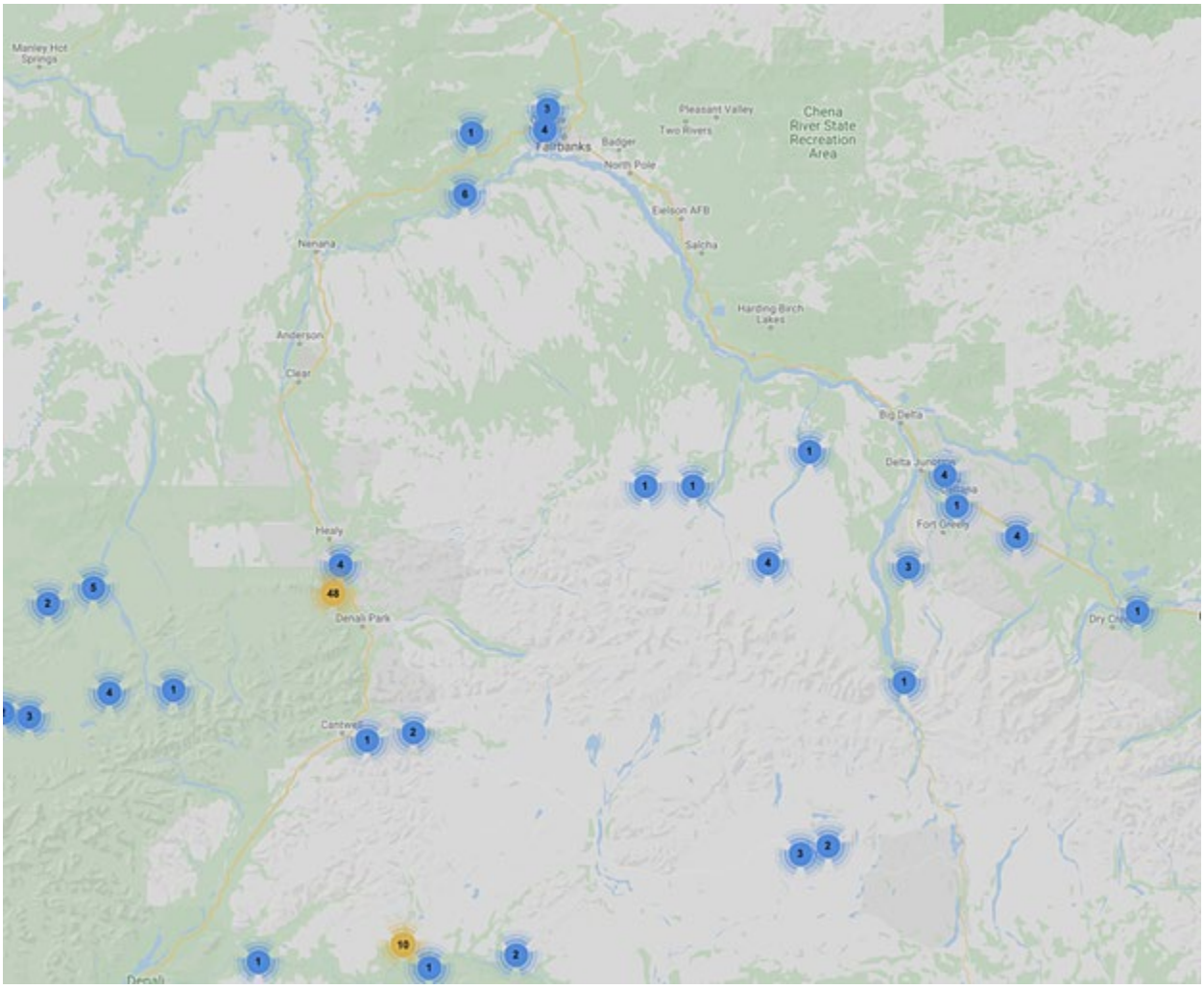


Figure 63. Museum occurrence locations of tundra shrew (Sorex tundrensis) denoting occurrence within the study area. Source: A. Gunderson, Collection Manager, Museum of the North, University of Alaska Fairbanks, contacted April 2021.

2.9.4.4 Total Wildlife Species

In sum, a total of 193 species of amphibian, birds, and mammals were included in the species occurrence lists, consisting of 166 mostly resident species and 27 avian migrant stopover species. A total of 57 taxonomic families of species were listed, including 49 families of mostly resident species and 8 families of avian migrant stopover species (Table 14).

Table 14. Numbers of wildlife species and taxonomic families included in the habitat projections.

	Amphibians	Birds	Mammals	TOTAL
Resident species	1	124	41	166
Migrant stopover species	0	27	0	27
Families of resident species	1	33	15	49
Families of migrant stopovers	0	8	0	8

2.9.4.5 Sign of Species Occurrence

Of value to determining presence of wildlife species within the study area is the variety of signs left behind by their various behaviors and functions, some of which were used upon opportunistic encounter in the current study to verify presence (Figures 64 and 65). References for identifying tracks, scats, and other wildlife signs includes Elbroch and McFarland, 2019; Halfpenny, 2019a, b; and Murie et al., 2005.)

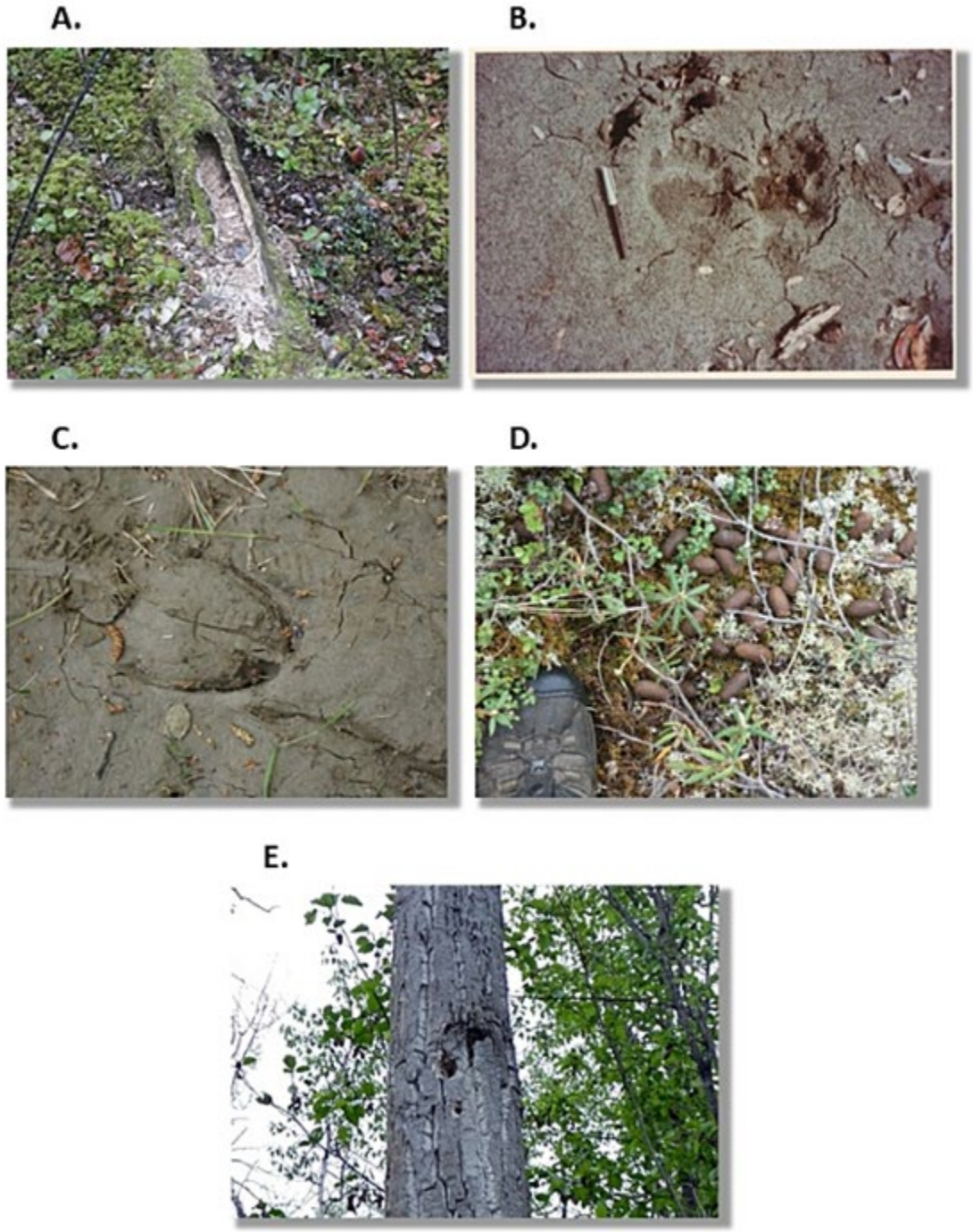


Figure 64. Examples of wildlife sign found within the study area: (A) down log torn apart likely by an American black bear (Ursus americanus) on the hunt for grubs to eat; (B) tracks of American black bear along a pond shoreline; (C) track of moose (Alces alces) along a river bank; (D) scat (droppings) of moose in an open black spruce woodland); (E) cavity and bark shredded in a cottonwood (Populus balsamifera) tree likely by an American three-toed woodpecker (Picoides dorsalis). Photos by Bruce G. Marcot.

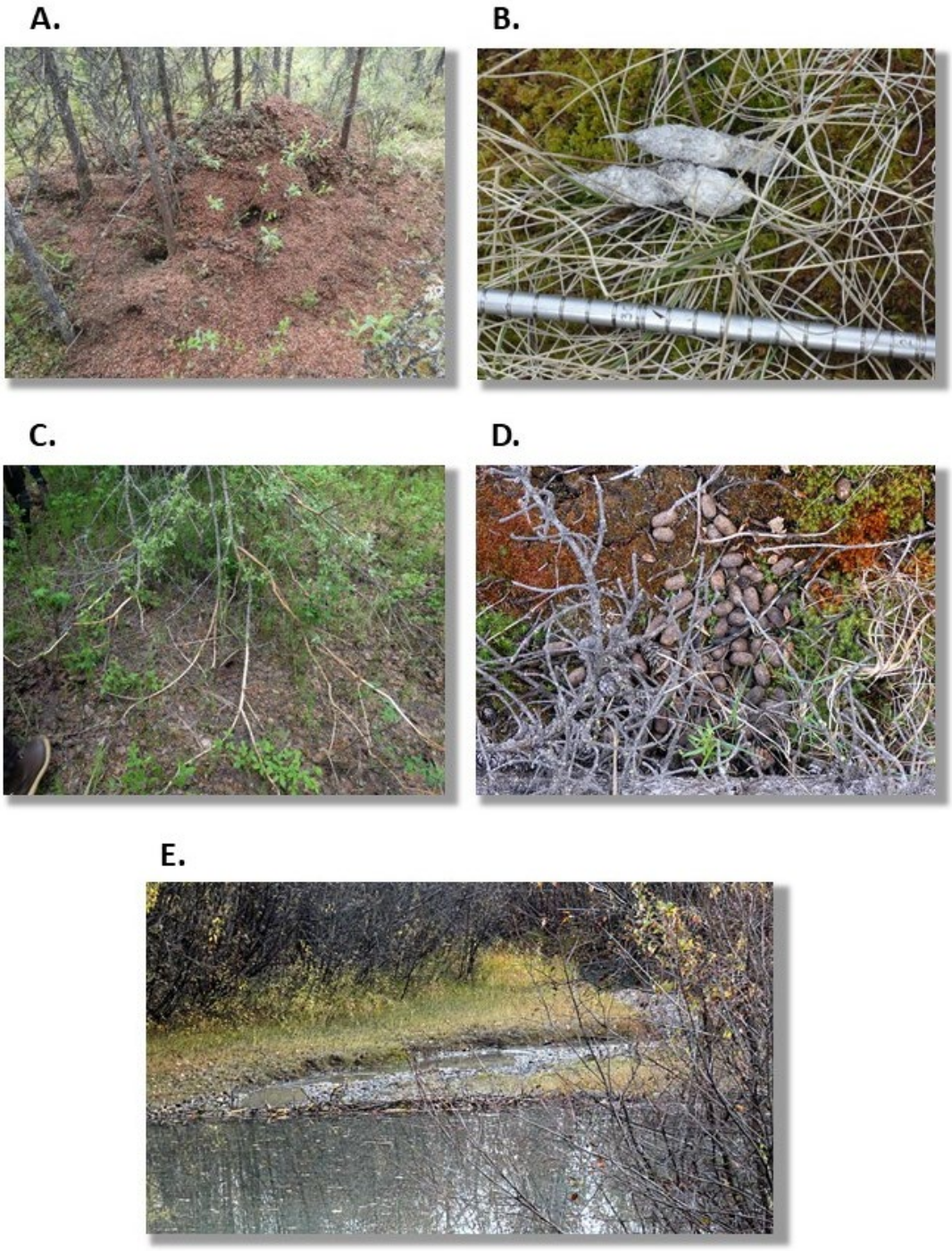


Figure 65. Further examples of wildlife sign found within the study area: (A) midden with multiple burrow entrances of an arctic ground squirrel colony (Urocitellus [Spermophilus] parryii) including a cache of spruce cones on top, in black spruce forest; (B) scat (droppings) of red fox (Vulpes vulpes); (C) browse of branches by snowshoe hare (Lepus americanus) who remove bark from low-hanging small branches of deciduous trees; (D) scat pile of snowshoe hare; (E) stream dam created by American beaver (Castor canadensis). Photos by Bruce G. Marcot.

2.9.4.6 Taxa Not Considered

This project was conceived to focus the analysis on wildlife species of the USAG-AK managed training lands study area. Faunal groups that were not included in the project analyses are invertebrates and fish.

- Invertebrates.
  -- Invertebrates can play key functional roles such as providing for health of riparian forests (Tolkkinen et al., 2020) and for pollination of flowering plants (Figure 66). Populations of various invertebrate taxa can be affected negatively (James et al., 2011) or positively (e.g., Nelson et al., 2021, Sandström et al., 2019) by human activities and by climate shifts (Pureswaran et al., 2015). Insect pest species are playing increasingly important roles in the region, such as with outbreaks of defoliators on trembling aspen (Boyd et al., 2019). Some moth species that induce tree mortality also can serve to reduce carbon storage and forest soil decomposition (Sandén et al., 2020). A fuller accounting of the status, potential impacts on populations, and ecological roles of invertebrates of the study area is beyond the scope of this report.



Figure 66. Example of a potentially key pollinator of flowering plants of the region is this butterfly, a common alpine (Erebia epipsodea, family Nymphalidae). Photo by Bruce G. Marcot.

- Fish:

-- Fish provide for important subsistence harvests for rural communities in the region (Fall, 2016), as well as providing important food sources for brown and black bears (Gende et al., 2001), bald eagles, kingfishers, and other species. Salmon in particular can serve as a source of nutrients for riparian forests (e.g., Helfield and Naiman, 2002, Siemens et al., 2020). As with invertebrates, a fuller accounting of the status and potential future changes in fish species and populations is beyond the scope of this report.

- Invasive and Introduced Species:

-- Not specifically included in the species lists for this project, except for a few minor exceptions, are invasive and introduced wildlife species. In a sense, the concept of invasive species becomes muddled when species may extend their distributional range as environmental conditions beyond current boundaries become more suitable for their persistence; the question becomes whether it is a natural change and expansion of their distribution, or an invasive expansion. Typically, however, invasive species are more often thought of as incursions from well outside their regional distributions, particularly when introduced by human intervention, and therein lies the overlap with deliberately or inadvertently introducing species.

Some invasive species may be difficult to detect, inventory, and monitor. An example from the invertebrate world is that of non-native anecic earthworms (Lumbricus terrestris) that have been shown to reduce germination and survival of boreal trees in Quebec, Canada (Drouin et al., 2014) and can adversely affect soil ecology in other boreal regions (Frelich et al., 2019).

Other invasive invertebrates difficult to monitor include species of ticks (Acari: Ixodidae) entering the region as ectoparasites of domestic dogs in Alaska and that could adversely affect human and animal health (Durden et al., 2016). In the Fairbanks area, recent reports of tularemia have been reported from hares, presumably originated from the native species of squirrel tick (Ixodes marxi; http://www.adfg.alaska.gov/static/species/disease/pdfs/tularemia_pet_owners _fact_sheet.pdf). Also, at least two non-native ticks (brown dog tick, Rhipicephalus sanguineus, and American dog tick, Dermacentor variabilis) have been documented as established in the Fairbanks area (http://www.adfg.alaska.gov/static/species/disease/pdfs/tularemia_pet_owners_ fact_sheet.pdf). Ticks can pass disease to hares and other wildlife such as moose, and eventually even to people, with potentially fatal results.

Introduced and invasive insects causing damage to some of the native forests of the study area include the amber-marked birch leaf miner (Profenusa thomsoni) that has been feeding on and defoliating native Alaska paper birch (Betula neoalaskana). Another species is the European yellow underwing (Noctua pronuba), the caterpillars of which feed on foliage and stems of a variety of horticultured and native plants of the region.

Among the set of wildlife taxa assessed in this report, several species may be expanding their range into, or further within, the study area, likely as a function of regional warming and associated increased access to suitable habitat conditions including food sources. These "naturally-invasive" species, so to speak, include black-billed magpies (Pica pica) which can be human commensals and occur near habitations, scavenging for food bits. Magpies seem to be recently expanding their range through much of Alaska (https://www.gi.alaska.edu/alaska-science-forum/magpies-more-common-sight-throughout-alaska). Magpies also increasingly serve as scavengers on moose carcasses, along with common ravens (Corvus corax), brown bears (Ursus arctos), black bears (Ursus amerianus), gray wolves (Canis lupus), and coyotes (Canis latrans; Lafferty et al., 2016). Coyotes themselves may be expanding their range in the region, possibly as a function of more moderating climates (Pozzanghera et al., 2016).

- Introduced species:

--Included in the mammal species list is bison (Bison bison). As reported by Anderson et al. (2000), bison are known to be introduced and to occur in natural habitats on DTAW and DTAE near Fort Greely. However, perhaps a more appropriate descriptor for the species in the region would be reintroduced, as it is known from archaeological surveys to have occurred in the

Tanana River valley dating ca. 14,000 to 9,000 B.P. (Holmes, 2001). Bison also have been introduced further southeast outside the study area https://www.adfg.alaska.gov/index.cfm?adfg=plainsbison.main).

2.9.5 Wildlife Species-Ecotype Relationships

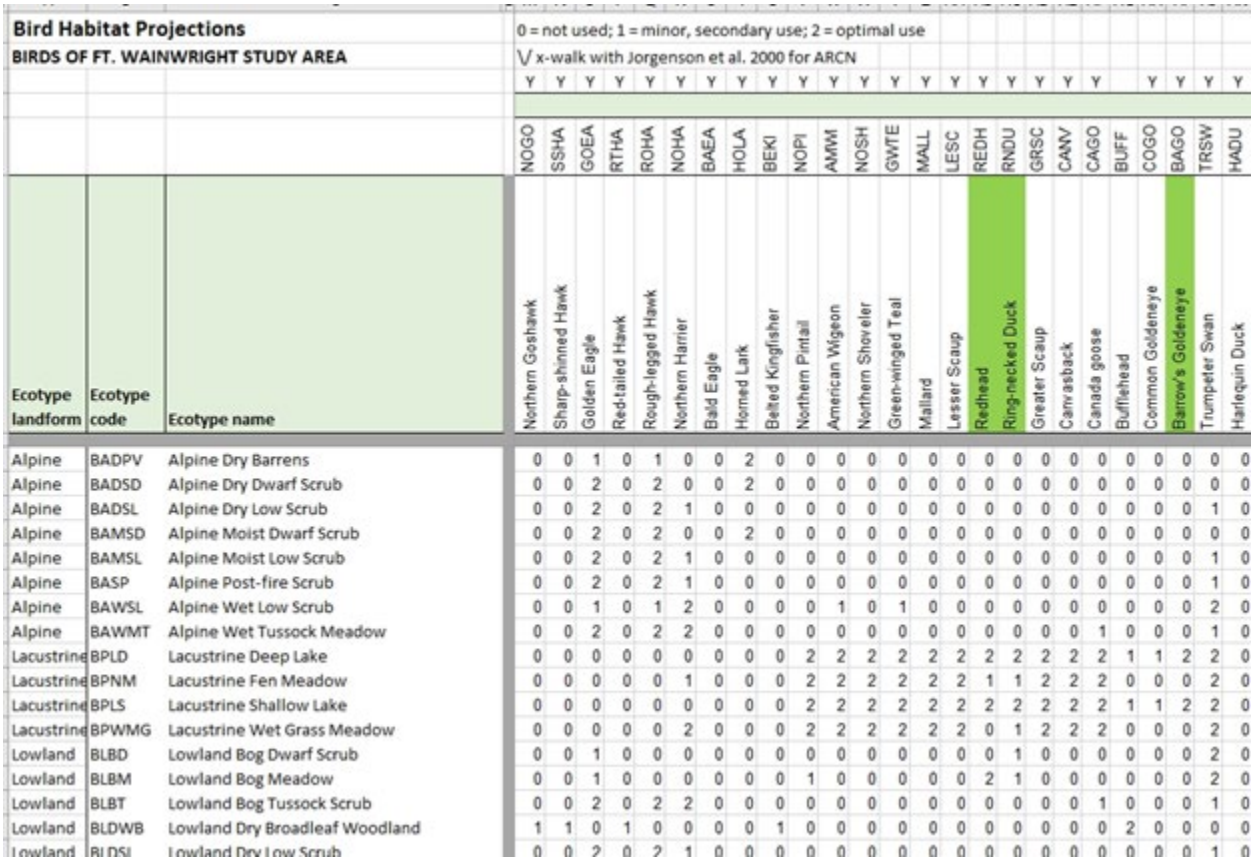
This section presents the procedures and results of developing tables of wildlife species-ecotype relationships to depict habitat conditions of each species, and current patterns of species richness among ecotypes. In general, the methods follow existing procedures for relating wildlife species to environmental conditions such as have been used in northwest Alaska (Marcot et al., 2015), Washington and Oregon (Johnson and O'Neill, 2001), the interior Columbia Basin (Marcot et al., 1997), and elsewhere.

2.9.5.1 Ecotypes Used

A set of 61 ecotypes identified as occurring within the study area were used as the basis for relating wildlife species use. A 62nd ecotype, Riverine Post-fire Scrub, was added too late to be incorporated into the wildlife response analyses. However, this ecotype is most similar to the Riverine Moist Tall Scrub ecotype that was used in the wildlife analyses. Wildlife species associated with that type thus could also associate with Riverine Post-fire Scrub.

2.9.5.2 Use of Ecotypes by Wildlife Species

The procedures generally entailed denoting one of three ordinal use levels of each ecotype by each wildlife species. The ordinal use levels are denoted in the wildlife-ecotype relationships tables as: 0 = not used, 1 = secondary use, 2 = primary use (e.g., see Figure 67). Secondary and primary use levels represent expected degrees of resource values sought and required by individuals. The species-ecotype relationships tables denoted 166 species of amphibian, birds, and mammals (Appendix Tables 1-2) by the 61 ecotype categories used here, thus totaling 10,126 entries (61 for wood frog, 7,564 for the 124 bird species, and 2,501 for the 41 mammal species).



Bird Habitat Projections			0 = not used; 1 = minor, secondary use; 2 = optimal use																							
BIRDS OF FT. WAINWRIGHT STUDY AREA			√ x-walk with Jorgenson et al. 2000 for ARCN																							
			Y	Y	Y	Y	Y	Y	Y	Y	Y	Y	Y	Y	Y	Y	Y	Y	Y	Y	Y	Y		Y	Y	Y	Y
			NOGO	SSHA	GOEA	RTHA	ROHA	NOHA	BAEA	HOLA	BEKI	NOPI	AMWI	NOSH	GWTE	MALL	LESC	REDH	RNDU	GRSC	CANV	CAGO	BUFF	COGO	BAGO	TRSW	HADU
Ecotype landform	Ecotype code	Ecotype name	Northern Goshawk	Sharp-shinned Hawk	Golden Eagle	Red-tailed Hawk	Rough-legged Hawk	Northern Harrier	Bald Eagle	Horned Lark	Belted Kingfisher	Northern Pintail	American Wigeon	Northern Shoveler	Green-winged Teal	Mallard	Lesser Scaup	Redhead	Ring-necked Duck	Greater Scaup	Canvasback	Canada goose	Bufflehead	Common Goldeneye	Barrow's Goldeneye	Trumpeter Swan	Harlequin Duck
Alpine	BADPV	Alpine Dry Barrens	0	0	1	0	1	0	0	2	0	0	0	0	0	0	0	0	0	0	0	0	0	0	0	0	0
Alpine	BADSD	Alpine Dry Dwarf Scrub	0	0	2	0	2	0	0	2	0	0	0	0	0	0	0	0	0	0	0	0	0	0	0	0	0
Alpine	BADSL	Alpine Dry Low Scrub	0	0	2	0	2	1	0	0	0	0	0	0	0	0	0	0	0	0	0	0	0	0	0	1	0
Alpine	BAMSD	Alpine Moist Dwarf Scrub	0	0	2	0	2	0	0	2	0	0	0	0	0	0	0	0	0	0	0	0	0	0	0	0	0
Alpine	BAMSL	Alpine Moist Low Scrub	0	0	2	0	2	1	0	0	0	0	0	0	0	0	0	0	0	0	0	0	0	0	0	1	0
Alpine	BASP	Alpine Post-fire Scrub	0	0	2	0	2	1	0	0	0	0	0	0	0	0	0	0	0	0	0	0	0	0	0	1	0
Alpine	BAWSL	Alpine Wet Low Scrub	0	0	1	0	1	2	0	0	0	0	1	0	1	0	0	0	0	0	0	0	0	0	0	2	0
Alpine	BAWMT	Alpine Wet Tussock Meadow	0	0	2	0	2	2	0	0	0	0	0	0	0	0	0	0	0	0	0	1	0	0	0	1	0
Lacustrine	BPLD	Lacustrine Deep Lake	0	0	0	0	0	0	0	0	0	2	2	2	2	2	2	2	2	2	2	2	1	1	2	2	0
Lacustrine	BPNM	Lacustrine Fen Meadow	0	0	0	0	0	1	0	0	0	2	2	2	2	2	2	1	1	2	2	2	0	0	0	2	0
Lacustrine	BPLS	Lacustrine Shallow Lake	0	0	0	0	0	0	0	0	0	2	2	2	2	2	2	2	2	2	2	2	1	1	2	2	0
Lacustrine	BPWMG	Lacustrine Wet Grass Meadow	0	0	0	0	0	2	0	0	0	2	2	2	2	2	2	0	1	2	2	2	0	0	0	2	0
Lowland	BLBD	Lowland Bog Dwarf Scrub	0	0	1	0	0	0	0	0	0	0	0	0	0	0	0	0	1	0	0	0	0	0	0	2	0
Lowland	BLBM	Lowland Bog Meadow	0	0	1	0	0	0	0	0	0	1	0	0	0	0	0	2	1	0	0	0	0	0	0	2	0
Lowland	BLBT	Lowland Bog Tussock Scrub	0	0	2	0	2	2	0	0	0	0	0	0	0	0	0	0	0	0	0	1	0	0	0	1	0
Lowland	BLDWB	Lowland Dry Broadleaf Woodland	1	1	0	1	0	0	0	0	1	0	0	0	0	0	0	0	0	0	0	0	2	0	0	0	0
Lowland	BLDSL	Lowland Dry Low Scrub	0	0	2	0	2	1	0	0	0	0	0	0	0	0	0	0	0	0	0	0	0	0	0	1	0

Figure 67. Extracted example of the wildlife species-ecotype relationships tables used to denote use levels of each ecotype by each species. This example shows only a partial list of the 61 ecotypes and 124 bird species in the study area. Within the Table, 0 denotes that an ecotype is generally not used by the species; 1 denotes secondary use; and 2 denotes primary use for resources. The full set of all ecotypes used by a given species at levels 1 or 2 (thus, omitting 0-coded entries) constitutes that species' habitat within the study area.

Data are essentially lacking on population density, status, trends, and other attributes of wildlife as related to the ecotype categories by which use levels would be quantified; thus, the ordinal scale substitutes as a framework for identifying presence-absence and the general value of each ecotype as habitat for each species. Also generally unavailable is information on which, if any, specific ecotypes may be critical to contribute to habitat for a given species, that is, if that ecotype were absent but other used ecotypes were present. As research provides more quantitative information on wildlife species' use of the ecotypes, the framework used in this analysis can be improved.

Identifying even the three ordinal-scale levels of wildlife species-ecotype relationships for the study area was a challenge, entailing extensive use of existing information on each species from the literature, peer reviews, audio recordings of selected locations, and opportunistic field observations. Of primary use were the analyses that some of us (Marcot and Jorgenson) had conducted in northwest Alaska (Marcot et al., 2015) that had produced similar species-ecotype relationships tables. For that use, we first had to develop reasonable cross-walks of the ecotypes of that region to those of the current study area. We then matched the wildlife species lists, excluding species found in northwest Alaska but not in the study area, and included

species of the study area not found in northwest Alaska. We then used the ordinal-scale use levels from the northwest Alaska databases as initial use values for the current study area for those wildlife species in common to both regions. Next, we consulted the literature and engaged in discussions with reviewers to correct use levels of the cross-walked data and to fill in values for the added species (see Appendix A.1 for lists of information sources used). Further improvements to the coding of some ecotype relationships could still be made, and we leave such refinement to next-generation updates of this information.

2.9.5.3 Patterns of Wildlife Species Richness by Ecotype

The number of species using a particular ecotype, as denoted in the species-ecotype relationships tables described above, constitutes that ecotype's species richness. Patterns of species richness varied among ecotypes and species groups, and are explored next.

Ecotypes with high species richness denote those conditions providing for greater levels of overall biodiversity. However, it should also be noted that ecotypes with low species richness does not mean that those ecotypes are unimportant to wildlife; they might provide critical resources for some species.

- Amphibian (wood frog) use of ecotypes.
  -- As there is only a single species of amphibian in the study area, wood frog, amphibian species richness obviously could not exceed one species. Shown in Figure 68 is the set of ecotypes used by wood frog in the study area at levels 1 (secondary) and 2 (primary). Wood frogs require aquatic and wet-site conditions adjacent vegetation, and are generally absent in alpine, scrub, barrens, most upland, and dry woodland and forests. According to the literature and research findings, primary-use ecotypes generally include standing water (ponds, lakes) for breeding and egg-laying, and other wet site conditions for dispersal; and secondary-use ecotypes include other conditions of running water (riverine), scrub, woodland, and forest conditions that generally occurring adjacent or near to the primary-use ecotype conditions. By this accounting, wood frogs use 13 ecotypes as primary habitat and another 13 as secondary habitat.

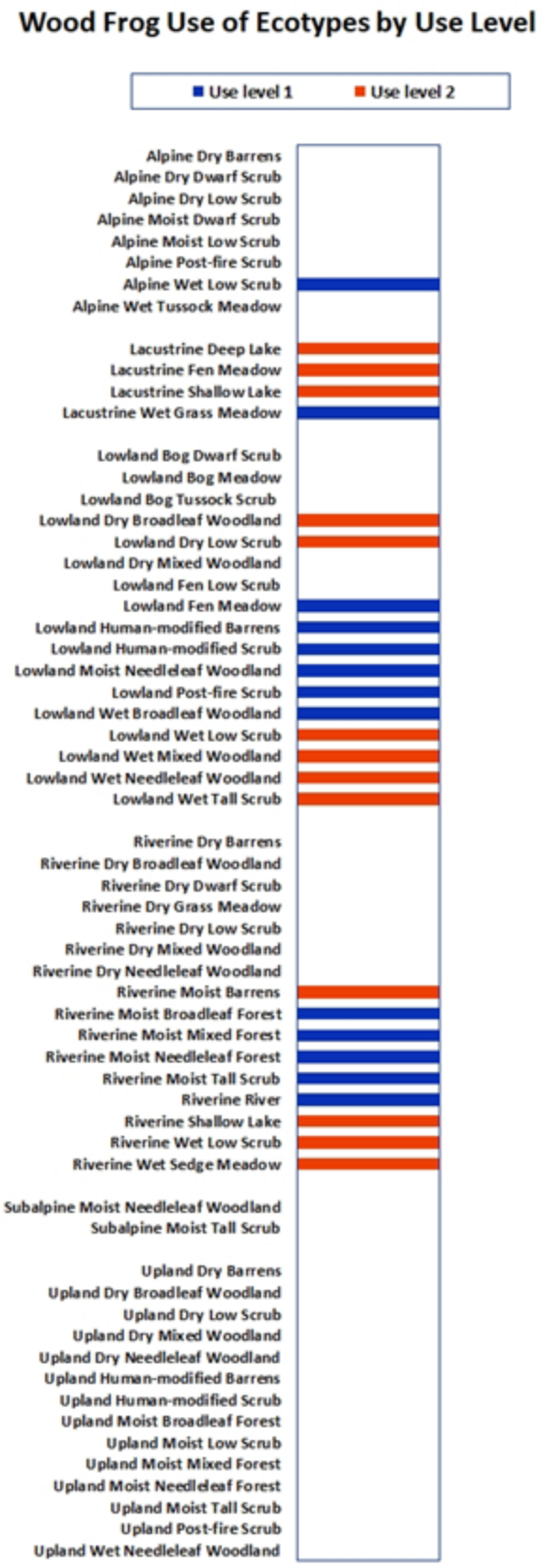


Figure 68. Ecotypes used by wood frogs in the study area, at use levels 1 (secondary habitat use) and 2 (primary habitat use). Blanks after ecotype names denote that they are generally not used.

- Bird species richness by ecotype.
  -- Bird species richness varied among the 61 ecotypes included in this analysis but nearly all ecotypes contributed primary habitat to some species (Figure 69). The most bird species-rich ecotypes, which also provided for the most bird species' primary habitats, included several riverine moist forest types (broadleaf, mixed, and needleleaf); lowland bog meadow and wet woodlands; upland moist and wet woodland and forest types; and lacustrine bog types.

The least bird species-rich ecotypes included lowland fen low scrub, and lowland and upland human-modified types. Ecotypes contributing little to no primary habitat for birds included lowland fen scrub and upland dry barrens.

The highest bird species richness among all ecotypes, for primary or secondary use levels, reached 56 species in riverine moist mixed forest, and lowest with only 3 bird species was lowland fen low scrub. Bird species richness among all 61 ecotypes averaged 32 species (median 33 species). Note the highest richness levels in various riverine forests, lowland and upland wet woodlands, meadows, and other ecotypes. Low richness levels occur in lowland fen low scrub and human-modified scrub and barrens.

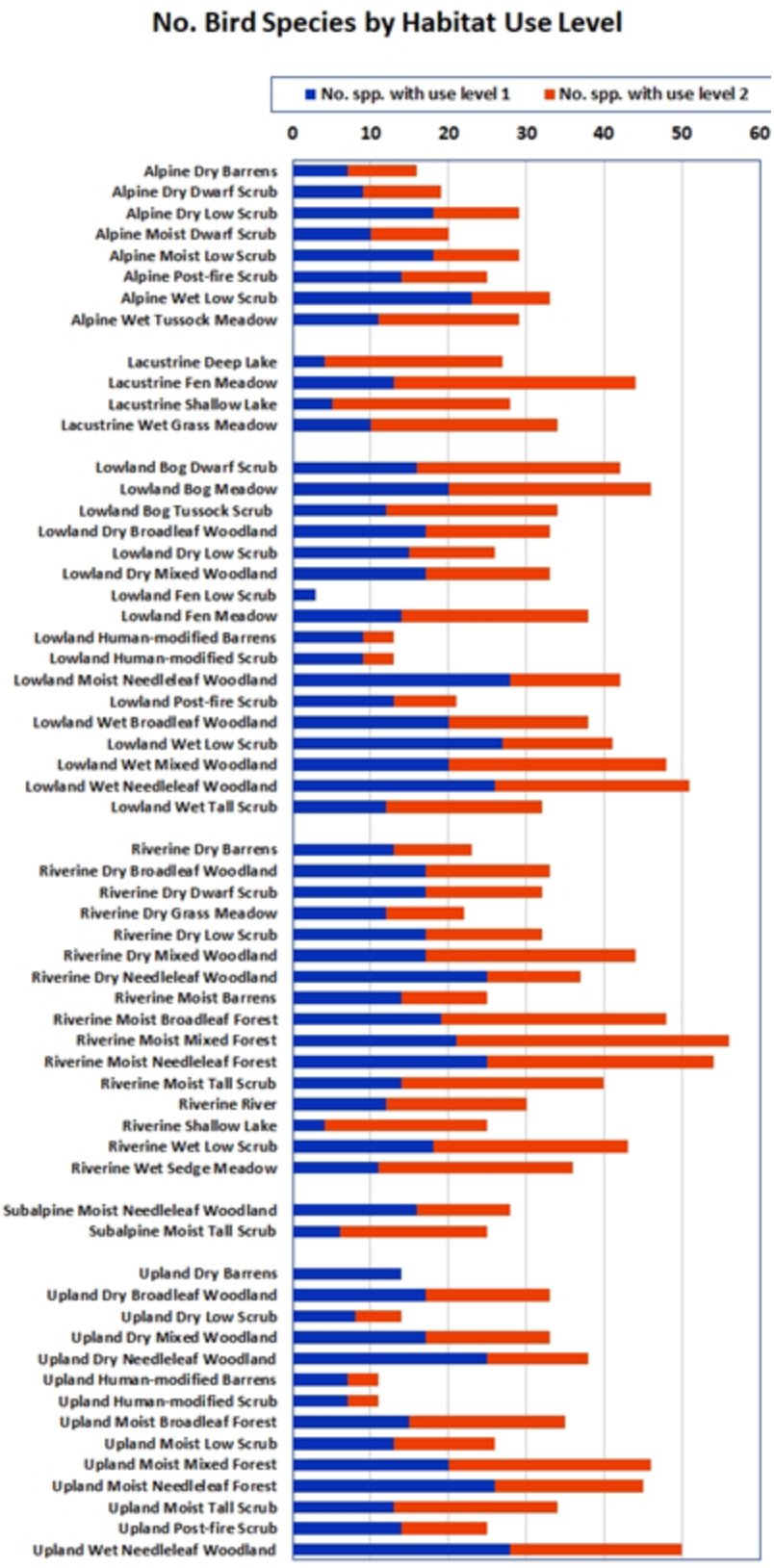


Figure 69. Bird species richness by ecotype and level of use (1 = secondary, 2 = primary).

Geographically, the highest bird species richness occurs in lowland and riverine environments of Tanana Flats and along river valleys of Donnelly Training Area West (Figure 70).

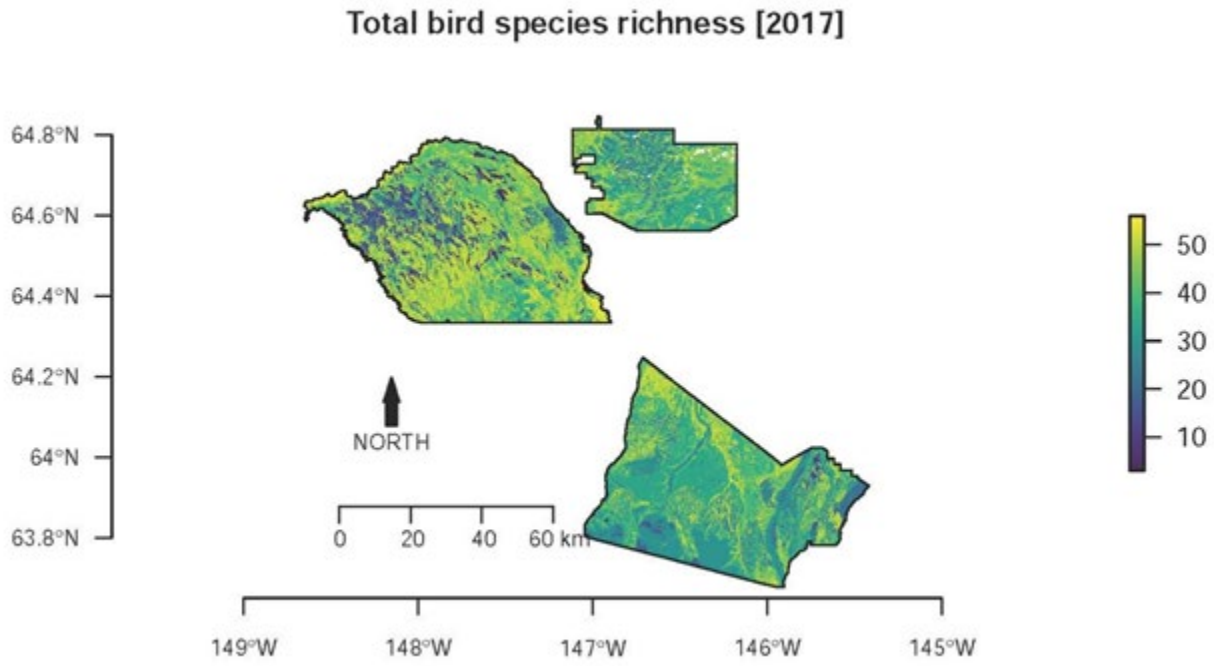


Figure 70. Total bird species richness (no. of species) combining secondary and primary habitat use levels of ecotypes, of the study area, based on vegetation maps of 2017, updated with recent fire events and other disturbances, and cross-indexed to the ecotypes used in this study.

- Migrant stopover bird groups by ecotype.
  -- Among the 6 migrant stopover bird groups included in this analysis, most occur in lacustrine, lowland, and riverine meadow ecotypes (Figure 71). None seems to particularly use alpine, scrub, post-fire, and barrens ecotypes. This is not unexpected, as bird species of these groups are largely tied to open water or vegetated, wet site conditions, as with waterfowl and shorebirds, or to woodland or forest conditions, as with songbirds (Appendix Table 2). Because this set of species includes waterfowl, shorebirds, species of some woodlands and forests, and others, they are most served by a variety of lake, wet site, and vegetated conditions among most landscapes except for alpine conditions.

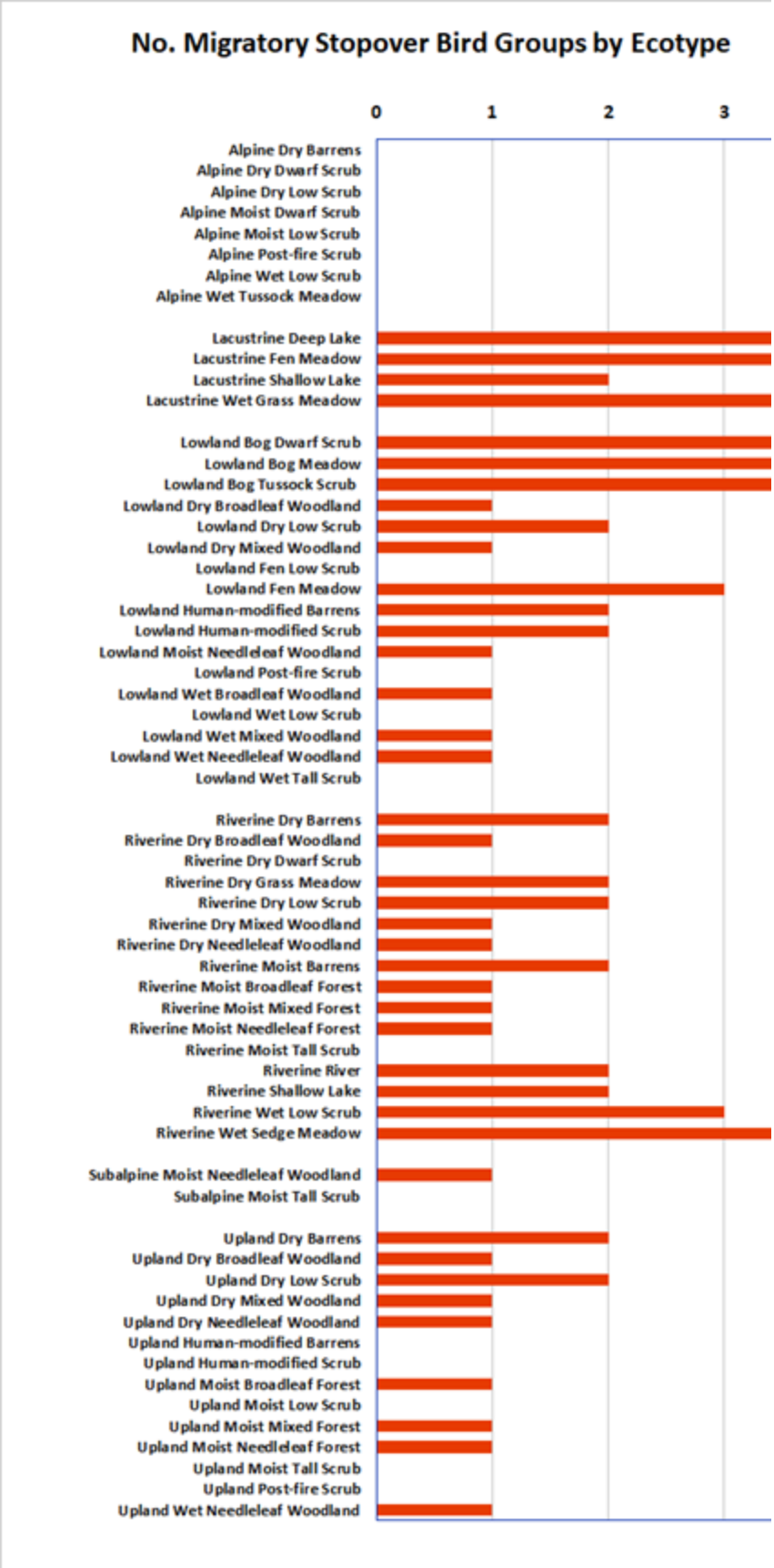


Figure 71. Number of migrant stopover bird groups by ecotype. See Table 13 for general categories of habitat associations, and Appendix Table 2 for the list of bird species in each migrant stopover group.

Geographically a greater number of migrant stopover bird groups, by secondary and primary habitat use levels combined, occurs largely in Donnelly Training Area West, in lowland tussock scrub bog (Figure 72).

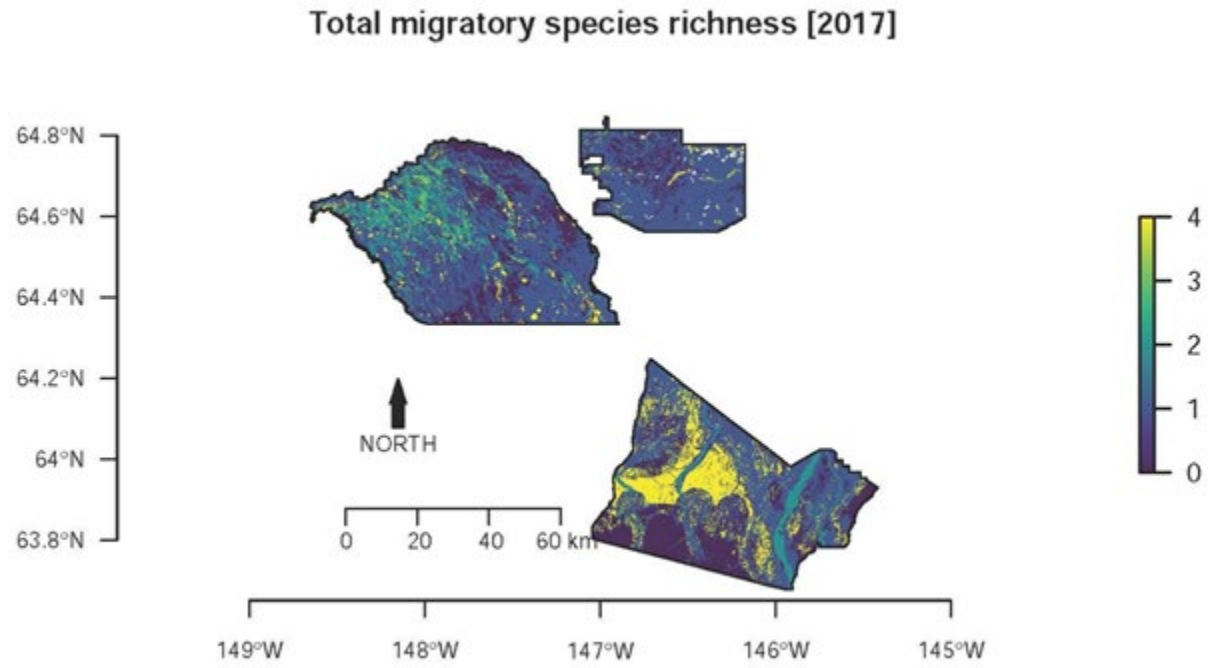


Figure 72. Number of migrant stopover bird groups' combined secondary and primary habitat use levels of ecotypes, of the study area, based on vegetation maps of 2017, updated with recent fire events and other disturbances, and cross-indexed to the ecotypes used in this study.

- Mammal species richness by ecotype.
  -- Mammal species richness was broadly distributed among the 61 ecotypes included in this analysis (Figure 73). Mammal species richness among all 61 ecotypes averaged 18 species (median 21 species). The highest mammal species richness among all ecotypes, for primary or secondary use levels, reached 30 species in riverine wet low scrub, and the lowest, with only 1 mammal species, was lowland post fire scrub. The most mammal species-rich ecotypes included lowland bog, wet, and meadow types; riverine wet scrub and meadows; and a variety of scrub, woodland, and forest types in riverine, lowland, upland, and subalpine landscapes. The most mammal species-poor ecotypes included barrens, scrub, and human-modified types found in lowland and upland landscapes. A number of these types provided no primary habitat conditions for mammals. Note that highest richness levels occur in lowland and riverine tussock and wet scrub, and lowest richness in human-modified, post-fire, and dry barren ecotypes.

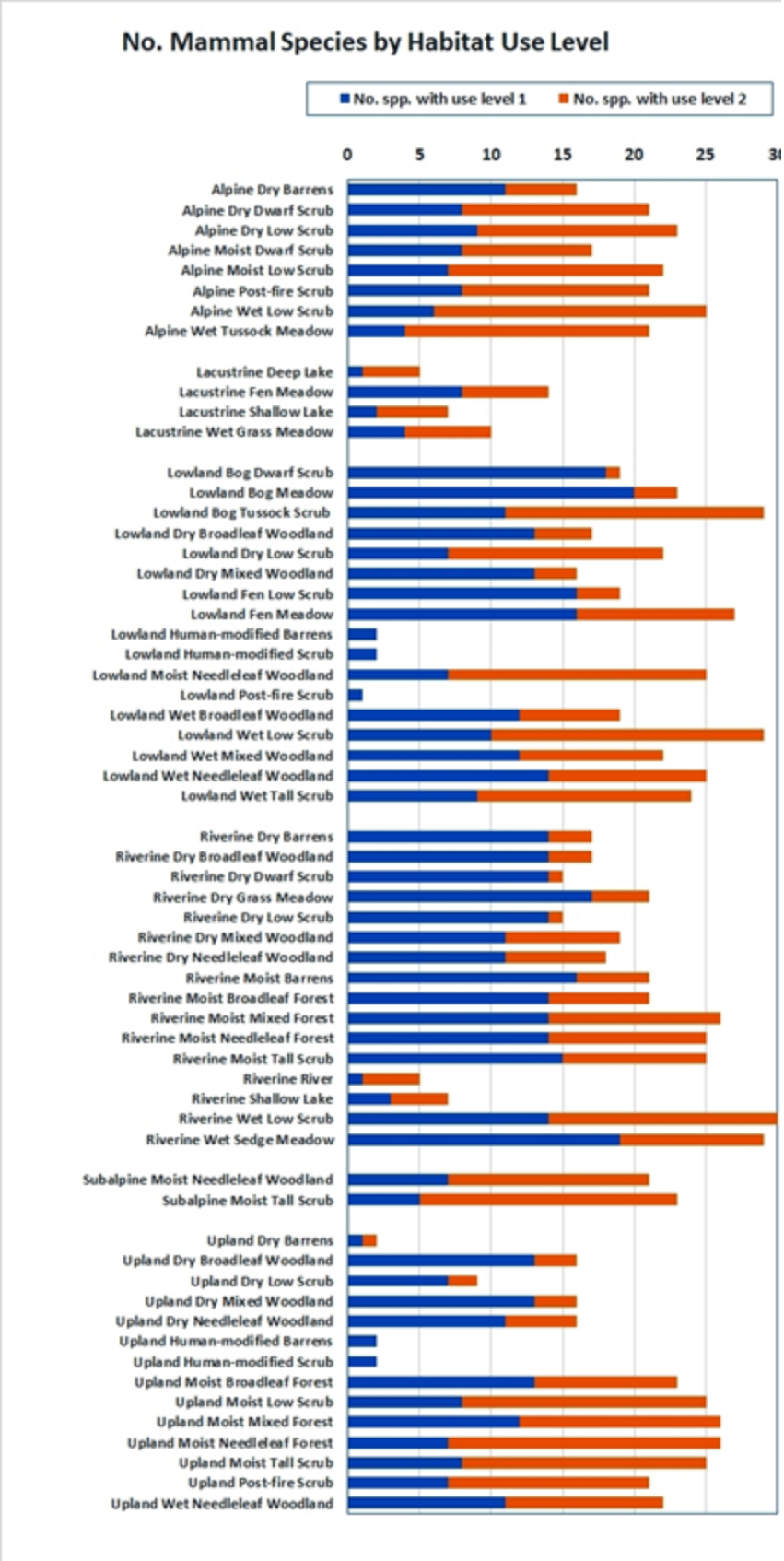


Figure 73. Mammal species richness by ecotype and level of use (1 = secondary, 2 = primary).

Geographically, the highest mammal species richness occurs in lowland and riverine environments of Tanana Flats and in upland forests of Donnelly Training Area West (Figure 74).

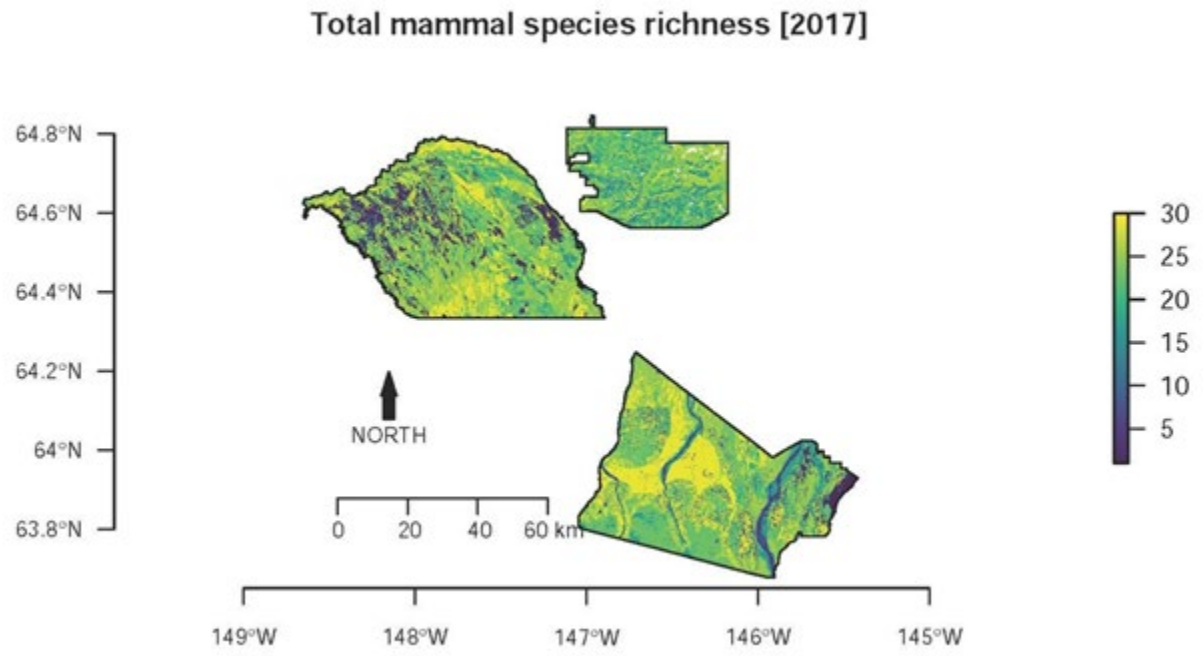


Figure 74. Total mammal species richness (no. of species) combining secondary and primary habitat use levels of ecotypes, of the study area, based on vegetation maps of 2017, updated with recent fire events and other disturbances, and cross-indexed to the ecotypes used in this study.

- Total wildlife species richness by ecotype:
  -- Summing total species among amphibian, bird, and mammal species (excluding the migrant stopover bird species groups), suggested that the collective set of ecotypes provide broadly for overall wildlife species richness (Figure 75). The most species-rich types included a variety of wet-site conditions such as meadow, riverine, and moist and wet forests and woodlands. The most species-poor types included human-modified barrens and scrub types, dry barrens types, and dry and post-fire low scrub types. Note that the most overall species-rich ecotypes include various wet woodland, moist forest, and meadow conditions in riverine, lowland, and upland landscapes.

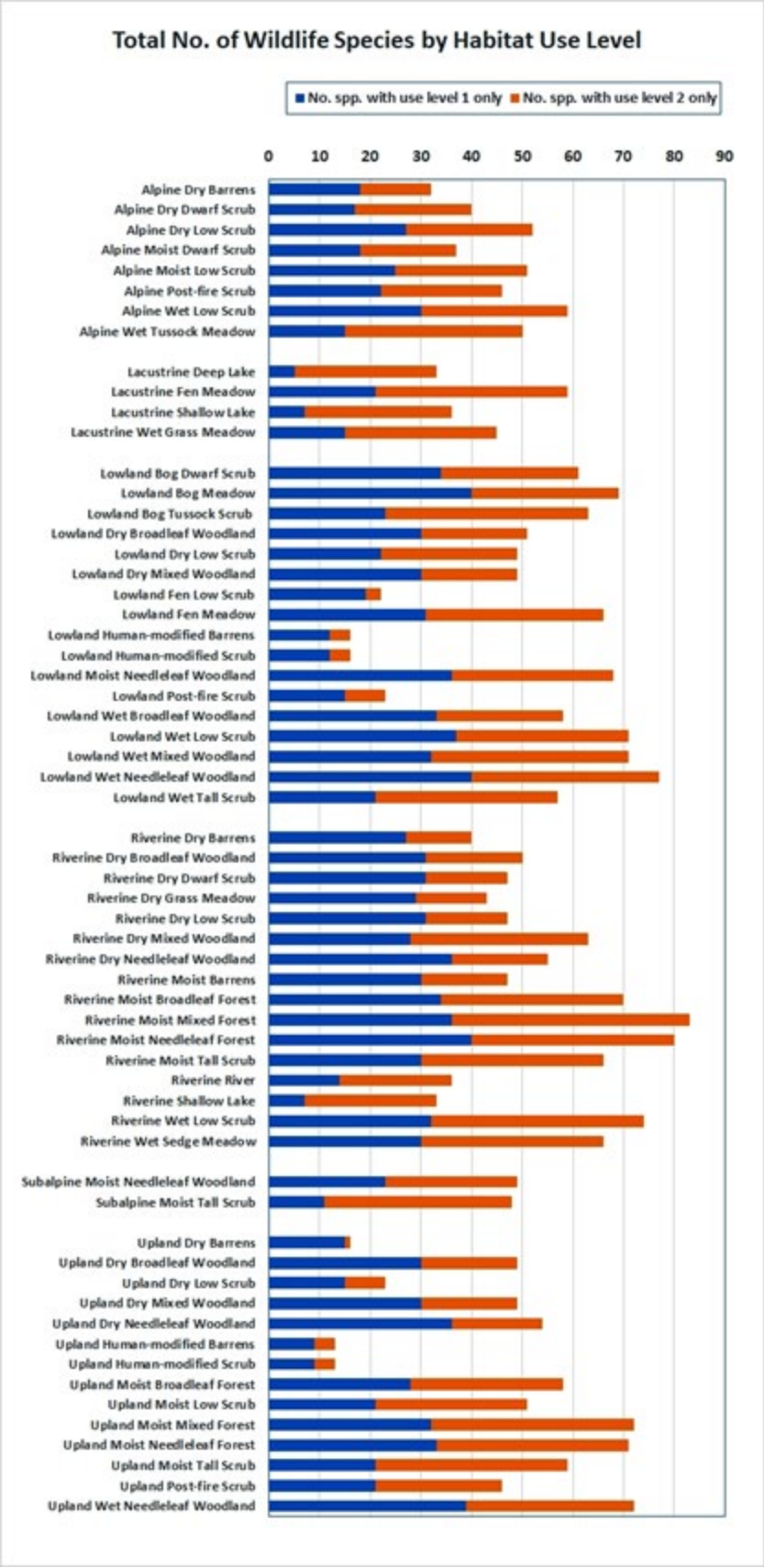


Figure 75. Total wildlife species richness, of all taxonomic groups (amphibian, birds, and mammals) by ecotype and level of use (1 = secondary, 2 = primary).

Geographically, highest overall wildlife species richness occurs broadly in multiple ecotypes throughout the study area, particularly in southern Tanana Flats and northern Donnelly Training Area East and West (Figure 76).

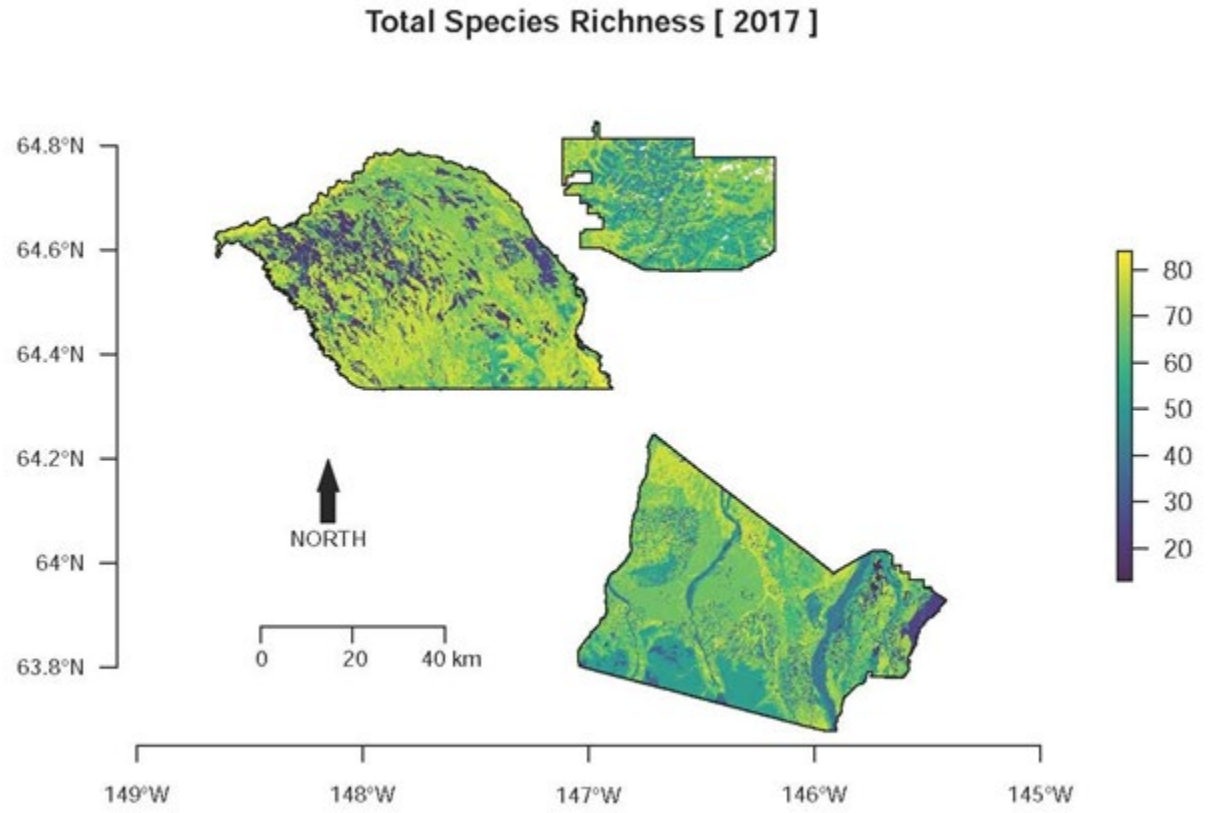


Figure 76. Total wildlife species richness (no. of species) of amphibians (wood frog) and all birds and mammals, combining secondary and primary habitat use levels of ecotypes, of the study area, based on vegetation maps of 2017, updated with recent fire events and other disturbances, and cross-indexed to the ecotypes used in this study.

2.9.5.4 Identifying Wildlife Habitat Specialists and Generalists

- Overall framework.

  -- The framework used here to match wildlife species to ecotypes also afforded the opportunity to identify species that use the fewest and the most ecotypes as an index to their habitat use breadth. Species using the fewest ecotypes are noted as those with the narrowest habitat use breadth and are habitat specialists; and those using the most ecotypes have the widest habitat use breadth and are habitat generalists. General patterns suggest the following differences among birds, mammals, and amphibian (wood frog).

- Bird species habitat specialists and generalists.
  -- Among birds, the number of species by number of ecotypes used follows a skewed normal distribution, with most species using between 7 and 13 ecotypes and fewest species using > 37 ecotypes (Figure 77). The number of ecotypes used by birds overall averaged 16 ecotypes.

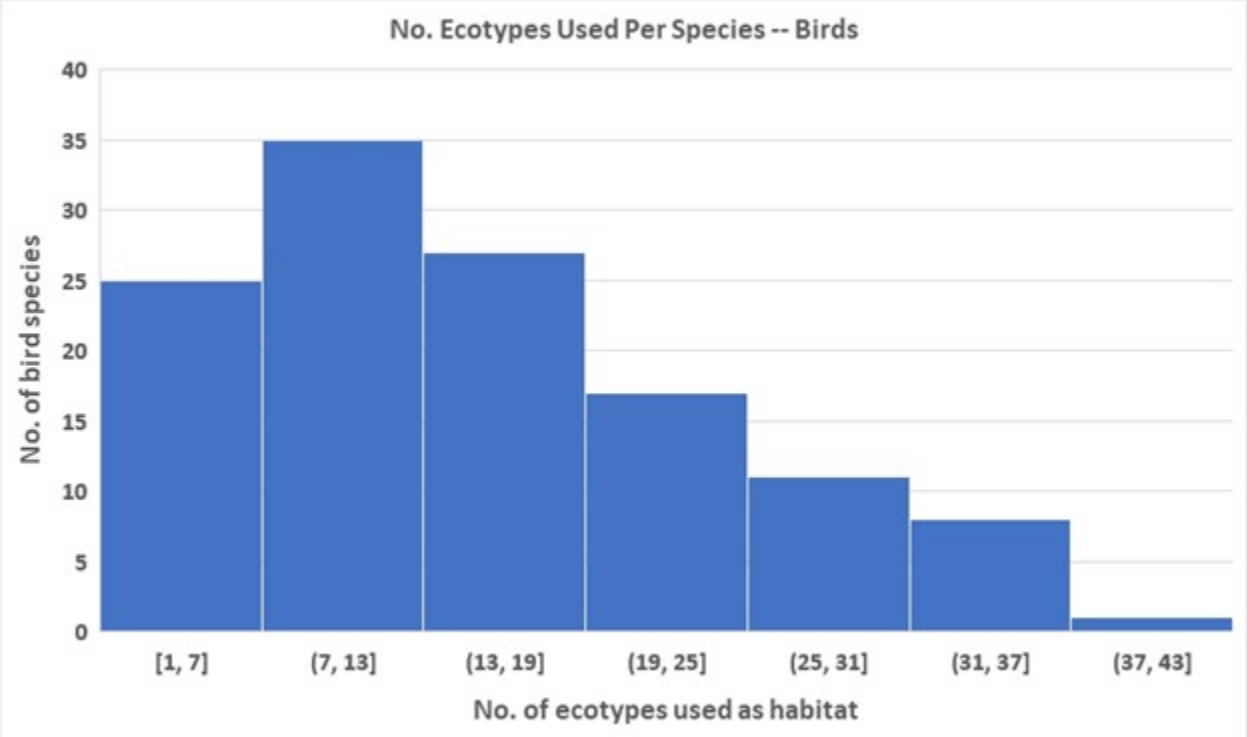


Figure 77. Frequency distribution of bird habitat use breadth, measured as number of ecotypes use as secondary or primary (level 1 or 2) habitat. This graph shows that most bird species each used < 20 ecotypes, and very few species used a broader set of ecotypes, e.g., > 30 ecotypes.

Bird species with the greatest habitat use breadth (no. of ecotypes used as habitat generalists) included mostly woodland and forest species of thrushes, sparrows, warbler, shrike, and others (Figure 78). Bird species with the narrowest habitat use breadth (habitat specialists) included some raptors, shorebirds, and open-site specialists such as horned lark and gray-crowned rosy finch. Rock dove appeared as a habitat specialist only because it tends to be a human habitation commensal, found within towns and cities, environments that are rare among the ecotypes of the study area but that are common just outside the study area. Rock doves are a highly resilient species and would not be expected to suffer from its scant, specific habitat within the study area. Bald eagles appear as a habitat specialist mostly because the species-ecotype relationships tables tie them solely to riverine moist broadleaf and moist mixed forests; they may also use additional ecotypes not so noted.

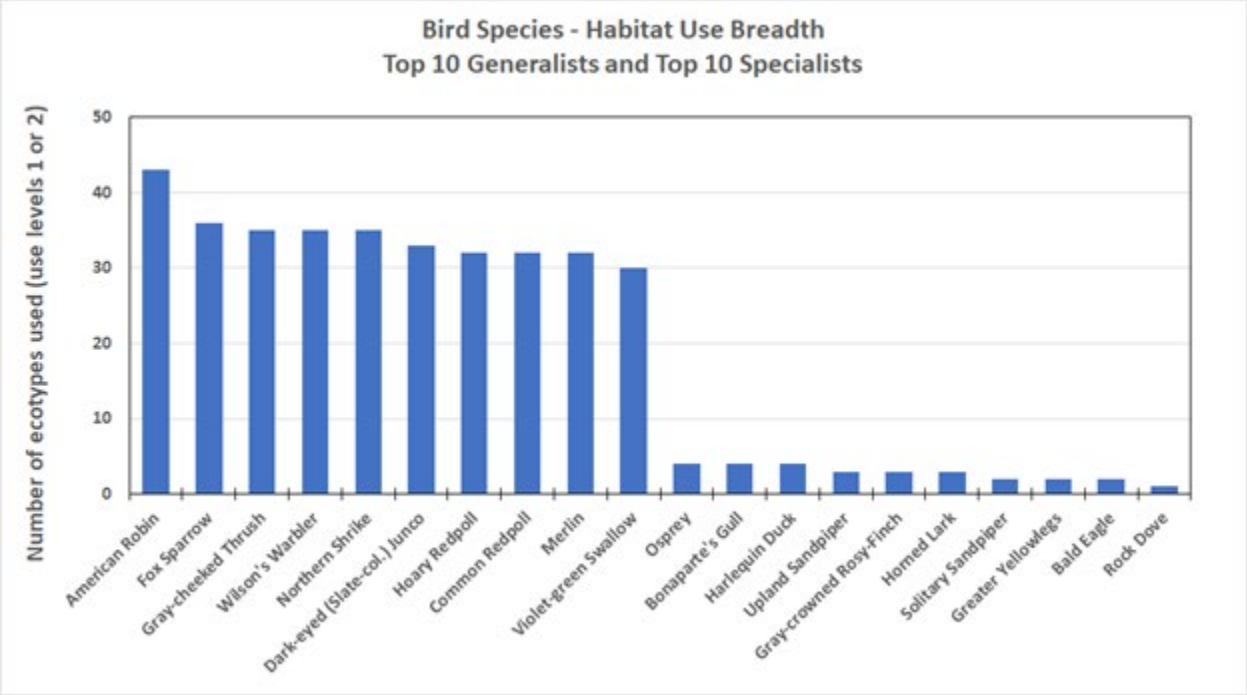


Figure 78. Bird species habitat use breadth, shown as number of ecotypes used at secondary or primary levels (use levels 1 or 2, respectively), of the top 10 generalists (most ecotypes used) and the top 10 specialists (least ecotypes used).

- Mammal species habitat specialists and generalists.
  -- Mammals, however, showed an unusual bimodal distribution of number of species by number of ecotypes used (Figure 79). This pattern may suggest a greater tendency toward some degree of either habitat specialization or habitat generalization than with birds, which may be a function of the life history patterns among mammals.

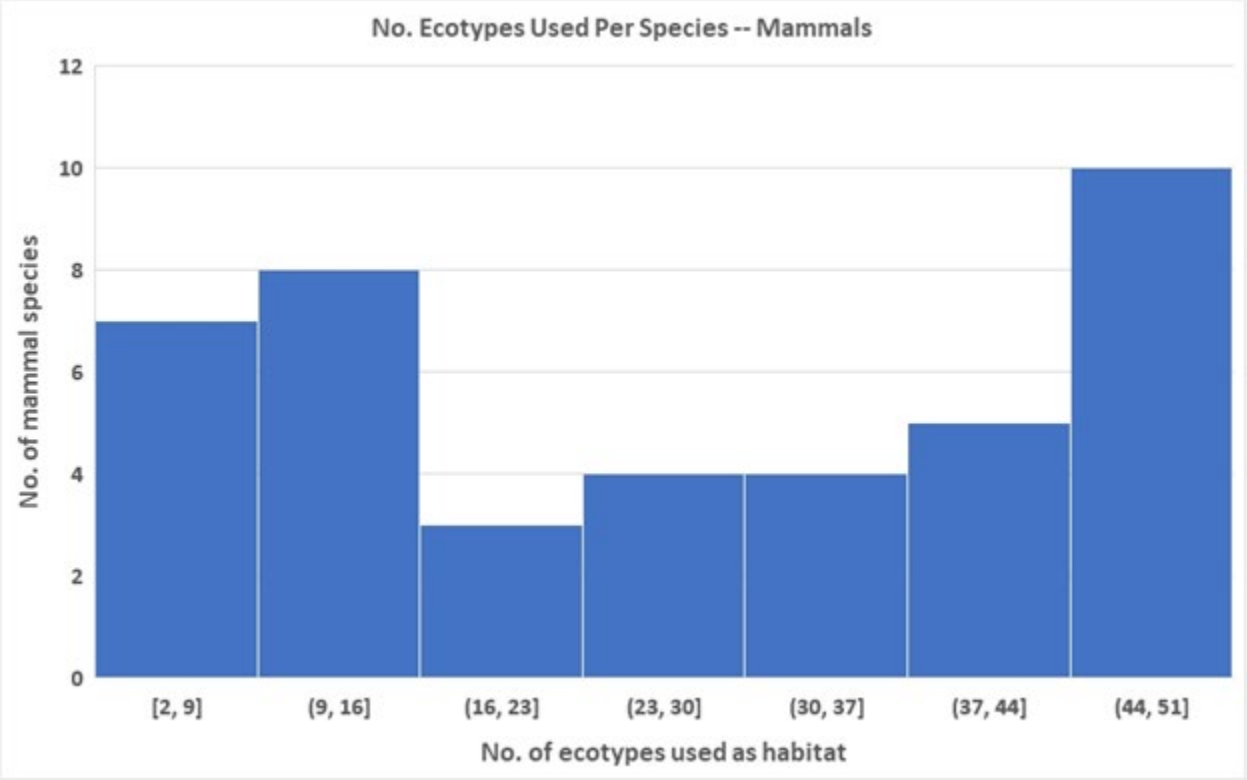


Figure 79. Frequency distribution of mammal habitat use breadth, measured as number of ecotypes use as secondary or primary (level 1 or 2) habitat. This graph shows that most mammal species use either a relatively few or many ecotypes, with fewer mammal species using a moderate number of ecotypes, suggesting greater degrees of habitat specialization and generalization than with birds (Figure 77).

Mammal species with the greatest habitat use breadth (highest no. of ecotypes used as habitat generalists) included a variety of carnivores and predators, such as brown and black bears, red fox, wolf, and lynx, along with mustelids including ermine and wolverine (Figure 80). Other notable habitat generalists included northern red-backed vole and snowshoe hare, each of which uses a wide variety of ecotypes among most landscape classes (alpine, lowland, riparian, and upland). Mammal species with the narrowest habitat use breadth (habitat specialists) included flying squirrel, bog lemming, bison, pika, mink, Dall sheep, and others. These are species mostly tied to specific environmental conditions, such as Dall sheep using mostly alpine types.

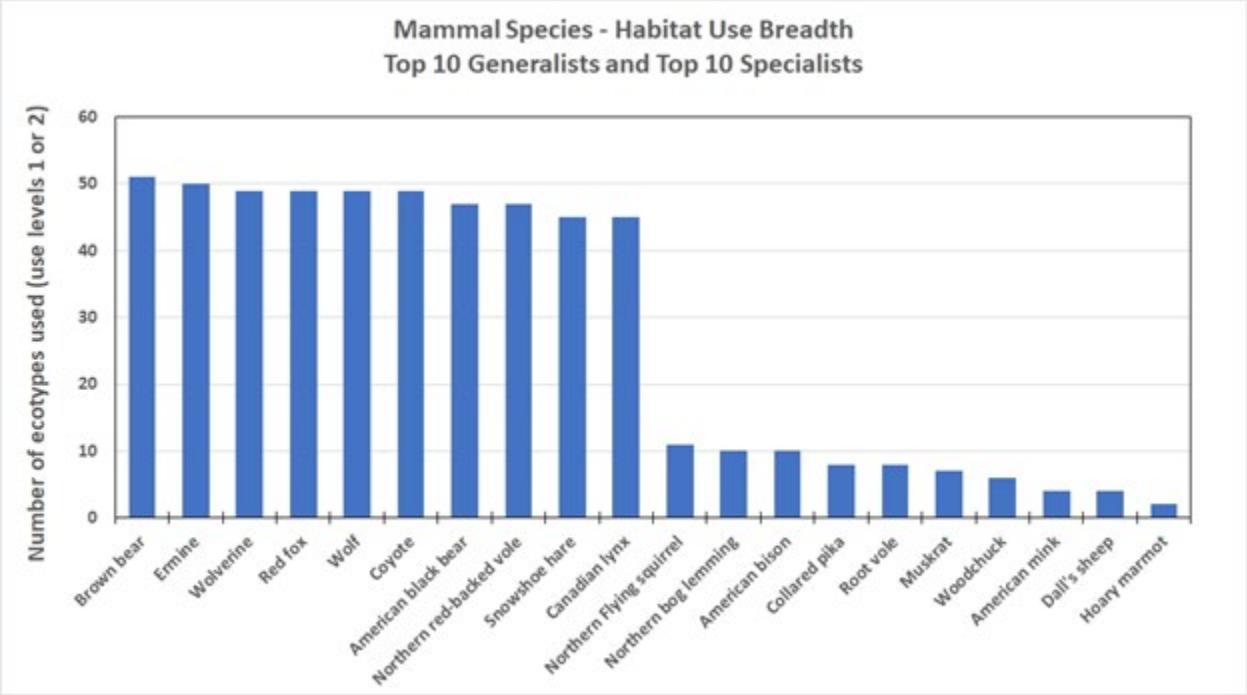


Figure 80. Mammal species habitat use breadth, shown as number of ecotypes used at secondary or primary levels (use levels 1 or 2, respectively), of the top 10 generalists (most ecotypes used) and the top 10 specialists (least ecotypes used).

- Wood frog by comparison.
  -- Wood frogs were denoted in the species-ecotype relationships tables as using 26 ecotypes for secondary or primary use (use levels 1 or 2), with 13 types each for secondary and primary use, mostly related to lacustrine, wet site, and adjacent conditions (Figure 68). As compared with birds and mammals, wood frog's habitat use breadth denotes neither a habitat specialist nor generalist, although of course wood frogs depend on aquatic and mostly wet-site conditions for their reproductive life history stage. This point highlights that indications of habitat specialization and generalization can depend on how, and how many, habitats -- in this case, ecotypes -- are denoted and differentiated. Wood frogs are indeed tied to aquatic and wet site conditions, and their quality, extent, and distribution across the landscape may most determine the frog's population status.

This section has summarized current conditions of amphibian, bird, and mammal species' documented, expected, or hypothesized use of ecotypes as indictors of habitat orientation, wildlife species richness among ecotypes, and species' habitat use breadth. The next section presents projections of wildlife species' habitat amounts to previous, current, and future time periods.

2.9.6 Bioacoustics of Interior Alaska Training Lands

This section presents methods, findings, and management implications of the bioacoustic analysis portion of the project. Discussed here are: (1) the objectives for identifying wildlife species and other site conditions through bioacoustic recordings; (2) the sampling design used for the bioacoustic recordings; (3) site conditions of the bioacoustic recording locations; (4) analysis of the audio recordings using machine learning approaches to identify wildlife species and other sound sources; and (5) discussion and potential implications for future inventory, monitoring, and research of biotic conditions on the training lands.

2.9.6.1 Identification of Wildlife Species and Other Site Conditions Through Bioacoustic Recordings

The objective of the bioacoustic recording study was to use audio recordings to help identify the occurrence of wildlife species at selected locations and ecotype conditions within the study area. Species identified through audio recordings were one source of information used to verify wildlife species presence by ecotype (see Figure 57). The audio recordings were also used for analyses of ecoacoustic soundscape conditions, presented in the next section further below.

Using audio recordings to identify species occurrence by site and selected ecotype condition assumes the following conditions. Sounds of individual animals, such as frog calls, bird songs, and squirrel calls, can be attributed to presence of the species in the specific ecotype in which the recording unit was placed. Sound occurrences provide evidence of a species' presence, whereas absence of a given species' sounds at a location does not provide sufficient evidence to conclude absence of the species per se at that site. Drawing from experience in bioacoustic recording in other locations, it is expected that sounds of individuals of wildlife species can be recorded from no more than 0.5 km distance from the recording unit, thus defining the radius of a roughly circular area within which a species presence can be verified, depending on local topography, intervening vegetation, and other site factors.

2.9.6.2. Sampling Design Used for the Bioacoustic Recordings

For the bioacoustic recording portion of this study, we secured 24 automated audio recording units (ARUs), model Cornell Swift, running STM32 Firmware Ver. 0.18.6.3, from Cornell Labs. Each unit was operated by 3 D-size batteries (alkaline, upon recommendation from Cornell Labs). Each ARU consisted of a weather-proof metal casing, straps for affixing to trees, integrated high-sensitivity microphones, and 64GB memory cards for storing sound files in Wave (.wav) file format.

The overall design was structured so as to sample sites in each of four major landscape types and their successional stages, with replicates. Specifically, the 24 ARUs were deployed in lowland, upland, riverine, and lacustrine landscapes, and within two or three of their successional stages (early, mid, and late; Table 15). The early stages of lowland sites were further specified as thermokarst or fire origins. All lacustrine early successional stage sites were of thermokarst origin. All upland early stages were in post-fire recovery. A mid-successional stage of lacustrine conditions was not identified in the study, and thus not sampled. This design also provided redundancy for each combination of landscape conditions and successional stage, with two ARUs set at different locations. Note that no ARUs were used in alpine landscapes, found in the southern extent of the study area, because of high difficulty of access to those remote sites for deployment, maintenance, and retrieval.

The ARUs were deployed during field seasons 2019 (June-August) and 2020 (April-September). Site conditions and other data were documented upon deployment of each ARU (Appendix Table 13). Specific GPS field locations of the ARUs were recorded (Appendix Table 12) to facilitate return for battery replacement, retrieval, and redeployment at the same sites in 2020.

Table 15. Deployment of 24 automated audio recording units (ARUs) in the study area. ARUs were used during field seasons 2019 (June-August) and 2020 (April-September) to record sounds useful for identifying wildlife species and soundscape conditions (discussed in section 2.10.4).

Landscape type	Successional stage				**No. of ARUs**
	Early		Mid	Late	
	Thermokarst	Fire			
Lowland	LDSB6 *y* LDSB2 *a*	LLSD1 *a* LLSD3 *a*	LWBF4 *y* LWBFX *t*	LWNF9 *y* LWNF1 *a*	**8 Lowland**
Upland	UMTLS7 *y* UMTLSX *y*		UMBF7 *y* UMBF6 *y*	UMNF5 *y* UMNF1 *a*	**6 Upland**
Riverine	RMTS3 *a* RMTS4 *t*		RMBF1 *a* RMBF5 *t*	RMNF1 *a* RMNF8 *t*	**6 Riverine**
Lacustrine	USTL1 *p* USTL2 *p*	(not applicable)	---	LDTL1 *c* LDTL2 *yh*	**4 Lacustrine**
No. of ARUs	**4 Early Thermokarst**	**2 Early Fire**	**---**	**---**	**---**
	10 Early		**6 Mid**	**8 Late**	**24 TOTAL**

Location codes:
a = APEX (Bonanza Creek)
c = Creamer's Field/Farmer's Loop
h = Husky Lake (located on Yukon Training Area)
p = Permafrost Tunnel (Glenn Creek)
t = Tanana Flats Training Area (TFTA), a.k.a. "The Bridge", near Salcha
y = Yukon Training Area (YTA), includes Transmitter Road & Johnson Road

Site names are coded as ecotypes as follows:
LDTL = Lowland Deep Thermokarst Lake
LDSB = Lowland Dwarf Scrub Bog
LLSD = Lowland Low Scrub Fire-Disturbed
LWBF = Lowland Wet Broadleaf Forest
LWNF = Lowland Wet Needleleaf Forest
RMTS = Riverine Moist Tall Scrub
RMBF = Riverine Moist Broadleaf Forest
RMNF = Riverine Moist Needleleaf Forest
UMTLS = Upland Moist Tall and Low Scrub
UMBF = Upland Moist Broadleaf Forest
UMNF = Upland Moist Needleleaf Forest
USTL = Upland Shallow Thermokarst Lake

We used the beta firmware provided from Cornell Labs to schedule audio recordings by each ARU. The units were programmed to record audio for 10 minutes at the top of each hour, 24 hours a day and 7 days a week. This provided samples of sounds throughout the 24-hour daily cycle which was important for capturing dawn and dusk bird choruses when many species were detected, as dawn and dusk times changed throughout the recording season. It also provided for nocturnal recordings for later analysis to potentially detect owls and other mostly nocturnal species. We deployed the ARUs much earlier in the spring season in 2020, starting in April, to be able to detect first-arrival dates of some of the migratory songbird species as a baseline from which to compare future data signaling phenological shifts likely caused by regional climate changes (analysis ongoing).

A consideration in the maintenance of the ARUs over the course of each recording season, affecting personnel time for upkeep, was battery life. As these recorders had not been used previously, we determined actual effective battery life based on ARU initial deployment and the start and end dates of the stored sound files when ARUs were first deployed and final recording when batteries failed (Appendix Table 14).

We found that battery life of the ARUs, using our hourly recording schedule noted above, averaged 60 days (+/- 1 day SD) and ranged 57 to 61 days. We also determined that battery life did not significantly vary by landscape or successional stage condition (Appendix Table 14). This information was used to subsequently schedule field visits for battery replacement to get full usage of the ARUs and to minimize ARU down time.

2.9.6.3. Site Conditions of the Bioacoustic Recording Locations

The ARU units were dispersed among the following field locations (Figures 81 and 82):

- Bonanza Creek LTER (Long Term Ecological Research) APEX (Alaska Peatland Experiment) - 8 ARUs
- Creamer's Field and Farmer's Loop - 1 ARU
- Yukon Training Area, at Transmitter Road and Johnson Road - 8 ARUs
- Yukon Training Area, at Husky Lake - 1 ARU
- Glenn Creek near the Permafrost Tunnel - 2 ARUs
- Tanana Flats Training Area (TFTA) near Salcha - 4 ARUs



Figure 81. A true color image of the region around Fairbanks and Fort Wainwright, Alaska identifying locations of the Automated Recording Units.

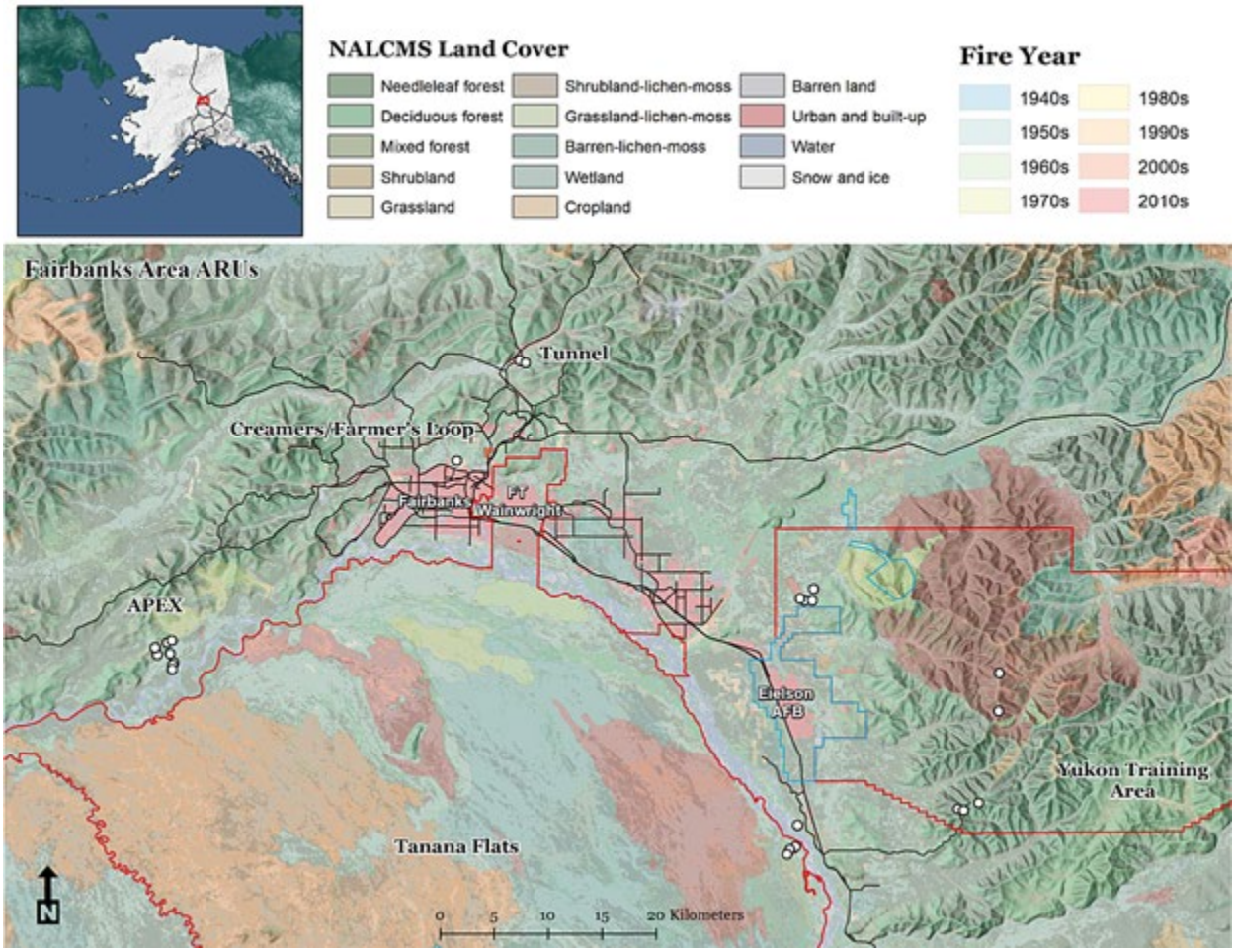


Figure 82. Deployment locations of 24 automated audio recording units (ARUs) in the study area for the bioacoustic recording study. (A) With satellite view from Google Earth; see Table 15 for code names, and landscape and successional stages at each site. (B) With North American Land Change Monitoring System (NALCMS) land cover conditions, with ARU placement locations shown as white circles.

Upon deployment of the ARUs, we documented conditions of vegetation cover at each site, by taking four horizontal digital photographs at 90-degree intervals around the tree to which each ARU was lashed, one photograph toward the zenith to document any canopy cover, and one photograph toward the nadir to document ground cover. This served to document visual conditions of cover as a baseline for conducting any future repeat studies at the same points, where vegetation and site conditions might change. An example of this site-specific photographic documentation is show in Figure 83.

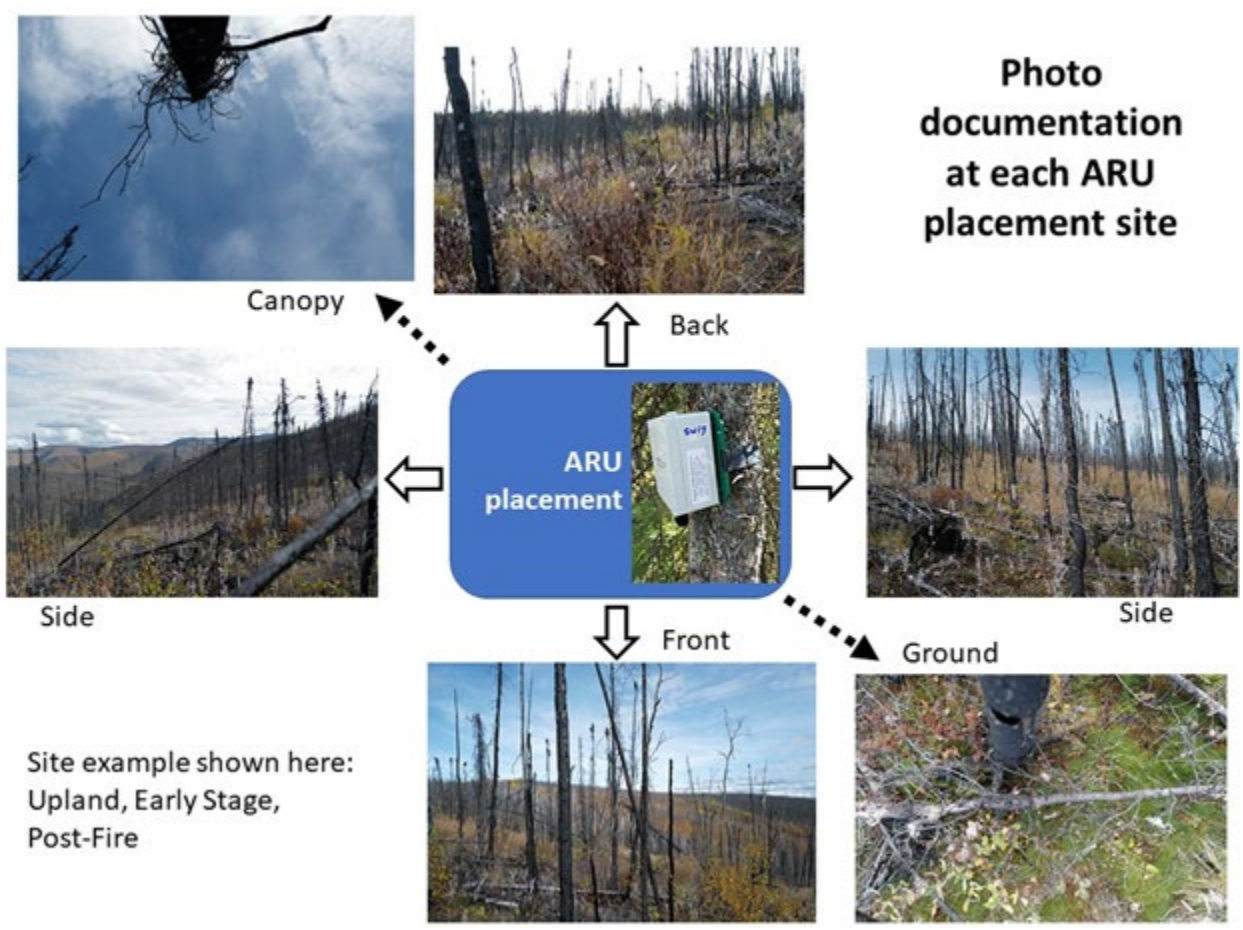


Figure 83. Example of photograph documentation done at each deployment site of the automated audio recording units (ARUs), showing four horizontal images taken at 90-degree intervals clockwise around each ARU unit lashed to trees at approximately head height, and images at zenith and nadir orientations to document canopy cover and ground cover, respectively.

Additionally, an ecological land survey was conducted at each ARU field site location (by M.T. Jorgenson). This consisted of an integrated sampling and investigation of geomorphology, hydrology, soils, and vegetation near to the actual ARU placement location. See prior sections of this report for details of methods. Results are available from the authors upon request.

GIS analysis was also used to characterize vegetation conditions within a 0.5-km radius of each ARU location, and landscape conditions within that distance and beyond (Figure 84). The ecological land survey and GIS analyses were used for the ecoacoustic soundscape analyses presented in the next section, below.

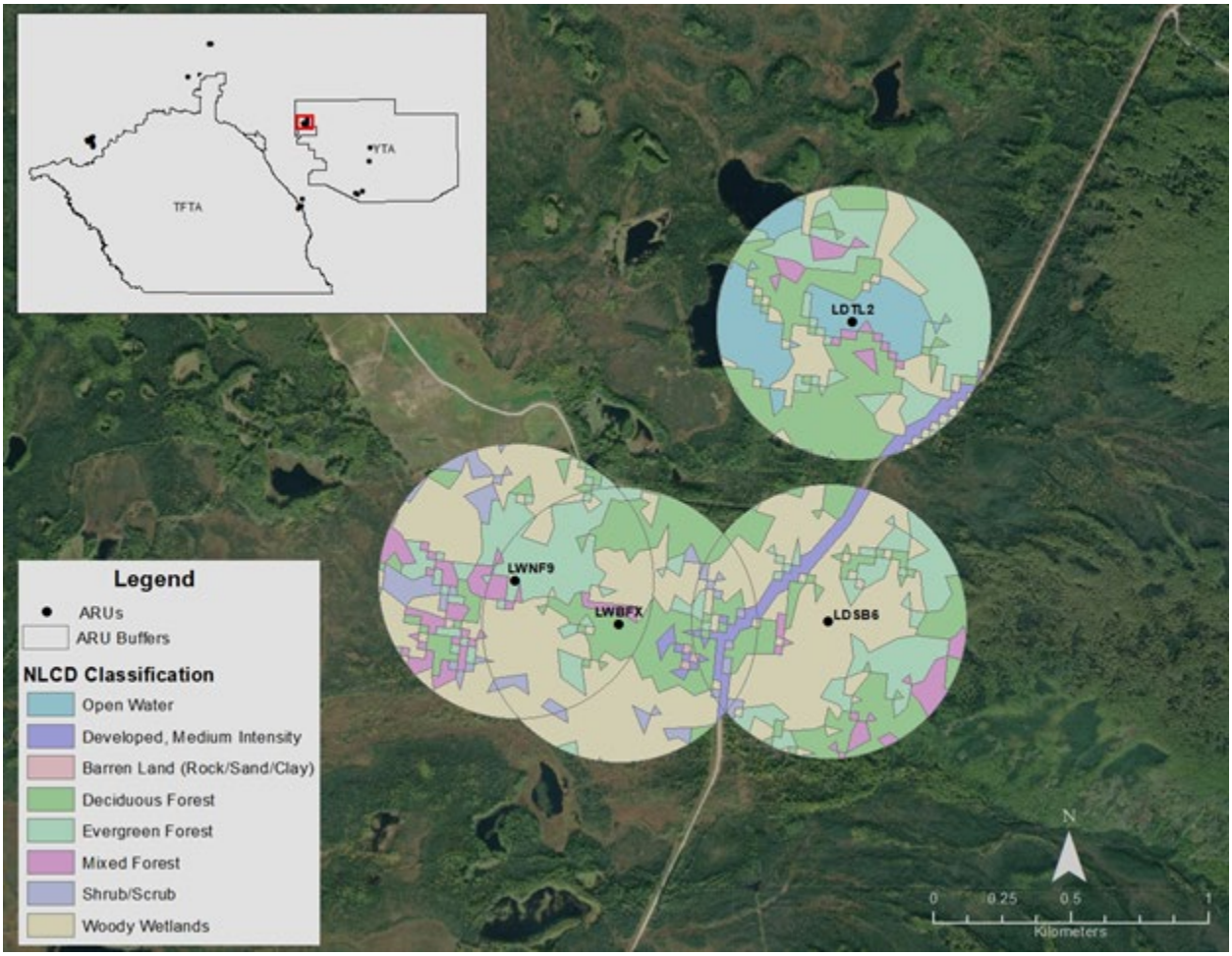


Figure 84. Examples of vegetation conditions within 0.5-km of four placements of automated audio recording units (ARUs) located in lowland landscapes of western Yukon Training Area (YTA). TFTA = Tanana Flats Training Area. Dots are the specific locations of the ARUs (see Table 3.2.1). LDTL = Lowland Deep Thermokarst Lake, LDSB = Lowland Dwarf Scrub Bog, LWNF = Lowland Wet Needleleaf Forest, LWBF = Lowland Wet Broadleaf Forest. The 0.5-km radius approximates the effective recording distance from each ARU location.

2.9.7 Analysis of Audio Recordings Using Machine Learning

Over field seasons 2019 and 2020, a total of 82,023 Wave sound files were recorded by the ARUs, totaling 2.80TB of data. Following the recording schedule we programmed into the ARUs, each Wave file consisted of a 10-minute audio recording starting at the top of each hour. The Wave files were sorted into 6,365 computer folders by recording year, landscape and successional stage, location by ecotype designation, and date.

The sound files were analyzed using Kaleidoscope Pro v. 5.4.2 (Wildlife Acoustics), a signal-detection, machine-learning program that statistically groups similar sounds into clusters (Knight et al., 2017). The individual samples of each cluster are then shown on screen as sound spectrograms (frequency as a function of time) and the audio of each recording can be played to aid in identification of the source, particularly wildlife species of birds and mammals. Using such machine-learning algorithms to identify birds and other sound sources is a relative recent technology but one fast becoming standard practice (Brooker et al., 2020, Ruff et al., 2020; Ntalampiras and Potamitis, 2021).

Identifications of bird sounds to species were made based on personal experience and knowledge (B. Marcot), and by comparing sounds to identified recordings from several on-line sources including xeno-canto (https://www.xeno-canto.org/), Macaulay Library of the Cornell Lab of Ornithology (https://www.macaulaylibrary.org/), and others.

Many non-biological sounds also were captured and clustered. Those sounds are not included in this bioacoustic species-recognition portion of the project, but are included in the ecoacoustic soundscape portion presented in the next section. Here, the focus is on clustering of similar sounds to identify wildlife species and to denote their association with landscape, successional stage, and ecotype designations by which to support or amend the species-ecotype relationships tables.

Several dozen species of wildlife were identified in the sound recordings that essentially supported the species-ecotype relationships designations developed from other source material. These species included sounds of wood frog, great horned owl, several species of thrushes (hermit, Swainson's, and varied thrushes; northern waterthrush; American robin), raptors (northern goshawk, red-tailed hawk, osprey), chickadees (black-capped and boreal), sparrows (golden-crowned, chipping), gulls, woodpeckers, sandhill crane, Canada goose, common raven, olive-sided flycatcher, red squirrels, and others (e.g., Figure 85). One bird species was discovered from the recordings and added after the list and analyses were complete (chipping sparrow; see Addendum at the end of Section 2.1.1).

The multiple bands appearing in some of these and subsequent plots (e.g., chickadee) are overtones or undertones, which help give some vocalizations their characteristic sound qualities that are uniquely identified by the machine-learning, sound-recognition program.

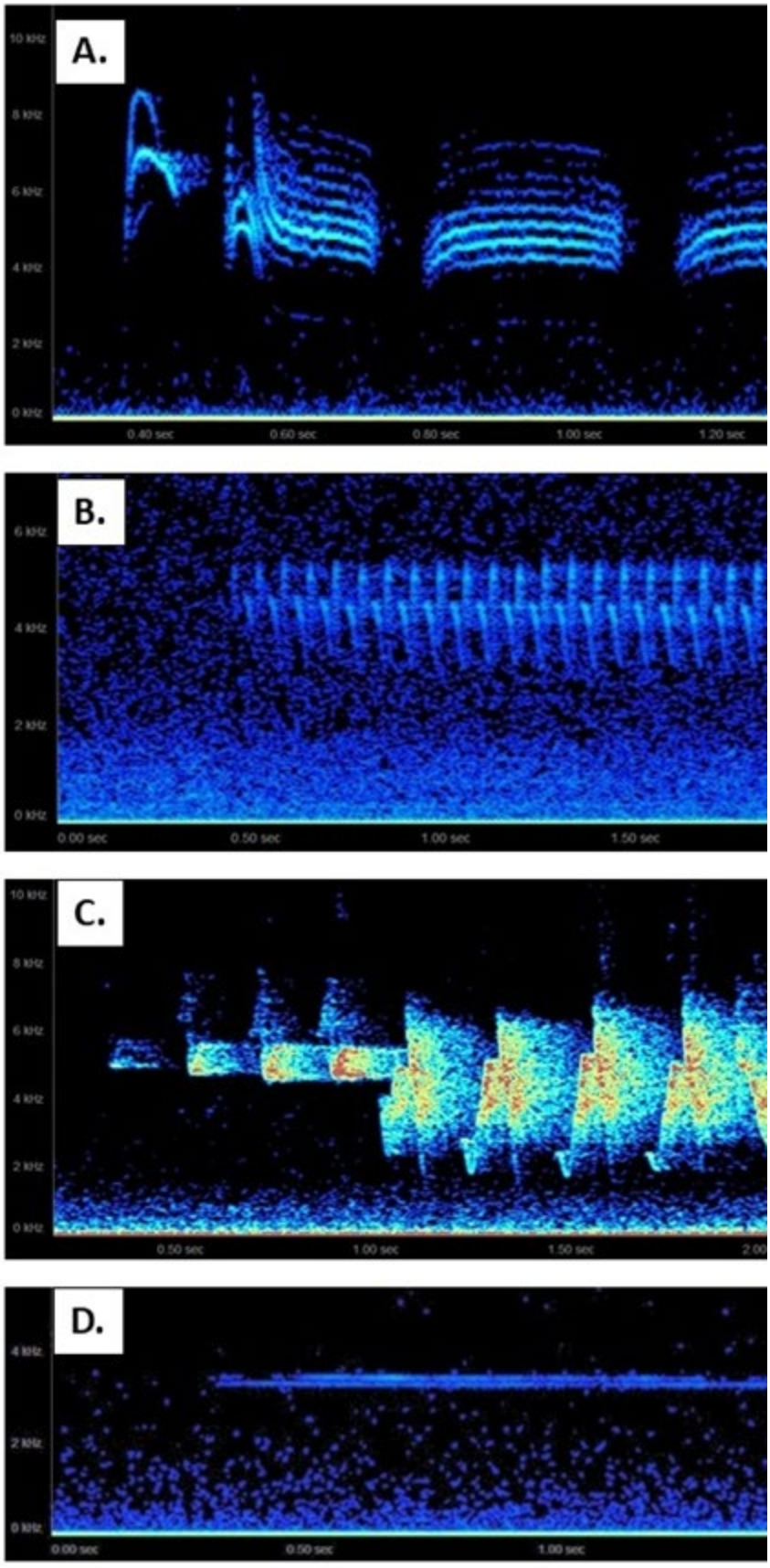


Figure 85. Examples of wildlife sound spectrograms of recordings from automated audio recording units (ARUs). (A) black-capped chickadee, (B) chipping sparrow,(C) northern waterthrush, (D) varied thrush (continued below). Ecotype associations: (A, D) Upland Moist Needleleaf Forest; (B) Lowland Deep Thermokarst Lake; (C) Upland Shallow Thermokarst Lake.

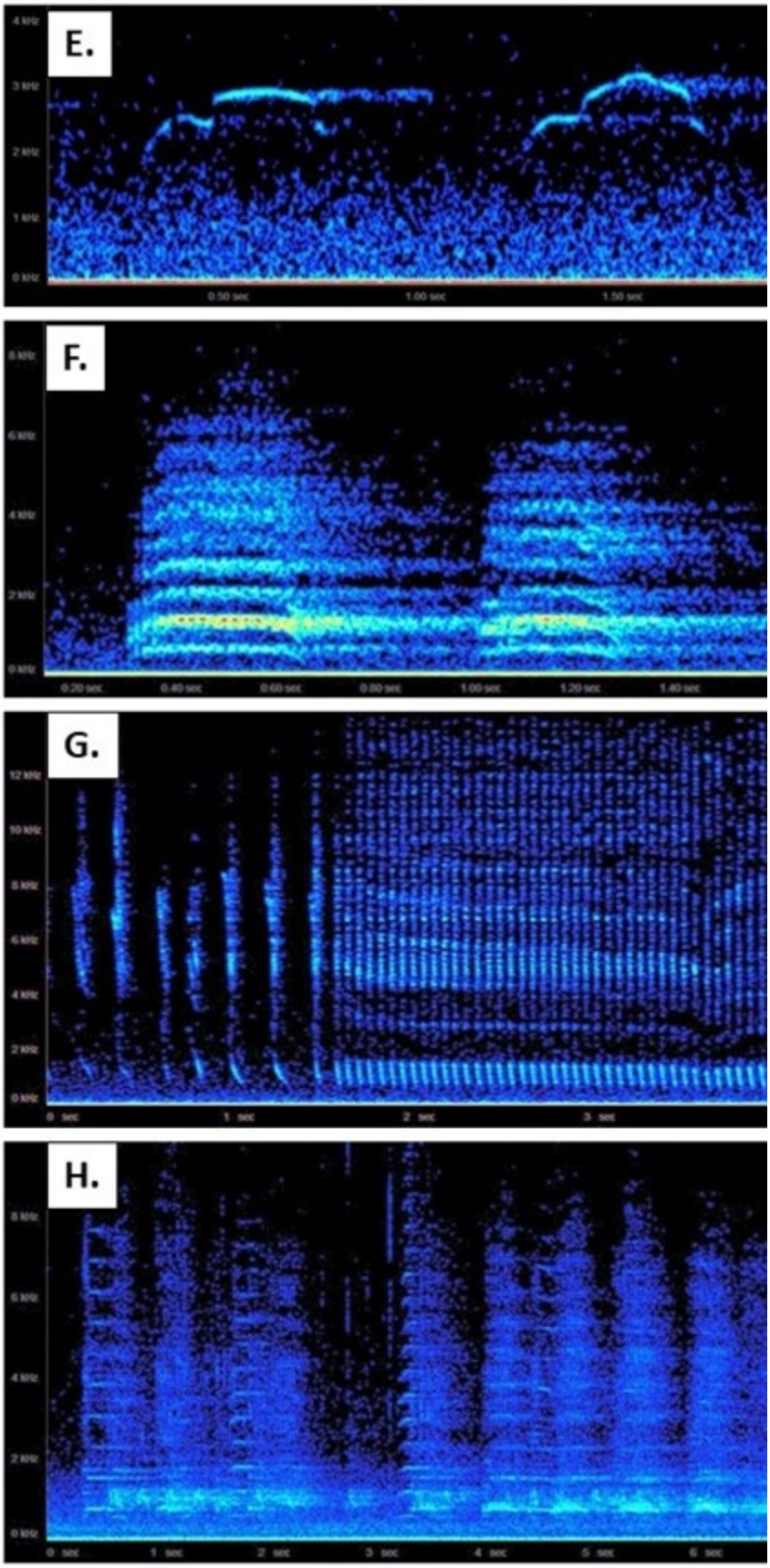


Figure 85. (continued) Examples of sound spectrograms of recordings from automated audio recording units (ARUs). (E) osprey, (F) common raven, (G) red squirrel, (H) sandhill crane. Ecotype associations: (E,H) Upland Shallow Thermokarst Lake, (F) Upland Moist Broadleaf Forest, (G) Upland Moist Needleleaf Forest.

Exploration of the recordings is continuing, to determine first-arrival dates of migratory songbirds of the region as a benchmark for potential future comparisons. Regional climate change may be advancing first-arrival times and a fostering northward spread of some species' distributions (e.g., black-billed magpie).

The entire set of the bioacoustic audio recordings, along with the clustering results from using Kaleidoscope Pro, are archived on external hard drives and can be made available for further analysis.

2.9.8 Ecoacoustic Study of the Soundscapes of USAG-AK Training Lands

This section presents methods and findings on the ecoacoustic study of the soundscapes on the training lands. Discussed are: (1) how the audio recorders were analyzed as indices of soundscape conditions; (2) categories of soundscape ecoacoustics; (3) analysis of the ecoacoustic indices; and (4) patterns of soundscapes on the training lands and implications for wildlife management.

2.9.8.1 Audio Recordings Analyzed as Indices of Soundscape Conditions

The objectives for this portion of the study was to explore the soundscapes of the ecotypes, vegetation conditions, and landscapes sampled with the automated audio recording units (ARUs) as presented in the previous section. Soundscapes are depictions of the array of sounds and their sources defining particular landscapes and sites. Soundscape analysis provides insight into the degree to which sites are natural or influenced by human presence and disturbances (Gómez et al., 2018; Pijanowski et al., 2011). Soundscapes can be analyzed by use of a variety of ecoacoustic indices (e.g,. Bradfer-Lawrence et al., 2020), which are calculations of sundry aspects of sound frequencies, amplitudes, occurrences, and their diversity over time.

Soundscapes unduly dominated by human activities can mark disturbances to some wildlife species such as for feeding, reproduction, and presence. Thus, an objective for this analysis is to determine which, if any, site conditions or landscape types sampled for sound in this study might be of conservation concern for disturbance to wildlife.

2.9.8.2 Categories of Ecoacoustics

Soundscapes can be characterized by a variety of categories of sounds that can be depicted with ecoacoustic analysis (Figure 86). The major division of acoustic categories is with natural versus anthropogenic (human-caused) sounds. Natural sound sources can be further divided into biophony or sounds created by non-human organisms such as birds, mammals, and insects; and geophony or other sounds of the natural world such as with wind, rain, thunder, and even silence. Anthropogenic sound sources can be further divided into anthrophony or sounds of people such as by walking or talking; and technophony or sounds of technological creations such as radios, aircraft, trains, road vehicles, gunshots, and much more.

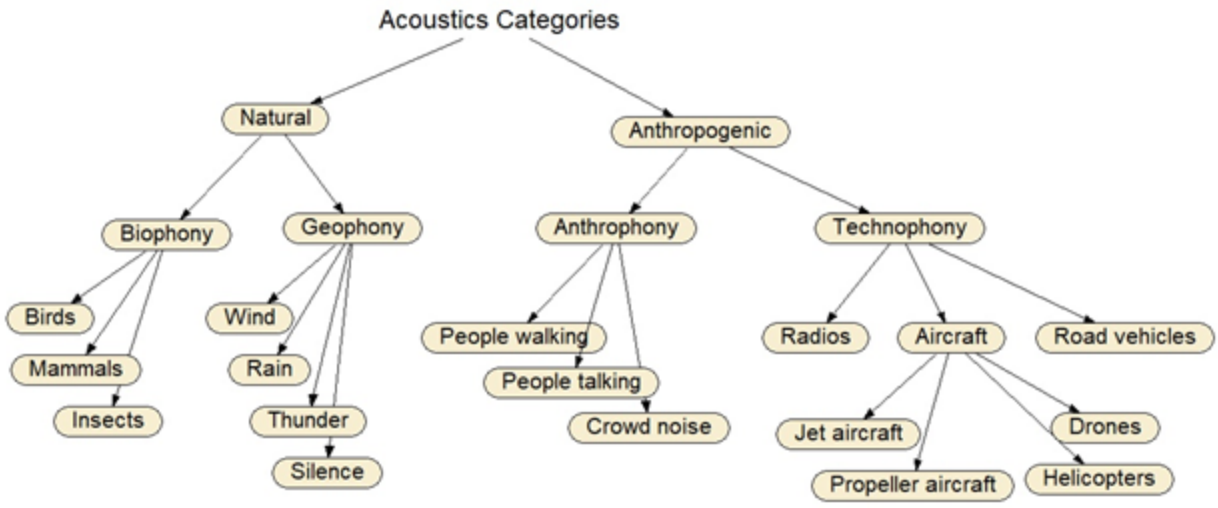


Figure 86. Categories of ecoacoustic sounds used in the soundscape analyses. Sounds can be generally classified as natural and anthropogenic (human-caused). Natural sounds can be further classified as caused by living organisms, including wildlife (biophony) or by abiotic conditions (geophony). Anthropogenic sounds can be further classified as sounds of people (anthrophony) or of their technologies, including vehicles (technophony). Sounds play important roles in ecological systems such as for species identification, and potentially as undue noise disturbance on wildlife from anthropogenic sources. See Appendix Table 15 for a variety of values for each ecoacoustic sound.

2.9.8.3 Examples of Ecoacoustic Categories

Each ecoacoustic category shown in Figure 86 has characteristic patterns of sound frequency, amplitude, and duration, and can be recognized in plots of sound spectrograms. Some 8 examples of biophony (insect, bird, and mammal sounds, songs, and calls) are presented in Figure 85. Additional examples of geophony, anthrophony, and technophony are presented in Figures 86, 87, and 88, respectively. The figures show amplitudes (loudness) of the sounds across the red graphs at the top (measured in decibel absolutes, dBA) and sound frequencies as a function of time on the bottom (color intensity corresponds to amplitude).

In the geophony examples, note how blustery wind (Figure 87 A) and thunder (Figure 86.D) differentiate from each other by the greater spread of more intense frequencies with wind, and how rain showers and heavy rain downpours (Figure 87 B,C) appear on the plots almost like falling rain itself because the sounds span a wide range of frequencies vertically on the spectrogram plots. Also, it is important to track the occurrence of silence (Figure 87 E) as a relatively uncommon sound pattern that is often interrupted by the many other sound sources and conditions.

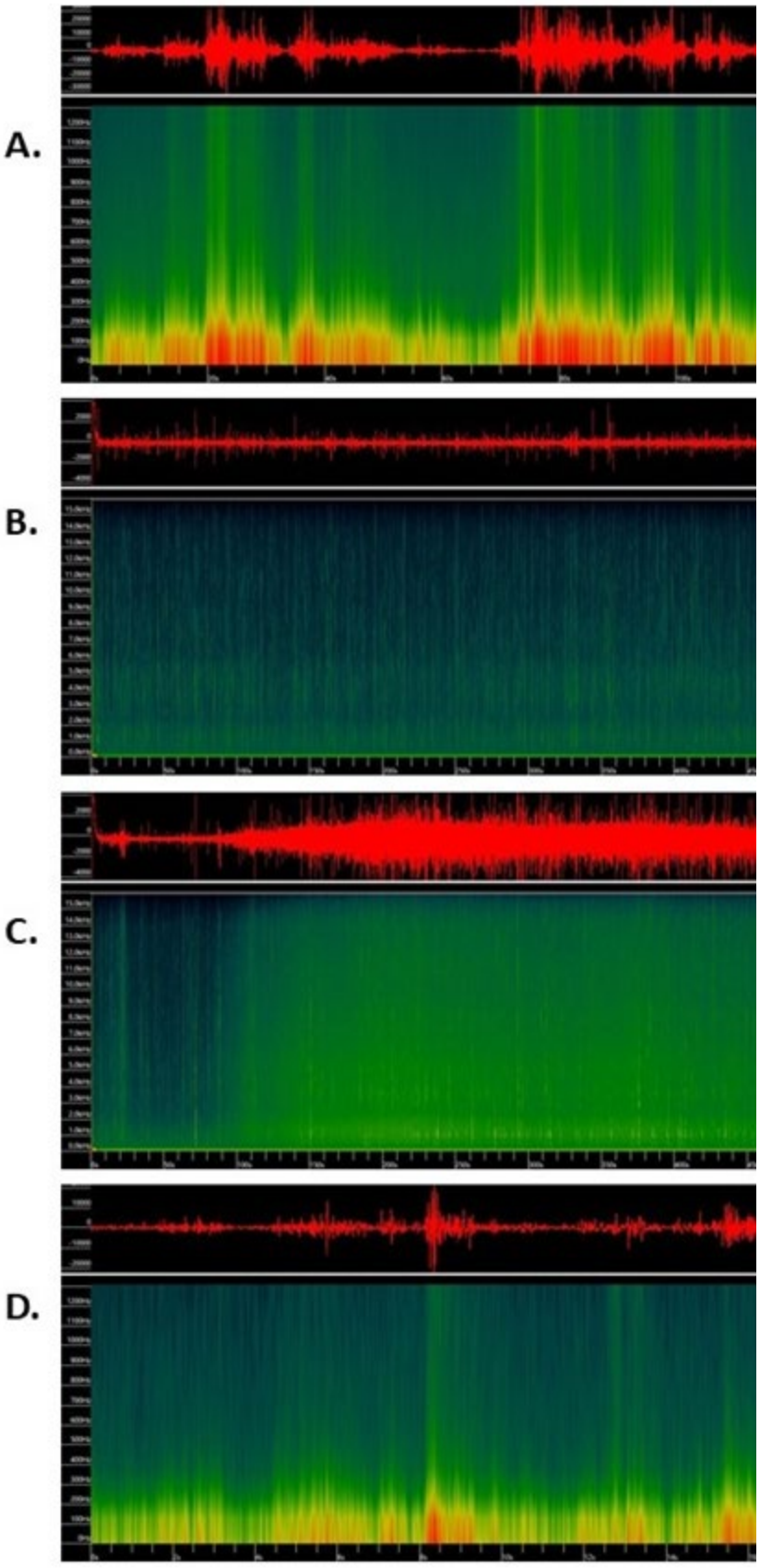


Figure 87. Examples of sound spectrograms of geophony conditions. (A) intermittent blustery wind, (B) rain, (C) heavy rain downpour, (D) thunder, (E) silence. The red traces at the top of each image denote sound amplitude, and the bottom part of the images denote frequency distributions, both as a function of time (x-axis). Continued below.

E.

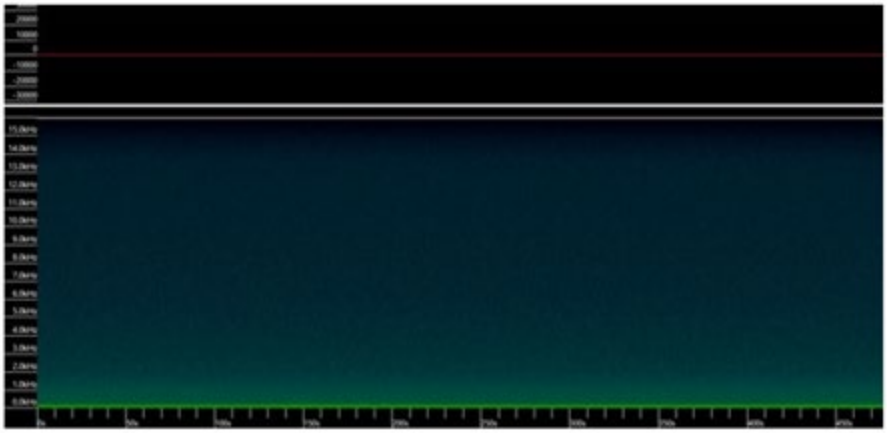


Figure 87, continued.

Differentiating some sound sources of anthrophony and geophony can be difficult. However, in the anthrophony example (Figure 88), note how the sounds of people talking and walking (through the bush, near the placed ARU recorder) produce more continuous amplitudes (the red band on the top of the Figure) than the geophony examples.

Lastly, the examples of technophony generally produce unique sound profiles. The passage of aircraft (Figures 89 A,B,C) can clearly show a Doppler effect of increasing and decreasing frequencies of overtones, although at different rates and frequency levels among the various kinds of aircraft. This is not particularly evident with road vehicles (Figure 89 D), at least the distances from the ARUs in this study.

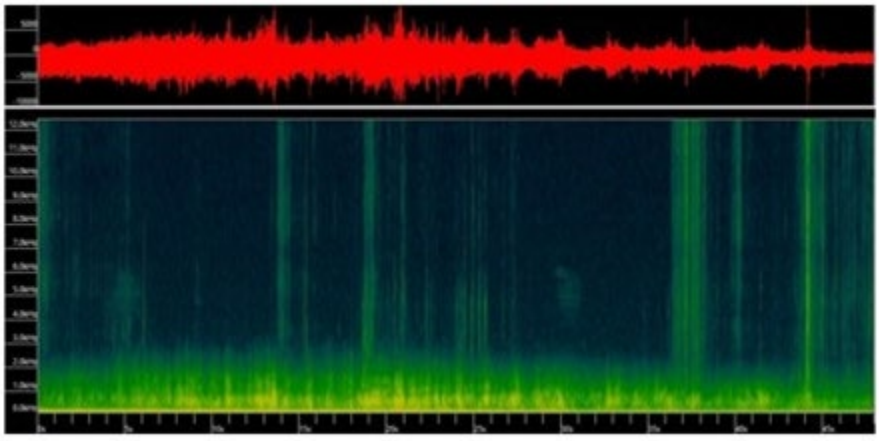


Figure 88. Examples of a sound spectrogram of an anthrophony condition of people talking and walking. Vocalizations produce the lower-frequency bands < ~1kHz, and walking -- here, through shrubs and vegetation cover, stepping on down twigs and branches -- appear as vertical bands covering a wide range of frequencies.

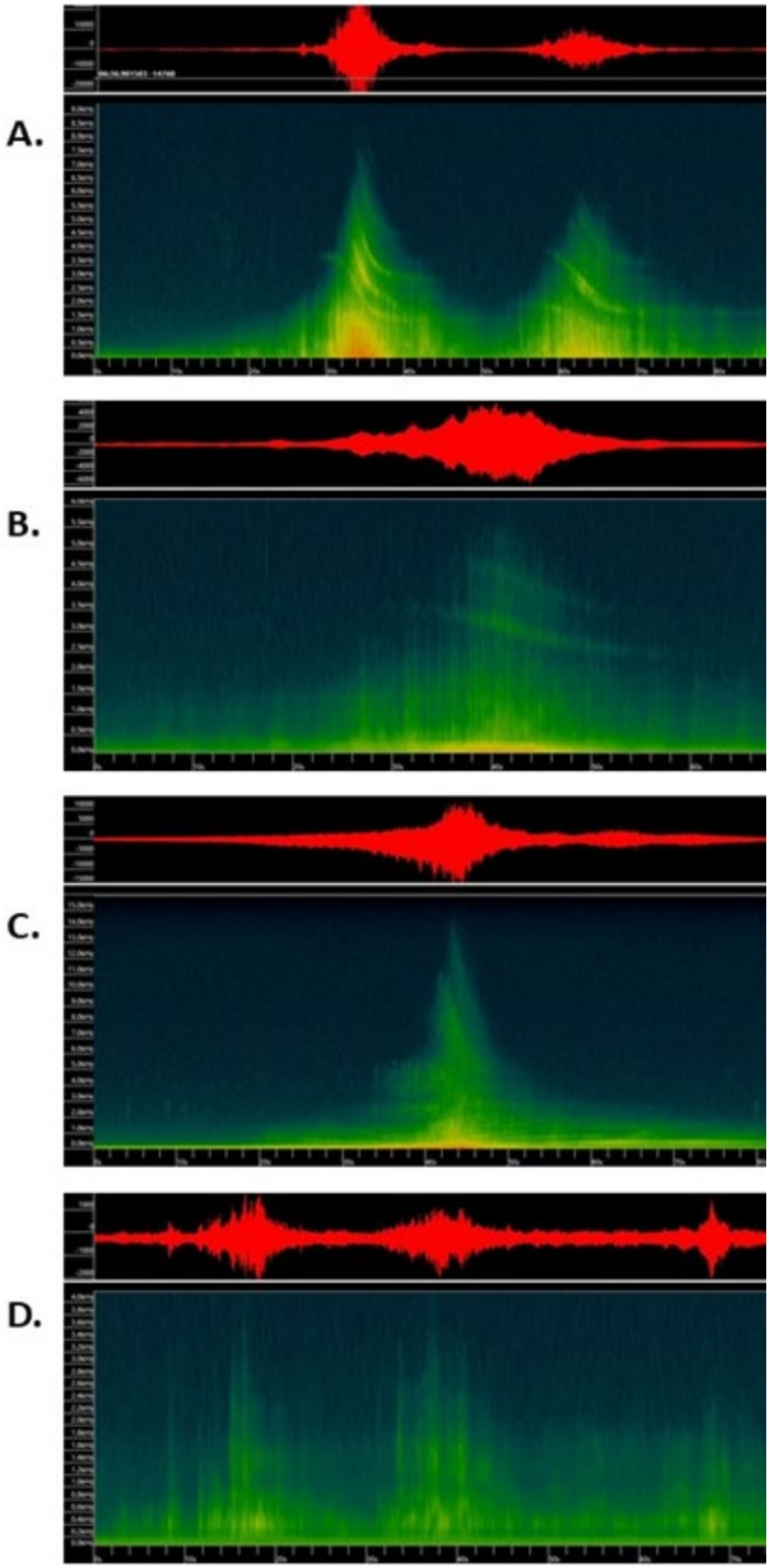


Figure 89. Examples of sound spectrograms of technophony conditions. (A) large jet aircraft, (B) small propeller airplane, (C) helicopter, (D) road vehicles. (continued below)

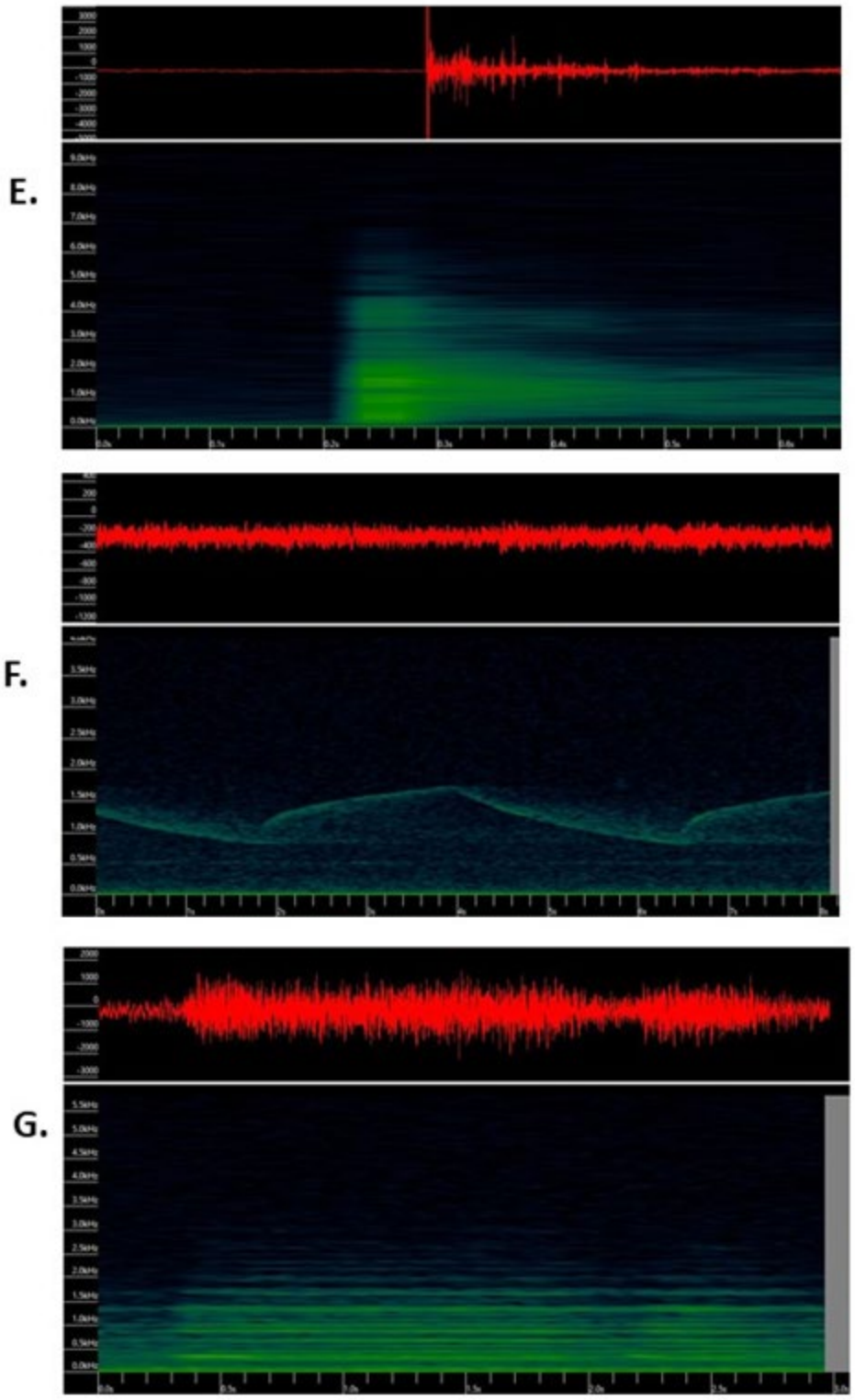


Figure 89, continued. Examples of sound spectrograms of technophony conditions. (E) gunshot (nearby), (F) vehicle siren, (G) train whistles.

Note the obvious changes in frequencies of the aircraft as they recede from the ARU audio recorder location; this is caused by the Doppler effect resulting in a drop in the amplitude-dominant frequencies (some recordings also show increases, as with approaching aircraft). This effect was not as evident with road vehicles, given the distance between ARU and road.

2.9.8.4 Analysis of Ecoacoustic Indices

We used the program Kaleidoscope Pro v. 5.4.2 (Wildlife Acoustics) to calculate ecoacoustic indices from the 2.80TB of Wave sound files collected from the 24 ARUs that we deployed during field seasons 2019 (June-August) and 2020 (April-September). We located the ARUs at sites representing 12 ecotypes in lowland, upland, riverine, and lacustrine landscape types and three successional stages (Table 15).

We initially calculated 13 ecoacoustic indices (Table 16) from the ARU field sound files, and also for specific examples of the main acoustic categories shown in Figure 86 (see Appendix Table 15 for example index values).

Table 16. Ecoacoustic indices calculated from field sound recordings. These 13 indices represent various dimensions of soundscape conditions, or patterns of sound frequencies, amplitudes, and temporal variations, from various natural and anthropogenic (human-caused) sources.

Form	Ecoacoustic index name	Description
NDSI	Normalized Difference Soundscape Index	weights higher frequencies of biophony with index values > 0, and lower frequencies of anthrophony with index values < 0
ACI	Acoustic Complexity Index	measures differences in amplitude across time segments of a sound file
ADI	Acoustic Diversity Index	Shannon diversity index of variations in sound frequencies among time segments of a sound file
AEI	Acoustic Evenness Index	Gini index of uniformity of sound frequencies among time segments of a sound file
BI	Bioacoustic Index	total amplitude content of a sound file; measures area under the amplitude spectrum curve
BGN	Background Noise Index	measures amplitude of background noise
SNR	Signal to Noise Ratio Index	calculates amplitudes of the primary signal to that of the background noise
ACT	Activity Index	measures the fraction of all sound contributed by a specified sound level above a specified threshold
EVN	Events Index	counts the number of acoustic events per second exceeding a specified amplitude threshold
LFC	Low-frequency Cover Index	measures the fraction of sound segments exceeding a specified amplitude (dB) threshold, in the 0-1 kHz frequency
MFCI	Mid-frequency Cover Index	measures the fraction of sound segments exceeding a specified amplitude (dB) threshold, in the 1-8 kHz frequency
HFCI	High-frequency Cover Index	measures the fraction of sound segments exceeding a specified amplitude (dB) threshold, in the 8-11.025 kHz frequency
CENT	Concentration Index	calculates the average frequency weighted by amplitudes for sounds ≥ 500 Hz

We next calculated Pearson correlation coefficients and Bonferonni probabilities among all 13 ecoacoustic index values calculated from all 82,023 field Wave recording files stratified by landscape and successional stage (see Table 15). We found 8 cases of significant correlation among pairs of 6 indices (Appendix Table 16). In the process of excluding indices that may be correlated with others, we pared the field down to two indices- the Normalized Difference Soundscape Index (NDSI) and the Acoustic Diversity Index (ADI)- that were uncorrelated with each other (Pearson correlation $r = 0.136$, $P = 1.000$).

The main analyses in this section include a focus on these two indice- NDSI and ADI -- that provide complementary information and insights into the soundscape conditions of the study area. NDSI values range [−1,+1] broadly representing the degree to which sounds pertain to biophony (values > 0) and anthrophony (values < 0) sources. ADI values theoretically range ≥ 0, but in practical application tend to range [0,~3], with higher values denoting a greater diversity of sound frequencies and, by inference, a greater variety of sound sources and conditions.

It should be noted that no ecoacoustic index is immune from conflation of different sound sources containing the same or very similar sound frequencies and amplitudes. This is especially the case with some categories of geophony such as wind and thunder (Figure 86) being confused with some categories of technophony such as aircraft and road vehicles (Figure 89). We explored these similarities.

A final note to mention here is the discovery of a sound "glitch" that occurred with the Cornell Swift ARUs' firmware that controlled the sleep and wake cycles of recordings. Upon awakening to do a recording, the firmware introduced an initial, anomalous "blip" sound into each recording, lasting only the first 4 seconds of the sound file. This glitch had no effect on the species-specific bioacoustic analyses presented in the previous section, but had a major effect on the calculated ecoacoustic indices used in this section. We employed a Python-coded program (provided by Zack Ruff, U.S. Forest Service, Corvallis Forestry Sciences Laboratory, Oregon) to delete the first 4 seconds from each Wave sound file, and recalculated all ecoacoustic indices and redid all analyses based on the cleaned sound files. These findings and analyses have been written in a separate journal manuscript and submitted for review (see Appendix A.2).

2.10 Task 3.2

Evaluate effects of projected change in ecotype distribution (Task 2.3) on wildlife.

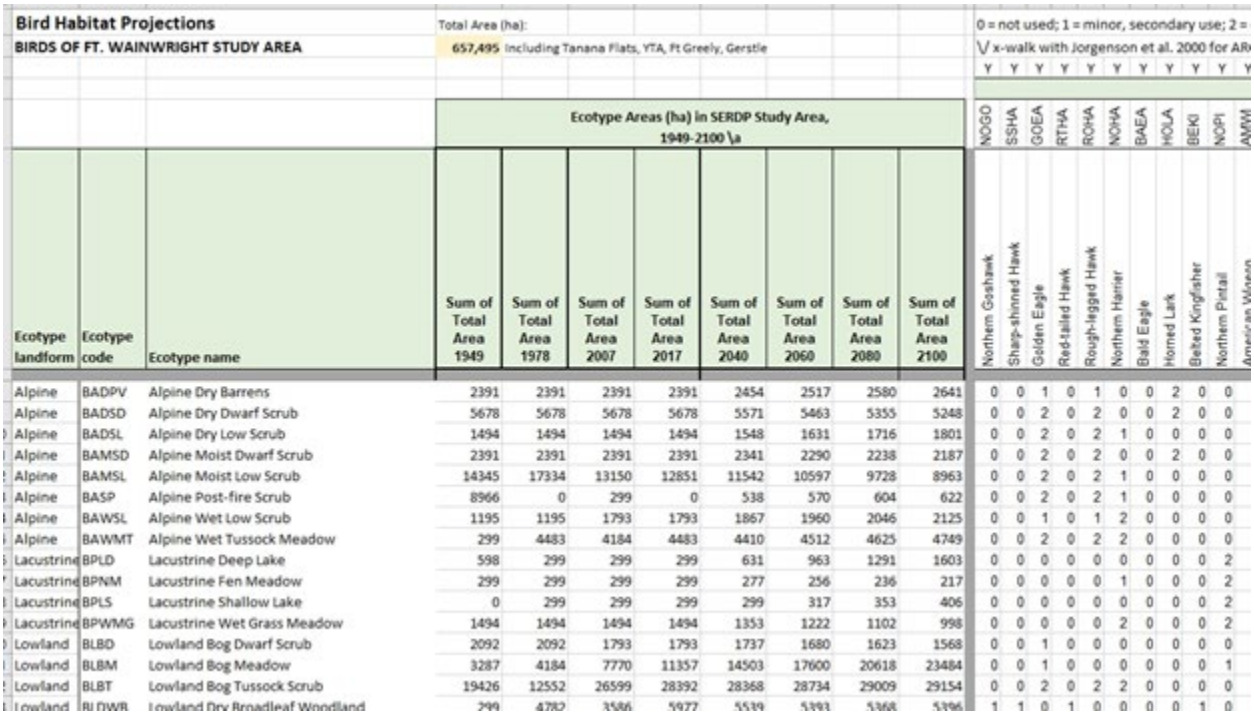
2.10.1 Species Habitats Over Past, Current, and Future Time Periods by Ecotype Projection Scenario

This section presents overall past, current, and future habitat trends of amphibian (wood frog), birds, and mammals, building on the base information from the previous sections. The next section explores these trends for selected species groups of ecological or potential conservation interest. Results presented here and in the next section address Project Objective 1: “Assessing habitat vulnerability to climate change and identify the factors that drive vulnerability."

In the ecotype projection scenarios, past time periods include years 1949, 1978, and 2007; current conditions are represented by year 2017; and future period projections include 2040, 2060, 2080, and 2100. Ecotype areas for past and current time periods are the same among the four scenarios. Ecotype areas for the four future time periods vary by scenario, being based on projections using climate model RCP 4.5, the driver-adjusted climate model RCP 6.0, climate model RCP 8.5, and the time model based on historic rates (see the sections of this report on explanation of these projection models). We focus here on comparing and summarizing species' habitat changes from 1949 to 2017, and from 2017 to 2100, with additional comparisons for 1949 to 2100 presented in appendices (cited below).

2.10.2 Integrating Ecotype Areas by Time Period

Expanding the previous example of a bird species-ecotype relationships table (Figure 67), here we show how the past, current, and future projections of areas of each ecotype were integrated into these relationships tables, using the climate model RCP 4.5 scenario projections as a case in point (Figure 90).



Bird Habitat Projections
BIRDS OF FT. WAINWRIGHT STUDY AREA
Total Area (ha): 657,495 including Tanana Flats, YTA, Ft Greely, Gerstle
0 = not used; 1 = minor, secondary use; 2 = ...
√ x-walk with Jorgenson et al. 2000 for AR...

Ecotype Areas (ha) in SERDP Study Area, 1949-2100 \a

Ecotype landform	Ecotype code	Ecotype name	Sum of Total Area 1949	Sum of Total Area 1978	Sum of Total Area 2007	Sum of Total Area 2017	Sum of Total Area 2040	Sum of Total Area 2060	Sum of Total Area 2080	Sum of Total Area 2100	NOGO Northern Goshawk	SSHA Sharp-shinned Hawk	GOEA Golden Eagle	RTHA Red-tailed Hawk	ROHA Rough-legged Hawk	NOHA Northern Harrier	BAEA Bald Eagle	HOLA Horned Lark	BEKI Belted Kingfisher	NOPI Northern Pintail	AMW...
Alpine	BADPV	Alpine Dry Barrens	2391	2391	2391	2391	2454	2517	2580	2641	0	0	1	0	1	0	0	2	0	0	
Alpine	BADSD	Alpine Dry Dwarf Scrub	5678	5678	5678	5678	5571	5463	5355	5248	0	0	2	0	2	0	0	2	0	0	
Alpine	BADSL	Alpine Dry Low Scrub	1494	1494	1494	1494	1548	1631	1716	1801	0	0	2	0	2	1	0	0	0	0	
Alpine	BAMSD	Alpine Moist Dwarf Scrub	2391	2391	2391	2391	2341	2290	2238	2187	0	0	2	0	2	0	0	2	0	0	
Alpine	BAMSL	Alpine Moist Low Scrub	14345	17334	13150	12851	11542	10597	9728	8963	0	0	2	0	2	1	0	0	0	0	
Alpine	BASP	Alpine Post-fire Scrub	8966	0	299	0	538	570	604	622	0	0	2	0	2	1	0	0	0	0	
Alpine	BAWSL	Alpine Wet Low Scrub	1195	1195	1793	1793	1867	1960	2046	2125	0	0	1	0	1	2	0	0	0	0	
Alpine	BAWMT	Alpine Wet Tussock Meadow	299	4483	4184	4483	4410	4512	4625	4749	0	0	2	0	2	2	0	0	0	0	
Lacustrine	BPLD	Lacustrine Deep Lake	598	299	299	299	631	963	1291	1603	0	0	0	0	0	0	0	0	0	2	
Lacustrine	BPNM	Lacustrine Fen Meadow	299	299	299	299	277	256	236	217	0	0	0	0	0	1	0	0	0	2	
Lacustrine	BPLS	Lacustrine Shallow Lake	0	299	299	299	299	317	353	406	0	0	0	0	0	0	0	0	0	2	
Lacustrine	BPWMG	Lacustrine Wet Grass Meadow	1494	1494	1494	1494	1353	1222	1102	998	0	0	0	0	0	2	0	0	0	2	
Lowland	BLBD	Lowland Bog Dwarf Scrub	2092	2092	1793	1793	1737	1680	1623	1568	0	0	1	0	0	0	0	0	0	0	
Lowland	BLBM	Lowland Bog Meadow	3287	4184	7770	11357	14503	17600	20618	23484	0	0	1	0	0	0	0	0	0	1	
Lowland	BLBT	Lowland Bog Tussock Scrub	19426	12552	26599	28392	28368	28734	29009	29154	0	0	2	0	2	2	0	0	0	0	
Lowland	BLDWB	Lowland Dry Broadleaf Woodland	299	4782	3586	5977	5539	5393	5368	5396	1	1	0	1	0	0	0	0	1	0	

Figure 90. An example of expanding the bird-ecotype relationships table (Figure 66) to include projections of the area coverage of each ecotype by 8 past, current, and future projected time periods. This example pertains to future projections (years 2040 to 2100) under the climate model RCP 4.5 scenario, and this figure shows just a small corner of the much larger table that includes 61 ecotypes (rows) and 124 bird species (columns). Ecotype amounts are the same under all four future climate projection scenarios for time periods 1949 to 2017, and they differ among all four scenarios for the future time periods of 2040 to 2100. In general, this table structure allows for matching of each wildlife species' ecotype use (at levels 1 and 2, secondary and primary habitats, respectively) for efficient calculation of total habitat areas by past, current, and future time period.

The above table structure allowed for efficient calculations of total habitat area for each wildlife species by each time period, based on use levels of each ecotype, by matching the use to each ecotype area (Figure 91).

Ecotype landform	Ecotype code	Ecotype name	Violet-green Swallow							
			1949	1978	2007	2017	2040	2060	2080	2100
Alpine	BADPV	Alpine Dry Barrens	2390.892	2390.892	2390.892	2390.892	2453.782	2516.837	2579.847	2641.286
Alpine	BADSD	Alpine Dry Dwarf Scrub	0	0	0	0	0	0	0	0
Alpine	BADSL	Alpine Dry Low Scrub	0	0	0	0	0	0	0	0
Alpine	BAMSD	Alpine Moist Dwarf Scrub	0	0	0	0	0	0	0	0
Alpine	BAMSL	Alpine Moist Low Scrub	0	0	0	0	0	0	0	0
Alpine	BASP	Alpine Post-fire Scrub	0	0	0	0	0	0	0	0
Alpine	BAWSL	Alpine Wet Low Scrub	0	0	0	0	0	0	0	0
Alpine	BAWMT	Alpine Wet Tussock Meadow	0	0	0	0	0	0	0	0
Lacustrine	BPLD	Lacustrine Deep Lake	0	0	0	0	0	0	0	0
Lacustrine	BPNM	Lacustrine Fen Meadow	0	0	0	0	0	0	0	0
Lacustrine	BPLS	Lacustrine Shallow Lake	0	0	0	0	0	0	0	0
Lacustrine	BPWMG	Lacustrine Wet Grass Meadow	0	0	0	0	0	0	0	0
Lowland	BLBD	Lowland Bog Dwarf Scrub	2092.03	2092.03	1793.169	1793.169	1736.568	1679.725	1623.111	1568.106
Lowland	BLBM	Lowland Bog Meadow	3287.476	4184.061	7770.398	11356.74	14503.47	17600.01	20618.47	23483.76
Lowland	BLBT	Lowland Bog Tussock Scrub	0	0	0	0	0	0	0	0
Lowland	BLDWB	Lowland Dry Broadleaf Woodland	298.8615	4781.783	3586.338	5977.229	5539.147	5392.975	5368.142	5396.007
Lowland	BLDSL	Lowland Dry Low Scrub	0	0	0	0	0	0	0	0
Lowland	BLDWM	Lowland Dry Mixed Woodland	3586.338	3885.199	3287.476	3287.476	3877.781	4313.196	4660.119	4945.151
Lowland	BLNS	Lowland Fen Low Scrub	0	0	0	0	0	0	0	0
Lowland	BLNM	Lowland Fen Meadow	0	0	0	0	0	0	0	0
Lowland	BLPU	Lowland Human-modified Barrens	0	298.8615	896.5844	896.5844	1022.914	1120.026	1192.425	1242.042
Lowland	BLSU	Lowland Human-modified Scrub	298.8615	896.5844	1195.446	1793.169	2308.991	2771.327	3181.881	3536.122
Lowland	BLMWN	Lowland Moist Needleleaf Woodland	2092.03	7172.675	3885.199	3885.199	4970.781	5796.555	6392.806	6798.547
Lowland	BLSP	Lowland Post-fire Scrub	0	0	0	0	0	0	0	0
Lowland	BLWWB	Lowland Wet Broadleaf Woodland	36162.24	35863.38	46921.25	45128.08	44372.71	43425.57	42277.31	41021.21

Figure 91. An example of using the table structure in Figure 90 to track the area of each ecotype, as used by each wildlife species, for the 8 time periods. This example shows the expected use of each ecotype by a bird species, violet-green swallow, for both secondary and primary levels of habitat use. Additional, similar tables track use for secondary and primary use levels separately; this table summed them. For the future time period values, this example pertains to the ecotype projections under the climate model RCP 4.5. The other projection scenarios are tracked in similarly-structured tables.

The final step was to sum the area of all ecotypes used by each species for each time period, as a final estimate of total habitat. This was done under each of four ecotype future projection scenarios mentioned further above. Then, calculations were made of the percent change in total habitat area of each species among selected time periods (Figure 92). In the following sections, we focus mostly on comparing changes from 1949 to 2017 (past to current), which do not vary among the four ecotype projection scenarios, and from 2017 to 2100 (current to future), which do vary among the four ecotype projection scenarios.

	Habitat (ha), Use ranks 2&1										
	1949	1978	2007	2017	2040	2060	2080	2100	Percent change 1949-2017	Percent change 2017-2100	Percent change 1949-2100
Northern Goshawk	320977.2	463833	406152.7	436337.7	424749.6	412908.3	402440.9	394558.4	35.9%	-9.6%	22.9%
Sharp-shinned Hawk	298861.5	379852.9	343690.7	333529.4	328433.9	323816.6	319231.6	314932.4	11.6%	-5.6%	5.4%
Golden Eagle	311114.8	227433.6	255825.4	252836.8	246173.8	243750.8	241070.9	238350.9	-18.7%	-5.7%	-23.4%
Red-tailed Hawk	298861.5	379852.9	343690.7	333529.4	328433.9	323816.6	319231.6	314932.4	11.6%	-5.6%	5.4%
Rough-legged Hawk	305735.3	221157.5	246261.8	239686.9	229933.7	224471.1	218829.3	213299	-21.6%	-11.0%	-30.2%
Northern Harrier	317092	233709.7	261802.6	258814	253467.2	252483.5	251334	250173.2	-18.4%	-3.3%	-21.1%
Bald Eagle	18529.41	17632.83	16138.52	15540.8	13782.7	12716.69	12351.28	12398.9	-16.1%	-20.2%	-33.1%
Horned Lark	10460.15	10460.15	10460.15	10460.15	10365.82	10269.6	10172.55	10077.02	0.0%	-3.7%	-3.7%
Belted Kingfisher	318586.3	396290.3	359530.3	348472.5	344223.1	340582.7	336410.7	332246.7	9.4%	-4.7%	4.3%
Northern Pintail	225042.7	333529.4	311712.5	336219.2	330559.8	328382.5	326972	327489.1	49.4%	-2.6%	45.5%
American Wigeon	49312.14	110578.7	92348.19	128510.4	124523.7	122588	121404.3	122235.6	160.6%	-4.9%	147.9%
Northern Shoveler	28989.56	30185.01	34667.93	39449.71	44533.94	49413.49	54213.81	58834.39	36.1%	49.1%	103.0%
Green-winged Teal	49312.14	110578.7	92348.19	128510.4	124523.7	122588	121404.3	122235.6	160.6%	-4.9%	147.9%
Mallard	40047.44	39449.71	41840.61	46323.53	51225.07	55899.51	60529.18	65018.13	15.7%	40.4%	62.4%
Lesser Scaup	28989.56	30185.01	34667.93	39449.71	44533.94	49413.49	54213.81	58834.39	36.1%	49.1%	103.0%
Redhead	23610.06	25702.09	32277.04	39449.71	47382	55340.75	63234.66	70837.94	67.1%	79.6%	200.0%
Ring-necked Duck	27794.12	29886.15	36162.24	43334.91	51069.1	58841.42	66562.85	74011.81	55.9%	70.8%	166.3%
Greater Scaup	28989.56	30185.01	34667.93	39449.71	44533.94	49413.49	54213.81	58834.39	36.1%	49.1%	103.0%
Canvasback	40047.44	39449.71	41840.61	46323.53	51225.07	55899.51	60529.18	65018.13	15.7%	40.4%	62.4%
Canada goose	60370.02	57082.54	73221.06	79796.01	84581.69	89706.38	94707.72	99449.97	32.2%	24.6%	64.7%
Bufflehead	55289.37	62462.05	62462.05	66048.38	62795.48	60149.42	58405.82	57278.05	19.5%	-13.3%	3.6%
Common Goldeneye	25702.09	24805.5	24805.5	25403.22	24417.37	23848.2	23887.81	24282.1	-1.2%	-4.4%	-5.5%
Barrow's Goldeneye	25702.09	24805.5	24805.5	25403.22	24417.37	23848.2	23887.81	24282.1	-1.2%	-4.4%	-5.5%

Figure 92. An example showing summed ecotype areas used by each species, by each time period, as measures of their total habitat area. This example shows habitat area based on secondary and primary use levels (levels 1 and 2 in the species-ecotype relationships tables), and the future time periods are based on the climate model 4.5 projection scenario. This is only a small part of the fuller table of all 124 bird species. Also shown in the right three columns are examples of calculated percent changes of habitat areas of each species, for three selected time-period comparisons.

2.10.3 Species Habitats Over Past, Current, and Future Time Periods

2.10.3.1 Wood frog

-- Between 1949 and 2017, wood frog habitat in the study area declined by 3%. Depending on the ecotype projection scenario, future wood frog habitat could remain unchanged (under the time model based on historic rates projection), could decline by an additional 4% (under RCP 4.5 and 8.5 climate projections), or could decline as much as 11% (under the driver-adjusted climate model RCP 6.0; Figure 93). No scenario projected an increase in habitat for this species, which is dependent on specific standing-water, and wet-site conditions that may undergo varying degrees of drying and drainage under the scenarios.

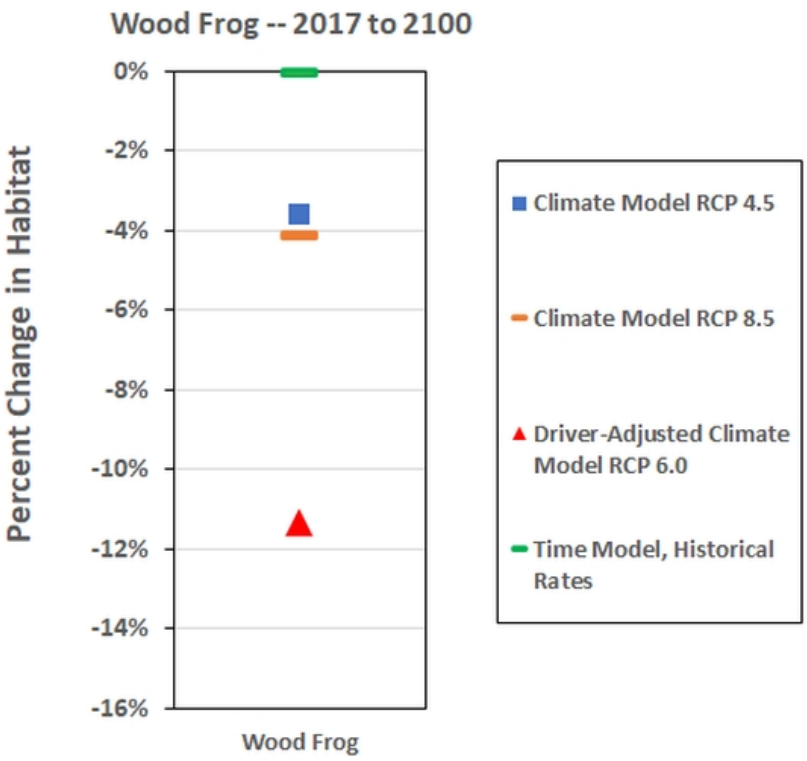


Figure 93. Projections of percent change in total habitat area for wood frog from 2017 to 2100, under the 4 ecotype projection scenarios. Note how the scenarios differ in degrees of changes in the ecotypes contributing to habitat for this species, and vary from essentially no change to as much as an 11% decline. These differences are due to the assumptions and factors considered in each of the ecotype projection scenarios.

2.10.3.2 Birds

-- Changes in ecotype areas from 1949 to 2017 provided gains in habitat for some bird species and losses for others (Appendix Table 4). The top 10 past habitat "gainer" bird species include associates of a variety of ecotypes that have most increased in area over this past time interval, such as lowland bogs, fens, and wet meadows (e.g., for sharp-tailed grouse, red-winged blackbird, Wilson's snipe), and low and tall scrub (e.g., for yellow warbler, golden-crowned sparrow, willow ptarmigan) (Figure 94). The top 10 past habitat "loser" bird species include associates of a mixed variety of ecotypes that have decreased in area over this past time interval, such as moist tall scrub (e.g., for arctic warbler, American tree sparrow), needleleaf woodland and forest (e.g., for black-backed woodpecker), post-fire scrub and barrens (e.g., for rough-legged hawk), and others (Figure 94).

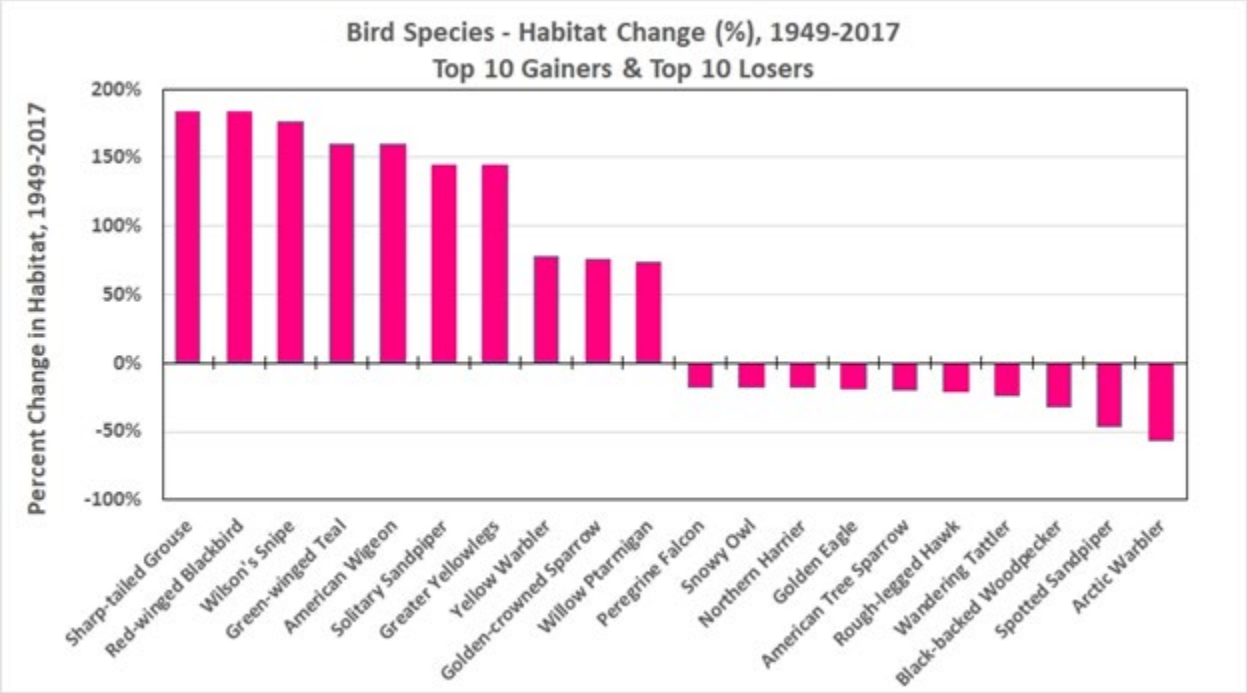
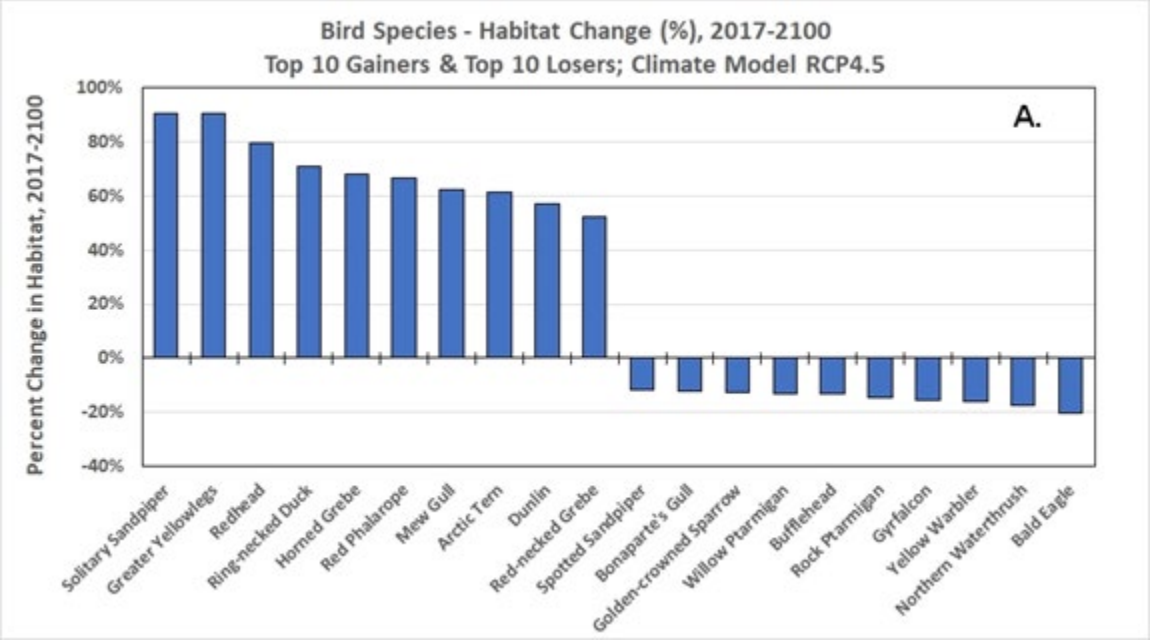
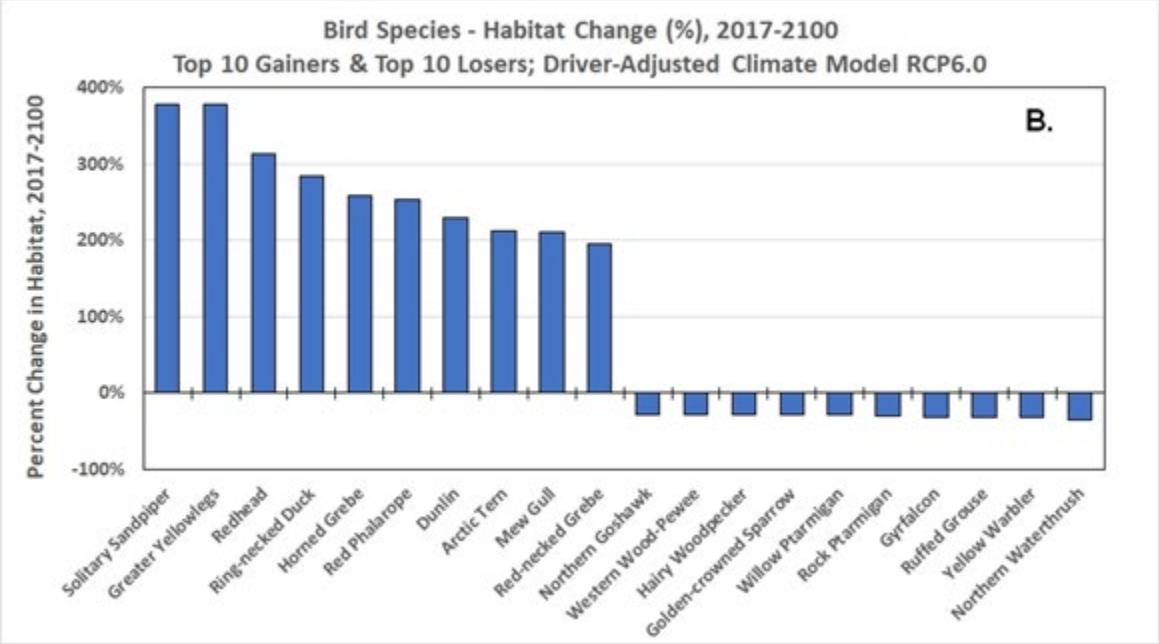


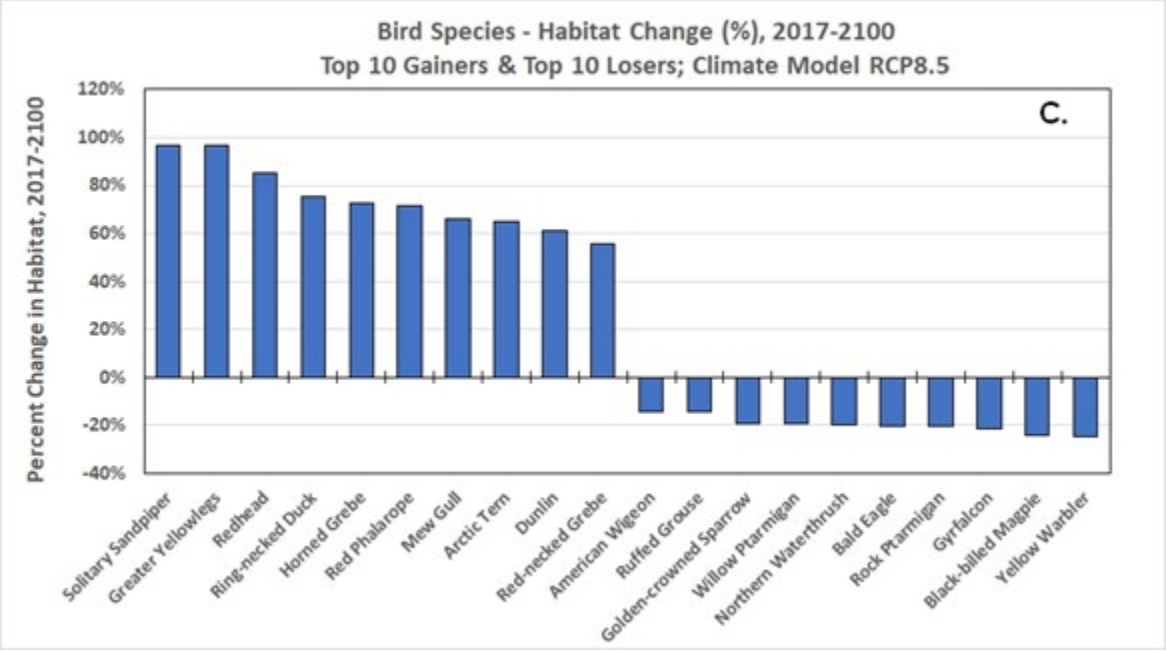
Figure 94. The top ten bird habitat "gainer" species and top ten "loser" species, over the historic time period of 1949 to 2017. Gainers generally include associates of lowland bogs, fens, wet meadows, and low and tall scrub that have increased in the study area. Losers include associates of other post-fire scrub conditions and needleleaf woodlands and forests that have decreased in area as they gave way to vegetation succession and other changes (see 2.4.3.1 Historical Ecotype Changes). Other bird species had less extreme habitat changes in the study area over this time period (Appendix Table 4).

Bird species projected to gain or lose habitat in the future, from 2017 to 2100, varied by ecotype projection scenario (Figures 95-97). The intensity of habitat gains and severity of habitat losses depended on the ecotype transitional changes that varied the projection scenarios. Greatest gains were for bird species associated with lowland bog meadow (e.g., greater yellowlegs, solitary sandpiper) that gained the most under the driver-adjusted climate model RCP 6.0 (Figure 95 B), although gains for these same conditions and species were far more modest under the climate model RCP 4.5 scenario (Figure 95 A). Losses of habitats were for some species variously associated with decreasing dry woodland environments near lakes (e.g., bufflehead, goldeneyes) and other conditions. Importantly, however, no bird species is projected for more than a 30% loss of habitat area.

Martin and Jochum (2017) identified seven species of shorebirds on the training lands, associated with barren/open mudflat and open water vegetation cover, as moderate to high conservation concern. These species included black-bellied plover, solitary sandpiper, lesser yellowlegs, upland sandpiper, whimbrel, dunlin, and Wilson’s snipe. However, we show potential future habitat gains for most of these seven species under one or more scenario projections (Figure 95).


Bird Species - Habitat Change (%), 2017-2100
Top 10 Gainers & Top 10 Losers; Climate Model RCP4.5
Percent Change in Habitat, 2017-2100
A.
100%
80%
60%
40%
20%
0%
-20%
-40%
Solitary Sandpiper
Greater Yellowlegs
Redhead
Ring-necked Duck
Horned Grebe
Red Phalarope
Mew Gull
Arctic Tern
Dunlin
Red-necked Grebe
Spotted Sandpiper
Bonaparte's Gull
Golden-crowned Sparrow
Willow Ptarmigan
Bufflehead
Rock Ptarmigan
Gyrfalcon
Yellow Warbler
Northern Waterthrush
Bald Eagle


Bird Species - Habitat Change (%), 2017-2100
Top 10 Gainers & Top 10 Losers; Driver-Adjusted Climate Model RCP6.0
Percent Change in Habitat, 2017-2100
B.
400%
300%
200%
100%
0%
-100%
Solitary Sandpiper
Greater Yellowlegs
Redhead
Ring-necked Duck
Horned Grebe
Red Phalarope
Dunlin
Arctic Tern
Mew Gull
Red-necked Grebe
Northern Goshawk
Western Wood-Pewee
Hairy Woodpecker
Golden-crowned Sparrow
Willow Ptarmigan
Rock Ptarmigan
Gyrfalcon
Ruffed Grouse
Yellow Warbler
Northern Waterthrush



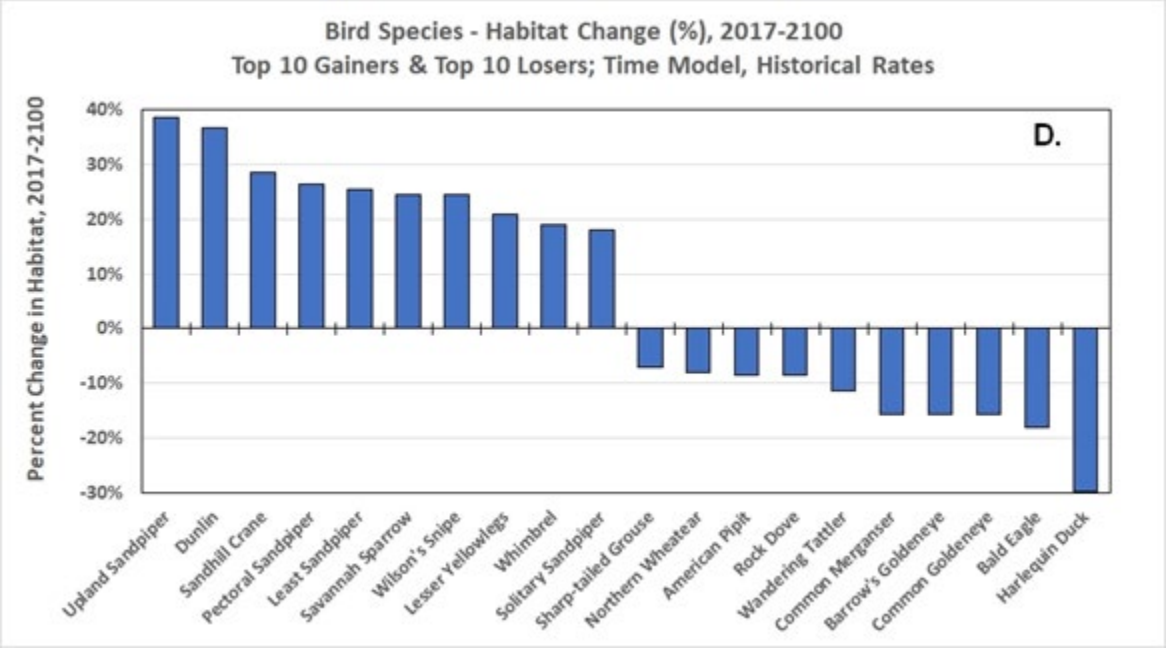


Figure 95. Top 10 bird species habitat gainers and top 10 habitat losers for the projected future time period of 2017 to 2100, among the four ecotype projection scenarios: (A) climate model RCP 4.5, (B) driver-adjusted climate model RCP 6.0, (C) climate model RCP 8.5, and (D) time model based on historic rates. Gainer and loser bird species varied among the projection scenarios depending on the severity of changes among ecotype conditions and disturbances considered in each scenario.

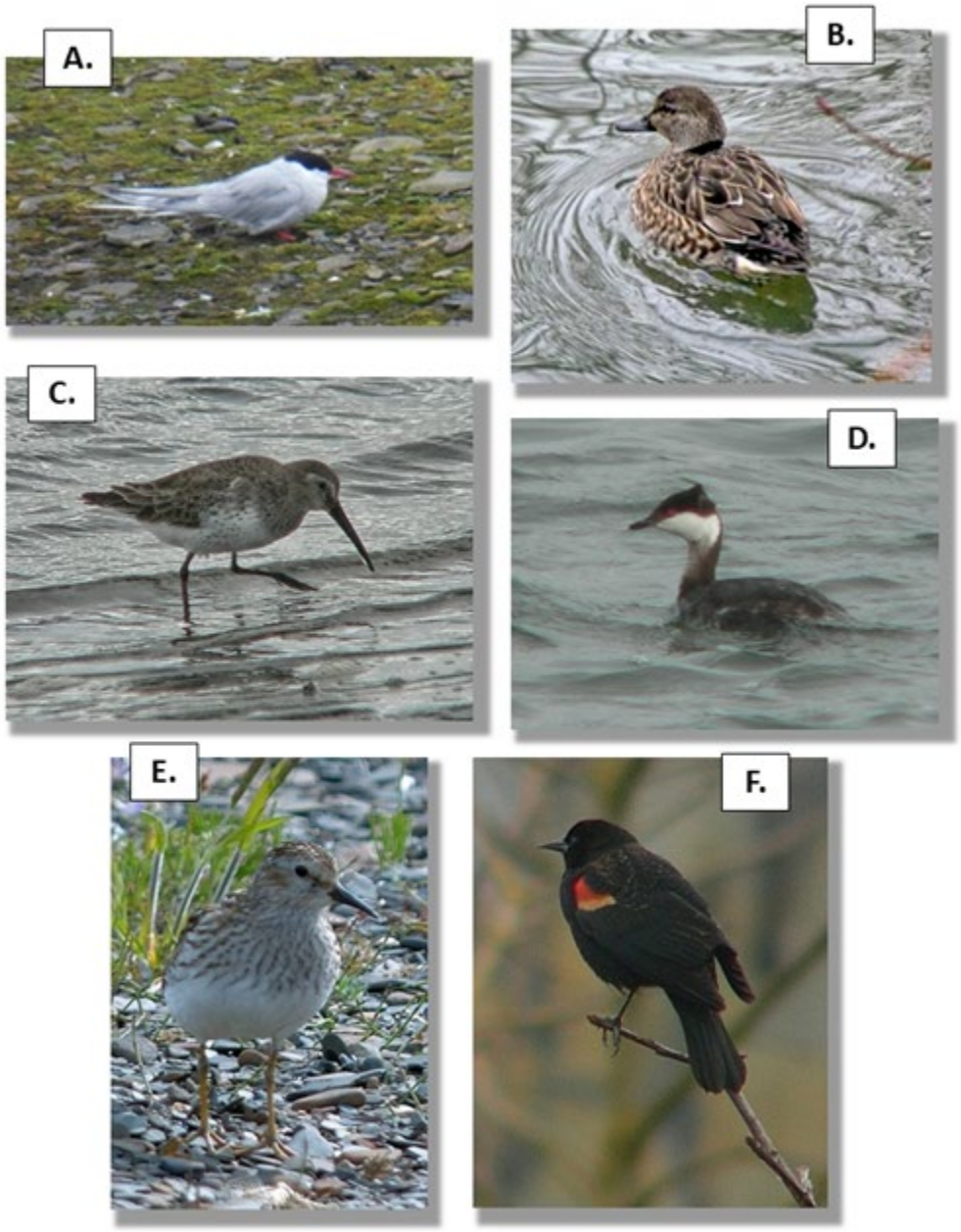


Figure 96. Examples of some bird species projected to gain habitat within the study area from 2017 to 2100 under one or more of the ecotype projection scenarios: (A) arctic tern, (B) green-winged teal, (C) dunlin, (D) horned grebe, (E) least sandpiper, (F) red-winged blackbird. Photos by Bruce G. Marcot.

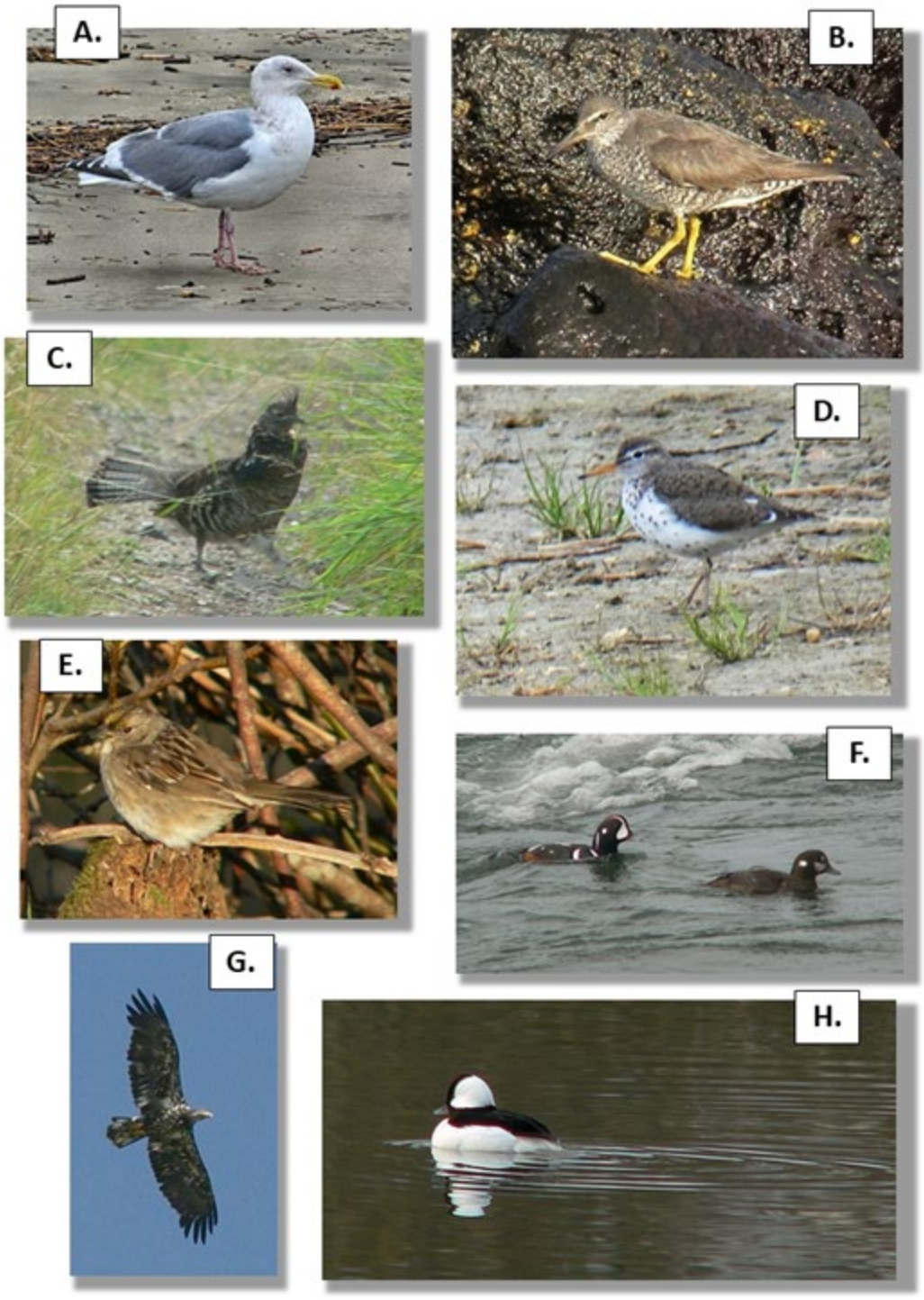


Figure 97. Examples of some bird species projected to lose habitat within the study area from 2017 to 2100 under one or more of the ecotype projection scenarios: (A) herring gull, (B) wandering tattler, (C) ruffed grouse, (D) spotted sandpiper, (E) golden-crowned sparrow, (F) harlequin duck, (G) bald eagle, (H) bufflehead. Photos by Bruce G. Marcot.

2.10.3.3 Mammals

Changes in ecotype areas from 1949 to 2017 provided gains in habitat for some mammal species and losses for other species (Appendix Table 5 and Appendix Figure 1). The top 10 past habitat "gainer" mammal species include associates of a variety of ecotypes that have most increased in area over this past time interval, such as post-fire recovery of open, short-vegetation ecotypes (Figure 98). The top 10 past habitat "loser" mammal species -- still gaining habitat historically but at the least rate- include associates of a mixed variety of ecotypes that have decreased in area over this past time interval.

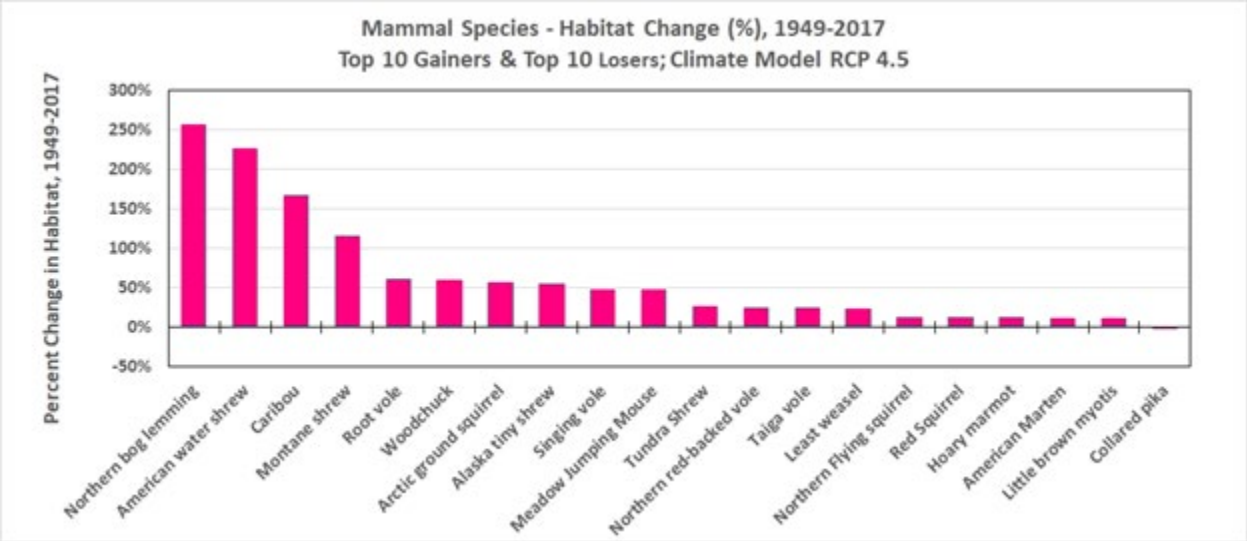
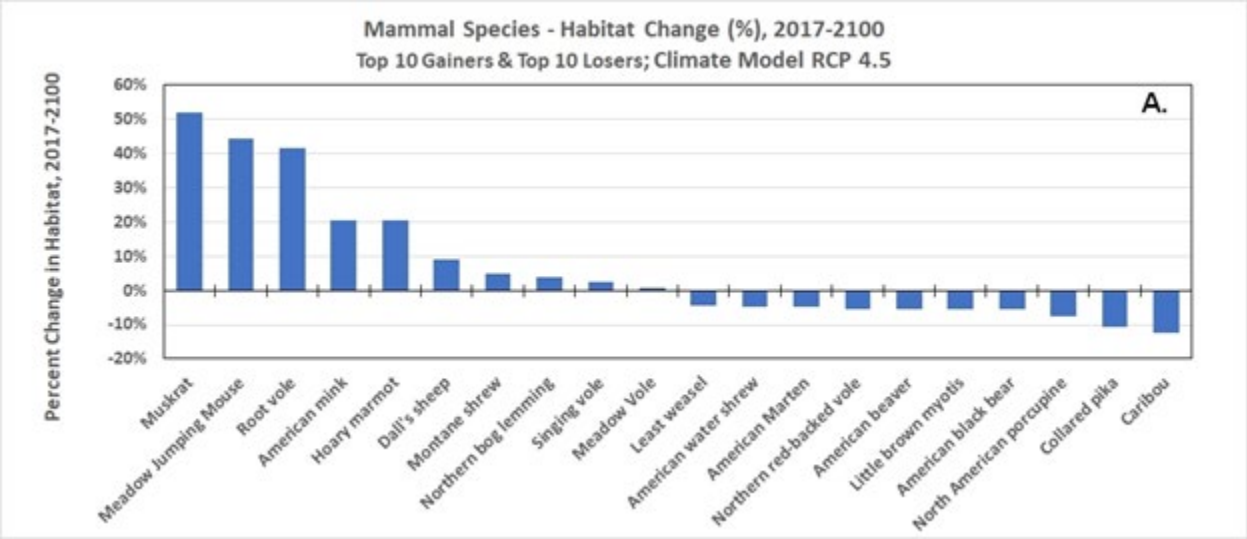
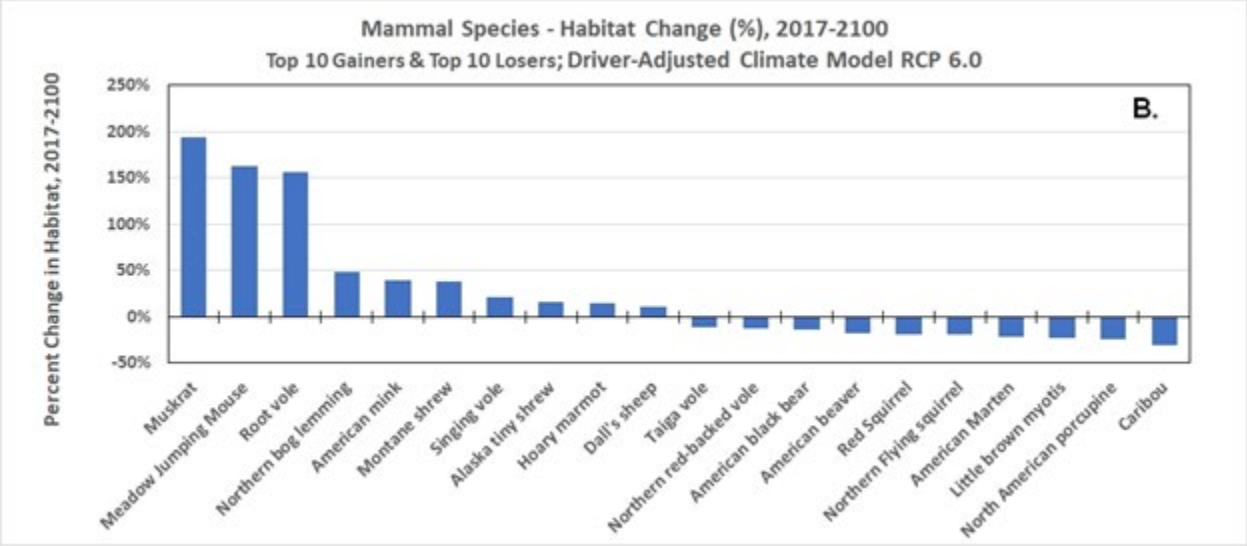


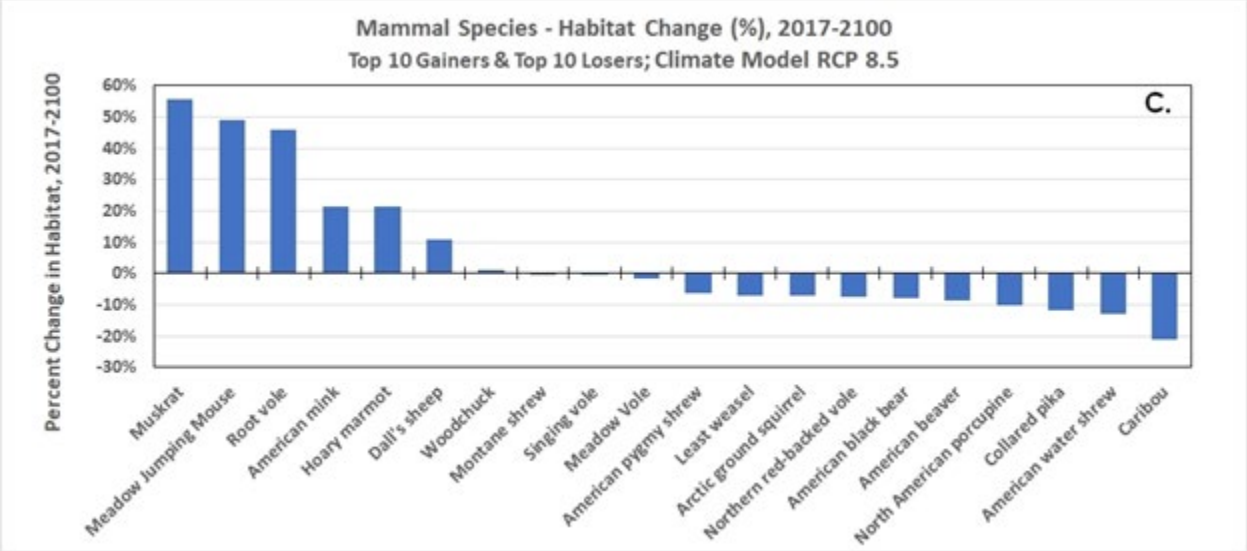
Figure 98. The top ten mammal habitat "gainer" species and top ten "loser" species, over the historic time period of 1949 to 2017. During this time period, no mammal species was projected to have lost habitat within the study area. Several small mammals (lemmings, shrews, voles) gained habitat conditions as a result of post-fire recovery of open, short-vegetation ecotypes, which also benefited grazing caribou. Most of the other mammal species had modest gains in their habitat conditions over this time period (Appendix Table 5).

Mammal species projected to gain or lose habitat in the future, from 2017 to 2100, varied by ecotype projection scenario (Figure 99). The intensity of habitat gains and severity of habitat losses depended on the ecotype transitional changes that varied the projection scenarios. Greatest habitat gains were under the driver-adjusted climate model RCP 6.0 for mammal species associated with lakes and fens (e.g., muskrat, mink); wet meadows, bogs, and fens (e.g., jumping mouse, root vole); and others (Figures 99 and 100). Dall sheep, which might show some habitat increase, are likely to be sensitivity in their northern range in central Alaska to changing snow conditions that can affect lamb recruitment (van de Kerk et al., 2018).

Greatest projected habitat losses for mammal species were most notably for caribou, pika, porcupine, and other species associated with alpine tussock and some scrub and woodland conditions. Habitat of caribou in boreal woodlands of Alberta, Canada, also was projected by Barber et al. (2018) to decline from effects of vegetation transitions and wildfire. Macander et al. (2020) established the critical need by caribou for quality lichen forage in interior Alaska, which can be greatly influenced by recovery processes following boreal wildfires (Greuel et al., 2021). Collared pika is largely an associate of alpine scrub conditions some of which are projected to decline because of expansion of tree cover. Overall, however, as with the bird species, no mammal species is projected for more than a 30% loss of habitat area over the coming century.


Mammal Species - Habitat Change (%), 2017-2100
Top 10 Gainers & Top 10 Losers; Climate Model RCP 4.5
A.
Percent Change in Habitat, 2017-2100
60%
50%
40%
30%
20%
10%
0%
-10%
-20%
Muskrat
Meadow Jumping Mouse
Root vole
American mink
Hoary marmot
Dall's sheep
Montane shrew
Northern bog lemming
Singing vole
Meadow Vole
Least weasel
American water shrew
American Marten
Northern red-backed vole
American beaver
Little brown myotis
American black bear
North American porcupine
Collared pika
Caribou


Mammal Species - Habitat Change (%), 2017-2100
Top 10 Gainers & Top 10 Losers; Driver-Adjusted Climate Model RCP 6.0
B.
Percent Change in Habitat, 2017-2100
250%
200%
150%
100%
50%
0%
-50%
Muskrat
Meadow Jumping Mouse
Root vole
Northern bog lemming
American mink
Montane shrew
Singing vole
Alaska tiny shrew
Hoary marmot
Dall's sheep
Taiga vole
Northern red-backed vole
American black bear
American beaver
Red Squirrel
Northern Flying squirrel
American Marten
Little brown myotis
North American porcupine
Caribou



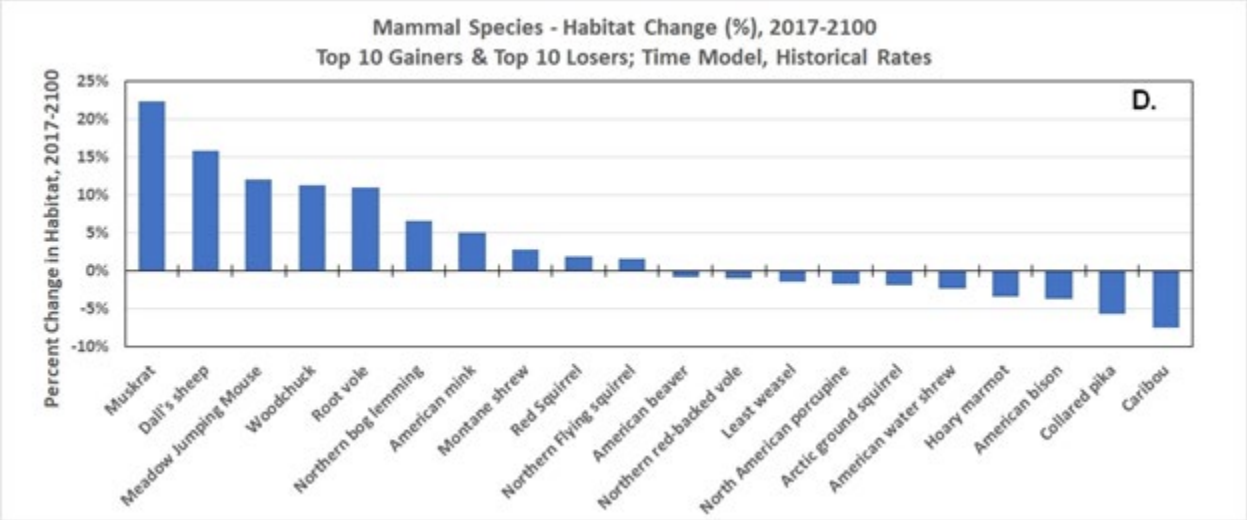


Figure 99. Top 10 mammal species habitat gainers and top 10 habitat losers for the projected future time period of 2017 to 2100, among the four ecotype projection scenarios: (A) climate model RCP 4.5, (B) driver-adjusted climate model RCP 6.0, (C) climate model RCP 8.5, and (D) time model based on historic rates. As with the bird species (Figure 95), gainer and loser mammal species and the severity of projected habitat changes varied among the projection scenarios depending on the intensity of changes among ecotype conditions and disturbances considered in each scenario.

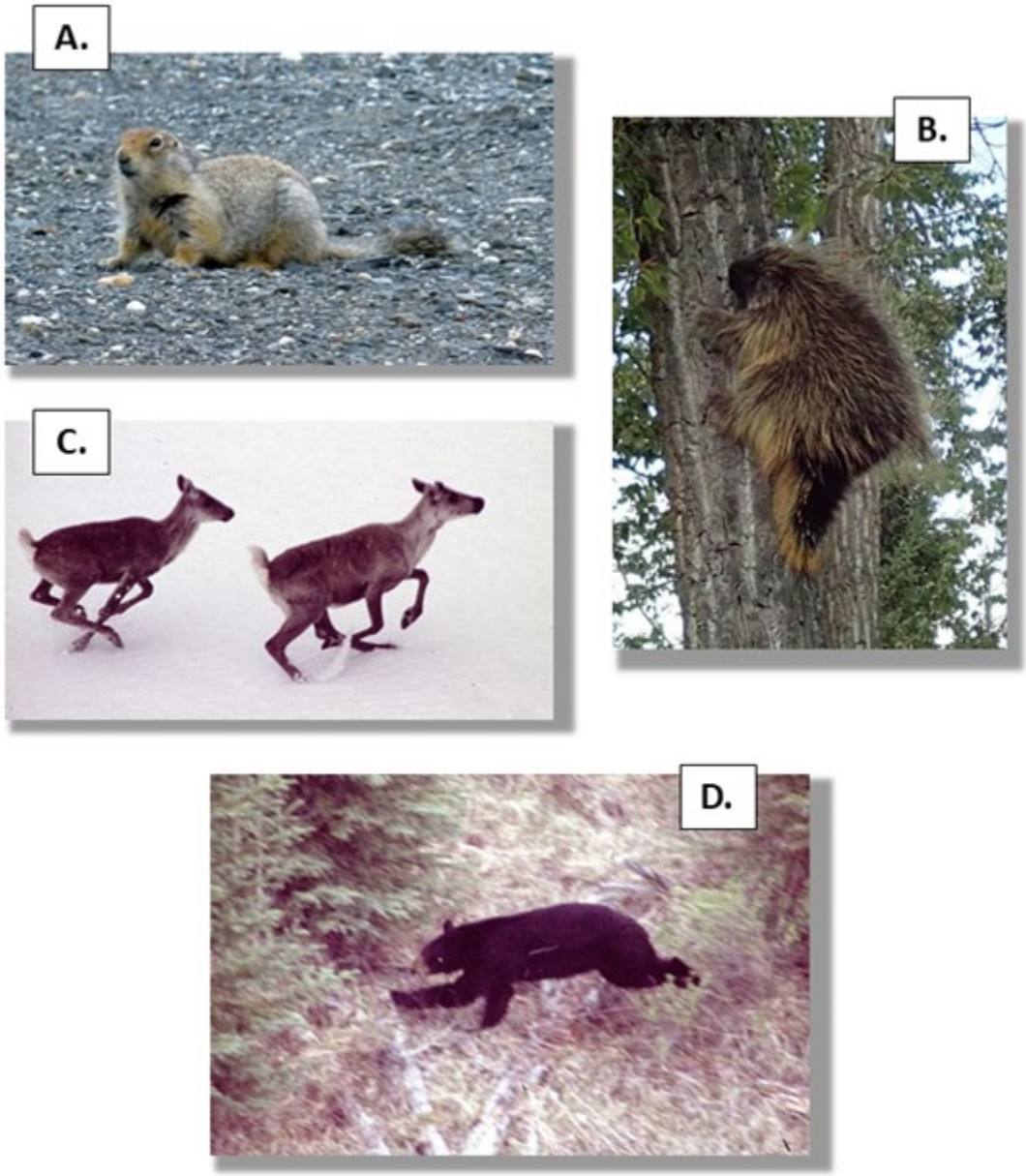


Figure 100. Examples of some mammal species projected to gain or lose habitat within the study area from 2017 to 2100 under one or more of the ecotype projection scenarios: (A) arctic ground squirrel, habitat gainer; (B) porcupine, habitat loser; (C) caribou, habitat loser; (D) black bear, habitat loser. Porcupine photo by M. Torre Jorgenson; other photos by Bruce G. Marcot.

The sole species of bat reported in the study area is the little brown myotis (little brown bat, Myotis lucifugus), predicted to incur habitat declines under all projection scenarios especially under the climate model RCP 4.5 and the driver-adjusted climate model RCP 6.0 scenarios (Figure 99). The species was surveyed in 2016 and 2017 on the training lands by Savory et al. (2017) using audio recording devices. They documented detections of the species and provided several management suggestions include minimizing disturbance of winter hibernacula and of maternity colonies, and to continue bat surveys in areas where they have not

been detected. They also concluded that most military activities conducted from October to March would be unlikely to impact populations of the species on the training areas. They also developed a habitat suitability index model that was used to map potential habitat across Tanana and Yukon Training Areas, suggesting a broad potential habitat distribution similar to the current study's species-ecotype relationships information, although in the current study, little brown myotis was designated only secondary habitat conditions because its occurrence in the study area apparently is at the very northern edge of its distributional range (MacDonald and Cook, 2009).

2.10.4. Patterns of Soundscapes in the Study Area and Implications for Wildlife Management

This section presents the findings of how the ecoacoustic indices reveal patterns of the soundscapes in the study area.

2.10.4.1 Overview of Ecoacoustic Indices by Soundscape Categories

We calculated values of the 13 ecoacoustic indices (16) for 150 Wave sound files selected to represent recordings of anthrophony, biophony, and geophony sources (Figure 86). Results (see Appendix Figure 2) suggest the following. The 13 ecoacoustic indices varied in terms of being able to differentiate among the three acoustic categories of anthrophony, biophony, and geophony. For example, NDSI and LFC best differentiated the general frequencies of anthrophony sounds (vehicles, planes, etc.) but they do not differentiate between biophony (animals) and geophony (weather) sounds. SNR, EVN, and perhaps ACT nicely differentiated geophony sounds from other sounds. Other indices, such as ACI and AEI, did not differentiate among any of the three general acoustic categories. Thus, depending on the purpose of the study, one would select indices accordingly. The main purpose of the current study, for example, was to determine which sites, landscapes, and conditions might have greater disturbance from anthropogenic sources, so NDSI would suffice as an indicator.

We can divide the three acoustic categories of anthrophony, biophony, and geophony further into their component sources. We calculated all 13 ecoacoustic index values for 6 example categories of anthrophony sounds (Appendix Figure 3). It is interesting to note how the various anthrophony sound sources can themselves be differentiated by the various ecoacoustic indices. For example, NDSI best differentiates road vehicles and helicopters; ACI, ADI, BGN, MFCI, and HFCI indices best differentiate sounds of people walking through the bush; CENT best differentiates radio noise; and others.

We then calculated all 13 ecoacoustic index values for 10 example categories of biophony sounds (Appendix Figure 4). NDSI and ACI best differentiated sounds of low-frequency bird calls and raptor calls from other sounds. ADI differentiated the mid- and high-frequency bird calls. SNR, ACT, and EVN best differentiated unidentified rustling (stomping through the brush and loud splashing in a lake, likely by moose). LFC nicely differentiated insect buzz sounds.

Lastly, we calculated all 13 ecoacoustic index values for 5 example categories of geophony sounds (Appendix Figure 5). NDI best differentiated sounds of silence and of wind from other sounds. The sound of rainfall was nicely differentiated by ACI, ACI, MFCI, HFCI, and CENT. Thunder and wind were differentiated by ACT and EVN.

This analysis was helpful for identifying specific ecoacoustic indices to use as sensitive markers of general acoustic categories or specific sound sources of those categories. The remainder of this analysis, however, focuses on use of the ADI and NDSI ecoacoustic indices as noted above to be uncorrelated with each other but correlated with all other indices.

2.10.4.2 The Daily Cycle of Sounds

Over the course of the 24-hour daily (diel) cycle, the amplitudes and frequencies of sounds of all sources tend to change, depending on the ecoacoustic category and the specific sound source. In particular, there is a well-documented daily cycle of bird vocalizations, such as has been recorded in subarctic tundra sites of Alaska (Thompson et al., 2017) and in ARU analyses of bird dawn choruses (Brooker et al., 2020).

Overall, daily trends can be seen with the Acoustic Diversity Index (Fig 100) where the diversity of sounds peaks in early morning hours (approx. 05:00-07:00) with the avian dawn chorus, reduces by mid-day (approx. 14:00-16:00), and then increases again into dusk (approx. 21:00-23:00). The high variation seen in the ADI plot in Figure 101 is from the change in timing of sunrise and sunset over the recording season (June-August 2019). Shown here are results from Riverine landscapes for the 3 successional stages of early (ecotype Riverine Moist Tall Scrub), mid (Riverine Moist Broadleaf Forest), and late (Riverine Moist Needleleaf Forest) over the entire 2019 recording season (June to August).

However, the Normalized Difference Soundscape Index does not show this same diel pattern (Figure 101). Rather, it suggests that the range of sound frequencies (increased standard deviation of NDSI values) increases during the mid-day hours, likely because of increased human activities of aircraft and road vehicles that add to the range of sound frequencies recorded.

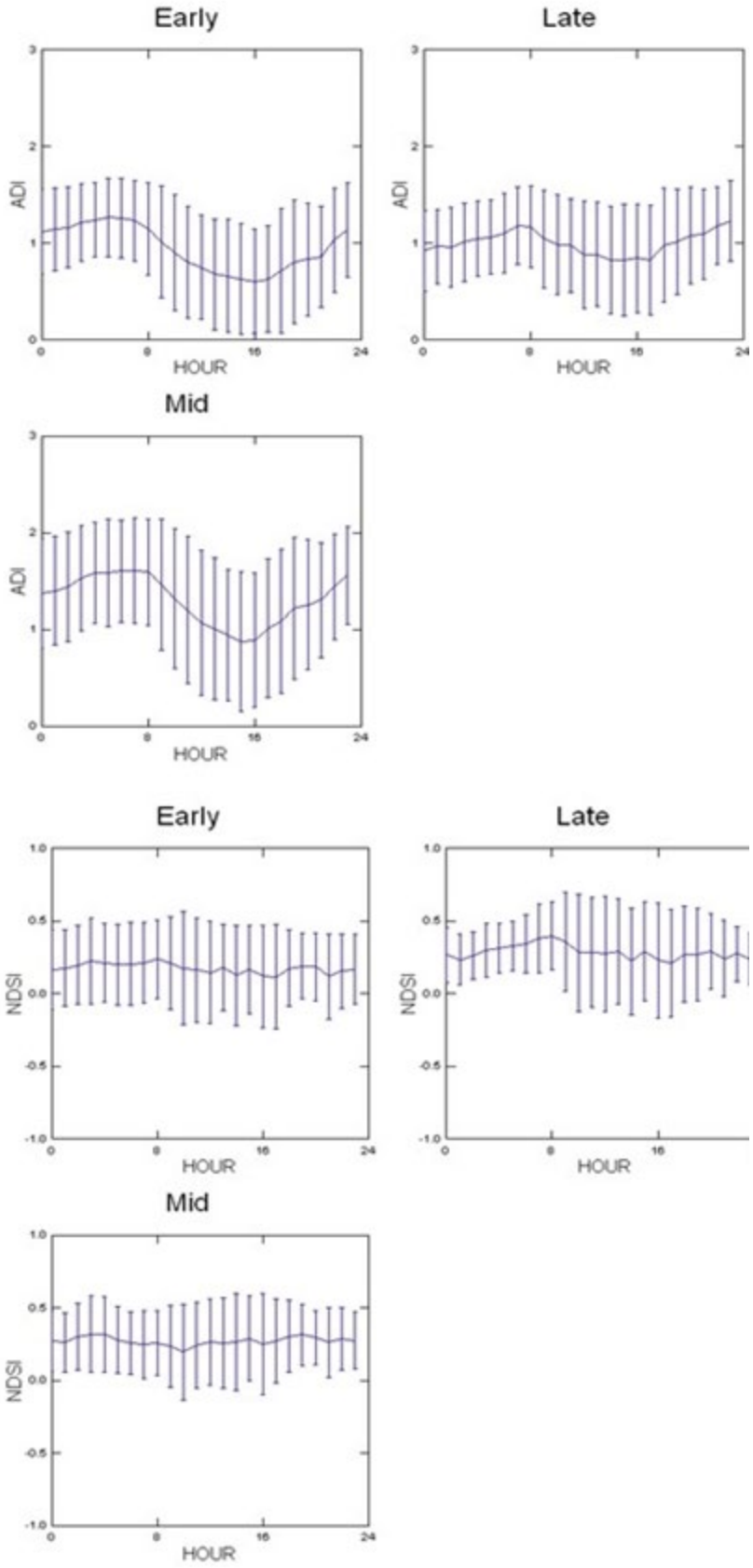


Figure 101. Example of variation in the values of two ecoacoustic indices — Acoustic Diversity Index (ADI) and Normalized Difference Soundscape Index (NDSI) — over the course of the 24-hour daily cycle. Curved lines are mean values and vertical bars are ±1 SD.

2.10.4.3 The Seasonal Cycle of Sounds

In addition to the daily cycle of sounds is the seasonal cycle of sounds. Recordings in this study, however, were made during the breeding and summer seasons (June-August 2019, and April-September 2020), so did not include fall, winter, and early spring conditions.

Values of the Acoustic Diversity Index fluctuated over the 2019 recording season, perhaps showing some tendency toward higher index values later in the season for some locations (e.g., Lacustrine early thermokarst stage, Riverine mid and late stages, and others; Appendix Figure 6). This could indicate a greater diversity of sound spectra perhaps from increased human activity as well as increased post-breeding movement of wildlife, especially songbirds, waterfowl, and others. At the same time, the Normalized Difference Soundscape Index showed little to no trends in values over the 2019 recording season (Appendix Figure 7), suggesting that the range of sound frequencies among all sound sources did not substantially shift; prevalence of actual sound sources may have changed but if they produced generally the same range of frequencies overall, NDSI index values would not show a trend. Again, this points out the value of using complementary ecoacoustic indexes.

The 2020 recording season was extended over that of 2019, beginning in April and ending in September. This afforded a greater opportunity to explore any seasonal cycles of sounds. Indeed, temporal values of the Acoustic Diversity Index suggests some possible trends (Figure 102) of lower sound diversity in mid-season (June-July) in lacustrine and riverine situations, little change in lowland sites, and increases in upland sites. These changes may have to do with post-breeding movement and dispersal of vocalizing birds, as well as differential degrees and types of human activities in each of these landscape conditions.

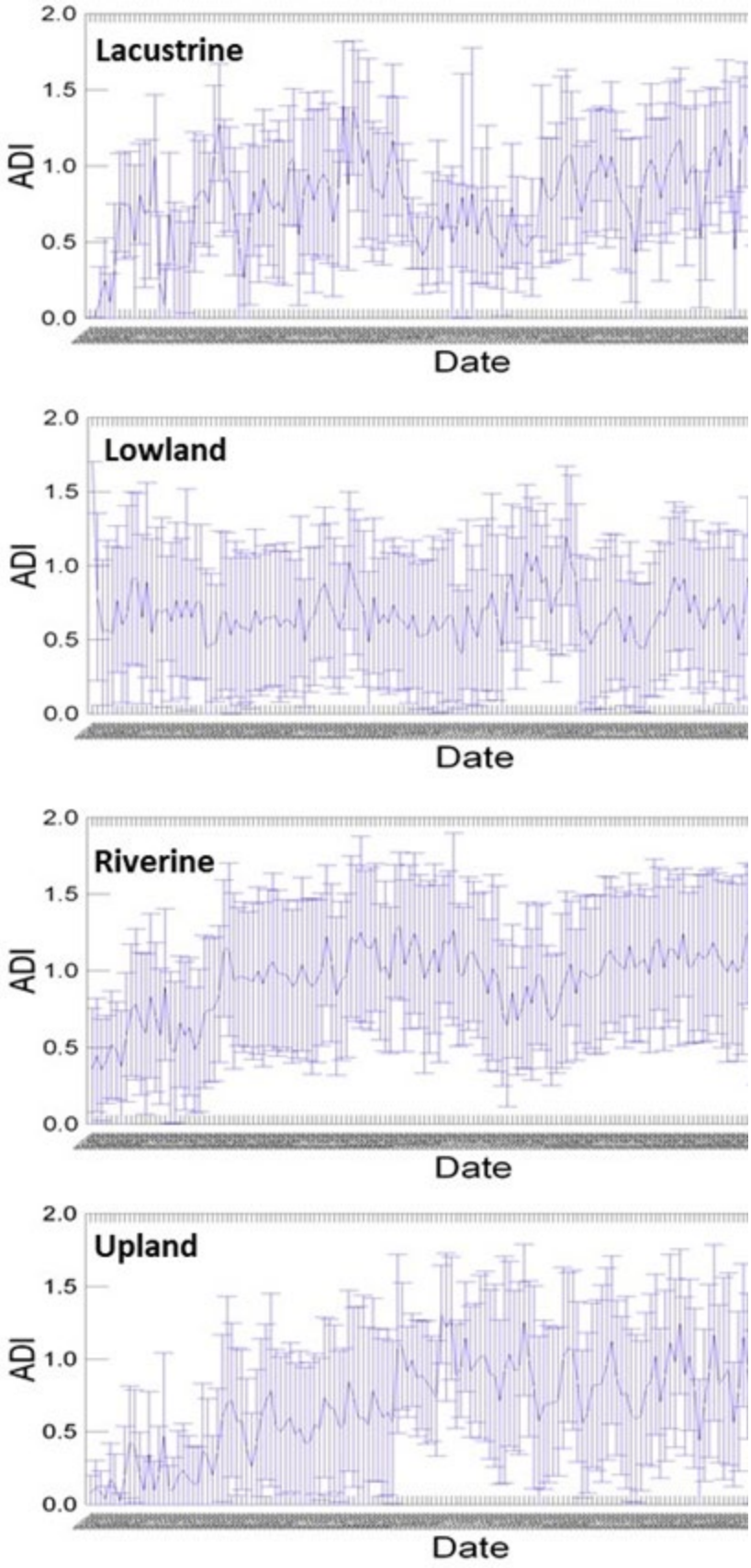


Figure 102. Values of the Acoustic Diversity Index (ADI) by date from April to September 2020, for four landscapes. Curved lines are mean values and vertical bars are ±1 SD.

2.10.4.4 Influence of Vegetation Conditions on Sounds

We also explored the potential correlation between the ADI and NDSI ecoacoustic index values and vegetation conditions among all sites studied, using results of the ecological land survey conducted at each ARU location.

Values of ADI were positively correlated with percent total conifer tree cover, total broadleaf tree cover, total tree cover, total tree and shrub cover, and total ground vegetation cover, and negatively correlated with total ground flat (unvegetated) cover (Figure 102). Overall, these patterns denote how the diversity of sound frequencies is greater at sites with fuller, and more mature, vegetation development, such as with late successional stages of riparian and upland forests. This makes ecological sense, as those are the conditions with a greater number of bird species (Figure 69) and with higher ADI values (Appendix Figure 6).

Values of NDSI were less strongly correlated with these same vegetation conditions (Figures 103 and 104), in part because NDSI values showed little difference between the older and younger successional stages of most landscape conditions except lacustrine (Appendix Figures 7 and 8). NDSI serves as an indicator of the relative dominance of biophony (values > 0) and anthrophony (values < 0) sound sources, so this pattern of less correlation with vegetation conditions generally suggests that anthropogenic sounds (e.g., aircraft, vehicles, etc.) are more or less equally prevalent in all landscape and successional stage conditions sampled in this ecoacoustic study.

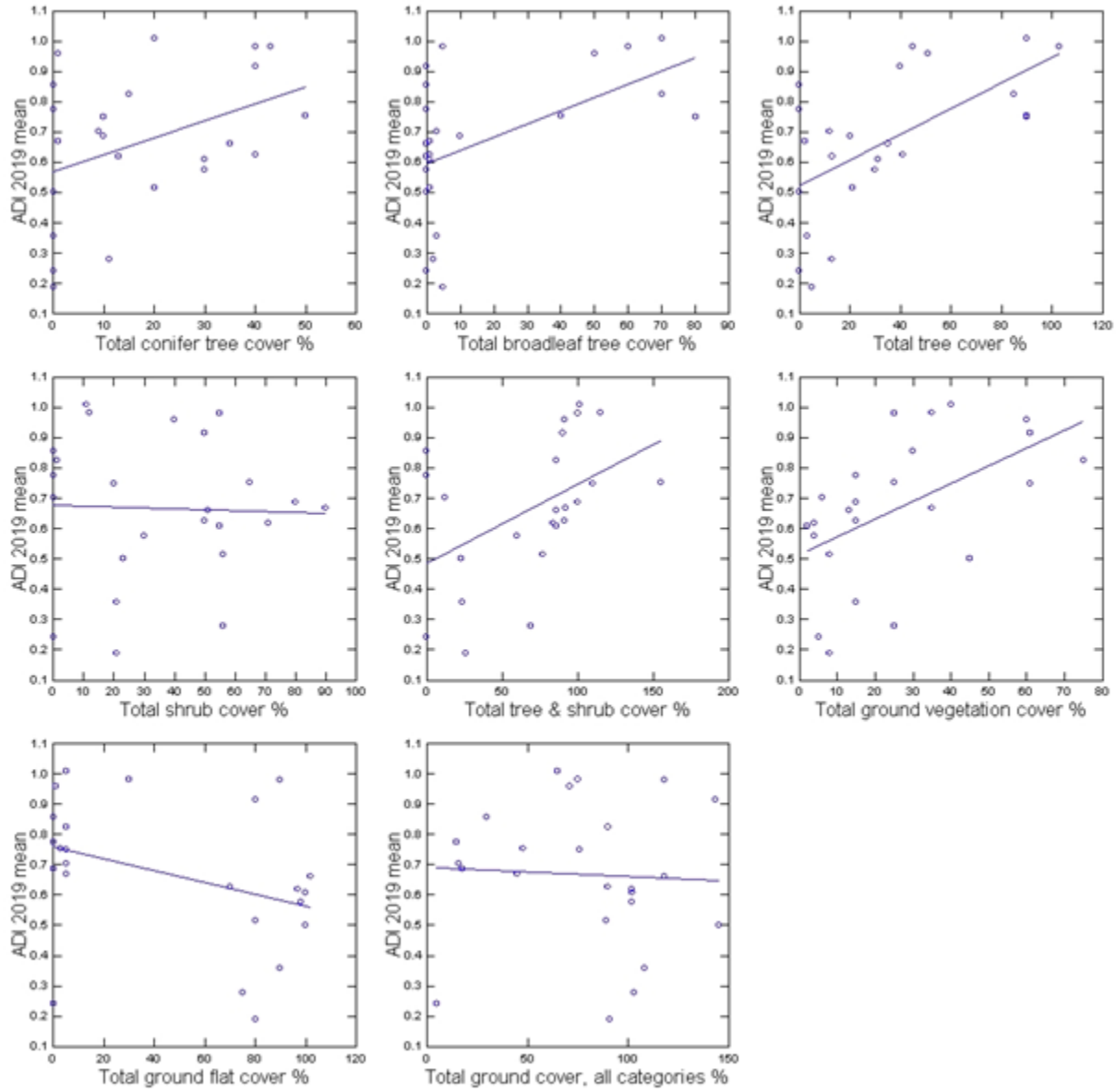


Figure 103. Values of the Acoustic Diversity Index (ADI) among all 24 automated audio recording unit (ARU) locations (Table 15), by 8 vegetation and ground cover covariates, from June-August 2019 audio recordings. Lines are best-fit linear regressions, dots are individual ARU locations. Patterns using the April-September 2020 ARU recordings also produced essentially the same patterns.

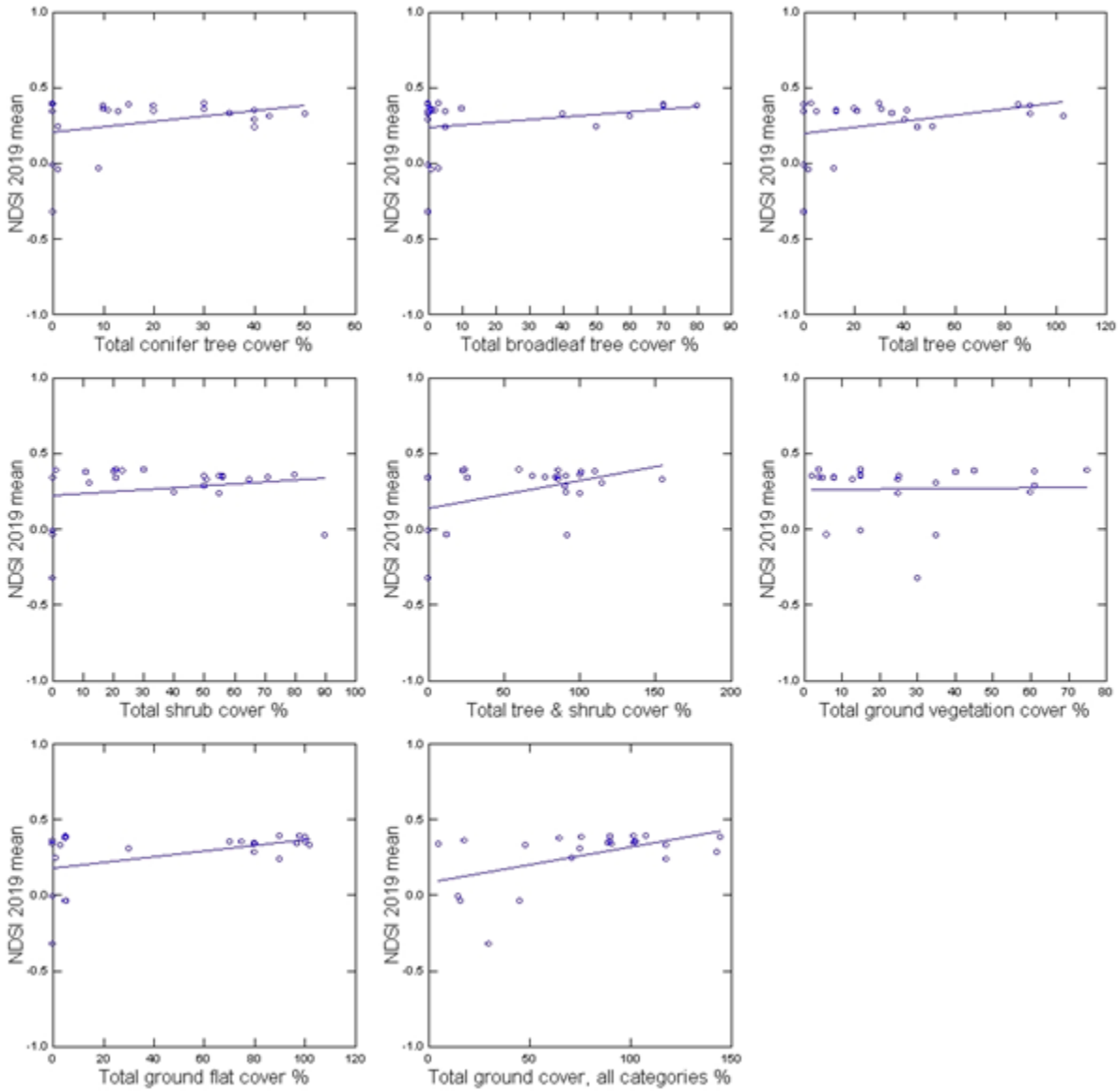


Figure 104. Values of the Normalized Difference Soundscape Index (NDSI) among all 24 automated audio recording unit (ARU) locations (Table 15), by 8 vegetation and ground cover covariates, from June-August 2019 audio recordings. Lines are best-fit linear regressions, dots are individual ARU locations. Patterns using the April-September 2020 ARU recordings also produced essentially the same patterns.

2.10.4.5 Influence on Sounds from Proximity to Human Activities

We next explored how soundscapes were influenced by proximity to various human activities. Using GIS, we measured distances from each ARU site location to the nearest main airport, primary road, any road, drop zone, firing site, flight line, development, landing zone, and range (Figure 106, Appendix Figure 6 and Appendix Table 17).

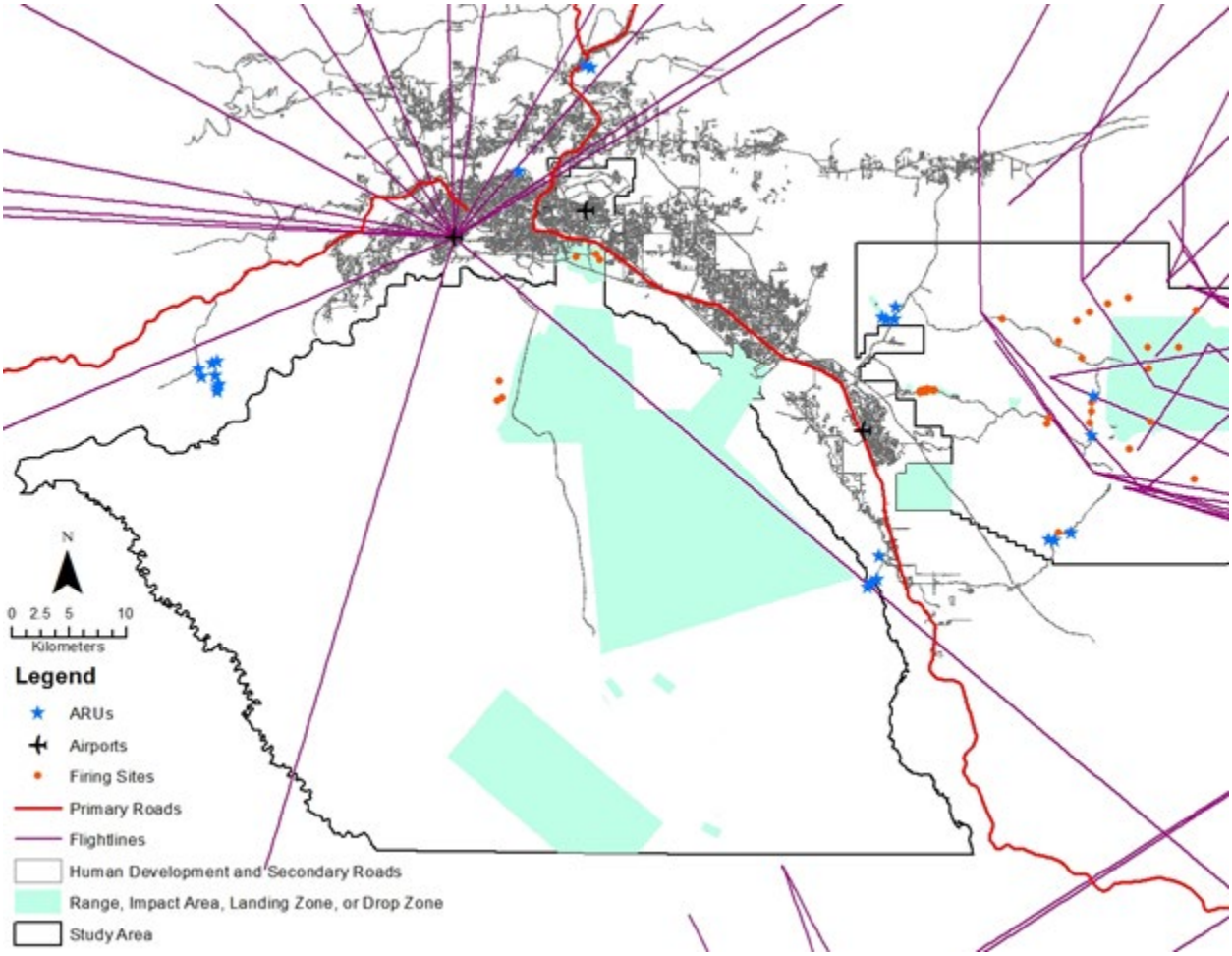


Figure 105. Locations of key human-created features in the portion of the study area with 24 automated audio recording units (ARUs). This was used to analyze the potential effects of distance to these features on soundscape attributes at each ARU location. The radial flight lines are from Fairbanks International Airport; flight lines on the right are military training flight paths.

Definitions are as follows. Main airports included Fairbanks International Airport, Eielson Air Force Base Airport, and Ladd Army Airfield on Fort Wainwright. Primary roads included mostly designated highways. Any roads included highways along with any and all additional primary, secondary, and other roads. Drop zones are designated areas where personnel and/or equipment may be delivered by parachute or by free drop. Firing sites are locations used for the firing of weapon systems. Flight lines were the main aircraft flight paths, constructed in GIS, originating from airports based on routes from OpenFlights.com, and further refined using military training routes from USAG-AK's database. Development refers to any development of human habitation (barracks, towns, etc.). Landing zones are locations where manned and unmanned aircraft can land or hover to pick up or offload troops or cargo; such sites are cleared of trees and other vertical hazards. Ranges are designated land or water areas set aside, managed, and used to conduct research on, develop, test, and evaluate military munitions and explosives and other ordnance or weapon systems, or to train military personnel in their use and handling.

Values of ADI were positively related to distance to firing ranges, flight lines, landings, and training ranges (Figure 106); that is, the nearer to these largely military activity categories,

the more the sounds were dominated by less diverse frequencies likely because these anthropogenic sound sources dominated the sound environment. ADI values were negatively related to distances to airports and primary roads, suggesting that closer proximity to aircraft and road vehicles contribute to a greater diversity of sound spectra (Appendix Figure 3). Using the inflection points of the power regression lines in Figure 105, main effects on the overall soundscapes varied by some human activity categories, with thresholds occurring at approximately 5,000 m distance to firing ranges and primary roads, and 1,000 m distance to flight lines, and with no clear distance threshold for other activity categories.

On the other hand, values of NDSI were positively related to distance to airports and primary roads (Appendix Figure 3), and showed little relationship to other activity categories (Figure 107). NDSI relationships suggested that proximity to aircraft and primary road vehicles skewed sounds toward being more dominated by lower frequencies (lower NDSI values), although vehicles along other roads did not show this relationship (Figure 107). Main effects on the overall soundscapes occurred within approximately 5,000 m to primary roads (as with the ADI index above), and perhaps 15,000 m to main airports, but there were no clear distance thresholds to other activity categories (power curve inflections in Figure 107).

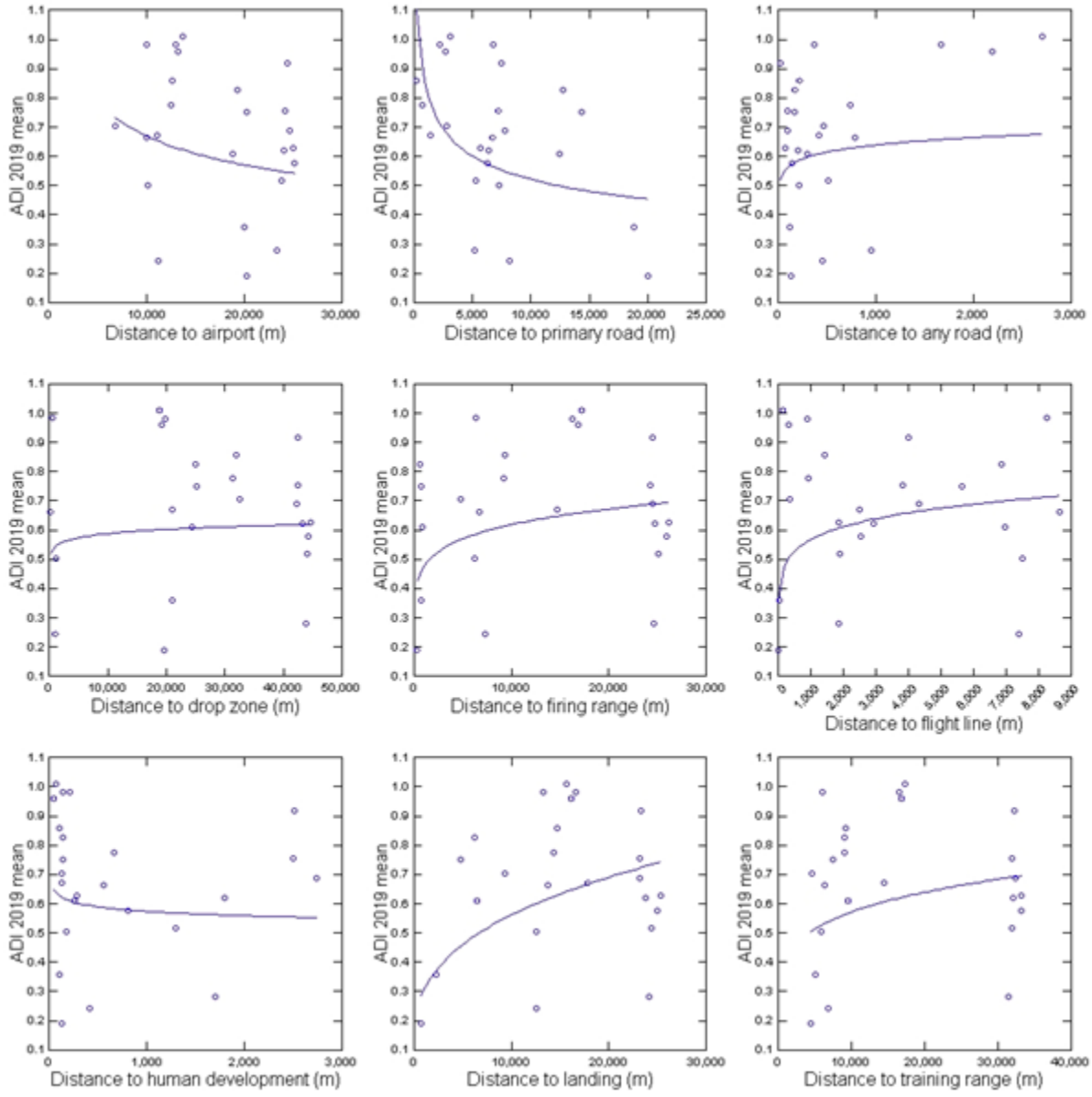


Figure 106. Values of the Acoustic Diversity Index (ADI) among all 24 automated audio recording unit (ARU) locations (Table 15), by distance from the recorder location to 9 categories of human activity (anthropogenic disturbance covariates), from June-August 2019 audio recordings. Lines are best-fit power regressions, dots are the individual ARU locations.

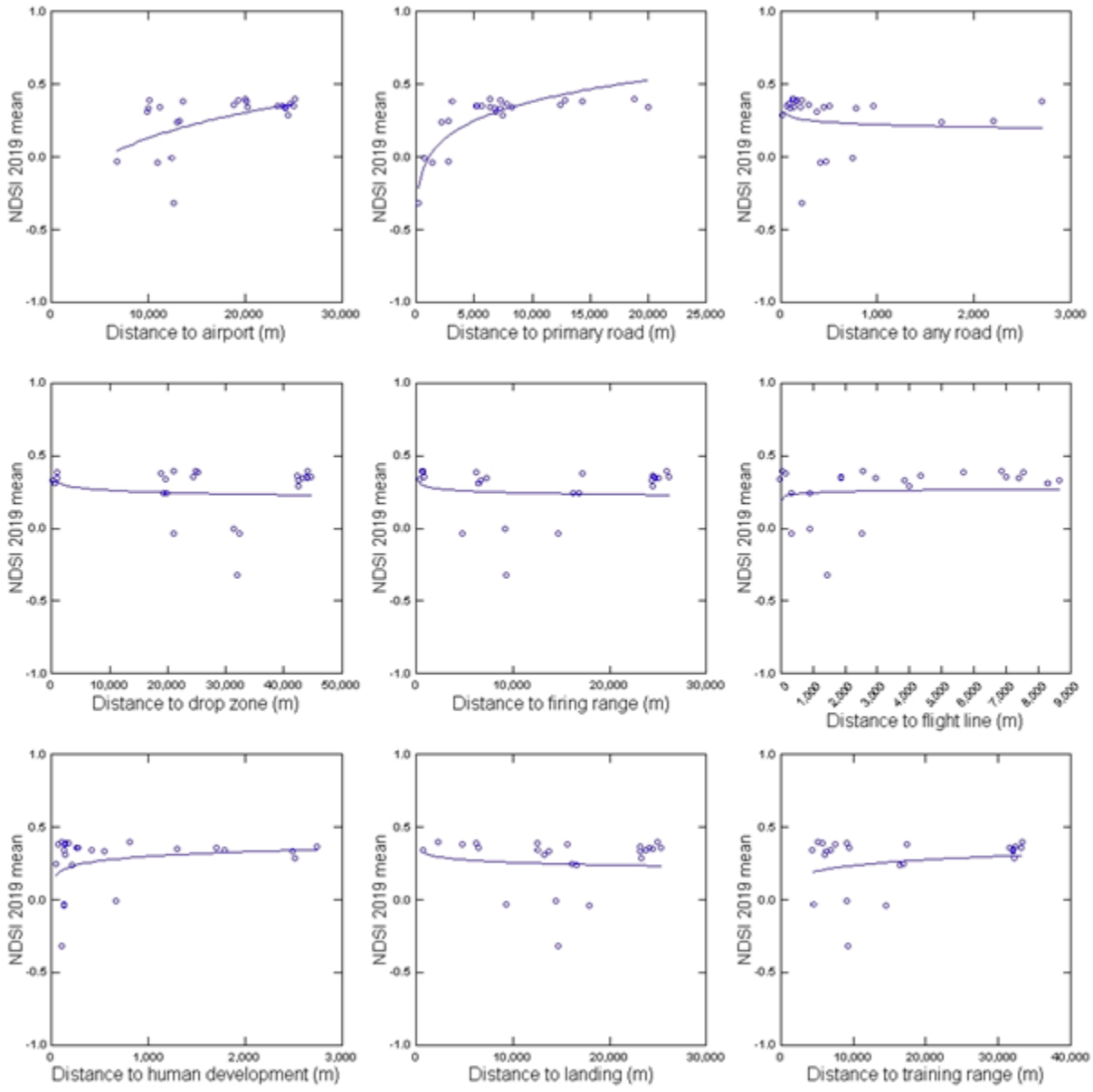


Figure 107. Values of the Normalized Difference Soundscape Index (NDSI) among all 24 automated audio recording unit (ARU) locations (Table 15), by distance from the recorder location to 9 categories of human activity (anthropogenic disturbance covariates), from June-August 2019 audio recordings. Lines are best-fit power regressions, dots are individual ARU locations.

We conducted a GIS analysis of the geographic locations within the threshold proximities to these sound sources, and tallied the individual areas affected by each source (Table 17). For example, 22% of the study area is within the 5,000 m threshold distance to firing sites. By buffering the respective threshold distances around each sound source and clipping to the boundary of the study area, we produced a map (Figure 108) that shows these areas and their intersections, denoting locations where noise effects may be more severe on wildlife resources, particularly where they overlap within their threshold distances. The complement, where distances to these sound sources exceed the thresholds noted above, denotes locations with

potentially less to little influence on wildlife by noise from these specific human activities. Such a map could help inform location planning for specific activities to avoid lesser-impacted sites of potentially high wildlife habitat value (see previous sections).

Table 17. R**egions of the study area that are within threshold distances of four anthropogenic sound sources or combinations thereof, that display distance threshold influences on the Acoustic Diversity Index (see Figure 106). Shown are non-mutually exclusive total areal coverage and percent of the total study area of each sound source individually and where they spatially overlap. Threshold buffer distances from each sound source are: primary road, 5,000 m; firing site, 5,000 m; main airport, 15,000 m; flight line, 1,000 m.**

Sound source(s), including buffer					
Primary road	Firing site	Main airport	Flight line	**Area (sq km)**	**Study area percent**
X				42.0	1%
	X			1,388.1	22%
		X		686.7	11%
			X	654.9	10%
X	X			25.2	0%
X		X		35.1	1%
X			X	2.3	<1%
	X	X		227.3	4%
	X		X	386.5	6%
		X	X	108.2	2%
	X	X	X	108.2	2%
X		X	X	2.3	<1%
X	X	X		25.2	<1%
X	X		X	0.0	0%
X	X	X	X	0.0	0%
			Total Feature Coverage:	2,031.4	32%
			Total Study Area:	6,389.5	100%

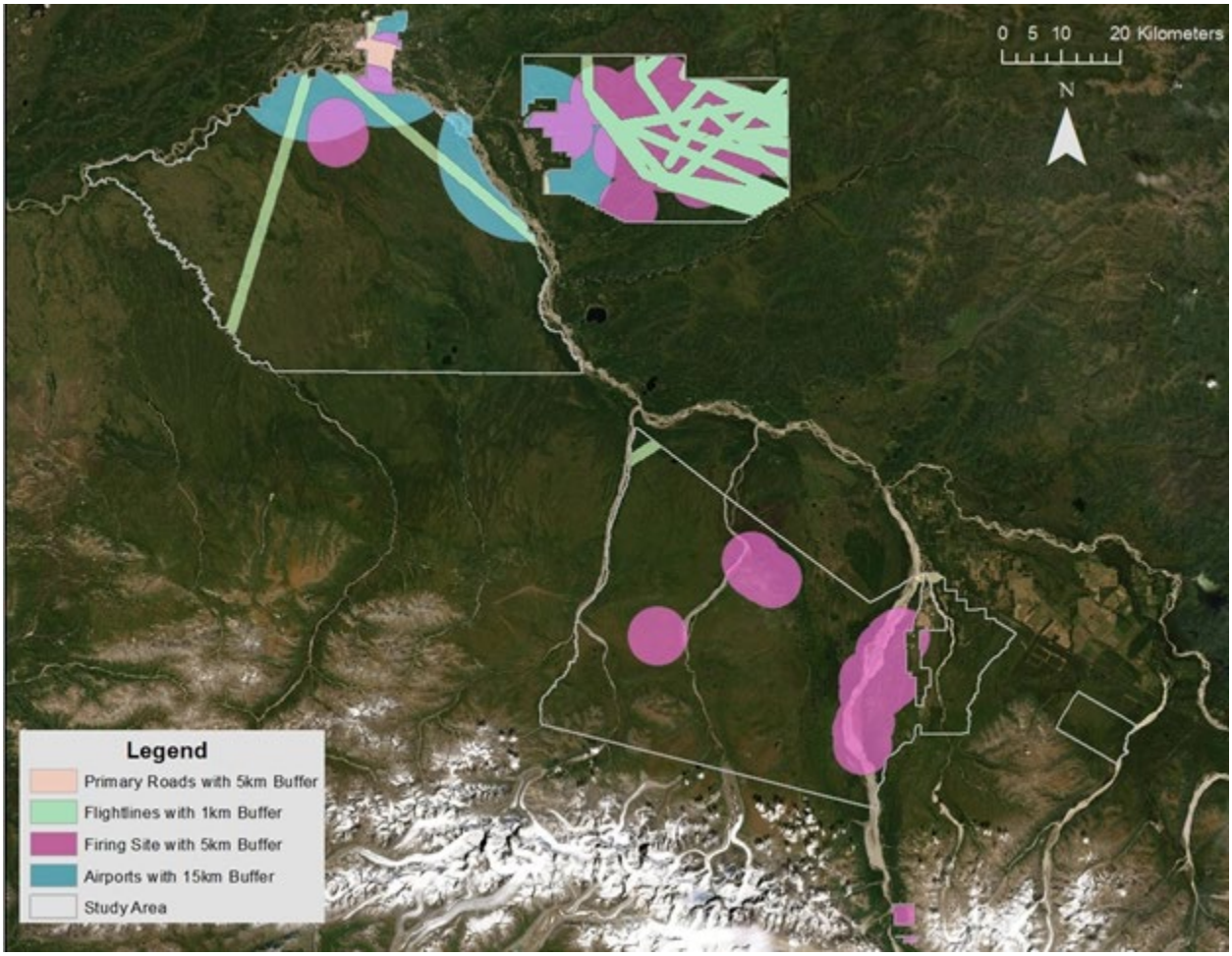


Figure 108. Areas within the study area within buffer threshold distances of four anthropogenic sound sources of primary roads (5,000 m), firing sites (5,000 m), main airports (15,000 m), and flight lines (1,000 m). These are sounds sources for which the Acoustic Diversity Index (ADI) shows curvilinear threshold distances within which effects on sound diversity greatly increase. Overlapping areas have >1 sound source within their respective threshold distances, and white areas are further than the threshold distances to all four of these sound sources where wildlife are likely the least impacted by noise of these human activities.

Finally, it should be mentioned that, although the plotted relationships of indices to distances suggest some positive and negative relationships (Figures 106 and 107). There was much variation among the audio sample locations. This resulted in linear regression correlations of both ADI and NDSI index values, with distances to each human activity category, strictly being statistically non-significant (ADI-distance R2 correlation coefficients ≤ 0.25, p ≥ 0.43; NDSI-distance R2 correlation coefficients ≤ 0.34, p ≥ 0.11). However, we have nonetheless noted here any potentially important overall trends in the data, particularly for distance threshold effects.

2.10.4.6 How Sounds Varied By Sampled Site

Finally, we explore here variations among the general audio-sampled locations. The 24 ARU sites were located in five general regions of the study area (Table 15): (1) Alaska Peatland Experiment (APEX) part of the Bonanza Creek Boreal Long-Term Ecological Research (LTER) site with lowland and riverine conditions; (2) Creamer's Field and Farmer's Loop lacustrine sites; (3) upslope from the Permafrost Tunnel, along Glenn Creek, thermokarst lacustrine sites; (4) Tanana Flats Training Area riparian and lowlands near Salcha; and (5) Yukon Training Area along Transmitter Road and Johnson Road, with lowland, upland, and lacustrine sites.

Soundscapes of Tanana Flats trended more toward greater acoustic diversity (higher ADI values) than did the other locations, which seems to also correspond to where much of the area is beyond key threshold distances to the four anthropogenic sound sources noted above (Figure 108). Soundscapes, however, of Creamer's Field and near the Permafrost Tunnel/Glenn Creek locations trended more toward human influence (lower NDSI values) than did the other locations (Figure 109), and these are also areas intersected by closer proximity to the distance-related anthropogenic sound sources (Figure 108).

Additionally, across the recording seasons, there was a greater range of acoustic diversity at the APEX and Yukon Training Area sites (broader spread of ADI values). These patterns suggest a complex interplay of natural and anthropogenic sound sources and activities, whereby APEX, Tanana Flats, and even the Yukon Training Area locations provided environments for more biotic, natural soundscape conditions, although the APEX and Yukon Training Area locations clearly varied greatly in how diverse those conditions remained over time.

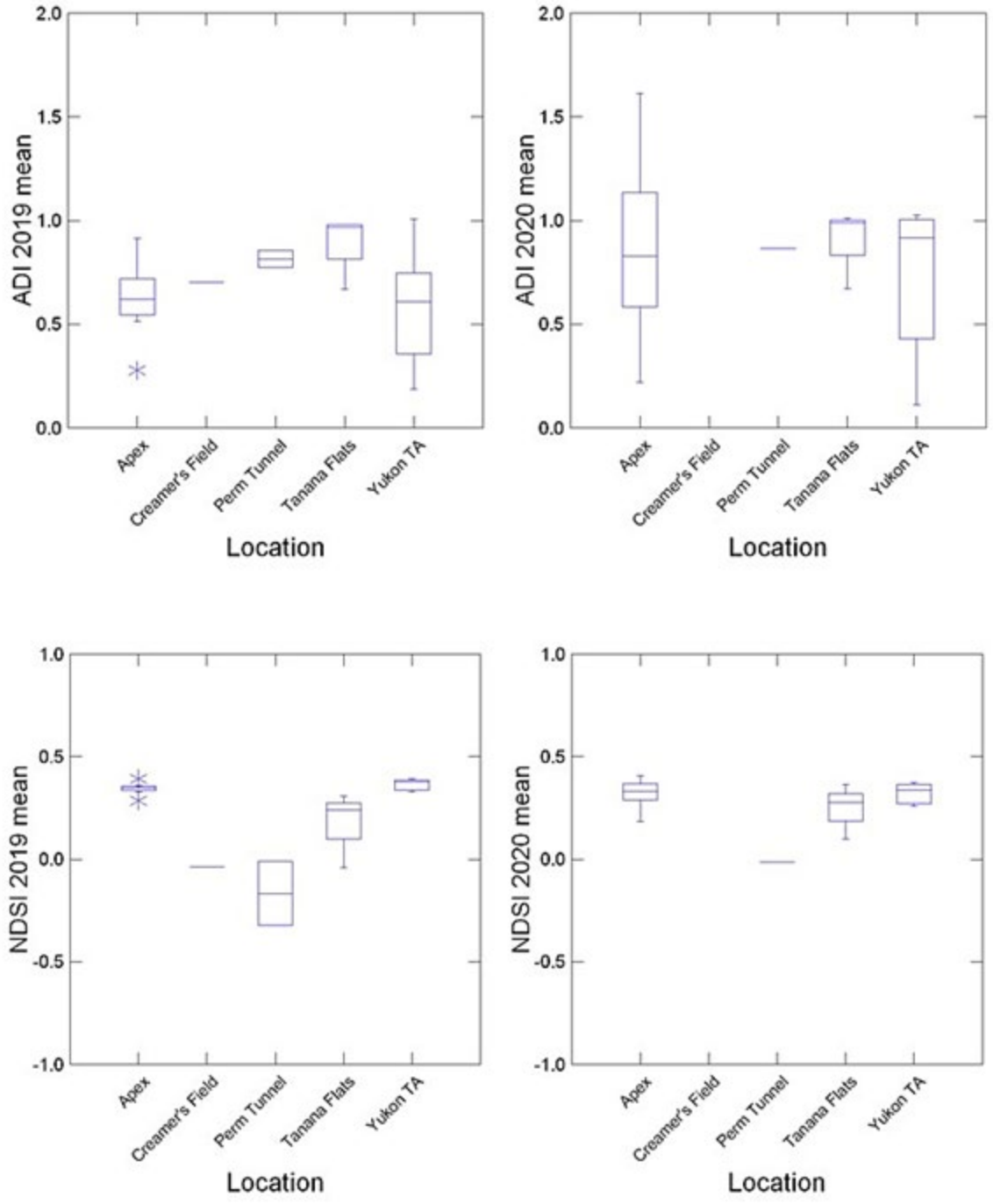


Figure 109. Variation in values of two ecoacoustic indices — Acoustic Diversity Index (ADI) and Normalized Difference Soundscape Index (NDSI) — among the 5 main geographic locations of deployment of the automated audio recording units (Table 15) during June-August 2019 and April-September 2020. (Note that, because of recorder scheduling problems, Creamer's field and the Permafrost Tunnel were inadequately sampled during 2020.) Center lines in the boxes are median values, box lengths are the range within the central 50% of values, and asterisks are outside values.

2.11 Task 3.3

Project and map the future distributions of wildlife habitats and assess changes in wildlife species' vulnerability by 2050 and 2100 through state-transition modeling and assess sensitivity of models to historical rates, temperature, and driver parameterization.

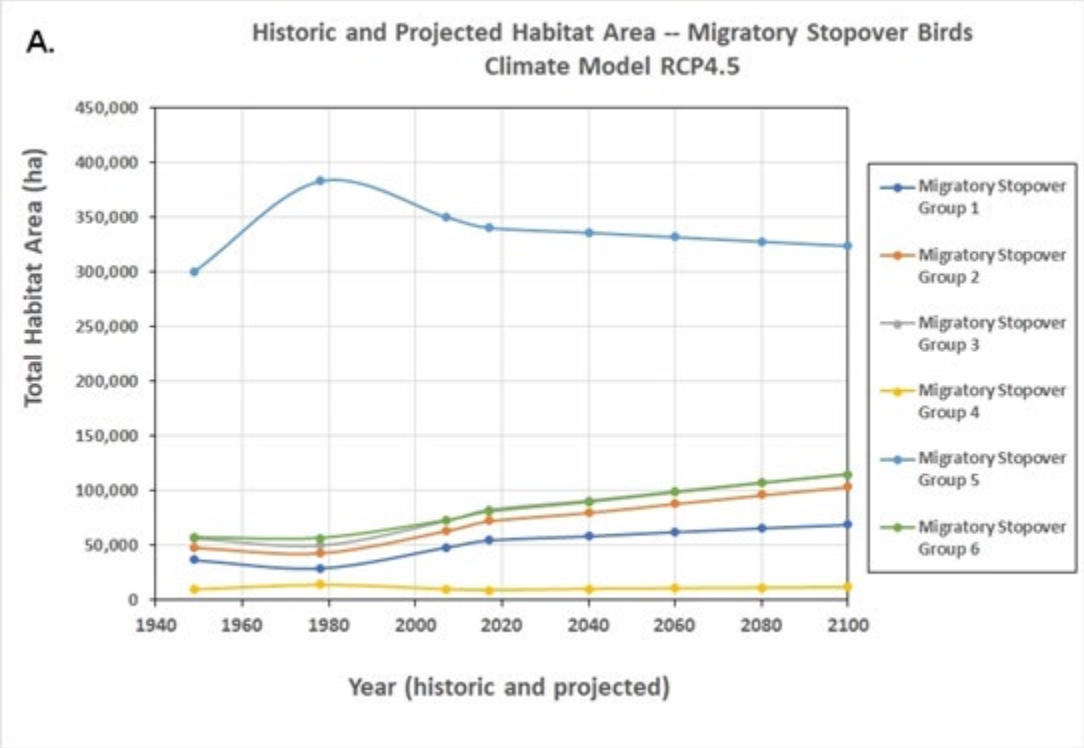
2.11.1 Habitat Trends of Key Selected Wildlife Species and Species Groups by Scenario

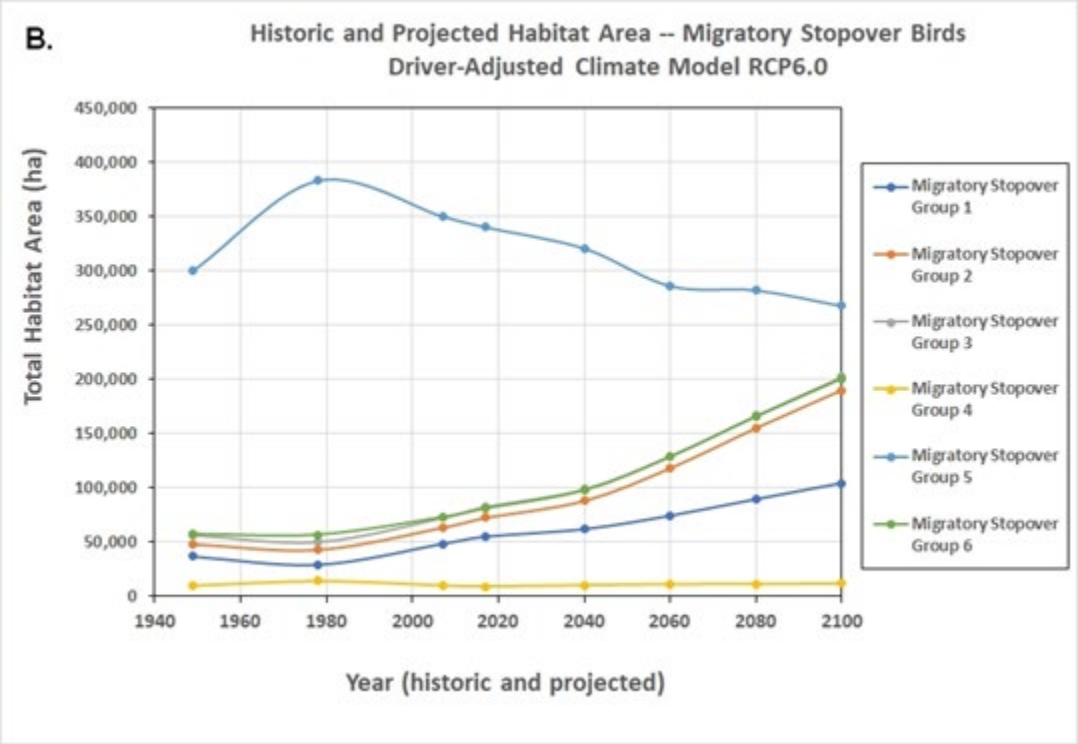
This section extends the above assessment of habitat amounts and changes for selected groups of wildlife species that may be of particular ecological or conservation interest and concern. As above, this section compares habitat amounts under the four ecotype projection scenarios, variously over past, current, and future time periods.

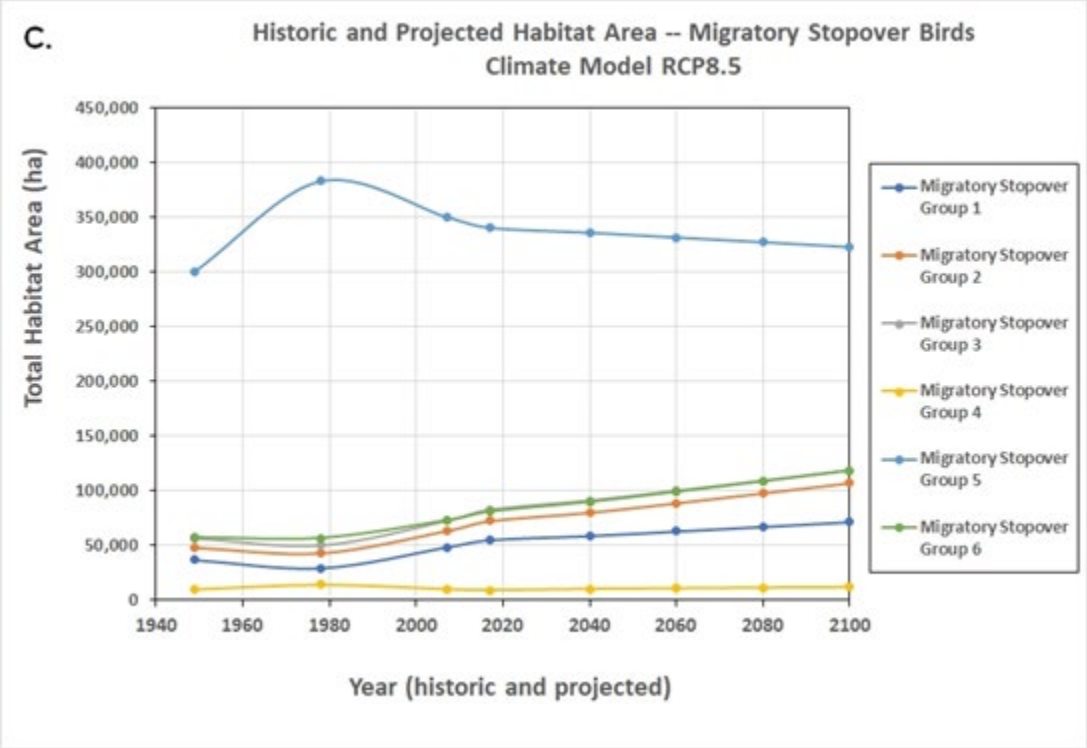
2.11.1.1 Bird Migrant Stopover Species Groups

As discussed above in section 2.9.4 Wildlife Species Occurring in the Project Area, some 27 bird species -- waterfowl, shorebirds, and a few forest and woodland species -- identified as seasonal migrant stopovers in the study area were placed into six species groups based on similar habitat associations (Figure 59, Table 13, and Appendix Table 2).

Habitat trends for the six bird migrant stopover species groups varied by time period and by ecotype projection scenario (Figure 110). Past conditions, 1940-2017, saw increases in habitats for migratory stopover groups 1,2, 3, and 6 that generally associate with wetlands, open water, and wet sites; a slight decrease for group 4 associated with dry open sites; and a large increase, then decrease, for group 5 associated with woodland and forest conditions (Figure 110).


A.
Historic and Projected Habitat Area -- Migratory Stopover Birds
Climate Model RCP4.5
Total Habitat Area (ha)
450,000
400,000
350,000
300,000
250,000
200,000
150,000
100,000
50,000
0
1940
1960
1980
2000
2020
2040
2060
2080
2100
Year (historic and projected)
Migratory Stopover Group 1
Migratory Stopover Group 2
Migratory Stopover Group 3
Migratory Stopover Group 4
Migratory Stopover Group 5
Migratory Stopover Group 6


B.
Historic and Projected Habitat Area -- Migratory Stopover Birds
Driver-Adjusted Climate Model RCP6.0
Total Habitat Area (ha)
450,000
400,000
350,000
300,000
250,000
200,000
150,000
100,000
50,000
0
1940
1960
1980
2000
2020
2040
2060
2080
2100
Year (historic and projected)
Migratory Stopover Group 1
Migratory Stopover Group 2
Migratory Stopover Group 3
Migratory Stopover Group 4
Migratory Stopover Group 5
Migratory Stopover Group 6



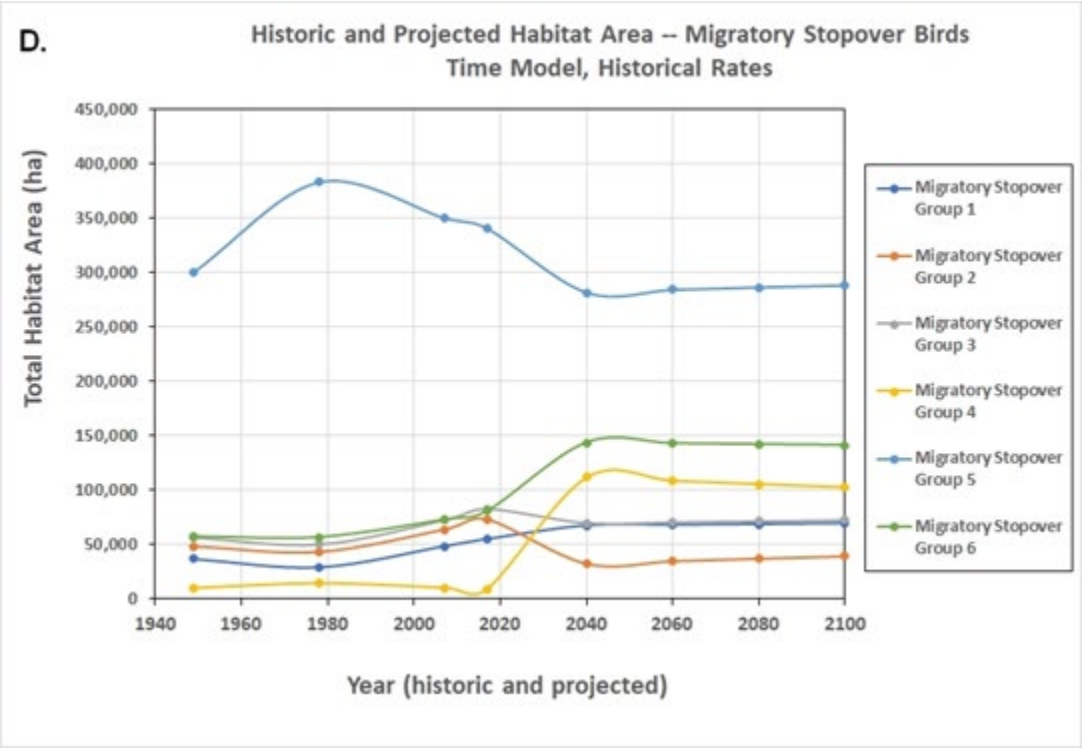


Figure 110. Past, present, and future habitat area of bird migrant stopover species groups (see Appendix Table 2 for species lists) under four ecotype projections: (A) climate model RCP 4.5, (B) driver-adjusted climate model RCP 6.0, (C) climate model RCP 8.5, (D) time model based on historic rates.

Future trends of the bird migrant stopover species groups are projected to vary by ecotype projection scenario. Increases in habitat are projected for groups 1, 2, 3, and 6, with the greatest increases projected under the driver-adjusted climate model RCP 6.0 scenario (Figure 110). Under the time model based on historic rates projection scenario, habitat for groups 4, 5, and 6 is anticipated to increase by 2040 but then generally level out thereafter; and habitat for groups 1, 2, and 3 will undergo various degrees of decline to 2040 and then level out thereafter. In general, as with the individual species of all of the bird migrant stopover groups, future projected habitat trends among the groups vary by habitat associations and the ecotype projection scenarios.

2.11.1.2 Bird Game Species

Alaska Department of Fish and Game provides a list of state bird game species (see Appendix A.1 for sources), specifying waterfowl, crane, grouse, and ptarmigan. Projected overall future outcomes, from 2017 to 2100, generally show equable or increasing habitat amounts for most of these species under most of the ecotype projection scenarios (Figure 111, Appendix Table 6). The driver-adjusted climate model RCP 6.0 scenario projects modest to high increases in habitat area for most waterfowl species, but decreases for grouse and ptarmigan except for increases for sharp-tailed grouse which is more associated with increasing lowland bog and meadow conditions. Changes are more moderate under the other projection scenarios for bird game species (Appendix Table 6).

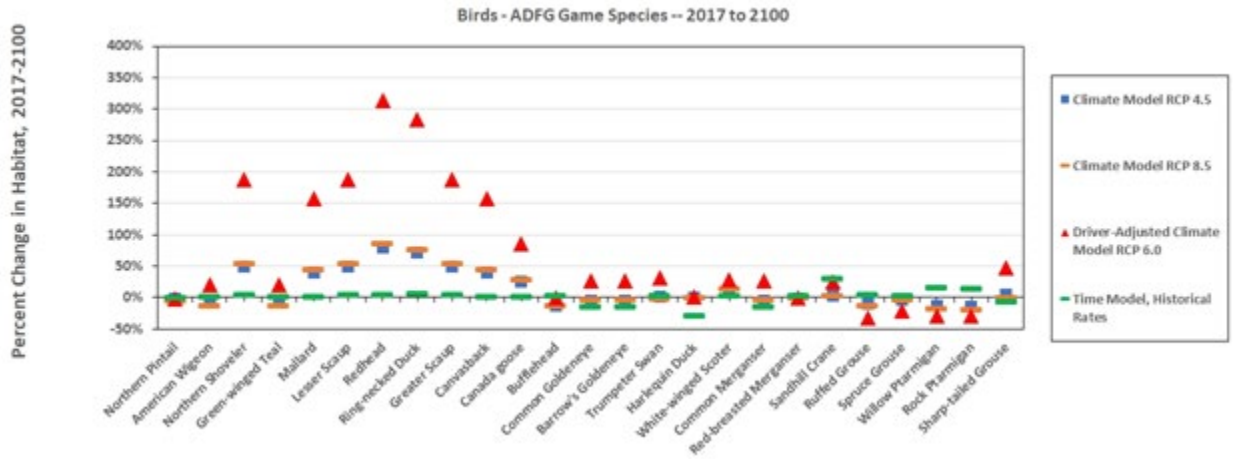


Figure 111. Percent change in future habitat, 2017 to 2100, of 25 bird game species (as listed by Alaska Department of Fish and Game; see Appendix A.1), under four ecotype projection scenarios. Note that most projections result in minor declines, no changes, or increases in habitat areas except for some scenarios projecting habitat decreases for harlequin duck and two species each of grouse and ptarmigan.

2.11.1.3 Bird Habitat Specialists

As discussed further above, we defined bird habitat specialists as those species that use five or fewer ecotypes at either secondary or primary use levels. The threshold of five ecotypes is subjective but serves to identify a small set of 14 bird species that can be further explored here. Among these 14 species, in recent history (1949-2017), for 10 of the bird habitat specialist species habitat increased, for two species (horned lark, gray-crowned rosy-finch) habitat remained constant, and for two other species (bald eagle, spotted sandpiper) habitat declined (Appendix Table 7).

Looking forward, 2017-2100 may see increases in habitat for some bird habitat specialist species under some ecotype projection scenarios (Figure 110). Greatest habitat gains may be forthcoming for some species of aquatic conditions (redhead, horned grebe, dunlin, greater yellowlegs, and solitary sandpiper), particularly under the driver-adjusted climate model RCP 6.0 projections, although that same project scenario suggests potential declines in habitat for a few other bird habitat specialist species such as rusty blackbird, Bonepart's gull, spotted sandpiper, and upland sandpiper (Figure 112).

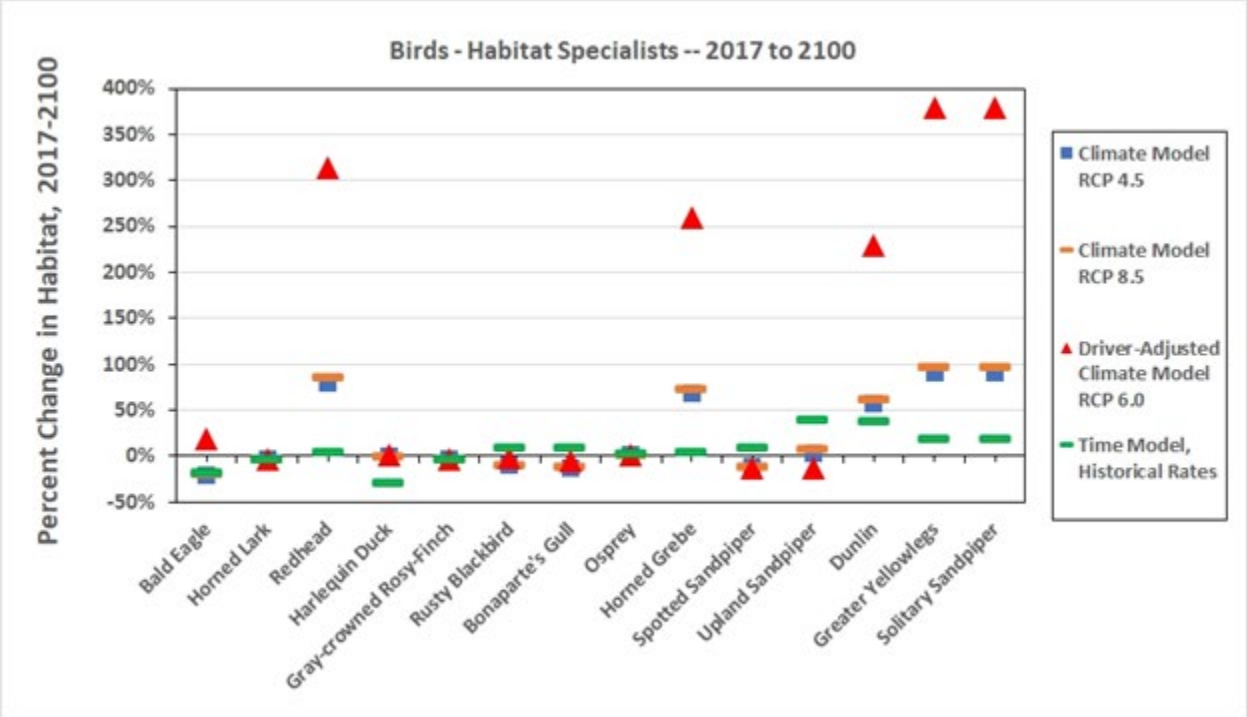


Figure 112. Percent change in future habitat, 2017 to 2100, of 14 habitat-specialist bird species, under four ecotype projection scenarios. Here, bird habitat specialists are defined as those species using 5 or fewer ecotype categories. Projections predict high increases in habitat for some aquatic-associated species, and possible declines for wetland and other wet-site vegetated conditions.

Smith et al. (2018) developed species distribution maps based on auditory point-count surveys of three species of conservation concern ─ rusty blackbird, blackpoll warbler, and olive-sided flycatcher ─ and reported that fens dominated by grasses and herbs near shrub and forest sites were important for all three species and are ubiquitous across Tanana Flats Training Area and Yukon Training Area. We projected various levels of future habitat increases for blackpoll warbler and olive-sided flycatcher under all four projection scenarios, and mixed results for rusty blackbird with projected decreases in habitat of about 6% by 2011 under the climate model RCP 4.5 and RCP 8.5 projection scenarios.

2.11.1.4 Other Bird Species Groups

Waterfowl.

-- Overall, future projections of habitat for ducks and geese look optimistic, with most species showing moderate to high increases in habitat under most of the ecotype projection scenarios, particularly under the driver-adjusted climate model RCP 6.0 scenario (Figure 113 A). Some

declines are predicted by time model based on historic rates scenario for harlequin duck and a few other species.

Grouse, ptarmigan.
-- Except for sharp-tailed grouse, habitat for the two grouse and two ptarmigan species of the study area are projected to maintain or slightly increase under the time model based on historic rates projection scenario, but decrease by up to more than 30% for the other ecotype projection scenarios (Figure 113 B). Sharp-tailed grouse, on the other hand, is predicted under the driver-adjusted climate model RCP 6.0 scenario to increase but otherwise remain mostly constant or slightly decrease under the other scenarios. The difference is that sharp-tailed grouse are more tied to lowland bog and scrub conditions than the other species of this set, and those conditions are expected to increase under the driver-adjusted climate model RCP 6.0 scenario over this century.

Raptors.
-- Nine of the 12 raptor species -- birds of prey -- are mostly predicted to experience habitat declines over this century under all but the time model based on historic rates projection scenario (Figure 113 C and Appendix Table 8). Among the other three raptor species, osprey is projected to show little to no change in habitat under all four ecotype projection scenarios, northern harrier may experience little change or a modest increase in habitat under the time model based on historic rates projection scenario, and bald eagle might experience either a 20% increase in habitat under the driver-adjusted climate model RCP 6.0 projection scenario or a 20% decline in habitat under the three other scenarios.

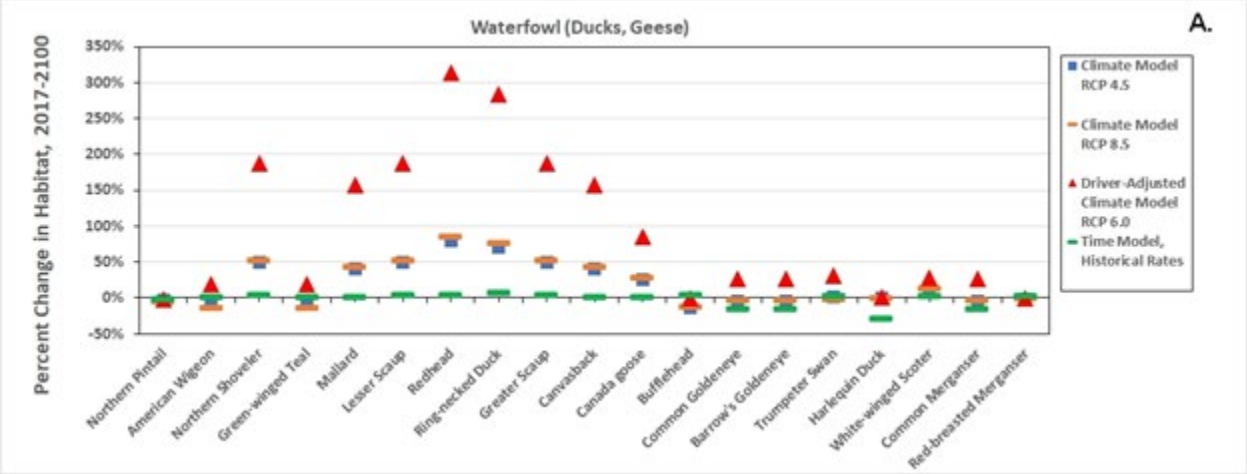
Owls.
-- Among the six owl species of the study area, two (short-eared owl, snowy owl) associate with very similar habitats consisting of various meadow and scrub ecotypes which may mostly remain constant or increase in area over this century under one or more ecotype projections scenarios (Figure 113 D). The four other owl species are more associated with various woodland and forest conditions which might decline the most under the driver-adjusted climate model RCP 6.0 scenario.

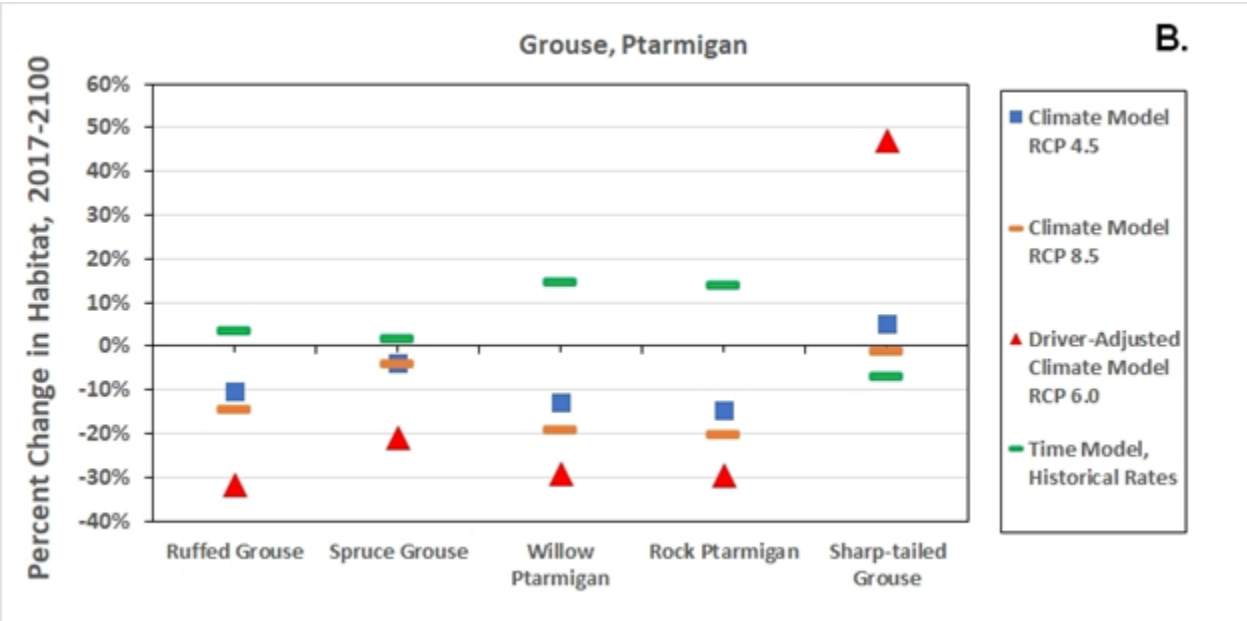
Woodpeckers.
-- Similar to the woodland- and forest-associated owl species are the five species of woodpeckers found in the study area (Figure 113 E). Their habitats are also projected to decline the most under the driver-adjusted climate model RCP 6.0 scenario.

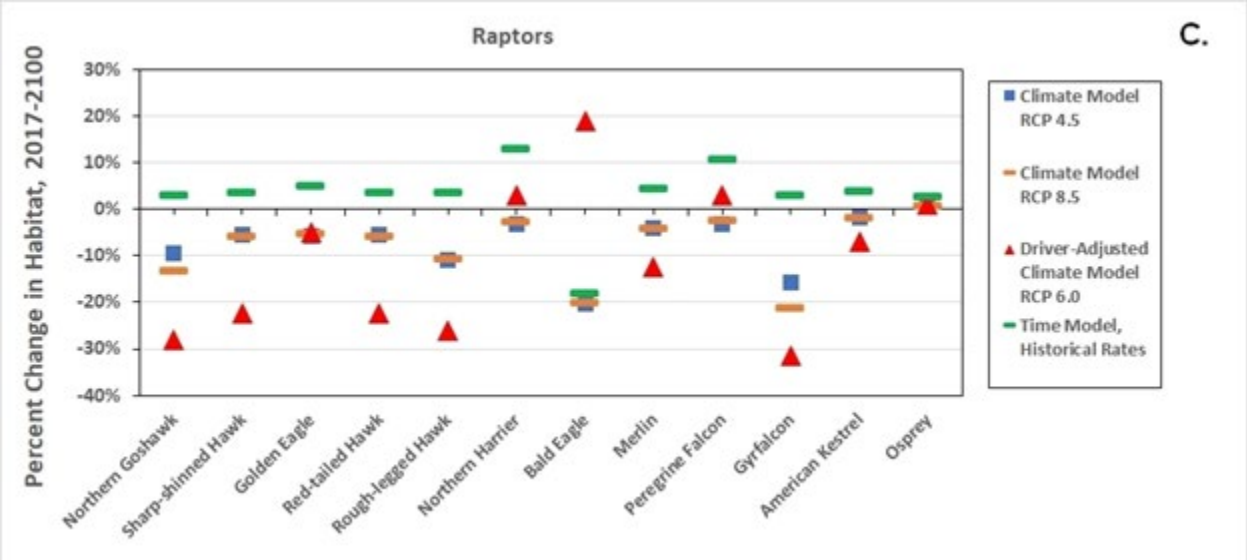
Thrushes and flycatchers.
-- Projections of habitats for the six species of thrushes and five species of flycatchers in the study area -- most of which are also woodland and forest associates -- follow projected habitat change patterns similar to those of the woodland- and forest-associated owls and woodpeckers (Figure 113 F). The exception is Say's phoebe that is more associated with open barrens and meadow environments that are projected to increase under all but the time model based on historic rates projection scenario.

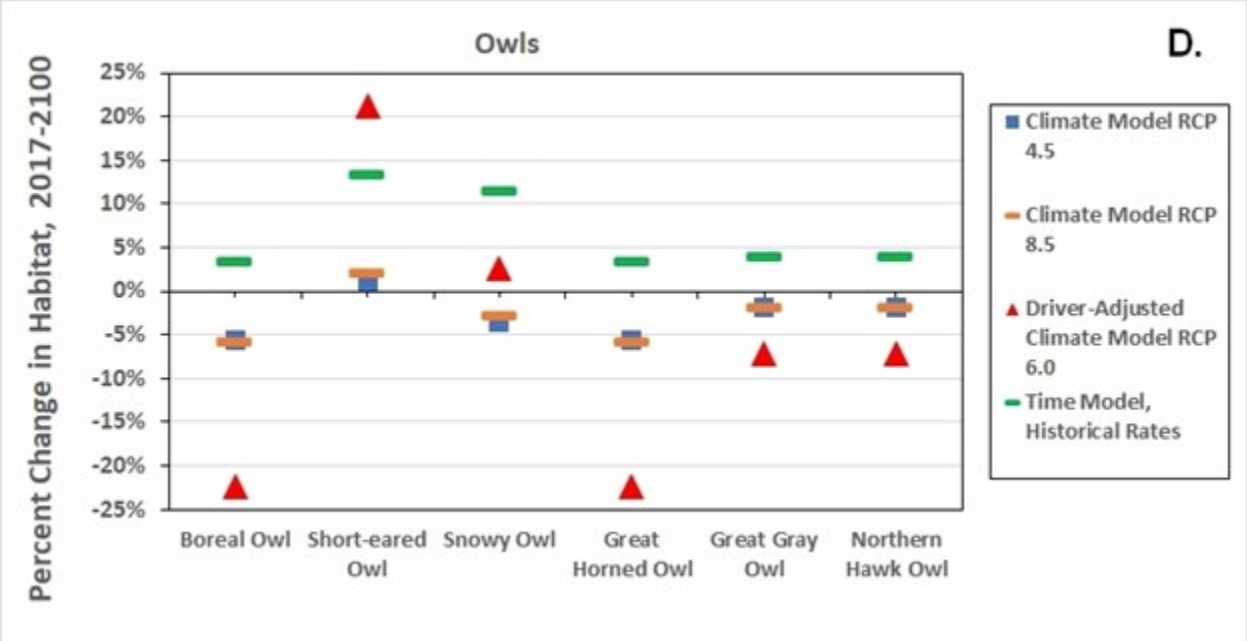
Warblers.
-- Most of the seven warbler species of the study area are associated with woodland and forest environments, and thus show patterns in expected habitat changes similar to the other woodland- and environment-associated bird species mentioned above. Again, greatest potential habitat declines may occur under the driver-adjusted climate model RCP 6.0 projection scenario (Figure 113 G).

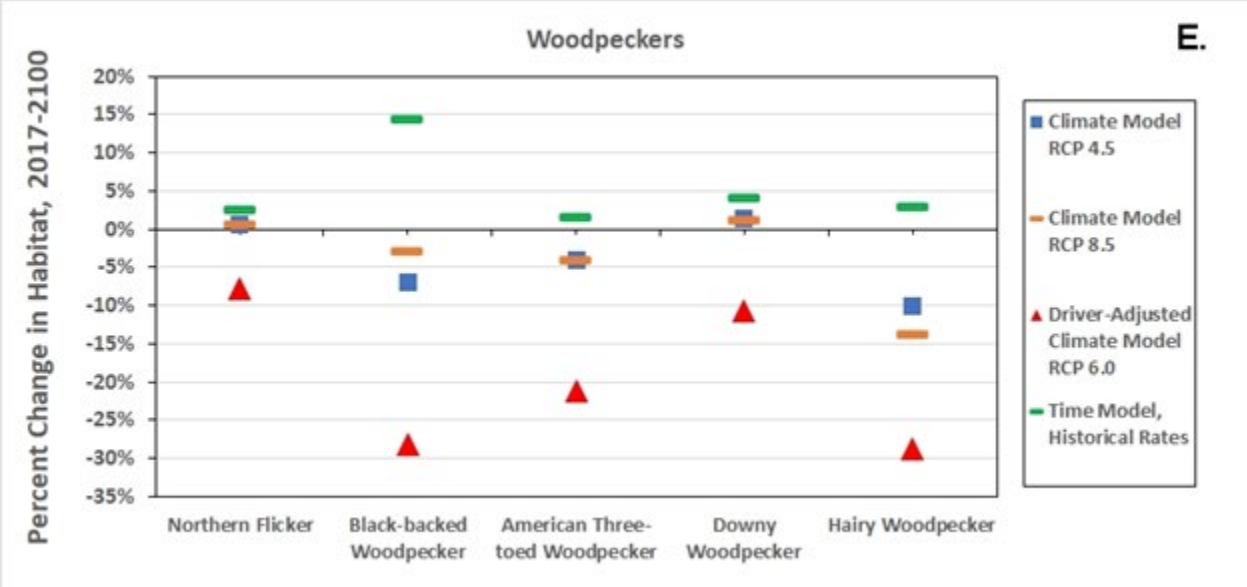
Sparrows, finches, and allies.
-- The pattern of woodland- and forest associates continues with many of the sparrows, finches, and allies, showing potential declines in their habitats particularly under the driver-adjusted climate model RCP 6.0 projection scenario (Figure 113 H). Species more associated with scrub and meadows, such as savannah sparrow, may experience habitat increases or at least no declines. Pine grosbeak -- associated with needleleaf or mixed woodland -- might experience low to moderate increases in habitat.

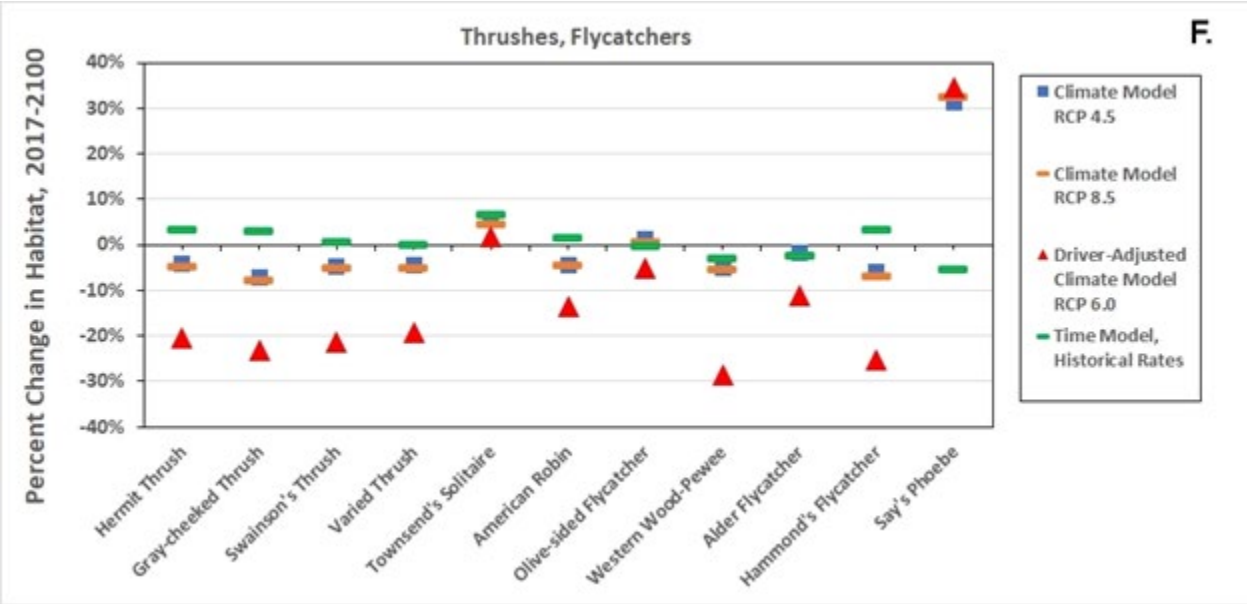





C.
Raptors
Percent Change in Habitat, 2017-2100
30%
20%
10%
0%
-10%
-20%
-30%
-40%
Northern Goshawk
Sharp-shinned Hawk
Golden Eagle
Red-tailed Hawk
Rough-legged Hawk
Northern Harrier
Bald Eagle
Merlin
Peregrine Falcon
Gyrfalcon
American Kestrel
Osprey
Climate Model RCP 4.5
Climate Model RCP 8.5
Driver-Adjusted Climate Model RCP 6.0
Time Model, Historical Rates


D.
Owls
Percent Change in Habitat, 2017-2100
25%
20%
15%
10%
5%
0%
-5%
-10%
-15%
-20%
-25%
Boreal Owl
Short-eared Owl
Snowy Owl
Great Horned Owl
Great Gray Owl
Northern Hawk Owl
Climate Model RCP 4.5
Climate Model RCP 8.5
Driver-Adjusted Climate Model RCP 6.0
Time Model, Historical Rates


Woodpeckers
E.
Percent Change in Habitat, 2017-2100
20%
15%
10%
5%
0%
-5%
-10%
-15%
-20%
-25%
-30%
-35%
Northern Flicker
Black-backed Woodpecker
American Three-toed Woodpecker
Downy Woodpecker
Hairy Woodpecker
Climate Model RCP 4.5
Climate Model RCP 8.5
Driver-Adjusted Climate Model RCP 6.0
Time Model, Historical Rates


Thrushes, Flycatchers
F.
Percent Change in Habitat, 2017-2100
40%
30%
20%
10%
0%
-10%
-20%
-30%
-40%
Hermit Thrush
Gray-cheeked Thrush
Swainson's Thrush
Varied Thrush
Townsend's Solitaire
American Robin
Olive-sided Flycatcher
Western Wood-Pewee
Alder Flycatcher
Hammond's Flycatcher
Say's Phoebe
Climate Model RCP 4.5
Climate Model RCP 8.5
Driver-Adjusted Climate Model RCP 6.0
Time Model, Historical Rates

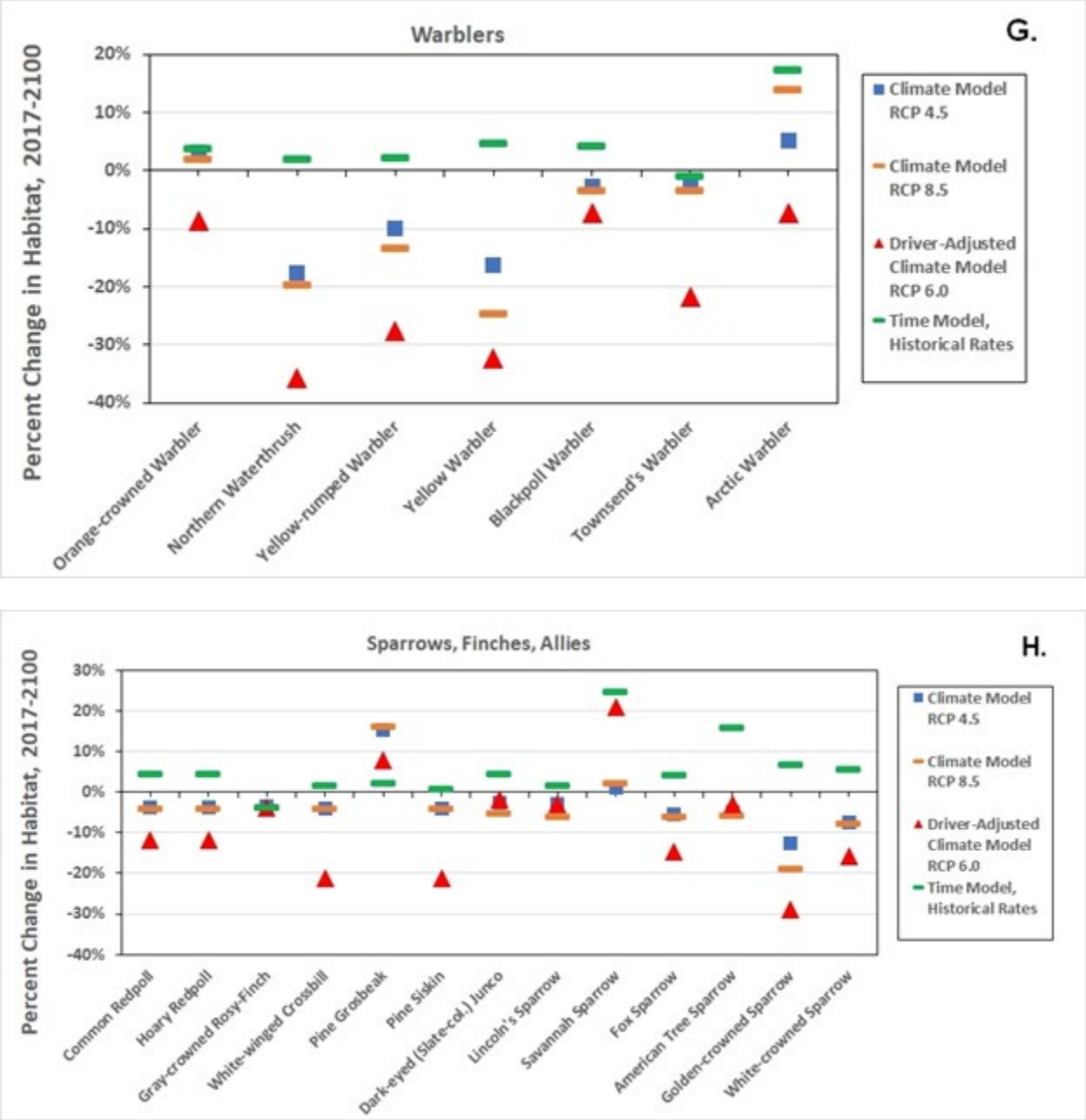


Figure 113. Percent change in future habitat, 2017 to 2100, of selected groups of bird species of potential management or conservation interest, under four ecotype projection scenarios: (A) waterfowl (ducks, geese), (B) grouse and ptarmigan, (C) raptors, (D) owls, (E) woodpeckers, (F) thrushes and flycatchers, (G) warblers, (H) sparrows, finches, and allies.

Rusty Blackbird.

-- Finally, of special conservation interest among the birds is the rusty blackbird, a species of freshwater wetlands of the boreal forest biome of North America and of Interior Alaska training lands in particular (Smith et al., 2018). Populations of rusty blackbird have experienced declines from 80% up to nearly 90% (https://www.audubon.org/field-guide/bird/rusty-blackbird) or higher (http://www.adfg.alaska.gov/index.cfm?adfg=wildlifenews.view_article

&articles_id=660), and had declined by 5 to 12% annually over 1970-2010 (Smith et al., 2018). Reasons for the declines are still being researched but might include lowered availability of their aquatic invertebrate prey; habitat loss and fragmentation; bioaccumulation of mercury as stored in and being released from thawing permafrost (Schuster et al., 2018) or from arctic snowmelt runoff (Douglas et al., 2017), although some evidence suggests this to be a greater concern for this species outside Alaska (Edmonds et al., 2010); and other factors. Our projections suggest that future habitat for rusty blackbird depends upon the ecotype projection scenario, with a modest gain of habitat under the time model based on historic rates, and with further habitat losses under the other scenarios, particularly another 10% or more loss of habitat under the climate model RCP 4.5 and RCP 8.5 projection scenarios (Figure 114).

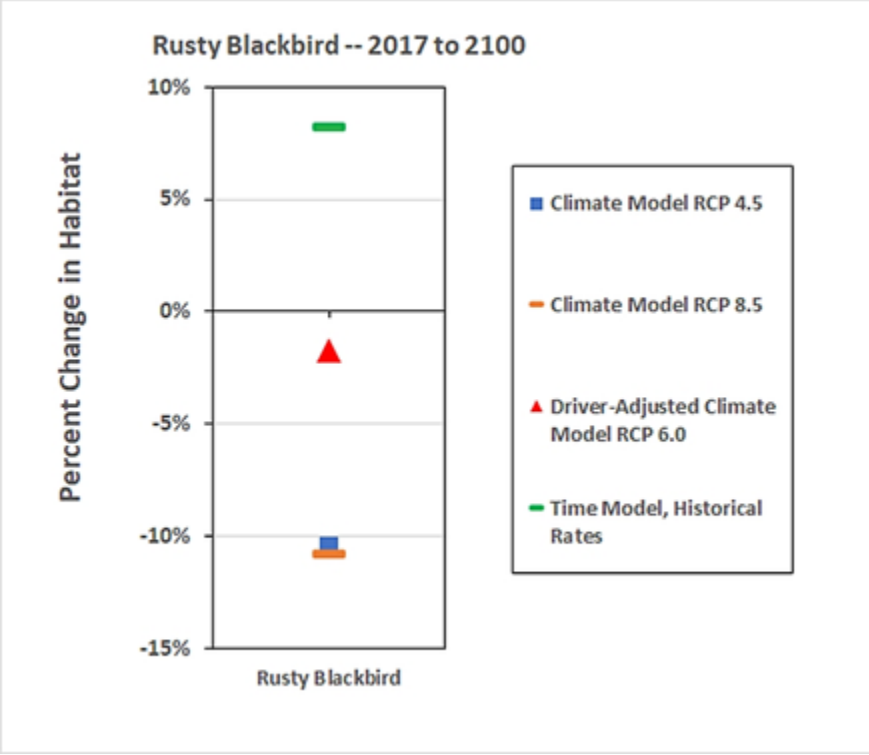


Figure 114. Percent change in future habitat, 2017 to 2100, of rusty blackbird, under four ecotype projection scenarios. Projections predict at much as a 10% increase or a 10% decrease depending on the scenario.

This is not an accounting of all the birds assessed (the complete accounting is found in Appendix Table 4). Next we explored habitat trends of selected mammal species groups.

2.11.1.5 Mammal Game Or Subsistence Species

Among mammal game or subsistence species listed by Alaska Department of Fish and Game (see Appendix A.1 for sources), habitat of caribou might decline the most over this century, particularly under the driver-adjusted climate model RCP 6.0 projection scenario (Figure 115, Appendix Table 9).

Within the study area, caribou are associated with various dwarf and low scrub and some meadow conditions as primary habitat for grazing, largely in alpine and upland landscapes although use of lowland areas also occurs. Under the driver-adjusted climate model RCP 6.0 projection scenario, a few of these conditions are projected to slightly increase over the century (alpine wet low scrub, alpine wet tussock meadow, and upland moist low scrub), but others may decline more severely (alpine dry and moist dwarf scrub, lowland bog tussock and wet low scrub), so that the collective area of all primary-use habitats will decline. It is unknown if caribou would compensate for such changes by being able to shift use of habitats among elevations.

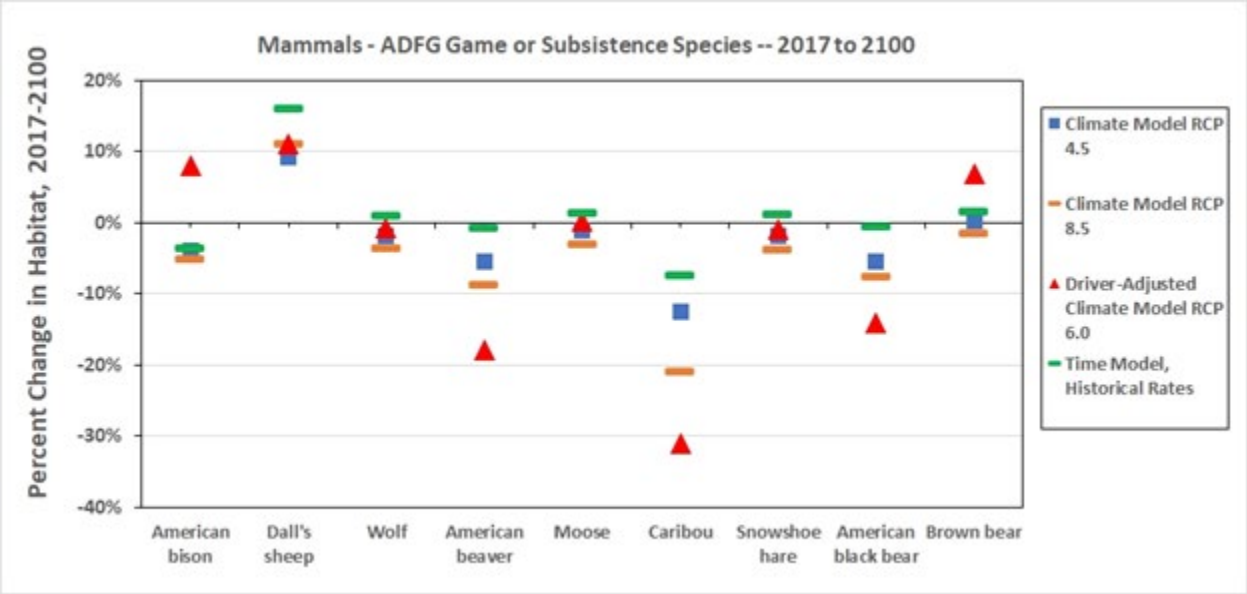


Figure 115. Percent change in future habitat, 2017 to 2100, of 9 mammal game or subsistence species (as listed by Alaska Department of Fish and Game; see Appendix A.1), under four ecotype projection scenarios. Note the projected, potential habitat decline for caribou, beaver, and black bear, although percent changes vary significantly among the four ecotype projection scenarios.

Habitat for beaver and black bear also might undergo some lesser decline or, as with the rest of the species of this group, remain constant, under some scenarios. For beaver, as with caribou, some habitats may increase (e.g., lacustrine shallow and deep lakes, lowland bog meadow) whereas others may decrease (e.g., lowland bog tussock scrub, lowland wet broadleaf woodland), leading to a net decrease in primary and secondary use habitats overall. Meanwhile, overall habitat for Dall sheep might increase mostly from moderate projected increases in alpine dry barrens and upland moist low scrub (Figure 116, Appendix Table 9).

2.11.1.6 Mammal Habitat Specialists

Here, habitat specialists among mammals were identified as those mammal species that use 10 or fewer ecotype categories. As with bird habitat specialists, this is a subjective threshold but also serves as a means by which to identify a set of species with the narrowest habitat use breadth that might be vulnerable to declines in the total amount of their habitat. Note that we use our subjectively-chosen thresholds of 10 or few ecotype categories for defining mammal habitat specialists and 5 or fewer for bird habitat specialists based on the rationale that birds tend to be

more vagile than mammals and can more readily cross poor- or non-habitat conditions, and thus providing a somewhat equivalent comparison between the taxa.

Among the top ten mammal species using the fewest number of ecotypes as explored above (Figure 80), nine of those species use 10 or fewer ecotypes in the study area. Encouragingly, however, little if any declines in the habitat of these nine mammal habitat specialists are projected over the century, with several species projected to experience 50% increases or more under some ecotype projection scenarios, such as with root vole, muskrat, and northern bog lemming (Figure 116, Appendix Table 10).

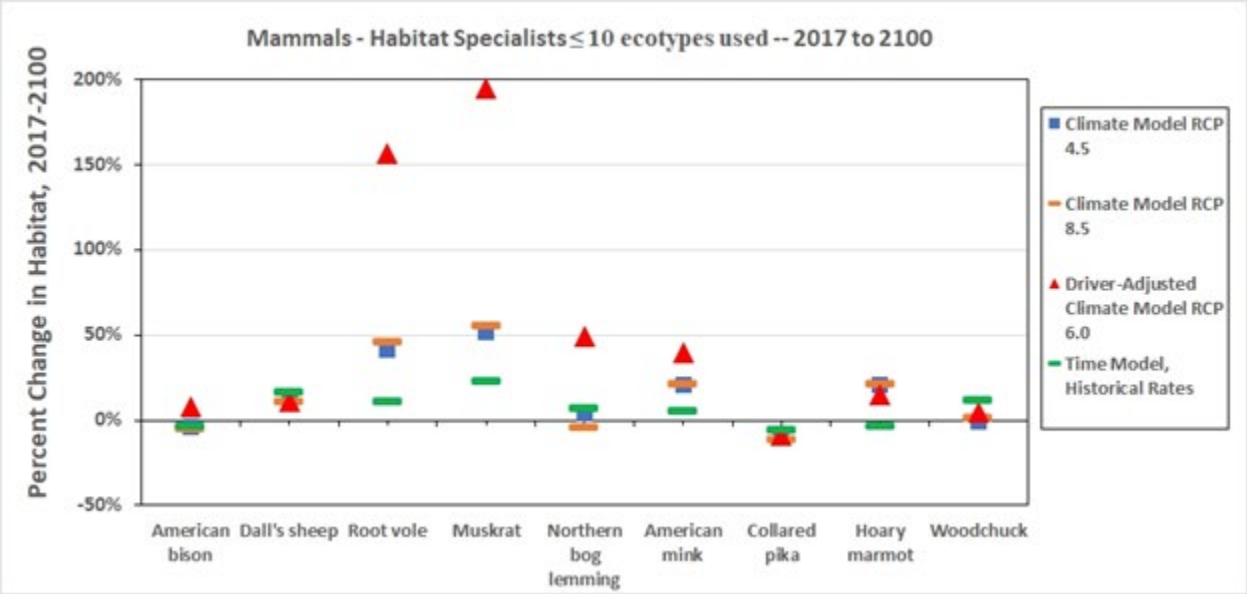


Figure 116. Percent change in future habitat, 2017 to 2100, of 9 mammal habitat specialist species, under four ecotype projection scenarios. Here, mammal specialists are defined as those species using 10 or fewer ecotype categories. Most species are projected with stable to increasing habitat amounts.

2.11.1.7 Mammal Carnivores And Top Predators

Another group of mammals of potential conservation interest is the set of 12 species of carnivores and top predators (order Carnivora) occurring the among families of Canidae, Felidae, Ursidae, and Mustelidae. Most of these species are projected to lose little habitat if at all, except for greater potential habitat losses for black bear and marten under the driver-adjusted climate model RCP 6.0 projection scenario, and mink is projected for approximately 5 to 40% habitat gain under various scenarios (Figure 117, Appendix Table 11).

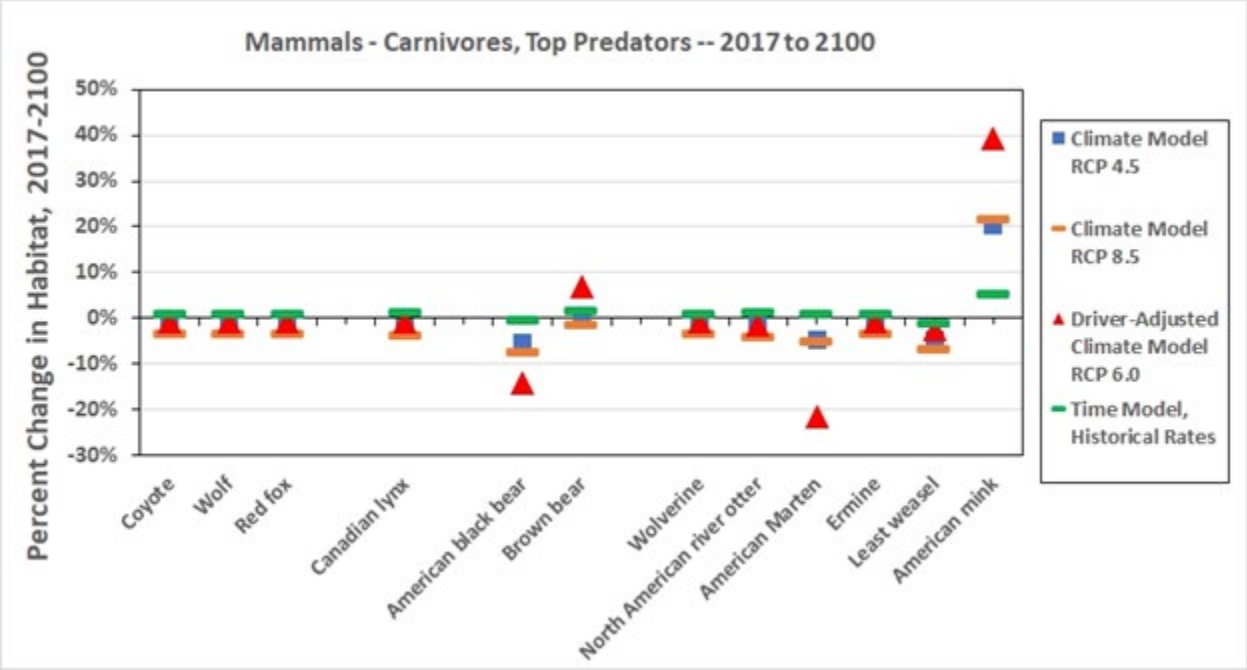


Figure 117. Percent change in future habitat, 2017 to 2100, of 12 species of mammalian carnivores, under four ecotype projection scenarios. The species listed here all belong to order Carnivora and in the families Canidae, Felidae, Ursidae, and Mustelidae.

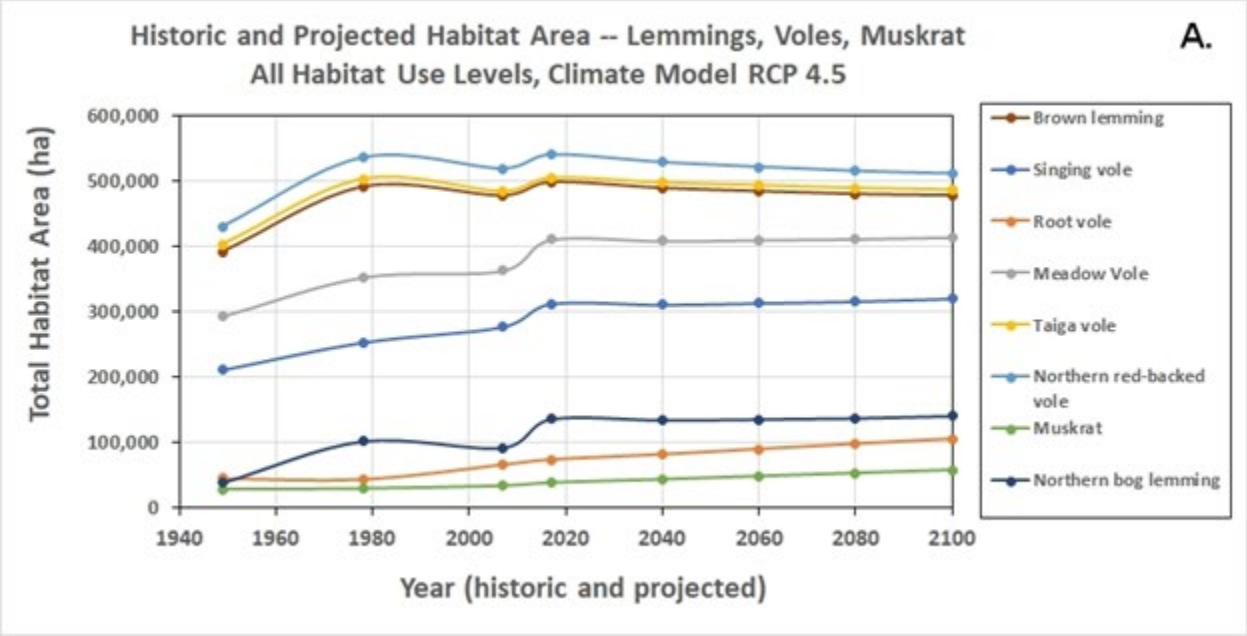
2.11.1.8 Examples Of Trends Of Mammals By Time Period

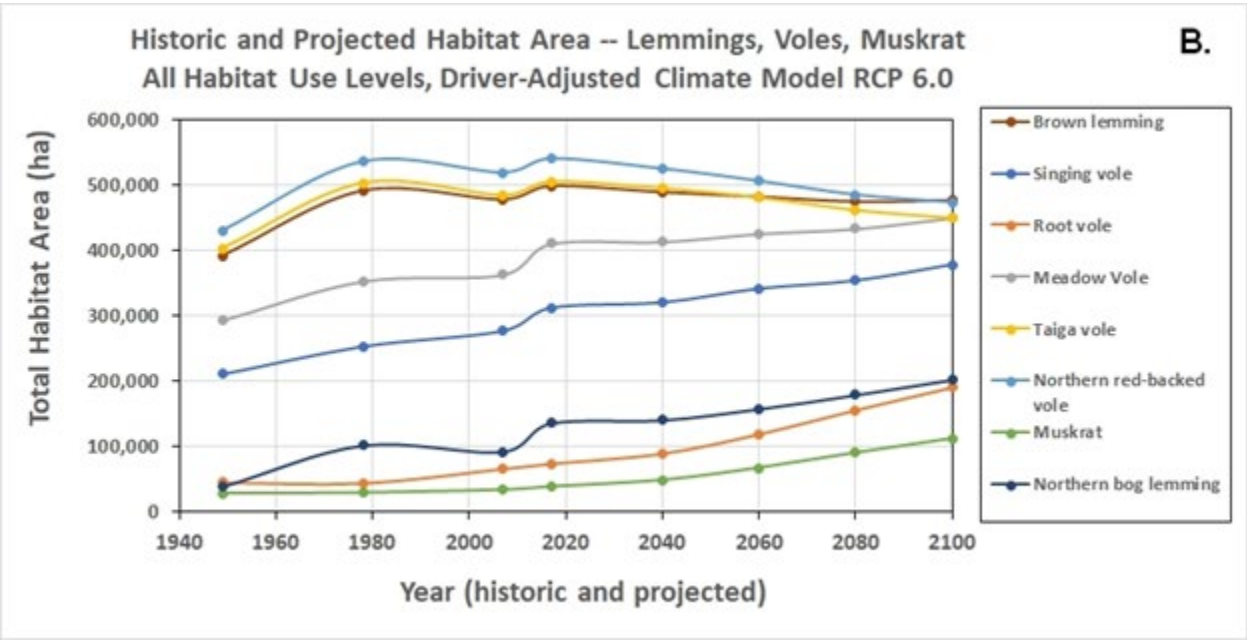
Finally, we close this section with a more detailed look at past-to-future projected habitat changes for the set of small mammals, the aquatic-associated muskrat, and ungulates.

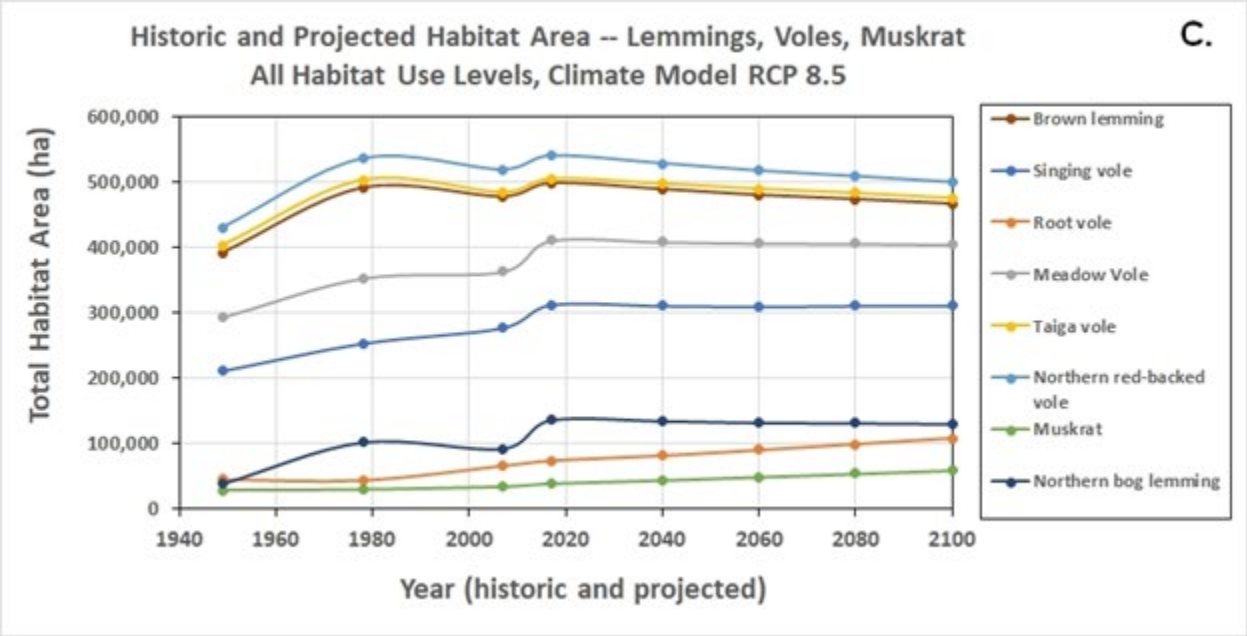
Lemmings, voles, muskrat.

-- The two species of lemmings and five species of voles in the study area are modeled to have gained habitat over the past time interval of 1949 to 2017 (Figure 118), largely due to post-fire recovery of open vegetation types. They are also projected to maintain much of their habitat area over the coming century, with some variations in some gains and losses especially under the driver-adjusted climate model RCP 6.0 projection scenario (Figure 118 B). However, trends may bear watching, as research on other lemming species elsewhere (e.g., collared lemming, Dicrostonyx groenlandicus, in northeast Greenland) suggest that patterns of snow cover can largely drive population response (Duncan et al., 2021).

Muskrat has experienced a slight past increase in habitat, with projected future increases as well (Figure 118). Small mammals such as those assessed here can serve as useful indicators of disturbance and stress on biodiversity from changes in climate (Hope et al., 2017), such as also suggested by Schmidt et al. (2017) for population cycles of hares and voles in central boreal Alaska. The set of small mammals also serves as a key prey base for mesocarnivores and can support their food webs and community trophic structures.


Historic and Projected Habitat Area -- Lemmings, Voles, Muskrat
All Habitat Use Levels, Climate Model RCP 4.5
A.
Total Habitat Area (ha)
600,000
500,000
400,000
300,000
200,000
100,000
0
1940
1960
1980
2000
2020
2040
2060
2080
2100
Year (historic and projected)
Brown lemming
Singing vole
Root vole
Meadow Vole
Taiga vole
Northern red-backed vole
Muskrat
Northern bog lemming


Historic and Projected Habitat Area -- Lemmings, Voles, Muskrat
All Habitat Use Levels, Driver-Adjusted Climate Model RCP 6.0
B.
Total Habitat Area (ha)
600,000
500,000
400,000
300,000
200,000
100,000
0
1940
1960
1980
2000
2020
2040
2060
2080
2100
Year (historic and projected)
Brown lemming
Singing vole
Root vole
Meadow Vole
Taiga vole
Northern red-backed vole
Muskrat
Northern bog lemming



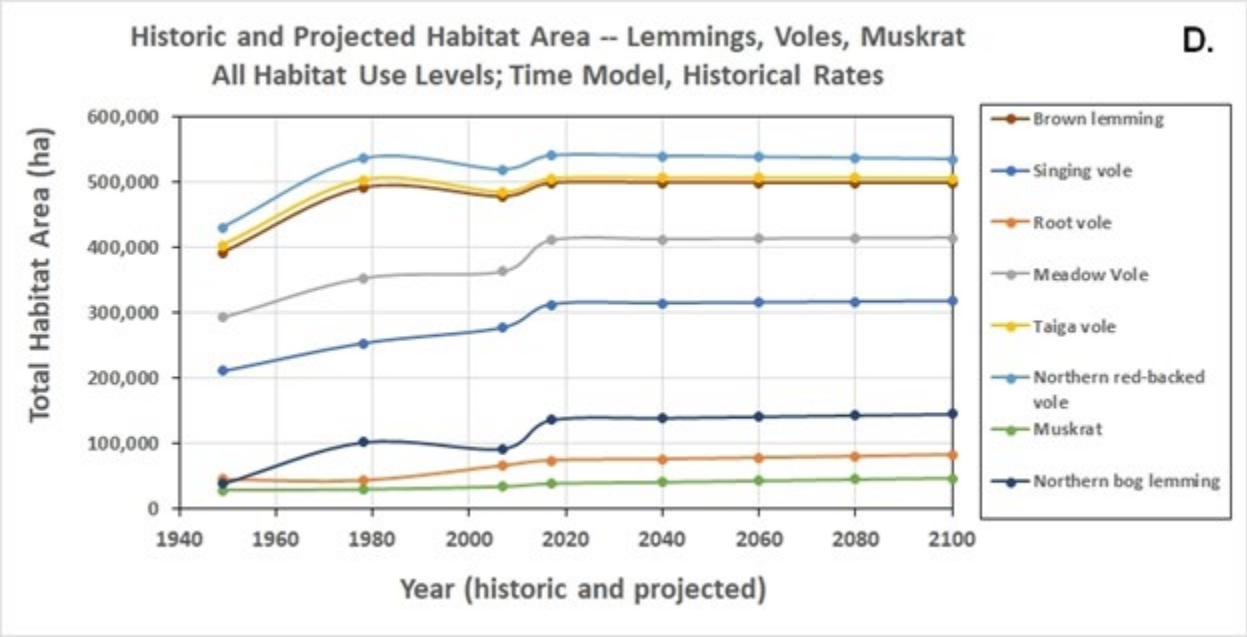
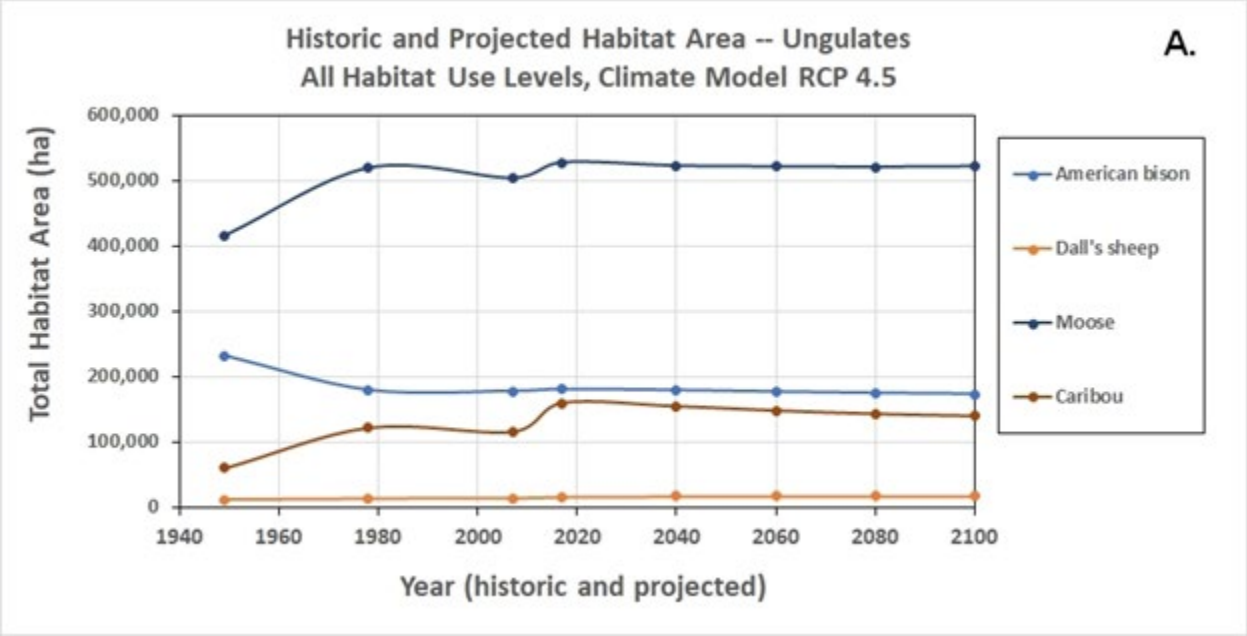
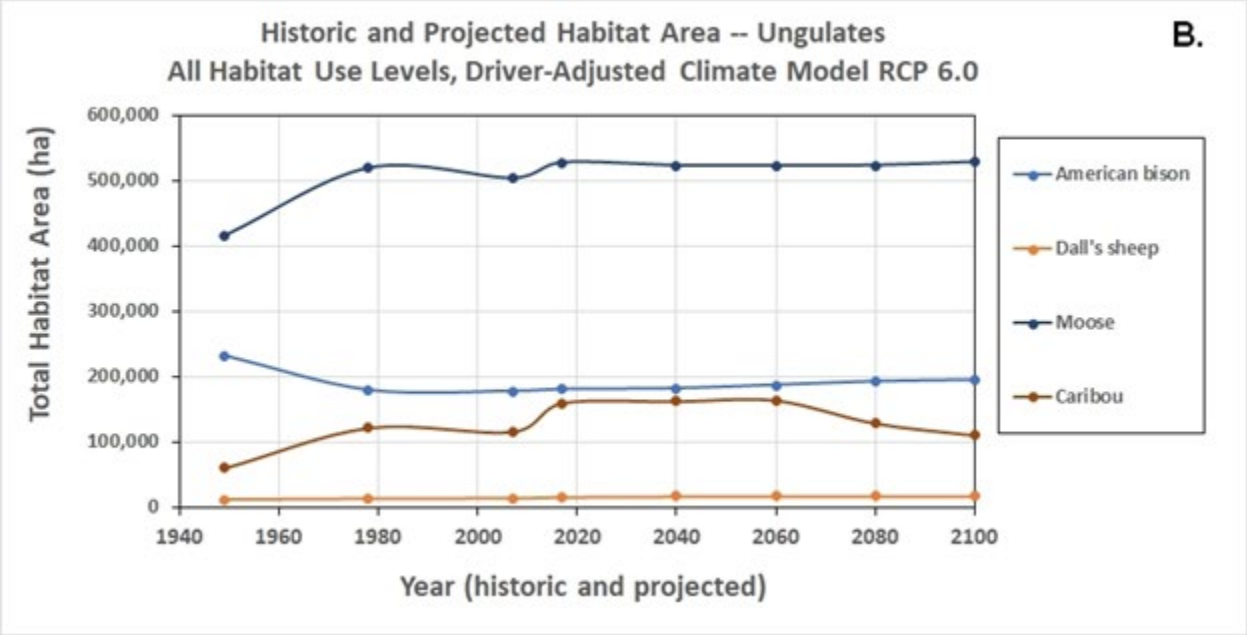


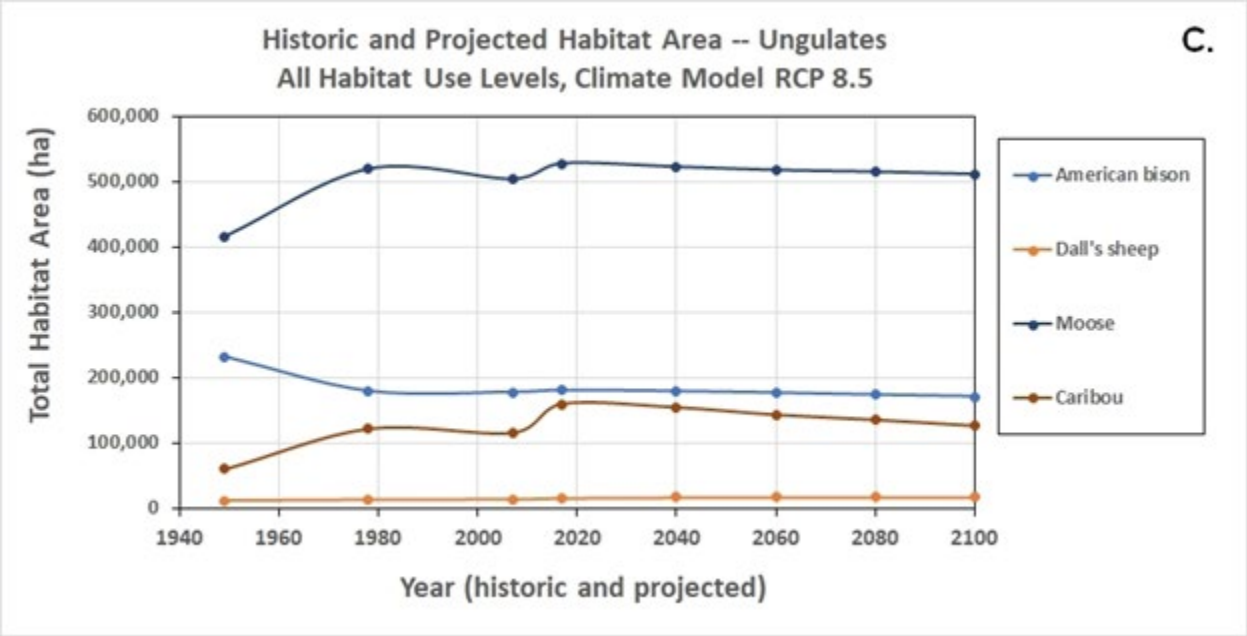
Figure 118. Past, present, and future habitat area of small mammals (lemmings and voles) and muskrat, under four ecotype projections: (A) climate model RCP 4.5, (B) driver-adjusted climate model RCP 6.0, (C) climate model RCP 8.5, (D) time model based on historic rates.

Ungulates.

-- Among the ungulates, habitat of moose and caribou were projected to have increased since 1949, and the more scant alpine habitat for Dall sheep has been essentially maintained (Figure 119). Future projections suggest potential decline in caribou habitat as discussed further above; little change in habitat amount for moose and bison; and a potential slight increase in habitat for Dall sheep.


A.
Historic and Projected Habitat Area -- Ungulates
All Habitat Use Levels, Climate Model RCP 4.5
Total Habitat Area (ha)
600,000
500,000
400,000
300,000
200,000
100,000
0
1940
1960
1980
2000
2020
2040
2060
2080
2100
Year (historic and projected)
American bison
Dall's sheep
Moose
Caribou


B.
Historic and Projected Habitat Area -- Ungulates
All Habitat Use Levels, Driver-Adjusted Climate Model RCP 6.0
Total Habitat Area (ha)
600,000
500,000
400,000
300,000
200,000
100,000
0
1940
1960
1980
2000
2020
2040
2060
2080
2100
Year (historic and projected)
American bison
Dall's sheep
Moose
Caribou



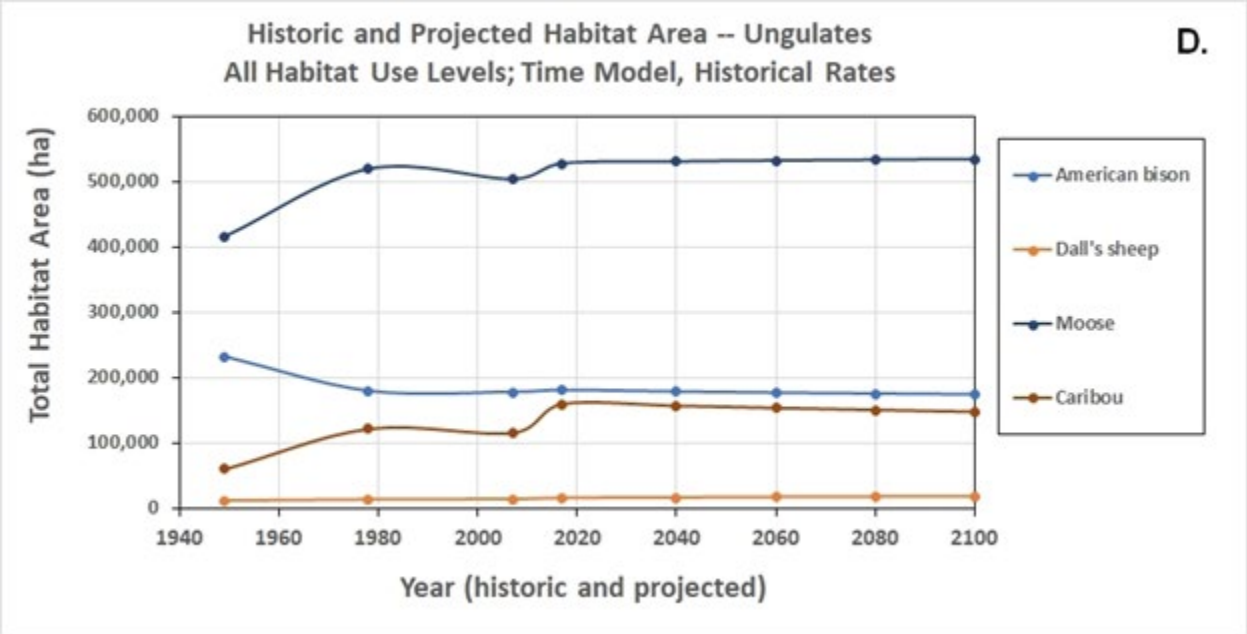


Figure 119. Past, present, and future habitat area of ungulate species, under four ecotype projections: (A) climate model RCP 4.5, (B) driver-adjusted climate model RCP 6.0, (C) climate model RCP 8.5, (D) time model based on historic rates.

This completes the presentations and summaries of identification of wildlife species occurrence; wildlife species-ecotype relationships; and past, current, and future changes in wildlife habitats of the study area. The final section, following, discusses general management and conservation implications of these findings.

Addendum: As suggested, the lists of wildlife species and their ecotype relationships in this study will doubtless be subject to edits and improvement over time. One key example is the omission of chipping sparrow (Spizella passerine) from the bird species list. This omission came to light upon a latent discovery of the call of this species from the audio recordings (see next section, below, on use of automated audio recording units) from a lakeside environment (ecotype Upland Shallow Thermokarst Lake, upslope from near the Permafrost Tunnel, along Glenn Creek); from an early-successional, post-fire lowland location (ecotype Lowland Low Scrub Fire-Disturbed, at APEX Bonanza Creek); and from a few other early, open sites. The presence of chipping sparrow in the general region (but not the training land study area per se) also had been reported from roadside North American Breeding Bird Survey results analyzed by Handel and Sauer (2017) and in the central boreal study area is likely near or at the northern edge of its distribution range (Chester, 2016).

2.12 Task 4

Developing technologies and methodologies and transferring results into operational routines useful for training land planning and develop adaptive management strategies to minimize impacts to vulnerable populations.

This Task is focused on aggregating geospatial information and modeling results into a decision-support system displaying projections of the distributions of ecotypes and wildlife habitats for individual species, particularly species of conservation concern, along with general probabilities of their future changes (gains and losses), under scenarios of future climate change and human activities. Ultimately, Task 4 encompasses synthesizing all four project objectives and providing useful and actionable information to training land managers.

We worked collaboratively with USAG-AK Directorate of Public Works and Range Control personnel throughout the project. Initially they helped us identify any potentially available field measurements on soils, permafrost, and vegetation/ecotype information from the Training Area domain. They provided us with data, Reports, and areas of concern and we integrated their data into our geospatial database and provided maps, ground survey measurement results, and habitat information to them. All project databases, geospatial layers, model outputs, wildlife information, and habitat projection information is being provided to them and any other State or Federal entity that has interest. Since CRREL has an office on Fort Wainwright we will work with them after project closeout to maintain this information exchange.

A main focus of the Task 4 information transfer efforts was to provide a risk assessment of projected outcomes with probabilities that can be used in risk management decision-making by comparing projected impacts of alternative future scenarios and human land-altering activities, displaying the degree to which wildlife conservation objectives would be met. We hope the system will be used to determine how human activities could be altered to better meet conservation objectives.

2.12.1 Discussion and Management Implications of the Wildlife Habitat Analyses

This section summarizes the basis and results of the wildlife-habitat analyses presented in sections A.1 through A.5, above, and suggests implications for habitat management and conservation. Here, we have highlighted in bold the major implications for management of wildlife habitats within the study area.

2.12.1.1 Assumptions and Caveats

Presented in the above sections are mostly hypotheses of species-habitat relationships and potential effects of climate change and disturbances on habitat conditions for wildlife. We have used much source material for constructing these relationships but much remains to be studied on population response to environmental conditions and changes for many, if not most, of the species assessed here. Representations of these hypotheses in the various species-ecotype relationships tables and subsequent change analyses can be updated and improved over time with new information and research findings.

This analysis does not address genetic diversity, the array of ecological functions of organisms, and other dimensions of biodiversity beyond species-habitat relationships. Also, the evaluation of habitat associations and projected past and future changes in habitat amounts does not consider changes and effects of habitat patch spatial configuration, patch size, fragmentation,

and connectivity, effects of which would need to be studied in depth and detail at the levels of individual species and populations.

2.12.1.2 Expectations of Ecotype Projection Scenarios

Overall, the driver-adjusted climate model RCP 6.0 projection scenario seemed to produce the greatest projected gains and losses of habitat. This is because this scenario modified the RCP 6.0 projections of ecotype transitions and coverages based empirically on key drivers of thermokarst activity, which was not included with the RCP 4.5 and RCP 8.5 projections. The RCP 6.0 projection scenario also is deemed to be the most likely of the four scenarios explored in this report because of the inclusion of thermokarst driver dynamics (see Table 10).

2.12.1.3 Species-Rich Ecotypes Depict Spatial Variability in Drivers of Vulnerability

We identified ecotypes that are most species-rich (number of species) as major contributors of biodiversity in the study area, including for birds (Figure 70), mammals (Figure 74), migrant stopover bird species groups (Figure 72), and all individual species combined (Figure 76). All ecotypes in the study area contribute in some degree to species richness, with the most contributions by lowland wet sites, riverine forests, and upland moist and wet forests.

The least contributions of ecotypes to wildlife species richness are in human-modified barrens and scrub conditions, in lowlands and uplands alike. This suggests that, to help maintain habitats for most species, it may be important to avoid or limit converting especially the higher species-rich ecotypes into human-modified barrens and scrub conditions. Such conversion can occur, for example, from road-building and from creating and maintaining impact clearings in the study area, activities of which tend to reduce or locally eliminate foraging, nesting, and breeding habitat for a variety of species. In general, these findings and suggestions are examples of the spatial variability in drivers of vulnerability across species' ranges, addressing Project Objective 2.

2.12.1.4 Understanding the Relationship Between Changing Climate and Key Ecological Processes

Although this study was not designed to explore specific ecological functions of species and impacts of disturbances including climate change on wildlife biotic processes per se, some results can be gleaned from patterns noted with selected wildlife species groups. In particular, it is encouraging to note that habitat of lemmings and voles, which constitute important prey for many of the mammalian carnivores of the region, are projected to generally maintain or increase in area over time (Figure 118). Further, habitat areas of the mammalian carnivore species are projected to generally maintain over time with a few exceptions by projection scenario (Figure 117).

However, many of the avian predators- the raptors, or birds of prey, and owls- are projected to decline in habitat area under most ecotype projection scenarios (Figure 113 C, Figure 113 D). It may be helpful to at least intermittently monitor the abundance of these species groups, particularly most of the raptors and the forest-associated owls. These findings and suggestions help address Project Objective 3, for developing an improved understanding of the relationship between changing climate and key ecological processes such as food webs.

2.12.1.5 Habitat Futures for Game and Subsistence Species

Much hunting and a little trapping of some game and subsistence species occur regularly within the study area, especially with moose hunting on Tanana Flats and along areas with road and river access. It is useful to consider how the area might contribute habitat to game and subsistence species within the study area and also for the broader region of central boreal Alaska.

It is encouraging that habitat of most of the bird game species, including waterfowl, will likely be maintained or increased over time (Figure 111, Figure 113 A). We note some cautionary exceptions, however, for potential habitat declines for harlequin duck and for grouse and ptarmigan (Figure 113 B) under most of the ecotype projection scenarios.

Mammalian game or subsistence species are more of a mixed set, with some species maintaining habitat but others likely to lose habitat under most scenarios (Figure 115). It may be useful to conduct at least intermittent surveys and monitor abundance of beavers, caribou, and black bears in the study area, which are projected to mostly decline in habitat under most scenarios, and, as feasible, monitor take for hunting and trapping by species.

2.12.1.6 Conservation and Protection of Key Ecotypes for the Most Vulnerable Species

Conservation and protection of habitat conditions for the most vulnerable wildlife species of the study area helps address Project Objective 4 for meeting conservation objectives. Potentially vulnerable species discussed here are bird and mammal habitat specialists, wood frog, rusty blackbird, and caribou.

Wildlife species with the narrowest habitat-use breadth- that is, that use the fewest number of ecotypes -- might constitute one set of species potentially and particularly vulnerable to declines in specific ecotype conditions. However, we found that the sets of 14 bird species (Figure 112, Appendix Table 7) and 9 mammal species (Figure 116, Appendix Table 10) that we defined as habitat specialists collectively use a wide array of ecotypes. The 14 bird habitat specialist species occur variously in 24 ecotypes (39% of all 61 ecotypes analyzed here); the 9 mammal habitat specialist species occur variously in 30 ecotypes (49% of all ecotypes); and collectively the 23 species of bird or mammal habitat specialists occur in 41 ecotypes (67% of all ecotypes). This suggests that no single, or small number, of ecotypes alone contributes to habitat-specialist species, but instead that, as feasible, maintaining the fuller array of all ecotypes across the landscape can best contribute to this set of potentially vulnerable species.

We also explored conditions of several individual species that may be of high conservation concern because of their recent or potentially impending declines in occurrence, habitats, or populations. It may be prudent to disturb the existing habitats of these species the least. These species include wood frog, rusty blackbird, and caribou, as follows.

We found that wood frogs may use some 26 ecotypes, but likely only 13 ecotypes as primary habitat (Figure 68) in lacustrine, lowland, and riverine environments, and only 5 of these are lake and wet meadow ecotypes used as primary breeding habitat. Further, only one ecotype projection scenario suggested little to no change in habitat area over the coming century, whereas the other three scenarios all predicted habitat declines of from about 4 to 11%. Monitoring especially the aquatic ecotype conditions for wood frog, and conducting calling surveys or recordings (see discussion below) during the breeding season, could usefully provide information on status of habitats and populations of this species.

Rusty blackbirds were also identified as a species of conservation concern because of its high decline in population abundance in recent decades. This species is noted as a habitat specialist mostly of lowland bogs and riverine moist tall scrub ecotypes which, collectively, are

projected to more likely decrease in area by at least 10% under some projection scenarios (Figure 114). Protecting these vulnerable habitats would serve to provide for rusty blackbird as well as a number of other species. In this way, the persistence of rusty blackbird populations could be used as an indicator of the health of this type of wet-site ecosystem for many other species.

Lastly, habitat of caribou, as noted in previous sections, is projected to decline over the century by as much as 20% (Figure 99, Figure 119). Caribou are a regionally and culturally important subsistence species. The study area provides habitat for caribou likely of the Delta herd, but also with some possible overlap with the Macomb and Nelchina herds (https://www.adfg.alaska.gov/static/species/speciesinfo/caribou/images/caribou_herds.jpg), as herd dynamics can be fluid (J. Smith, pers. comm.). Caribou in the study area mostly use alpine and upland scrub and barrens environments for grazing. Maintaining these higher-elevation grazing environments free from shrub encroachment could help maintain habitat for caribou in the study area, thereby contributing to maintaining the species more broadly throughout the central boreal region of Alaska.

2.12.1.7 Effects on Wildlife Habitat From Environmental Disturbances

Comparing the results of species-habitat projections among the four ecotype projection scenarios helps to identify how wildlife habitats can be affected by various disturbances, including climate, fire, thermokarst-forming processes, and other drivers, that could result in increases or decreases of habitats of dependent wildlife species. Specifically, among the four ecotype projection scenarios, the driver-adjusted climate model RCP 6.0 scenario is likely the most realistic, and which often results in the greatest projections of future habitat gains or losses. Further, information on habitat-use breadth (number of ecotypes used by species) provides some insight into species' ecological flexibility that could help buffer habitat declines. This directly addressed Project Hypothesis 3.

2.12.1.8 Considering Habitat Fragmentation and Connectivity

Some final considerations in this section pertain to how spatial patterns of habitats can affect wildlife species persistence. There may be unintended consequences of development that would sever the more fragile and scarce environments of the study area, fragmenting habitats into smaller and disjunct patches. This might have adverse effects in wood frog habitat, natural alpine environments, riparian vegetative cover, and other situations, including for terrestrial species with low vagility and poor dispersal capabilities. Retaining or restoring connectivity of these and other scarce ecotypes may be part of a general wildlife habitat conservation strategy (e.g., for wolverine; Balkenhol et al., 2020).

Ecotypes to disturb the least may include the small ponds, fens, bog and wet meadows, and riparian woodlands. These conditions are most susceptible to change and loss of habitat values from local disturbance such as drainage and road-building, and contribute key habitats for rusty blackbird, wood frog, and many other species.

2.12.1.9 How Wildlife Behaviors Can Alter Habitat

A final topic here not explicitly included in the species-habitat relationships assessments is how specific behaviors of organisms- key ecological functions of wildlife- can, in turn, provide or detract habitat conditions for other species (e.g., Marcot and Vander Heyden, 2001; Marcot and Aubry, 2003). This is known for large ungulates such as caribou and moose whose grazing and browsing can change successional vegetation trajectories (e.g., Joly et al., 2009,

Kolstad et al., 2018). It is less well known for a wide range of species that can play other key roles that can enhance habitat conditions for other species. Examples are functions of seed caching and dispersal (Figure 65), creation of tree cavities or ground burrows used by secondary cavity-nesters and other species (Figure 64), disintegration of down wood and underground burrowing to facilitate organic input into soil (Figure 64), movement of fish caught from streams up into the riparian zone providing soil nutrients, and much more. How wildlife behaviors can influence habitat may become an important part of future ecosystem-based habitat projections, particularly under habitat-change dynamics, but much remains to be learned and quantified about these influences.

2.12.2 Summary

It should be made clear that this analysis was designed to project amounts and, to some degree, distributions of wildlife species' habitats, not to predict sizes and trends of wildlife populations. Populations can change from more than just the availability of habitat, such as by changes in food and prey sources, presence or absence of disturbances, climate conditions, and other factors. A case in point may be expansions in occurrence or distributions of black-billed magpies and coyotes, among other species, in central boreal Alaska, and potential reduction in other species.

It is heartening to have learned that few wildlife species are projected to suffer major habitat loss over the coming century under the four ecotype projection scenarios assessed in this report, although historic declines in some species' habitats has been documented here. Still, if the objective is to minimize further habitat declines, particularly for at-risk and vulnerable species, then planning for further site development or for maintenance of existing developed lands might incorporate consideration for the more vulnerable habitats and species as noted above, and, in general, with a vision to maintain the existing diversity and connectivity of ecotypes within the study area.

2.12.3 Discussion and Potential Implications for Future Inventory, Monitoring, and Research

Few studies have been conducted on bioacoustics of wildlife in central boreal Alaska on USAG-AK training lands. We found value in conducting this part of the study, although it took special preparation to program the ARUs, to identify the appropriate variety of field conditions and locations for recording, and to deploy, maintain, and retrieve the ARUs in the field. Also, for various reasons over the course of the study, we encountered occasional, unexpected problems of access to some field locations for deployment or retrieval of ARUs (e.g., live fire training on the Yukon Training Area and on Tanana Flats at Bonanza Creek).

It may be useful to continue bioacoustic studies in selected ecotypes and environments that are (1) least known and researched as to wildlife occurrence and use, and (2) potentially subject to disturbances from development (e.g., roads, impact clearings, drainage of ponds, lakes, and fens, etc.). Bioacoustic studies of wood frog may be particularly useful to better determine its distribution and to refine understanding of habitat associations over the course of the breeding season.

2.12.4 Conclusions and Management Implications of the Soundscape Analyses

In summary, the quality of the individual soundscapes of the sampled locations seemed influenced by a complex combination of sounds of various ecoacoustic categories and specific sound sources, particularly as influenced by presence and changes in human activities over the

course of the recording seasons. The natural biophony sources of bird songs and calls, squirrel calls, and other organisms generally contributed to a different ecoacoustic profile than when the sound profiles were interrupted or dominated by anthrophony sources of human activities.

Although this was not a direct study of potential noise impacts on wildlife, many studies have established that undue anthropogenic noise can be a major disturbance to wildlife occurrence, movement, feeding, and reproduction (e.g., Barber et al., 2011; Brown et al., 2012, Dooling and Popper, 2007; Kunc and Schmidt, 2019; Francis and Barber, 2013), including adverse effects on wood frogs (Tennessen et al,. 2018), wolves and elk (Creel et al., 2002), owls (Mason et al., 2016), and other species. Dumyahn and Pijanowski (2011) suggested treating soundscapes as "common-pool resources" whereby the collective effects of all natural and artificial sound sources be considered in management and planning for conservation objectives. Francis et al. (2017) argued generally for designation of areas to be protected from undue human impacts on natural soundscapes.

Despite the high variation in sound structures among the 24 audio recording sites samples, some distance threshold effects can be suggested from the analysis. We noted potentially adverse influence of sites within approximately 5 km to firing ranges and primary roads, 1 km to flight lines, and 15 km to main airports. Our GIS map of the locations and overlap of these sound sources could be used to identify ecological areas already affected by higher levels of anthropogenic noise, and to identify areas not yet so affected where undue noise could be averted.

2.12.5 Applications for Future Change-Detection Studies

As noted throughout this section, the low-level aerial photographic transects could be repeated at future intervals along the same flight paths to facilitate change-detection studies of relatively fine-grained landscape features.

The objective would be to aid in identifying early warning signals and evidence of more subtle landscape changes such as thermokarst slumps, spread of effects of insect defoliators, rates of pond and lake formation and drying or draining, shifts in river courses and riparian conditions, and much more.

3. CONCLUSIONS AND RECOMMENDATIONS FOR TRAINING RANGE MANAGEMENT

1) In developing our database of all known measurements of permafrost presence/absence, soil type, and vegetation characteristics across the USAG-AK training land domain we identified many hundreds of measurements that the Army does not currently have in their geospatial datasets. These included measurements from a variety of studies that were not known to us or the Army or from contractors that had not finalized their datasets and/or had not shared them. Due to the remote nature of the training lands and the high time and monetary cost of these types of data this expanded geospatial dataset has high value. There are other information sources still to be integrated but this is an exciting outcome both for our modeling needs (i.e., it provided more data than we knew existed), but also for the Army to have access to the broadest measurements available.
2) Our repeat LiDAR analyses have identified many areas where permafrost thaw and degradation are occurring. They also provide an established means of rapidly assessing landscape change. This is part of a natural cycle in some places and is the result of fire or infrastructure disturbance in others. However, there are also some hot spots of thaw at our field sites and identifiable from remote sensing that are likely the result of changing climate in the region. Areas of recent large scale thawing and degradation in ice rich permafrost are evident on the Tanana Flats Training Area, on the Yukon Training Area, above the Permafrost Tunnel, and at the Creamer's Field site. None of these sites have been disturbed by fire or infrastructure. Further focus this upcoming year will be on identifying how/where these ecosystem changes may lead to changing habitat use or affect infrastructure. Since the Army has started airborne LiDAR acquisitions over their lands the repeat imagery analysis process we used provides utility in rapidly identifying places of high likelihood of thermokarst development or landscape change.
3) At all of our field sites, permafrost temperatures have increased over the past 10 years with a more abrupt increase in the past three to five years. At most of our sites we have identified the formation of a variety of thermokarst features. At sites disturbed by wildfire or infrastructure thermokarst development and top-down thaw are greater than at non-disturbed locations.
4) Fens on Tanana Flats are expanding laterally due to permafrost thaw. These fens are projected to triple in extent to cover 11% of the military lands. As the fens maintain groundwater movement throughout the winter and provide a barrier to travel in the summer, this expanding ecotype has the potential to affect the training mission and infrastructure in lowland areas. Expanding fens will be an issue for expanding airboat use, hunter access, and wildlife disturbance. The fens provide important moose and waterfowl habitat and are probably very important for wood frog habitat, a species of concern.
5) Our first Normalized Difference Vegetation Index (NDVI) change detection analysis (for the western portion of Tanana Flats) shows a moderate increase in vegetation density on the north slopes of the Alaska Range (Figure 30). This may be due an increase in top-down thaw of permafrost allowing for more vibrant rooting and, in some areas, surface drying. However, we have few ground-based measurements of vegetation and soil characteristics over time in that area due to its' remoteness. Of particular note is that the southern portion of Tanana Flats has experienced a small to moderate increase in NDVI

over the time of record. This is an area with ice-rich permafrost that has been identified for expanded infrastructure including 40 km of potential all season road access and expanded Air Force targeting facilities.

6) Where resources are available, we will look further into how this changing vegetation regime may affect habitats in these areas.
7) The first application of the Integrated Ecosystem Model to our areas of interest showed that areas where wetlands are expanding are in high ice content permafrost (Figure 31). This is what we expected because high ice content permafrost is most vulnerable to climatic or ecosystem changes. However, we also found increasing wetland areas in parts of the eastern portion of Donnelly Training Area West that we did not expect to have high ice content permafrost. This is an area of proposed expansion of training activities and the potential high ice content permafrost will provide a challenge to infrastructure siting and design. We can use recently acquired satellite imagery and the large geospatial database of point based ground measurements to refine this model result (if needed) or verify it (where possible).
8) The first runs of the Alaska Thermokarst Model show promise in applying the model parameters in Interior Alaska. The comparison between modeled and observed rates of permafrost plateau loss shows strong statistically significant correlation (Figure 40).
9) Based on our current Alaska Thermokarst Model outputs (Figures 53-54) there is a wide discrepancy in future wetland areal extent which is driven by uncertainties in future greenhouse gas atmospheric concentration scenarios (i.e. Representative Concentration Pathways). The ecotype and habitat projections rely on assessment of wetland characteristics so this uncertainty in future scenario planning (i.e. keyed to emissions inventories) provides a stark reminder that a warming climate will be felt strongest in high latitudes.
10) Our land cover change model output (Figures 53 and 54) shows that paludification and thermokarst are the largest projected drivers of landscape (and thus habitat) change. Habitat modeling identified relationships with these ecotypes to develop future habitat use projections (14 and 15 below).
11) Historical rates of ecosystem change from time series analyses and ecotype projections show that 68% of the landscape exhibited ecotype changes over a 68-yr interval, with cumulative changes of 49.6%, 52.4%, and 25.0%, respectively, during the 1949-1978, 1978-2007, and 2007-2017 time intervals. Most of the changes resulted from increases in upland and lowland forest types, with an accompanying decrease in upland and lowland scrub types as post-fire succession led to late-successional stages. There also were smaller losses of forest ecotypes to river erosion, and increases in riverine scrub with accompanying decreases in riverine gravelly barrens. Fire was by far the largest driver of landscape change, affecting 47.3% of the region overall from 1949 to 2017. Thermokarst was notable in that affected areas have nearly doubled from 3.7% area in 1949 to 6.0% in 2017.
12) Fire will continue to be a huge challenge for land managers. Our research indicates that lowland forest (dominated by fire prone black spruce and ericaceous shrubs) has the highest fire cycle, but also that upland broadleaf forest are also quite fire-prone. The landscape change analysis found that 49% of the military lands had burned shortly before 1949, leaving a legacy of mid- and late-successional forest by the end of the 2000s that

have set the stage for more frequent fires. The expansion of thermokarst-related ecotypes will slowly reduce fire-prone ecotypes over the next century.

13) Permafrost degradation and thermokarst will become an increasingly more difficult issue for land managers over the next century. Ice-rich permafrost is extensive in lowland terrain on all of the training areas. This will be of large concern for infrastructure stability. Because of climate warming, there will be limited ability to stabilize permafrost and prevent infrastructure damage on ice-rich terrain. Future construction of roads, pads, trails, powerlines, and buildings must take into account the projected marked increase in climate warming and landscape instability. Of particular concern is the zone of extremely ice-rich Pleistocene silt along Transmitter Road in the heavily used Yukon Training Area. If fully thawed, the ground can collapse 5-10 m due to large syngenetic ice wedges. Expansion of facilities on this terrain should be avoided to the extent possible. In addition, permafrost degradation will open up new subterrain pathways for water movement that will be of concern for groundwater movement and the potential migration of contaminants.
14) Our studies did not identify any specific ecotypes/habitats that are projected to be substantially gained or severely diminished by climate change during the next century. Ecotypes on the Interior Alaska military lands are diverse and highly patchily distributed. They have been affected by a wide range of disturbance drivers, predominantly wildfire, for the past hundred years and this will continue. The disturbance and recovery of this patchy mosaic of differing ages creates a fairly stable composition of heterogeneous ecotypes across the entire area. However, there will be substantial increases in some ecotypes, such a Lowland Fen and Bog meadows, which will mostly be at the expense of diminishing Lowland Wet Needleleaf Forest and Scrub, both of which are currently abundant and not of a near future conservation concern. While drainage of Lacustrine Deep and Shallow lakes are a high conservation concern, the loss will be somewhat offset by development of new lakes from thermokarst. The highest potential risk to species using these habitats would be if migration corridors disappear or if certain important ecotypes are relegated to specific locations that limit usage/expansion by some species due to lack of access.
15) Across the Interior Alaska training range domain we compiled habitat (ecotype) use information on 193 species. This included 1 amphibian, 151 birds, and 41 mammals present across 61 ecotypes. The species of concern for land management that might lose the most habitat over the coming century, particularly under climate model RCP 6.0 projections, include wood frogs, woodland birds (e.g., yellow warbler, northern waterthrush), porcupine, caribou, and marten. Birds and mammals that we expect to gain habitats are associated with lowland bogs, fens, wet meadows, scrub, and post-fire recovery of open, short-vegetation types. Among habitat specialists, potential habitat-losers, to varying degrees, include wood frog, rusty blackbird, caribou, pica, and others. Although by 2100 we project substantial declines compared to historic (1949-2017) habitat availability (e.g., > 25%) for some bird species, overall, few wildlife species are projected to suffer major habitat loss over the coming century.

REFERENCES CITED

Anderson, B. A., R. J. Ritchie, B. E. Lawhead, J. R. Rose, A. M. Wildman, and S. F. Schlentner. 2000. Wildlife studies at Fort Wainwright and Fort Greely, Central Alaska, 1998. Final Report Prepared for U.S. Army Cold Regions Research and Engineering Laboratory, and United States Army Alaska. Fairbanks, Alaska. 105 pp.

Arendt, A. A., K. A. Echelmyer, W. D. Harrison, C. S. Lingle and V. B. Valentince. 2002. Rapid wastage of Alaska glaciers and their contribution to rising sea level. Science 297 382-386.

Balkenhol, N., M. K. Schwartz, R. M. Inman, J. P. Copeland, J. S. Squires, N. J. Anderson, and L. P. Waits. 2020. Landscape genetics of wolverines (Gulo gulo): Scale-dependent effects of bioclimatic, topographic, and anthropogenic variables. Journal of Mammalogy 101(3):790-803.

Barber, J. R., C. L. Burdett, S. E. Reed, K. A. Warner, C. Formichella, K. R. Crooks, D. M. Theobald, and K. M. Fristrup. 2011. Anthropogenic noise exposure in protected natural areas: estimating the scale of ecological consequences. Landscape Ecology 26(9):1281-1295.

Barber, Q. E., M.-A. Parisien, E. Whitman, D. Stralberg, C. J. Johnson, M.-H. St-Laurent, E. R. DeLancey, D. T. Price, D. Arseneault, X. Wang, and M. D. Flannigan. 2018. Potential impacts of climate change on the habitat of boreal woodland caribou. Ecosphere 9(10):e02472.

Barrett, K., A. D. McGuire, E. E. Hoy and E. Kasischke. 2011. Potential shifts in dominant forest cover in interior Alaska driven by variations in fire severity. Ecological Applications 21 (7): 2380–2396.

Berg, E. E., J. D. Henry, C. L. Fastie, A. D. De Volder and S. M. Matsuoka. 2006. Spruce beetle outbreaks on the Kenai Peninsula, Alaska, and Kluane National Park and Reserve, Yukon Territory: Relationships to summer temperatures and regional differences in disturbance regimes. Forest Ecology and Management 227: 219-232.

Boike, J., Roth, K., and Overduin, P. P.. 1998. Thermal and hydrologic dynamics of the active layer at a continuous permafrost site (Taymyr Peninsula, Siberia), Water Resourc. Res., 34(3), 355-63.

Boyd, M. A., L. T. Berner, P. Doak, S. J. Goetz, B. M. Rogers, D. Wagner, X. J. Walker, and M. C. Mack. 2019. Impacts of climate and insect herbivory on productivity and physiology of trembling aspen (Populus tremuloides) in Alaskan boreal forests. Environmental Research Letters 14(8):085010. DOI: 10.1088/1748-9326/ab215f.

Bradfer-Lawrence, T., N. Bunnefeld, N. Gardner, S. G. Willis, and D. H. Dent. 2020. Rapid assessment of avian species richness and abundance using acoustic indices. Ecological Indicators 115:art. no. 106400.

Brooker, S. A., P. A. Stephens, M. J. Whittingham, and S. G. Willis. 2020. Automated detection and classification of birdsong: An ensemble approach. Ecological Indicators 117:art. no. 106609.

Brown, C. L., A. R. Hardy, J. R. Berber, K. M. Fristrup, K. R. Crooks, and L. M. Angeloni. 2012. The effect of human activities and their associated noise on ungulate behavior. PLoS ONE 7(7):doi.org/10.1371/journal.pone.0040505.

Brown, D. R. N., Jorgenson, M. T., Douglas, T. A., Romanovsky, V., Kielland, K., and Euskirchen, E. 2015. Vulnerability of permafrost to fire-initiated thaw in lowland forests of the Tanana Flats, interior Alaska, J. Geophys. Res. Biogeosci., doi: 10.1002/2015JG003033,.

Brown, D. R., T. J. Brinkman, W. R. Bolton, C. L. Brown, H. S. Cold, T. N. Hollingsworth and D. L. Verbyla. 2020. Implications of climate variability and changing seasonal hydrology for subarctic riverbank erosion. Climatic Change 162:1-20.
Chapin III, F. S., M. W. Oswood, K. Van Cleve, L. A. Viereck and D. L. Verbyla. 2006. Alaska's Changing Boreal Forest. Oxford University Press, New York. 354 p.
Chasmer, L. and Hopkinson, C.: Threshold loss of discontinuous permafrost and landscape evolution, Glob. Change Biol., 23, 2672-2686, doi:10.1111/gcb.13537, 2017.
Chester, S. 2016. The Arctic guide. Wildlife of the far north. Princeton University Press, Princeton, New Jersey. 542 pp.
Circumpolar Active Layer Monitoring Network, www2.gwu.edu/~calm/data/north.htm, 2020.
Creel, S., J. E. Fox, A. Hardy, J. Sands, B. Garrott, and R. O. Peterson. 2002. Snowmobile activity and glucocorticoid stress responses in wolves and elk. Conservation Biology 14(3):809-814.
Dooling, R. J., and A. N. Popper. 2007. The effects of highway noise on birds. The California Department of Transportation, Division of Environmental Analysis. Sacramento CA. 74 pp.
DeGange, A. R., B. G. Marcot, J. Lawler, T. Jorgenson, and R. Winfree. 2014. Predicting the effects of climate change on ecosystems and wildlife habitat in northwest Alaska: results of the WildCast project. Alaska Park Science 12(2):66-73.
DeWilde, L. and F. S. Chapin. 2006. Human Impacts on the Fire Regime of Interior Alaska: Interactions among Fuels, Ignition Sources, and Fire Suppression. Ecosystems 9: 1342–1353.
Douglas, T. A., Jorgenson, M. T., Kanevskiy, M. Z., Romanovsky, V. E., Shur, Y., and Yoshikawa, K.: Permafrost dynamics at the Fairbanks Permafrost Experimental Station near Fairbanks, Alaska, Proceedings of the Ninth International Conference on Permafrost, D. Kane, and K. Hinkel, eds. pp. 373, 2008.
Douglas, T. A., Fortier, D., Shur, Y. I., Kanevskiy, M. Z., Guo, L., Cai, Y., and Bray, M.: Biogeochemical and geocryological characteristics of wedge and thermokarst-cave ice in the CRREL Permafrost Tunnel, Alaska, Permafrost Periglac. Process., doi: 10.1002/ppp.709, 2011.
Douglas, T.A., M.C. Jones, C.A. Hiemstra, J.R. Arnold. 2014. Sources and sinks of carbon in boreal ecosystems of interior Alaska: A review. Elementa: Science of the Anthropocene, 2(1), p.000032.
Douglas, T. A., Jorgenson, M. T., Brown, D. R. N., Campbell, S. W., Hiemstra, C. A., Saari, S. P., Bjella, K., and Liljedahl, A. K.: Degrading permafrost mapped with electrical resistivity tomography, airborne imagery and LiDAR, and seasonal thaw measurements, Geophysics, 81, WA71–WA85, https://doi.org/10.1190/GEO2015-0149.1, 2016.
Douglas, T.A., and Mellon, M.T. 2019. Sublimation of terrestrial permafrost and the implications for ice-loss landforms on Mars. Nature Communications 10(1):1716. Doi: 10.1038/s41467-019-09410-8.
Douglas, T. A., M. R. Turetsky and C. D. Koven. 2020. Increased rainfall stimulates permafrost thaw across a variety of Interior Alaskan boreal ecosystems. Nature Climate and Atmospheric Change 3:28.
Douglas, T.A., Hiemstra, C.A. Anderson, J.E., Barbato, R.A., Bjela, K.L., Deeb, E.J., Gelvin, A.B., Newman, S.D., Saari, S.P., Wagner, A.M. (2021) Recent degradation of Interior Alaska permafrost mapped with geophysics, airborne LiDAR, ground surveys, and drilling. The Cryosphere Discussions.1-39.

Douglas TA, Zhang C. (2021) Machine learning analyses of remote sensing measurements establish strong relationships between vegetation and snow depth in the boreal forest of Interior Alaska. Environmental Research Letters.
Drouin, M., R. Bradley, L. Lapointe, and J. Whalen. 2014. Non-native anecic earthworms (Lumbricus terrestris L.) reduce seed germination and seedling survival of temperate and boreal trees species. Applied Soil Ecology 75:145-149.
Dumyahn, S. L., and B. C. Pijanowski. 2011. Beyond noise mitigation: managing soundscapes as common-pool resources. Landscape Ecology 26(9):1311-1326.
Duncan, R. J., M. E. Andrew, and M. C. Forchhammer. 2021. Snow mediates climatic impacts on Arctic herbivore populations. Polar Biology 44:1251-1271.
Durden, L. A., K. B. Beckmen, and R. F. Gerlach. 2016. New records of ticks (Acari: Ixodidae) from dogs, cats, humans, and some wild vertebrates in Alaska: invasion potential. Journal of Medical Entomology 53(6):1391-1395.
Edmonds, S. T., D. C. Evers, D. A. Cristol, C. Mettke-Hofmann, L. L. Powell, A. J. McGann, J. W. Armiger, O. P. Lane, D. F. Tessler, P. Newell, K. Heyden, and N. J. O'Driscoll. 2010. Geographic and seasonal variation in mercury exposure of the declining Rusty Blackbird. Condor 112(4):789-799.
Eidenshink J, Schwind B, Brewer K, Zhu ZL, Quayle B, Howard S. A project for monitoring trends in burn severity. Fire ecology. 2007 Jun;3(1):3-21.
Elbroch, M., and C. McFarland. 2019. Mammal tracks & sign. a guide to North American species. Stackpole Books, Mechanicsburg, PA. 680 pp.
Euskirchen ES, McGuire AD, Chapin III FS, Yi S, Thompson CC. Changes in vegetation in northern Alaska under scenarios of climate change, 2003–2100: implications for climate feedbacks. Ecological applications. 2009 Jun;19(4):1022-43.
Fall, J. A. 2016. Regional patterns of fish and wildlife harvests in contemporary Alaska. Arctic 69(1):47-64.
Francis, C. D., and J. R. Barber. 2013. A framework for understanding noise impacts on wildlife: an urgent conservation priority. Frontiers in Ecology and the Environment 11(6):305-313.
Francis, C. D., P. Newman, B. D. Taff, C. White, C. A. Monz, M. Levenhagen, A. R. Petrelli, L. C. Abbott, J. Newton, S. Burson, C. B. Cooper, K. M. Fristrup, C. J. W. McClure, D. Mennitt, M. Giamellaro, and J. R. Barber. 2017. Acoustic environments matter: Synergistic benefits to humans and ecological communities. Journal of Environmental Management 203:245-254.
Frelich, L. E., B. Blossey, E. K. Cameron, A. Dávalos, N. Eisenhauer, T. Fahey, O. Ferlian, P. M. Groffman, E. Larson, S. R. Loss, J. C. Maerz, V. Nuzzo, K. Yoo, and P. B. Reich. 2019. Side-swiped: ecological cascades emanating from earthworm invasions. Frontiers in Ecology and the Environment 17(9):502-510.
Fresco, N. 2019. Interactions among drivers in the Northwest Boreal Region. In Drivers of Landscape Change in the Northwest Boreal Region. S. e. al., eds. University of Alaska Press: 159-165.
Gende, S. M., T. P. Quinn, and M. F. Willson. 2001. Consumption choice by bears feeding on salmon. Oecologia 128(1):372-382.
Genet, H., A. D. McGuire, K. Barrett, A. Breen, E. S. Euskirchen, J. F. Johnstone, E. S. Kasischke, A. M. Melvin, A. Bennett, M. C. Mack and T. S. Rupp. 2013. Modeling the effects of fire severity and climate warming on active layer thickness and soil carbon storage

of black spruce forests across the landscape in interior Alaska. Environmental Research Letters 8(4): 045016.
Genet H., McGuire A.D.M., Romanovsky V., Bolton W., Lara M., Zhang Y. 2014. Alaska Thermokarst Predisposition Model. Scenario Network for Alaska Planning, Fairbanks, Alaska, USA. http://ckan.snap.uaf.edu/dataset/thermokarst-formation
Gómez, W. E., C. V. Isaza, and J. M. Daza. 2018. Identifying disturbed habitats: A new method from acoustic indices. Ecological Informatics 45:16-25.
Greuel, R. J., G. E. Degré-Timmons, J. L. Baltzer, J. F. Johnstone, E. J. B. McIntire, N. J. Day, S. J. Hart, P. D. McLoughlin, F. K. A. Schmiegelow, M. R. Turetsky, A. Truchon-Savard, M. D. van Telgen, and S. G. Cumming. 2021. Predicting patterns of terrestrial lichen biomass recovery following boreal wildfires. Ecosphere 12(4):e03481.
Grosse, G., V. Romanovsky, T. Jorgenson, K. W. Anthony and J. Brown. 2011. Vulnerability and feedbacks of permafrost to climate change. Eos Trans. AGU 92 (9): 73-80.
Gustine DD, Brinkman TJ, Lindgren MA, Schmidt JI, Rupp TS, Adams LG. Climate-driven effects of fire on winter habitat for caribou in the Alaskan-Yukon Arctic. PloS one. 2014 Jul 3;9(7):e100588.
Halfpenny, J. 2019a. Scats and tracks of Alaska including the Yukon and British Columbia: a field guide to the signs of sixty-nine wildlife species. Second edition. Falcon Guides, Helena, MT. 184 pp.
Halfpenny, J. 2019b. Scats and tracks of North America: a field guide to the signs of nearly 150 wildlife species. Falcon Guides, Helena, MT. 344 pp.
Handel, C. M., and J. R. Sauer. 2017. Combined analysis of roadside and off-road Breeding Bird Survey data to assess population change in Alaska. Condor 119(3):557-575.
Helfield, J. M., and R. J. Naiman. 2002. Salmon and alder as nitrogen sources to riparian forests in a boreal Alaskan watershed. Oecologia 133(4):573-582.
Hinkel, K. M. and Nelson, F. E.: Spatial and temporal patterns of active layer thickness at Circumpolar Active Layer Monitoring (CALM) sites in northern Alaska, 1995–2000, J. Geophys. Res., 108, 8168, https://doi.org/10.1029/2001JD000927, 2003.
Holmes, C. E. 2001. Tanana River valley archaeology circa 14,000 to 9000 B.P. Arctic Anthropology 38(2):154-170.
Homer C, Dewitz J, Fry J, Coan M, Hossain N, et al. 2007. Completion of the 2001 National Land Cover Database for the Counterminous United States. Photogramm Eng Rem S 73(4): 337.
Hope, A. G., E. Waltari, N. R. Morse, J. A. Cook, M. J. Flamme, and S. L. Talbot. 2017. Small mammals as indicators of climate, biodiversity, and ecosystem change. Alaska Park Science 16(1):70-76.
Hubbard, S. S., Gangodagamage, C., Dafflon, B., Wainwright, H., Peterson, J., Gusmeroli, A., Ulrich, C., Wu, Y., Wilson, C., Rowland, J., Tweedie, C., and Wullscheleger, S. D.: Quantifying and relating land-surface and subsurface variability in permafrost environments using LiDAR and surface geophysical datasets, Hydrogeol. J., 21, 1, 149-169, 2013.
IPCC. 2014. Climate Change 2014: Synthesis Report, Geneva, Switzerland. Contribution of Working Groups I, II and III to the Fifth Assessment Report of the Intergovernmental Panel on Climate Change. 151 pgs.
Jafarov, E. E., Romanovsky, V. E, Genet, H., McGuire, A. D., Marchenko, S. S.: The effects of fire on the thermal stability of permafrost in lowland and upland black spruce forests of interior Alaska in a changing climate, Environ. Res. Lett., 8,3, 035030, 2013.

James, P. M. A., M.-J. Fortin, B. R. Sturtevant, A. Fall, and D. Kneeshaw. 2011. Modelling spatial interactions among fire, spruce budworm, and logging in the boreal forest. Ecosystems 14(1):60-75.
Jafarov, E. E., V. E. Romanovsky, H. Genet, A. D. McGuire and S. S. Marchenko. 2013. The effects of fire on the thermal stability of permafrost in lowland and upland black spruce forests of interior Alaska in a changing climate. Environ. Res. Lett. 8 (035030): 11 pp.
Joly, K., R. R. Jandt and D. R. Klein. 2009 Decrease of lichens in Arctic ecosystems: the role of wildfire, caribou, reindeer, competition and climate in north-western Alaska. Polar Research 28 433–442.
Johnson, D., and T. O'Neill, ed. 2001. Wildlife-habitat relationships in Oregon and Washington. Oregon State University Press, Corvallis OR.
Johnstone, J. F., Chapin, F. S., Hollingsworth, T. N., Mack, M. C., Romanovsky, V., Turetsky, M.: Fire, climate change, and forest resilience in interior Alaska, Canadian J. For. Res., 40,7, 1302-12, 2010.
Johnstone JF, Rupp TS, Olson M, Verbyla D. Modeling impacts of fire severity on successional trajectories and future fire behavior in Alaskan boreal forests. Landscape Ecology. 2011 Apr;26(4):487-500.
Johnstone, J. F., X. Walker and T. N. Hollingsworth. 2019. Wildfire in the Northwest Boreal Region. In Drivers of Landscape Change in the Northwest Boreal Region. A. L. Sesser and A. P. Rockhill, eds. University of Alaska Press: pp. 15-19.
Joly, K., R. R. Jandt, and D. R. Klein. 2009. Decrease of lichens in Arctic ecosystems: the role of wildfire, caribou, reindeer, competition and climate in north-western Alaska. Polar Research 28:433-442.
Jones, B. M., G. Grosse, A. C. D., M. C. Jones, K. M. Walter Anthony, and others. 2011. Modern thermokarst lake dynamics in the continuous permafrost zone, northern Seward Peninsula, Alaska. Journal of Geophysical Research - Biogeosciences 116 G00M03.
Jones, B. M., Stoker, J. M., Gibbs, A. E., Grosse, G., Romanovsky, V. E., Douglas, T. A., Kinsman, N. E. M., and Richmond, B. M.: Quantifying landscape change in an arctic coastal lowland using repeat airborne LiDAR, Environ. Res. Lett., 8, 045025, doi:10.1088/1748-9326/8/4/045025, 2013.
Jorgenson, M. T., J. E. Roth, M. Raynolds, M. D. Smith, W. Lentz, and others. 1999. An ecological land survey for Fort Wainwright, Alaska. U.S. Army Cold Regions Research and Engineering Laboratory, Hanover, NH. CRREL Report 99-9, 83 p.
Jorgenson, M. T., J. E. Roth, B. A. Anderson, M. D. Smith, B. E. Lawhead, and others. 2000. An ecological land evaluation for the Yukon Training Area on Fort Wainwright: permafrost, disturbance, and habitat use. Final Report for U.S. Army Alaska, Anchorage, AK by ABR, Inc., Fairbanks, AK 88 p.
Jorgenson, M. T., C. H. Racine, J. C. Walters and T. E. Osterkamp. 2001a. Permafrost degradation and ecological changes associated with a warming climate in central Alaska. Climatic Change 48(4): 551-579.
Jorgenson, M. T., J. E. Roth, M. D. Smith, S. Schlentner, W. Lentz, and others. 2001b. An ecological land survey for Fort Greely, Alaska. U.S. Army Cold Regions Research and Engineering Laboratory, Hanover, NH. ERDC/CRREL TR-01-04., 85 p.
Jorgenson, M. T. and T. E. Osterkamp. 2005. Response of boreal ecosystems to varying modes of permafrost degradation. Canadian Journal of Forest Research 35 2100-2111.

Jorgenson, M. T., Y. L. Shur and E. R. Pullman. 2006. Abrupt increase in permafrost degradation in Arctic Alaska. Geophysical Research Letters 33: L02503.
Jorgenson, M. T., Y. L. Shur and T. E. Osterkamp. 2008. Thermokarst in Alaska. In D. L. Kane and K. M. Hinkel, eds., Proceedings Ninth International Conference on Permafrost. Institute of Northern Engineering, University of Alaska, Fairbanks, AK. pp. 869-876.
Jorgenson, M. T., Yoshikawa, K., Kanevskiy, M., Shur, Y., Romanovsky V, Marchenko S, Grosse G, Brown J, Jones B.: Permafrost characteristics of Alaska, Proceedings of the Ninth International Conference on Permafrost, edited by D. Kane, and K. Hinkel, Vol. 29, p. 121-122, 2008.
Jorgenson, M. T., J. E. Roth, P. F. Miller, M. J. Macander, M. S. Duffy, A. F. Wells, G. V. Frost and E. R. Pullman. 2009. An Ecological Land Survey and Landcover Map of the Arctic Network. National Park Service, Ft Collins, CO. Natural Resources Technical Report NPS/ARCN/NRTR—2009/270. 307 pgs.
Jorgenson, M. T., V. Romanovsky, J. Harden, Y. Shur, J. O'Donnell, E. A. G. Schuur, M. Kanevskiy and S. Marchenko. 2010. Resilience and vulnerability of permafrost to climate change. Canadian Journal of Forest Research 40: 1219-1236.
Jorgenson, M. T., M. Kanevskiy, Y. Shur, T. Osterkamp, D. Fortier, and others. 2012. Thermokarst Lake and Shore Fen Development in Boreal Alaska. Salekhard, Russia. Vol. 1, 179-184 p.
Jorgenson, M. T., J. Harden , M. Kanevskiy, J. O'Donnell, K. Wickland, and others. 2013. Reorganization of vegetation, hydrology and soil carbon after permafrost degradation across heterogeneous boreal landscapes. Environmental Research Letters 8 (035017): 13.
Jorgenson, M. T., B. G. Marcot, D. K. Swanson, J. C. Jorgenson, and A. R. DeGange. 2015a. Projected changes in diverse ecosystems from climate warming and biophysical drivers in northwest Alaska. Climatic Change 130(2):131-144.
Jorgenson, M T., M. Kanevskiy, Y. Shur, J. Grunblatt, C.L. Ping, and others. 2015b. Permafrost database development, characterization, and mapping for northern Alaska. Report for Arctic Landscape Conservation Cooperative by Alaska Ecoscience and University of Alaska Fairbanks. 46 p. http://www.gina.alaska.edu/projects/permafrost-database-and-maps-for-northern-alaska, 46 p.
Jorgenson, M. T., T. A. Douglas, A. K. Liljedahl, J. E. Roth, T. C. Cater, W. A. Davis, G. V. Frost, P. F. Miller and C. H. Racine. 2020. The roles of climate extremes, ecological succession, and hydrology in repeated permafrost aggradation and degradation in fens on the Tanana Flats, Alaska. JGR Biogeosciences JGRG21762.
Kasischke, E. S. and Johnstone, J. F.: Variation in postfire organic layer thickness in a black spruce forest complex in interior Alaska and its effects on soil temperature and moisture, Can. J. For. Res., 35, 9, 2164-77, 2005.
Kasischke, E. S., D. L. Verbyla, T. S. Rupp, A. D. McGuire, K. A. Murphy, and others. 2010. Alaska's changing fire regime — implications for the vulnerability of its boreal forests. Can. J. For. Res. 40 1313–1324.
Knight, E. C., K. C. Hannah, G. J. Foley, C. D. Scott, R. M. Brigham, and E. Bayne. 2017. Recommendations for acoustic recognizer performance assessment with application to five common automated signal recognition programs. Avian Conservation and Ecology 12(2):14. https://doi.org/10.5751/ACE-01114-120214.
Kokelj, S. V. and Jorgenson, M. T.: Advances in Thermokarst Research, Permafrost Periglac. Process., 24, 108–119, 2013.

Kolstad, A. L., G. Austrheim, E. J. Solberg, L. De Vriendt, and J. D. M. Speed. 2018. Pervasive moose browsing in boreal forests alters successional trajectories by severely suppressing keystone species. Ecosphere 9(10):e02458.
Kreig, R. A. and R. D. Reger. 1982. Air-photo analysis and summary of landform soil properties along the route of the Trans-Alaska Pipeline System. Alaska Div. of Geological and Geophysical Surveys, Fairbanks, AK. Geologic Report 66. 149 p.
Kropp, H., and 48 others Vegetation stature controls air-soil temperature coupling across pan-Arctic ecosystems, Environ. Res. Lett. Doi: 10.1088/1748-9326/abc994, 2020.
Kunc, H. P., and R. Schmidt. 2019. The effects of anthropogenic noise on animals: a meta-analysis. Biology Letters 15(11):https://doi.org/10.1098/rsbl.2019.0649.
Lafferty, D. J. R., Z. G. Loman, K. S. White, A. T. Morzillo, and J. L. Belant. 2016. Moose (Alces alces) hunters subsidize the scavenger community in Alaska. Polar Biology 39(4):639-647.
Lara, M.J., Genet, H., McGuire, A.D., Euskirchen, E.S., Zhang, Y., Brown, D.R.N., Jorgenson, M.T., Romanovsky, V., Breen, A., Bolton, W.R., 2016. Thermokarst rates intensify due to climate change and forest fragmentation in an Alaskan boreal forest lowland. Glob Change Biol 22, 816–829. doi:10.1111/gcb.13124
Lewkowicz, A. G., Etzelmüller, B., and Smith, S.L.: Characteristics of discontinuous permafrost based on ground temperature measurements and electrical resistivity tomography, southern Yukon, Canada, Permafrost Periglac. Process., 22, 4, 320-342, 2011.
Lewkowicz, A. G., Way, R. G.: Extremes of summer climate trigger thousands of thermokarst landslides in a High Arctic environment, Nature Comm., 10, 1, 2019.
Liston, G. E., Hiemstra, C.A.: The changing cryosphere: Pan-Arctic snow trends (1979–2009). J. Climate, 1;24(21), 5691-712, 2011.
Loranty, M. M. and 18 others: Changing ecosystem influences on soil thermal regimes in northern high-latitude permafrost regions. Biogeosci., doi: 10.5194/bg-15-5287-2018, 2018.
Macander, M. J., E. C. Palm, G. V. Frost, J. D. Herriges, P. R. Nelson, C. Roland, K. L. M. Russell, M. J. Suitor, T. W. Bentzen, K. Joly, S. J. Goetz, and M. Hebblewhite. 2020. Lichen cover mapping for caribou ranges in interior Alaska and Yukon. Environmental Research Letters 15(5):055001.
MacDonald, S. O., and J. A. Cook. 2009. Recent mammals of Alaska. University of Alaska Press, Fairbanks, Alaska. 300 pp.
Manies KL, Harden JW, Hollingsworth TN. Soils, Vegetation, and Woody Debris Data from the 2001 Survey Line Fire and a Comparable Unburned Site, Tanana Flats Region, Alaska. US Department of the Interior, US Geological Survey; 2014.
Marcot, B. G., and M. Vander Heyden. 2001. Key ecological functions of wildlife species. Pp. 168-186 in: D. H. Johnson and T. A. O'Neill, editors. Wildlife-habitat relationships in Oregon and Washington. Oregon State University Press, Corvallis OR.
Marcot, B. G., M. A. Castellano, J. A. Christy, L. K. Croft, J. F. Lehmkuhl, R. H. Naney, K. Nelson, C. G. Niwa, R. E. Rosentreter, R. E. Sandquist, B. C. Wales, and E. Zieroth. 1997. Terrestrial ecology assessment. Pp. 1497-1713 in: T. M. Quigley and S. J. Arbelbide, editors. An assessment of ecosystem components in the interior Columbia Basin and portions of the Klamath and Great Basins. Volume III. USDA Forest Service General Technical Report PNW-GTR-405. USDA Forest Service Pacific Northwest Research Station, Portland, OR. 1713 pp.

Marcot, B. G., and M. Vander Heyden. 2001. Key ecological functions of wildlife species. Pp. 168-186 in: D. H. Johnson and T. A. O'Neil, Technical Coordinators. Wildlife-habitat relationships in Oregon and Washington. Oregon State University Press, Corvallis, Oregon.
Marcot, B. G., and K. B. Aubry. 2003. The functional diversity of mammals in coniferous forests of western North America. Pp. 631-664 in: C. J. Zabel and R. G. Anthony, eds. Mammal community dynamics: management and conservation in the coniferous forests of western North America. Cambridge University Press, Cambridge UK. 709 pp.
Marcot, B. G., M. T. Jorgenson, and A. R. DeGange (2014) Low-altitude photographic transects of the Arctic Network of national park units and Selawik National Wildlife Refuge, Alaska, July 2013. USGS Data Series 846. http://dx.doi.org/10.3133/ds846. Anchorage, AK. 44 pp.
Marcot, B. G., M. T. Jorgenson, and A. R. DeGange. 2014. Low-altitude photographic transects of the Arctic Network of national park units and Selawik National Wildlife Refuge, Alaska, July 2013. USGS Data Series 846. http://dx.doi.org/10.3133/ds846. Anchorage, AK. 44 pp.
Marcot, B. G., M. T. Jorgenson, J. Lawler, C. M. Handel, and A. R. DeGange. 2015. Projected changes in wildlife habitats in Arctic natural areas of northwest Alaska. Climatic Change 130(2):145-154.
Mason, J. T., C. J. W. McClure, and J. R. Barber. 2016. Anthropogenic noise impairs owl hunting behavior. Biological Conservation 199:29-32.
Martin, E., and K. Jochum. 2017. Fauna planning level surveys of shorebirds in Tanana Flats Training Area, Fort Wainwright, Alaska. Final Report Scope of Work 14-25. Center for Environmental Management of Military Lands, Colorado State University. 36 pp.
Martin, P. D., J. L. Jenkins, F. J. Adams, M. T. Jorgenson, A. C. Matz, and others. 2009. Wildlife responses to environmental Arctic change. U.S. Fish and Wildlife Service, Fairbanks, AK. 138 p.
Minsley, B., Wellman, T. P., Walvoord, M. A., Revil, A.: Sensitivity of airborne geophysical data to sublacustrine and near-surface permafrost thaw, The Cryosphere 9(2), 781-94, 2015.
Moore, R. D., S. W. Fleming, B. Menounos, R. Wheate, A. Fountain, and others. 2009. Glacier change in western North America: influences on hydrology, geomorphic hazards and water quality. Hydrol. Process. 23 42–61.
Murie, O. J., M. Elbroch, and R. T. Peterson. 2005. Peterson field guide to animal tracks. Third edition. Houghton Mifflin Harcourt, Boston MA. 432 pp.
Myers-Smith, I., Harden, J., Wilmking, M., Fuller, C., McGuire, A, and Chapin, F. S.: Wetland succession in a permafrost collapse: interactions between fire and thermokarst, Biogeosc., 5, 5, 2008.
Myers-Smith, I. H., B. C. Forbes, M. Wilmking, M. Hallinger and T. C. Lantz. 2012. Shrub expansion in tundra ecosystems: Dynamics, impacts and research priorities. Environmental Research Letters 6: 045509.
Nelson, C. J., C. M. Frost, and S. E. Nielsen. 2021. Narrow anthropogenic linear corridors increase the abundance, diversity, and movement of bees in boreal forests. Forest Ecology and Management 489:art. no. 119044.
Nicholas, J. R. and Hinkel, K. M.: Concurrent permafrost aggradation and degradation induced by forest clearing, central Alaska, USA, Arctic, Ant., Alp. Res., 28, 1996.
Nilsson, C., R. Jansson, L. Kuglerová, L. Lind and L. Ström. 2013. Boreal riparian vegetation under climate change. Ecosystems 16 (3): 401-410.

Nitze, I., G. Grosse, B. M. Jones, C. D. Arp, M. Ulrich, A. Fedorov and A. Veremeeva. 2017. Landsat-based trend analysis of lake dynamics across northern permafrost regions. Remote Sensing 9(7): 640.

Nossov, D. R., M. T. Jorgenson, K. Kielland and M. Z. Kanevskiy. 2013. Edaphic and microclimatic controls over permafrost response to fire in interior Alaska. Environ. Res. Lett. 8 035013 (12 p.).

Ntalampiras, S., and I. Potamitis. 2021. Acoustic detection of unknown bird species and individuals. [Early view]. CAAI Transactions on Intelligence Technology 2021:1-10.

Olefeldt, D., S. Goswami, G. Grosse, D.J. Hayes, G. Hugelius, P. Kuhry, B. Sannel, E.A.G. Schuur, and M.R. Turetsky. 2016. Arctic Circumpolar Distribution and Soil Carbon of Thermokarst Landscapes, 2015. ORNL DAAC, Oak Ridge, Tennessee, USA. http://dx.doi.org/10.3334/ORNLDAAC/1332

Osterkamp, T. and Romanovsky, V.: Evidence for warming and thawing of discontinuous permafrost in Alaska, Permafrost Periglac. Process., 10, 1, 17–37, 1999.

Osterkamp T, Jorgenson J. 2006.Warming of permafrost in the Arctic National Wildlife Refuge, Alaska. Permafrost Periglac 17(1): 65–69.

Ostrom, C. 2020. FWA_SDE_40.GDB, Military Ranges and Training, SDSFIE-V 4.0.2 Army Adaptation. USAG Alaska Fort Wainwright IGI&S Program, Fort Wainwright, Alaska. https://atlas.obs.army.mil/portal/home/

Panda, S. K., S. S. Marchenko and V. E. Romanovsky. 2014. High-Resolution Permafrost Modeling in Denali National Park and Preserve National Park Service, Fort Collins, Colorado. NPS/CAKN/NRTR–2014/858. 115 p.

Pastick, N. J., M. T. Jorgenson, B. K. Wylie, S. J. Nield, K. D. Johnson and A. O. Finley. 2015. Distribution of near-surface permafrost in Alaska: estimates of present and future conditions. Remote Sensing of Environment 168: 301–315.

Pijanowski, B. C., A. Farina, S. H. Gage, S. L. Dumyahn, and B. L. Krause. 2011. What is soundscape ecology? An introduction and overview of an emerging new science. Landscape Ecology 26(9):1213-1232.

Potter, C., S. Li and R. Crabtree. 2013. Changes in Alaskan Tundra Ecosystems Estimated from MODIS Greenness Trends, 2000 to 2010. J. Geophys Remote Sensing 2 (107): 6.

Pozzanghera, C. B., K. J. Sivy, M. S. Lindberg, and L. R. Prugh. 2016. Variable effects of snow conditions across boreal mesocarnivore species. Canadian Journal of Zoology 94(10):697-705.

Pureswaran, D. S., L. De Grandpré, D. Paré, A. Taylor, M. Barrette, H. Morin, J. Régnière, and D. Kneeshaw. 2015. Climate-induced changes in host tree–insect phenology may drive ecological state-shift in boreal forests. Ecology 96(6):1480-1491.

Racine, C. H. and Walters, J. C.: Groundwater-discharge fens in the Tanana Lowlands, Interior Alaska, U.S.A., Arctic Alpine Res., 26, 4, 418-426, 1994.

Raich JW, Rastetter EB, Melillo JM, Kicklighter DW, Steudler PA, Peterson BJ, Grace AL, Moore III B, Vorosmarty CJ. Potential net primary productivity in South America: application of a global model. Ecological applications. 1991 Nov;1(4):399-429.

Raynolds, M. K., D. A. Walker, K. J. Ambrosius, J. Brown, K. R. Everett, M. Kanevskiy, G. P. Kofinas, V. E. Romanovsky, Y. Shur and P. J. Webber. 2014. Cumulative geoecological effects of 62 years of infrastructure and climate change in ice-rich permafrost landscapes, Prudhoe Bay Oilfield, Alaska. Global Change Biology 20(4): 1211–1224.

Rey, D. M., Walvoord, M. A., Minsley, B. J., Ebel, B. A., Voss, C. I., and Singha, K.: Wildfire initiated talik development exceeds current thaw projections: Observations and models from Alaska's continuous permafrost zone, Geophys. Rese. Lett., e2020GL087565, 2020.
Roach, J., Griffith, B., Verbyla, D., & Jones, J. 2011. Mechanisms influencing changes in lake area in the Alaskan boreal forest. Global Change Biology, 17(8), 2567–2583. https://doi.org/10.1111/j.1365-2486.2011.02446.x
Roach, J. K., Griffith, B. and Verbyla, D. 2013. Landscape influences on climate-related lake shrinkage at high latitudes. Glob Change Biol, 19: 2276–2284. doi:10.1111/gcb.12196
Riordan, B., D. Verbyla and A. D. McGuire. 2006. Shrinking ponds in subarctic Alaska based on 1950-2002 remotely sensed images. Journal of Geophysical Research 111: G04002.
Ruff, Z. J., D. B. Lesmeister, L. S. Duchac, B. K. Padmaraju, and C. M. Sullivan. 2020. Automated identification of avian vocalizations with deep convolutional neural networks. Remote Sensing in Ecology and Conservation 6(1):79-92.
Rupp TS, Chapin III FS, Starfield AM. Response of subarctic vegetation to transient climatic change on the Seward Peninsula in north-west Alaska. Global Change Biology. 2000 Jun;6(5):541-55.
Sandén, H., M. Mayer, S. Stark, T. Sandén, L. O. Nilsson, J. U. Jepsen, P. R. Wäli, and B. Rewald. 2020. Moth outbreaks reduce decomposition in subarctic forest soils. Ecosystems 23:151-163.
Sandström, J., C. Vernes, K. Junninen, A. Lõhmus, E. Macdonald, J. Müller, and B. G. Jonsson. 2019. Impacts of dead wood manipulation on the biodiversity of temperate and boreal forests. A systematic review. Journal of Applied Ecology 56:1770-1781.
Savory, G. A., V. Anderson, and J. Smith. 2017. Evaluating bat habitat on Fort Wainwright, Alaska. Final Report Scope of Work 14-70. Center for Environmental Management of Military Lands, Colorado State University. 27 pp.
Schmidt, J. H., E. A. Rexstad, C. A. Roland, C. L. Mcintyre, M. C. MacCluskie, and M. J. Flamme. 2018. Weather-driven change in primary productivity explains variation in the amplitude of two herbivore population cycles in a boreal system. Oecologia 186(2):435-446.
Schuster, P. F., K. M. Schaefer, G. R. Aiken, R. C. Antweiler, J. F. Dewild, J. D. Gryziec, A. Gusmoreli, G. Hugelius, E. Jaforov, D. P. Krabbenhoft, L. Liu, N. Herman-Mercer, C. Mu, D. A. Roth, T. Schaefer, R. G. Striegl, K. P. Wickland, and T. Zhang. 2018. Permafrost stores a ViereckShikglobally significant amount of mercury. Geophysical Research Letters 45:1463-1471.
Schuur, E. A. and M. C. Mack. 2018. Ecological response to permafrost thaw and consequences for local and global ecosystem services. Annual Review of Ecology, Evolution, and Systematics 49: 279-301.
Selkowitz DJ, Stehman SV. Thematic accuracy of the National Land Cover Database (NLCD) 2001 land cover for Alaska. Remote Sensing of Environment. 2011 Jun 15;115(6):1401-7.
Shiklomanov, N. I., Streletskiy, D. A., Nelson, F. E., Hollister, R. D., Romanovsky, V. E., Tweedie, C. E., Bockheim, J. G., and Brown, J.: Decadal variations of active-layer thickness in moisturecontrolled landscapes, Barrow Alaska, J. Geophys. Res., 115, G00I04, https://doi.org/10.1029/2009JG001248, 2010.
Shur, Y. L., Hinkel, K. M., and Nelson, F. E.: The transient layer: Implications for geocryology and global-change science, Permafrost Periglac. Process., 16, 5–17, 2005.
Shur, Y. and Jorgenson, M.: Patterns of permafrost formation and degradation in relation to climate and ecosystems, Permafrost Periglac. Process., 18, 1, 7–19, 2007.

Siemens, L. D., A. M. Dennert, D. S. Obrist, and J. D. Reynolds. 2020. Spawning salmon density influences fruit production of salmonberry (Rubus spectabilis). Ecosphere 11(11):e03282.
Smith, L. C., Sheng, Y., MacDonald, G. M., and Hinzman, L 2005. Disappearing Arctic lakes, Science, 308, 1429–1429.
Smith, J., G. Preston, and G. Savory. 2018. Neotropical bird habitat assessment, Fort Wainwright, Alaska. Final Report Scope of Work 15-49. Center for Environmental Management of Military Lands, Colorado State University. 44 pp.
Strauss, J., Schirrmeister, L., Grosse, G., Wetterich, S., Ulrich, M., Herzschuh, U., Hubberten, H. W.: The deep permafrost carbon pool of the Yedoma region in Siberia and Alaska, Geophys. Res. Lett., 40(23), 6165-70, 2013.
Strauss, J., Laboor, S., Fedorov, A. N.: Database of ice-rich Yedoma permafrost (IRYP), PANGAEA, https://doi.org/10.1594/PANGAEA.861733, 2016.
Sturm, M., C. Racine and K. Tape. 2001. Increasing shrub abundance in the Arctic. Nature 411: 546.
Sturm, M., J. Schimel, G. J. Michaelson, J. M. Welker, S. F. Oberbauer, and others. 2005. Winter biological processes could help convert Arctic tundra to shrubland. BioScience 55:17-26.
Suarez, F., D. Binkley, M. W. Kaye and R. Stottlemyer. 1999. Expansion of forest stands into tundra in the Noatak National Preserve, northwest Alaska. Écoscience 6 (3): 465-470.
Trammell, E. J. and M. Aisu. 2015. Development of a landscape integreting dataset for the Alaska Crucial Habitat Assessment Tool. Alaska Center for Conservation Science, Univ. of Alaska Anchorage, Anchorage, AK. 13 pgs.
Tennessen, J. B., S. E. Parks, L. Swierk, L. K. Reinert, W. M. Holden, L. A. Rollins-Smith, K. A. Walsh, and T. Langkilde. 2018. Frogs adapt to physiologically costly anthropogenic noise. Proceedings of the Royal Society B 285(1891):https://doi.org/10.1098/rspb.2018.2194.
Thomas, T. A., M. Sturm, J. D. Blum, C. Polashenski, S. Stuefer, C. Hiemstra, A. Steffen, S. Filhol, and R. Prevost. 2017. A pulse of mercury and major ions in snowmelt runoff from a small Arctic Alaska watershed. Environmental Science & Technology 51(19):11145-11155.
Thompson, S. J., C. M. Handel, and L. B. McNew. 2017. Autonomous acoustic recorders reveal complex patterns in avian detection probability. Journal of Wildlife Management 81(7):1228-1241.
Tolkkinen, M. J., J. Heino, S. H. K. Ahonen, K. Lehosmaa, and H. Mykrä. 2020. Streams and riparian forests depend on each other: A review with a special focus on microbes. Forest Ecology and Management 462:art. no. 117962.
van de Kerk, M., D. Verbyla, A. W. Nolin, K. J. Sivy, and L. R. Pruch. 2018. Range-wide variation in the effect of spring snow phenology on Dall sheep population dynamics. Environmental Research Letters 13(7):075008.
Van Cleve, K., L. A. Viereck and C. T. Dyrness. 1996. State factor control of soils and forest succession along the Tanana River in interior Alaska, USA. Arctic and Alpine Research 28 388-400.
Viereck, L. A., C. T. Dyrness and M. J. Foote. 1993. An overview of the vegetation and soils of the floodplain ecosystems of the Tanana River, interior Alaska. Canadian Journal of Forest Research 23 (5): 889-898.
Walker, D. A., P. J. Webber, E. F. Binnian, K. R. Everett, N. D. Lederer, and others. 1987. Cumulative impacts of oil fields on northern Alaskan landscapes. Science 238: 757-761.

Walsh, J. E., U. S. Bhatt, J. S. Littell, M. Leonawicz, M. Lindgren, T. A. Kurkowski, P. A. Bieniek, R. Thoman, S. Gray and T. S. Rupp. 2018. Downscaling of climate model output for Alaskan stakeholders. Environmental Modelling & Software 110: 38-51.

Walvoord, M. A., C. I. Voss and T. P. Wellman. 2012. Influence of permafrost distribution on groundwater flow in the context of climate-driven permafrost thaw: Example from Yukon Flats Basin, Alaska, United States. Water Resources Journal 48 W07524.

Wang, J.A., D. Sulla-Menashe, C.E. Woodcock, O. Sonnentag, R.F. Keeling, and M.A. Friedl. 2019. ABoVE: Landsat-derived Annual Dominant Land Cover Across the ABoVE Core Domain, 1984-2014. ORNL DAAC, Oak Ridge, Tennessee, USA. https://doi.org/10.3334/ORNLDAAC/1691.

Wendler G, Shulski M. 2009. A century of climate change for Fairbanks, Alaska. Arctic 62(3).

Yi S, McGuire AD, Harden J, Kasischke E, Manies K, Hinzman L, Liljedahl A, Randerson J, Liu H, Romanovsky V, Marchenko S. Interactions between soil thermal and hydrological dynamics in the response of Alaska ecosystems to fire disturbance. Journal of Geophysical Research: Biogeosciences. 2009 Jun;114(G2).

Yi, Y., Kimball, J. S., Chen, R., Moghaddam, M., Reichle, R. H., Mishra, U., Zona, D., and Oechel, W. C.: Characterizing permafrost active layer dynamics and sensitivity to landscape spatial heterogeneity in Alaska, The Cryosphere, 12, 1, 145, 2018.

Yoshikawa, K., Hinzman, L. D.: Shrinking thermokarst ponds and groundwater dynamics in discontinuous permafrost near Council, Alaska, Permafrost Periglac. Proc., (2), 151-60, 2003.

Yoshikawa, K., Leuschen, C., Ikeda, A., Harada, K., Gogineni, P., Hoekstra, P., Hinzman, L., Sawada, Y., and Matsuoka, N.: Comparison of geophysical investigations for detection of massive ground ice (pingo ice), J. Geophys. Res.: Planets (1991–2012), 111 E6, 2006.

4. ADDRESSING COMMENTS FROM THE INTERIM REPORT
SERDP Interim Report comments are in bold; our responses follow.

Clarify the discrepancy in lowland scrub
When comparing areal extents of ecotypes from our grid photo-interpretation with those from previous mapping efforts, values were similar for Lowland Wet Needleleaf Forest (21.6% from grid vs 20.1% previous mapping), Lowland Wet Low Scrub (10.5% vs 13.4%), Lowland Wet Broadleaf Woodland (5.5% vs 5.1%), Upland Moist Mixed Forest (3.8% vs 4.3%), Upland Moist Needleleaf Forest (6.5% vs 3.0%), and Upland Dry Broadleaf Woodland (3.1 vs 2.7%). There were, however, a couple of ecotypes with widely varying extents between the two methods, including Lowland Bog Tussock Scrub (1.9% vs 10.3%) and Lowland Post-fire Scrub (12.7% vs 1.3%). We attribute this large discrepancy to misclassification between these two classes during automated spectral image classification for the two training lands near Fort Greely (Donnnelly Training Area West and East). Overall, values indicate that the results from systematic grid assessment was broadly representative of the terrain conditions quantified through intensive mapping.

Consider vulnerabilities definitions for the different wildlife types
Here, we identify potentially vulnerable wildlife species based on multiple criteria such as degree of habitat specialization, designated game and subsistence status, recognized vulnerability from small population size, and other factors.

The outcome of this part of the project pertains to much of the four main project objectives of: assessing habitat vulnerability to climate change and identifying the factors that drive vulnerability; developing an improved understanding of the spatial variability in drivers of vulnerability across a species' range; developing an improved understanding of the relationship between changing climate and key ecological processes such as fire regimes, hydrological regime or food webs; and development of methodologies, tools, and guidance to translate research on these issues into practical information for improving adaptive management of sensitive habitats to meet conservation objectives.

We also identified habitat specialists among mammals as those mammal species that use 10 or fewer ecotype categories. As with bird habitat specialists, this is a subjective threshold but also serves as a means by which to identify a set of species with the narrowest habitat use breadth that might be vulnerable to declines in the total amount of their habitat.

A section entitled "Species-Rich Ecotypes Depict Spatial Variability in Drivers of Vulnerability" that briefly summarizes activities to avoid in species-rich ecotypes, concludes " In general, these findings and suggestions are examples of the spatial variability in drivers of vulnerability across species' ranges, addressing Project Objective 2."

Describe vulnerability criteria as related to changes in species density.
It is not quite clear what is meant by "species density." Assuming it refers to species richness (i.e. the number of species), this addressed in detail in the section "Patterns of Wildlife Species Richness by Ecotype." We address richness both from the point of individual wildlife species, that is, habitat-use breadth, where species with narrow habitat-use breadth (that use the fewest

ecotype categories) may be more vulnerable to disturbances; and from the point of ecotype species richness, that is, which ecotypes have the most, or the fewest, associated wildlife species, and which may be vulnerable to human activities.

It seems there is some overlap and confusion between tasks as well. In going through the report multiple times, the tasks themselves are not very clearly or consistently defined (in Table 2, and in the individual task sections in the report.) The section on task 3.2, although very well-written, is actually the summary for the work that should be done in task 1.2 – it says nothing about the effect of the modeled changes in ecotypes on habitat availability for wildlife, and doesn't provide any info on future projections of ecotype distribution and abundance. Task references in the text are occasionally wrong or messed up; a "Task 3.4" is referenced a couple times in one section, but currently there is no Task 3.4.

There are a few methodology or analysis concerns as well – especially with interpretation of ecotype changes. The ecotype changes from a couple different analyses don't seem consistent with each other; looks like one showed much more wetland formation/thermokarst formation than the other in 1.2 and 3.2.
The full analyses were completed for this Final Report and all results have been updated.

Content of figures generally on track, but captions, axes labeling, etc. need significant work for ease of understanding in many instances. Check citations and references – for example, where is Jorgensen et al. 2018 in ref list. Check all acronyms, make sure they're spelled out the first time.
The references have been newly cross-referenced and updated and acronyms have been updated.

The report needs extensive copy-editing throughout as well; nearly every single paragraph and figure caption has some sort of typo or verb tense issue or other error.
We have diligently tried to identify and correct grammar.

All figures and captions should be revisited to ensure clarity, and that the critical information is being conveyed.
This Final Report was developed with this in mind.

Objective
Before the figures and tables in this section, I'd recommend adding a brief paragraph introducing the ecotypes that are being evaluated through much of this project.
We added a table cross-walking the new statewide ecotype classification that we developed with the old ecotypes as described in earlier reports for Ft Wainwright and Ft Greely. As the description of ecotypes would be very lengthy, we refer the reader to those reports.

Hypothesis 1
Example of vague writing: (a) Fire is the most rapid driver of ecological changes compared to other primary drivers such as thermokarst and hydrologic change on interior Alaska DoD lands. (b) But thermokarst, driven by a set of physical characteristics including altered surface vegetation from wildfires or changing environmental conditions, will lead to the most dramatic, long-lasting ecological changes."

My understanding is that "thermokarst" is a sort of landform, that develops as permafrost thaws. A landform – a mountain, a kettle moraine, thermokarst – in itself isn't an ecological process. Permafrost thaw and associated thermokarst development or formation is an ecological process. I may just not be familiar with the common usage, but it seems strange to refer to thermokarst as a process. It seems more appropriate – when referencing the ecological process (rather than just the landform itself) – to call it thermokarst formation, or thermokarst development – or even directly reference permafrost thaw, or permafrost degradation. This is an issue that should be addressed throughout the entire report (assuming I'm not wrong about the common usage, which is certainly possible).
Thermokarst is typically used as a general term to describe a variety of landforms that result from ground collapse during thawing of ice-rich permafrost (see definition provided in Jorgenson, 2020). But as a general term, it can also be used as a verb to describe the thawing and collapse of frozen ground. This is siilar to the way "fire" is used as both a noun and a verb.

Tasks
For the final report, please add a table to summarize data collected, analyses completed, etc. for each task section of the report. This will help clarify each task as a whole and its relationship to previous and subsequent tasks. It will also provide a useful framework for simple documentation of the status of/progress on data collection and analysis for each analysis. The dataset listed in each row should be clear – either the official name of the dataset, or the specific variable it measures or characterizes (not something vague like "soil characteristics"). Not sure of best headings for additional columns but ensure those are clear and each cell is completed.
We have provided this information where relevant.

Please make the task list (Table 2) and the task summary descriptions for each task section more consistent and clear; they're currently inconsistent and often vague.
This has been addressed.

Task 1.1
For example, in table 2, task 1.1 reads as: "Develop a database of critical physical characteristics (e.g. permafrost ice content, topography, soil texture) and the distribution and classification of thermokarst formations and ecotypes across the landscape." In the section on task 1.1, it reads as: "*Development of a database of critical environmental characteristics and the distribution and classification of thermokarst formation across main ecological units"*
A database can imply a relational database (like Access or Oracle) that can be queried, so that's confusing if you're just collecting datasets. Or building a geodatabase of spatial datasets.

If I'm interpreting correctly, Task 1.1. would be clearer as something like "Compile geospatial datasets on the environmental characteristics (elevation (or landform/geomorphology/topography), temperature, precipitation, permafrost ice content, soil texture, vegetation cover, etc.) that drive thermokarst formation and distribution across the landscape."

This is a great suggestin. We have changed the text description for Task 1.1 (also see comment below) to:
"*Development of a database of critical environmental characteristics useful in evaluating the distribution and classification of thermokarst formation across main ecological units.*"

We have also added the following paragraph to introduce Task 1.1 and provide the characteristics suggested:
"We compiled a broad variety of geospatial information for the training lands and field sites that represent training land permafrost, ecology, and hydrology. The most relevant environmental characteristics for thermokarst assessment include topography, temperature, permafrost ice content, soil composition, vegetation cover, and hydrologic conditions. Data from field surveys and instrumentation deployed at point locations were compiled into several relational databases in ArcGIS and Microsoft Access. Spatial data involving remote sensing imagery and geographic information systems (GIS) vector data were compiled into geodatabases. Field surveys of seasonal thaw depths, permafrost geophysical characteristics and borehole samples were used to quantify rates of top-down and lateral thaw and to track thermokarst feature development. The field measurements and database properties are described first and some field site measurements of thermokarst processes follow."

In reading just the brief task description, I'm still not clear on whether the team is proposing to develop a classification of thermokarst features, and map them across the study area, or simply compile datasets on the features that shape thermokarst formation and distribution. I have to carefully read through the narrative, and it still isn't 100% clear if this is a data collection task or a data collection and analysis task.
Good point necessitating clarification and we appreciate the comment. Accordingly, we revised the header as "*Task 1.1: Development of a database of critical environmental characteristics useful in evaluating the distribution and classification of thermokarst formation across main ecological units*." This clarifies that the objective was to compile and standardize available data into a database. This database can then be used in support of other objectives.

Task 1.2
Example of inconsistency:
In table 2: "Analyze historical rates of change in the distribution of ecotypes, in response to fire, thermokarst and hydrologic change by field survey and photointerpretation of a time-series of high-resolution imagery from the 1950s to the late 2010s."
In the Task 1.2 section: "*Analysis of rates of historical ecotype change and associated biophysical drivers using field surveys and time-series photointerpretation of high-resolution imagery"*
We have made the Task description consistent for all mentions.

Following Figure 4, recommend inserting brief text explaining that Figures 5-8 illustrate preliminary results for one of the field sites, Creamers Field Migratory Refuge and moving that first small paragraph after Figure 8 to just before Figure 5.
This part of the Report has been completely rewritten and new maps have been added for clarity.

As currently written, after Figure 8, the report states "It is clear from the airborne LiDAR, photos, and ground temperatures the permafrost at this site has warmed dramatically and has started to degrade. We plan to acquire another airborne LiDAR measurement over the site…" But the reader doesn't immediately know which site is being discussed.
We have provided more specific location informatio and some new maps where relevant to reduce confusion on site names and locations.

Task 2.2 (1.2?
This task seems to accomplish what Task 3.2 claims it will – it generates projected land cover / ecotypes out to the year 2100.
These Task titles and their activities have been more clearly explained to show they are quite different.

Figure 24: The combination of four emission scenarios and five global climate models should have 20 lines on the graph and a legend for the line colors that shows all 20 combinations. At a minimum, the figure should be enlarged, and the colors should clearly show the 20 combos. For final report, you might consider doing one figure for each of the five climate models (so just four lines per graph, one for each scenario).
That was a preliminary Figure for the Interim Report. That entire section has been updated and the Figure is no longer relevant.

Figure 25: "Cumulated", do you mean *Simulated* or *Cumulative*?
As pointed out by the reviewer there was some overlap between the objectives of Task 1.2 and Task 3.3 objectives to project and map the future distributions of wildlife habitats and assess changes in wildlife species' vulnerability by 2050 and 2100 through state-transition modeling and assess sensitivity of models to historical rates, temperature, and driver parameterization. We better partitioned this effort by including the state-transition modeling of ecotype/habitat changes in Task 1.2 so that both the historical and projected changes can be in the same section. Thus, Task 3.3 can use those projection and just focus on wildlife specie vulnerability.

Task 2.1
References Task 3.4 a couple times, however there is no Task 3.4.
We have fixed this in the Final Report.

Figure 12
This figure highlights an issue throughout much of this report. The figure illustrates changes in ecotype, at point locations, throughout the study area. It notes that only 23% of the points showed no change from 1949 to 2017. In a boreal landscape shaped by fire, insect outbreaks, variable hydrologic regimes, permafrost dynamics, and other ecosystem processes, it would be surprising if most of those points didn't change in that roughly 70-year period. The key seems to be which of those changes are a result of anthropogenic climate change – presumably much or most of the thermokarst formation, and SOME of the fire-associated succession.
Our research has quantified the extent of ecotype changes associated with 17 geomorphic and ecological drivers of change. In our projects of ecotype changes from 2017 to 2100 we are able to compare the changes that would be expected to occur at historical rates, before there was

much influence of anthropogenic climate change, with three climate warming scenarios developed for various greenhouse gas emission scenarios. The intermediate scenario that includes rate adjustments to the disturbance drivers expects net changes from the driver-adjusted RCP6.0 temperature model (31%) to be nearly three fold higher than the time (historical rate) model (12%), mostly driven by a fast acceleration in thermokarst, while fire effects on overall ecotype composition are diminished because the landscape is comprised on a highly patchy mosaic of differing aged stands in differing stages of post-fire recovery. We evaluate the relative effects of climate change, fire, thermokarst, hydrology, and human impacts in Task 2.3.

Task 3.1

The ARU data collection is interesting, but is not clearly tied into determining species-habitat relationships (at least as the report is written). Will these data be used to help identify species-habitat relationships? It's not clear that these data are well suited for linking individual species to individual ecotypes with a high level of confidence.

As of writing the Interim Report we had not finished the ARU data collection and had only done a preliminary analysis. In this Report we have far more results from the ARU measurements and analyses and we provide more specific links between the ARU results and the overall habitat assessment work.

Task 3.2

Example of vagueness:

Task 3.2 in Table 2 reads as "Evaluate effects of projected change in ecotype distribution (Task 2.3) on wildlife."

In the section on task 3.2, it reads as: "*Projection of future ecotype and wildlife changes through state- transition modeling"*

Please provide a more clear and specific definition of what is being evaluated.

These Task titles and their activities have been more clearly explained to show they are quite different.

Decide whether the team is going to include full mini-report for each task or not; be consistent for all tasks. Task 3.2 is the one task where there's a complete draft report for the task. This is by far the best-written section, and the content (background, methods, results, discussion, etc.) will be along the lines of what is needed for the final report. However, for this progress report, seems unnecessary to provide a complete draft report on each task – especially with 11 tasks to report on. Suggest removing most of the background, methods, summary, conclusions, etc, and stick with a simple table, brief supporting narrative explaining data collection and analysis progress/status, and brief overview of results to date. In addition, this narrative makes no mention of correlating ecotype change to habitat availability for wildlife, so it seems very similar to task 1.2.

For the interim Report many of the Tasks were only partially complete and some had not started in earnest. For this Final Report we have provided more information specific to eash Task. We also show how/where some efforts in a given Task build toward other Tasks and the final overall assessments.

What is process-based IEM under Task 3.2?

IEM stands for the Integrated Ecosystem Model. It couples two models that were used in this project: GIPL and TEM. GIPL is a permafrost dynamic model and TEM is a terrestrial ecosystem model.

ACKNOWLEDGMENTS

T. Douglas acknowledges the project team that helped lead and perform the duties that supported this effort. A variety of collaborators provided guidance, ideas, data, and supported field measurements. Their efforts are greatly appreciated. B. Marcot expresses his appreciation to: Amal Ajmi (U.S. Fish and Wildlife Service), Aren Gunderson (University of Alaska, Fairbanks), and Justin Smith (USAG-FWA) for reviews of the wildlife species lists; Deanna Klobuchar, Stephen Klobucar Knut Kielland, and Ken Tape (University of Alaska Fairbanks), Jeffrey Falke (U.S. Geological Survey) and Melanie Flamme (National Park Service), for discussions and exchanges on wildlife, habitats, and changing conditions; Robert Koch (Cornell Labs) for guidance on preparing and updating the "Swift" automated audio recording units; John Chase (U.S. Forest Service) for providing forest inventory information; Chris Hiemstra, Tricia Nelsen, Taylor Sullivan, and Dragos Vas (CRREL) and Damon Lesmeister (U.S. Forest Service) for help with deploying, retrieving, and other related field operations with the automated audio recording units; and Jamie Hollingsworth and Teresa Nettleton Hollingsworth (U.S. Forest Service) for providing a field inspection to the Bonanza Creek Experimental Forest. Marcot acknowledges support from Pacific Northwest Research Station, U.S. Forest Service, Portland, Oregon. Mention of commercial products or services does not necessarily constitute endorsement by U.S. Department of Agriculture.

PEER REVIEWED PUBLICATIONS AND PRESENTATIONS SUPPORTED BY THIS PROJECT

Published

Douglas, T.A., Hiemstra, C.A. Anderson, J.E., Barbato, R.A., Bjela, K.L., Deeb, E.J., Gelvin, A.B., Newman, S.D., Saari, S.P., Wagner, A.M. (2021) Recent degradation of Interior Alaska permafrost mapped with geophysics, airborne LiDAR, ground surveys, and drilling. The Cryosphere Discussions.1-39.

Douglas TA, Zhang C. (2021) Machine learning analyses of remote sensing measurements establish strong relationships between vegetation and snow depth in the boreal forest of Interior Alaska. Environmental Research Letters.

Zhang C, Douglas TA, Anderson JE. (2021) Modeling and mapping permafrost active layer thickness using field measurements and remote sensing techniques. International Journal of Applied Earth Observation and Geoinformation. 102:102455.

Creamean J., Hill T., DeMott P.J., Uetake J., Kreidenweis S., Douglas T.A. (2020) Thawing permafrost: an overlooked source of seeds for Arctic cloud formation. Environmental Research Letters, doi: 10.1088/1748-9326/ab87d3.

Douglas, T.A., Turetsky, M.R., Koven, C.D. (2020) Increased rainfall stimulates permafrost thaw across a variety of Alaskan ecosystems. Nature Climate and Atmospheric Change. 10.1038/s41612-020-0130-4.

Holloway, J.E., Lewkowicz, A.G., Douglas, T.A., Li, X., Turetsky, M.R., Baltzer, J.L., Jin, H. (2020) Impact of wildfire on permafrost landscapes: a review of recent advances and future prospects. Permafrost and Periglacial Processes, doi: 10.1002/ppp.2048.

Jorgenson, M. T. 2021. Thermokarst. In Treatise on Geomorphology, 2nd Edition. J. Schroeder, eds. Elsevier, San Diego. Vol. 4 Cryospheric Geomorphology: pp. 1-22.

Jorgenson, M. T., T. A. Douglas, A. K. Liljedahl, J. E. Roth, T. C. Cater, W. A. Davis, G. V. Frost, P. F. Miller and C. H. Racine. 2020. The roles of climate extremes, ecological succession, and hydrology in repeated permafrost aggradation and degradation in fens on the Tanana Flats, Alaska. JGR Biogeosciences JGRG21762.

Kropp, H., and 48 others Shallow soils are warmer under trees and tall shrubs across Arctic and Boreal ecosystems. (2020) Environmental Research Letters. Doi: 10.1088/1748-9326/abc994.

Leewis, M.-C., Berlemont, R., Podgorski, D.C., Srinivas, A., Zito, P., Spencer, R.G., McFarland, J., Douglas, T.A., Conaway, C., Waldrop, M.P., Mackelprang, R. (2020) Life at the frozen limit: Microbial Carbon Metabolism Across a Late Pleistocene Permafrost Chronosequence. Frontiers in Microbiology 11:1753; doi: 10.3389/fmicb.2020.01753.

Messan, K.S., Jones, R.M., Doherty, S.J., Foley, K., Douglas, T.A., Barbato, R.A. (2020) The role of a changing temperature in microbial metabolic processes during permafrost thaw. PLOS One, doi: 10.1371/journal.pone.0232169.

O'Donnell J., Douglas T., Barker A., Guo L. (2020) Changing Biogeochemical Cycles of Organic Carbon, Nitrogen, Phosphorus, and Trace Elements in Arctic Rivers. In: Yang D., Kane D. (eds) Arctic Hydrology, Permafrost and Ecosystems. Springer, Cham. https://doi.org/10.1007/978-3-030-50930-9_11.

Sowers, T.D., Wani, R., Coward, E.K., Fischel, M.H.H., Betts, A.R., Douglas, T.A., Duckworth, O.W., Sparks, D.L. (2020) Spatially-resolved carbon interactions with iron phases across a permafrost chronosequence. Environmental Science and Technology. es-2019-06558v.R2.

Anderson, J.E., Douglas, T.A., Barbato, R.A., Saari, S., Edwards, J.D., Jones, R.M. (2019) Vegetation Mapping and Seasonal Thaw Estimates in Interior Alaska Permafrost. Remote Sensing of Environment, 233(111363). Doi:10.1016/j.rse.2019.111363, 14 pages.

Douglas TA, Mellon MT (2019) Sublimation of terrestrial permafrost and the implications for ice-loss processes on Mars. Nature Communications 10(1):1716. This paper was supported by project activities that included ice content measurements at multiple locations in the CRREL Permafrost Tunnel.

McPartland, M, et al. (2019) Characterizing boreal peatland community composition and biodiversity with hyperspectral remote sensing. Remote Sensing, 1685; doi:10.3390/rs11141685.

Treat CC, Kleinen T, Broothaerts N, Dalton AS, Dommain R, Douglas TA, Drexler JZ, Finkelstein SA, Grosse G, Hope G, Hutchings J (2019) Widespread global peatland establishment and persistence over the last 130,000 y. Proceedings of the National Academy of Sciences. 116(11):4822-7. This paper was supported by project activities that included a variety of cores collected at field sites in the project study domain.

Burkert A, Douglas TA, Waldrop MP, Mackelprang R. (2018) Changes in the Active, Dead, and Dormant Microbial Community Structure Across a Pleistocene Permafrost Chronosequence. Applied Environmental Microbiology 85(7): e02646-18. This paper was supported by project activities that included ice content measurements at multiple locations in the CRREL Permafrost Tunnel.

In Review

Barbato, R, Jones, R., Douglas, T., Esdale, J., Foley, K., Perkins, E., Rosten, S., Garcia-Reyero, N. Alaskan paleosols in modern times: deciphering unique microbial ecology within the late Holocene. In review, Molecular Ecology.

Barbato, R.A., Douglas, T., Doherty, S., Jones, R., Foley, K., Messan, K., Perkins, E., Vinas, N. Not all permafrost microbiomes are created equal: starting inoculum drives microbial community succession during permafrost thaw. In review, The Holocene.

Coward, E.K., Sowers, T.D., Wani, R.P., Thompson, A., Douglas, T.A., Sparks, D.L. Iron complexation constrains organic carbon abundance and molecular composition across a permafrost chronosequence. In review, Environmental Science and Technology.

Miller, C., and 42 others. The ABoVE L-band and P-band Airborne SAR Surveys. In review, Earth System Science Data.

In Preparation

Cox, W.D., Dieleman, C.M., Doulgas, T.A., Kane, E.S., Turetsky, M.R. Plant community shifts as early indicators of abrupt permafrost thaw and associated carbon release in interior Alaska lowlands. In preparation for submission to the Journal of Geophysical Research Biogeosciences.

Douglas, T.A. Stable water isotopes of precipitation and permafrost in Interior Alaska. In preparation for submission to Permafrost and Periglacial Processes.

Douglas, T.A., Jorgenson, M.T., Sullivan, T., Saari, S. Zhang, C. Permafrost degradation in Interior Alaska quantified by repeat electrical resistivity tomography. In preparation for submission to Ecological Research Letters.

Jorgenson, M. T., D. Brown, C. Hiemstra, H. Genet, R. Murphy, T. Douglas and B. Marcot. In Prep. Patterns and rates of landscape change in central Alaska: fires more widespread but thermokarst more transformative. Environ. Res. Lett.

Kanevskiy, M., Shur, Y., Bigelow, N.H., Bjella, K.L., Douglas, T.A., Jones, B.M., Jorgenson, M.T., Fortier, D. Yedoma cryostratigraphy of recently excavated sections of the CRREL Permafrost Tunnel near Fairbanks, Alaska. In preparation for submission to the Journal Frontiers in Earth Science.

Genet, H., M.T. Jorgenson, T. Douglas, B. Marcot, P. Nelson. Modeling historical and future effects of climate change, wildfire and thermokarst disturbances on land cover dynamics in boreal Alaskan peatlands. Frontiers in Ecology and the Environment.

Genet, H., H. Greaves, N. Pastick, M.T. Jorgenson, T. Douglas, B. Marcot, P. Nelson. Assessing the consequences of permafrost thaw on soil moisture dynamic across boreal and arctic Alaska: a synthesis of long term historical in-situ observations. Environ. Res. Lett.

Presentations attributable to this project

Note that many of these presentations are collaborative with other people and projects and SERDP funding was only used for a few of the meetings attended.

Murphy, R., M. T. Jorgenson, B. G. Marcot, T. A. Douglas and H. Genet. (2021). Drivers of Landscape Change Across Diverse Boreal Ecosystems in Central Alaska Documented with High-resolution Photographs, Fairbanks, AK. Poster presented at IBFRA21. 1 pgs.

Genet, H., M.T. Jorgenson, T. Douglas, B. Marcot, P. Nelson, H. Greaves (2021). Modeling land cover dynamic in response to climate change, wildfire and thermokarst in boreal Alaska peatlands. Yukon Flats NWR Fire Management Workshop, Alaska Fire Science Consortium (virtual).

Douglas, T.A. (2020) The current and projected future state of permafrost in the north with a focus on the carbon cycle. Invited, Alaska Geological Society (virtual).

Douglas, T.A., Hiemstra, C.A., ANderson, J., Zhang, X. (2020) Identifying vegetation-geomorphology relationships in permafrost with airborne LiDAR, electrical resistivity tomography, seasonal thaw depth measurements, and machine learning. European GEophysical Union Annual Meeting. Vienna, Austria (virtual).

Cox, W., Dieleman, C.M., Douglas, T.A., Turetsky, M.R. (2020) As above, so below: Linkages between ground-layer plant communities and subsurface permafrost characteristics in interior Alaska lowlands. Fall Meeting of the American Geophysical Union. San Francisco, CA (virtual).

Nicolsky, D., Farquharson, L.M., Robert, Z.V., Hasson, N., Romanovsky, V.E., Douglas, T.A., Schmidt, J. (2020) Permafrost hazard mapping in the discontinuous permafrost zone of Alaska. Fall Meeting of the American Geophysical Union. San Francisco, CA (virtual).

Barbato, R.A., Messan, K., Jones, R.,Doherty, S., Douglas, T., (2020) The role of changing temperature in microbial metabolic processes during permafrost thaw. Fall Meeting of the American Geophysical Union. San Francisco, CA (virtual).

Douglas, T.A., Hiemstra, C.A., Sullivan, T., Jorgenson, M.T., Genet, H., Marcot, B. Identifying areas at risk of permafrost degradation and habitat change in Interior Alaska by integrating

information from remote sensing, field measurements, and ecological modelling. SERDP/ESTCP Annual Meeting, Washington, DC (virtual).
Zhang, C., Douglas, T.A., Anderson, J. (2020) Modeling and Mapping Permafrost Thaw Depth in Interior Alaska Using a Remote Sensing Data Fusion Approach. American Association of Geographers Annual Meeting (virtual).
Zhang, C., Douglas, T.A., Anderson, J. (2020) Mapping vegetation and seasonal thaw depths in central Alaska using airborne hyperspectral and LiDAR data. IEEE Geoscience and Remote Sensing Society (virtual).
Cox, W., Turetsky, M.R., Douglas, T.A., Dieleman, C.M., Kane, E.S. (2019) Plant community shifts as early indicators of abrupt permafrost thaw and thermokarst development in interior Alaska lowlands. Fall Meeting of the American Geophysical Union. San Francisco, CA.
Douglas, T.A., Barker, A.J., Gelvin, A.B., Barbato, R.A. (2019) Biogeochemical Characteristics of Ancient Permafrost in Newly Excavated Sections of the Fox Tunnel, Alaska. V.M. Goldschmidt Conference on Geochemistry. Barcelona, Spain.
Douglas, T.A., Bjella, J., Larsen, G.W. (2019) Ongoing expansion of the Cold Regions Research and Engineering Laboratory's Permafrost Tunnel. Arctic Futures 2050 Conference. Washington, DC.
Douglas, T.A., Turetsky, M.R., Jorgenson, M.T., Genet, H. (2019) Identifying risk factors for permafrost thaw and degradation on U.S. Army Alaska training lands. Arctic Futures 2050 Conference. Washington, DC.
Douglas, T.A., and Turetsky, M.R. (2019) Links between increased summer and winter precipitation and enhanced seasonal thaw of permafrost across a variety of Alaskan ecosystems. Southern Conference on Permafrost. Queensland, New Zealand.
Douglas, T.A., and Mellon, M. (2019) Sublimation in the CRREL permafrost Tunnel-implications for ice-loss landforms on Mars. Southern Conference on Permafrost. Queensland, New Zealand.
Douglas, T.A. (Invited; 2019) Ecosystem Changes: What are the microbial threats we know are in the environment? Understanding and Responding to Global Health Security Risks from Microbial Threats in the Arctic. National Academies of the U.S. and German Science Federation Meeting. Hannover, Germany.
Douglas, T.A., Barker, A.J., Gelvin, A.B., Barbato, R. (2019) Biogeochemical Characteristics of Ancient Permafrost in Newly Excavated Sections of the Fox Tunnel, Alaska. V.M. Goldschmidt Conference on Geochemistry. Barcelona, Spain August.
Douglas, T.A., Bjella, K., Larsen, G.W. (2019) Ongoing expansion of the Cold Regions Research and Engineering Laboratory's Permafrost Tunnel Arctic Futures Conference Washington, DC September.
Douglas, T.A., Turetsky, M.T., Jorgenson, M.T., Genet, H. (2019) Identifying risk factors for permafrost thaw and degradation on U.S. Army Alaska training lands. Arctic Futures Conference Washington, DC September.
Du, J., Potter, S., Watts, J., Rogers, B., Natali, S., Douglas, T.A., Kimball, J. (2019) Multi-scale satellite observations of river ice and vegetation conditions in Interior Alaska during the spring landscape freeze/thaw transition. NASA Arctic Boreal Vulnerability Experiment Workshop La Jolla, CA.
Genet, H., Jorgenson, M.T., Douglas, T.A., Greaves, H., Hiemstra, C.A., Marcot, B.G., Turetsky, M.R. (2019) Assessing land cover change and lowland vulnerability to permafrost thaw,

altered fire regime, and hydrologic changes on Interior Alaska. Fall Meeting of the American Geophysical Union. San Francisco, CA.
Hiemstra, C.A., Douglas, T.A., Gelvin, A.B., Liddle-Broberg, K., Cook, B., Vas, T. (2019). Time Series Analyses of Interior Alaska Thermokarst Using Airborne and Terrestrial Lidar. Fall Meeting of the American Geophysical Union. San Francisco, CA.
Jorgenson, MT (2019) Past and projected trends in Alaska habitats stressed by rapid climate change. In 18th Alaska Bird Conference, 4. Alaska Songbird Institute.
Sullivan, T.D., Parsekian, A., Douglas, T.A., Schaefer, K.M., Michealides, R.J., Saari, S., Liddle-Broberg, K., Westenhoff, J., Schaefer, S. (2019) Geophysical Observations of Organic Matter and Soil Moisture Interactions during Freezing and Thawing of Alaskan Boreal Permafrost. Fall Meeting of the American Geophysical Union. San Francisco, CA.
Barbato, R.N., Jones, R.M., Anderson, J., Douglas, T.A., Jarvis, S., Foley, K.L. (2018) Shifts in microbial and plant diversity above thawing discontinuous permafrost in high latitude ecotones. Polar and Alpine Microbiology Conference Nuuk, Greenland.
Douglas, T. (2018) Ecosystem controls on seasonal thaw depths, snowpack characteristics, and the soil thermal regime in boreal biome permafrost of interior Alaska. Ecological Society of America Annual Meeting. New Orleans, LA.
Douglas, T.A., Turetsky, M.R. (2018) Thermokarst in pingos and adjacent collapse scar bogs in interior Alaska. NASA Arctic Boreal Vulnerability Experiment Annual Meeting. Seattle, Washington.
Douglas, T.A., Anderson, J., Barbato, R., Barker, A., Beal, S., Deeb, E., Gelvin, A., Hiemstra, C., Jones, R. Newman, S., Parker, N., Saari, S., Staples, A. (2018) CRREL permafrost field sites in Interior Alaska. NASA Arctic Boreal Vulnerability Experiment Annual Meeting. Boulder, Colorado.
Natali, S., et al. (2018) Detecting Recent Changes in Vegetation, Landscape Water Availability and Freeze/Thaw Characteristics in Interior Alaska Using VIS-NIR-TIR and Microwave Remote Sensing Fall Meeting of the American Geophysical Union. Washington, DC.
Sullivan, T., et al. (2018) Geophysical Investigation of Soil Moisture Distribution and Behavior in Permafrost Soils from Interior Alaska. Fall Meeting of the American Geophysical Union. Washington, DC.
Turetsky, M., et al. (2018) New Insights Test our Fundamental Understanding of How Thermokarst Influences Permafrost Peatlands. Fall Meeting of the American Geophysical Union. Washington, DC.
Yang, Ji-W., et al. (2018) Greenhouse gases (CO_2, CH_4, and N_2O) entrapped in Alaskan and Siberian ice wedges: a direct evidence of the microbial activity within ground ice. European Geophysical Union Annual Meeting. Vienna, Austria.

5. APPENDICES

Appendix A.1. References Consulted for Determining Wildlife Species Occurrence and Habitat Use on Fort Wainwright

[A] = amphibians, [B] = birds, [M] = mammals

Smith, J., G. Preston, and G. Savory. 2018. Neotropical bird habitat assessment, Fort Wainwright, Alaska. Final Report Scope of Work 15-49. Center for Environmental Management of Military Lands, Colorado State University. 44 pp. [B]

Websites:
All accessed through May 2, 2021

Game Species - https://www.adfg.alaska.gov/index.cfm?adfg=hunting.species [B,M]
Small Game Species - https://www.adfg.alaska.gov/index.cfm?adfg=smallgamehunting.species [B,M]
Subsistence species - https://www.adfg.alaska.gov/index.cfm?adfg=subsistence.hunting [M]
eBird. Electronic database of observations. Hosted by Audubon and Cornell Lab of Ornithology. https://ebird.org/home [B]
The Cornell Lab, All About Birds, https://www.allaboutbirds.org/news/ [B]
xeno-canto. Bird sounds (recordings), https://www.xeno-canto.org/ [B]
Macaulay Library of the Cornel Lab of Ornithology. Bird sounds (recordings), https://www.macaulaylibrary.org/ [B]
Alaska Department of Fish and Game. Checklists of species of Alaska:
Wood Frog https://www.adfg.alaska.gov/static-f/species/speciesinfo/_aknhp/Wood_Frog.pdf [A]
Birds https://www.adfg.alaska.gov/index.cfm?adfg=animals.listbirds [B]
Mammal https://www.adfg.alaska.gov/index.cfm?adfg=animals.listmammals [M]

Personal communications for information on species occurrence:

Justin Smith
Natural Resource Specialist
Directorate of Public Works Environmental Division
USAG Alaska
907-361-4539
justin.a.smith230.civ@mail.mil

Amal Ajmi
Fish & Wildlife Biologist
Planning and Consultation
US Fish & Wildlife Service
101 12th Ave, Room 110
Fairbanks, AK 99701
907-456-0324 (Office)
907-456-0208 (Fax)

amal_ajmi@fws.gov

Aren M. Gunderson, M.S.
Collection Manager
Museum of the North
University of Alaska Fairbanks
Office: 004 Museum, (907) 474-6947
Lab: 013 Museum, (907) 474-1883
Email: amgunderson@alaska.edu
https://www.uaf.edu/museum/

Publications and reports on ecological land classification:

Anderson, B. A., R. J. Ritchie, B. E. Lawhead, J. R. Rose, A. M. Wildman, and S. F. Schlentner. 2000. Wildlife studies at Fort Wainwright and Fort Greely, Central Alaska, 1998. Final Report Prepared for U.S. Army Cold Regions Research and Engineering Laboratory, and United States Army Alaska. Fairbanks, Alaska. 105 pp. (sections numbered separately)

Jorgenson, M. T., J. E. Roth, M. K. Raynolds, M. D. Smith, W. Lentz, A. L. Zusi-Cobb, and C. H. Racine. 1999. An ecological land survey for Fort Wainwright, Alaska. CRREL Report 99-9, US Army Corps of Engineers, Cold Regions Research & Engineering Laboratory. Fairbanks, Alaska. 83 pp.

Jorgenson, M. T., J. E. Roth, B. A. Anderson, M. D. Smith, B. E. Lawhead, and S. F. Schlentner. 2000. Ecological land evaluation for the Yukon Training Area on Fort Wainwright, Alaska: permafrost, disturbance, and habitat use. Final report prepared for U.S. Army Cold Regions Research and Engineering Laboratory, and Unites States Army Alaska. Fairbanks, AK. 88 pp.

Jorgenson, M. T., J. E. Roth, J. D. Smith, S. Schlentner, W. Lentz, E. R. Pullman, and C. H. Racine. 2001. An ecological land survey for Fort Greely, Alaska. Laboratory Technical Report ERDC/CRREL TR-01-4, Cold Regions Research and Engineering. 82 pp.

Appendix Table 1. List of 124 bird species included in the species-specific habitat projections.

\1 = game species (Alaska Department of Fish and Game, https://www.adfg.alaska.gov/index.cfm?adfg=hunting.species);

\2 = small game species (Alaska Department of Fish and Game, https://www.adfg.alaska.gov/index.cfm?adfg=smallgamehunting.species)

\3 = habitat specialists, use ≤ 5 ecotypes

Family	Species Code	Common Name	Scientific Name
Accipitridae	NOGO	Northern Goshawk	*Accipiter gentilis*
Accipitridae	SSHA	Sharp-shinned Hawk	*Accipiter striatus*
Accipitridae	GOEA	Golden Eagle	*Aquila chrysaetos*
Accipitridae	RTHA	Red-tailed Hawk	*Buteo jamaicensis*
Accipitridae	ROHA	Rough-legged Hawk	*Buteo lagopus*
Accipitridae	NOHA	Northern Harrier	*Circus cyaneus*
Accipitridae	BAEA	Bald Eagle \5	*Haliaeetus leucocephalus*
Alaudidae	HOLA	Horned Lark \5	*Eremophila alpestris*
Alcedinidae	BEKI	Belted Kingfisher	*Megaceryle alcyon*
Anatidae	NOPI	Northern Pintail \1	*Anas acuta*
Anatidae	AMWI	American Wigeon \1	*Anas americana*
Anatidae	NOSH	Northern Shoveler \1	*Anas clypeata*
Anatidae	GWTE	Green-winged Teal \1	*Anas crecca*
Anatidae	MALL	Mallard \1	*Anas platyrhynchos*
Anatidae	LESC	Lesser Scaup \1	*Aythya affinis*
Anatidae	REDH	Redhead \1, \5	*Aythya americana*
Anatidae	RNDU	Ring-necked Duck \1	*Aythya collaris*
Anatidae	GRSC	Greater Scaup \1	*Aythya marila*
Anatidae	CANV	Canvasback \1	*Aythya valisineria*
Anatidae	CAGO	Canada goose \1	*Branta canadensis*
Anatidae	BUFF	Bufflehead \1	*Bucephala albeola*
Anatidae	COGO	Common Goldeneye \1	*Bucephala clangula*
Anatidae	BAGO	Barrow's Goldeneye \1	*Bucephala islandica*
Anatidae	TRSW	Trumpeter Swan \1	*Cygnus buccinator*
Anatidae	HADU	Harlequin Duck \1, \5	*Histrionicus histrionicus*
Anatidae	WWSC	White-winged Scoter \1	*Melanitta fusca [deglandi]*
Anatidae	COME	Common Merganser \1	*Mergus merganser*
Anatidae	RBME	Red-breasted Merganser \1	*Mergus serrator*
Bombycillidae	BOWA	Bohemian Waxwing	*Bombycilla garrulus*
Charadriidae	AGPL	American Golden-Plover	*Pluvialis dominica*
Cinclidae	AMDI	American Dipper	*Cinclus mexicanus*
Columbidae	RODO	Rock Dove	*Columba livia*
Corvidae	CORA	Common Raven	*Corvus corax*
Corvidae	GRAJ	Gray Jay	*Perisoreus canadensis*

Corvidae	BBMA	Black-billed Magpie	*Pica pica*
Falconidae	MERL	Merlin	*Falco columbarius*
Falconidae	PEFA	Peregrine Falcon	*Falco peregrinus*
Falconidae	GYRF	Gyrfalcon	*Falco rusticolus*
Falconidae	AMKE	American Kestrel	*Falco sparverius*
Fringillidae	CORE	Common Redpoll	*Acanthis flammea*
Fringillidae	HORE	Hoary Redpoll	*Acanthis hornemanni*
Fringillidae	GCRF	Gray-crowned Rosy-Finch \5	*Leucosticte tephrocotis*
Fringillidae	WWCR	White-winged Crossbill	*Loxia leucoptera*
Fringillidae	PIGR	Pine Grosbeak	*Pinicola enucleator*
Fringillidae	PISI	Pine Siskin	*Spinus pinus*
Gaviidae	COLO	Common Loon	*Gavia immer*
Gaviidae	PALO	Pacific Loon	*Gavia pacifica*
Gruidae	SACR	Sandhill Crane \1	*Grus canadensis*
Hirundinidae	CLSW	Cliff Swallow	*Petrochelidon pyrrhonota*
Hirundinidae	BANS	Bank Swallow	*Riparia riparia*
Hirundinidae	TRES	Tree Swallow	*Tachycineta bicolor*
Hirundinidae	VGSW	Violet-green Swallow	*Tachycineta thalassina*
Icteridae	RWBL	Red-winged Blackbird	*Agelaius phoeniceus*
Icteridae	RUBL	Rusty Blackbird \5	*Euphagus carolinus*
Laniidae	NOSK	Northern Shrike	*Lanius excubitor*
Laridae	BOGU	Bonaparte's Gull \5	*Chroicocephalus philadelphia*
Laridae	MEGU	Mew Gull	*Larus canus*
Laridae	HEGU	Herring Gull	*Larus smithsonianus*
Laridae	ARTE	Arctic Tern	*Sterna paradisaea*
Motacillidae	AMPI	American Pipit	*Anthus rubescens*
Muscicapidae	NOWH	Northern Wheatear	*Oenanthe oenanthe*
Pandionidae	OSPR	Osprey \5	*Pandion haliaetus*
Paridae	BCCH	Black-capped Chickadee	*Poecile atricapillus*
Paridae	BOCH	Boreal Chickadee	*Poecile hudsonicus*
Parulidae	WIWA	Wilson's Warbler	*Cardellina pusilla*
Parulidae	OCWA	Orange-crowned Warbler	*Oreothlypis celata*
Parulidae	NOWA	Northern Waterthrush	*Parkesia noveboracensis*
Parulidae	YRWA	Yellow-rumped Warbler	*Setophaga coronata*
Parulidae	YEWA	Yellow Warbler	*Setophaga petechia [aestiva]*
Parulidae	BLPW	Blackpoll Warbler	*Setophaga striata*
Parulidae	TOWA	Townsend's Warbler	*Setophaga townsendi*
Passerellidae	DEJU	Dark-eyed Junco (Slate-colored)	*Junco hyemalis*
Passerellidae	LISP	Lincoln's Sparrow	*Melospiza lincolnii*

Passerellidae	SASP	Savannah Sparrow	*Passerculus sandwichensis*
Passerellidae	FOSP	Fox Sparrow	*Passerella iliaca*
Passerellidae	ATSP	American Tree Sparrow	*Spizella arborea*
Passerellidae	GCSP	Golden-crowned Sparrow	*Zonotrichia atricapilla*
Passerellidae	WCSP	White-crowned Sparrow	*Zonotrichia leucophrys*
Phasianidae	RUGR	Ruffed Grouse \2	*Bonasa umbellus*
Phasianidae	SPGR	Spruce Grouse \2	*Falcipennis canadensis*
Phasianidae	WIPT	Willow Ptarmigan \2	*Lagopus lagopus*
Phasianidae	ROPT	Rock Ptarmigan \2	*Lagopus muta*
Phasianidae	STGR	Sharp-tailed Grouse \2	*Tympanuchus phasianellus*
Phylloscopidae	ARWA	Arctic Warbler	*Phylloscopus borealis*
Picidae	NOFL	Northern Flicker	*Colaptes auratus*
Picidae	BBWO	Black-backed Woodpecker	*Picoides arcticus*
Picidae	ATTW	American Three-toed Woodpecker	*Picoides dorsalis*
Picidae	DOWO	Downy Woodpecker	*Picoides pubescens*
Picidae	HAWO	Hairy Woodpecker	*Picoides villosus*
Podicipedidae	HOGR	Horned Grebe \5	*Podiceps auritus*
Podicipedidae	RNGR	Red-necked Grebe	*Podiceps grisegena*
Regulidae	RCKI	Ruby-crowned Kinglet	*Regulus calendula*
Scolopacidae	SPSA	Spotted Sandpiper \5	*Actitis macularia*
Scolopacidae	UPSA	Upland Sandpiper \5	*Bartramia longicauda*
Scolopacidae	DUNL	Dunlin \5	*Calidris alpina*
Scolopacidae	PESA	Pectoral Sandpiper	*Calidris melanotos*
Scolopacidae	LESA	Least Sandpiper	*Calidris minutilla*
Scolopacidae	SEPL	Semipalmated Plover	*Charadrius semipalmatus*
Scolopacidae	COSN	Wilson's Snipe	*Gallinago delicata*
Scolopacidae	WHIM	Whimbrel	*Numenius phaeopus*
Scolopacidae	REPH	Red Phalarope	*Phalaropus fulicarius*
Scolopacidae	RNPH	Red-necked Phalarope	*Phalaropus lobatus*
Scolopacidae	LEYE	Lesser Yellowlegs	*Tringa flavipes*
Scolopacidae	WATA	Wandering Tattler	*Tringa incana*
Scolopacidae	GRYE	Greater Yellowlegs \5	*Tringa melanoleuca*
Scolopacidae	SOSA	Solitary Sandpiper \5	*Tringa solitaria*
Sittidae	RBNU	Red-breasted Nuthatch	*Sitta canadensis*
Strigidae	BOOW	Boreal Owl	*Aegolius funereus*
Strigidae	SEOW	Short-eared Owl	*Asio flammeus*
Strigidae	SNOW	Snowy Owl	*Bubo scandiacus*
Strigidae	GHOW	Great Horned Owl	*Bubo virginianus*
Strigidae	GGOW	Great Gray Owl	*Strix nebulosa*
Strigidae	NOHO	Northern Hawk Owl	*Surnia ulula*

Turdidae	HETH	Hermit Thrush	*Catharus guttatus*
Turdidae	GCTH	Gray-cheeked Thrush	*Catharus minimus*
Turdidae	SWTH	Swainson's Thrush	*Catharus ustulatus*
Turdidae	VATH	Varied Thrush	*Ixoreus naevius*
Turdidae	TOSO	Townsend's Solitaire	*Myadestes townsendi*
Turdidae	AMRO	American Robin	*Turdus migratorius*
Tyrannidae	OSFL	Olive-sided Flycatcher	*Contopus cooperi*
Tyrannidae	WWPE	Western Wood-Pewee	*Contopus sordidulus*
Tyrannidae	ALFL	Alder Flycatcher	*Empidonax alnorum*
Tyrannidae	HAFL	Hammond's Flycatcher	*Empidonax hammondii*
Tyrannidae	SAPH	Say's Phoebe	*Sayornis saya*

Appendix Table 2. List of 27 species of migrant stopover-birds assessed in the habitat projections under six habitat-association groups. See main text Table 13 for information on these six groups.

Family	Species Code	Common Name	Scientific Name	General habitat associations	Migrant Stopover Group No. (MSG#) \1
Anatidae	BWTE	Blue-winged Teal	*Anas discors*	marshes, ponds, lakes in open country; migrants use marshes, vegetated wetlands around lakes	MSG1
Anatidae	GWFG	Greater White-fronted Goose	*Anser albifrons*	lakes, ponds, wet meadows in tundra & forest-tundra; aquatic; grazes on land; tall grass, hummocks near water; during migration forage in wet sedge meadows, tidal mudflats, ponds, lakes, wetlands	MSG3
Anatidae	CKGO	Cackling Goose	*Branta hutchinsii*	similar to Canada goose; breeds in coastal marshes, along tundra ponds and streams, and steep turf slopes above rocky shores	MSG3
Anatidae	SNGO	Snow Goose	*Chen caerulescens*	open tundra near ponds, streams; marshes, wet grasslands, flooded fields; shallow water, wet soil; during spring and fall migration, use open areas of lakes, farm fields, freshwater & brackish marshes, sluggish rivers, & sandbars	MSG1
Anatidae	LTDU	Long-tailed Duck, Oldsquaw	*Clangula hyemalis*	aquatic; ponds, wet tundra, willow or birch scrub (nesting); freshwater wetlands, lakes	MSG1
Anatidae	TUSW	Tundra Swan	*Cygnus columbianus*	tundra, sheltered marshes; shallow ponds, lakes; wetlands in boreal forests (fall migration)	MSG1

Anatidae	BLSC	Black Scoter	*Melanitta americana*	aquatic; tundra (nests); ponds, lakes; late autumn migration on lakes, large rivers	MSG1
Anatidae	SUSC	Surf Scoter	*Melanitta perspicillata*	tundra & wooded areas near water (nests); ponds, lakes; lakes, usually coastal	MSG1
Calcariidae	SNBU	Snow Bunting	*Plectrophenax nivalis*	tundra, talus (nesting); shores, sand dunes, beaches, weedy fields & grain stubble, open agriculture, along roadsides (migration); prefers barren rocky areas; patches of sedges and other vegetation (foraging)	MSG4
Charadriidae	PGPL	Pacific Golden-Plover	*Pluvialis fulva*	less-vegetated slopes; tundra (nesting); on migration found in prairie, pastures, farmland, airports, mudflats, shorelines, beaches	MSG4
Charadriidae	BBPL	Black-bellied Plover	*Pluvialis squatarola*	tundra (nesting); sandy beaches, estuaries, mudflats (wintering); migration primary coastal; migrants use lowlands, wet & flooded agricultural fields, wet prairies, muddy or gravelly edges of lakes, ponds, rivers	MSG2
Gaviidae	RTLO	Red-throated Loon	*Gavia stellata*	migrates coastally, casual inland; ponds, lakes; ponds, lakes; rugged tundra & taiga wetlands (breeding)	MSG1
Laridae	GWGU	Glaucous-winged Gull	*Larus glaucescens*	rare inland	MSG1
Laridae	GLGU	Glaucous Gull	*Larus hyperboreus*	migrants stay near water, likely ponds, lakes, rivers	MSG1

Parulidae	TEWA	Tennessee Warbler	*Oreothlypis peregrina*	coniferous & mixed woodlands (summer); mixed open woodlands & brushy areas (fall migration); clearings in spruce-fir forest, along margins of spruce-tamarack bogs, 2nd growth forests with balsam poplar (nesting); boreal forests of coniferous or mixed deciduous-coniferous trees, younger or middle-aged woodlands regenerating from disturbance, with open areas & dense shrubs (nesting); in migration not picky, found in many types of wooded habitats in eastern North America	MSG5
Passerellidae	CHSP	Chipping Sparrow	*Spizella passerina*	lawns, fields, woodland edges, pine-oak forests; low vegetation; grassy forests, woodlands and edges; evergreens but also aspen, birch, oak; up to treeline	MSG4
Scolopacidae	SURF	Surfbird	*Aphriza virgata*	mountain tundra (nesting); barren, rocky alpine tundra (nesting); stony alpine tundra (nesting)	MSG4
Scolopacidae	RUTU	Ruddy Turnstone	*Arenaria interpres*	rare inland migrant; tundra or gravel ridges; during migration along mudflats and shorelines of lakes	MSG6
Scolopacidae	DUNL	Dunlin	*Calidris alpina*	tundra (nesting); during migration use moist harvested agricultural fields, rivers, lakes, shallow water areas	MSG3

Scolopacidae	BASA	Baird's Sandpiper	*Calidris bairdii*	lakeshores, wet fields; migrants use variety of habitats, often near freshwater wetlands, including edges of lakes and rivers, pastures, drying lake beds	MSG3
Scolopacidae	WRSA	White-rumped Sandpiper	*Calidris fuscicollis*	mudflats (feeding); tundra hummocks near marshy ponds (nesting); during migration use wide variety of freshwater habitats including wet agricultural fields, freshwater impoundments, marshes with muddy margins	MSG3
Scolopacidae	STSA	Stilt Sandpiper	*Calidris himantopus*	grassy pools, shores of ponds and lakes; sedge meadow; migrants use freshwater environments of marshes, ponds, pools, and also flooded pastures, wet agricultural fields, impoundments	MSG3
Scolopacidae	WESA	Western Sandpiper	*Calidris mauri*	similar to Semipalmated Sandpiper; sand flats, mudflats; dwarf birch, grassy vegetation; during migration use river deltas, sandflats, agricultural fields, muddy river and lake margins, freshwater marshes	MSG3
Scolopacidae	SESA	Semipalmated Sandpiper	*Calidris pusilla*	mudflats (feeding); marsh edges, lakeshores, near ponds; dwarf willows, dwarf birch (nesting); migrates along mudflats, sandy beaches, shores of lakes and ponds, wet meadows	MSG3

Scolopacidae	LBDO	Long-billed Dowitcher	*Limnodromus scolopaceus*	mud or shallow water; wet grassy tundra (nesting); during migration use freshwater environments including lakes, ponds, marshes, flooded fields, also river margins	MSG3
Scolopacidae	HUGO	Hudsonian Godwit	*Limosa haemastica*	wet tundra, sedgy marshland (nesting); wetlands; small ponds, wet meadows; during migration use wetlands including lakes, pools, flooded agricultural areas, freshwater impoundments, wet pastures	MSG3
Scolopacidae	BBSA	Buff-breasted Sandpiper	*Tryngites subruficollis*	agricultural fields; tundra, sedge meadow (nesting); during migration use dry flat habitats including prairies, agricultural fields, pastures, grasslands	MSG4

Appendix Table 3. List of 41 mammal species included in the species-specific habitat projections.

\1 = introduced species;
\2 = game species (Alaska Department of Fish and Game, https://www.adfg.alaska.gov/index.cfm?adfg=hunting.species);
\3 state subsistence species (Alaska Department of Fish and Game, https://www.adfg.alaska.gov/index.cfm?adfg=subsistence.hunting);
\4 = small game species (Alaska Department of Fish and Game, https://www.adfg.alaska.gov/index.cfm?adfg=smallgamehunting.species).
\5 = habitat specialists, use ≤ 10 ecotypes

Family	Species Code	Common name	Scientific name
Bovidae	BISBIS	American bison \1, \2, \5	*Bison bison*
Bovidae	OVIDAL	Dall's sheep \2, \3, \5	*Ovis dalli*
Canidae	CANLAT	Coyote	*Canis latrans*
Canidae	CANLUP	Wolf, Gray wolf \2	*Canis lupus*
Canidae	VULVUL	Red fox	*Vulpes vulpes*
Castoridae	CASCAN	American beaver \3	*Castor canadensis*
Cervidae	ALCALC	Moose \2, \3	*Alces alces* [*americanus*]
Cervidae	RANTAR	Caribou \2, \3	*Rangifer tarandus*
Cricetidae	LEMTRI	Brown lemming	*Lemmus trimucronatus*
Cricetidae	MICMIU	Singing vole	*Microtus miurus*
Cricetidae	MICOEC	Root vole, Tundra vole, \5	*Microtus oeconomus*
Cricetidae	MICPEN	Meadow Vole	*Microtus pennsylvanicus*
Cricetidae	MICXAN	Taiga vole, Yellow-cheeked vole	*Microtus xanthrognatus*
Cricetidae	MYORUT	Northern red-backed vole	*Myodes rutilus*
Cricetidae	ONDZIB	Muskrat, \5	*Ondatra zibethicus*
Cricetidae	SYNBOR	Northern bog lemming, \5	*Synaptomys borealis*
Dipodidae	ZAPHUD	Meadow Jumping Mouse	*Zapus hudsonius*
Erethizontidae	EREDOR	North American porcupine	*Erethizon dorsatum*
Felidae	LYNCAN	Canadian lynx	*Lynx canadensis*
Leporidae	LEPAME	Snowshoe hare \4	*Lepus americanus*
Mustelidae	GULGUL	Wolverine	*Gulo gulo*
Mustelidae	LONCAN	North American river otter, Northern river otter	*Lontra canadensis*
Mustelidae	MARAME	American Marten	*Martes americana*
Mustelidae	MUSERM	Ermine, Short-tailed weasel	*Mustela erminea*
Mustelidae	MUSNIV	Least weasel	*Mustela nivalis*
Mustelidae	NEOVIS	American mink, \5	*Neovison vison*
Ochotonidae	OCHCOL	Collared pika, \5	*Ochotona collaris*
Sciuridae	GLASAB	Northern Flying squirrel	*Glaucomys sabrinus*

Sciuridae	MARCAL	Hoary marmot, \5	*Marmota caligata*
Sciuridae	MARMON	Woodchuck, \5	*Marmota monax*
Sciuridae	TAMHUD	Red Squirrel	*Tamiasciurus hudsonicus*
Sciuridae	UROPAR	Arctic ground squirrel	*Urocitellus parryii*
Soricidae	SORCIN	Cinereous shrew, Masked shrew, Common shrew	*Sorex cinereus*
Soricidae	SORHOY	American pygmy shrew	*Sorex hoyi*
Soricidae	SORMON	Montane shrew	*Sorex monticolus*
Soricidae	SORPAL	American water shrew, Northern water shrew	*Sorex palustris*
Soricidae	SORTUN	Tundra Shrew	*Sorex tundrensis*
Soricidae	SORYUK	Alaska tiny shrew	*Sorex yukonicus*
Ursidae	URSAME	American black bear \2, \3	*Ursus americanus*
Ursidae	URSARC	Brown bear \2, \3	*Ursus arctos*
Vespertilionidae	MYOLUC	Little brown myotis	*Myotis lucifugus*

Appendix Table 4. Percent change (Weber fraction) in habitat area of all 124 bird species over three time periods and four ecotype projection scenarios.

	Percent change 1949-2017	Percent change 2017-2100				Percent change 1949-2100			
Species	All models	Climate Model RCP 4.5	Climate Model RCP 8.5	Driver-Adjusted Climate Model RCP 6.0	Time Model, Historical Rates	Climate Model RCP 4.5	Climate Model RCP 8.5	Driver-Adjusted Climate Model RCP 6.0	Time Model, Historical Rates
Northern Goshawk	35.9%	-9.6%	-13.3%	-28.1%	2.9%	22.9%	17.9%	-2.2%	8.9%
Sharp-shinned Hawk	11.6%	-5.6%	-5.9%	-22.3%	3.4%	5.4%	5.0%	-13.3%	20.5%
Golden Eagle	-18.7%	-5.7%	-5.3%	-5.0%	4.9%	-23.4%	-23.0%	-22.8%	22.0%
Red-tailed Hawk	11.6%	-5.6%	-5.9%	-22.3%	3.4%	5.4%	5.0%	-13.3%	20.5%
Rough-legged Hawk	-21.6%	-11.0%	-10.9%	-26.1%	3.4%	-30.2%	-30.1%	-42.1%	13.7%
Northern Harrier	-18.4%	-3.3%	-2.7%	3.0%	12.7%	-21.1%	-20.6%	-15.9%	41.3%
Bald Eagle	-16.1%	-20.2%	-20.2%	19.0%	-18.2%	-33.1%	-33.0%	-0.2%	-31.4%
Horned Lark	0.0%	-3.7%	-3.9%	-3.7%	-3.9%	-3.7%	-3.9%	-3.7%	-3.9%
Belted Kingfisher	9.4%	-4.7%	-5.0%	-20.2%	3.1%	4.3%	3.9%	-12.7%	18.2%
Northern Pintail	49.4%	-2.6%	-6.1%	-1.1%	-1.8%	45.5%	40.3%	47.7%	8.6%
American Wigeon	160.6%	-4.9%	-14.1%	19.7%	0.2%	147.9%	123.8%	212.0%	60.3%
Northern Shoveler	36.1%	49.1%	52.4%	187.2%	3.1%	103.0%	107.4%	290.8%	58.6%
Green-winged Teal	160.6%	-4.9%	-14.1%	19.7%	0.2%	147.9%	123.8%	212.0%	60.3%
Mallard	15.7%	40.4%	43.1%	157.6%	0.5%	62.4%	65.5%	198.0%	53.0%
Lesser Scaup	36.1%	49.1%	52.4%	187.2%	3.1%	103.0%	107.4%	290.8%	58.6%
Redhead	67.1%	79.6%	85.0%	313.5%	3.4%	200.0%	209.1%	590.9%	68.0%
Ring-necked Duck	55.9%	70.8%	75.7%	283.8%	5.9%	166.3%	173.9%	498.4%	91.4%
Greater Scaup	36.1%	49.1%	52.4%	187.2%	3.1%	103.0%	107.4%	290.8%	58.6%
Canvasback	15.7%	40.4%	43.1%	157.6%	0.5%	62.4%	65.5%	198.0%	53.0%
Canada goose	32.2%	24.6%	27.8%	86.2%	0.6%	64.7%	68.9%	146.2%	54.0%

Bufflehead	19.5%	-13.3%	-13.3%	0.3%	2.9%	3.6%	3.6%	19.8%	29.5%
Common Goldeneye	-1.2%	-4.4%	-4.0%	26.9%	-15.8%	-5.5%	-5.1%	25.5%	-5.2%
Barrow's Goldeneye	-1.2%	-4.4%	-4.0%	26.9%	-15.8%	-5.5%	-5.1%	25.5%	-5.2%
Trumpeter Swan	53.0%	0.9%	-2.6%	30.9%	2.6%	54.4%	48.9%	100.3%	33.7%
Harlequin Duck	48.1%	0.0%	-0.4%	0.8%	-29.8%	48.1%	47.6%	49.3%	-37.2%
White-winged Scoter	30.0%	12.4%	12.9%	28.7%	1.5%	46.1%	46.7%	67.3%	53.2%
Common Merganser	-1.2%	-4.4%	-4.0%	26.9%	-15.8%	-5.5%	-5.1%	25.5%	-5.2%
Red-breasted Merganser	16.7%	-1.0%	-0.8%	-0.3%	2.0%	15.5%	15.7%	16.3%	36.6%
Bohemian Waxwing	40.6%	-6.0%	-9.0%	-16.1%	3.3%	32.2%	27.9%	17.9%	12.0%
American Golden-Plover	-14.0%	3.2%	4.1%	22.2%	4.6%	-11.3%	-10.5%	5.1%	93.4%
American Dipper	34.6%	16.8%	17.5%	11.7%	-3.8%	57.2%	58.2%	50.3%	94.9%
Rock Dove	n/a \1	38.5%	37.6%	25.3%	-8.4%	n/a \1	n/a \1	n/a \1	877.8%
Common Raven	9.7%	-3.0%	-3.2%	-18.1%	0.2%	6.5%	6.2%	-10.1%	37.1%
Gray Jay	18.0%	-0.9%	-1.5%	-6.2%	3.7%	17.0%	16.3%	10.7%	13.8%
Black-billed Magpie	521.2%	-11.7%	-24.4%	3.3%	14.8%	448.5%	369.7%	541.8%	151.8%
Merlin	-5.7%	-4.0%	-4.2%	-12.4%	4.4%	-9.4%	-9.6%	-17.4%	11.2%
Peregrine Falcon	-17.9%	-3.2%	-2.6%	2.9%	10.6%	-20.5%	-20.0%	-15.5%	34.5%
Gyrfalcon	61.1%	-15.8%	-21.2%	-31.3%	2.9%	35.7%	26.9%	10.6%	12.8%
American Kestrel	13.9%	-1.9%	-2.0%	-7.1%	3.9%	11.7%	11.7%	5.9%	23.1%
Common Redpoll	-4.3%	-3.9%	-4.1%	-11.7%	4.2%	-8.0%	-8.2%	-15.5%	13.9%
Hoary Redpoll	-4.3%	-3.9%	-4.1%	-11.7%	4.2%	-8.0%	-8.2%	-15.5%	13.9%
Gray-crowned Rosy-Finch	0.0%	-3.7%	-3.9%	-3.7%	-3.9%	-3.7%	-3.9%	-3.7%	-3.9%
White-winged Crossbill	12.1%	-4.0%	-4.2%	-21.0%	1.5%	7.7%	7.5%	-11.4%	35.9%
Pine Grosbeak	25.7%	15.3%	16.0%	8.0%	2.0%	45.0%	45.8%	35.7%	34.3%
Pine Siskin	12.2%	-4.2%	-4.3%	-21.2%	0.7%	7.5%	7.3%	-11.7%	34.9%
Common Loon	36.8%	49.9%	53.2%	190.1%	3.1%	105.1%	109.6%	296.9%	59.6%
Pacific Loon	36.1%	49.1%	52.4%	187.2%	3.1%	103.0%	107.4%	290.8%	58.6%
Sandhill Crane	-11.3%	2.5%	2.5%	26.1%	28.5%	-9.1%	-9.1%	11.8%	217.7%
Cliff Swallow	9.1%	39.2%	40.3%	43.2%	-5.8%	51.9%	53.0%	56.2%	98.9%
Bank Swallow	9.1%	39.2%	40.3%	43.2%	-5.8%	51.9%	53.0%	56.2%	98.9%
Tree Swallow	15.9%	0.2%	0.1%	-4.6%	0.7%	16.0%	16.0%	10.6%	40.1%

Violet-green Swallow	13.6%	0.2%	0.1%	-4.5%	0.6%	13.8%	13.8%	8.5%	39.4%
Red-winged Blackbird	183.5%	6.1%	-0.2%	47.5%	-5.0%	200.8%	183.1%	318.2%	-14.9%
Rusty Blackbird	5.2%	-10.5%	-10.8%	-1.7%	8.2%	-5.8%	-6.1%	3.4%	83.6%
Northern Shrike	-6.4%	-7.9%	-8.5%	-18.6%	5.4%	-13.7%	-14.4%	-23.8%	15.1%
Bonaparte's Gull	7.3%	-12.3%	-12.6%	-4.9%	8.8%	-5.9%	-6.2%	2.1%	117.6%
Mew Gull	30.7%	62.4%	65.9%	211.1%	-2.2%	112.2%	116.8%	306.6%	90.6%
Herring Gull	46.3%	41.7%	45.9%	147.7%	-3.6%	107.4%	113.5%	262.5%	-45.8%
Arctic Tern	38.3%	61.4%	65.1%	212.4%	-2.2%	123.1%	128.2%	332.0%	93.9%
American Pipit	21.7%	-0.1%	2.3%	-10.7%	-8.4%	21.6%	24.6%	8.7%	10.9%
Northern Wheatear	45.7%	0.4%	3.0%	-11.0%	-8.1%	46.2%	50.1%	29.7%	15.4%
Osprey	4.1%	0.7%	0.6%	0.9%	2.7%	4.8%	4.7%	5.0%	10.5%
Black-capped Chickadee	40.2%	-6.4%	-9.8%	-15.9%	3.7%	31.3%	26.5%	18.0%	13.6%
Boreal Chickadee	17.3%	2.4%	1.6%	4.3%	2.9%	20.1%	19.3%	22.4%	12.2%
Wilson's Warbler	-5.5%	-7.6%	-8.3%	-23.9%	5.8%	-12.7%	-13.4%	-28.1%	15.8%
Orange-crowned Warbler	26.2%	3.0%	1.9%	-8.6%	3.7%	30.0%	28.6%	15.3%	7.7%
Northern Waterthrush	5.9%	-17.6%	-19.9%	-35.6%	1.8%	-12.8%	-15.2%	-31.8%	-13.1%
Yellow-rumped Warbler	35.4%	-9.9%	-13.5%	-27.6%	2.1%	22.0%	17.1%	-1.9%	8.8%
Yellow Warbler	78.2%	-16.3%	-24.7%	-32.3%	4.5%	49.2%	34.2%	20.7%	-18.2%
Blackpoll Warbler	18.4%	-2.7%	-3.6%	-7.3%	4.0%	15.1%	14.2%	9.7%	11.2%
Townsend's Warbler	16.2%	-2.6%	-3.5%	-21.6%	-1.0%	13.2%	12.2%	-9.0%	1.0%
Dark-eyed (Slate-col.) Junco	37.9%	-2.7%	-5.3%	-1.8%	4.2%	34.1%	30.6%	35.3%	14.5%
Lincoln's Sparrow	36.7%	-2.9%	-6.2%	-3.0%	1.5%	32.7%	28.2%	32.6%	6.3%
Savannah Sparrow	-15.8%	1.0%	1.9%	20.8%	24.6%	-14.9%	-14.2%	1.8%	90.6%
Fox Sparrow	-4.1%	-5.6%	-6.2%	-14.5%	4.1%	-9.5%	-10.1%	-18.1%	13.7%
American Tree Sparrow	-20.5%	-5.0%	-5.9%	-3.0%	15.6%	-24.4%	-25.1%	-22.9%	10.3%
Golden-crowned Sparrow	75.7%	-12.7%	-19.0%	-28.9%	6.5%	53.4%	42.4%	25.0%	-14.9%
White-crowned Sparrow	-6.6%	-7.5%	-7.8%	-15.8%	5.6%	-13.6%	-13.9%	-21.3%	15.9%
Ruffed Grouse	38.1%	-10.6%	-14.4%	-31.5%	3.5%	23.5%	18.2%	-5.4%	8.9%
Spruce Grouse	12.1%	-4.0%	-4.2%	-21.0%	1.5%	7.7%	7.5%	-11.4%	35.9%
Willow Ptarmigan	74.1%	-13.1%	-19.3%	-29.0%	14.7%	51.4%	40.5%	23.6%	4.1%
Rock Ptarmigan	57.0%	-14.7%	-20.2%	-29.6%	13.9%	33.8%	25.2%	10.5%	35.0%

Sharp-tailed Grouse	183.6%	5.1%	-1.3%	47.2%	-7.0%	198.2%	179.8%	317.3%	-62.8%
Arctic Warbler	-56.9%	5.1%	13.9%	-7.3%	17.2%	-54.8%	-50.9%	-60.1%	-0.2%
Northern Flicker	14.9%	0.6%	0.4%	-7.8%	2.4%	15.6%	15.4%	6.0%	13.0%
Black-backed Woodpecker	-32.0%	-6.9%	-3.0%	-28.1%	14.2%	-36.7%	-34.1%	-51.1%	70.8%
American Three-toed Woodpecker	12.1%	-4.0%	-4.2%	-21.0%	1.5%	7.7%	7.5%	-11.4%	35.9%
Downy Woodpecker	18.3%	1.3%	1.1%	-10.7%	3.9%	19.9%	19.7%	5.6%	17.7%
Hairy Woodpecker	38.6%	-10.1%	-13.9%	-28.6%	2.8%	24.6%	19.4%	-1.1%	8.9%
Horned Grebe	37.7%	68.1%	72.8%	259.4%	3.1%	131.4%	137.9%	394.8%	71.8%
Red-necked Grebe	38.0%	52.4%	55.9%	195.8%	2.5%	110.4%	115.2%	308.3%	56.7%
Ruby-crowned Kinglet	15.7%	1.3%	1.5%	1.5%	3.2%	17.2%	17.4%	17.3%	44.4%
Spotted Sandpiper	-47.4%	-11.8%	-12.6%	-13.2%	9.0%	-53.6%	-54.0%	-54.3%	9.0%
Upland Sandpiper	65.7%	2.9%	6.7%	-12.7%	38.7%	70.4%	76.7%	44.6%	259.3%
Dunlin	41.7%	57.0%	61.0%	229.4%	36.7%	122.4%	128.1%	366.6%	302.8%
Pectoral Sandpiper	31.8%	25.5%	29.1%	93.7%	26.5%	65.5%	70.1%	155.4%	184.5%
Least Sandpiper	61.3%	37.8%	42.0%	146.4%	25.4%	122.4%	129.1%	297.6%	203.7%
Semipalmated Plover	0.0%	39.5%	40.6%	44.0%	-1.5%	39.5%	40.6%	44.0%	122.0%
Wilson's Snipe	176.7%	3.8%	-1.9%	41.5%	24.5%	187.3%	171.4%	291.6%	217.6%
Whimbrel	66.4%	1.2%	-2.4%	32.3%	19.0%	68.5%	62.4%	120.1%	68.3%
Red Phalarope	36.6%	66.7%	71.3%	254.1%	3.1%	127.7%	134.1%	383.7%	70.5%
Red-necked Phalarope	13.6%	46.4%	49.4%	174.3%	2.1%	66.3%	69.8%	211.6%	52.7%
Lesser Yellowlegs	19.8%	1.8%	3.0%	32.5%	20.9%	21.9%	23.3%	58.7%	181.5%
Wandering Tattler	-23.9%	4.5%	3.8%	12.1%	-11.3%	-20.4%	-21.0%	-14.7%	-11.3%
Greater Yellowlegs	144.4%	90.5%	96.6%	379.1%	18.2%	365.7%	380.5%	1071.2%	181.8%
Solitary Sandpiper	144.4%	90.5%	96.6%	379.1%	18.2%	365.7%	380.5%	1071.2%	181.8%
Red-breasted Nuthatch	12.1%	-4.0%	-4.2%	-21.0%	1.5%	7.7%	7.5%	-11.4%	35.9%
Boreal Owl	11.6%	-5.6%	-5.9%	-22.3%	3.4%	5.4%	5.0%	-13.3%	20.5%
Short-eared Owl	-15.7%	1.2%	2.1%	21.2%	13.3%	-14.7%	-13.9%	2.2%	48.8%
Snowy Owl	-17.9%	-3.5%	-2.9%	2.7%	11.4%	-20.8%	-20.3%	-15.7%	36.6%
Great Horned Owl	11.6%	-5.6%	-5.9%	-22.3%	3.4%	5.4%	5.0%	-13.3%	20.5%
Great Gray Owl	13.9%	-1.9%	-2.0%	-7.1%	3.9%	11.7%	11.7%	5.9%	23.1%

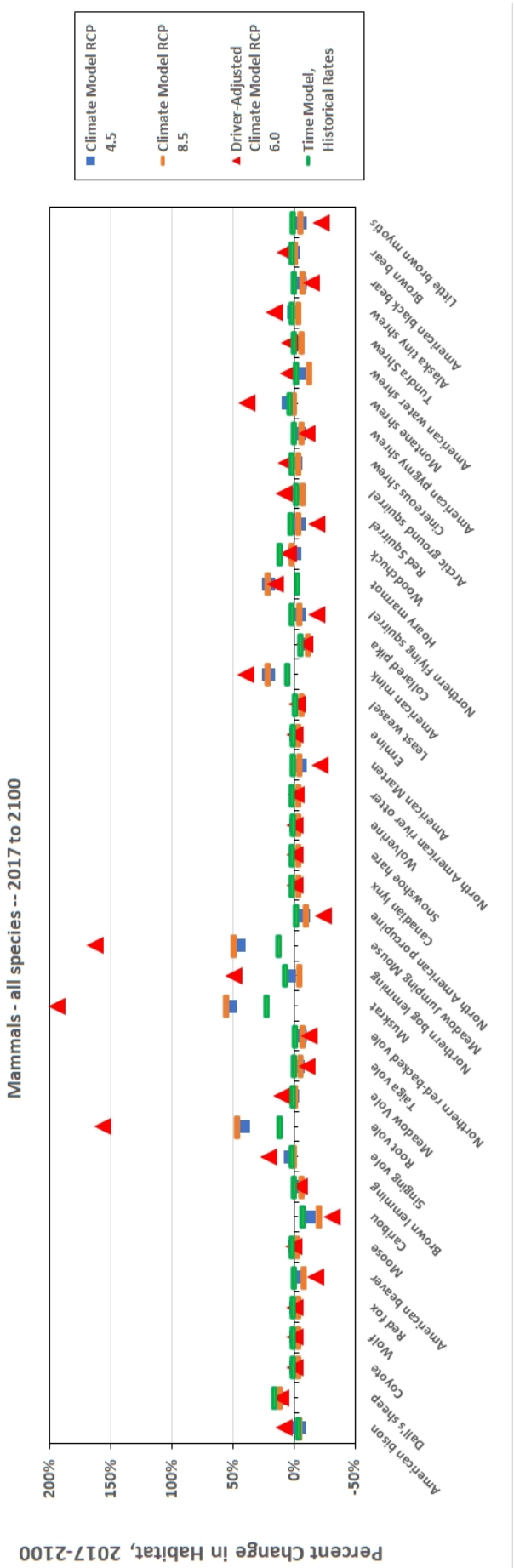
Northern Hawk Owl	13.9%	-1.9%	-2.0%	-7.1%	3.9%	11.7%	11.7%	5.9%	23.1%
Hermit Thrush	15.9%	-4.2%	-5.0%	-20.4%	3.3%	11.0%	10.1%	-7.7%	11.6%
Gray-cheeked Thrush	-5.4%	-7.2%	-7.8%	-23.2%	2.9%	-12.2%	-12.9%	-27.4%	-17.4%
Swainson's Thrush	11.7%	-4.8%	-5.1%	-21.3%	0.3%	6.3%	6.0%	-12.1%	-21.0%
Varied Thrush	14.4%	-4.4%	-5.2%	-19.3%	0.0%	9.4%	8.4%	-7.6%	-21.2%
Townsend's Solitaire	70.5%	5.4%	4.4%	1.8%	6.6%	79.7%	78.0%	73.5%	-11.1%
American Robin	-1.5%	-4.4%	-4.6%	-13.5%	1.4%	-5.8%	-6.1%	-14.8%	-16.3%
Olive-sided Flycatcher	15.9%	1.1%	0.4%	-5.2%	-0.5%	17.1%	16.4%	9.8%	2.9%
Western Wood-Pewee	16.5%	-5.1%	-5.4%	-28.5%	-3.2%	10.5%	10.3%	-16.7%	8.7%
Alder Flycatcher	23.6%	-1.7%	-2.5%	-11.1%	-2.7%	21.5%	20.5%	9.9%	-3.5%
Hammond's Flycatcher	15.2%	-6.1%	-7.0%	-25.3%	3.2%	8.2%	7.1%	-14.0%	6.6%
Say's Phoebe	-5.8%	31.4%	32.3%	34.5%	-5.5%	23.8%	24.7%	26.7%	92.4%

\1 n/a = calculation of percent change is not applicable because initial habitat amount (the denominator in the change calculation) is zero.

Appendix Table 5. Percent change (Weber fraction) in habitat area of all 41 mammal species over three time periods and four ecotype projection scenarios.

	Percent change 1949-2017	Percent change 2017-2100				Percent change 1949-2100			
Species	All models	Climate Model RCP 4.5	Climate Model RCP 8.5	Driver-Adjusted Climate Model RCP 6.0	Time Model, Historical Rates	Climate Model RCP 4.5	Climate Model RCP 8.5	Driver-Adjusted Climate Model RCP 6.0	Time Model, Historical Rates
American bison	-22.3%	-3.9%	-5.1%	8.0%	-3.6%	-25.3%	-26.2%	-16.1%	-25.1%
Dall's sheep	35.1%	9.2%	11.0%	11.1%	15.9%	47.6%	49.9%	50.1%	56.7%
Coyote	27.7%	-1.8%	-3.6%	-0.6%	0.8%	25.4%	23.1%	26.9%	28.8%
Wolf	27.7%	-1.8%	-3.6%	-0.6%	0.8%	25.4%	23.1%	26.9%	28.8%
Red fox	27.7%	-1.8%	-3.6%	-0.6%	0.8%	25.4%	23.1%	26.9%	28.8%
American beaver	39.7%	-5.4%	-8.8%	-17.9%	-0.7%	32.1%	27.4%	14.6%	38.7%
Moose	26.8%	-1.1%	-3.1%	0.2%	1.2%	25.4%	22.8%	27.0%	28.4%
Caribou	167.3%	-12.5%	-21.0%	-30.9%	-7.4%	134.0%	111.2%	84.6%	147.5%
Brown lemming	27.1%	-4.1%	-6.3%	-4.4%	0.0%	22.0%	19.1%	21.6%	27.2%
Singing vole	47.9%	2.5%	-0.5%	21.1%	1.7%	51.7%	47.2%	79.1%	50.4%
Root vole	62.1%	41.6%	46.1%	156.8%	11.0%	129.6%	136.7%	316.2%	80.0%
Meadow Vole	40.2%	0.9%	-1.5%	9.6%	1.0%	41.4%	38.1%	53.6%	41.5%
Taiga vole	25.3%	-3.6%	-5.8%	-11.0%	0.1%	20.8%	17.9%	11.4%	25.4%
Northern red-backed vole	25.6%	-5.4%	-7.5%	-12.4%	-1.0%	18.9%	16.2%	10.1%	24.4%
Muskrat	37.6%	52.0%	55.5%	194.3%	22.5%	109.2%	114.0%	305.1%	68.5%
Northern bog lemming	257.5%	3.7%	-4.3%	49.2%	6.7%	270.7%	242.0%	433.3%	281.4%
Meadow Jumping Mouse	47.9%	44.4%	49.1%	162.9%	12.1%	113.6%	120.5%	288.8%	65.7%

North American porcupine	28.3%	-7.7%	-10.1%	-24.0%	-1.7%	18.3%	15.3%	-2.5%	26.1%
Canadian lynx	26.7%	-1.9%	-3.8%	-0.8%	1.1%	24.2%	21.9%	25.6%	28.0%
Snowshoe hare	26.7%	-1.9%	-3.8%	-0.8%	1.1%	24.2%	21.9%	25.6%	28.0%
Wolverine	27.7%	-1.8%	-3.6%	-0.6%	0.8%	25.4%	23.1%	26.9%	28.8%
North American river otter	39.8%	-1.2%	-4.1%	-1.5%	1.1%	38.1%	34.1%	37.6%	41.3%
American Marten	11.7%	-4.8%	-5.1%	-21.3%	0.8%	6.3%	6.0%	-12.1%	12.6%
Ermine	27.7%	-1.8%	-3.6%	-0.6%	0.8%	25.4%	23.1%	26.9%	28.8%
Least weasel	22.9%	-4.6%	-6.9%	-2.3%	-1.3%	17.3%	14.5%	20.1%	21.3%
American mink	37.5%	20.5%	21.4%	39.4%	5.2%	65.7%	66.9%	91.7%	44.6%
Collared pika	-1.1%	-10.6%	-11.6%	-9.0%	-5.7%	-11.6%	-12.5%	-10.0%	-6.7%
Northern Flying squirrel	12.7%	-4.4%	-4.5%	-18.7%	1.7%	7.8%	7.6%	-8.4%	14.6%
Hoary marmot	12.5%	20.3%	21.3%	15.2%	-3.3%	35.3%	36.5%	29.6%	8.7%
Woodchuck	60.0%	-0.4%	1.2%	4.5%	11.4%	59.3%	61.9%	67.2%	78.2%
Red Squirrel	12.7%	-4.2%	-4.3%	-18.6%	2.0%	8.0%	7.8%	-8.2%	15.0%
Arctic ground squirrel	56.5%	-2.7%	-7.2%	7.8%	-1.8%	52.3%	45.3%	68.7%	53.6%
Cinereous shrew	30.0%	-1.7%	-3.6%	6.1%	1.1%	27.8%	25.3%	37.9%	31.4%
American pygmy shrew	28.8%	-4.2%	-6.4%	-11.0%	0.1%	23.4%	20.5%	14.6%	28.9%
Montane shrew	116.2%	5.0%	-0.1%	38.7%	2.9%	126.9%	116.0%	199.8%	122.4%
American water shrew	227.2%	-4.6%	-12.9%	4.6%	-2.3%	212.1%	185.1%	242.2%	219.7%
Tundra Shrew	26.1%	-3.8%	-6.2%	4.1%	-0.3%	21.3%	18.4%	31.3%	25.7%
Alaska tiny shrew	55.8%	-0.2%	-3.6%	15.9%	1.2%	55.5%	50.2%	80.6%	57.7%
American black bear	26.2%	-5.5%	-7.7%	-14.0%	-0.5%	19.2%	16.5%	8.4%	25.5%
Brown bear	28.9%	0.2%	-1.6%	7.0%	1.5%	29.2%	26.8%	37.9%	30.8%
Little brown myotis	11.4%	-5.5%	-5.8%	-22.2%	0.6%	5.3%	4.9%	-13.3%	12.0%



Appendix Figure 1. Projected future changes in habitat, 2017 to 2100, of all 41 mammal species of the Fort Wainwright study area, under four ecotype projection scenarios.

Appendix Table 6. Percent change (Weber fraction) in habitat area of 25 bird species denoted by Alaska Department of Fish and Game as game species or small game species, over three time periods and four ecotype projection scenarios. See Appendix Table 1 for source.

	Percent change 1949-2017	Percent change 2017-2100				Percent change 1949-2100			
Species	All models	Climate Model RCP 4.5	Climate Model RCP 8.5	Driver-Adjusted Climate Model RCP 6.0	Time Model, Historical Rates	Climate Model RCP 4.5	Climate Model RCP 8.5	Driver-Adjusted Climate Model RCP 6.0	Time Model, Historical Rates
Northern Pintail	49.4%	-2.6%	-6.1%	-1.1%	-1.8%	45.5%	40.3%	47.7%	8.6%
American Wigeon	160.6%	-4.9%	-14.1%	19.7%	0.2%	147.9%	123.8%	212.0%	60.3%
Northern Shoveler	36.1%	49.1%	52.4%	187.2%	3.1%	103.0%	107.4%	290.8%	58.6%
Green-winged Teal	160.6%	-4.9%	-14.1%	19.7%	0.2%	147.9%	123.8%	212.0%	60.3%
Mallard	15.7%	40.4%	43.1%	157.6%	0.5%	62.4%	65.5%	198.0%	53.0%
Lesser Scaup	36.1%	49.1%	52.4%	187.2%	3.1%	103.0%	107.4%	290.8%	58.6%
Redhead	67.1%	79.6%	85.0%	313.5%	3.4%	200.0%	209.1%	590.9%	68.0%
Ring-necked Duck	55.9%	70.8%	75.7%	283.8%	5.9%	166.3%	173.9%	498.4%	91.4%
Greater Scaup	36.1%	49.1%	52.4%	187.2%	3.1%	103.0%	107.4%	290.8%	58.6%
Canvasback	15.7%	40.4%	43.1%	157.6%	0.5%	62.4%	65.5%	198.0%	53.0%
Canada goose	32.2%	24.6%	27.8%	86.2%	0.6%	64.7%	68.9%	146.2%	54.0%
Bufflehead	19.5%	-13.3%	-13.3%	0.3%	2.9%	3.6%	3.6%	19.8%	29.5%
Common Goldeneye	-1.2%	-4.4%	-4.0%	26.9%	-15.8%	-5.5%	-5.1%	25.5%	-5.2%
Barrow's Goldeneye	-1.2%	-4.4%	-4.0%	26.9%	-15.8%	-5.5%	-5.1%	25.5%	-5.2%
Trumpeter Swan	53.0%	0.9%	-2.6%	30.9%	2.6%	54.4%	48.9%	100.3%	33.7%
Harlequin Duck	48.1%	0.0%	-0.4%	0.8%	-29.8%	48.1%	47.6%	49.3%	-37.2%
White-winged Scoter	30.0%	12.4%	12.9%	28.7%	1.5%	46.1%	46.7%	67.3%	53.2%

Common Merganser	-1.2%	-4.4%	-4.0%	26.9%	-15.8%	-5.5%	-5.1%	25.5%	-5.2%
Red-breasted Merganser	16.7%	-1.0%	-0.8%	-0.3%	2.0%	15.5%	15.7%	16.3%	36.6%
Sandhill Crane	-11.3%	2.5%	2.5%	26.1%	28.5%	-9.1%	-9.1%	11.8%	217.7%
Ruffed Grouse	38.1%	-10.6%	-14.4%	-31.5%	3.5%	23.5%	18.2%	-5.4%	8.9%
Spruce Grouse	12.1%	-4.0%	-4.2%	-21.0%	1.5%	7.7%	7.5%	-11.4%	35.9%
Willow Ptarmigan	74.1%	-13.1%	-19.3%	-29.0%	14.7%	51.4%	40.5%	23.6%	4.1%
Rock Ptarmigan	57.0%	-14.7%	-20.2%	-29.6%	13.9%	33.8%	25.2%	10.5%	35.0%
Sharp-tailed Grouse	183.6%	5.1%	-1.3%	47.2%	-7.0%	198.2%	179.8%	317.3%	-62.8%

Appendix Table 7. Percent change (Weber fraction) in habitat area of 14 bird species denoted as habitat specialists (i.e., that each use ≤ 5 ecotypes; see Appendix A.2.1).

	Percent change 1949-2017	Percent change 2017-2100				Percent change 1949-2100			
Species	All models	Climate Model RCP 4.5	Climate Model RCP 8.5	Driver-Adjusted Climate Model RCP 6.0	Time Model, Historical Rates	Climate Model RCP 4.5	Climate Model RCP 8.5	Driver-Adjusted Climate Model RCP 6.0	Time Model, Historical Rates
Bald Eagle	-16.1%	-20.2%	-20.2%	19.0%	-18.2%	-33.1%	-33.0%	-0.2%	-31.4%
Horned Lark	0.0%	-3.7%	-3.9%	-3.7%	-3.9%	-3.7%	-3.9%	-3.7%	-3.9%
Redhead	67.1%	79.6%	85.0%	313.5%	3.4%	200.0%	209.1%	590.9%	68.0%
Harlequin Duck	48.1%	0.0%	-0.4%	0.8%	-29.8%	48.1%	47.6%	49.3%	-37.2%
Gray-crowned Rosy-Finch	0.0%	-3.7%	-3.9%	-3.7%	-3.9%	-3.7%	-3.9%	-3.7%	-3.9%
Rusty Blackbird	5.2%	-10.5%	-10.8%	-1.7%	8.2%	-5.8%	-6.1%	3.4%	83.6%
Bonaparte's Gull	7.3%	-12.3%	-12.6%	-4.9%	8.8%	-5.9%	-6.2%	2.1%	117.6%
Osprey	4.1%	0.7%	0.6%	0.9%	2.7%	4.8%	4.7%	5.0%	10.5%
Horned Grebe	37.7%	68.1%	72.8%	259.4%	3.1%	131.4%	137.9%	394.8%	71.8%
Spotted Sandpiper	-47.4%	-11.8%	-12.6%	-13.2%	9.0%	-53.6%	-54.0%	-54.3%	9.0%
Upland Sandpiper	65.7%	2.9%	6.7%	-12.7%	38.7%	70.4%	76.7%	44.6%	259.3%
Dunlin	41.7%	57.0%	61.0%	229.4%	36.7%	122.4%	128.1%	366.6%	302.8%
Greater Yellowlegs	144.4%	90.5%	96.6%	379.1%	18.2%	365.7%	380.5%	1071.2%	181.8%
Solitary Sandpiper	144.4%	90.5%	96.6%	379.1%	18.2%	365.7%	380.5%	1071.2%	181.8%

Appendix Table 8. Percent change (Weber fraction) in habitat area of 12 raptor bird species.

	Percent change 1949-2017	Percent change 2017-2100				Percent change 1949-2100			
Species	All models	Climate Model RCP 4.5	Climate Model RCP 8.5	Driver-Adjusted Climate Model RCP 6.0	Time Model, Historical Rates	Climate Model RCP 4.5	Climate Model RCP 8.5	Driver-Adjusted Climate Model RCP 6.0	Time Model, Historical Rates
Northern Goshawk	35.9%	-9.6%	-13.3%	-28.1%	2.9%	22.9%	17.9%	-2.2%	8.9%
Sharp-shinned Hawk	11.6%	-5.6%	-5.9%	-22.3%	3.4%	5.4%	5.0%	-13.3%	20.5%
Golden Eagle	-18.7%	-5.7%	-5.3%	-5.0%	4.9%	-23.4%	-23.0%	-22.8%	22.0%
Red-tailed Hawk	11.6%	-5.6%	-5.9%	-22.3%	3.4%	5.4%	5.0%	-13.3%	20.5%
Rough-legged Hawk	-21.6%	-11.0%	-10.9%	-26.1%	3.4%	-30.2%	-30.1%	-42.1%	13.7%
Northern Harrier	-18.4%	-3.3%	-2.7%	3.0%	12.7%	-21.1%	-20.6%	-15.9%	41.3%
Bald Eagle	-16.1%	-20.2%	-20.2%	19.0%	-18.2%	-33.1%	-33.0%	-0.2%	-31.4%
Merlin	-5.7%	-4.0%	-4.2%	-12.4%	4.4%	-9.4%	-9.6%	-17.4%	11.2%
Peregrine Falcon	-17.9%	-3.2%	-2.6%	2.9%	10.6%	-20.5%	-20.0%	-15.5%	34.5%
Gyrfalcon	61.1%	-15.8%	-21.2%	-31.3%	2.9%	35.7%	26.9%	10.6%	12.8%
American Kestrel	13.9%	-1.9%	-2.0%	-7.1%	3.9%	11.7%	11.7%	5.9%	23.1%
Osprey	4.1%	0.7%	0.6%	0.9%	2.7%	4.8%	4.7%	5.0%	10.5%

Appendix Table 9. Percent change (Weber fraction) in habitat area of 9 mammal species denoted by Alaska Department of Fish and Game as game or subsistence species, over three time periods and four ecotype projection scenarios. See Appendix A.2.3 for source.

	Percent change 1949-2017	Percent change 2017-2100				Percent change 1949-2100			
Species	All models	Climate Model RCP 4.5	Climate Model RCP 8.5	Driver-Adjusted Climate Model RCP 6.0	Time Model, Historical Rates	Climate Model RCP 4.5	Climate Model RCP 8.5	Driver-Adjusted Climate Model RCP 6.0	Time Model, Historical Rates
American bison	-22.3%	-3.9%	-5.1%	8.0%	-3.6%	-25.3%	-26.2%	-16.1%	-25.1%
Dall's sheep	35.1%	9.2%	11.0%	11.1%	15.9%	47.6%	49.9%	50.1%	56.7%
Wolf	27.7%	-1.8%	-3.6%	-0.6%	0.8%	25.4%	23.1%	26.9%	28.8%
American beaver	39.7%	-5.4%	-8.8%	-17.9%	-0.7%	32.1%	27.4%	14.6%	38.7%
Moose	26.8%	-1.1%	-3.1%	0.2%	1.2%	25.4%	22.8%	27.0%	28.4%
Caribou	167.3%	-12.5%	-21.0%	-30.9%	-7.4%	134.0%	111.2%	84.6%	147.5%
Snowshoe hare	26.7%	-1.9%	-3.8%	-0.8%	1.1%	24.2%	21.9%	25.6%	28.0%
American black bear	26.2%	-5.5%	-7.7%	-14.0%	-0.5%	19.2%	16.5%	8.4%	25.5%
Brown bear	28.9%	0.2%	-1.6%	7.0%	1.5%	29.2%	26.8%	37.9%	30.8%

Appendix Table 10. Percent change (Weber fraction) in habitat area of 9 mammal species denoted as habitat specialists (i.e., that each use ≤ 10 ecotypes; see Appendix A.2.3).

	Percent change 1949-2017	Percent change 2017-2100				Percent change 1949-2100			
Species	All models	Climate Model RCP 4.5	Climate Model RCP 8.5	Driver-Adjusted Climate Model RCP 6.0	Time Model, Historical Rates	Climate Model RCP 4.5	Climate Model RCP 8.5	Driver-Adjusted Climate Model RCP 6.0	Time Model, Historical Rates
American bison	-22.3%	-3.9%	-5.1%	8.0%	-3.6%	-25.3%	-26.2%	-16.1%	-25.1%
Dall's sheep	35.1%	9.2%	11.0%	11.1%	15.9%	47.6%	49.9%	50.1%	56.7%
Root vole	62.1%	41.6%	46.1%	156.8%	11.0%	129.6%	136.7%	316.2%	80.0%
Muskrat	37.6%	52.0%	55.5%	194.3%	22.5%	109.2%	114.0%	305.1%	68.5%
Northern bog lemming	257.5%	3.7%	-4.3%	49.2%	6.7%	270.7%	242.0%	433.3%	281.4%
American mink	37.5%	20.5%	21.4%	39.4%	5.2%	65.7%	66.9%	91.7%	44.6%
Collared pika	-1.1%	-10.6%	-11.6%	-9.0%	-5.7%	-11.6%	-12.5%	-10.0%	-6.7%
Hoary marmot	12.5%	20.3%	21.3%	15.2%	-3.3%	35.3%	36.5%	29.6%	8.7%
Woodchuck	60.0%	-0.4%	1.2%	4.5%	11.4%	59.3%	61.9%	67.2%	78.2%

Appendix Table 11. Percent change (Weber fraction) in habitat area of 12 carnivore mammal species (Appendix A.2.3).

	Percent change 1949-2017	Percent change 2017-2100				Percent change 1949-2100			
Species	All models	Climate Model RCP 4.5	Climate Model RCP 8.5	Driver-Adjusted Climate Model RCP 6.0	Time Model, Historical Rates	Climate Model RCP 4.5	Climate Model RCP 8.5	Driver-Adjusted Climate Model RCP 6.0	Time Model, Historical Rates
Coyote	27.7%	-1.8%	-3.6%	-0.6%	0.8%	25.4%	23.1%	26.9%	28.8%
Wolf	27.7%	-1.8%	-3.6%	-0.6%	0.8%	25.4%	23.1%	26.9%	28.8%
Red fox	27.7%	-1.8%	-3.6%	-0.6%	0.8%	25.4%	23.1%	26.9%	28.8%
Canadian lynx	26.7%	-1.9%	-3.8%	-0.8%	1.1%	24.2%	21.9%	25.6%	28.0%
American black bear	26.2%	-5.5%	-7.7%	-14.0%	-0.5%	19.2%	16.5%	8.4%	25.5%
Brown bear	28.9%	0.2%	-1.6%	7.0%	1.5%	29.2%	26.8%	37.9%	30.8%
Wolverine	27.7%	-1.8%	-3.6%	-0.6%	0.8%	25.4%	23.1%	26.9%	28.8%
American river otter	39.8%	-1.2%	-4.1%	-1.5%	1.1%	38.1%	34.1%	37.6%	41.3%
American Marten	11.7%	-4.8%	-5.1%	-21.3%	0.8%	6.3%	6.0%	-12.1%	12.6%
Ermine	27.7%	-1.8%	-3.6%	-0.6%	0.8%	25.4%	23.1%	26.9%	28.8%
Least weasel	22.9%	-4.6%	-6.9%	-2.3%	-1.3%	17.3%	14.5%	20.1%	21.3%
American mink	37.5%	20.5%	21.4%	39.4%	5.2%	65.7%	66.9%	91.7%	44.6%

Appendix Table 12. Form used for deploying automated audio recording units (ARUs) on Fort Wainwright study area, with data dictionary definitions.

ARU DEPLOYMENT AND RETRIEVAL -- DoD, U.S. Army, Fort Wainwright, Fairbanks AK

Field Form v. 22 May 2019 [190522]

Units: Cornell University Labs Swift ARUs (automated audio recording units)

Bruce G. Marcot, US Forest Service, bruce.marcot@usda.gov, 503-347-2277

AUTOMATED AUDIO RECORDING UNIT (ARU) DEPLOYMENT	
SITE DATA	
from Field Form v. 22 May 2019 [190522]	
Bruce G. Marcot, US Forest Service, bruce.marcot@usda.gov, 503-347-2277	
Variable name	**Definition**
ARU no. (SWxx)	each Swift ARU unit is given a unique number, as per SW01, SW02, …
SD Card no.	each SD card is given a unique number conforming to the Swift it is in, as per SW01, SW02 …
Date deployed (YYMMDD)	date that the Swift ARU is affixed to a tree in the field at the appropriate site location
Person(s) deploying	name(s) of the person(s) doing the ARU field deployment
Ecotype name	full name of the ecotype as per: Jorgenson, M. T., and D. Brown. n.d. Patterns and rates of landscape change in central Alaska. Unpublished report. 14 pp.
Ecotype general description	brief description of dominant tree species, age class, and site condition
UTM X	corresponding to longitude, from GPS
UTM Y	corresponding to latitude, from GPS
Elevation (m)	elevation ASL, from GPS
Location name (site ID)	code name of ecotype and site ID
ARU compass direction (N, NE, E, etc.)	degrees azimuth that the ARU is facing when deployed (strapped to a tree)
ARU slope direction (U,C,D: Up, Contour, Down)	degrees azimuth of the slope (if any) of the overall site (would be the same as ARU compass direction, above, if the ARU was pointed straight downhill)
Stream noise? (Y/N)	Y if any obvious, persistent stream sounds; N otherwise
Human noise? (Y/N)	Y if any obvious, persistent anthropogenic sounds; N otherwise
Photos taken at ARU point? (Y/N)	Y if all eight photos are taken at the ARU deployment site (see "Deployment Scheme of ARUs 190610.docx"); N otherwise

Site access notes (unit, road, mile, up/downslope, etc.)	brief description of site access
Comments	other misc. observations

Appendix Table 13. Locations of the 24 automated audio recording units (ARUs) used for bioacoustic and ecoacoustic studies of the Fort Wainwright study area, determined in the field using Garmin GPS units. See text Table 15 for further descriptions of ecotypes and site conditions of each recorder location.

Landscape type	ARU name	Latitude	Longitude
Lacustrine	LDTL1	64.867676	-147.73871
Lacustrine	LDTL2	64.763294	-147.04178
Lacustrine	USTL1	64.951332	-147.61775
Lacustrine	USTL2	64.94959	-147.60653
Lowland	LDSB2	64.703792	-148.29058
Lowland	LDSB6	64.75354	-147.04365
Lowland	LLSD1	64.712898	-148.29677
Lowland	LLSD3	64.71483	-148.28822
Lowland	LWBFX	64.753437	-147.05964
Lowland	LWFB4	64.542975	-147.09265
Lowland	LWNF1	64.702731	-148.31627
Lowland	LWNF9	64.754845	-147.0676
Riverine	RMBF1	64.696389	-148.28298
Riverine	RMBF5	64.546829	-147.08703
Riverine	RMNF1	64.694197	-148.28612
Riverine	RMNF8	64.549591	-147.0761
Riverine	RMTS3	64.690932	-148.2864
Riverine	RMTS4	64.567261	-147.07264
Upland	UMBF6	64.579254	-146.75142
Upland	UMBF7	64.585374	-146.72225
Upland	UMNF1	64.708563	-148.32045
Upland	UMNF5	64.580633	-146.76182
Upland	UMTLS7	64.661427	-146.68262
Upland	UMTLSX	64.692933	-146.68046

Appendix Table 14. Calculation of battery life of the Cornell Swift automated audio recording units (ARUs). Determining expected battery life was important for scheduling field visits to replace batteries in the ARUs so as to lose as little recording time as possible. These calculations were based on the Swift ARU units being programmed to audio-record for 10 minutes at the top of each hour, 24 hours a day and 7 days a week. Battery life did not vary significantly among landscape, successional stage, or disturbance conditions.

				Dates (m/d/y)		Ordinal date		No. days batteries last
Landscape	Successional Stage	Disturbance	Site	Start	End	Start	End	Difference (End-Start)
Lacustrine	Early	Thermokarst	USTL1	6/21/19	8/19/19	172	231	59
Lacustrine	Early	Thermokarst	USTL2	6/21/19	8/19/19	172	231	59
Lacustrine	Late	n/a	LDTL1	6/11/19	8/8/19	162	220	58
Lacustrine	Late	n/a	LDTL2	6/11/19	8/10/19	162	222	60
Lowland	Early	Fire	LLSD1	6/8/19	8/5/19	159	217	58
Lowland	Early	Fire	LLSD3	6/8/19	8/6/19	159	218	59
Lowland	Early	Thermokarst	LDSB2	6/8/19	8/6/19	159	218	59
Lowland	Early	Thermokarst	LDSB6	6/8/19	8/5/19	159	217	58
Lowland	Late	n/a	LWNF1	6/8/19	8/4/19	159	216	57
Lowland	Late	n/a	LWNF9	6/8/19	8/5/19	159	217	58
Lowland	Mid	n/a	LWBF4	6/8/19	8/8/19	159	220	61
Lowland	Mid	n/a	LWBFX	6/11/19	8/9/19	162	221	59
Riverine	Early	n/a	RMTS3	6/8/19	8/6/19	159	218	59
Riverine	Early	n/a	RMTS4	6/11/19	8/9/19	162	221	59
Riverine	Late	n/a	SW13	6/8/19	8/7/19	159	219	60
Riverine	Late	n/a	SW06	6/11/19	8/10/19	162	222	60
Riverine	Mid	n/a	RMBF1	6/8/19	8/6/19	159	218	59
Riverine	Mid	n/a	RMBF5	6/11/19	8/9/19	162	221	59
Upland	Early	n/a	UMTLS7	6/8/19	8/4/19	159	216	57
Upland	Early	n/a	UMTLSX	6/8/19	8/6/19	159	218	59
Upland	Late	n/a	UMNF1	6/8/19	8/6/19	159	218	59
Upland	Late	n/a	UMNF5	6/8/19	8/5/19	159	217	58
Upland	Mid	n/a	UMBF6	6/8/19	8/4/19	159	216	57
Upland	Mid	n/a	UMBF9	6/8/19	8/7/19	159	219	60

Appendix Table 15. Values of ecoacoustic indices calculated for 13 example sounds among acoustic categories (see main text Figure 86 for categories of acoustic types, and text Table 16 for names and descriptions of each ecoacoustic index shown here).

Acoustic Type	Category	Example	NDSI	ACI	ADI	AEI	BI	BGN	SNR	ACT	EVN	LFC	MFCI	HFCI	CENT
Anthrophony	aircraft	helicopter	-0.285	160.518	0.186	0.889	33.456	-33.920	10.320	0.098	0.910	0.135	0.037	0.018	0.112
Anthrophony	aircraft	jets	-0.077	159.069	0.279	0.875	45.981	-35.298	12.352	0.097	0.400	0.154	0.036	0.014	0.096
Anthrophony	aircraft	propeller	0.143	155.443	0.243	0.881	36.820	-38.770	8.703	0.065	0.086	0.097	0.028	0.013	0.116
Anthrophony	people	walking	-0.032	180.976	0.592	0.819	17.180	-29.550	12.820	0.044	0.468	0.150	0.150	0.150	0.114
Anthrophony	people	radio	0.066	156.097	0.462	0.825	38.669	-34.560	6.250	0.005	0.073	0.092	0.027	0.013	0.157
Anthrophony	vehicles	road	0.620	162.771	0.452	0.830	36.869	-33.855	5.985	0.014	0.088	0.113	0.023	0.013	0.129
Biophony	bird song	gulls & wind	0.487	156.116	0.040	0.898	74.570	-31.950	9.730	0.032	0.448	0.076	0.067	0.029	0.097
Biophony	bird song	high freq	0.476	158.791	0.324	0.849	42.618	-38.658	11.190	0.028	0.369	0.063	0.016	0.017	0.160
Biophony	bird song	low freq	0.055	151.789	0.190	0.888	21.488	-35.610	6.040	0.005	0.002	0.082	0.014	0.013	0.090
Biophony	bird song	cross freq	0.827	159.519	0.591	0.801	41.745	-36.840	6.373	0.003	0.017	0.064	0.059	0.016	0.136
Biophony	bird song	mid freq	0.679	157.817	0.561	0.794	36.304	-39.125	7.420	0.015	0.209	0.060	0.033	0.013	0.168
Biophony	birds	raptor call	-0.125	152.234	0.239	0.882	19.301	-32.310	6.120	0.004	0.002	0.090	0.016	0.013	0.067
Biophony	birds	woodpecker	0.483	162.597	0.072	0.896	59.373	-38.640	7.740	0.014	0.250	0.065	0.013	0.014	0.178
Biophony	insect	buzz	0.456	156.303	0.370	0.848	27.606	-35.905	9.240	0.026	0.186	0.139	0.025	0.015	0.114
Biophony	mammal	squirrel	0.684	160.831	0.420	0.828	46.941	-37.690	7.497	0.007	0.034	0.074	0.021	0.019	0.126
Biophony	rustling	moose	0.820	161.286	0.000	0.900	52.420	-36.830	14.500	0.041	0.603	0.081	0.016	0.015	0.102
Geophony	weather	rainfall	0.465	172.108	0.788	0.765	32.758	-37.022	20.047	0.056	0.402	0.076	0.059	0.054	0.231
Geophony	weather	rain plunks	0.511	158.946	0.316	0.858	53.327	-32.950	15.620	0.026	0.330	0.064	0.015	0.014	0.122
Geophony	weather	thunder	0.608	158.353	0.049	0.895	44.538	-35.570	20.419	0.194	1.815	0.093	0.023	0.017	0.099
Geophony	weather	wind	0.360	158.898	0.161	0.878	54.237	-27.153	19.823	0.180	1.822	0.118	0.030	0.023	0.055
Geophony	weather	silence	0.760	156.594	0.580	0.786	28.331	-40.817	4.350	0.002	0.001	0.054	0.013	0.013	0.186

Appendix Table 16. Correlation of 13 ecoacoustic indices (see text Figure 86 for categories of acoustic types, and text Table 16 for names and descriptions of each ecoacoustic index shown here).

Pearson correlation coefficient

Pearson Correlation Matrix	NDSI	ACI	ADI	AEI	BI	BGN	SNR	ACT	EVN	LFC	MFCI	HFCI	CENT
NDSI	1.000												
ACI	-0.008	1.000											
ADI	0.136	0.443	1.000										
AEI	-0.333	-0.391	-0.970	1.000									
BI	0.402	-0.145	-0.507	0.382	1.000								
BGN	-0.426	0.220	-0.205	0.297	0.062	1.000							
SNR	0.047	0.387	-0.163	0.147	0.271	0.378	1.000						
ACT	-0.164	0.086	-0.383	0.378	0.213	0.397	0.769	1.000					
EVN	-0.023	0.123	-0.433	0.381	0.305	0.469	0.789	0.938	1.000				
LFC	-0.624	0.291	-0.076	0.231	-0.289	0.541	0.197	0.426	0.284	1.000			
MFCI	-0.232	0.761	0.369	-0.276	-0.184	0.437	0.180	0.055	0.060	0.406	1.000		
HFCI	-0.242	0.856	0.359	-0.267	-0.319	0.416	0.265	0.055	0.089	0.385	0.915	1.000	
CENT	0.361	0.331	0.630	-0.702	-0.066	-0.646	-0.110	-0.394	-0.377	-0.476	0.003	0.048	1.000

Bonferroni probabilities; values < 0.05 denote significant correlations between denoted indices, shown here in yellow highlight (excluding indices correlated with themselves, as shown on the diagonal axis).

Matrix of Bonferroni Probabilities	NDSI	ACI	ADI	AEI	BI	BGN	SNR	ACT	EVN	LFC	MFCI	HFCI	CENT
NDSI	0.000												
ACI	1.000	0.000											
ADI	1.000	1.000	0.000										
AEI	1.000	1.000	0.000	0.000									
BI	1.000	1.000	1.000	1.000	0.000								
BGN	1.000	1.000	1.000	1.000	1.000	0.000							
SNR	1.000	1.000	1.000	1.000	1.000	1.000	0.000						
ACT	1.000	1.000	1.000	1.000	1.000	1.000	0.004	0.000					
EVN	1.000	1.000	1.000	1.000	1.000	1.000	0.002	0.000	0.000				
LFC	0.197	1.000	1.000	1.000	1.000	0.877	1.000	1.000	1.000	0.000			
MFCI	1.000	0.005	1.000	1.000	1.000	1.000	1.000	1.000	1.000	1.000	0.000		
HFCI	1.000	0.000	1.000	1.000	1.000	1.000	1.000	1.000	1.000	1.000	0.000	0.000	
CENT	1.000	1.000	0.173	0.030	1.000	0.121	1.000	1.000	1.000	1.000	1.000	1.000	0.000

Appendix A.2. Issue with Cornell Swift ARU audio recording anomalies

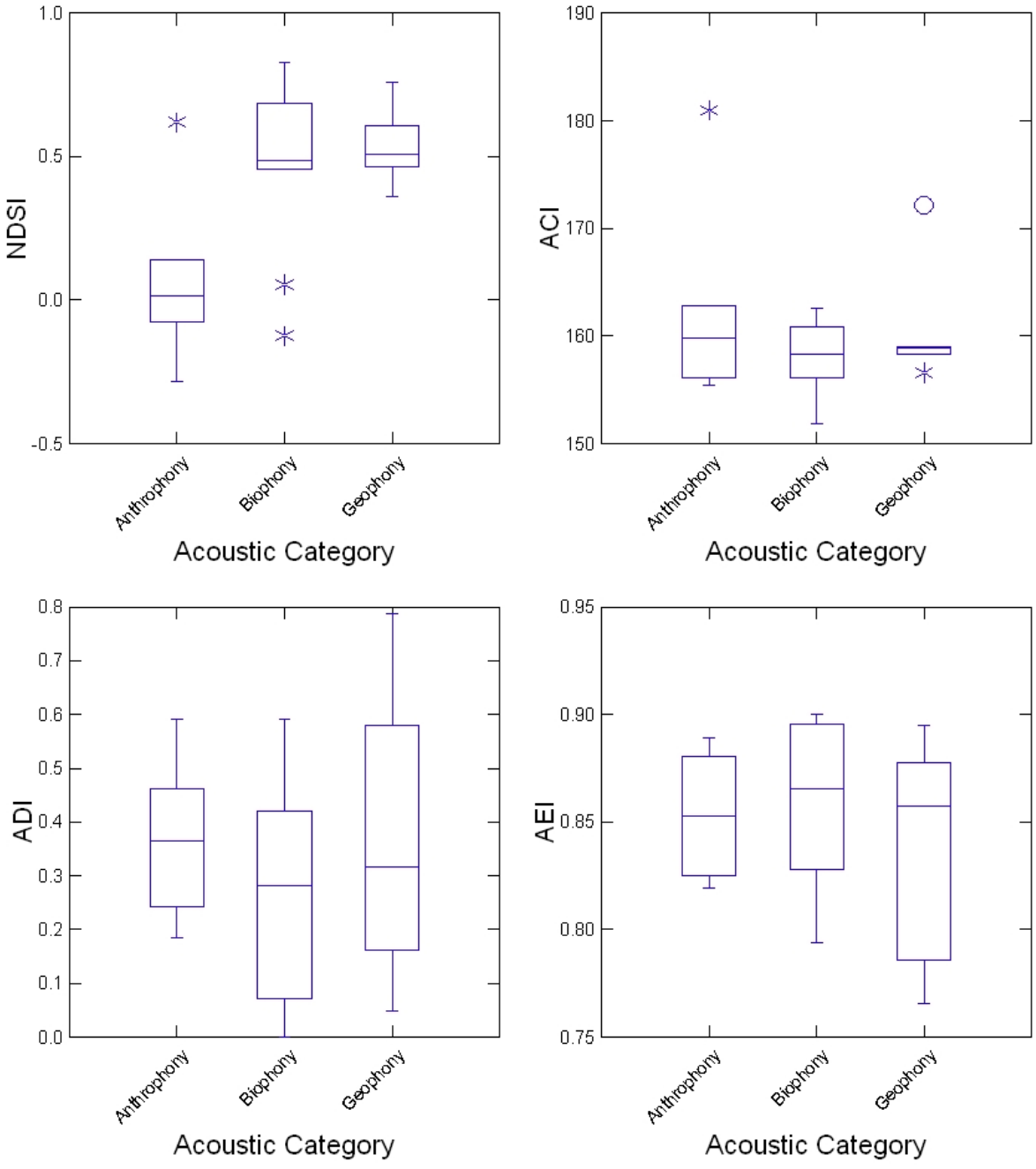
Following is the abstract of a manuscript produced and submitted for potential journal publication on a sound recording anomaly discovered with the Cornell Swift automatic audio recording units.

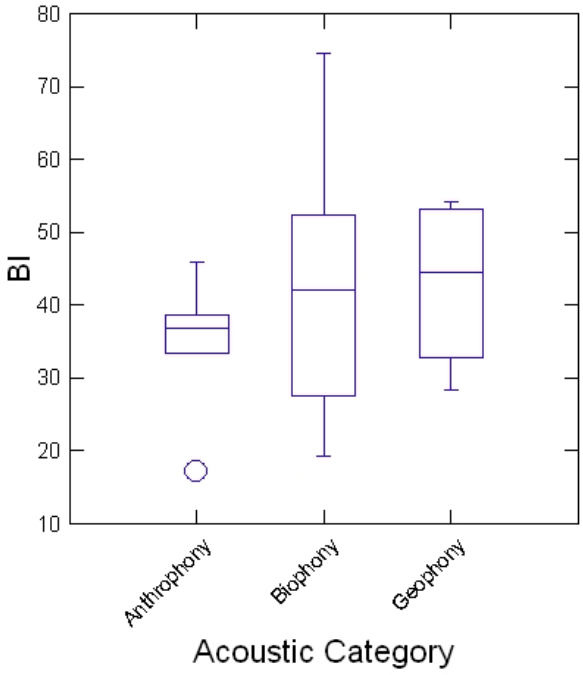
Marcot, B. G. Submitted. Sound anomalies of Cornell Swift recorders affect ecoacoustic studies, and a workaround solution.

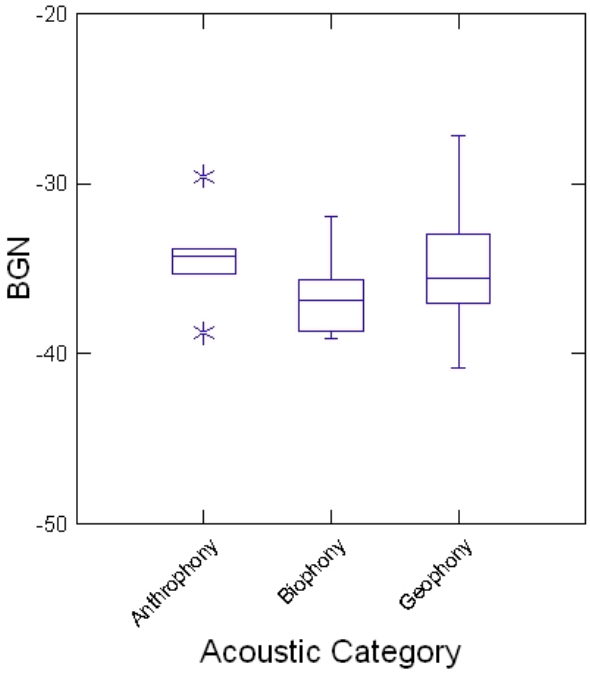
Abstract

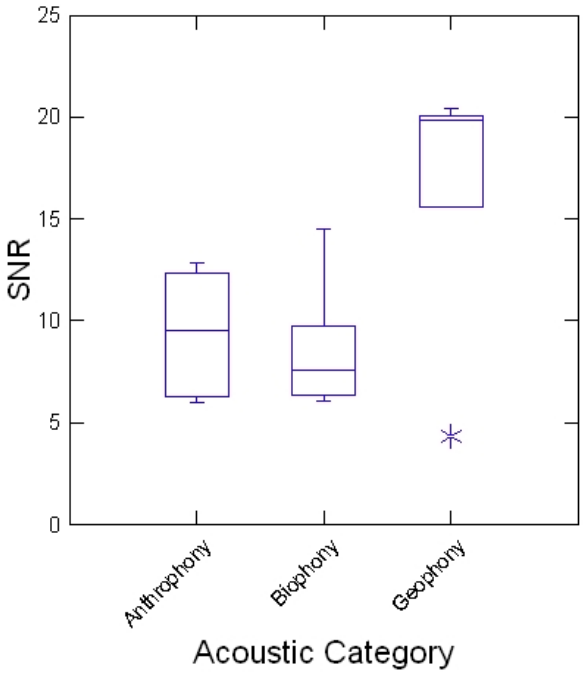
I discovered that the Swift Terrestrial Passive Acoustic Recording Unit from The Cornell Lab of Ornithology, running firmware v. STM32 0.18.6.3, produced an initial 4-sec sound anomaly in each sound (wave file) recording, created by the power-saving features of the unit as it switches from standby to record mode. The sound anomaly has a statistically significant impact on a number of soundscape indices calculated from the recordings. Here, I dissect the nature of the anomaly and analyze the highly variable effects it has on calculated ecoacoustic soundscape indices. I used a sample of 150 sound files, recorded during my ongoing ecoacoustics study in central boreal Alaska, stratified by several landscape conditions and by types of sounds representing anthrophony, biophony, and geophony conditions. The sound anomaly statistically significantly affected calculations of 7 of 13 ecoacoustic indices analyzed from all of these landscape and soundscape conditions. There is no simple correction factor that can be applied to calculated index values to account for effects of the anomaly. I suggest several workarounds, notably to automate a procedure to delete a specified initial segment of each sound file to eliminate the anomaly prior to soundscape analysis.

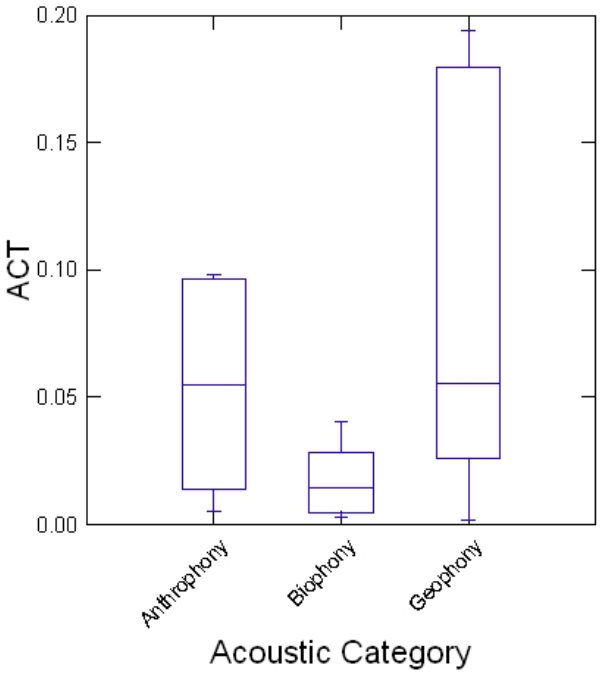
Appendix Figure 2. Values of 13 ecoacoustic indices (see main text Table 16), calculated from 150 audio samples across recording stations in the Fort Wainwright study (text Table 15), representing ecoacoustic categories of anthrophony (human-source), biophony (wildlife and other organisms), and geophony (natural abiotic environmental sources) sound sources (text Figure 86). Center lines in the boxes are median values, box lengths are the range within the central 50% of values, and asterisks are outside values.

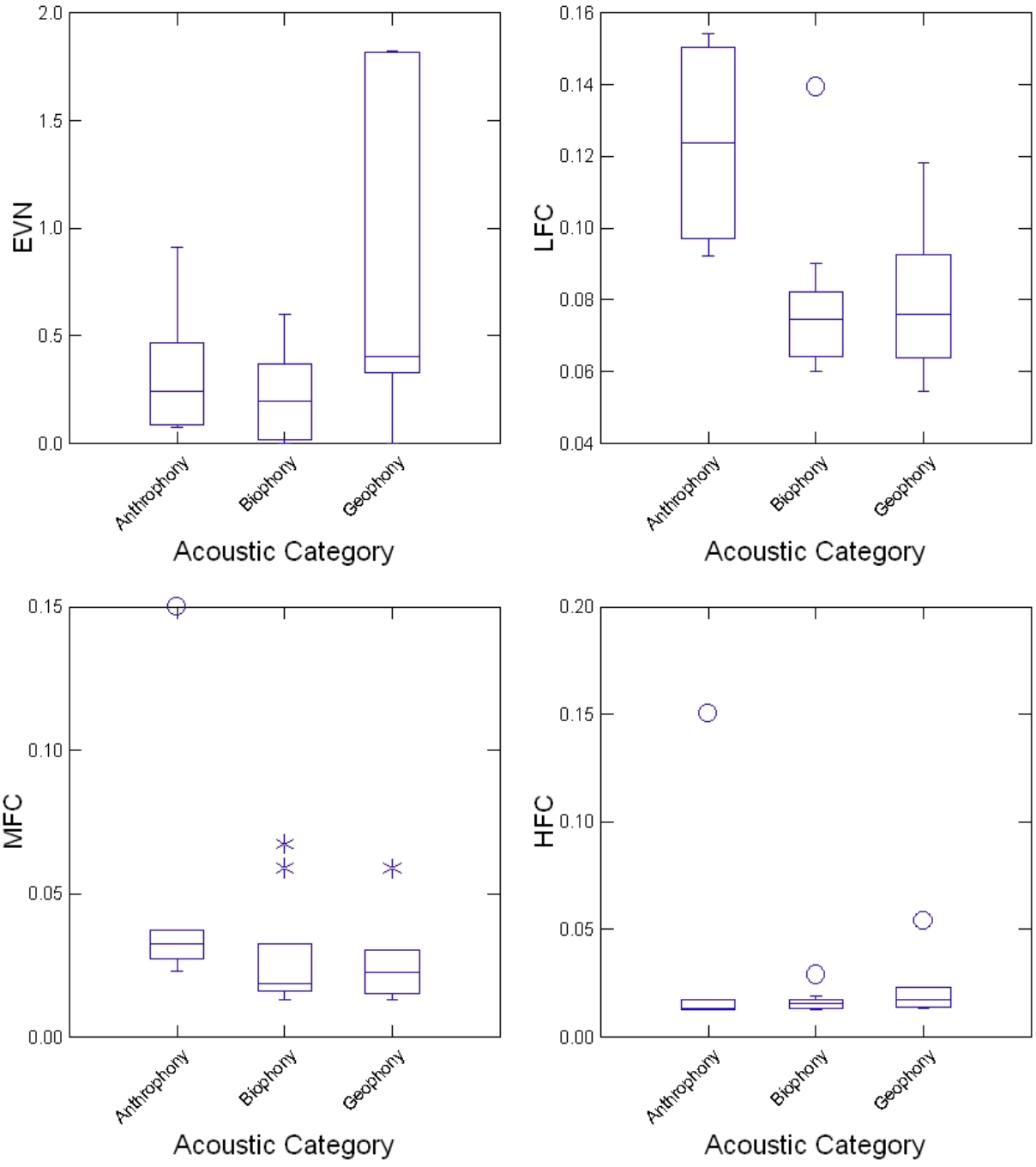


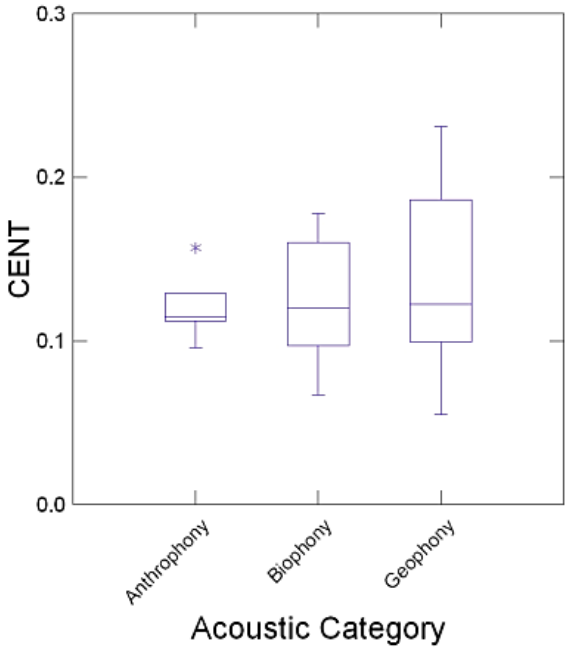

BI
80
70
60
50
40
30
20
10
Anthrophony
Biophony
Geophony
Acoustic Category


BGN
-20
-30
-40
-50
Anthrophony
Biophony
Geophony
Acoustic Category

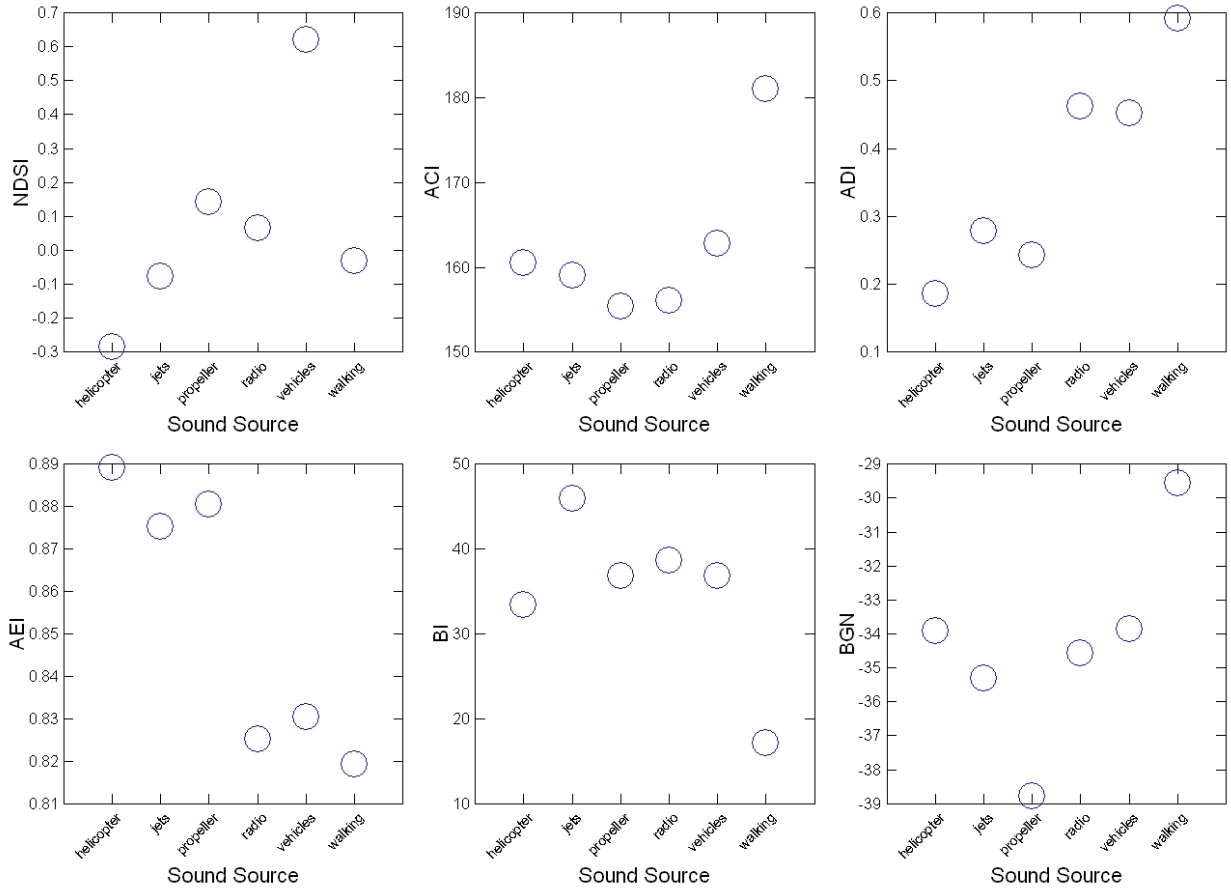

SNR
25
20
15
10
5
0
Anthrophony
Biophony
Geophony
Acoustic Category

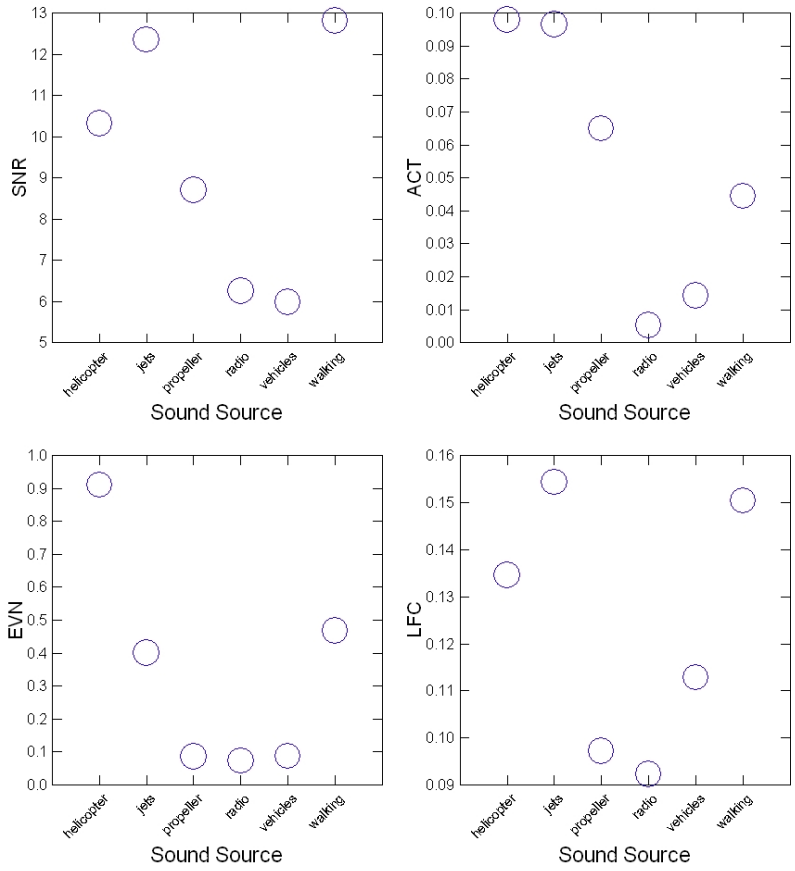

ACT
0.20
0.15
0.10
0.05
0.00
Anthrophony
Biophony
Geophony
Acoustic Category

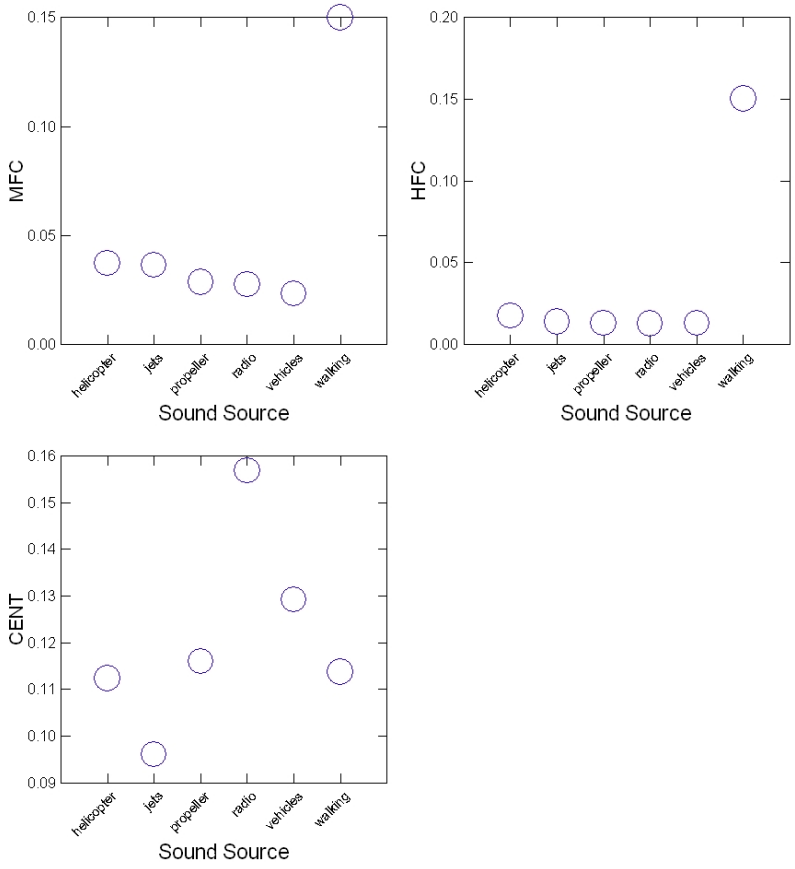

EVN
2.0
1.5
1.0
0.5
0.0
Anthrophony
Biophony
Geophony
Acoustic Category
LFC
0.16
0.14
0.12
0.10
0.08
0.06
0.04
Anthrophony
Biophony
Geophony
Acoustic Category
MFC
0.15
0.10
0.05
0.00
Anthrophony
Biophony
Geophony
Acoustic Category
HFC
0.20
0.15
0.10
0.05
0.00
Anthrophony
Biophony
Geophony
Acoustic Category


0.3
0.2
0.1
0.0
CENT
Anthrophony
Biophony
Geophony
Acoustic Category

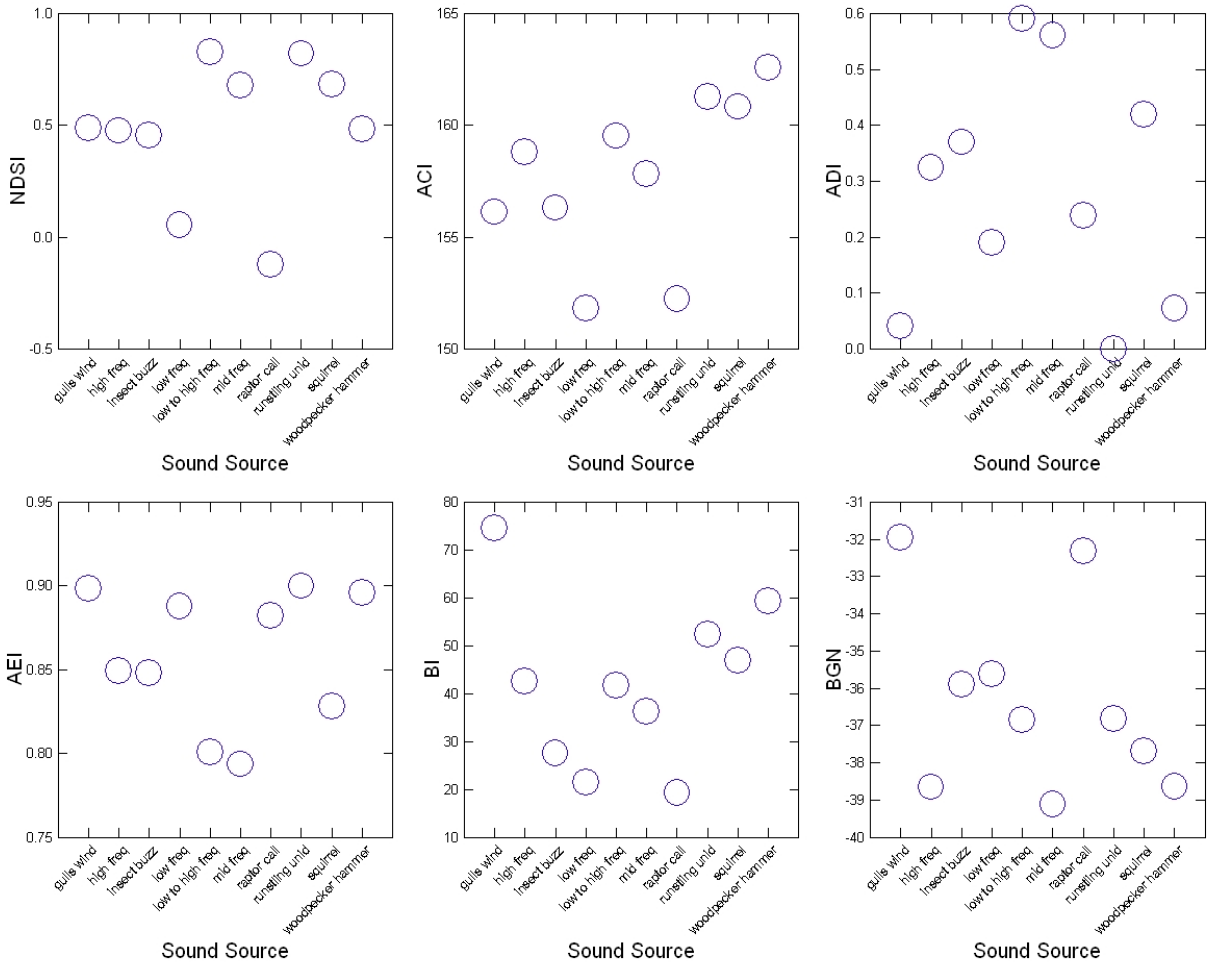
Appendix Figure 3. Values of 13 ecoacoustic indices (see main text Table 16) of 6 example categories of anthrophony (human-source) sound sources. Each circle denotes an individual, selected sound file pertaining to the specified sound source.

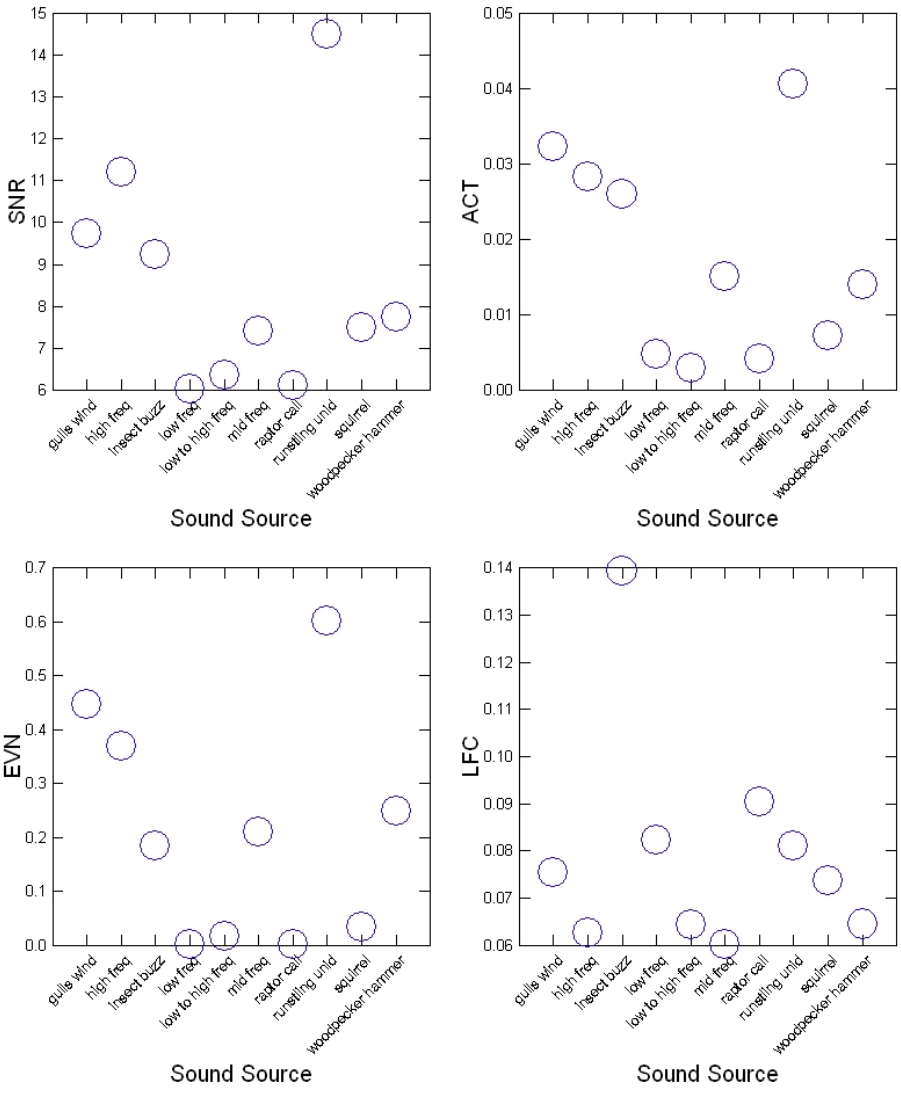


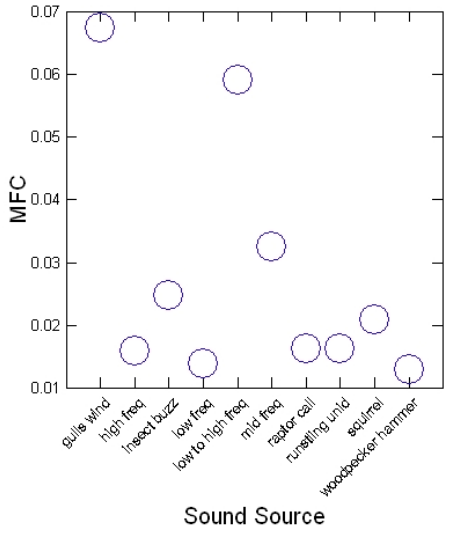

SNR
13
12
11
10
9
8
7
6
5
helicopter
jets
propeller
radio
vehicles
walking
Sound Source
ACT
0.10
0.09
0.08
0.07
0.06
0.05
0.04
0.03
0.02
0.01
0.00
helicopter
jets
propeller
radio
vehicles
walking
Sound Source
EVN
1.0
0.9
0.8
0.7
0.6
0.5
0.4
0.3
0.2
0.1
0.0
helicopter
jets
propeller
radio
vehicles
walking
Sound Source
LFC
0.16
0.15
0.14
0.13
0.12
0.11
0.10
0.09
helicopter
jets
propeller
radio
vehicles
walking
Sound Source

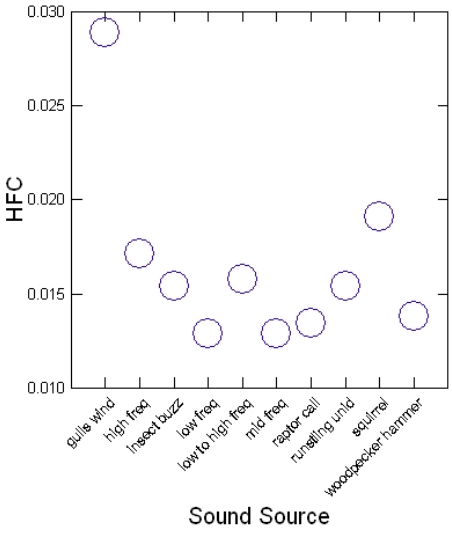

MFC
0.15
0.10
0.05
0.00
helicopter
jets
propeller
radio
vehicles
walking
Sound Source
HFC
0.20
0.15
0.10
0.05
0.00
helicopter
jets
propeller
radio
vehicles
walking
Sound Source
CENT
0.16
0.15
0.14
0.13
0.12
0.11
0.10
0.09
helicopter
jets
propeller
radio
vehicles
walking
Sound Source

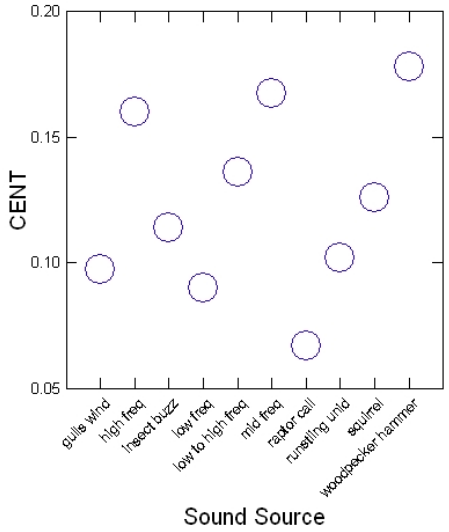
Appendix Figure 4. Values of 13 ecoacoustic indices (see main text Table 16) of 10 example categories of biophony (wildlife and other organisms) sound sources. Each circle denotes an individual, selected sound file pertaining to the specified sound source.



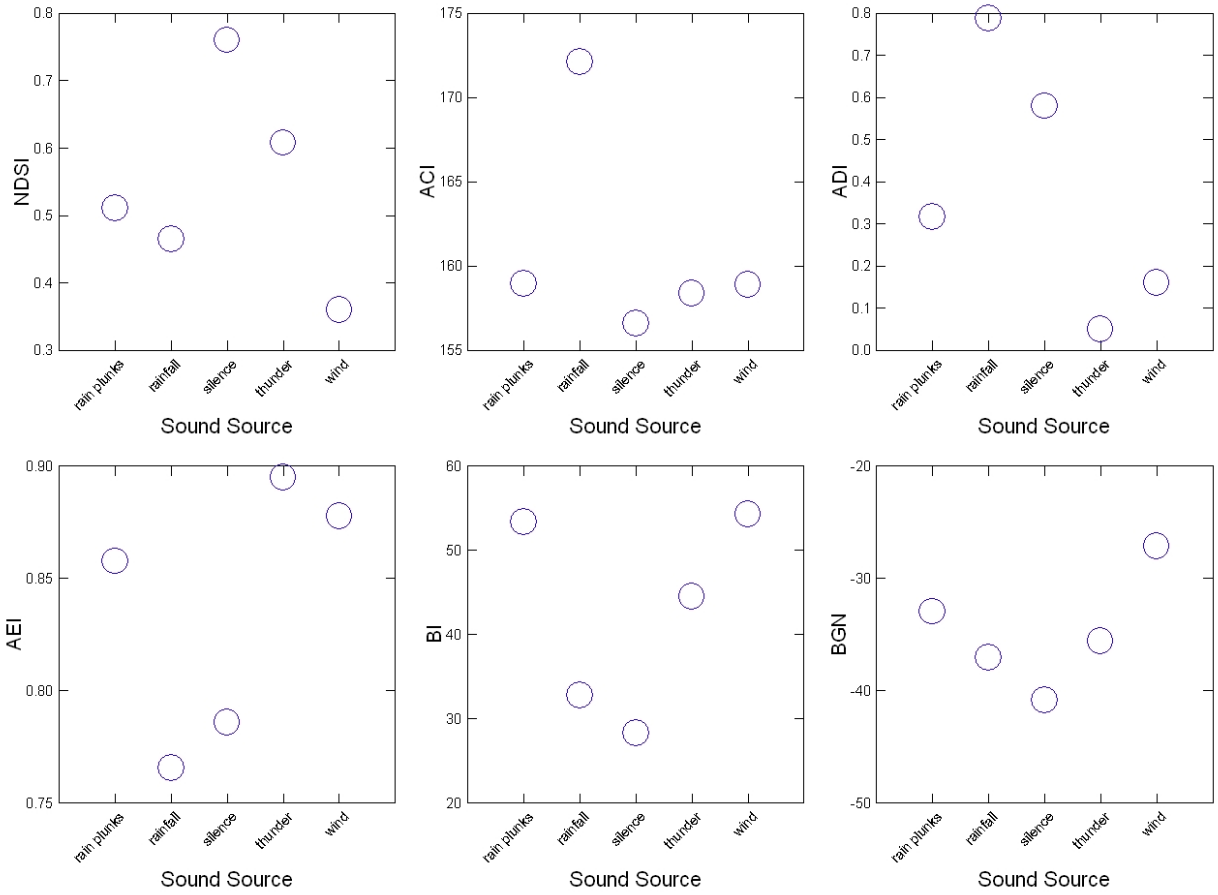

SNR
ACT
EVN
LFC
Sound Source
gulls wind
high freq
insect buzz
low freq
low to high freq
mid freq
raptor call
rustling unid
squirrel
woodpecker hammer

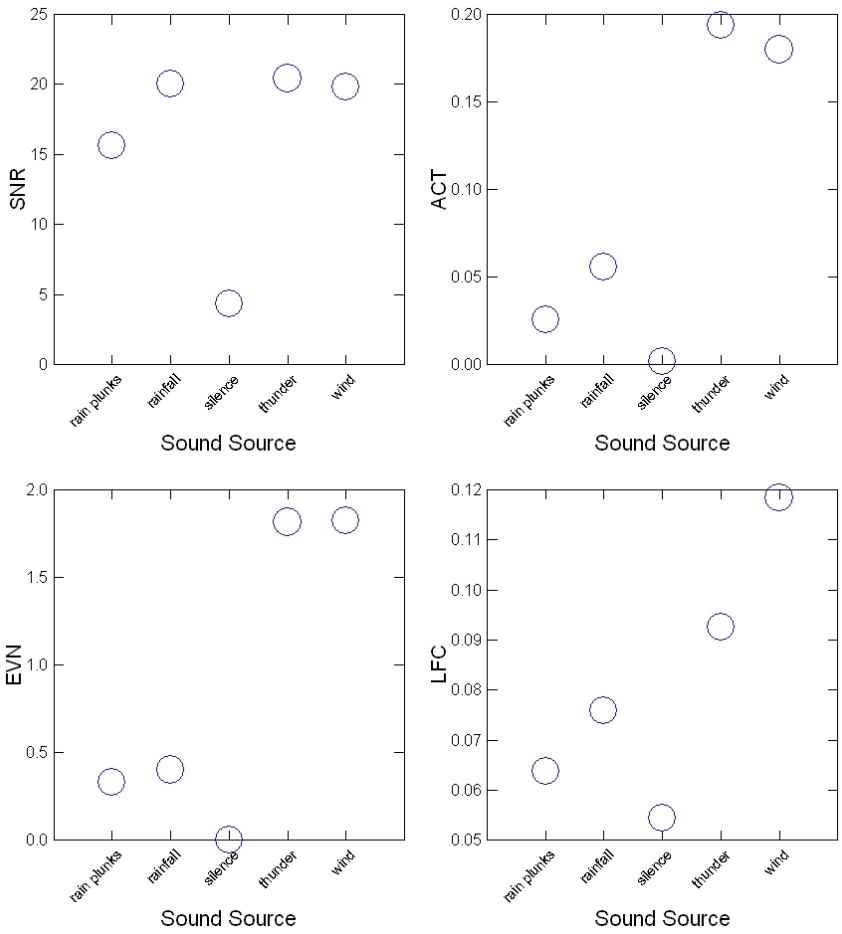

MFC
0.07
0.06
0.05
0.04
0.03
0.02
0.01
gulls wind
high freq
insect buzz
low freq
low to high freq
mid freq
raptor call
rustling unid
squirrel
woodpecker hammer
Sound Source

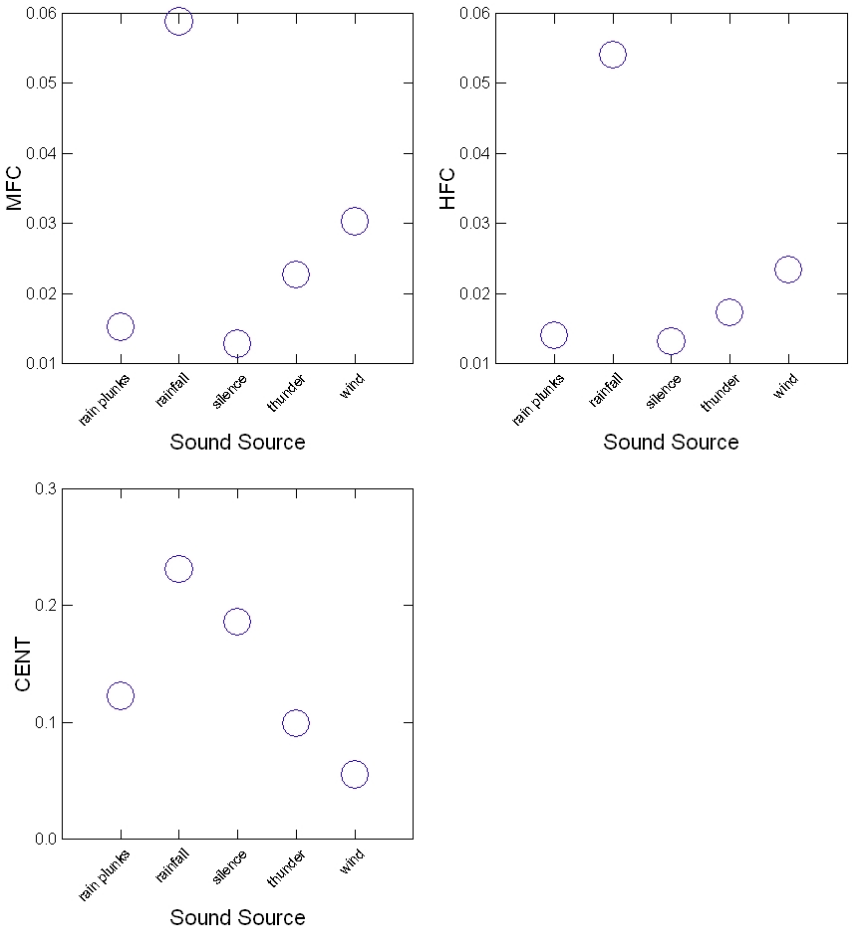

HFC
0.030
0.025
0.020
0.015
0.010
gulls wind
high freq
insect buzz
low freq
low to high freq
mid freq
raptor call
rustling unid
squirrel
woodpecker hammer
Sound Source


CENT
0.20
0.15
0.10
0.05
gulls wind
high freq
insect buzz
low freq
low to high freq
mid freq
raptor call
rustling unid
squirrel
woodpecker hammer
Sound Source

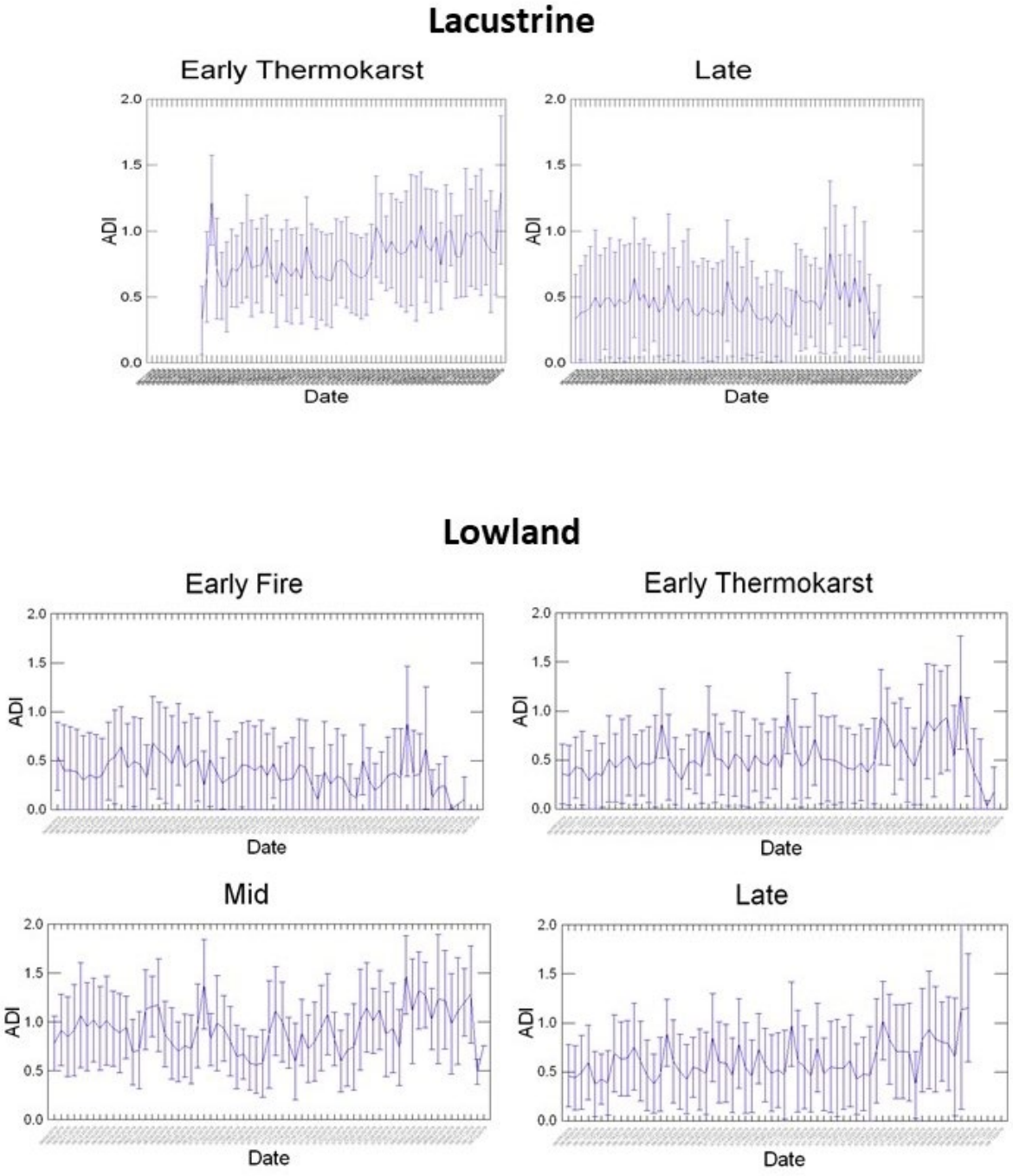
Appendix Figure 5. Values of 13 ecoacoustic indices (see main text Table 16) of 5 example categories of geophonic (natural abiotic environmental) sound sources. Each circle denotes an individual, selected sound file pertaining to the specified sound source.



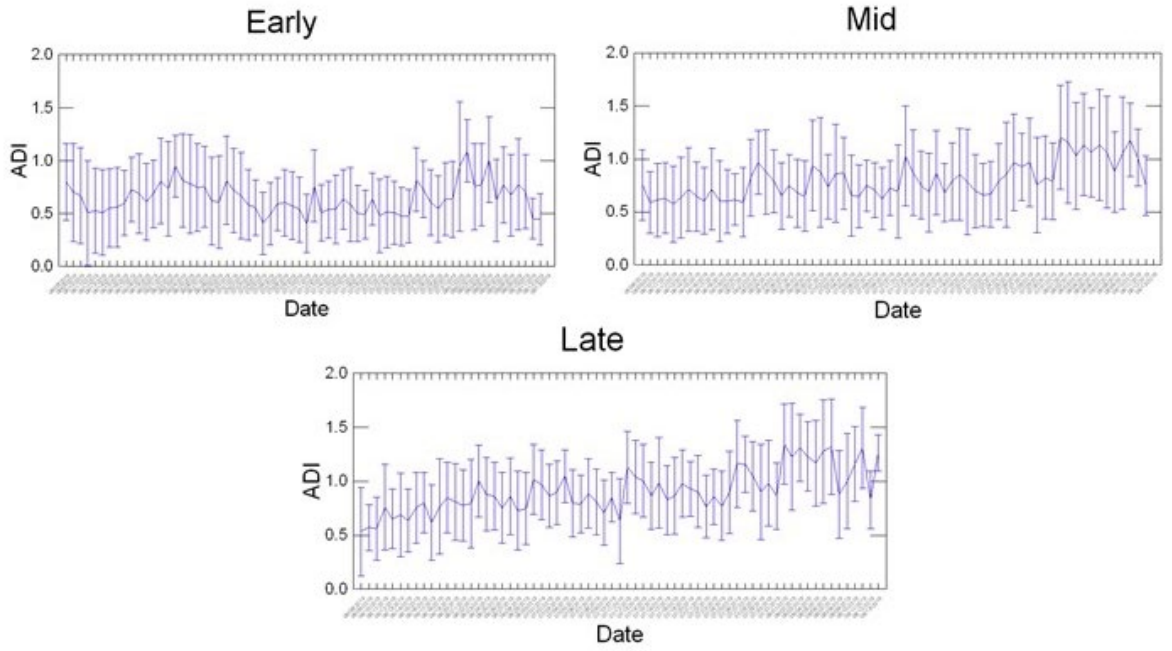

SNR
25
20
15
10
5
0
rain plunks
rainfall
silence
thunder
wind
Sound Source
ACT
0.20
0.15
0.10
0.05
0.00
rain plunks
rainfall
silence
thunder
wind
Sound Source
EVN
2.0
1.5
1.0
0.5
0.0
rain plunks
rainfall
silence
thunder
wind
Sound Source
LFC
0.12
0.11
0.10
0.09
0.08
0.07
0.06
0.05
rain plunks
rainfall
silence
thunder
wind
Sound Source


MFC
0.06
0.05
0.04
0.03
0.02
0.01
rain plunks
rainfall
silence
thunder
wind
Sound Source
HFC
0.06
0.05
0.04
0.03
0.02
0.01
rain plunks
rainfall
silence
thunder
wind
Sound Source
CENT
0.3
0.2
0.1
0.0
rain plunks
rainfall
silence
thunder
wind
Sound Source

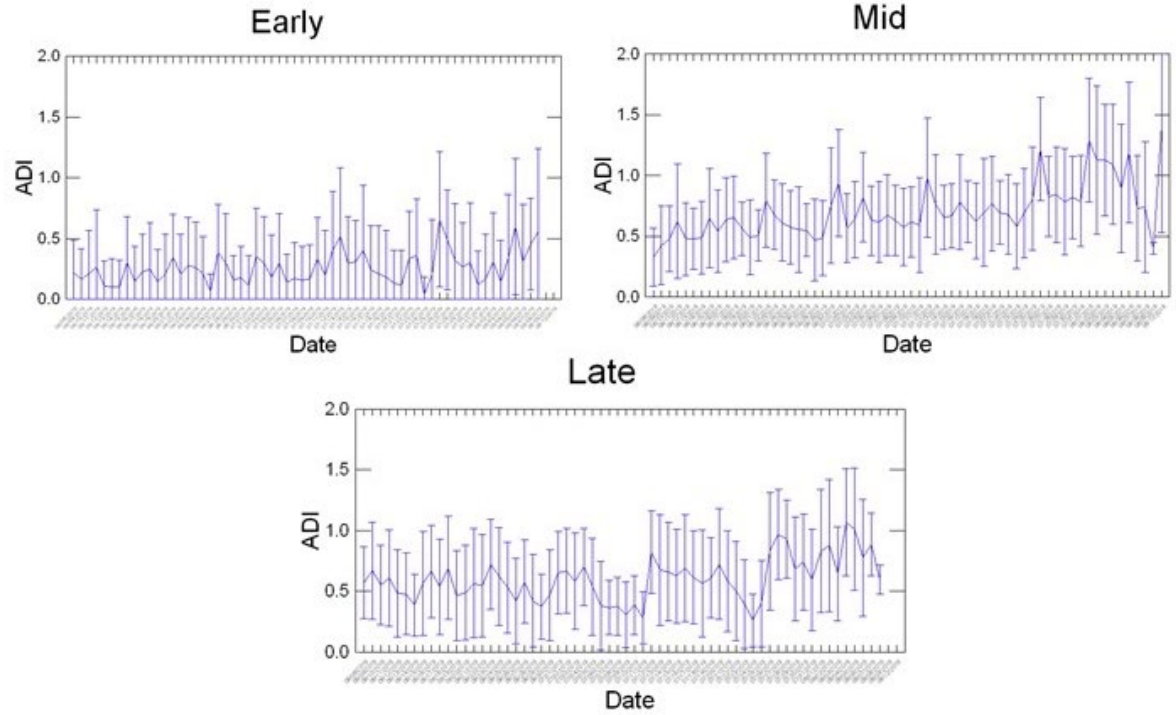
Appendix Figure 6. Values of the Acoustic Diversity Index (ADI) by date (June-August 2019) for lacustrine, lowland, riverine, and upland landscapes and their successional stages (continued below). Curved lines are mean values and vertical bars are ±1 SD.



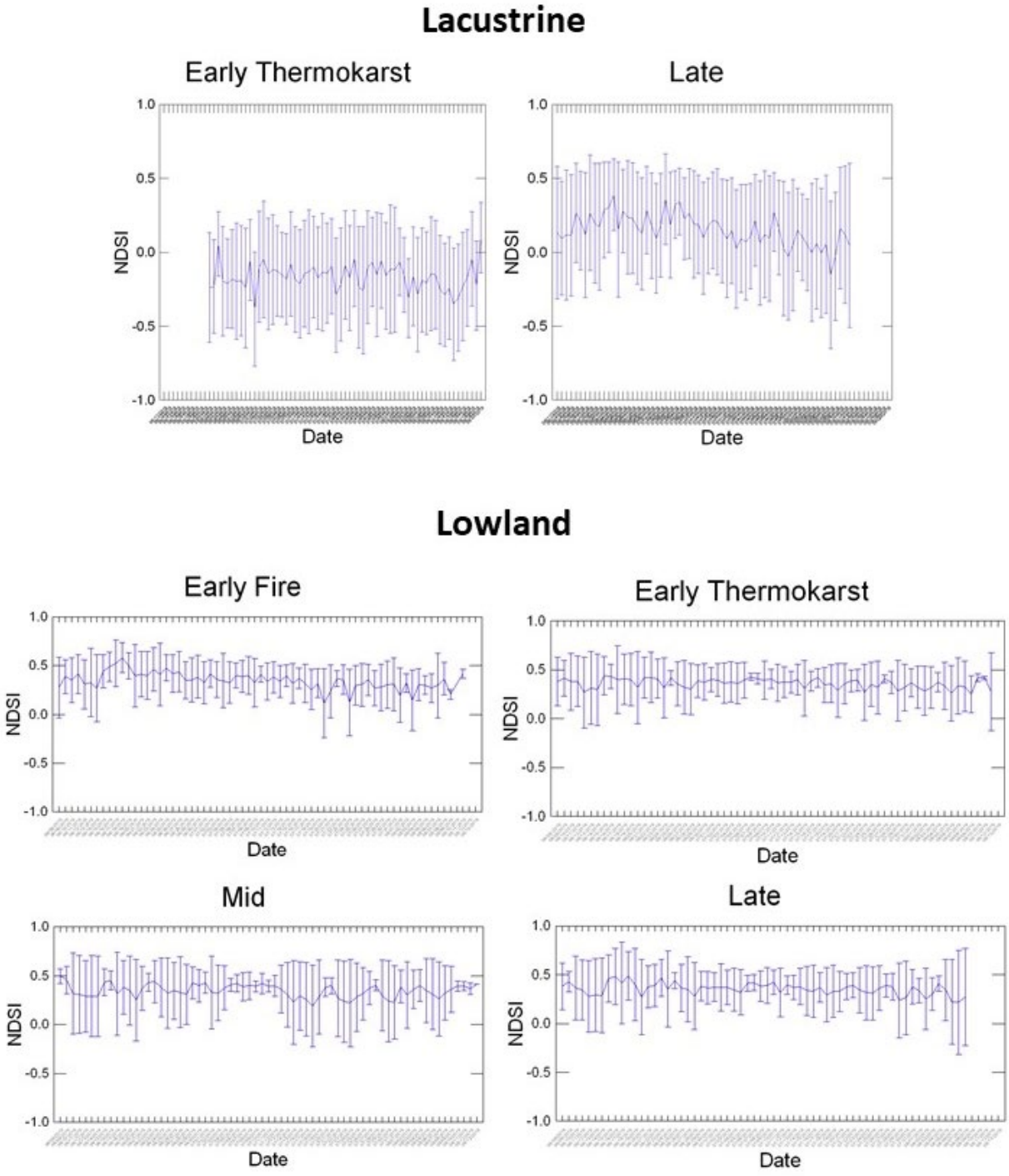
Riverine

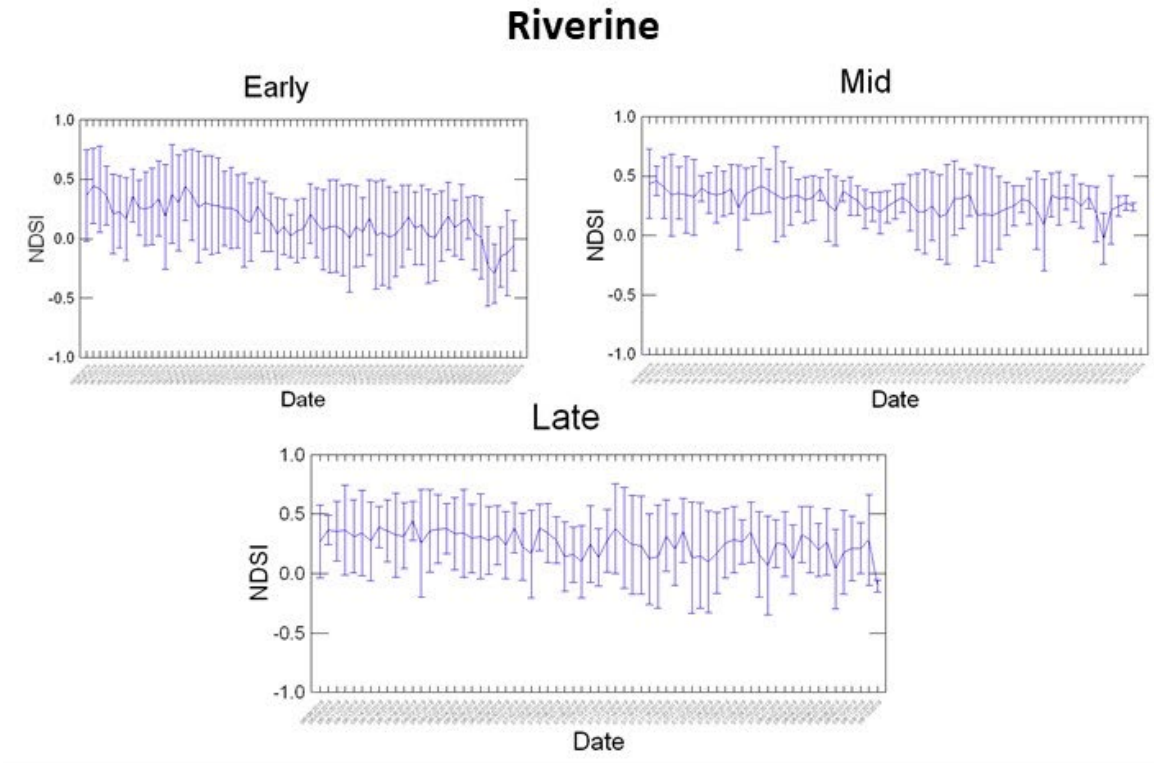


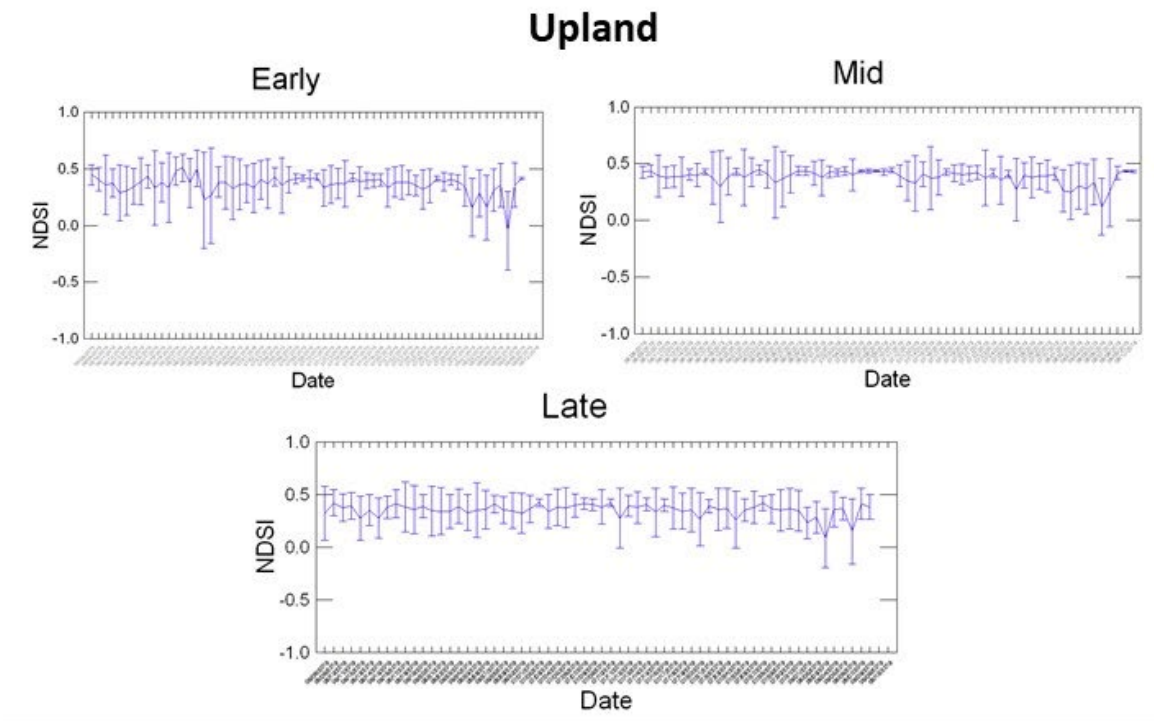
Upland



Appendix Figure 7. Values of the Normalized Difference Soundscape Index (NDSI) by date (June-August 2019) for lacustrine, lowland, riverine, and upland landscapes and their successional stages (continued below). Curved lines are mean values and vertical bars are ±1 SD.




Riverine
Early
Mid
Late
NDSI
Date
1.0
0.5
0.0
-0.5
-1.0


Upland
Early
Mid
Late
NDSI
Date
1.0
0.5
0.0
-0.5
-1.0

Appendix Table 17. Locations of the 24 automated audio recording units (ARU) and distances to each of 9 categories of human activity. See main text for definitions of the activity categories, and text Table 15 for definitions of ARU names and for ARU locations by landscape and successional stage deployment.

	Distance to Nearest Human Activity (m)								
ARU	Airport	Primary Road	Any Road	Drop Zone	Firing Site	Flight Line	Develop-ment	Landing Zone	Range
LDSB2	24113	6412	211	43375	24759	2955	1798	23846	32126
LDSB6	10177	7354	223	1127	6299	7531	184	12606	5922
LDTL1	6803	2875	470	32541	4821	358	134	9377	4666
LDTL2	11248	8260	455	1105	7361	7413	421	12652	6967
LLSD1	23863	5371	513	44227	25096	1908	1305	24481	32059
LLSD3	23402	5209	962	44039	24699	1878	1709	24184	31603
LWBF4	13684	3185	2711	18866	17235	160	74	15696	17443
LWBFX	9984	6871	380	642	6459	8291	146	13364	6134
LWNF1	25228	6376	143	44289	25973	2562	812	24966	33315
LWNF9	10069	6783	788	307	6723	8660	556	13754	6420
RMBF1	24247	7279	101	42591	24352	3856	2502	23237	32093
RMBF5	13267	2801	2204	19304	16860	342	47	16199	16964
RMNF1	24506	7499	24	42567	24494	4017	2518	23306	32325
RMNF8	12999	2212	1670	19911	16275	915	217	16700	16555
RMTS3	24720	7858	96	42365	24499	4344	2748	23212	32480
RMTS4	11060	1490	418	21049	14711	2531	130	17921	14592
UMBF6	19336	12841	177	24982	626	6875	147	6268	9148
UMBF7	20245	14381	167	25308	780	5678	144	4811	7593
UMNF1	25085	5761	75	44834	26209	1887	283	25367	33283
UMNF5	18829	12516	300	24565	887	6998	267	6536	9535
UMTLS7	20031	18855	127	21164	820	55	111	2362	5225
UMTLSX	20344	20013	136	19672	383	8	137	796	4455
USTL1	12687	225	225	32007	9416	1455	112	14711	9327
USTL2	12497	745	745	31473	9288	928	666	14454	9196

Appendix Table 18. Total area of each land cover and vegetation condition represented in 6,063 GoPro camera photographs taken during two low-altitude photographic flight transects in Fort Wainwright (see text Figs. D.1.1, D.1.2). Values here are total m2 of each cover category summed across all photos.

Cover category	Flight Path 1	Flight Path 2	SUM
Agriculture-Cultivated Crops and Irrigated Agriculture	44,266	483,244	527,510
Agriculture-Pasture and Hay	0	9,972	9,972
Alaskan Boreal Dry Aspen Forest	253,513	35,820	289,333
Alaskan Maritime Western Hemlock - Sitka Spruce Rainforest	0	0	0
Alaskan-Yukon Boreal Black Spruce Wet Forest	174,105,786	175,802,286	349,908,072
Alaskan-Yukon Boreal Flooded & Rich Swamp	79,524,807	63,516,579	143,041,386
Alaskan-Yukon Boreal Montane Alder - Willow Shrubland	19,520,438	165,414	19,685,852
Alaska-Yukon Northern Boreal Mesic Woodland	0	0	0
Arctic Herbaceous Tundra	912,275	33,159	945,434
Arctic Low Shrub Tundra	14,572,441	8,379,939	22,952,379
Central Alaskan Boreal Montane Woodland	37,816,683	448,889	38,265,572
Central Alaskan-Yukon Boreal Mesic Forest	884,096,598	610,162,013	1,494,258,611
Developed-High Intensity	11,382,780	4,960,785	16,343,565
Developed-Low Intensity	36,330,366	17,978,417	54,308,782
Developed-Medium Intensity	12,253,384	5,174,425	17,427,809
Developed-Open Space	22,910,005	17,632,069	40,542,074
Developed-Roads	28,849,009	15,349,830	44,198,839
North American Glacier and Ice Field	591,168	0	591,168
Open Water	194,333,623	68,571,996	262,905,620
Quarries-Strip Mines-Gravel Pits-Energy Development	1,874,970	1,306,729	3,181,699
Recently Burned-Herb and Grass Cover	18,063,412	4,910,934	22,974,346
Recently Burned-Shrub Cover	133,906,307	12,272,376	146,178,682
Recently Burned-Tree Cover	12,438,093	2,753,995	15,192,087
Recently Disturbed Other-Herb and Grass Cover	0	0	0
Recently Disturbed Other-Shrub Cover	0	0	0
Recently Logged-Herb and Grass Cover	0	37,662	37,662
Recently Logged-Shrub Cover	0	0	0
Southern Alaskan Boreal Mesic Forest	0	0	0
Southern Alaskan Boreal Montane Woodland	21,520,050	0	21,520,050
Western Boreal Alpine Acidic Mesic Meadow	8,221,733	12,159	8,233,892
Western Boreal Alpine Cliff, Scree & Rock Vegetation	105,147,011	146,581	105,293,592
Western Boreal Alpine Dwarf-shrubland	69,003,678	2,900,093	71,903,771
Western Boreal Alpine Mesic Dwarf Birch - Willow Shrubland	285,517,117	239,411	285,756,528
Western Boreal Cliff, Scree & Rock Vegetation	54,170,295	1,224,678	55,394,973
Western Boreal Dry Shrubland & Grassland	1,081,118	439,868	1,520,985
Western Boreal Dune Shrubland & Grassland	1,270,856	348,165	1,619,021
Western Boreal Mesic Alder - Willow Shrubland	22,794,767	757,786	23,552,553
Western Boreal Mesic Birch - Willow Low Shrubland	59,939,238	63,630,018	123,569,256
Western Boreal Mesic Grassland & Meadow	3,670,464	4,969,441	8,639,905
Western Boreal Wet Alder - Willow Tall Shrub Swamp	103,071,600	70,173,874	173,245,474
Western Boreal Wet Birch - Willow Low Shrubland	2,596,284	404,308	3,000,592
Western Boreal Wet Meadow & Marsh	16,420,501	34,116,417	50,536,918
Western North American Boreal Alkaline Fen	207,178	36,672	243,850
Western North American Boreal Bog & Acidic Fen	280,183,815	396,757,282	676,941,098

7. PERFORMING ORGANIZATION NAME(S) AND ADDRESS(ES)

Cold Regions Research and Engineering Laboratory
U.S. Army Engineer Research and Development Center
9th Avenue, Building 4070, Fort Wainwright, AK 99703

Alaska Ecosience
2332 Crodes Way, Fairbanks, AK 99709

U.S. Forest Service Pacific Northwest, Portland Forestry Sciences Laboratory
620 SW Main St #400, Portland, OR 97205

Institute of Arctic Biology, University of Alaska Fairbanks
2140 Koyukuk Drive, Fairbanks, AK 99775